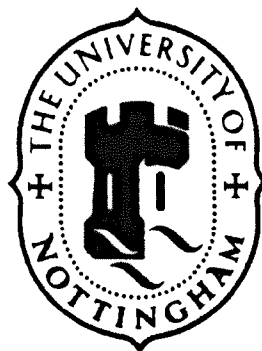


**University of Nottingham**  
**School of Chemical, Environmental and Mining Engineering**



**THE APPLICATION OF ROCK MASS  
CLASSIFICATION PRINCIPLES TO COAL MINE  
DESIGN**

**By**

**David N. Whittles  
B.Sc.(Hons), M.Sc., FGS**

**Thesis submitted to the University of Nottingham  
for the degree of Doctor of Philosophy**

**November 1999**

*....this thesis is dedicated to my parents.*

## **CONTENTS**

<b>Abstract.....</b>	i
<b>Affirmation.....</b>	iii
<b>List of Figures.....</b>	iv
<b>List of Tables.....</b>	xi

### **CHAPTER 1**

#### **AN INTRODUCTION TO THE THESIS**

<b>1.1 INTRODUCTION.....</b>	1
<b>1.2 OBJECTIVES OF THESIS.....</b>	4

### **CHAPTER 2**

#### **GEOLOGY OF THE UNITED KINGDOM COAL MEASURES**

<b>2.1 GENERAL STRATIGRAPHY.....</b>	7
<b>2.1.1 Introduction.....</b>	7
<b>2.1.2 Depositional Environments Of The UK Coal Measures .....</b>	8
<b>2.1.2.1 Sedimentary Province.....</b>	9
<b>2.2 DIAGENESIS.....</b>	9
<b>2.2.1 Introduction.....</b>	9
<b>2.2.2 Diagenesis Of Sandstones.....</b>	10
<b>2.2.3 Diagenesis Of Mudrocks.....</b>	12
<b>2.3 TECTONIC EVENTS.....</b>	13
<b>2.4 UK COAL MEASURE ROCK TYPES.....</b>	15
<b>2.4.1 Sandstones.....</b>	15
<b>2.4.2 Mudrocks.....</b>	15
<b>2.4.2.1 Siltstone.....</b>	16
<b>2.4.2.2 Mudstones.....</b>	16
<b>2.4.2.3 Claystones and Seatearths.....</b>	17
<b>2.4.2.4 Shale.....</b>	17
<b>2.4.3 Coal.....</b>	17
<b>2.5 SEDIMENTARY STRUCTURES.....</b>	18
<b>2.5.1 Introduction.....</b>	18
<b>2.5.2 Bedding.....</b>	18
<b>2.5.2.1 Massive Bedding.....</b>	19

<b>2.5.2.2 Cross Bedding.....</b>	<b>19</b>
<b>2.5.2.3 Graded Bedding .....</b>	<b>19</b>
<b>2.5.2.4 Laminations.....</b>	<b>19</b>
<b>2.5.3 Soft Sediment Structures.....</b>	<b>19</b>
<b>2.5.3.1 Convolute Bedding.....</b>	<b>20</b>
<b>2.5.3.2 Convolute Laminations.....</b>	<b>20</b>
<b>2.5.3.3 Load Casts and Pseudo Nodules.....</b>	<b>20</b>
<b>2.5.3.4 Slump Structures.....</b>	<b>21</b>
<b>2.5.3.5 Organic Sedimentary Structures.....</b>	<b>21</b>
<b>2.5.4 Sedimentary Structures Affecting Coal Seams.....</b>	<b>21</b>
<b>2.5.4.1 Washouts.....</b>	<b>21</b>
<b>2.5.4.2 Roof Rolls.....</b>	<b>21</b>
<b>2.5.4.3 Swilles.....</b>	<b>22</b>
<b>2.5.4.4 Seam Splits.....</b>	<b>22</b>
<b>2.5.4.5 Dirt Partings.....</b>	<b>22</b>
<b>2.6 NON-SEDIMENTARY STRUCTURES.....</b>	<b>23</b>
<b>2.6.1 Introduction.....</b>	<b>23</b>
<b>2.6.2 Discontinuities.....</b>	<b>23</b>
<b>2.6.2.1 Joints.....</b>	<b>23</b>
<b>2.6.2.1.1 Mechanism of joint formation.....</b>	<b>24</b>
<b>2.6.2.1.2 Coal cleat.....</b>	<b>27</b>
<b>2.6.2.1.3 Joint spacing distributions.....</b>	<b>28</b>
<b>2.6.2.1.4 Average joint spacing.....</b>	<b>28</b>
<b>2.6.2.1.5 Joint spacing in thick beds.....</b>	<b>30</b>
<b>2.6.2.2 Faults.....</b>	<b>31</b>
<b>2.6.2.2.1 Origin of faults.....</b>	<b>32</b>
<b>2.6.3 Folding.....</b>	<b>32</b>
<b>2.7 IN-SITU STATE OF STRESS WITHIN UK COAL MEASURES.....</b>	<b>34</b>
<b>2.7.1 Introduction.....</b>	<b>34</b>
<b>2.7.2 Sources Of In-Situ Stress.....</b>	<b>34</b>
<b>2.7.2.1 Gravitational Stress.....</b>	<b>35</b>
<b>2.7.2.1.1 The affect of surface topography.....</b>	<b>36</b>
<b>2.7.2.2 Tectonic Stress.....</b>	<b>36</b>
<b>2.7.2.3 Structural Stress.....</b>	<b>37</b>
<b>2.7.2.4 Residual Stress.....</b>	<b>37</b>

<b>2.7.3 Global In-Situ Stress.....</b>	<b>37</b>
<b>2.7.4 In-Situ Stress Within The United Kingdom.....</b>	<b>38</b>
<b>2.7.5 In-Situ Stress Within The UK Coal Measures.....</b>	<b>41</b>
<b>2.8 CONCLUSION.....</b>	<b>42</b>

## CHAPTER 3

### UK COAL MINING AND COAL MINE STABILITY

<b>3.1 LONGWALL EXTRACTION TECHNIQUES.....</b>	<b>43</b>
<b>3.1.1 Introduction.....</b>	<b>43</b>
<b>3.1.2 Longwall Advance Methods.....</b>	<b>43</b>
<b>3.1.3 Longwall Retreat Methods.....</b>	<b>44</b>
<b>3.1.3.1 Semi Retreat Methods.....</b>	<b>45</b>
<b>3.1.3.2 Single Entry Longwalls.....</b>	<b>45</b>
<b>3.1.4 Layout Of Longwalls.....</b>	<b>45</b>
<b>3.2 MINING INDUCED STRESS.....</b>	<b>46</b>
<b>3.2.1 Introduction.....</b>	<b>46</b>
<b>3.2.2 Stress Distributions Around a Simplified Excavations In Homogeneous Medium.....</b>	<b>47</b>
<b>3.2.2.1 Stresses at the Excavation Boundary.....</b>	<b>48</b>
<b>3.2.2.2 Stress Change with Increasing Distance from the Excavation Boundary.....</b>	<b>49</b>
<b>3.2.3 Stress Distributions Around Rectangular Excavations In An Homogeneous Elastic Medium.....</b>	<b>50</b>
<b>3.2.4 Influence Of A Yield Zone On Stress Distributions Around A Circular Excavation.....</b>	<b>51</b>
<b>3.2.5 Stress Distributions Around Longwall Panels In Coal Measure Strata.....</b>	<b>52</b>
<b>3.2.5.1 Vertical Stress Distributions.....</b>	<b>52</b>
<b>3.2.5.1.1 Front abutment.....</b>	<b>54</b>
<b>3.2.5.1.2 Flank abutments.....</b>	<b>54</b>
<b>3.2.5.1.3 Rear abutments.....</b>	<b>54</b>
<b>3.2.5.1.4 Wilson's equations.....</b>	<b>55</b>

<b>3.2.6 Affect Of Differential Horizontal In-Situ Stresses On Stress Distributions Around Longwall Panels.....</b>	58
<b>3.2.7 Affect Of Stress Interactions With Adjacent Workings.....</b>	58
<b>3.2.7.1 Neighbouring Panels.....</b>	58
<b>3.2.7.1.1 Vertical stress interaction.....</b>	58
<b>3.2.7.1.2 Horizontal stress interaction.....</b>	60
<b>3.2.7.2 Overlying and Underlying Workings.....</b>	60
<b>3.2.7.2.1 Pillars.....</b>	60
<b>3.2.7.2.2 Goafs.....</b>	62
<b>3.3 ROADWAY AND GATE ROAD STABILISATION TECHNIQUES.....</b>	63
<b>3.3.1 Introduction.....</b>	63
<b>3.3.2 Free Standing Supports.....</b>	64
<b>3.3.3 Rock Reinforcement Techniques.....</b>	65
<b>3.3.3.1 Roof Bolting.....</b>	65
<b>3.3.3.2 Cable Bolting.....</b>	66
<b>3.3.3.3 Rib Bolting.....</b>	68
<b>3.3.4 Road Side Packs.....</b>	68
<b>3.4 CHARACTERISTIC MECHANISM OF STRATA DEFORMATION WITHIN COAL MINES.....</b>	71
<b>3.4.1 Introduction.....</b>	71
<b>3.4.2 Roof Deformation Mechanisms.....</b>	72
<b>3.4.3 Floor Deformation Mechanisms.....</b>	74
<b>3.4.3.1 The Affect of Water on Clay Rich Mudrocks.....</b>	74
<b>3.4.3.2 Floor Deformation Mechanisms.....</b>	76
<b>3.4.4 Rib Deformation Mechanisms.....</b>	79
<b>3.5 CONCLUSIONS.....</b>	81

## **CHAPTER 4**

### **CHARACTERISATION OF THE MECHANICAL PROPERTIES OF ROCK AND ROCK MASSES**

<b>4.1 INTRODUCTION.....</b>	83
<b>4.2 MECHANICAL PROPERTIES OF INTACT ROCK.....</b>	83
<b>4.2.1 Stress-Strain Behaviour Of Intact Rock.....</b>	84
<b>4.2.2 Elastic Properties Of Intact Rock.....</b>	86

<b>4.2.3 Intact Rock Failure.....</b>	87
<b>4.2.3.1 Influencing Parameters.....</b>	87
<b>4.2.3.1.1 <i>Confining pressure.....</i></b>	87
<b>4.2.3.2 Failure Criteria.....</b>	88
<b>4.2.3.3 Theoretical Failure Criteria.....</b>	88
<b>4.2.3.3.1 <i>Coulomb's theory and criterion.....</i></b>	89
<b>4.2.3.3.2 <i>Mohr's failure criterion.....</i></b>	91
<b>4.2.3.3.3 <i>Griffith's theory and criterion for brittle fracture.....</i></b>	92
<b>4.2.3.4 Empirical Failure Criteria.....</b>	94
<b>4.2.3.4.1 <i>Murrel's criterion.....</i></b>	95
<b>4.2.3.4.2 <i>Bieniawski's criterion.....</i></b>	95
<b>4.3 MECHANICAL PROPERTIES OF ROCK MASSES.....</b>	97
<b>4.3.1 Introduction .....</b>	97
<b>4.3.2 Stiffness Properties Of Rock Masses.....</b>	98
<b>4.3.3 Rock Mass Failure Criteria.....</b>	101
<b>4.3.3.1 Hoek–Brown Criterion.....</b>	101
<b>4.3.3.2 Bieniawski-Yudhibr Criterion.....</b>	105
<b>4.3.3.3 Ramamurthy's Criterion.....</b>	105
<b>4.3.4 Application of Rock Mass Failure Criteria to the UK</b>	
<b>Coal Measure Strata.....</b>	106
<b>4.3.4.1 Development of a Rock Mass Failure Criteria for UK</b>	
<b>Coal Measure Strata.....</b>	107
<b>4.3.4.2 Evaluation of Most Suitable Criterion for Predicting</b>	
<b>Failure of Coal Measure Strata.....</b>	109
<b>4.4 MECHANICAL PROPERTIES OF ANISOTROPIC ROCKS.....</b>	111
<b>4.4.1 Introduction.....</b>	111
<b>4.4.2 Elastic Properties Of Stratified Rocks.....</b>	111
<b>4.4.2.1 Orthotropy.....</b>	111
<b>4.4.2.2 Transverse Isotropy .....</b>	112
<b>4.4.3 Failure Criteria For Anisotropic Rocks.....</b>	113
<b>4.5 ROCK MASS CLASSIFICATIONS.....</b>	114
<b>4.5.1 Introduction.....</b>	114
<b>4.5.2 Terzaghi's Rock Load Height Classification.....</b>	115
<b>4.5.3 Lauffer's Classification.....</b>	118
<b>4.5.4 Rock Quality Designation (RQD) Index.....</b>	118

<b>4.5.5 Rock Structure Rating (RSR).....</b>	<b>119</b>
<b>4.5.6 Rock Mass Rating (Geomechanics Classification).....</b>	<b>122</b>
<b>4.5.7 NGI Tunneling Quality Index ('Q' Index).....</b>	<b>126</b>
<b>4.5.8 The Utilisation Of Rock Mass Classification In Coal Mine Design.....</b>	<b>132</b>
<b>4.5.9 USBM Coal Mine Roof Rating Classification.....</b>	<b>140</b>
<b>4.5.9.1 USBM Floor Quality Classification.....</b>	<b>143</b>
<b>4.6 CONCLUSIONS.....</b>	<b>143</b>

## **CHAPTER 5**

### **DEVELOPMENT OF A ROCK MASS CLASSIFICATION FOR UK COAL MINE DESIGN**

<b>5.1 INTRODUCTION.....</b>	<b>145</b>
<b>5.2 SELECTION OF CLASSIFICATION STRUCTURE.....</b>	<b>145</b>
<b>5.3 IDENTIFICATION OF THE KEY CLASSIFICATION PARAMETERS...147</b>	
<b>5.3.1 Introduction.....</b>	<b>147</b>
<b>5.3.2 Conceptual Mechanisms Of Strata Deformation.....</b>	<b>148</b>
5.3.2.1 Roadway Floor Deformation Mechanisms.....	149
5.3.2.2 Roadway Roof Deformation Mechanisms.....	150
5.3.2.2 Coal Face Deformation Mechanisms.....	151
5.3.2.3 Pillar / Rib Side Deformation Mechanisms.....	152
<b>5.3.3 Parameter Assessment.....</b>	<b>157</b>
5.3.2.4 Path 1: Assessment of Parameters Used in Existing Rock Mass Classification Systems.....	157
5.3.2.5 Path 2: Assessment of Parameters Used in Existing Coal Mine Classifications Systems.....	159
5.3.2.6 Path 3: Review of Lithological Classification Systems and Coal Measure Rock Types.....	161
<b>5.3.4 Synthesis Of Parameters.....</b>	<b>161</b>
<b>5.4 DESCRIPTION OF IDENTIFIED CLASSIFICATION PARAMETERS...163</b>	
<b>5.4.1 Introduction.....</b>	<b>163</b>
<b>5.4.2 Unconfined Compressive Strength (UCS).....</b>	<b>163</b>
5.4.2.1 Point Load Test.....	163
5.4.2.2 NCB Cone Indenter.....	166
<b>5.4.3 Joint Properties.....</b>	<b>168</b>

<b>5.4.3.1 Number of Joint/Cleat Sets.....</b>	168
<b>5.4.3.2 Joint Spacing.....</b>	169
<b>5.4.3.3 Joint Roughness.....</b>	169
<b>5.4.3.4 Joint Persistence.....</b>	170
<b>5.4.3.5 Cleat Dominance.....</b>	170
<b>5.4.3.6 Joint/Cleat Orientation.....</b>	171
<b>5.4.4 Bedding And Lamination Plane Characteristics.....</b>	171
<b>5.4.4.1 Bedding / Lamination Plane Strength.....</b>	171
<b>5.4.4.2 Bedding / Lamination Spacing.....</b>	172
<b>5.4.5 Fissility.....</b>	172
<b>5.4.6 Groundwater Flow.....</b>	173
<b>5.4.7 Moisture Sensitivity.....</b>	173
<b>5.5 DERIVATION OF PARAMETER IMPORTANCE RATINGS.....</b>	175
<b>5.5.1 Introduction.....</b>	175
<b>5.5.2 Maximum Importance Rating.....</b>	176
<b>5.5.3 Rating Scales.....</b>	180
<b>5.5.4 Adjustment For Joint/Cleat Orientation.....</b>	181
<b>5.6 OUTLINE OF THE COAL MINE CLASSIFICATION.....</b>	181
<b>5.6.1 Introduction.....</b>	181
<b>5.6.2 Characterisation Of Strata Anisotropy Using Coal Mine Classification Rating.....</b>	186
<b>5.6.3 Applying The Coal Mine Classification.....</b>	188
<b>5.7 CONCLUSIONS.....</b>	189

## **CHAPTER 6**

### **APPLICATION OF THE COAL MINE CLASSIFICATION TO UK COAL MINES**

<b>6.1 INTRODUCTION.....</b>	192
<b>6.1.1 Data Uncertainty.....</b>	192
<b>6.2 APPLICATION OF THE COAL MINE CLASSIFICATION TO RICCALL MINE, NORTH YORKSHIRE.....</b>	192
<b>6.2.1 Introduction.....</b>	192
<b>6.2.2 General Strata Sequence Adjacent To The Barnsley Seam.....</b>	193
<b>6.2.3 Location Of Case Studies.....</b>	193

<b>6.2.4 Roadway Dimensions.....</b>	198
<b>6.2.5 Installed Supports.....</b>	198
6.2.5.1 Primary Support.....	199
6.2.5.2 Secondary Support.....	199
<b>6.2.6 Monitoring Data.....</b>	199
<b>6.2.7 In-Situ Stress.....</b>	199
<b>6.2.8 Mining Interactions.....</b>	200
<b>6.2.9 Intact Rock Properties.....</b>	200
6.2.9.1 Triaxial Strength.....	201
6.2.9.2 Young's Modulus.....	201
<b>6.2.10 Application Of The Coal Mine Classification.....</b>	203
6.2.10.1 Case Study Locality 1: Panel 438, Main Gate 214 Metre Mark.....	204
6.2.10.2 Case Study Locality 2: Panel 478, Main Gate 31 Metre Mark.....	206
6.2.10.3 Case Study Locality 3: Panel 478, Main Gate 110 Metre Mark.....	207
6.2.10.4 Case Study Locality 4: Panel 478, Main Gate 387 Metre Mark.....	208
6.2.10.5 Case Study Locality 5: Panel 478, Main Gate 486 Metre Mark.....	209
6.2.10.6 Case Study Locality 6: Panel 478, Main Gate 587 Metre Mark.....	210
6.2.10.7 Case Study Locality 7: Panel 478, Main Gate 710 Metre Mark.....	211
6.2.10.8 Case Study Locality 8: Panel 505, Tail Gate 353 Metre Mark.....	212
6.2.10.9 Case Study Locality 9: Panel 505, Tail Gate 922 Metre Mark.....	213
6.2.10.10 Case Study Locality 10: Panel 505, Main Gate 669 Metre Mark.....	214
6.2.10.11 Case Study Locality 11: Panel 505, Main Gate 902 Metre Mark.....	215
6.2.10.12 Case Study Locality 12:	

Panel 505, Main Gate 1583 Metre Mark.....	216
<b>6.3 APPLICATION OF THE COAL MINE CLASSIFICATION TO DAW</b>	
MILL MINE, WARWICKSHIRE.....	217
<b>6.3.1 Introduction.....</b>	217
<b>6.3.2 General Strata Sequence Adjacent To The Warwickshire Thick Seam.....</b>	217
<b>6.3.3 Structure Of The Warwickshire Thick Coal.....</b>	219
<b>6.3.4 Roadway Dimensions.....</b>	219
<b>6.3.5 Installed Supports.....</b>	219
<b>6.3.5.1 Roof Bolt Bond Strength.....</b>	219
<b>6.3.6 Monitoring Data.....</b>	220
<b>6.3.7 In-Situ Stress.....</b>	221
<b>6.3.8 Mining Interaction.....</b>	221
<b>6.3.9 Intact Rock Properties.....</b>	221
<b>6.3.9.1 Triaxial Strength.....</b>	221
<b>6.3.9.2 Young's Modulus.....</b>	223
<b>6.3.10 Application Of The Coal Mine Classification.....</b>	223
<b>6.4 APPLICATION OF THE COAL MINE CLASSIFICATION</b>	
<b>TO ROSSINGTON MINE, SOUTH YORKSHIRE.....</b>	225
<b>6.4.1 Introduction.....</b>	225
<b>6.4.2 General Strata Sequence Adjacent To The Barnsley Seam.....</b>	228
<b>6.4.3 Roadway Dimensions.....</b>	228
<b>6.4.4 Installed Supports.....</b>	228
<b>6.4.5 Monitoring Data.....</b>	229
<b>6.4.5.1 Roof Displacement.....</b>	229
<b>6.4.5.2 Rib Displacement.....</b>	230
<b>6.4.6 In-Situ Stress.....</b>	231
<b>6.4.7 Mining Interactions.....</b>	231
<b>6.4.8 Intact Rock Properties.....</b>	232
<b>6.4.8.1 Triaxial Strength of Roof Strata.....</b>	232
<b>6.4.8.2 Triaxial Strength of the Barnsley Seam.....</b>	232
<b>6.4.8.3 Elastic Modulus.....</b>	233
<b>6.4.9 Application Of The Coal Mine Classification.....</b>	233
<b>6.4.9.1 Classification of the Roof Strata.....</b>	233
<b>6.4.9.2 Classification of the Barnsley Seam.....</b>	236

## CHAPTER 7

### NUMERICAL MODELLING STUDIES

<b>7.1 INTRODUCTION.....</b>	<b>238</b>
<b>7.2 STRATA MODELLING TECHNIQUES.....</b>	<b>238</b>
<b>    7.2.1 Closed Form Techniques.....</b>	<b>238</b>
<b>    7.2.2 Limit Equilibrium Techniques.....</b>	<b>239</b>
<b>    7.2.3 Photo-Elastic Techniques.....</b>	<b>239</b>
<b>    7.2.4 Physical Modelling Techniques.....</b>	<b>240</b>
<b>7.3 COMPUTER BASED NUMERICAL MODELLING METHODS.....</b>	<b>241</b>
<b>    7.3.1 Introduction.....</b>	<b>241</b>
<b>    7.3.2 Solution Techniques.....</b>	<b>242</b>
<b>    7.3.3 Numerical Modelling Methodologies.....</b>	<b>242</b>
<b>        7.3.3.1 Boundary-Element Method.....</b>	<b>242</b>
<b>        7.3.3.2 Distinct-Element Method.....</b>	<b>243</b>
<b>        7.3.3.3 Finite Element Method.....</b>	<b>243</b>
<b>        7.3.3.4 The Finite Difference Method.....</b>	<b>244</b>
<b>7.4 FAST LANGRANGIAN ANALYSIS     OF CONTINUA (FLAC).....</b>	<b>245</b>
<b>    7.4.1 Introduction.....</b>	<b>245</b>
<b>    7.4.2 The Finite Difference Grid.....</b>	<b>247</b>
<b>    7.4.3 FLAC Constitutive Models.....</b>	<b>247</b>
<b>        7.4.3.1 Null Model.....</b>	<b>247</b>
<b>        7.4.3.2 Elastic Model Group.....</b>	<b>248</b>
<b>            7.4.3.2.1 <i>Elastic isotropic model</i>.....</b>	<b>248</b>
<b>            7.4.3.2.2 <i>Elastic, transversely isotropic model</i>.....</b>	<b>248</b>
<b>            7.4.3.3 Plasticity Models.....</b>	<b>248</b>
<b>                7.4.3.3.1 <i>Mohr-Coulomb model</i>.....</b>	<b>248</b>
<b>                7.4.3.3.2 <i>Ubiquitous joint model</i>.....</b>	<b>249</b>
<b>                7.4.3.3.3 <i>Strain-softening model</i>.....</b>	<b>249</b>
<b>                7.4.3.3.4 <i>Other plastic models provided for in FLAC</i>.....</b>	<b>249</b>
<b>    7.4.4 Model Boundary Conditions.....</b>	<b>250</b>

<b>7.4.5 Initial Stress Conditions.....</b>	250
<b>7.4.6 FLAC Modelling Methodology.....</b>	250
<b>7.5 NUMERICAL MODELLING OF GATE ROAD DEFORMATIONS WITHIN UK COAL MINES.....</b>	253
<b>7.5.1 Introduction.....</b>	253
<b>7.5.2 Numerical Modelling Of Gate Road Deformation, Riccall Colliery.....</b>	254
<b>7.5.2.1 Establishment of a Modelling Methodology.....</b>	254
<b>7.5.2.1.1 Roof deformation characteristics, 922 mm tail gate, 505 panel, Riccall.....</b>	254
<b>7.5.2.1.2 Selection of constitutive material model.....</b>	255
<b>7.5.2.2 Modelling Input Parameters.....</b>	256
<b>7.5.2.2.1 Elastic parameters.....</b>	256
<b>7.5.2.2.2 Strength properties.....</b>	258
<b>7.5.2.2.3 Density.....</b>	258
<b>7.5.2.2.4 Modelling of support elements.....</b>	258
<b>7.5.2.2.5 The finite difference grid.....</b>	261
<b>7.5.2.2.6 Boundary conditions.....</b>	261
<b>7.5.2.2.7 Running the simulation.....</b>	261
<b>7.5.2.2.8 Time dependency.....</b>	263
<b>7.5.2.2.9 Analysis of results.....</b>	263
<b>7.5.2.3 Numerical Modelling of Case Study Localities at the Riccall Mine Site.....</b>	264
<b>7.5.2.3.1 Analysis of results.....</b>	264
<b>7.5.3 Numerical Modelling Of Gate Roads Within Daw Mill Colliery, Warwickshire.....</b>	277
<b>7.5.3.1 Installed Roadway Supports.....</b>	277
<b>7.5.3.2 Results of Numerical Modelling.....</b>	278
<b>7.5.3.3 Sensitivity of Model to Shear Strength of Rock/Grout Bond.....</b>	278
<b>7.5.4 Numerical Modelling Of The Tail Gate, B3 Panel, Rossington Colliery, Yorkshire.....</b>	281
<b>7.5.4.1 Introduction.....</b>	281
<b>7.5.4.2 Modelling of B3 Panel Main Gate 24 Metre Mark.....</b>	282
<b>7.5.4.3 Modelling of B3 Panel Main Gate 408 Metre Mark.....</b>	282
<b>7.5.4.4 Modelling of B3 Panel Main Gate 594 Metre Mark.....</b>	285

<b>7.5.4.5 Modelling of Rib Displacement in B3 Panel, Main Gate, 24 Metre Mark.....</b>	<b>289</b>
<b>7.5.4.6 Modelling of Rib Displacement in B3 Panel Main Gate, 415 Metre Mark.....</b>	<b>294</b>
<b>CONCLUSIONS.....</b>	<b>294</b>

## **CHAPTER 8**

### **GENERAL CONCLUSIONS AND RECOMMENDATIONS**

<b>8.1 GENERAL CONCLUSIONS.....</b>	<b>295</b>
<b>8.2 RECOMMENDATIONS FOR FUTURE STUDIES.....</b>	<b>299</b>
<b>REFERENCES.....</b>	<b>301</b>

### **ACKNOWLEDGEMENTS**

### **APPENDIX 1**

-Stress Strain Plots For Roof Strata Samples, Panels 478 and 505, Riccall Mine

### **APPENDIX 2**

-Application of Rock Mass Failure Criteria to Triaxial Data

### **APPENDIX 3**

-Summary Sheets of Rock Test Results and Coal Mine Classification Data Sheets

## **ABSTRACT**

This thesis aims to develop a rock mass classification system for UK Coal Measure strata such that the output from the classification system may provide a means by which the strength and stiffness properties of Coal Measure strata encountered within UK coal mines may be predicted.

The development of the Coal Mine Classification system is described within this thesis. A structured methodology utilising a database of information obtained from 118 different rock mass classifications, together with consideration of the typical mechanisms of strata deformation within coal mines, was employed to determine the parameters of the Coal Measure strata that have the greatest influence on the engineering properties of the strata. These identified parameters have formed the basis of the Coal Mine Classification system. By comparison to a series of conceptual models of strata deformation that occur within the roof ,floor, ribs of roadways and within the region of the coal face, relative importance weightings and rating scales for the identified classification parameters have been proposed.

The anisotropic nature of the UK Coal Measures is characterised within the Coal Mine Classification by the calculation of separate ratings for directions parallel to and perpendicular to bedding.

An appraisal of the optimum method of using the classification ratings, determined by the Coal Mine Classification, to predict the strength properties of individual strata units was undertaken. Rock mass failure criteria that utilise outputs from existing rock mass classification systems to determine the rock mass strength, have been reviewed. Utilising published triaxial data the rock mass failure criterion that best predicts the failure characteristics of UK Coal Measure strata was identified. From this study the Hoek-Brown rock mass failure criterion was identified as the optimum existing criterion for predicting the intact strength and rock mass strength of Coal Measure strata. However this criterion was still found not to produce a close fit in many cases to the intact failure strength of the strata. A modified Coal Measure Failure criterion has been developed, which for a wide range of Coal Measure rock types was found to produce a better prediction of the intact strength of Coal Measure strata than any of the existing rock mass failure criteria.

To determine the efficacy of the Coal Mine Classification system as a means of predicting the strength and stiffness properties of the rock mass the Coal Mine Classification was applied to the strata at case study localities within rock bolted roadways within three UK mine sites.

Numerical models of the case study localities were developed using the FLAC finite difference code utilising a ubiquitous jointed elastic-perfectly plastic material model to simulate strata behaviour. The output from the modelling included predicted roof and rib side displacements, and these displacements were compared to the actual monitoring data for the case study localities.

The results of the numerical modelling indicate that the predictions produced by the numerical models reflected the pattern and scale of deformations actually measured in-situ within the coal mine roadways, thus indicating that the Coal Mine Classification system provides a means of predictively determining the engineering properties of the in-situ Coal Measure strata.

The modelling also indicated that time delays related to the installation of the roof extensometers may under predict that actual roof deformation that occurs within the roadway roof.

## AFFIRMATION

The following publications include the findings and results obtained during the research for this thesis:

“The Application of Rock Mass Classification Principles to Coal Mine Design” The 5<sup>th</sup> International Conference on Mining, Petroleum and Metallurgical Engineering, Suez Canal University, Feb. 24<sup>th</sup> to 26<sup>th</sup> 1997, R.K. Dunham, P.W. Lloyd, D.J. Reddish and D.N. Whittles.

“Anisotropic Strength and Stiffness Properties of Some UK Coal Measure Siltstones”, unpublished paper, (submitted to the Quarterly Journal of Engineering Geology) E. Yasar, D.N Whittles, P.W. Lloyd and D.J Reddish.

## LIST OF FIGURES

- Figure 2.1 Westphalian Paleogeography of the United Kingdom
- Figure 2.2 Progressive Compaction of Mudrocks with Depth
- Figure 2.3 Surface Features on a Joint Plane
- Figure 2.4 Variation in Stress Due to Simple Uplift
- Figure 2.5 Variation in Stress Due to Tectonic Compression and Uplift
- Figure 2.6 Faulting and its Relationship to the Principal Stresses at Failure.
- Figure 2.7 Vertical Stress Against Depth Below Surface
- Figure 2.8 Ratio of Average Horizontal Stress to Vertical Stress With Depth Below Surface
- Figure 2.9 Orientation of the Maximum Principal Stress in North West Europe
- Figure 3.1 'Z' Semi-Retreat System
- Figure 3.2 Variation in Tangential and Radial Stress in a Sidewall of a Circular Tunnel Under Vertical Uniaxial Loading
- Figure 3.3 Theoretical Stress Distribution Around a Rectangular Opening in an Homogeneous Elastic Medium.
- Figure 3.4 Stresses Around a Circular Roadway Surrounded by a Yield Zone.
- Figure 3.5 Vertical Stress Distribution Around a Retreat Longwall Panel
- Figure 3.6 Stress Distributions along Figure 3.5
- Figure 3.7 Horizontal Stress Redistribution Around a Longwall Retreat Panel
- Figure 3.8 Induced Vertical Stress in Strata Above an Underlying Pillar
- Figure 3.9 Vertical Stress Trajectories; Panel Moving Towards Goaf
- Figure 3.10 Vertical Stress Trajectories; Panel Moving Away from Goaf
- Figure 3.11 Features of a Full Column Grouted Steel Rock Bolt
- Figure 3.12 Typical Load-Displacement Curves for Cable and Rock Bolts
- Figure 3.13 Detached Block Theory
- Figure 3.14 Stages of Strata Movement According to Roof Beam Tilt Theory

Figure 3.15 Load Characteristics of Pack Supports.

Figure 3.16 Redistribution of Stresses Around a Coal Mine Roadway.

Figure 3.17 Failure of a Coal Mine Roadway Due to Cutter Roof

Figure 3.18 Mineralogy of UK Coal Measure Spoil

Figure 3.19 Mechanism of Deformation of a Coal Mine Floor.

Figure 3.20 Lateral Gateroad Closure Expressed as a Percentage of the Original Width

Figure 3.21 Rib Extrusion With Layers of Different Engineering Properties

Figure 3.22 Rib Extrusion Within Homogeneous Coal Seams

Figure 3.23 Rib Extrusion Within Coal Seam Consisting of Hard and Soft Layers

Figure 4.1 Typical Stress-Strain Behavior of Intact Rock

Figure 4.2 Stress Strain Curve for a Brittle Material

Figure 4.3 Stress Strain Curve for a Elastic-Perfectly Plastic Material

Figure 4.4 Stress-Strain Curve for a Strain Hardening Material

Figure 4.5 Stress-Strain curve for a Strain Softening-Perfectly Plastic Material

Figure 4.6 Stress Conditions in a Biaxial Stress Field

Figure 4.7 Coulomb-Navier Failure Envelope

Figure 4.8 Mohr's Failure Envelope

Figure 4.9 Griffith Crack in a Biaxial Compressive Stress Field

Figure 4.10 Transition from Intact Rock to a Heavily Jointed Rock Mass With Increasing Sample Size

Figure 4.11 Plot of  $\sigma_3/\text{ucs}$  'v'  $(\sigma_1/\text{ucs}-\sigma_3/\text{ucs})^2$

Figure 4.12 A Transversely Isotropic Body for Which the x,y Plane is the Plane of Isotropy

Figure 4.13 Application of Anisotropic Failure Theories to a Middle Coal Measure Laminated Siltstone

Figure 4.14 The Tunnel Rock-Load Concept of Terzaghi

Figure 4.15 Relationship Between Active Span, Rock Class and Stand Up Time

**Figure 4.16 Adjustments to the RMR System for Mining**

**Figure 4.17 Relationship Between the Maximum Equivalent Dimension De of an Unsupported Excavation and the 'Q' Index**

**Figure 4.18 Adjustment to RMR to Account for In-Situ Stress Condition**

**Figure 4.19 The Different Components of the Coal Mine Roof Rating**

**Figure 5.1 Flow Chart Illustrating Coal Mine Classification Development**

**Figure 5.2 Buckling by Horizontal stress**

**Figure 5.3 Swelling of Seatearth**

**Figure 5.4 Deformation Along Shear Planes**

**Figure 5.5 Extrusion of Seatearth into Roadway**

**Figure 5.6 Bearing Capacity Failure**

**Figure 5.7 Buckling of Roof Beds**

**Figure 5.8 Self Weight Bending**

**Figure 5.9 Shear Failure**

**Figure 5.10 Shear/Parting Plane Failure**

**Figure 5.11 Wedge/Block Failure**

**Figure 5.12 Spalling of Coal Face**

**Figure 5.13 Bearing Capacity Failure**

**Figure 5.14 Collapse of Immediate Roof**

**Figure 5.15 Wedge/Block Failure**

**Figure 5.16 Cantilevering of Roof Beds**

**Figure 5.17 Tensile Cracking**

**Figure 5.18 Coal Cleat Dilation**

**Figure 5.19 Shear Failure**

**Figure 5.20 Wedge/Block failure**

**Figure 5.21 Yield Zone Development**

**Figure 5.22 Parameter Evaluation Proforma**

Figure 5.23 Rock Mass Parameters Adopted Within Existing Classifications developed for Coal Mining/Coal measure Strata.

Figure 5.24 Point Load Test System

Figure 5.25 Diametrical Point Load Test

Figure 5.26 Axial Point Load Test

Figure 5.27 Point Load Lump Test

Figure 5.28 The NCB Cone Indenter

Figure 5.29 Barton's Joint Roughness Coefficient, JRC

Figure 5.30 Geodurability Classification

Figure 5.31 Cell and Specimen Assembly for Unconfined Swelling Test.

Figure 5.32 Methodology Developed to determine Maximum Importance Ratings

Figure 5.33 Linear Scales

Figure 5.34 Non-Linear Scales

Figure 5.35 Rating Scale for Unconfined Compressive Strength

Figure 5.36 Rating Scale for Joint/Cleat Spacing

Figure 5.37 Rating Scale for Joint/Cleat Roughness

Figure 5.38 Rating Scale for Bedding Plane Spacing

Figure 5.39 Rating Scale for Bedding Plane Cohesion

Figure 5.40 Rating Scale for Bedding Plane Roughness

Figure 5.41 Rating Scale for Fissility

Figure 5.42 Rating Scale for Moisture Sensitivity

Figure 5.43 Adjustment Rating for Cleat/Joint Orientation in Rib/Pillar

Figure 5.44 Adjustment Rating for Cleat/Joint Orientation in Roof/Floor

Figure 5.45 Structure of the Coal Mine Classification System

Figure 5.46 Calculation of Rating Perpendicular to Bedding.

Figure 5.47 Calculation of Rating Parallel to Bedding

**Figure 5.48 Coal Mine Classification Data Entry Sheet**

**Figure 6.1 Riccall Mine, Panel 438 Layout**

**Figure 6.2 Riccall Mine, Panel 478 Layout**

**Figure 6.3 Riccall Mine, Panel 505 Layout**

**Figure 6.4 Primary Supports, Riccall Mine**

**Figure 6.5 Triaxial Envelope: Mudstone, Riccall 478 Panel**

**Figure 6.6 Triaxial Envelope: Mudstone, Riccall 505 panel**

**Figure 6.7 Triaxial Envelope: Siltstone, Riccall 478 panel**

**Figure 6.8 Triaxial Envelope: Siltstone, Riccall 505 panel**

**Figure 6.9 Triaxial Envelope: Laminated siltstone, Riccall 478 panel**

**Figure 6.10 Triaxial Envelope: Sandstone, Riccall 478 panel**

**Figure 6.11 Roof Core from the Main Gate of Panel 438 at 214 Metre Mark**

**Figure 6.12 Roof Core from the Main Gate of Panel 478 at 31 Metre Mark**

**Figure 6.13 Roof Core from the Main Gate of Panel 478 at 387 Metre Mark**

**Figure 6.14 Roof Core from the Main Gate of Panel 478 at 486 Metre Mark**

**Figure 6.15 Roof Core from the Main Gate of Panel 478 at 587 Metre Mark**

**Figure 6.16 Roof Core from the Main Gate of Panel 478 at 710 Metre Mark**

**Figure 6.17 Roof Core from the Tail Gate of Panel 505 at 353 Metre Mark**

**Figure 6.18 Roof Core from the Tail Gate of Panel 505 at 922 Metre Mark**

**Figure 6.19 Roof Core from the Main Gate of Panel 505 at 669 Metre Mark**

**Figure 6.20 Roof Core from the Main Gate of Panel 505 at 902 Metre Mark**

**Figure 6.21 Roof Core from the Main Gate of Panel 505 at 1583 Metre Mark**

**Figure 6.22 Daw Mill Panel 94 Layout**

**Figure 6.23 Generalized Lithology 90's Area**

**Figure 6.24 Roof Displacement, Daw Mill, 94's Coal Gate, 588 metre mark.**

**Figure 6.25 Failure Envelope for Daw Mill Mudstone.**

Figure 6.26 Failure Envelope for Sandstone/Siltstone.

Figure 6.27 Failure Envelope for the Warwickshire Thick Seam.

Figure 6.28 Geotechnical Roof Log, 94's Tail Gate, 210 Metre Mark

Figure 6.29 Rossington Mine, Panel B3 Layout

Figure 6.30 Section Close to Barnsley Seam, Finningley No.2 Borehole, Rossington

Figure 6.31 Roof Displacement, 24 Metre Mark

Figure 6.32 Roof Displacement 408 Metre Mark

Figure 6.33 Roof Displacement, 594 Metre Mark

Figure 6.34 Left Rib Displacement, 24 Metre Mark, B3's Main Gate

Figure 6.35 Right Rib Displacement, 24 Metre Mark, B3's Main Gate

Figure 6.36 Left Rib Displacement, 415 Metre Mark, B3's Main Gate

Figure 6.37 Right Rib Displacement, 415 Metre Mark , B3's Main Gate

Figure 6.38 Intact Failure Envelope for the Barnsley Coal.

Figure 6.39 Geotechnical Log for B2's Tail Gate, 865 Metre Mark.

Figure 7.1 Sequence of Calculation, Finite Difference Method

Figure 7.2 FLAC Model Components

Figure 7.3 Holling's Conceptual Classification of Modelling Problems

Figure 7.4 Spectrum of Modelling Situations

Figure 7.5 Roof Extensometer 922mm, Tail Gate 505 Panel, Riccall

Figure 7.6 Relationship Between Rock Mass Ratings and Deformation Modulus  
(Young's Modulus = 20 GPa)

Figure 7.7 FLAC's Cable Bolt Parameters

Figure 7.8 Schematic of the Finite Difference Grid Used in the Modelling of Coal Mine Gateroads

Figure 7.9 Comparison Between FLAC Prediction and Monitored Roof Displacement at 922 Metre Mark, 505 Panel, Riccall

Figure 7.10 Comparison Between FLAC Prediction and Monitored Roof Displacement at 31 Metre Mark, Main Gate, 478 Panel, Riccall

Figure 7.11 Comparison Between FLAC Prediction and Monitored Roof Displacement at 110 Metre Mark, Main Gate of 478 Panel, Riccall

Figure 7.12 Comparison Between FLAC Prediction and Monitored Roof Displacement at 387 Metre Mark, Main Gate of 478 Panel, Riccall

Figure 7.13 Comparison Between FLAC Prediction and Monitored Roof Displacement at 486 Metre Mark, Main Gate of 478 Panel, Riccall

Figure 7.14 Comparison Between FLAC Prediction and Monitored Roof Displacement at 587 Metre Mark, Main Gate of 478 Panel, Riccall

Figure 7.15 Comparison Between FLAC Prediction and Monitored Roof Displacement at 710 Metre Mark, Main Gate of 478 Panel, Riccall

Figure 7.16 Comparison Between FLAC Prediction and Monitored Roof Displacement at 353 Metre Mark, Tail Gate of 505 Panel, Riccall

Figure 7.17 Comparison Between FLAC Prediction and Monitored Roof Displacement at 669 Metre Mark, Main Gate of 505 Panel, Riccall

Figure 7.18 Comparison Between FLAC Prediction and Monitored Roof Displacement at 902 Metre Mark, Main Gate of 505 Panel, Riccall

Figure 7.19 Comparison Between FLAC Prediction and Monitored Roof Displacement at 1583 Metre Mark, Main Gate of 505 Panel, Riccall

Figure 7.20 Comparison Between FLAC Prediction and Monitored Roof Displacement: Coal Gate of 94 Panel, Daw Mill

Figure 7.21 Roof Displacement of the Coal Gate of 94 Panel, Daw Mill

Figure 7.22 Comparison Between FLAC Prediction and Monitored Roof Displacement at 24 Metre Mark, Main Gate, B3 Panel, Rossington

Figure 7.23 Predicted Shear Strain: 24 Metre Mark, Main Gate, B3 Panel, Rossington

Figure 7.24 Comparison Between FLAC Prediction and Monitored Roof Displacement 408 Metre Mark, Main Gate, B3 Panel, Rossington

Figure 7.25 Predicted Shear Strain:408 Metre Mark, Main Gate, B3 Panel, Rossington

Figure 7.26 Comparison Between FLAC Prediction and Monitored Roof Displacement 594 Metre Mark, Main Gate, B3 Panel, Rossington

Figure 7.27 Predicted Shear Strain:594 Metre Mark, Main Gate, B3 Panel, Rossington

Figure 7.28 Comparison Between FLAC Predictions With Different Orientation Adjustment Ratings and Monitored Rib Displacement; 24 Metre Mark, Main Gate, B3 Panel, Rossington

Figure 7.29 Revised Orientation Adjustment Ratings for Rib Side Strata

## LIST OF TABLES

Table 2.1 Classification of Mudrocks

Table 2.2 Soft Sediment Structures

Table 4.1 Factors Influencing the Strength of Intact Rock

Table 4.2 Material Constants

Table 4.3 Material Constants for UK Coal Measure Rocks

Table 4.4 Relationship Between RMR Deformation Modulus and Poisson's Ratio

Table 4.5  $m_i$  Values for Intact Rock

Table 4.6 Coefficients of Determination Calculated for Hoek-Brown Failure Criterion

Table 4.7 Terzaghi's Recommendations of Support in Steel Arch Supported Tunnels

Table 4.8 Relationship Between RQD Index and the Engineering Quality of the Rock Mass

Table 4.9 Rock Structure Rating, Parameter A

Table 4.10 Rock Structure Rating, Parameter B

Table 4.11 Rock Structure Rating, Parameter C

Table 4.12 1976 Rock Mass Rating System

Table 4.13 1989 Rock Mass Rating System

Table 4.14 Joint Orientation Adjustment Rating

Table 4.15 Relationship Between RMR and Rock Mass Quality

Table 4.16 Stand Up Time and Rock Strength for Different Rock Classes

Table 4.17 Joint Orientation for Tunnelling

Table 4.18 Rock Mass Rating Extensions

Table 4.19 The NGI Tunnelling Quality ('Q') Index

Table 4.20 ESR Values

Table 4.21 Cavability Classification

Table 4.22 Lithological Index Classification

Table 4.23 Weathering Index Classification

**Table 4.24 Discontinuity Index Classification**

**Table 4.25 Parameter Weightings CMRS Classification**

**Table 4.26 Relationship Between Unit Roof Rating and Rock Class**

**Table 4.27 Floor Classification**

**Table 4.28 Stratification Parameter**

**Table 4.29 Adjustment for Cleat Orientation**

**Table 4.30 CMRR Cohesion-Roughness Rating**

**Table 4.31 CMRR Spacing-Persistence Rating**

**Table 4.32 CMRR Multiple Discontinuity Set Adjustment**

**Table 4.33 CMRR Strength Rating**

**Table 4.34 CMRR Moisture Sensitivity Rating**

**Table 5.1 Existing Classification Systems for Coal Mining**

**Table 5.2 Identified Potential Classification Parameters**

**Table 5.3 Final List of Classification Parameters**

**Table 5.4 Classification of Point Load Strength Anisotropy for Foliated Rocks**

**Table 5.5 Importance Ratings for Rock Mass Parameters Within Roadway Floor**

**Table 5.6 Importance Ratings for Rock Mass Parameters Within Roadway Roof**

**Table 5.7 Importance Ratings for Rock Mass Parameters Within Coal Face**

**Table 5.8 Importance Ratings for Rock Mass Parameters Within Rib or Coal Face**

**Table 5.9 Average Importance Rating for Roof/Floor**

**Table 5.10 Average Importance Ratings Coal Pillar/Rib/Face**

**Table 5.11 Ratings for Number of Joint Cleat Sets**

**Table 5.12 Ratings for Joint Persistence**

**Table 5.13 Ratings for Joint Dominance**

**Table 5.14 Ratings for Bedding Plane Topography**

**Table 5.15 Ratings for Groundwater Conditions**

**Table 6.1 Section of Skipwith No.1 Borehole Adjacent to the Barnsley Seam, Riccall**

**Table 6.2 Case Study Locations Riccall Mine**

**Table 6.3 In-Situ Stress Results 505 Panel Tail Gate**

**Table 6.4 mi Variables for Riccall Lithologies**

**Table 6.5 Young's Modulus for Riccall Basic Lithologies**

**Table 6.6 Classification Ratings for Roadway Roof, Panel 438 at 214 Metre Mark**

**Table 6.7 Coal Mine Classification Ratings Main Gate, Panel 478 at 31 Metre Mark**

**Table 6.8 Coal Mine Classification Ratings Main Gate, Panel 478 at 110 Metre Mark**

**Table 6.9 Coal Mine Classification Ratings Main Gate, Panel 478 at 387 Metre Mark**

**Table 6.10 Coal Mine Classification Ratings, Main Gate, Panel 478, 486 Metre Mark**

**Table 6.11 Coal Mine Classification Ratings, Main Gate, Panel 478, 587 Metre Mark**

**Table 6.12 Coal Mine Classification Ratings, Main Gate, Panel 478, 710 Metre Mark**

**Table 6.13 Coal Mine Classification Ratings, Tail Gate, Panel 505, 353 Metre Mark**

**Table 6.14 Coal Mine Classification Ratings, Tail Gate, Panel 505, 922 Metre Mark**

**Table 6.15 Coal Mine Classification Ratings, Main Gate, Panel 505, 669 Metre Mark**

**Table 6.16 Coal Mine Classification Ratings, Main Gate, Panel 505, 902 Metre Mark**

**Table 6.17 Coal Mine Classification Ratings, Main Gate, Panel 505, 1583 Metre Mark**

**Table 6.18 Summary of Pull Test Data for 95 Tail Gate Roof Strata**

**Table 6.19 In-Situ Stress Results 90's Tail Gate**

**Table 6.20 Coal Measure Failure Criterion Material Parameters  $m_{i1}$  and  $m_{i2}$**

**Table 6.21 Classification Ratings for Roadway Roof of the Tail Gate, Panel 94 at 210 Metre Mark**

**Table 6.22 In-Situ Stresses, Rossington Mine**

**Table 6.23 Hoek-Brown  $m_i$  Parameter for Rossington Roof Strata**

**Table 6.24 Typical Young's Modulus of Rossington Roof Strata**

**Table 6.25 Classification Ratings for Roadway Roof at the Tail Gate of B2 Panel**

**Table 6.26 Estimated Classification Ratings for the Rib Side Strata (Barnsley Seam)  
B3 Panel, Rossington Mine**

**Table 7.1 Strata Properties: Immediate Roof 922 Metre Mark, Tail Gate, 505 Panel,  
Riccall**

**Table 7.2 Properties of 2.4 Metres Long Steel Roof Bolts**

**Table 7.3 Properties of 1.8 Metres Long Rib Bolts**

**Table 7.4 Roof Strap Properties**

**Table 7.5 End Plate Properties**

**Table 7.6 Properties of Cable Bolts**

**Table 7.7 Strata Properties, Roof Strata, 94 Panel, Daw Mill**

**Table 7.8 Roof Strata Properties, B3 Panel, Rossington**

**Table 7.9 Strata properties, Coal Rib B3 Panel, Rossington (Barnsley Seam)**

# **CHAPTER ONE**

## **AN INTRODUCTION TO THE THESIS**

### **1.1 INTRODUCTION**

A rock mass represents the in-situ condition of the rock material. Rock masses are almost always ubiquitously fractured and often consist of different rock types. The complexity of the rock mass prohibits, due to expense and time, the description and analysis of each individual feature that effects the rock masses engineering behaviour.

Rock mass classifications provide an alternative method of predicting the engineering behaviour of the in-situ rock material. Such classifications are typically derived by undertaking an assessment of the relative importance, on the effect of the rock masses behaviour, of five or six parameters of the rock mass that have been identified as having the greatest influence. The relative importance of each of the parameters is normally expressed as a weighted parameter rating and a combination of the weighted parameter ratings produces a final classification value of the rock mass.

Rock mass classifications were initially developed over 50 years ago by Karl Terzaghi (1946) as a means of predicting the behaviour of rock masses within tunnelling projects. Subsequently development of many new classification systems has occurred. These classification systems have been mainly developed for and applied to tunnelling. Traditionally rock mass classifications have provided an empirical means of directly predicting support requirements and approximate stand up times of civil engineering tunnels.

Although the early rock mass classifications were utilised to determine the stand up times and support requirements of sub surface excavations, more recent developments have put increased emphasis on using rock mass classifications to estimate, more representatively, in-situ strength and stiffness properties of the rock mass. These parameters used in conjunction with numerical modelling techniques have allowed for the development of a sophisticated methodology for determining stress and displacements within the rock masses surrounding underground excavations.

Rock mass classification principles have also been applied to other rock engineering applications such as predicting the stability of rock slopes and determining the bearing capacities of rock in foundation design. On a worldwide scale, modifications of existing classifications have allowed the application of rock mass classification techniques in the design of both hard rock mining and in 'soft rock' coal mining environments. Rock mass classifications have been developed in several countries worldwide to specifically classify coal measure strata. These classification systems have been mainly utilised to predict the roof stability and support requirements within the coal mines and in civil engineering tunnels excavated in coal measure rock.

Coal mining within the UK is characterised by the relatively weak nature of the immediate strata surrounding the coal seams and by the high in-situ stress environment due to the depth of mining and horizontal stress regime, and by the method of mining itself. It is desirable to have a dedicated classification for UK Coal Measure strata due to the distinctive characteristic features of UK Coal Measure strata that effect its deformational and strength behaviour. Typically the UK Coal Measures are characterised by a distinctive sequence of strata layers known as a cyclothem. These strata layers are often laterally extensive but vertically variable and bedding planes in between each strata layer often provides planes of weakness. The strata often contains systematic jointing perpendicular to bedding. The intact coal measure rock itself can vary between being very weak to very strong but with the majority of the strata sequence typically being weak to moderately weak in strength. Due to the characteristics of the cyclothem the weakest strata frequently occurs immediately above and below the coal horizons.

The UK coal industry in the last fifteen years has endured rapid rationalisation and restructuring. The highly competitive world market for coal and the reduced home market associated with the electricity generating industry, has meant that the remaining major coal producing mines within the UK are fewer but must be high production units. To be economically viable these units must have longwalls that allow the rapid production of coal without interruption. This has triggered the need for improved ground control within the roadways and faces of the mine with reduced costs. As a response to this requirement advanced rockbolting practices have been introduced, mainly replacing free standing supports with roof, rib and cable bolts in

gate roads. This new technology has allowed the rapid development of roadways and reduced the considerable cost of the supports and their installation. Although this new technology has brought about savings in money and time it has also brought about the need for detailed design and monitoring of the installed supports.

This fact has been recognised by the Health and Safety Executive (HSE) and new regulations relating to the control of Ground Movement within mines have been constructed to incorporate safe practice associated with the new mining technology. These new regulations were due to come into enforcement towards the end of 1999 and at the time of writing this thesis were provided as guideline recommendations. These regulations will place a duty of the manager of every mine to ensure that such ground control measures are taken as may be necessary for keeping every road, drive and place in a mine secure. The HSE regulations will state that in order to ensure the security of a mine a geotechnical assessment must be initially undertaken. The geotechnical assessment is a type of risk assessment and the new regulations require that a suitable geotechnical assessment is undertaken before commencing any new roadway or place of work. The regulations will specifically state that where rockbolts are to be used in the relatively weak or variable ground found in coal mining the assessment will need to be suitably detailed and technical.

At the present time the geotechnical assessment is normally undertaken by either the mines own geotechnical staff or by independent consultants commissioned by the mine. The assessments are normally based on geotechnical logs of rock cores of the immediate roof taken at regular intervals along the mines roadways. Intact samples from the rock cores are often taken to determine the strength and deformation properties of the intact strata. The geotechnical assessment may also include in-situ stress measurements. However as was found during research for this thesis the assessment lacked structural data such as joint orientation, which have been identified to have a significant effect on the strata behaviour.

The HSE regulations will state that once the geotechnical assessment has been completed then the next step is to consider the design of the ground control measures in the area to be worked and specifically for rock bolting roadways this design should include monitoring of strata deformations.

At the present time this design process is undertaken using both knowledge of the required reinforcement used previously in conditions similar to the expectant prevailing conditions and the utilisation of semi-analytic predictive techniques such as numerical modelling. Numerical modelling techniques however require a wide range of parameters that represent the in-situ stress conditions, shape of excavation, installed supports and the material properties of the rock strata. Quantification of these parameters is often difficult and there is at present a large degree of uncertainty in relation to some of the required parameter values. This is especially true of the strata properties as there are many influencing factors on the strata behaviour such as degree of jointing and strength of bedding. Due to the uncertainty in the accuracy of the input parameters of numerical models the models parameters are usually adjusted to fit measurements taken for the existing excavations they are modelling. These calibrated models are then developed for a region within a mine and also utilized as a basis for parametric studies undertaken as an aid to judging support requirements within that region. However there are several limitations with this method of back analysis. These include the fact that different combinations of input parameters can give very similar deformation results, which may therefore produce incorrect predictions when applied to a different area. Models constructed using this method may only be utilised for the conditions which it has been calibrated which restricts its application of use. A methodology that allows more realistic input parameters to be predicted is more desirable as a universal method of numerical modelling. To characterise the rock strata in terms of its fabric and structure and through a systematic process develop this into the representative predicted strength and stiffness parameters is more desirable, and would allow a true predictive approach to numerical modelling of coal mine roadways.

## **1.2 OBJECTIVES OF THE THESIS**

The main objectives of this thesis is to develop a methodology of classifying the Carboniferous Coal Measure strata typically encountered within UK coal mines such that the output of the classification can be used to determine the strength and stiffness properties of the strata. These parameters can then be used within numerical models to allow the strata behaviour within coal mine roadways to be predicted and to allow a predictive method for the design of support requirements.

The development of such a classification requires a clear understanding of the lithological nature and characteristic structural features of the U.K. Coal Measures. Chapter 2 aims to review the lithological and structural characteristic features of UK Coal Measures and describes their modes of formation and the mechanism of development of the structures typically found within coal measure rock masses. Currently coal mining in the UK takes place at depths of between, approximately, 600m to 1000m. The in-situ stress fields at these depths has a large affect on the deformation behaviour of the strata. An understanding of the in-situ stress fields is required and has been reviewed in Chapter 2.

Chapter 3 focuses on the typical features of UK coal mining. Stress redistribution around longwall panels is described and roadway and gateroad stabilisation techniques are detailed. Important in determining which parameters have the greatest effect on strata behaviour is an understanding of the characteristic strata deformation mechanisms that occur in UK coal mines. Typical mechanisms of deformation are described in Chapter 3.

Chapter 4 aims to describe the mechanical behaviour of intact and rock masses and reviews methods used to define their mechanical properties. This chapter also reviews existing rock mass classification techniques with a special emphasis on those classifications that have been developed worldwide for the characterisation of rock strata within coal mining environments.

Chapter 5 details the actual development of a rock mass classification for use in UK coal mine design. This chapter describes the determination of the influencing factors on the rock strata and the development of initial weightings for the influencing factors. Practical means of quantification of the parameters are given and the final structure of the classification and the incorporation of anisotropy into the classification are described.

Chapter 6 describes the application of the Coal Mine Classification to sites at three different UK coal mines to allow case studies to be undertaken to evaluate the

efficacy of the Coal Mine Classification in predicting the strength and stiffness parameters of the in-situ rock strata.

Chapter 7 details the numerical modelling of the case study localities described in Chapter 6. Within this chapter strata modelling techniques are reviewed and modelling methodologies utilised within rock engineering are described. The results of the extensive numerical modelling programme using the FLAC finite difference code of each of the case study localities described within Chapter 6 are presented and compared to actual in-situ monitoring data for validation. This allows initial conclusions to be drawn on the effectiveness of the Coal Mine Classification in determining the in-situ strata properties.

Finally Chapter 8 draws general conclusions on the research work described in this thesis and gives recommendations for future work to progress this field of research.

## **CHAPTER 2** **GEOLOGY OF THE UNITED KINGDOM COAL MEASURES**

### **2.1 GENERAL STRATIGRAPHY**

#### **2.1.1 Introduction**

During the Carboniferous period the British Isles formed part of the southern edge of a landmass known as the Old Red Sandstone Continent. This continent encompassed areas of Northwest Europe, Greenland and the Eastern Seaboard of Canada and the United States of America. A marine transgression during lower Carboniferous times (Dinantian) flooded the margins of the Old Red Sandstone Continent and a block and basin system developed with extensive carbonate deposition occurring in the marine basins. During late Lower Carboniferous times a major phase of uplift occurred which lead to the development of extensive river systems draining off the land mass areas into the basins. The river systems drained mainly from sources in the Northern landmass, but also from an upland area passing through Central England known as St. George's Land or the Wales-Brabant Landmass (Williamson 1967, Anderton et al 1979) (Figure 2.1).

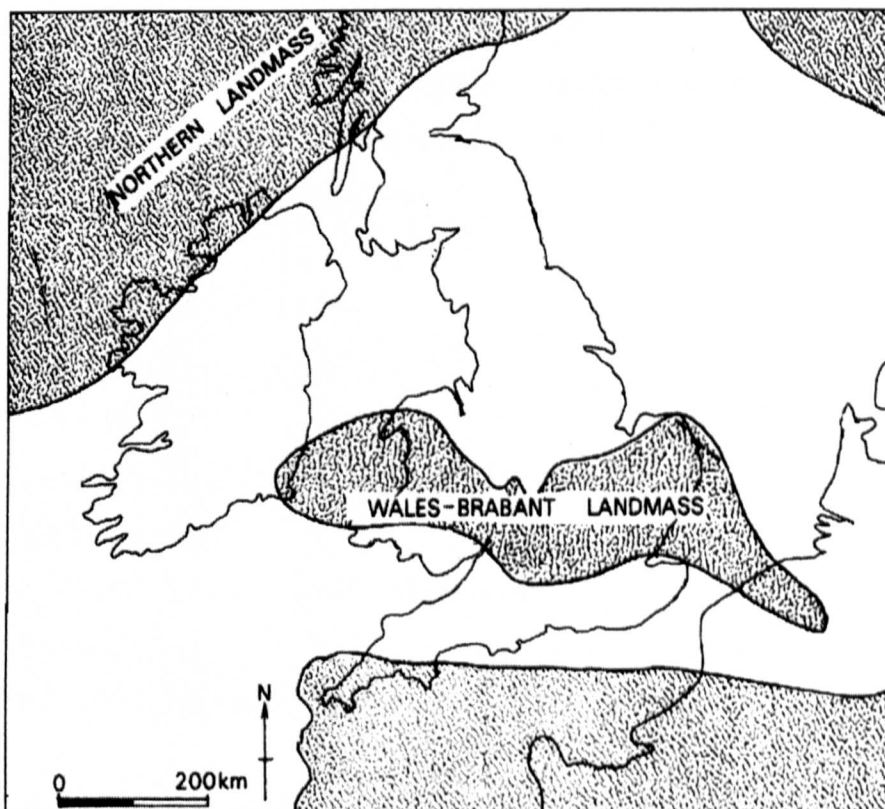


Figure 2.1. Westphalian paleogeography of the United Kingdom  
(after Anderton et al 1979)

The river systems spread into the basins depositing a large thickness of coarse angular sandstone to form extensive deltas on the margins of the landmasses. By Upper Carboniferous times (Westphalian) subaerially exposed deltaic plains covered much of the British Isles.

### **2.1.2 Depositional Environments Of The UK Coal Measures**

The UK Coal Measures have been interpreted as representing the product of delta top environments (Williamson 1967). Enormous low lying fluvio-deltaic plains lay over much of the United Kingdom during the Westphalian stage. At this time the United Kingdom was situated at a latitude of approximately 10° south of the Equator and experienced a tropical climate (Fookes 1998). The delta tops for the majority of the Westphalian were sub-aerially exposed, however marine incursions occurred with some nineteen widespread examples known (Anderton et al 1979). The large lateral extent of these marine incursions indicate a uniformity in the depositional levels on the delta tops. The environments on the delta tops consisted of rivers, peat swamps and lagoons (Anderton et al 1979). It is also conjectured by Williamson (1967) that low sand barriers may have separated lagoonal areas from the open sea. The depositional process that occurred on the delta tops can be inferred from the cyclic nature of sections through coal measure rocks. The clastic facies can be divided into upward coarsening and upward fining units. Typically upward coarsening units are between two to thirty metres in thickness

The complete sequence is as follows: -

- Coal
- Seatearths
- Fine and medium grained cross-stratified sandstones
- Flaggy sandstones
- Alternating thin sandstones and siltstones
- Siltstones
- Shales and mudstones

Only very rarely is this complete sequence present. This sequence is known as a cyclothem and represents a phase of subsidence of the delta top leading to the flooding and formation of delta top lakes. Rivers on the delta top drained into the general lake body leading to the deposition of successive argillaceous and arenaceous

beds until the surface was built up above the water level and allowed vegetation to form (Moore 1958, Reading 1982).

Upward fining units are also present within Coal Measure sequences. These units are normally sharp based, lenticular in section and ribbon shaped in plan. They are normally arenaceous, show cross stratification and are between 1 to 20 metres in thickness. They are considered to be of fluvial origin formed by the deposition of sands within a migrating delta distributary channels and with the finer grained argillaceous section representing flood plain deposition (Reading 1982).

#### **2.1.2.1 Sedimentary Province**

The presence of two separate landmasses led to the formation of three different sedimentary provinces (Williamson 1967).

Southern Province	South Wales, Forest of Dean, Somerset and Kent
Midland Province	Lancashire, North Wales, Yorkshire, Nottinghamshire, Derbyshire, Leicestershire, Staffordshire, Shropshire and Warwickshire
Northern Province	Cumberland, Durham, Northumberland and Scotland.

Within each province the coal seams form at similar stratigraphic levels and can often be correlated across the province. The degree of subsidence associated with the delta tops is illustrated by the fact that 1060 metres of coal measures are preserved in the Midland Valley of Scotland, 3050 metres in the Lancashire- North Staffordshire area, 2440 metres in South Wales and 60 metres in Kent (Anderton et al 1979).

## **2.2 DIAGENESIS**

### **2.2.1 Introduction**

Diagenesis can be defined as the changes which occur in the character and composition of sediments beginning from the moment of deposition and lasting until the resulting rocks are either moved into the realm of metamorphism or become exposed to the effects of atmospheric weathering (Larsen and Chilingar 1979). Tucker (1981) stated that the diagenetic processes are compaction, recrystallisation, dissolution, replacement, authigenesis (precipitation of new minerals within pore spaces) and cementation. More limited definitions of diagenesis exist for instance

Selley (1982) in his study of sandstone lithification used the definition that diagenesis refers to chemical processes that take place between mineral grains or between mineral grain and the pore fluids. This essentially eliminates physical processes such as compaction, which is the dominant lithification process within certain rock types. Larsen and Chilingar (1979) using diagenesis defined in its broadest sense stated that diagenesis of sediments can be broken down into three general stages. The earliest stage occurs within the layer of recently deposited sediment within an oxidising or reducing environment (Selley 1982). It has been found that in sediments within a normal oxygen regime that this layer is approximately 100-150 mm thick, but in an oxygen deficient depositional environment this layer is only a few cm thick or is completely absent (Larsen and Chilingar 1979). This stage is dominated by oxidation and reduction reactions and bacterial activity. These processes have the effect of reducing pore water pH and the production of early diagenetic material such as iron sulphide and the solution of certain minerals such as silica and carbonates into the pore water. The second stage commenced with the termination of bacterial activity. This stage is characterised by the formation of local cementation and concretions. The third stage of diagenesis involved compaction of sediments by the squeezing out of pore water due to the weight of the overlying sediments and extensive cementation of the sediments by precipitation of minerals out of migrating pore water solutions. This stage unlike the previous two stages can operate down to a great depth (for example 10 km) and over a long period of time (100 million years). Pressure and temperature are the controlling factors, with the pressure of the overlying sediments resulting in compaction and simultaneous expulsion of pore fluids, This in turn leads to a large scale migration of pore fluids through the sequence. These migrating fluids may have reacted chemically with the sediments and rocks resulting in either dissolution or precipitation of various minerals. With increasing depth and hence pressure the pore volume is reduced to a point where pore connections are closed. The closure of these pore connections effectively ends the diagenetic processes and demarks the boundary between diagenesis and metamorphism.

### **2.2.2 Diagenesis Of Sandstones**

The processes of diagenesis and the resulting characteristics of the lithified sandstones are dependent on the particle size distribution of the original sediment and the percentage of clay mineral present. Two categories of sandstone can be identified which have undergone very different diagenetic processes and produce rock types of

different engineering properties. The types are identified as those, which have a large percentage of clay minerals, and those that have a narrow range of sand sized particles. The first type tend to be matrix supported and are called wackes whilst the latter tend to be grain supported and are called arenites.

Within the wacke framework lithification occurs generally by the binding of sand grains by the clay minerals. Overburden pressure squeezes out water from the pores and from the clay mineral crystal matrix framework. The reduction in water content of clay minerals increases the bond strength leading to lithification of the sediment. Such a rock, however, if immersed in water, some of the water would be adsorbed by osmosis into the clay minerals crystal structure. This process increases the spacing of the clay minerals lattice and reduces the strength. This eventually leads to the breakdown of the clay bond and disintegration of the rock. However other cement bonds exist in wacke sandstones that prevent the complete disintegration of the sandstone into a soil. Hydration structures can develop on the surfaces of quartz grains. This hydrated silica layer approximates to a clay mineral structure thus allowing the hydrated outer surfaces of clay minerals to become orientated on the surface of a quartz grain in the form of a lattice intergrowth. This effectively welds the clay mineral to the surface of the quartz grain. The transition from the simple clay bond to the quartz-clay intergrowth is a progressive change due to diagenetic modification (Larsen and Chilingar 1979).

Different processes are involved in the diagenesis of grain supported arenite sandstones. As for the wacke sandstones the initial stages of compaction, dewatering and local cementation are present. However large pore spaces free of clay minerals allow the precipitation and crystallisation of mineral cement. The most common mineral cements are silica, calcite, dolomite, siderite, iron oxides, anhydrite and gypsum. The type of mineral cement precipitated is dependant on both the initial composition of the sediment and the origin of the pore water as this affects the EH, pH and mineral content of water (Selley 1982).

Cements found in arenite sandstones may be termed compatible or incompatible. Compatible cements are in crystallographic continuity to the crystal lattice of the grains and are usually formed when the cementing agent is of the same mineral composition as the grain, for instance quartz grains and silica cement. These cements

may form strong welded boundaries between adjacent grain cements, however pressure solution between the cement boundaries may lead to weaker interpenetrated or stylotic (sharply undulating) grain boundaries (Tucker 1981). Non compatible cements are usually of a different mineral composition than the grain. A sharp discordant crystallographic boundary exists between the grain and the cement and acts as a cementing agent by surrounding the grains (Larsen and Chilingar 1979).

### 2.2.3 Diagenesis Of Mudrocks

Diagenesis of the finer grained clay rich argillaceous rocks is dominated by compaction through overburden pressure and associated expulsion of pore water. Upon deposition argillaceous sediments contain between 50 to 90 % water (Tucker 1981, Selley 1982). Compaction soon removes most of the water so that at depths of 1 km or so mudrocks contains 30% water, much of which is contained within the clay minerals crystal lattice as interlayer water. Further compaction through water loss requires temperatures approaching 100 °C and these are typically obtained through burial between 2 to 4 km depth. Compaction to give a mudrock with only a few percent water requires a much longer period of overburden pressure and raised temperature (Figure 2.2).

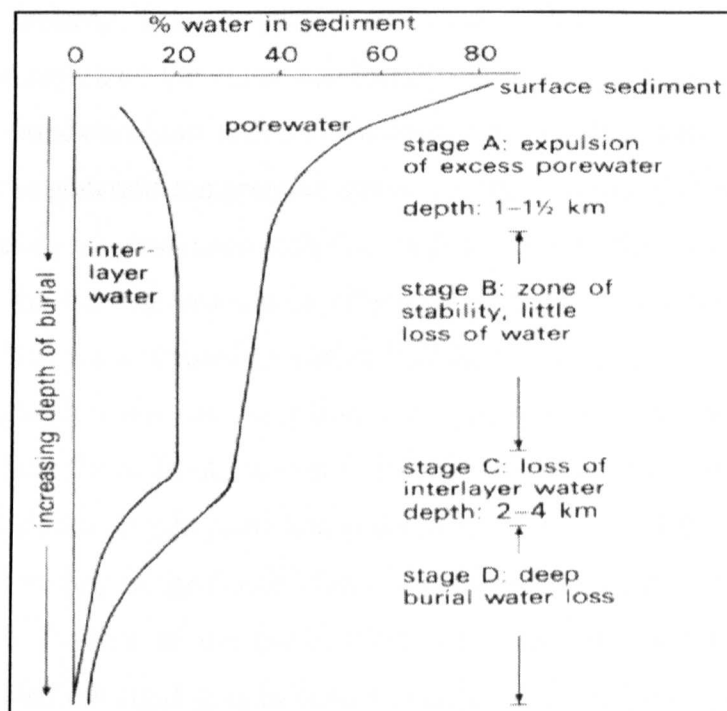


Figure 2.2. Progressive compaction of mudrocks with depth (after Tucker 1981)

A manifestation of the deposition and compaction of argillaceous deposits is the preferred orientation of the clay mineral particles. Clay minerals are plate like structures. On deposition they may flocculate to form peds of roughly orientated clay particles or dispersion may occur to form randomly oriented deposits. Compaction and associated dewatering also produces a parallel alignment of the clay minerals (Bell 1986). Alteration of the clay mineralogy during diagenesis takes place due to temperature increases associated with depth of burial. The main change that occurs is an alteration of montmorillonite to illite via a mixed layer illite-montmorillonite stage. The temperature where montmorillonite disappears is approximately 70 to 95 °C i.e. 2 to 3 km depths. At greater depths and higher temperatures kaolinite is replaced by illite and chlorite (Tucker 1981).

### **2.3 TECTONIC EVENTS**

In the subsequent 300 million years since their deposition, the Carboniferous Coal Measures have been subjected to phases of both compression and tensional stress of tectonic origin that have folded and faulted them (Anderton 1979 et al). The Coal Measures were deposited during a time of intensive tectonic activity known as the Hercynian Orogeny. This Orogeny is associated with the closure of an ocean (Rheic Ocean) that separated the super continents of Eurasia (Europe, North America and Asia) and Gondwanaland (Africa, Australia and South America). Such orogenic events tend to generate compressive stresses within the Earth's crust. Three phases of tectonic activity are associated with this orogeny with the final phase occurring during the end of the Carboniferous thus affecting the newly deposited Westphalian Coal Measures. This phase caused extensive folding and thrusting especially in the South West of England, where the thrust front is conjectured to have existed. Immediately to the north of the thrust front, basinal Carboniferous successions are now much folded and deformed into upright folds due to the effect of this orogeny. The large degree of faulting and folding of the South Wales Coal Measure province is due to the phase of compression. Further to the north, block and basin successions formed with the underlying shallow rigid granite basement cushioning and protecting them from the full effect of the orogeny. The block and basin structure was developed along pre-existing normal faults and were only gently tilted. Other major structures in the Coal Measures formed by the late Hercynian deformation are the Pennines Anticline and

the South Wales Syncline. Although east-west compression produced the major Pennines structure, the local interplay of blocks and basins further to the north gave rise to many local variations of fold and fault structures within this region.

Early Jurassic times marked the opening of the Central Atlantic. This event was associated with crustal tension in North West Europe. The Paleozoic floor already possessed its own structural grain and movements along these ancient lines were triggered by the tensional stresses. Tensional rifting and associated uplifting of the central North Sea basin also occurred at approximately this time. Stratigraphical, sedimentological and igneous evidence suggest that periodically, since the opening of the North Atlantic, sectors of the European lithosphere have been locally upwarped eg North Sea (Hallam & Sellwood 1976). Tensile stress and the downward propagation of normal faults would have accompanied these movements.

A new cycle of uplifting and rifting west of Britain is postulated to have occurred in the early Cretaceous. Periodic and local upwarping of the lithosphere was accompanied by tension and occasionally volcanism. Active sea floor spreading of the North Atlantic began in the late Cretaceous and continues to the present day. Evidence of the tensional stresses associated can be seen in the Northern Ireland - Hebrides region. Here plateau lava lie in shallow folded basins associated major faults that represent reactivated ancient structures. This lava, and also a wider belt of dykes also of tertiary age with a north west to south east trend, indicate a major tensional phase with stresses operating in a north east to south west direction (i.e. oblique to the Atlantic-Continental margin). Much of the British Isles became land during the earliest Tertiary and Britain began to assume its present tectonic style with uplift in the north west and subsidence in the south east.

As the Atlantic opened the southern European Ocean separating Europe from Africa, known as the Tethys, closed. The compression associated with this tectonic event culminated in the main alpine orogeny. In southern alpine Europe the tensional regime that had typified most of the period subsequent to the Carboniferous was replaced by a phase of compression. The Tethys began to narrow, as its oceanic crust was subducted. The Alps and Carpathian Chains are believed to represent the remains of the peripheral mobile belt that existed on the border of the margin of the European continent. The presence of these compression forces within the British Isles can be

illustrated by the rejuvenation of existing Paleozoic structures. For instance the Sticklepath-Lustleigh dextral wrench fault, which exists in the Bristol Bay area. Reactivation of this fault during the Oligocene generated approximately 30 km of movement within the South West of England (Anderton et al 1979).

## **2.4 UK COAL MEASURES ROCK TYPES**

The UK Coal Measures mainly comprise of terrigenous clastic sedimentary rocks (rocks comprised of grains or clasts derived from pre-existing rocks). Such rocks are classified in terms of their grain size and vary in the Coal Measures from coarse grained sandstone to finer grained mudrocks. Coal itself is predominantly non-clastic and is organic in origin. Inter-lamination of one rock type with another and the lack of distinct lithological boundaries, when one rock type grades imperceptibly with another can create problems in the lithological identification of strata units in Coal Measure sequences (Williamson 1967).

### **2.4.1 Sandstones**

Sandstones can be defined very broadly as sedimentary rocks where greater than 50% of the grains are between 0.06mm and 2mm in diameter (BS5930 Site Investigations 1981). Sandstones can be classified as being fine, medium or coarse grained where the sand sized grains are predominantly less than 0.2mm, between 0.2mm and 0.6mm and predominantly greater than 0.6mm respectively. Mineralogically sandstones are usually comprised of sub-angular quartz grains with small amounts of feldspar and mica. There are various types of cement; common cements are silica, calcite, iron compounds or clay minerals. The sandstone structure and the cement type has an important influence on the sandstone strength, for example silica cements in arenites can produce very strong rock types as in the case of the Pennant Sandstone of the South Wales coalfield. Those sandstones with a high percentage of clay mineral matrix may be weak or very sensitive to moisture content (Hawkins and McConnell 1992). Sandstones vary from being thinly bedded to massive and may display a variety of internal structures including cross and graded bedding.

### **2.4.2 Mudrocks**

These are the lithic rock types where at least 50 percent of the grains are smaller than 0.06 mm (BS5930 Site Investigations 1981). Mudrocks encompass the siltstones and finer grained rock types and also fissile rocks of these types such as shale. Several

different lithological classifications have been developed for the engineering classification of mudrocks (BS5930 1981, Hawkins and Pinches 1992, Dick and Shakoor 1992). Hawkins and Pinches (1992) have proposed a three-fold classification in terms of clay content. This classification was developed to differentiate mudrocks into groups with similar geomechanical properties, in particular its durability and is shown in Table 2.1 below.

<b>MUDROCK</b>  (50% grains < 0.06mm in diameter)	<b>SILTSTONE (&lt;25 % clay fraction)</b>
	<b>MUDSTONE (25 to 40 % clay fraction)</b>
	<b>CLAYSTONE (&gt; 40 % clay fraction)</b>
	<b>SHALE (mudrock with fissile planes &lt; 20mm apart)</b>
	<b>METAMUDROCK (mudrock subjected to low grade metamorphism)</b>

Table 2.1 Classification of Mudrocks (after Hawkins and pinches 1992)

#### 2.4.2.1 Siltstone

Siltstones are recorded as being common members of the interseam sequence and occur either as thick groups of sediments passing upwards into sandstone or as relatively thin beds or laminations interbedded or interlaminated with sandstone (Williamson 1967, Clarke 1963). Mineralogically the silt and coarser grains are dominantly quartz whilst clay minerals make up the finer fraction. The degree of cementation of mudrocks is related to total porosity and effective pore size. In siltstone the cement can penetrate with relative ease and thus produce a thick and continuous bonding. Siltstones tend to form thick laminations and thin beds and due to the presence of platy clay minerals may have a coarse fissility parallel to bedding. Due to their inert mineralogy, large grain contact and relatively large degree of cementation the siltstones tend to be the strongest of the mudrocks. Due to their low percentage of clay minerals siltstones have a low swelling potential.

#### 2.4.2.2 Mudstones

The mineralogy of mudstones is the same as that of the siltstones but with a higher clay mineral content. The swelling potential of mudstones is lower than claystones due to both the lower percentage of clay minerals and the higher degree of cementation inhibiting swelling. Mudstones units themselves may be massive or they

may be interlaminated with siltstone. Due to the presence of platy clay minerals they may have a poorly developed fissility parallel to bedding.

#### 2.4.2.3 Claystones and Seatearths

These are classified as having > 40% clay fraction. This boundary is considered to be the point at which the geomechanical properties of the rock are dominated by the clay minerals (Hawkins and Pinches 1992). During diagenesis compaction is dominant with cementation only playing a minor role. This creates a weaker and less durable mudrock (Dick and Shakoor 1992). The major clay minerals in UK Coal Measures are illite and kaolinite with a smaller percentage of mixed layer clays and chlorite (Taylor and Spears 1970, Taylor 1988). A characteristic feature of rocks with a high clay content is the increase in bulk volume (swelling) and a corresponding decrease in shear strength due to water uptake. Repeated wetting and drying of rocks susceptible to swelling may lead to breakdown of the rock in a process known as slaking. Of the common clay minerals present within UK Coal Measures only the mixed layer clay mineral (illite-montmorillonite) swell in a physico-chemical manner therefore mechanical swelling is probably dominant. Bedding and lamination planes are often absent in claystones. Due to the parallel alignment of the clay minerals during diagenesis a fissility is often generated within the rock material. Seatearths containing a high percentage of clay minerals, although often massive or thickly bedded, can contain smooth, striated undulating planes known as listric planes which may have been produced by movements of strata during diagenesis (Taylor and Spears 1970).

#### 2.4.2.4 Shale

Shale represents the fissile mudrocks with a highly developed parallel alignment of clay minerals. It was recommended by Hawkins and Pinches (1992) that the term shale be used to prefix the mudrock subdivision when the mudrock has fissile planes that are spaced at less than 20 mm apart. Fissile planes are planes of very low cohesion and therefore the rock can be easily parted along such planes.

### 2.4.3 Coal

Coal is a carbonaceous sedimentary rock that is comprised of both organic and clastic constituents. Coal can be divided into two basic groups, the humic coals and the sapropelic or cannel coals. The sapropelic coals contain no stratification, usually have a dull lustre, and fine grained uniform texture and conchoidal fracture. Humic coals

are classified in terms of their degree of coalification due to burial and low-grade metamorphism (Williamson 1967). This is termed the coals rank and can be related to the reflectance of certain constituents and to the volatility of the coal. In ascending orders of rank the basic coal types are peat, brown coal, lignite, sub-bituminous, bituminous, semi-anthracite, anthracite and meta-anthracite (Williamson 1967). The major constituents of humic coal are vitrain, which is glossy and vitreous, clarain which has a pronounced surface lustre, durain, which is dull and granular in appearance, and fusain which contains fibrous strands. Humic coal normally consists of bright and dull bands with vitrain and clarain forming the bright bands and durain forming the dull bands.

## **2.5 SEDIMENTARY STRUCTURES**

### **2.5.1 Introduction**

These are structures within sedimentary rocks that are visible to the naked eye and are formed during or shortly after deposition (Selley 1982). They are formed mainly from physical processes but structures of chemical (for instance ironstone concretions) or organic origin (burrow structures) can occur. Sedimentary structures vary in scale from tens of metres down to a few millimetres (e.g. thickness of lamination planes). A hierarchy of scale exists and smaller scale structures may form within a larger scale structure, for instance laminations within a thick bed of siltstone. In engineering terms many sedimentary structures form planes of reduced strength that have a directional significance and thus impart a structural anisotropy into the rock.

### **2.5.2 Bedding**

Beds are layers of rock usually deposited horizontally and are found within most sedimentary rocks. The minimum thickness for a bed has been given as 1 cm (Tucker 1981, Selley 1982). However a commonly accepted classification for bedding spacing defines bedding as being greater than 60 mm (Anon 1970). Bed boundaries are usually defined by a bedding plane which represents changes in grain size, grain orientation or sediment composition. They may also represent periods of no deposition and the plane may represent an erosion surface. Reworking of the surface by the movement of water across the top of the exposed plane may create surface lineaments and ripple/wave effects.

Several types of bedding exist with the main types described as follows:

#### **2.5.2.1 Massive Bedding**

This refers to beds without any apparent internal structure. Thick and massive beds are usually a product of rapid deposition of sediment. It may also be due to the internal removal of structure by the action of burrowing animals (Selley 1982).

#### **2.5.2.2 Cross Bedding**

Cross bedding is characterised by parallel intra-bed planes inclined at an angle of about 30 degrees to the bedding planes (Williamson 1967). The structure is formed by the downstream migration of sand waves and sand dunes under conditions of net sedimentation (Tucker 1981).

#### **2.5.2.3 Graded Bedding**

A graded bed occurs when there is a gradual decrease in the whole grain size upward through the bed. This structure is formed due to a gradual reduction in the flow energy during sedimentation (Selley 1982).

#### **2.5.2.4 Laminations**

Laminations are planes within the rock that are classified by being less than approximately 1 cm apart. Laminations arise from changes in grain size during sedimentation, size grading within laminations or changes in mineral or colour composition. Laminations typically occur in the finer grained sediments. In such cases they are usually formed through deposition from suspension. The surface of the laminations may be coated with parallel-aligned mica. This mica coating can substantially reduce the shear strength of the plane (Williamson 1967). Cross lamination can occur and is mainly produced by migration of ripple structures formed by the flow of water. Where mud deposition is intermittent with ripple migration the mud tends to be concentrated in the ripple troughs. Laminations may occasionally be formed within sandstones due to deposition of the sand by turbulent, high flow velocity currents (Tucker 1981).

### **2.5.3 Soft Sediment Structures**

Post depositional disturbance of the sediment can create characteristic structures. They may be a result of either physical processes or as a result of disturbance by

living organisms. Selley (1982) subdivided physically generated structures into three groups according to whether the sense of movement was dominantly vertical or dominantly lateral and whether the sediment deformed physically in an unconsolidated state or whether it was sufficiently consolidated to shear along slide planes (Table 2.2).

Sense of movement	Structure	Nature of deformation
<b>Dominantly vertical</b>	Convolute bedding	Plastic (sediment lacks strength)
	Convolute laminations	
	Load and pseudo nodules	
<b>Dominantly horizontal</b>	Slumps	Brittle (sediment possess shear strength)
	Slides	

Table 2.2 Soft Sediment Structures (after Selley 1982)

#### 2.5.3.1 Convolute Bedding

Typically appears in beds of sandstone up to 1 metre thick as series of synclines separating sharp peaked anticlines. This structure is caused by the vertical passage of water through loosely packed sand, which generates plastic deformation of the sand bed.

#### 2.5.3.2 Convolute Laminations

Similar to convolute bedding but on a smaller scale. Convolute laminations occur in laminated fine sands and silts as a series of local small scale folds often truncated by overlying planar laminations. Again generally recognised to originate by the vertical dewatering of the sediment.

#### 2.5.3.3 Load Casts and Pseudo Nodules

These occur at the interface where sands overlie mud and are generated by the differential loading of waterlogged sand on unconsolidated mud. Load casts are irregular lobes of sand penetrating into the underlying mud whilst pseudo nodules occur where the lobes separate from the sand interface and form discrete balls of sand within the mud layer.

#### **2.5.3.4 Slump Structures**

Crumpling and folding of the sediment can take place due to slumping of the sediment deposited on slopes. Slump folds are usually associated with low angle soft sediment faulting which provides evidence of lateral movement of the sediment. Lateral movement may be spontaneous or may be triggered by earthquake activity.

#### **2.5.3.5 Organic Sedimentary Structures**

Structures formed within the sediment by the action of living organisms are known as trace fossils and consist of animal borings, footprints etc. Trace fossils tend to destroy the primary sedimentary structures such as bedding (Selley 1982).

### **2.5.4 Sedimentary Structures Affecting Coal Seams**

These structures vary in scale from regional in the case of seam splits to local in the case of roof rolls, swilles etc.

#### **2.5.4.1 Washouts**

Areas of the seam where the coal is totally or partially replaced by non-carbonaceous sediment are known as washouts. The sediment that forms the washout is usually, fairly coarse grained. Washouts tend to be relatively narrow compared to their lengths. They are a manifestation of river channels that cut across the top of the peat deposit eroding the peat and depositing typically sand sized sediment. Normally the junction between the washout and the coal is irregular due to undercutting of the peat by stream erosion. In other cases the interface between the washout and the coal is sharp and possibly slickensided. Washouts may also affect more than one seam. Powerful deeply eroding rivers form such structures. High energy rivers would be unlikely on the low lying delta plains and so they may be associated with local uplift or rapid subsidence which would generate steep gradients (Williamson 1967).

#### **2.5.4.2 Roof Rolls**

These are projections into the top of the coal seam formed by the undersurface of the roof strata replacing the upper layers of the coal. Roof rolls can be either elongate or more equidimensional in plan. Elongate roof rolls are formed by erosion of a minor stream channel in the soft upper layers of the peat. Equidimensional roof rolls are considered to have been formed by localised sinking of the overlying sediment into the peat (Williamson 1967).

#### **2.5.4.3 Swilles**

Swilles are elongated hollows in the seatearth that directly underlies the coal seam and are subsequently infilled with coal. They are considered to be formed by rivers eroding channels in the top of the seatearth prior to peat deposition. (NCB 1984).

#### **2.5.4.4 Seam Splits**

Commonly a single coal seam may be split into two or more separate ‘leaves’ separated by lenticular shaped interseam sediment. Seam splits typically occur on a regional scale and are considered to be a result of variations in subsidence rates in different parts of the coal forming basins. It is considered that subsidence was greatest towards the centre of the basins and the marginal basin areas were usually stable.

Initially no differential subsidence occurs and the peat forms a continuous horizontal horizon. (stage 1). By stage 2 subsidence has occurred over part of the peat forming area. This zone would then have flooded leading to deposition of sediment and cessation of peat formation. The adjacent, more stable area would have remained above the water level and peat formation would have continued. Eventually subsidence would have ceased and peat again would have extended across the whole region to form the continuous upper leaf of the seam (stage 3). Multi seam splits occurred when subsidence was more intermittent and several coal seams laterally join to form one seam. Linear splits are more local in extent and tend to form elongated and narrow features. They are attributed to river channels being diverted across the peat area restricting peat formation over its length. After channel abandonment peat would have extended across the river deposits so that the upper coal would have formed a continuous bed (Williamson 1967).

#### **2.5.4.5 Dirt Partings**

These are horizons, a few centimetres thick within coal seams. They are usually comprised of argillaceous rock types such as claystones, shale and mudstones. The partings are a result of temporary flooding of the coal forming peat, from adjacent river channels. The low topography of the delta surfaces resulted in widespread flooding. The floodwater would usually have been of low velocity thus typically only fine grained sediment would have been deposited.

## **2.6 NON-SEDIMENTARY STRUCTURES**

### **2.6.1 Introduction**

Structures present within sedimentary rock masses that are developed after diagenesis and are usually a result of deformation and/or brittle fracturing of the rock mass under the influence of a differential stress field. Such structures can be subdivided into either discontinuous structures such as joints, coal cleat and faults which are a result of brittle failure of the rock material and continuous structures such as folds which are a product of ductile deformation of the rock material.

### **2.6.2 Discontinuities**

The characterisation of discontinuous structures within rock masses is of fundamental importance in rock engineering as these structures adversely affect the engineering performance of the rock structure.

#### **2.6.2.1 Joints**

Joints are extremely common and are developed in all competent rock types exposed at the surface. They are cracks and fractures along which there has been extremely little or no movement. There is no universal formal definition of joints (Park 1983, Laderia and Price 1981) due to their differing modes of formation and wide range of scales and forms. However a general terminology exists that is used to classify and describe joints. A group of planar joints that run approximately parallel to each other are said to be systematic and form a single joint set. A joint system occurs when two or more joint sets intersect. A conjugate joint system occurs when two joint sets intersect about a structural plane or line. The size of the joint plane varies over a large range. Generally joints can be divided into master joints which penetrate several rock horizons and persist for hundreds of metres, major joints which are an order of magnitude smaller. Smaller non-persistent structures are termed minor joints whilst minor fractures only a few mm in size are known as micro joints (Bell 1986). Bedded sedimentary rocks often contain orthogonal joint sets perpendicular to bedding consisting of an early systematic set and non-systematic joints extending across intervals between the joint set (Gross 1992). Joint faces are often irregular so that the adjacent walls are interlocking. The dominant features on a systematic joint plane are plumose markings with the axis of the plume parallel to bedding. Price (1966) considered that these structures are a result of the linking of micro-fractures during joint development (Figure 2.3).

On the edges of a joint plane a fringe area may exist where the plume structures terminate against a system of small scale joints usually at an angle of 5 to 25 degrees to the main joint surface.

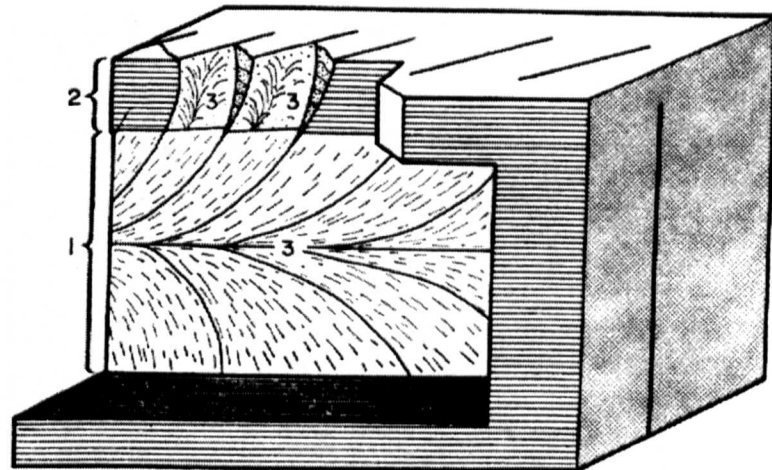


Figure 2.3 Surface features on a joint plane. 1) main joint face, 2) fringe, 3) plumose Structures. (after Price 1966)

#### *2.6.2.1.1 Mechanism of joint formation*

Price (1959, 1966) suggested a mechanism for the formation of ubiquitous tension and shear joints within sedimentary rocks. His model requires that two processes occur. He considered that during tectonic deformation or burial, rocks undergo progressive compaction and strain, which in turn increases their elastic and strength properties. The rocks final properties are reached at depths of maximum burial and tectonic compression. This hardening process leads to locked-in residual stresses, which represent in direction and amount the stress field at the time the final elastic properties were obtained. The other concept he used to generate his model of joint formation is of lateral stretching of the strata during uplift. He stated that during uplift the effective lateral extent of the strata increased due to the effective increase in circumference of the earth's crust. He calculated that the decrease in lateral stress due to this stretching is approximately equal in value to but opposite in sign, to half the decrease in vertical load, which occurs during uplift. Models of joint formation were constructed for the case of simple burial and uplift and for the case of tectonic compression and subsequent uplift.

### Model 1. Simple burial and uplift.

Price assumed that during burial over a long period of time stresses that develop in the rock might be very close to being hydrostatic. Figure 2.4 illustrates the variation in stress within such a rock mass during uplift.

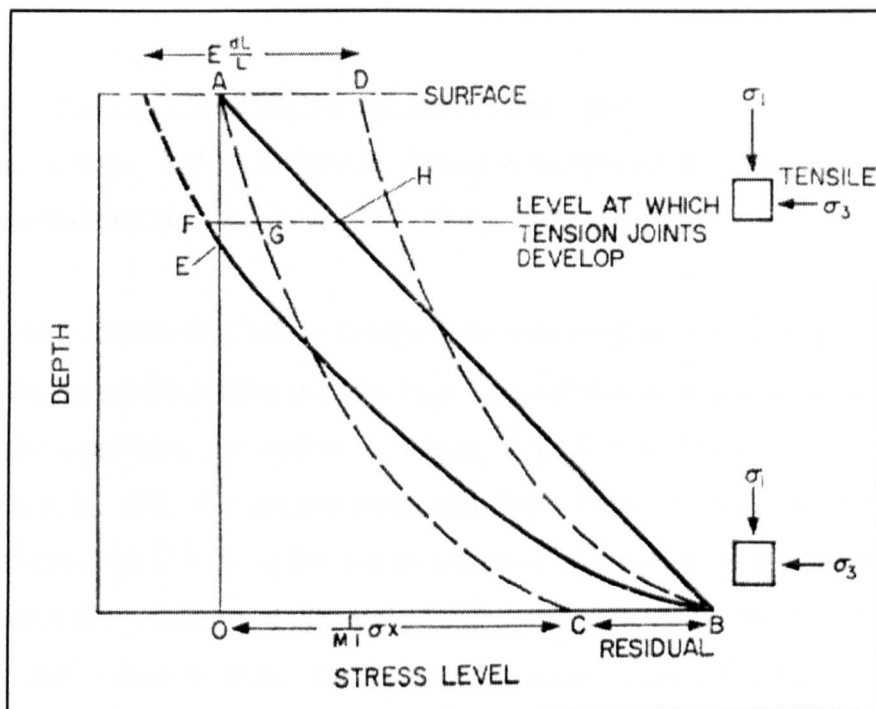


Figure 2.4. Variation in stress due to simple uplift (after Price 1959).

The stress value obtained in all directions at the maximum depth of burial are represented by point B and is hydrostatic. Line B to A represents the decrease in the gravitational load during uplift. The curve C to A represents the predicted way that the lateral stresses decay during uplift if the rocks elastic modulus was constant during burial. Distance CB represents the 'locked in' residual stress due to the increase in elastic modulus at point O. The curve BD represents the change in lateral stress during uplift in the rock mass taking into account residual stress. As previously stated Price (1959,1966) suggested that the lateral stretching of the strata during uplift brought about a further decrease in horizontal stress. If this is taken into consideration the variation of horizontal stress during uplift is given by curve BEF. It can be seen from the figure that at point E lateral stress is zero and at shallower depths the rock will go into tension. Normally the horizontal principal stresses will not be exactly equal and when the tensile stress of the minimum principal stress reaches the tensile strength of the rock, tension joints will form perpendicular to the axis of the lowest principal stress. The tensile stress is immediately relieved in this direction and is

probably replaced by a compressive stress which can have a maximum value of  $\sigma_v \cdot v$  where  $\sigma_v$  = the vertical stress and  $v$  = Poisson's Ratio. The other horizontal principal stress now becomes the minimum principal stress and further uplift can eventually cause a second set of tension joints to develop with the two sets forming an orthogonal system.

### Model 2 . Tectonic Compression and Subsequent Uplift

Tectonic stresses, which developed during a compressive phase, are suggested to remain as residual stresses (Price 1959,1966).

This model assumes that lateral compression was unequal and that the vertical stress acts as the minimum principal stress ( $\sigma_3$ ). The variations in stress due to uplift from this initial condition are shown in Figure 2.5. The maximum principal stress is represented by OF, the intermediate principal stress by OB and the minimum principal stress by OA. As uplift occurs the two horizontal stresses change as indicated by the curve FH and BD and the vertical stress as indicated by line AK. At level C the vertical load changes from being the minor principal stress to being the intermediate principal stress. This condition must be satisfied prior to vertical fracturing occurs. With further uplift the ratio between the two horizontal stress increases. At the point D in the diagram the stress conditions are such that the shear strength of the rock is exceeded and vertical shear joints form. The angle between the two sets of shear joints is bisected by the two horizontal principal stresses. The shearing is also conjectured to release residual stresses in the vicinity of individual joint planes (Price 1966). A large number of joints need to form in order to dissipate the residual stress over a large area. Eventually the vertical stress may become the major principal stress or further uplift may cause the rock to pass into tension and tension joints may form.

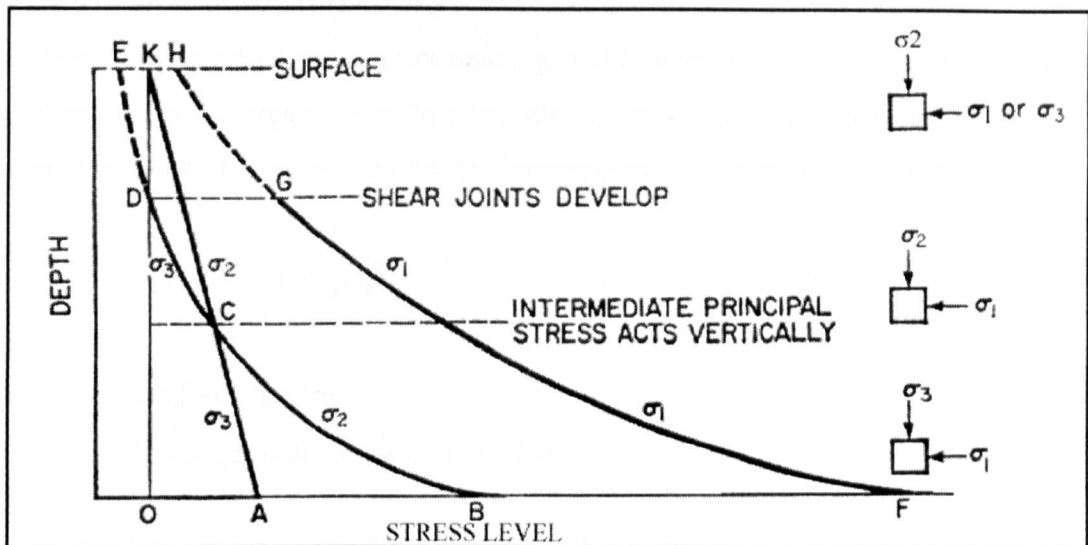


Figure 2.5 Variation in stress due to tectonic compression and uplift (after Price 1959)

#### 2.6.2.1.2 Coal cleat.

Joints within coal seams are commonly called cleat. Typically, as with most joints in sedimentary rocks, there are usually two sets of cleat both dipping vertically and striking perpendicular to each other. Usually one set is better developed and is called the main, face, or primary cleat. The other set is called the butt, cross or tertiary cleat (Macrae and Lawson 1956, Williamson 1967, NCB 1984). Cleat planes tend to be more closely spaced than the jointing in adjacent strata. Typical spacings measured within some Yorkshire coal seams being 40mm to 250mm (Macrae and Lawson 1956). The cleat spacing can vary within different layers within a seam and tends to be closest in bright coal horizons. The trend of cleat planes can be constant over a wide area and also between different coal seams (USBM 1984). The origin of cleat has been much debated. An early theory (Kendall and Briggs 1933) states that cleat forms due to torsional stresses regularly oriented and operating continuously. They identified the semi-diurnal east to west tide as the source of the stress. The theory considers that such a small stress but endlessly repeated at high frequency may create fatigue joints. Other theories of cleat formation can be divided into either endogenetic or exogenetic origin. Endogenetic theories relate the origin of cleat to compaction, dewatering and coalification processes. Exogenetic theories claim that cleat is formed by tectonic and stress generated during uplift by the same mechanisms as the jointing in the adjacent strata.

#### *2.6.2.1.3 Joint spacing distributions*

The frequency distribution of joint spacing within a rock unit is not uniform. Priest and Hudson (1976) suggest that the distribution considering all joints measured along a scan line is best represented by a negative exponential function (Equation 2.1).

$$f(x) = \lambda e^{(-\lambda x)} \quad (2.1)$$

Where  $x$  is the joint spacing

$\lambda$  is the inverse of the mean joint spacing.

The frequency distribution has also been represented by a log-normal distribution (Bridges 1976). The frequency of joint spacing within a single set is probably best represented by a normal distribution.

#### *2.6.2.1.4 Average joint spacing*

The average spacing of joint planes within a joint set has long been established to be related to the thickness and competency of the lithological unit (Laderia and Price 1981). An empirical relationship (Equation 2.2) was established in the 1940's for sandstones and limestone in Russia (referred to in Price 1966, Laderia and Price 1981)

$$S = K \cdot B_t \quad (2.2)$$

Where  $S$  = mean spacing between fractures

$K$  = constant relating to the lithology of the strata unit

$B_t$  = bed thickness

Various theories have been developed to explain the relationship between rock lithology, bed thickness and mean joint spacing.

Price's theory for joint formation (Price 1966):

Price suggests that the number of joints developed in a rock is directly related to overall strain energy stored in the rock. He states that strain energy is equal to the work done in producing a given amount of strain. In a unit cube the strain energy is given by Equation 2.3.

$$w = \frac{1}{2} \cdot \sigma \cdot \varepsilon \quad (2.3)$$

Where  $w$  = strain energy

$\sigma$  = applied stress

$\varepsilon$  = resulting strain

Under triaxial compression the strain energy in a unit cube is given by:-

$$\omega = \frac{1}{2E} [\sigma_1^2 + \sigma_2^2 + \sigma_3^2 - \frac{2}{M} (\sigma_1\sigma_2 + \sigma_1\sigma_3 + \sigma_2\sigma_3)] \quad (2.4)$$

Where  $E$ = Young's Modulus

$M$ = Poisson's Number

$\sigma_1, \sigma_2$  and  $\sigma_3$  are the principal stresses

The strain energy is therefore related to the Young's Modulus and Poisson's Ratio of the rock beds. Even if the stresses within adjacent rock beds are the same more strain energy is stored in the rock units with lower Young's Modulus. Price (1966) considers the most striking example of this relationship is in the ratio between cleat spacing in coal seams and the corresponding joint spacing in the adjacent non coal rock units.

Price (1966) states that the relationship between thickness of the bed or rock unit and joint frequency is related to the frictional forces which exist between adjacent beds. He stated that after development of an initial fracture within a bed a minute amount of bedding plane slip occurs at the interfaces at the top and bottom of the bed. The movement relieves the tensional stresses in the vicinity of the joint. He believed that at some horizontal distance from the joint the shear forces along the bedding surface are sufficient to maintain the stress, which existed just prior to the first joint forming. This distance represents the limit of influence of the joint and the tensile stress is sufficient to form a second joint. Price concluded that frictional shear force resisting bedding plane slip must balance the total horizontal force within the jointed bed. The horizontal force within the bed increase proportionally with increasing bed thickness thus the distance along the bedding plane before sufficient shear resistance is obtained for a further joint to form is directly related to bed thickness.

### Hobbs' theory for joint formation (After Hobbs 1967):

Hobbs proposed an alternative mechanism for the formation of tension joints in sedimentary rocks. He considered during uplift of sedimentary lithologys there was an increase in the lateral tensile stress. Eventually the tensile stress may have reached the tensile strength of a rock unit and a vertical joint forms in the beds at its weakest point. If the beds adjacent have a higher tensile strength, joints will not form within these units but there will be an increase in the shear stress in the neighbouring beds in the regions of the boundaries of the joint. The increase in shear stress is directly related to the force generated within the jointed bed, thus the jointed bed thickness. Hobbs argued that the shear stress decreased both with vertical distance from the jointed bed and with horizontal distance from the rock joint. The shear stress produces corresponding shear strains within the unjointed beds. If the unjointed beds have high shear modulus then the low shear strains produced in the unjointed beds allows a rapid increase, with horizontal distance from the joint, of tensile stress within the jointed bed. At a critical distance from the joint the tensile stress in the unjointed bed is sufficient to cause a further joint to form.

#### *2.6.2.1.5 Joint spacing in thick beds*

In an investigation between fracture spacing and bed thickness (Laderia and Price 1981) on Carboniferous turbidities of Portugal and the Carboniferous flysch of Devon and Cornwall (UK) it was found that there was a linear relationship between spacing and bed thickness for thin beds. However it was found that the fracture spacing is approximately constant for bed thickness greater than 1 metre for the UK flysch and 2.0 metres for the Portuguese turbidities. The authors using data obtained by McQuillan (1973) for joint spacing in the Asmari Limestone of the Zagros Range found that again joint spacing was approximately constant after 1.5 metres bed thickness. Laderia and Price (1981) considered that in thin beds the joint separation is influenced by traction at the bed interfaces however at a certain bed thickness this mechanism is superceded by the hydraulic fracturing of the beds to produce the jointing. They stated that hydraulic fracturing occurs when the fluid pressure in the rock exceeds the minor principal stress by an amount equal to the tensile strength of the rock. After initial fracture the fluid pressure in the vicinity of the joint is reduced, a fluid pressure gradient occurs perpendicular to the joint plane and at a critical distance the fluid pressure is sufficient to cause further hydraulic fracturing.

### 2.6.2.2 Faults

Discontinuities where there is measurable displacement across the fracture plane are termed faults (Park 1983). Faults occur on a continuum of scales from structures, which form the boundary of tectonic plates to small-scale features where the relative displacements may only be a few mm. Faults have a large affect on the viability of mining a coal seam. Not only is the displacement of the seam problematical to mining but there is a tendency for poor mining conditions to be present within the vicinity of the fault due to fracturing parallel to the main fault plane and the possible presence of residual stresses. Faults, like joints, are the result of brittle or semi-brittle fracture of the Earth's crust, usually under the influence of stresses of tectonic origin. They therefore form in the upper zone of the crust where the temperature and pressure are low enough for the crust to behave in a brittle manner.

Faults are classified in terms of the orientation of the fault plane and the sense of movement of the adjacent strata. Where the fault plane is non-vertical the block above the fault is referred to as the hanging wall and the block below the fault is called the foot wall. The dip of the fault plane is called the hade. If the direction of movement is parallel to the fault plane the fault is termed strike-slip. Faults where the movement is parallel to the dip are termed dip slip faults. The horizontal and vertical displacements associated with dip slip faults are termed the faults heave and throw respectively. When the hanging wall moves down relative to the footwall the fault is termed normal and where the hangingwall moves up relative to the footwall the fault is termed reverse. Reverse faults where the hade is less than 45° are called thrusts (Park 1983) (Figure 2.6).

The patterns of tectonic faulting within UK Coal Measures can be divided into the following Hierarchy (NCB 1984):

- (1) Master fault/fold belts. Typically form the boundaries of tectonic blocks. For example the Alston Block and its extension into the North East coalfield. The major boundary faults of some coalfields fall into this category. These faults are readily detected by reconnaissance seismic surveys (NCB 1984).
- (2) Main faults. These are evenly spaced across blocks in one set or two conjugate sets and pass through most of the coal seams within that block. A set is defined as any group of faults having similar orientations, age and other characteristics suggesting a common origin (NCB 1984).

- (3) Splay faults. They are off shoots associated with the main faults. Displacement along the fault plane decreases rapidly with distance from the main fault and these faults are prone to change vertically with strata of different competence.
- (4) Isolated faults. Faults that cannot be included with any well represented set and usually pass through only a few seams.

#### *2.6.2.2.1 Origin of faults.*

Faults are a result of brittle shear failure of the rock mass. The orientation, dip of the fault plane and relative movements of the rock on either side of the fault plane are related to the orientation and magnitude of the principal stresses at failure (Figure 2.6). Normal faulting occurs when the major principal stress is vertical which is typical of tensional tectonic conditions (Park 1988). Reverse faulting occurs when the intermediate principal stress is vertical and the maximum and minimum principal stresses act horizontally, which is typical of compressional tectonic conditions (Park 1988).

### **2.6.3 Folding**

A fold is a structure produced when an originally planar surface becomes bent or curved as a result of deformation. Folds are a product of ductile deformation of rock strata. Ductile deformation is associated with conditions of high temperatures and confining pressures and thus usually occurs at depths greater than approximately 10 km (Park 1983). Folds represent crustal shortening under the influence of horizontal compressive stresses usually of tectonic origin. Within coal seams folds can have a large influence on the viability of mining the seams by creating sharply undulating or steeply dipping seams which may prove problematical, expensive or impossible to mine.

Folds consist of a hinge area, which is the zone of maximum curvature, bounded by two limbs. The orientation and inclination of the fold is defined by reference to an imaginary plane which is equidistant from each limb and which bisects the angle between them. This plane is called the axial plane. The trend of the fold is the azimuth of the strike of the axial plane. The wavelength and amplitude of the folded strata are used to quantify the size of the fold. The wavelength is defined as the distance between adjacent hinge lines and the amplitude represents half the height of the fold. The fold's wavelength can range from 100 km's to a few mm's. The limbs of

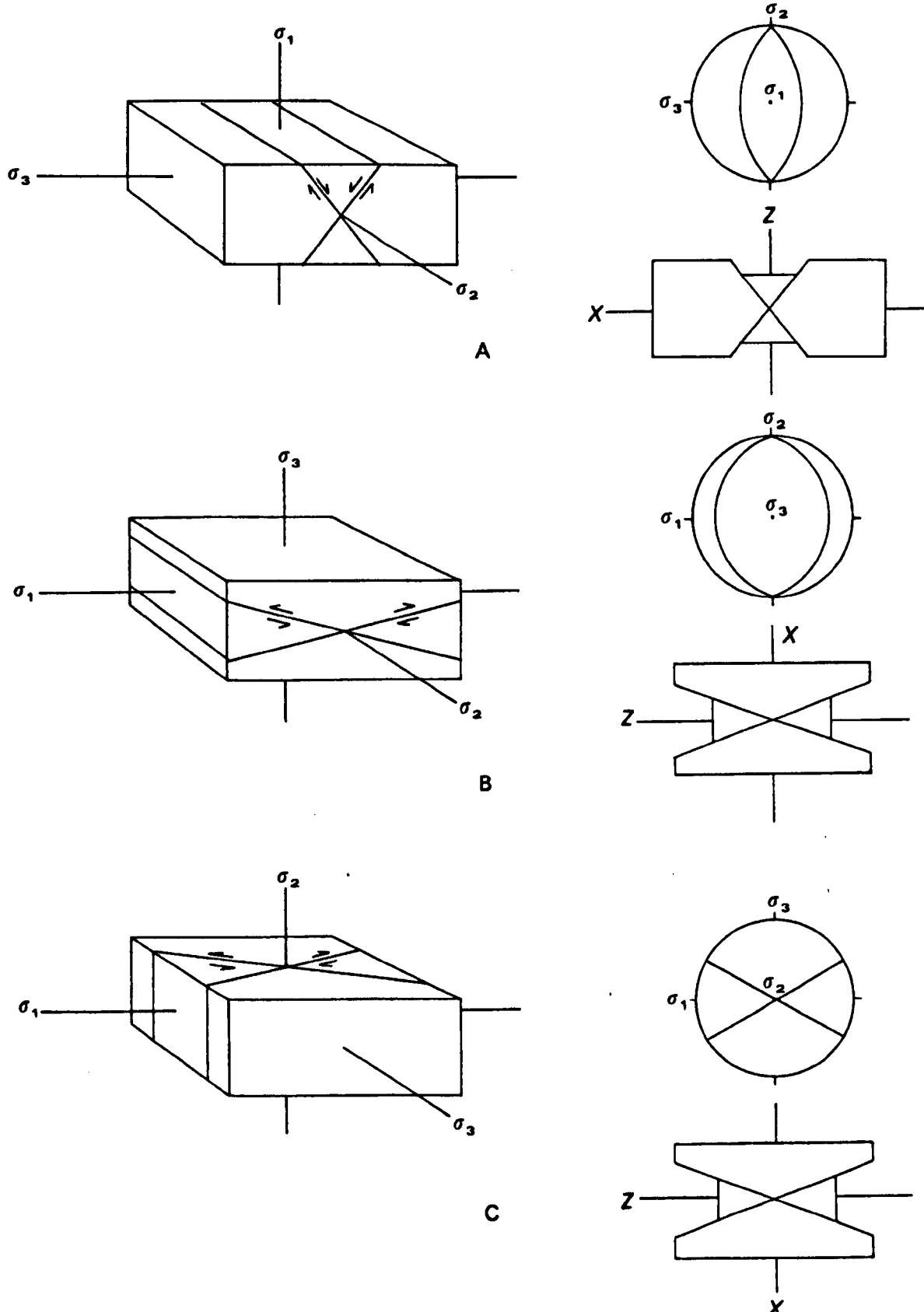


Figure 2.6 Faulting and its relationship to the principal stresses at failure.  
**A** Normal faulting, **B** Reverse/thrust faulting, **C** Lateral faulting

the fold may themselves be folded by smaller wavelength folds, termed parasitic folds. Complex deformational structures can occur when previously folded strata are subjected to further phases of folding (Park 1983).

Two basic types of fold are recognised, folds where the limbs dip away from the hinge are termed antiforms and folds where the limbs dip towards the hinge area are termed synforms. Normally the bedding becomes younger upwards; in this situation an antiform will contain older rocks within its core and is called an anticline, likewise a synform will contain younger rock within its core and is called a syncline. When the angle between the folds axial plane and each limb is different the fold is said to be asymmetrical. Plunging folds occur when the hinge line of the fold dips.

## **2.7 INSITU STATE OF STRESS WITHIN UK COAL MEASURES**

### **2.7.1 Introduction**

The state of stress within a rock mass prior to excavation is known as the in-situ stress. The in-situ stress is directly responsible for the magnitudes and orientations of the induced stress around an excavation; thus it is an important influencing factor on the deformation and failure of the rock mass adjacent to an underground excavation (Hoek and Brown 1980).

Coal mining within the UK takes place at depths below the surface of approximately 1000 metres, within the strong outer layer of the Earth's crust known as the lithosphere. The lithosphere is approximately 100 – 150 km thick (Park 1988) and can be subdivided into a brittle outer layer known as the upper lithosphere and a deeper layer which behaves as a ductile material. The transition from brittle to ductile behaviour takes place at elevated temperatures and high confining pressures (Jaeger and Cook 1979). The transition has been found to occur when the peak strength of the rock becomes approximately 3.4 times the confining pressure at failure (Mogi 1966). This indicates that Coal Mining within the UK is within the brittle upper lithosphere.

### **2.7.2 Sources Of In-Situ Stress**

There are several sources of stress within the lithosphere and the total state of stress within the rock mass is the sum of the stress generated from all sources.

Park (1988) states that source of stresses affecting the lithosphere can be divided into renewable and non-renewable types. Renewable stresses are those that persist as a result of the continued presence or reapplication of the causative forces even though the strain energy are progressively dissipated. Examples of renewable stress sources are plate boundary forces and surface loading from features that are in isostatic equilibrium. Non-renewable stresses are those that are dissipated by release of the strain energy originally present. These sources include bending forces by surface loads which are not in isostatic equilibrium, membrane stresses created by the change in curvature of a tectonic plate as it migrates towards or away from the poles and thermal stress created by the cooling of oceanic crust. Sources of stress include gravitational stresses, tectonic stresses, structural stresses and residual stresses (Klein and Brown 1983).

#### 2.7.2.1 Gravitational Stresses

These are generated by the weight of the overlying rocks. The vertical gravitational stress is given by Equation 2.5 (Jaeger and Cook 1979):

$$\sigma_z = \gamma z \quad (2.5)$$

Where  $\sigma_z$  is the vertical stress (MPa)

$\gamma$  is the unit weight of rock (MN/m<sup>3</sup>)

$z$  is depth (m)

The horizontal stress generated by the weight of the overlying load, assuming the rock mass to be isotropic, linearly elastic and with complete lateral restraint is given by Equation 2.6 (Terzaghi and Ricard 1952).

$$\sigma_h = \left( \frac{\nu}{1-\nu} \right) \sigma_z \quad (2.6)$$

Where  $\sigma_h$  is the horizontal stress (MPa)

$\nu$  is the Poisson's Ratio

#### *2.7.2.1.1 The affect of surface topography*

Gravitational stresses will vary if the surface topography is irregular. For example in the case of a v-notch valley the vertical stress below the bottom of the valley is reduced with respect to the horizontal stresses which are a result of loading by the valley shoulders. However the effect of such a feature on the state of stress will decrease rapidly as the distance below ground level increases (Brady and Brown 1985). Uneven surface loading by features greater than about 50 km wide (Park 1988) will produce bending stresses within the lithosphere beneath the feature. These stresses will cause the region to be in tension relative to adjacent regions.

#### **2.7.2.2 Tectonic Stresses**

Tectonic stresses are generated on a regional scale and can be both compressive and tensional in nature. Typically they generate an altered horizontal stress field and can be characterized by the occurrence of one sub-horizontal stress component significantly greater than both the overburden stress and the other horizontal component (Brady and Brown 1985). Plate tectonics describes the lithosphere as being divided into a number of thin, rigid plates that move tangentially to each other. Six major plates have been identified (Rice 1977). The plate boundaries may be either conservative or destructive. Destructive boundaries occur where lithospheric material is destroyed. Oceanic crustal rocks are denser than continental rocks and if a plate of oceanic material collides with a continental plate the density of the oceanic plate leads to the plate being forced down into the earth's interior in a processes called subduction. Tensional stresses acting perpendicular to the subduction zone are induced into the plate being subducted by the pull of the subducted slab (Park 1988). Tensional stresses are also induced in the overlying plate by a subduction trench suction force. Where two continental plates collide neither plate is subducted and compression of the plate boundaries occurs. This process is called orogenies and leads to the formation of major mountain chains. Orogenies generates horizontal compressive stresses perpendicular to the collision zone on a regional scale. New lithospheric material is created at spreading centers, for instance the rifted ridge that runs parallel to the axis of the Atlantic. The new material pushes the plate on either side in opposite directions to generate horizontal compression perpendicular to the ridge. The stress for ridge push has been calculated to be between 20-30 MPa in magnitude across the entire thickness of the lithosphere. However the lower lithosphere is not capable of holding large stress and the stress is redistributed into the

more brittle upper lithosphere by a process known as stress amplification. The stress generated may be sufficiently high to overcome the strength of the rocks of the upper lithosphere (Park 1988). Price (1959) has suggested a further source of tectonic stress. He states that if a rock mass is uplifted there is an increase in the lateral extent of the rock mass. This induces stretching and thus tensile stresses within the rock mass.

#### 2.7.2.3 Structural stresses

Rock masses with different elastic modulus may generate differential stresses with the stiffer rock units experiencing elevated stress levels relative to the adjacent rock units. This has been observed to occur in layered sedimentary rocks (Bush and Meyer 1988). Hydraulic fracture data compiled worldwide for minimum, horizontal stress measurements suggest that stress magnitude is lithology dependent (Bush and Meyer 1988).

#### 2.7.2.4 Residual stresses

Residual stresses can occur within a rock body and remain present even after the source of the stress has been removed. They arise by a variety of mechanisms, such as phase changes of minerals, changes in the rocks elastic properties (Price 1966), unloading and loading during glaciation and temperature reduction with overburden removal. Residual stresses are also associated with fault zones. One likely mechanism for the presence of residual stress is that of a visco-elastic effect caused by erosion (Jaeger and Cook 1979). Erosion may remove the overburden relatively quickly compared to the viscous dissipation of stress within the rock body. A further effect of time dependent stress changes within weak rock, such as coal measures has been suggested to cause lateral and vertical stresses to equalize over periods of geological time (Wilson 1980). This is known as Heim's Rule, that suggests that weak rock was unable in the long term to support large stress differences (Hoek and Brown 1980, Jaeger and Cooke 1979).

### 2.7.3 Global In-Situ Stress

In a review of literature relating to in-situ stress measurement at the time Hoek and Brown (1980) selected 116 stress measurements for sites worldwide which they considered were outside unusual geological situations in order to characterise the general state of stress within the earth's lithosphere. From this analysis they constructed two plots one showing the change in vertical stress (Figure 2.7) with

depth the other plotting  $k$ , the ratio of average horizontal stress to vertical stress against depth ( $z$ ) (Figure 2.8). They concluded that the measured vertical stresses were in general agreement with the vertical stress predicted by Equation 2.7. They found that most values of  $k$  lay within the limits defined by:

$$\frac{100}{z} + 0.3 < k < \frac{1500}{z} + 0.5 \quad (2.7)$$

The plot also indicates that at depths of less than 500 metres the horizontal stresses are significantly greater than the vertical stress. They also conclude that the wide variation in horizontal stress measurements precludes the prediction of horizontal stress at a site by the use of simple theory.

#### 2.7.4 In-Situ Stress Within The United Kingdom

In a review of the available data on in-situ stress measurements in the United Kingdom, Klein and Brown (1983) found only six sets of measurements, which included complete information. From this very limited data set they concluded that the principal stresses were always close to either the vertical or horizontal and that the principal stress closest to the vertical in all but one case corresponded closely to the weight of the overlying rock. They tentatively concluded that the minimum horizontal stress was approximately 65% of the vertical stress and that the maximum horizontal stress exhibits a large scatter and no simple relationship can be used to describe it. Considering the UK within the context of North West Europe they state that the maximum horizontal stress trends in a NNW to SSE direction. This they stated was due to the push of the African plate against the Eurasian plate.

Brereton and Evans (1987) analysed eighty on shore UK boreholes for breakout orientations and inferred that the regional minimum principal stress orientation was approximately 54°/234°.

In an overview of the current state of knowledge of in-situ stress within the United Kingdom (Hudson and Cooling 1988) stated that at that present time there was insufficient data to provide a clear understanding of the stress state throughout the United Kingdom. The authors also concluded that when the available data was considered there appeared to be a tendency for the maximum principal stress to be horizontal and to trend in a NW-SE direction. (Figure 2.9).

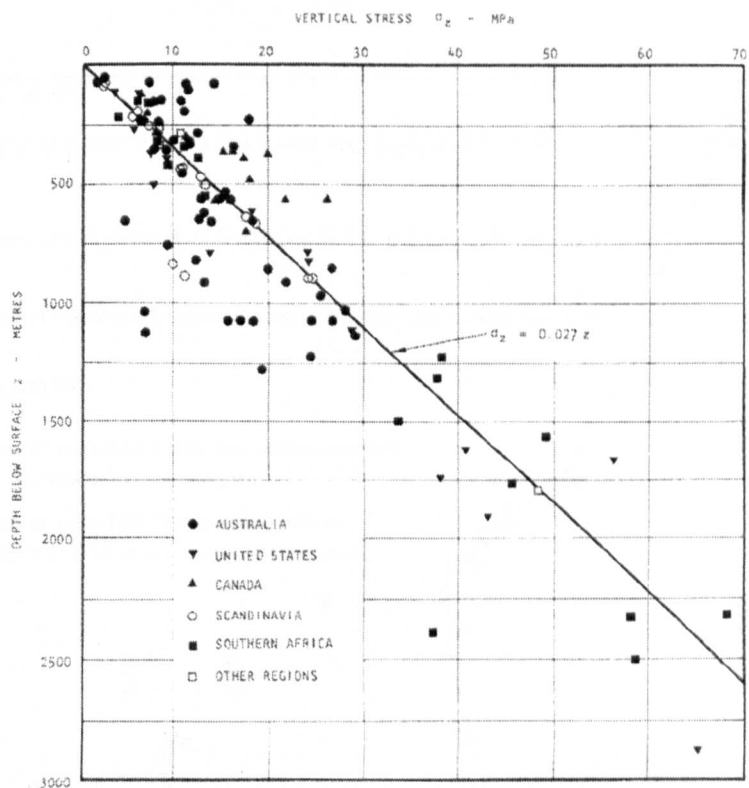


Figure 2.7 Vertical stress against depth below surface (after Hoek and Brown 1980)

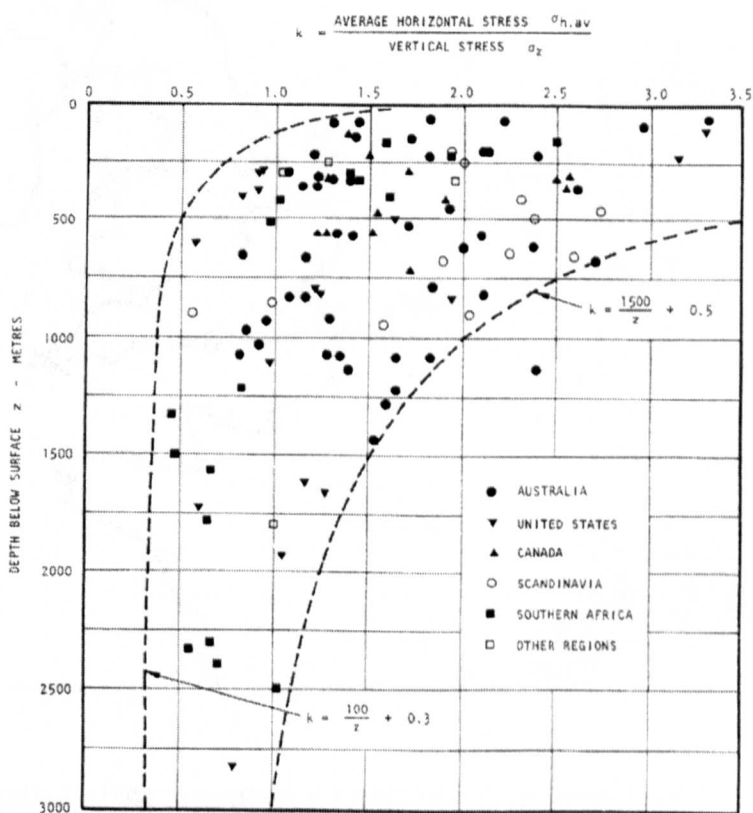


Figure 2.8. Ratio of average horizontal stress to vertical stress with depth below surface. (after Hoek and Brown 1980)

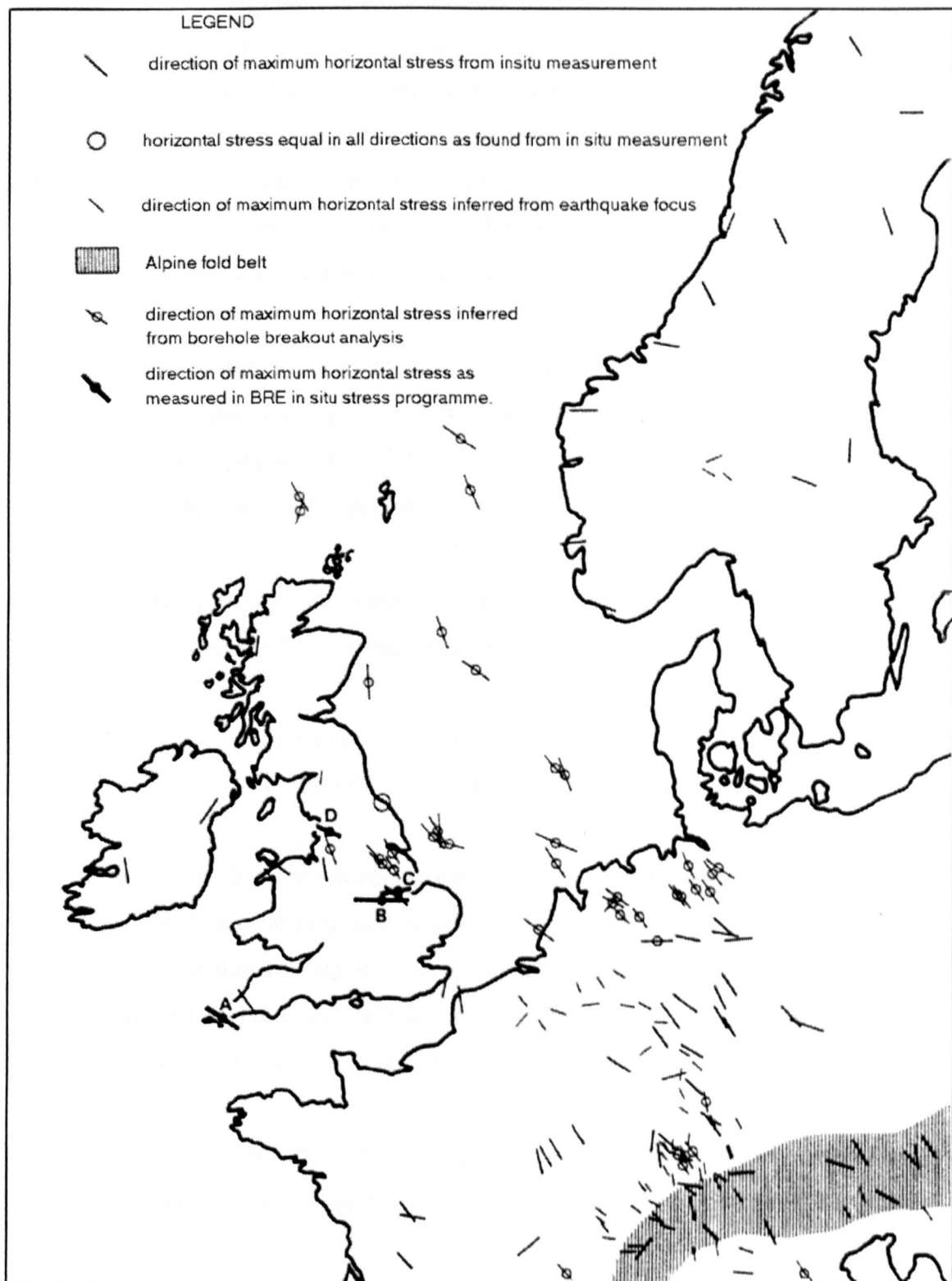


Figure 2.9 Orientation of the maximum principal stress in North West Europe  
 (after Klein and Barr 1986, new data added by Hudson and Cooling 1988)

## 2.7.5 In-Situ Stress Within The UK Coal Measures

In-situ stress measurements undertaken in eight mines mostly within the East Pennine coal field indicated that the in-situ stress field present within the UK Coal Measures was anisotropic (Bigby et al 1992). The general NNW trend of the major horizontal stress was confirmed to be present within the Coal Measures. The measurement sites varied between 440 metres and 987 metres below surface and the vertical stress was indicated to increase linearly with depth. However the authors found that there was no correlation with horizontal stress and depth, but their results indicated that there was a correlation between elastic modulus of the strata and the horizontal stress.

A further investigation of the state of in-situ stress within UK coal mines was undertaken at 16 mine sites throughout the United Kingdom (Bigby et al 1995). From the results of the measurements the researchers reached a number of conclusions concerning the state of in-situ stress within UK Coal Measures.

- (i) As generally accepted worldwide the vertical stress varies linearly with depth. The unit weight of overburden was found to be  $0.027 \text{ MN/m}^3$
- (ii) The ratio of maximum to minimum horizontal stress component, after ignoring 3 highly anomalous readings, was fairly constant at 1.68.
- (iii) The magnitude of horizontal stress, especially the maximum horizontal stress concluded to now vary as a function of both depth and strata stiffness. They considered that the variation of horizontal stress with strata stiffness was a result of tectonic strain, which was conjectured to be approximately constant for all the Coal Measure rock types.
- (iv) An equation was derived, relating maximum horizontal stress ( $\sigma_H$ ) in UK Coal Measures to the depth (z), elastic modulus (E) and Poisson's Ratio ( $\nu$ ), of the form:

$$\sigma_H = a_1.z.(\nu/1-\nu) + a_2.E - a_3 \quad (\text{Mpa}) \quad (2.9)$$

- (v) Using data for all the mine sites they produced the following relationship:

$$\sigma_H = 0.009.z.(\nu/1-\nu) + 0.779.E - 3.998 \quad (\text{MPa}) \quad (2.10)$$

(vii) For English mines only there was an improved fit using the relationship:

$$\sigma_H = 0.009.z.(v/1-v) + 0.803.E - 4.567 \quad (\text{MPa}) \quad (2.11)$$

(viii) There was too much scatter in the relationship between minimum horizontal stress, depth and elastic modulus for a meaningful relationship to be derived.

## 2.8 CONCLUSION

The typical lithological and structural characteristics of the UK Coal measures are a manifestation of their depositional environment, subsequent burial and diagenesis and the effects of the stresses that they have been subjected to from their deposition in the Carboniferous to the present day. The stresses, that have been of both compressional and tensional in nature, have folded, faulted and fractured the strata.

This chapter describes the processes that have formed the Coal Measures and the resulting characteristic features of the Coal Measures. Knowledge is thus gained of the nature of the Coal Measures that can be utilised as a basis of predicting the factors that effect the Coal Measures' engineering properties.

The characteristics of the in-situ stresses within the UK Coal Measures has been reviewed. The review indicated that the principal stresses generally acted in vertical and horizontal directions. The magnitude of the vertical in-situ stress has been concluded to be directly related to the thickness and density of the overlying strata. The magnitude of the horizontal principal stresses was concluded to be harder to predict but has been tentatively correlated with depth and strata stiffness.

## **CHAPTER 3**

### **UK COAL MINING AND COAL MINE STABILITY**

#### **3.1 LONGWALL EXTRACTION TECHNIQUES**

##### **3.1.1 Introduction**

Longwall mining involves the underground working of coal on a face or wall that is longer than 100 metres (Massey 1977) and typically in the United Kingdom 200 metres long. Longwall mining is considered to have originated in the early 18<sup>th</sup> century in Shropshire where it was known as the Shropshire or Longway method (Mills 1985). It has therefore been used for over 200 years and is now accepted as the most economic method of exploitation for the majority of seams found in Britain (Whittaker and Hodgkinson 1971, RJB 1999). It is currently practiced in large scale, heavily mechanised mines in many places worldwide and is the dominant method of underground coal mining within the United Kingdom. However the method relies upon uniform geological conditions over the length of the panel and also involves initial large scale investment. Therefore small mines or mines in heavily faulted and folded strata may adopt other mining methods (Roberts 1994).

Access to a longwall face is usually provided by two 'gate road' tunnels, which run down either side of the coal panel being extracted. The gate roads connect into the main roadways of the mine and provide a circuit for ventilation at the face. The air intake gate road is known variously as the main gate, loader gate or coal gate and the air return gate road is called the tail gate or supply gate. The main gate is usually used for the transportation of extracted coal whilst the tail gate is usually used for materials supply.

There are two basic types of longwall mining; advance longwall and retreat longwall.

##### **3.1.2 Longwall Advance Methods**

Longwall advance has been the traditional method of longwall coal mining within the UK, however over the last thirty years there has been a gradual change in favour of longwall retreat methods (Massey 1977, Mills 1985, RJB 1999). Longwall advance involves the formation of the gate roads simultaneously with coal extraction. Normally the gate roads are initially driven from the main roadways to form a

partition pillar and are connected to a face drivage from a face entry. From the face entry the face advances into the panel and the gate roads are usually formed at the face ends as the face advances. The unsupported roof behind the face line collapses into the void left behind by coal extraction, to a height usually corresponding to a major bedding plane or more competent horizon. This broken material is known as the goaf or gob whilst the roof that collapses is often termed the immediate roof. The gate roads are protected by the construction of pack supports on the goaf side of the gate road. Packs can be constructed from broken rock produced by ripping from the roof or floor (dinting) of the roadway or from timber or concrete chocks. A more modern technique of packing is known as pump packing, which involves the pumping of cement and clay slurry into bags hung in the pack area. This technique produces high resistance packs, which aid in controlling roof deformation within the gate roads (Newson 1983). With face advance the pack forms a continuous wall along the side of the gate road separating it from the goaf. Longwall advance has the advantage of rapid initial development in comparison to retreat mining but there is an element of uncertainty of geological conditions within the panel which in turn may delay or make production impossible.

### **3.1.3 Longwall Retreat Methods**

Longwall retreat mining separates the process of roadway drivage from that of coal production. In longwall retreat, the gate roads are driven the full length of the panel and then connected together at the far end by a face heading. The face supports, shearer, conveyors etc are taken down the gate roads and assembled in the face heading. The face then retreats back between the two gateroads towards the main roadways. As the faceline retreats back, the gate roads behind the faceline are allowed to collapse and are abandoned. A major advantage of retreat mining is that the geological features such as faults or seam splits and washouts will be identified during roadway drivage, which allows time to adjust the mining method to account for the feature. However, retreat mining prohibits rapid initial development of the panel. Thus a considerable investment has to be made prior to coal production. A further problem is that the gate roads may have to stand for a considerable period of time.

### 3.1.3.1 Semi Retreat Methods

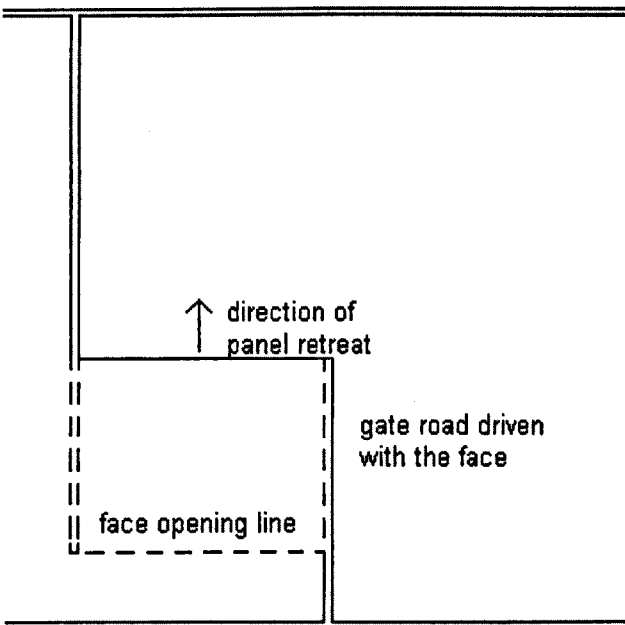


Figure 3.1 'Z' Semi-retreat system

An alternative to conventional retreat mining is a semi-retreat method known as the 'Z System' (Figure 3.1). The system requires one gate road to be driven before the face is worked. The other gate is driven from a main roadway behind the face opening line and then formed with the face as it retreats back. Usually the main gate is driven as the retreat gate while the tail gate is driven with the face. This method was sometimes used at mines practicing retreat mining for the first time (Daws 1973).

### 3.1.3.2 Single Entry Longwalls

This technique involves the drivage of only one gate roadway, thus greatly reducing the amount of development work that is required. However the gate road has to be multi-purpose, providing adequate ventilation, man access, supplies and coal removal. Because of this single entry longwall mining is only suitable for small shallow mines where ventilation requirements are low (Roberts 1994).

### 3.1.4 Layout Of Longwalls

The mine layout includes consideration of the panel size, panel position, method of coal extraction (i.e. retreat or advance), position of the main haulage and gate roadways and position and size of any rib pillars. Mills (1985) stated that the basic selection criterion for the mining system is that the method must achieve higher bulk

outputs at lower costs than any other method. Thus the mining layout should be designed to fulfill this criteria under the prevailing working conditions. The NCB working party report of 1972 states that the possible arrangement of longwall layout is limited. Blades and Whittaker (1974) state there are four main types of longwall panel layout which are: (1) conventional longwall advance with rib pillars (2) conventional longwall retreat with rib pillars (3) Z semi retreat system and (4) panel retreat between two adjacent advance panels to give total extraction.

Rib pillars are generally left between adjacent faces for the purpose of protecting the gate roadways from excessive deformation due to the presence of stress abutments from the adjacent panel (Daws 1973). There are two types of rib pillar which are; wide pillars and narrow pillars. Wide pillars are designed to accept the total load transfer from adjacent panels whilst narrow pillars are designed to yield in a controlled manner under the imposed stresses. An alternative to leaving rib pillars is total extraction of the coal. Total extraction involves the complete removal of coal from an area and thus involves gate roads being reused twice. Daws considered the secondary reuse of the roadway by an advancing face would not be feasible because of severe deformation within the roadway. Thus normally the secondary reuse of the roadway should be by a retreat face.

### **3.2 MINING INDUCED STRESS**

#### **3.2.1 Introduction**

As previously stated underground excavations generate a redistribution of the in-situ stress within the vicinity of the excavation. New stresses are induced in the rock mass in the immediate vicinity of the opening. Zones of enhanced compression, tension and shear are created. The reason why this occurs can be illustrated using the following analogy between streamlines within a river and imaginary lines along which the principal stresses act (principal stress trajectories) (Hoek and Brown 1980). When a cylindrical object is placed into a river the water flows around the obstacle and the streamlines are deflected. Immediately upstream and down stream from the obstacle the water is slowed and the streamlines are spread outwards. This is analogous to the separation of the principal stress trajectories around a circular tunnel, which occurs in the zones of tension. In the areas either side of the obstruction the water flow has to speed up to catch up with the rest of the stream. Here the streamlines are crowded

together. This is analogous to the crowding of the stress trajectories, which occurs in zones of increased compression.

According to Hoek and Brown (Hoek and Brown 1980) the limit of stress disturbance created by an excavation is a distance from the excavation approximately equal to three times the diameter of the excavation. The inner zone of disturbance is sometimes referred to as the near field and the outer zone where the stresses are undisturbed is known as the far field (Hudson 1996). A knowledge of far-field stress conditions are important when analysing the stress and deformation around a mining excavation as they define the external boundary conditions, which must be satisfied for a correct analytical solution.

### **3.2.2 Stress Distributions Around a Simplified Excavation In a Homogeneous Medium**

The simplest example that can be used to illustrate theoretical stress distribution around an underground excavation is for the case of a circular excavation within a linear homogeneous elastic medium under a state of biaxial stress. It is worth noting at this stage that the solution for stress and displacement distributions within an elastic medium is based upon the satisfaction of a set of equations relating to the following points (Brady and Brown 1993):

- (a) the boundary conditions of the problem
- (b) differential equations of equilibrium
- (c) the constitutive equations for the material
- (d) The strain compatibility equations.

The boundary conditions relate to both the internal loading of the excavation by supports etc and the far field external boundary stresses. The differential equations of equilibrium have to be satisfied for static equilibrium and are related to the rate of change of normal and shear stress throughout the body. The constitutive equations for the material are based on stress-strain relationships, for instance Poisson's Ratio and Young's Modulus. Strain compatibility has to be satisfied as the strains within an elastic body are not independent (Jaeger and Cooke 1979). These equations and the process involved in obtaining solutions to elastic problems are beyond the scope of

this work. The interested person can find such information in Jaeger and Cook (1979) and Timoshenko and Goodyear (1970).

The solution, that satisfies the four sets of criteria, for the case of the circular opening under a state of biaxial stress is given as equations 3.1, 3.2 and 3.3. The solution was originally published by Kirsch in 1898 and is now generally known as the Kirsch Equations (Hoek and Brown 1980).

$$\sigma_{rr} = \frac{p}{2} \left[ (1+K) \left( 1 - \frac{a^2}{r^2} \right) - (1-K) \left( 1 - 4 \frac{a^2}{r^2} + \frac{3a^4}{r^4} \right) \cos 2\theta \right] \quad (3.1)$$

$$\sigma_{\theta\theta} = \frac{p}{2} \left[ (1+K) \left( 1 + \frac{a^2}{r^2} \right) + (1-K) \left( 1 + \frac{3a^4}{r^4} \right) \cos 2\theta \right] \quad (3.2)$$

$$\sigma_{r\theta} = \frac{p}{2} \left[ (1-K) \left( 1 + \frac{2a^2}{r^2} - \frac{3a^4}{r^4} \right) \cos 2\theta \right] \quad (3.2)$$

Where  $\sigma_{rr}$  is the radial normal stress

$\sigma_{\theta\theta}$  is the tangential or hoop normal stress

$\sigma_{r\theta}$  is the tangential shear stress

$r$  is the distance from the center of the circular excavation

$a$  is the radius of the circular excavation

$p$  is the principal stress acting parallel to the y axis

$K$  is the ratio between the principle stresses acting parallel to the x-axis and y-axis

$\theta$  is the angle between the x axis and the radial line from the point of interest

### 3.2.2.1 Stresses at the Excavation Boundary

Equations 3.2 and 3.3 indicate that that the radial normal stress and the tangential shear stress are zero at the excavation boundary. This is also true of any shape of excavation providing the excavation is free from internal loading (Hoek and Brown 1980).

The tangential stress on the boundary is given by Equation 3.4

$$\sigma_\theta = p[(1+K) - 2(1-K)\cos 2\theta] \quad (3.4)$$

In the roof and floor of the opening (i.e.  $\theta = 0^\circ$  and  $180^\circ$  respectively) Equation 3.4 reduces to Equation 3.5

$$\sigma_\theta = p(3K - 1) \quad (3.5)$$

Thus under uniaxial loading in the vertical direction (i.e. when  $K = 0$ ) the stresses in the roof and floor are tensile. When  $K = 0.33$  the stresses in the roof and floor are zero and for greater values of  $K$  all tangential stresses on the boundary are compressive.

### 3.2.2.2 Stress Change With Increasing Distance From the Excavation Boundary.

With increasing distance the affect of the opening on the rock stresses decrease (Figure 3.2).

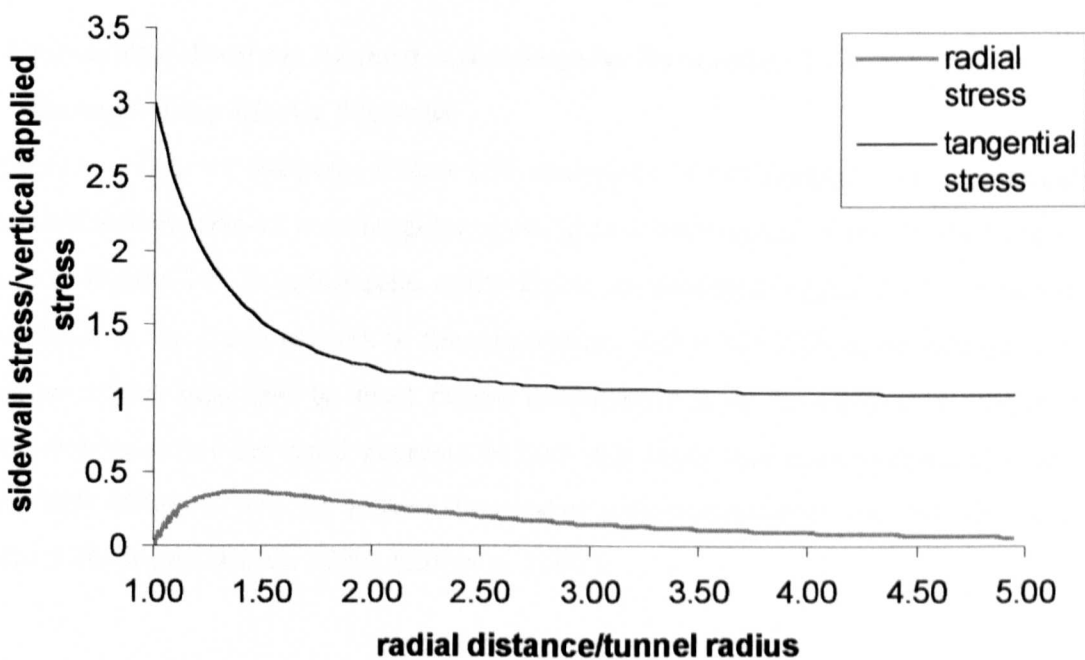


Figure 3.2 Variation in tangential and radial stress in sidewall of a circular tunnel under vertical uniaxial loading

Figure 3.2 illustrates that the stress concentration decays rapidly with increasing distance from the tunnel at a rate that is dependent on the size of the tunnel. The effect

of the excavation is minimal at distances from the centre of the tunnel greater than 3 times the tunnel radius (Hoek and Brown 1980, Brady and Brown 1993).

As Equations 3.1, 3.2 and 3.3 do not include any parameters relating to the elastic properties of the rock material the distribution and magnitude of the stresses are therefore independent of the elastic properties of the material.

Figure 3.2 illustrates that although the rates of change of the stresses due to the excavation are influenced by the size of the excavation the actual magnitude of the stresses are independent of excavation size. Hoek and Brown (1980) state that this fact has lead in the past to some underground excavation engineers to assume that the stability of an excavation is also independent of the excavation size. However these designers did not take into account that rock masses contain jointing and other discontinuities and the stability of the excavation is also dependent on the ratio between joint spacing and excavation size.

### **3.2.3 Stress Distributions Around A Rectangular Excavation In A Homogeneous Elastic Medium**

A common shape of roadway within UK coalmines is rectangular. The theoretical stress distribution around a rectangular opening in a homogeneous elastic medium is shown in Figure 3.3. In rectangular excavations, as indicated by Figure 3.3, stresses concentrate in the sharp corners of the excavation. Relatively high shear stresses are generated which may lead to shear failure propagating from the excavation corners. However because of the rapid decrease in both the major and minor principal stress values with distance from the corners the zone of over-stressed rock may only be very limited. ( Hoek and Brown 1980, Frith et al 1990 ).

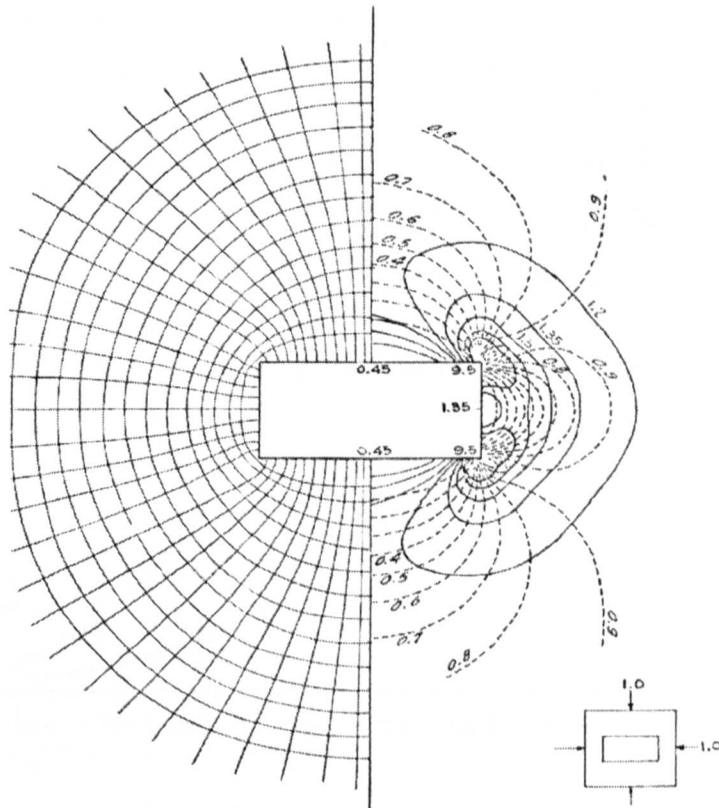


Figure 3.3 The theoretical stress distribution around a rectangular opening in a homogeneous elastic medium is shown (after Hoek and Brown 1980)

### **3.2.4 Influence Of A Yield Zone On The Stress Distribution Around A Circular Excavation**

At depth typical of coal mining within the UK the stress redistributed around excavations within the Coal Measures will generally exceed the strength of the average Coal Measure rock mass. (Wilson 1983, Farmer et al 1972). A zone of failed, fractured rock occurs adjacent to the excavation boundary. This zone is generally known as a yield zone and has reduced strength properties compared to the unfailed rock mass. If failure occurs the stress distribution adjacent to the excavation becomes dependent on the strength criteria of both the unfailed and failed rock mass. The general distribution of the stresses around a circular excavation with a yield zone is shown in Figure 3.4. The stress distributions are derived from relationships for the stress conditions in the yield and elastic zones (Wilson 1983, Hoek and Brown 1980). Figure 3.4 indicates that the stress within the yield zone is reduced in comparison with the pure elastic case. The position of the maximum tangential stress occurs at the yield/elastic boundary

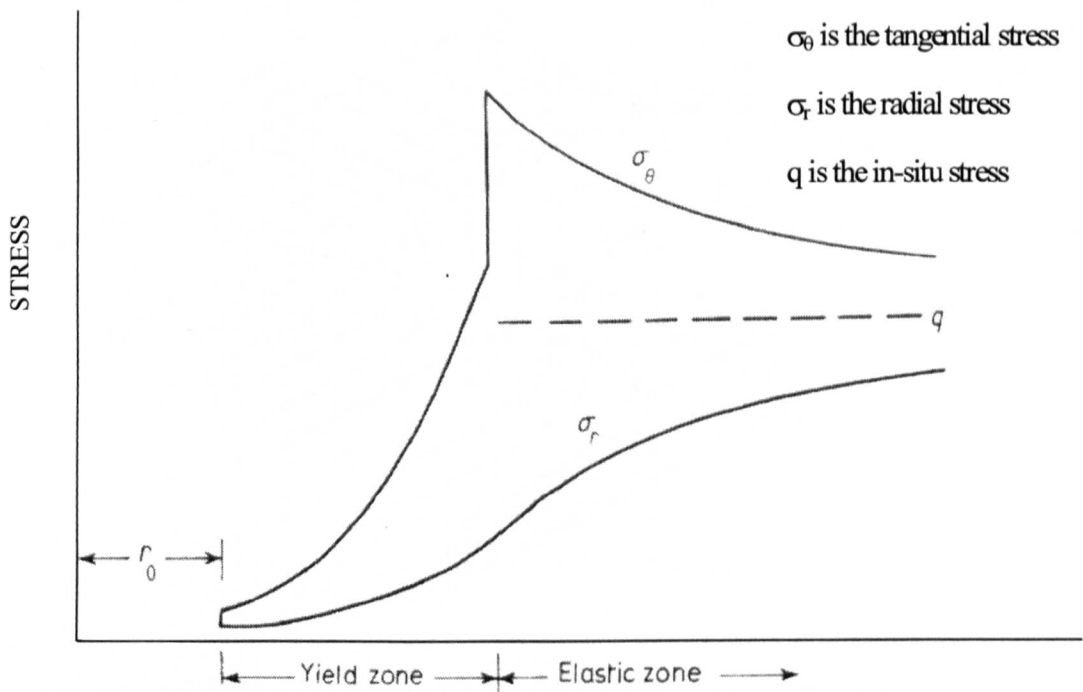


Figure 3.4 Stresses around a circular roadway surrounded by a yield zone ( $\sigma_1 = \sigma_3$ )  
(after Wilson 1983)

### 3.2.5 Stress Distributions Around Longwall Panels In Coal Measure Strata

#### 3.2.5.1 Vertical Stress Distribution

The extraction of coal in a longwall panel leads to the redistribution of the in-situ vertical stress into the strata on the periphery of the panel. Enhanced zones of stress relative to the in-situ stress are created close to the periphery of the extracted area and reduced stress zones are created within the worked out area (Figure 3.5) (Blades and Whittaker 1974). Immediately adjacent to the panel the increase in vertical load leads to rock failure and yield zone development. The yielded zone is an area of reduced vertical stress and thus permits the successful operation of support systems on the coalface and in the roadways.

Prior to suitable pressure monitoring methods the vertical stress distribution through a longwall face was predicted using arch theory (Jacobi 1956). This predicted that the

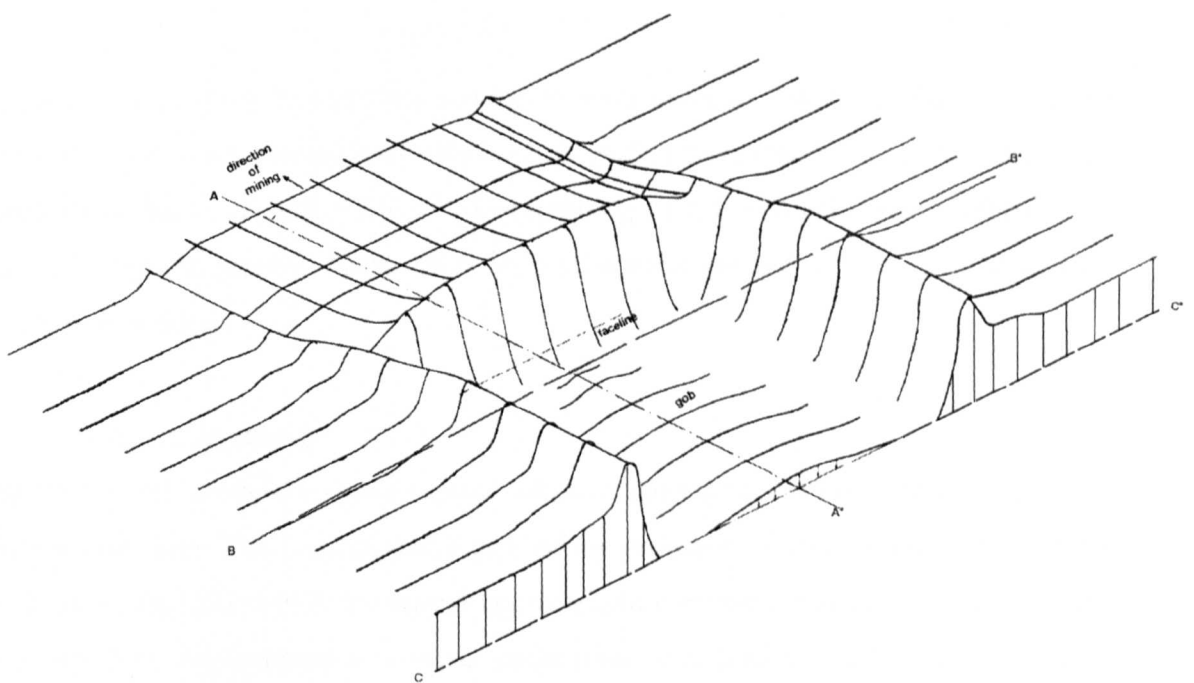


Figure 3.5 Vertical stress distribution around a retreat longwall panel  
(after Peng and Chiang 1984)

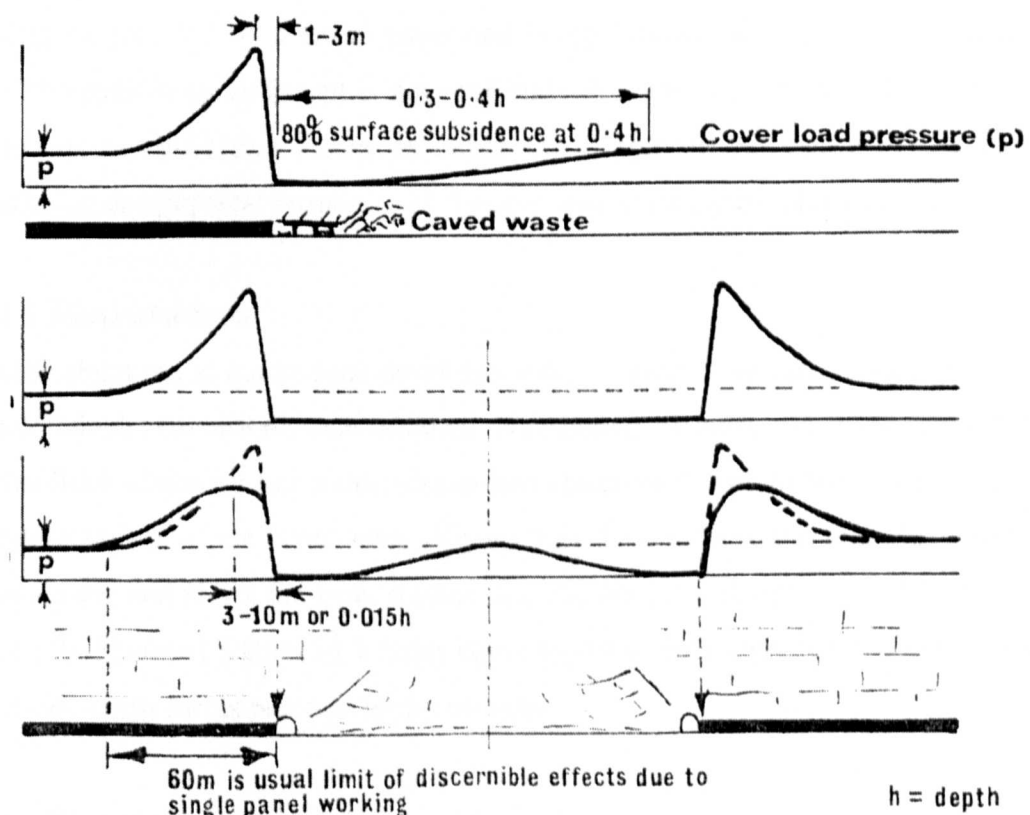


Figure 3.6 Stress distributions along Figure 3.5 Section line A-A\* (top), B-B\* (middle) and C-C\* (bottom) (after Whittaker 1974)

strata immediately in front of the face and at some distance behind the face, within the goaf area act as abutments where the excess load is transferred. Stress measurements techniques have allowed a better understanding of the vertical stress redistribution around longwall panels. Three zones exist where the vertical stress may be enhanced upon coal extraction.

### *3.2.5.1.1 Front abutment*

Jacobi (1956) analysed measurements taken of the vertical stress within the seam in front of the face. The measurements proved the presence of a stress abutment directly in front of the face which decreased approximately exponentially with distance from the face line. An increase in vertical stress over overload was found to occur upto about 100 metres in front of the face (Creuels and Hermes 1956). The peak pressure of the front abutment has been recorded to occur approximately 1 to 3 metres in front of the longwall face (Figure 3.6) (Daws 1973, Whittaker 1974, Blades and Whittaker 1974). The magnitude of the peak is governed by the strength of the coal and surrounding rock (Whittaker 1974, Wilson 1983) with typically for UK Coal Measures values of 3 to 5 times overload being typical (Wilson 1972, Whittaker 1974). The peak front abutment is not uniformly distributed in front of the face line. The maximum stress may occur at either the corner or the centre of the panel dependant on the physical properties of the roof rock (Peng and Chiang 1984).

### *3.2.5.1.2 Flank abutment*

The flank abutment is continuous down the sides of each panel and, unlike the front abutment which moves with face advance, is stationary (Blades and Whittaker 1974). Thus the flank abutment has a time-dependant effect on the strata which may lead to progressive failure of the panel sides (Figure 3.6). This reduces the magnitude of the peak abutment and shifts the peak further into the rib sides (Figure 3.6). Wilson and Ashwin (1972) stated values of 4 times cover load for flank abutment magnitude and 0.015 times depth for its position in the rib side.

### *3.2.5.1.3 Rear abutment*

The goaf undergoes progressive compaction with increasing distance from the face line due to the uncollapsed (bridging) beds above the goaf, lowering and loading the

goaf. With compaction the load bearing capacity of the goaf increases. Prior to stress measurements it was presumed that a pressure arch occurred over the extracted longwall face with one abutment of the pressure arch occurring in the solid immediately in front of the face and the other abutment occurring at some distance back from the face line within the goaf area (Jacobi 1956). However stress measurement within the goaf area indicated that the vertical stress within the goaf does not exceed cover load (Jacobi 1956). Roadway crush, which occurs between 70 to 100 metres behind a longwall face, has been attributed to the presence of a rear abutment. However Blades and Whittaker (1974) state that such deformation is due solely to goaf settlement behind the face and that no rear abutment in excess of coverload may exist in the goaf as a consequence of working that face. Whittaker states that the vertical stress eventually reaches that coverload at a distance from the face line equal to 0.3 to 0.4 times the mining depth (Figure 3.6). Blades and Whittaker (1974), based on the critical width of maximum subsidence, state that the only condition under which cover load pressure may be regained in the goaf is when the panel width/depth ratio reaches 1.4. Wilson (1983) however argued that the critical panel width/depth condition for cover load to be reached in the goaf is 0.6.

### *3.2.5.1.4 Wilson's equations*

Wilson (1983) developed a series of equations for determining the vertical stress distributions around a longwall panel. His equations are based on a stress balance approach where the total aggregate downward force remains that of the cover load and any stress rise over the rib side must be compensated for by an equivalent stress reduction over the caved waste. He assumes that stress rise within the caved waste is of a linear form and reaches coverload at a distance from the rib sides of 0.3 times the panel depth. The load reduction ( $A_w$ ) in the waste can be calculated using Equations 3.6 and 3.7.

For  $w > 0.6h$

$$A_w = 0.15\gamma h^2 \quad (3.6)$$

For  $w < 0.6h$

$$A_w = \frac{1}{2} w\gamma \left( h - \frac{w}{1.2} \right) \quad (3.7)$$

Where  $w$  = width of panel

$h$  = depth of panel

$\gamma$  = unit density of overburden

As previously stated, stress in the yield zone reaches a maximum in the order of 3 to 5 times the cover load. Wilson (1983) conjectured this is due to the build up of lateral constraint within the failed rock with increasing depth into the rib. Eventually the lateral confinement equals the original virgin horizontal stress. This point represents the yield/elastic boundary and the peak stress is determined by the failure criteria of the elastic rock. The stress rise within the yield zone takes an exponential form.

Wilson (1983) developed equations for two sets of strata conditions.

One condition is where the seam is weak relative to the roof and floor with yield taking place preferentially in the weak stratum. For this condition the vertical stress ( $\sigma_{zz}$ ), peak abutment stress ( $\sigma_y$ ), width of yield zone ( $x_b$ ) and vertical force ( $A_b$ ) carried by the yield zone are calculated using Equation 3.8, Equation 3.9, Equation 3.10 and Equation 3.11 respectively

$$\sigma_{zz} = kp \cdot \exp\left(\frac{xF}{m}\right) \quad (3.8)$$

$$\sigma_y = C_o + kp \quad (3.9)$$

$$x_b = \frac{m}{F} \ln\left(\frac{p}{p^*}\right) \quad (3.10)$$

$$A_b = \frac{m}{F} k(p - p^*) \quad (3.11)$$

The other condition is where the roof, seam and floor are all soft. Yield will also occurs in the floor and roof and the rate of stress rise will be lower. The vertical stress, peak abutment stress, width of yield zone and vertical force carried by the yield zone are calculated using Equations 3.12, 3.13, 3.14 and 3.15 respectively.

$$\sigma_{zz} = kp^* \exp\left(\frac{2x}{m} + 1\right)^{k-1} \quad (3.12)$$

$$\sigma_y = C_0 + kp \quad (3.13)$$

$$x_b = \frac{m}{2} \left[ \left( \frac{p}{p^*} \right)^{\frac{1}{k-1}} - 1 \right] \quad (3.14)$$

$$A_b = \frac{m}{2} p^* \left[ \left( \frac{p}{p^*} \right)^{\frac{1}{k-1}} - 1 \right] \quad (3.15)$$

Where  $\sigma_y$  = peak abutment stress

$x_b$  = width of yield zone

$\sigma_{zz}$  is the vertical stress,

$k$  is the triaxial stress factor,

$p = \gamma h$  ie vertical stress remote from excavation

$p^*$  is the support pressure plus the unconfined compressive strength of the broken material at the rib side

$x$  is the distance from the rib side

$m$  is the height of extraction

$$F = \frac{k-1}{\sqrt{k}} \left( 1 + \frac{k-1}{\sqrt{k}} \tan^{-1} \sqrt{k} \right)$$

Wilson (1983) assumed that the stress beyond the peak stress decays asymptotically towards the cover load stress (Equation 3.16). The rate of stress decay is dependant on the amount of stress outstanding above the overload.  $C$  is a constant that satisfies the stress balance (Equation 3.17).

$$(\sigma_{zz} - p) = (\sigma_y - p) \exp\left(\frac{x_b - x}{C}\right) \quad (3.16)$$

$$C = \frac{A_w + px_b - A_b}{\sigma_y - p} \quad (3.17)$$

### 3.2.6 Affect Of Differential Horizontal In-Situ Stresses On Stress Redistributions Around Longwall Panels

Horizontal stresses are redirected around the goaf of a longwall panel. Due to tectonic activity the horizontal stresses can often exceed the vertical stress. The two principal horizontal stresses are also often unequal (Siddall and Gale 1992). If the panel orientation is angled to the principal horizontal stress direction then the horizontal stress becomes concentrated against one corner of the face line of the panel whilst in the opposite corner of the face line the horizontal stress is reduced (Siddall and Gale 1992)(Figure 3.7). The degree of stress concentration depends on the angle the panel makes with the major horizontal stress. Stress concentration is greatest when the angle between the major horizontal stress and the panel is between 60° to 70° (Waite 1997). The concentration of horizontal stress generates greater deformation within the roof and floor of the panel's gateroads. Thus the gate road on the stress concentrated (notched) side of the panel usually experience greater deformation and requires more support than the gate road on the stress relieved side. The same effect occurs around single roadways driven into the solid, which are inclined to the major horizontal stress and the stress notched side of the roadway usually requires additional support.

### 3.2.7 Affect Of Stress Interactions With Adjacent Workings

Interactions of the redistributed stresses between adjacent and overlying/ underlying mine workings generates new stress conditions. Stress interactions may occur with adjacent panels working the same seam or with overlying or underlying workings of different seams. The zone of significant influence of a mine panel may extend for over a 100 metres horizontally whilst vertically the zone may extend for several hundred metres above and below the panel (NCB 1972).

#### 3.2.7.1 Neighbouring Panels

##### 3.2.7.1.1 Vertical stress interaction

Interaction between the panel abutments of adjacent panels generates elevated vertical stress conditions. The effect of this increases the size of the yield zone around the

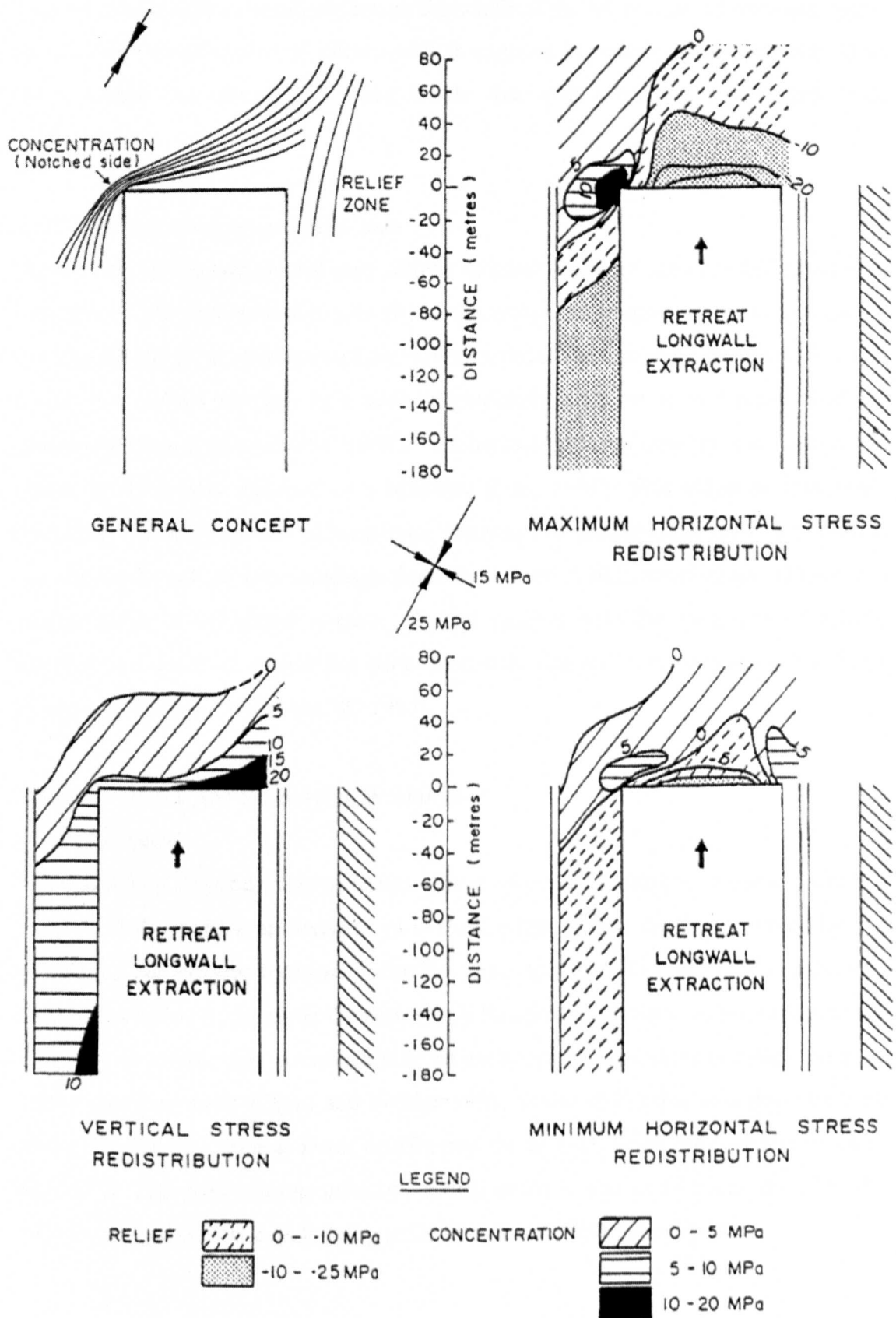


Figure 3.7 Horizontal stress redistribution around a longwall retreat panel.  
(After Siddall and Gale 1992)

panel and its gate road and produces greater deformation within the gate road. The level of stress increase is dependant on the width of the rib pillars left between panels thus careful consideration of pillar width is required in order to maximise extraction ratios whilst not generating stress levels that will adversely affect gate road performance.

### *3.2.7.1.2 Horizontal stress interaction*

Yielded and collapsed ground only allows reduced levels of stress to be transmitted through it. The redistribution into the strata above and below the caved waste or above and below the yield zone of a roadway reduces the horizontal stress, which acts across the yielded ground, in a zone immediately adjacent to the panel roadway creating a stress shadow (ECSC 1995). This horizontal stress relief may occur upto 30 metres to 40 metres adjacent to a roadway (Gale 1991). This effect is sometimes utilised by the construction of sacrificial roadways to protect other critical roadways and drivages such as face headings from the effect of horizontal stress. However a concentration of horizontal stresses, aligned parallel with the long axis of pillars, between two adjacent panels has been observed. The stress concentration has been termed a 'letter box' effect (ECSC 1995).

## **3.2.7.2 Overlying and Underlying Workings**

### *3.2.7.2.1 Pillars*

The effect of old pillars left in seams above or below a current longwall panel or roadway is to produce an increase in vertical stress within the area covered by the pillar with the highest increase occurring close to the pillars edge. The enhanced vertical stress due to the pillar decreases as a function of distance above or below the pillar. Stress greater than overload may be experienced in workings outside the edge of the overlying pillar (Oram and Ponder 1995, Waite 1997) due to a pressure bulb effect. The induced vertical stress distribution for an underlying pillar is illustrated in Figure 3.8. The peak mining induced vertical stress is shown to occur at  $11^\circ$  to the vertical inclined over the underlying pillar (Blades and Whittaker 1974).

The effect that overlying or underlying pillars have on the vertical stress within a roadway has been concluded to depend upon how the roadway approaches the pillar (ECSC 1995). Higher stress concentrations were observed to occur if the face of the panel travels towards the goaf of the underlying or overlying panel. This has been attributed to the vertical stress being concentrated within a decreasing area of pillar support between the panels (Figure 3.9). However if the panel moves towards the pillar of the underlying or overlying workings after passing beneath the goaf of the old workings the stress concentration ahead of the face was considered to be the same magnitude as that for the face above or below (Figure 3.10).

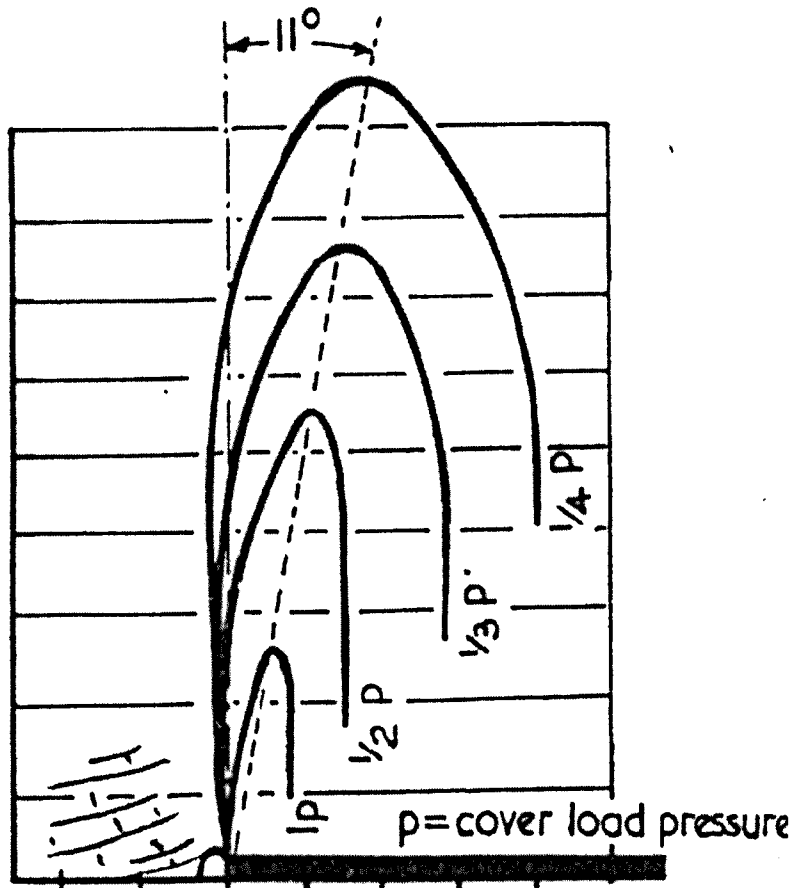


Figure 3.8 Induced vertical stress in strata above an underlying pillar (after Blades and Whittaker 1974)

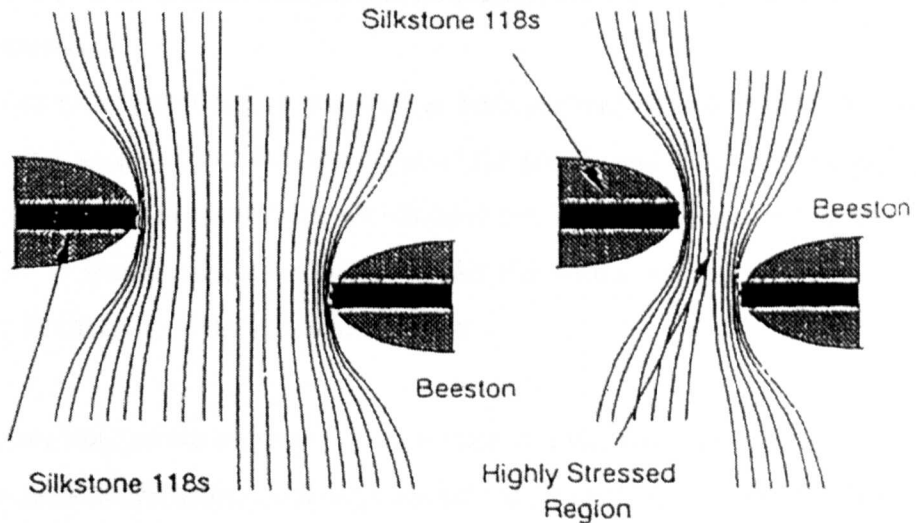


Figure 3.9 Vertical stress trajectories panel moving towards goaf

(After ECSC 1995)

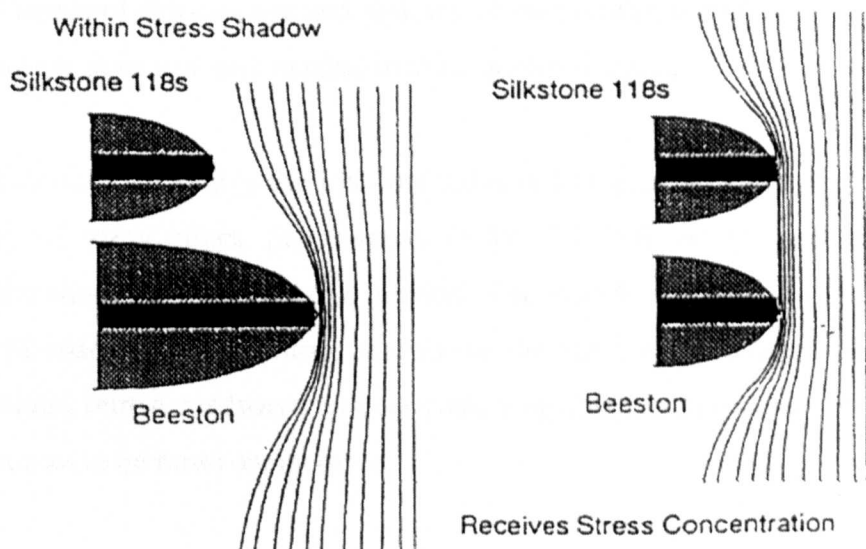


Figure 3.10 Vertical stress trajectories panel moving away from goaf

(After ECSC 1995)

### 3.2.7.2.2 Goafs

Goafs generate vertical stress shadows in the underlying and overlying strata thus panels and roadways lying above or below goafs tend to experience reduced vertical stress.

### **3.3 ROADWAY AND GATE ROAD STABILISATION TECHNIQUES**

#### **3.3.1 Introduction**

Stabilisation of mine roadways is required to both prevent excessive deformation of the roadway that would effect the operation of the panels and to ensure the safety of the mine personnel against roof falls, rib collapse etc. There is a legal requirement for mine managers to install suitable supports under the Mines and Quarries Act 1954, where, under Section 48 of the Act which states:

*“It shall be the duty of the manager of every mine to take, with respect to every road and working place in the mine, such steps by way of controlling movement of strata in the mine and supporting the roof and sides of the road or working place as may be necessary for keeping the road or working place secure”*

According to Farmer et al (1972) the selection of a support system depends on the mode and extent of deformation and yielding of the peripheral rocks and the degree of convergence or deformation tolerable in the completed tunnel.

Since the mid to late 1980's the UK coal industry has undergone great changes with the closure of many mines, privatisation of the UK coal industry and the need to compete economically on the world market. The introduction of new technological methods of roadway stabilisation, mainly in the form of rock and cable bolting systems within retreat roadways reduces costs associated with roadway support thus allowing mines to be more competitive.

In order to design or validate a support system a geotechnical assessment must be undertaken. The assessment includes all factors that have a bearing on the security of any new roadway that is proposed and is therefore a form of risk assessment (Wing 1997). The design of a support system is also dependent on the function and possible life of the different roadways. Based on these criteria roadways can be classified into three types (British Coal 1997).

### (1) Main truck roadways

These provide a strategic route for the transportation of coal, materials and men and are generally classified as long life roadways. The installed supports are therefore required to produce maximum roadway stability throughout its working life.

### (2) District Access Roadways

District access roadways provide a link between the main trunk roadways and the production districts and as such their life is dependant upon the reserves within the district. Typical life spans for such roadways maybe upto 10 years. These roadways may be driven in-seam.

### (3) Face Gate Roadways.

These are normally driven in seam and normally have only a short life span varying from 0.5 to 3 years. However stability is important and the roadways are often of minimal width. The support requirements are also dependent on the method of working i.e. retreat or advance. Advance face roadways have the special requirement of goaf side support.

The main support categories that are presently used in UK coalmines are: free standing supports, roof bolting, rib bolting, floor reinforcement and roadside packs

#### **3.3.2 Free Standing Supports**

These are steel supports of an arch or square profile normally of 'H' section steel. For the past 70 years the majority of roadways in United Kingdom coalmines have been supported by means of steel supports and hence are frequently called conventional supports. The arch supports vary between two to four piece forms having semi-circular crowns and legs splayed at between 6° and 6° 45' to the vertical. The pieces are connected by fishplate joints. The square profile supports are three pieces with either flat or cambered beams and either straight or splayed legs. To aid in spacing of the arches, and to increase the support strength parallel to the road axis, steel struts connecting the arch supports are employed. Freestanding supports are used when long term stability of the tunnel is required or where strata conditions are not conducive to other support types. Arch supports are the normal means of support for main trunk roadways and advance panel gate roads. Arch and square profile supports are used for district access roadways whilst where required square profile supports are used for

retreat panel roadways. The disadvantages of free standing supports include their relatively high cost and difficulty of transportation.

In order to minimise strata yield and hence deformation of the strata around the tunnel it is important that the support is set as soon after tunnel excavation as possible and that maximum contact is made between the support and the strata. The aim is to help the rock support its self by the provision of a radial confinement to the periphery of the tunnel. Free standing supports act in a passive manner as the support reaction is generated by the deformation and loading of the strata onto the support.

### **3.3.3 Rock Reinforcement Techniques**

Rock reinforcement has become an established means of support in British mines over the last nine years (Bigby 1997). Unlike conventional supports rock reinforcement elements are installed into the rock rather than in the tunnel and operates by generating confinement within the rock around the periphery of the tunnel and thus to increase the strength of the rock mass.

#### **3.3.3.1 Roof Bolting**

Roof bolting was first introduced into British mines in the 1940's as a result of steel shortages during and shortly after the 2<sup>nd</sup> world war (Siddall and Gale 1992). However these bolts were mechanically anchored into the strata at the end only and thus had to be sited in strong competent strata to operate effectively. It became apparent that such bolts were unsuitable for use within the 'soft' British Coal Measures and the use of roof bolts as a supporting medium virtually died out after 1963. The development of new bolting technology based on full column grouted roof bolts was undertaken overseas during the 1970's and 1980's mainly by the United States Bureau of Mines (USBM) and the Commonwealth Scientific and Industrial Research Organisation of Australia (CSIRO).

The suitability of this technology was assessed for use within UK coal mines and introduced in the late 1980's. The success of this technology is illustrated by the fact that full column resin grouted roof bolts are now used in over 90% of retreat longwall gate roads (Bigby 1997). Figure 3.11 shows the general features of a full column resin grouted roof bolts. The resin and catalyst are contained in a plastic cylindrical

shaped capsule that is inserted into the pre-drilled bolt hole. The rigid steel roof bolt bar is then inserted by rotation into the bolt-hole splitting the plastic and mixing the resin and catalyst. The specification for roof bolt consumables is detailed in a British Standard (BS7861). Typically the roof bolt has a diameter of approximately 22 mm and is 2.4 metres long.

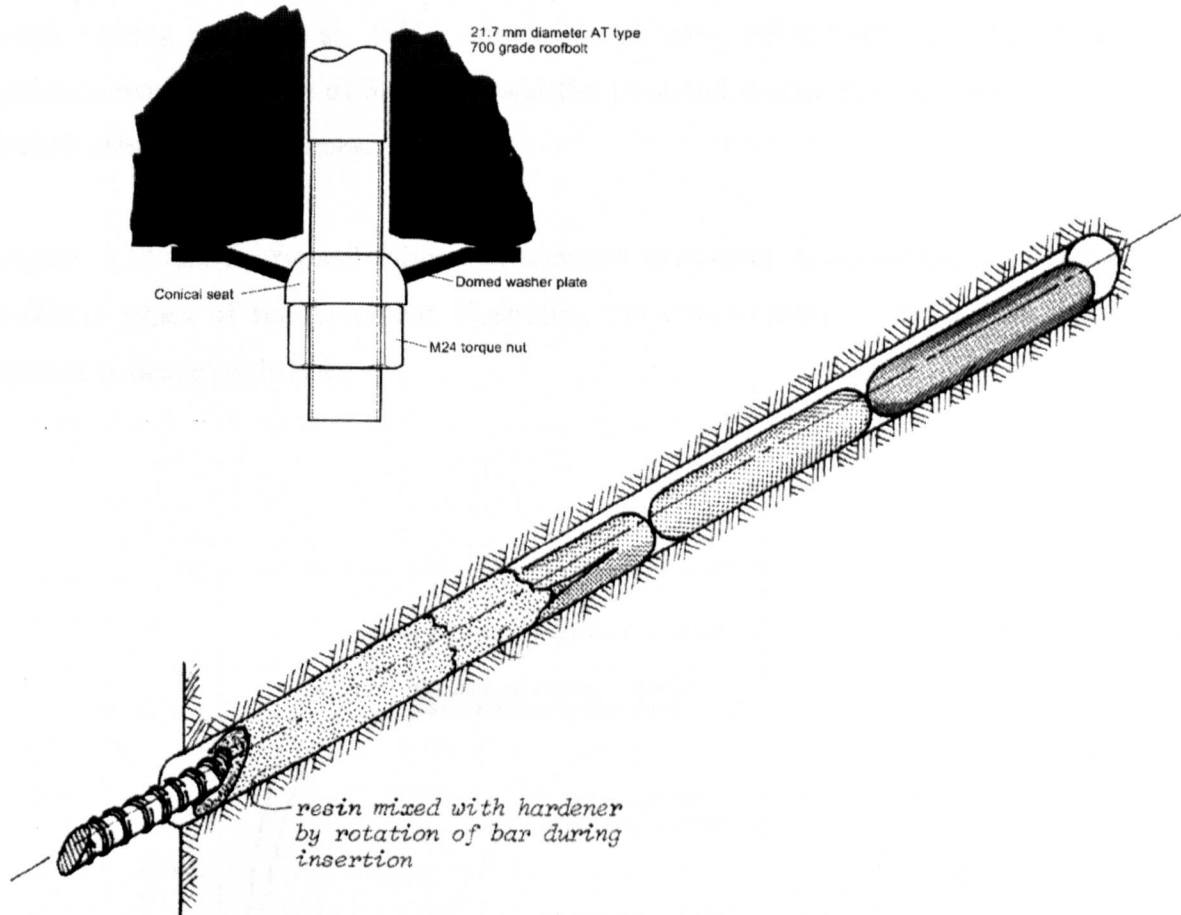


Figure 3.11 Features of a full column grouted steel rock bolt (After Hoek-Brown 1980 and Health and Safety Executive 1994)

### 3.3.3.2 Cable Bolting

Cable bolts are required when significant strata deformation occurs above the height of the roof bolts. The length of steel roof bolts is limited by the height of the roadway, with standard bolts being 2.4 metres long. Cable bolts used within UK coal mines are manufactured from steel Dyform wire strands and due to their flexibility there are no restrictions on length. However, normally, 6 to 12 metres long cables are used. The cable itself consists of seven strands twisted together. Partial unwinding of the cable produces an open structure, which allows complete encapsulation by the grout. Such

cables are termed ‘birdcaged’ and produce a reinforcement system with high bond strength. Two cables are often combined in a single hole to produce a ‘double birdcaged’ cable bolt with enhanced properties. The cable bolt is installed into pre-drilled 55 mm diameter hole and then fully encapsulated with a cementitious grout.

High strength and stiffness grouts with a rapid cure time have been developed for cable bolting (Kent et al, 1997). Single, seven wire, cable bolts have a nominal ultimate tensile strength of 30 tonnes and the 14 strand double birdcage bolts have a tensile strength of 60 tonnes.

Figure 3.12 shows typical laboratory derived axial-load displacement curves for different types of reinforcement illustrating the effectiveness of the birdcage and double birdcage cable bolt.

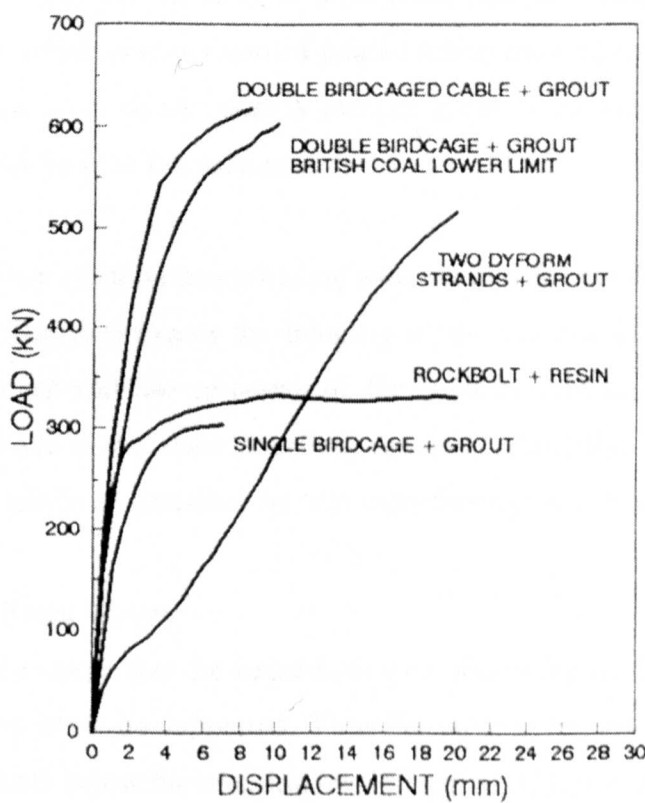


Figure 3.12 Typical load-displacement curves for cable and rock bolts  
(after Kent 1997)

### **3.3.3.3 Rib Bolting**

Rib bolt reinforcement adds confinement to the coal within the rib side, thus increasing the effective strength of the coal decreasing the extent of yield zone development and thus reducing rib side deformation. Typically within retreat gate roadways steel 1.8m long full column grouted rock bolts are used within the solid rib side. On the panel side the rib will eventually form part of the face and the coal extracted. To avoid damage to coal cutting equipment the rib bolts are made out material which has low shear strength. Wooden dowels have been used for this purpose but now have been generally superceded by full column grouted fiberglass GRP bolts.

### **3.3.4 Road Side Packs**

Roadside packs are used in advance longwall systems to separate the roadway from the goaf area. Packs construction includes hand built packs of rock waste, wooden cribs, man made aerated blocks etc. Monolithic pumped pack systems have been used since 1973. Several varieties of monolithic pumped pack systems exist. In general bulk filler, which may consists of graded run of mine material or of bentonitic clay, is slurried and then mixed with a cement grout. This mixture is then pumped into shuttering or bags in the pack area.

The main aim of strata control using packs is to offer resistance to the lowering of the roof beds and to preserve the integrity of the immediate roof. Two stages of pack loading occur and the response of the pack is critical to ensure stability of the roadway both in the short and long term. Deformation of the roadway and pack behaviour has been described by two main theories which are as follows:

#### **Detached Block Theory**

This theory states that the immediate roof above the roadways on either end of the caving zone must be supported. Thus the pack is required to support the load of a block of strata below the bridging beds (Figure 3.13). In order to achieve this the pack must offer immediate resistance after installation (Clarke and Newson 1985).

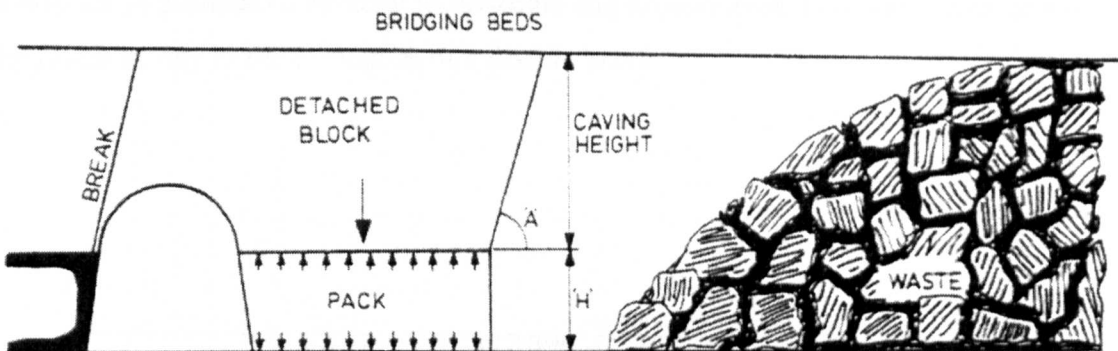


Figure 3.13 Detached block theory (after Clarke and Newson 1985)

### Roof Beam Tilt Theory

The gradual downward movement of the bridging beds as it lowers onto the caved waste can be considered to be the development of an underground subsidence profile that migrates over the ribside which fails progressively inwards (Smart et al 1982). The movement itself is irresistible as it involves the full weight of the cover load, but the final tilt of the beds over the roadway can be controlled by the strength of the pack (Clarke and Newson 1985). The movement of the beds immediately above the roadway can be described in terms of a tilting beam extending from the waste edge spanning the pack and roadway to a imaginary pivot point at some distance under the rib (Smart and Haley 1987). The tilt angle and pivot point position change with face advance and undergo three distinct stages of strata movement if convergence is not limited by sufficient pack resistance. (Smart and Haley, 1987).

#### Stage 1

During this stage the tilt angle increases with greatest convergence of the roof and floor occurring at the waste edge of the pack. The pivot point remains stationary at approximately 4 metres into the rib side.

#### Stage 2

At a critical tilt angle, identified to be around  $2.5^\circ$  (Smart and Haley, 1987 Clarke and Newson 1985) the pivot point begins to migrate further into the rib side. The tilt angle itself during this stage remains constant and thus the roof to floor convergence remains constant across the roadway.

### Stage 3

The final stage produces a reversal in tilt angle and an acceleration of the convergence in the roadway due to the formation of a ribside break

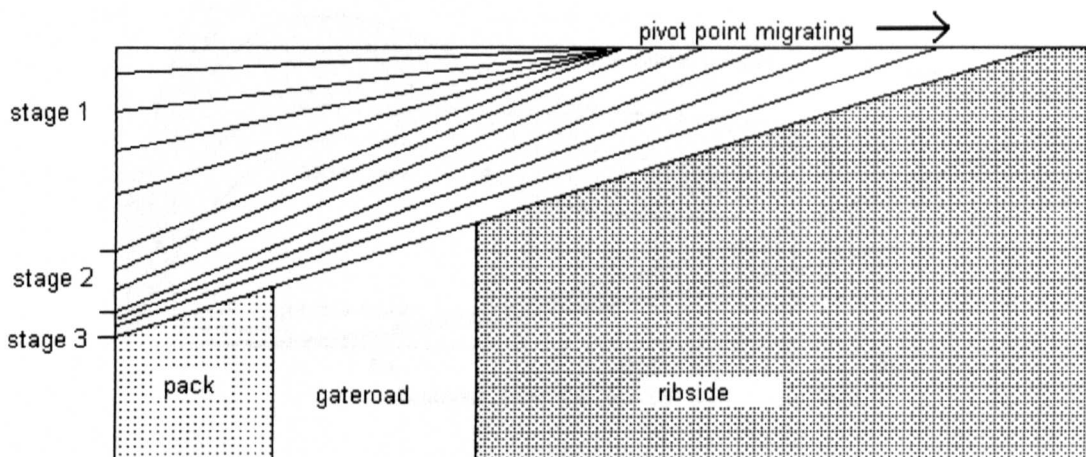


Figure 3.14 Stages of strata movement according to roof beam tilt theory  
(after Smart and Haley 1987)

For long term stability of the roadway the pack system should be designed to limit the roof beam tilt to below  $2.5^\circ$  and to yield gradually under load to prevent bearing capacity failure of the floor and immediate roof.

The pack load characteristics of various packs is shown in Figure 3.15. It can be seen that wooden packs have the greatest load bearing characteristics but do not yield and can fail catastrophically whilst resistance generated by hand built packs is very slow to build up. Monolithic pumped packs show very good characteristics with a rapid build up of resistance but yielding to prevent excessive pack stress.

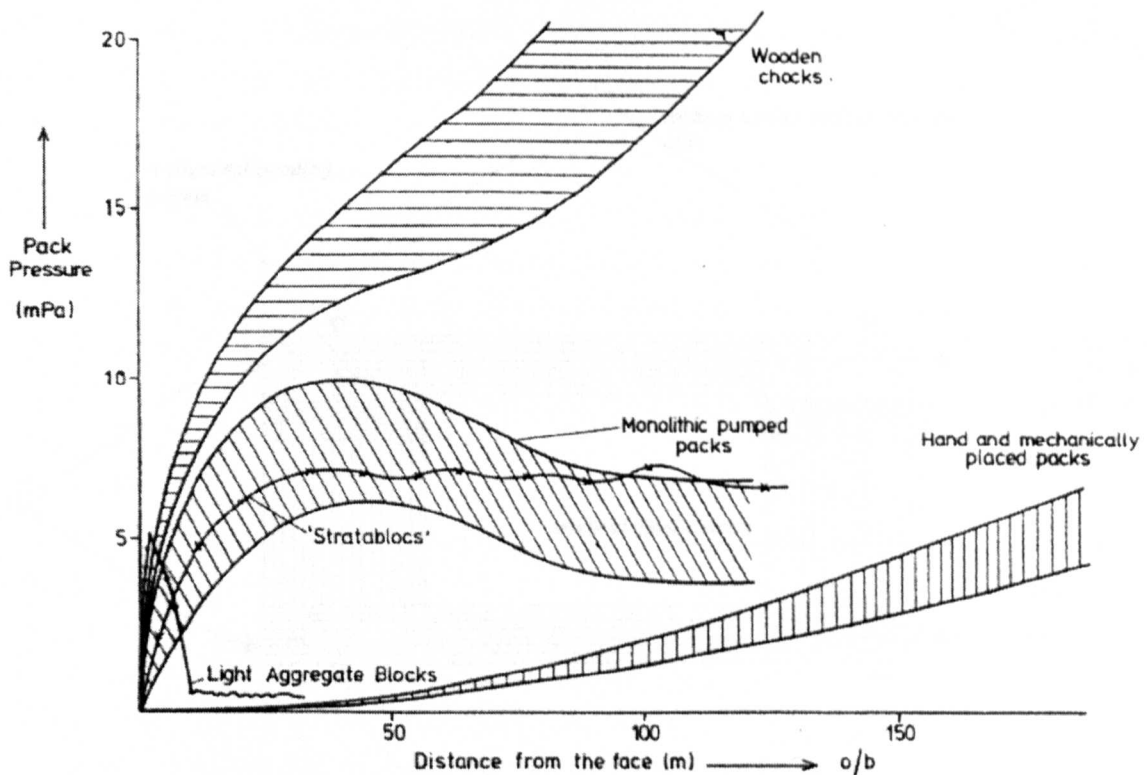


Figure 3.15 Load characteristics of pack supports (After Clarke and Newson 1985)

### 3.4 CHARACTERISTIC MECHANISM OF STRATA DEFORMATION WITHIN COAL MINES

#### 3.4.1 Introduction

A knowledge of the major mechanisms of failure and deformation that occur within UK coal mines is a prerequisite for the determination of critical influencing factors and an assessment of their relative importance.

The deformation mechanisms around a coal mine roadway can be divided by consideration of where they occur. Within a coal mine the mechanisms can logically be divided into those that occur either at the rib/coal face, within the coal mine floor and within coal mine roof.

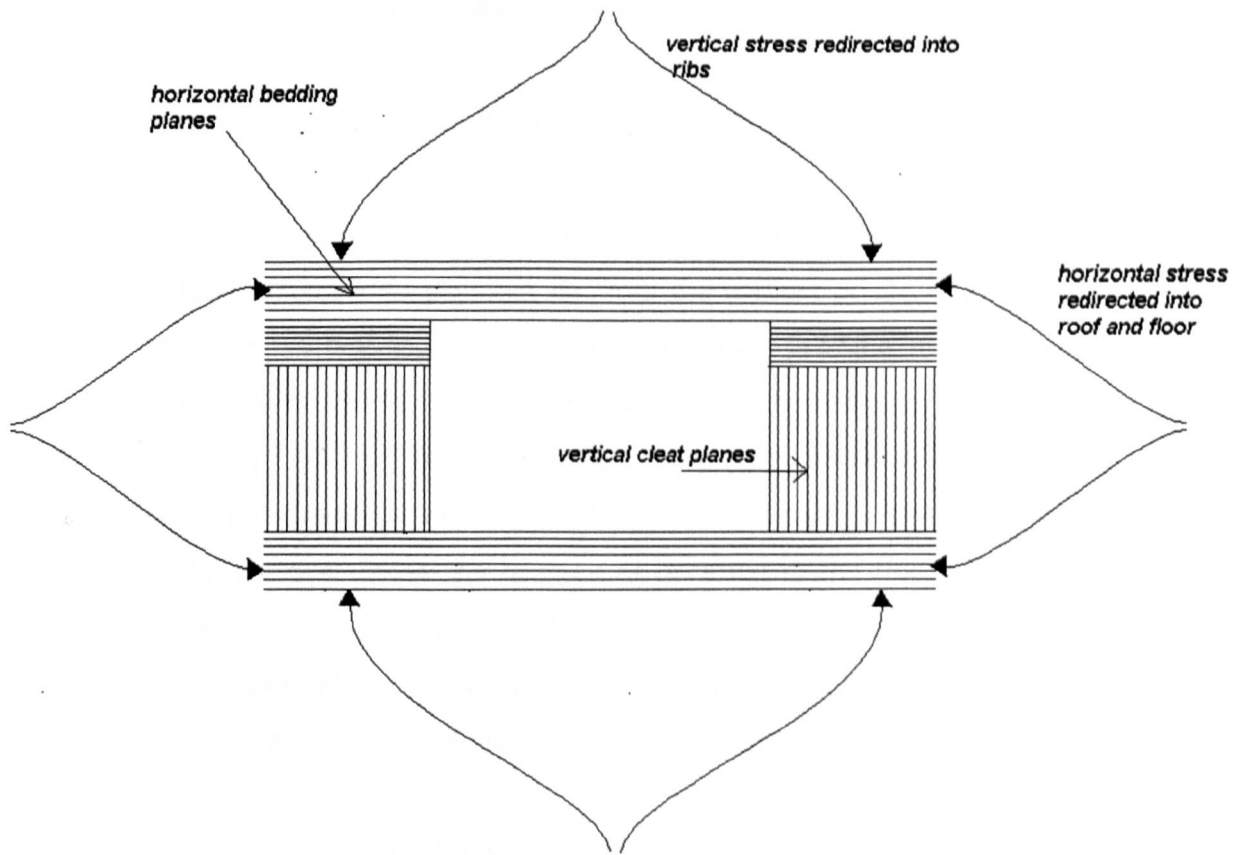


Figure 3.16 Redistribution of stresses around a coal mine roadway.

Vertical stress concentrates in the ribs and horizontal stress concentrates in the roof and floor (Figure 3.16). Characteristically floor strata tends to be of weak seatearth whilst the ribs are normally situated within the coal seam. The roof strata can be variable consisting of interbedded siltstones, mudstones and sandstones. The immediate roof often tends to be of a weak nature.

### 3.4.1 Roof Deformation Mechanisms

Roof deformation is dependant on the magnitude of the horizontal stresses acting across the roof. Thus the roadways direction to the maximum horizontal stress is an important factor when considering mine layouts.

The deformation of coal mine roofs has been attributed to the following six mechanisms (Caudle 1974).

- i) Immediate roof may delaminate under its own weight and fail in bending
- ii) The immediate roof under the influence of horizontal stress may delaminate and fail by buckling.
- iii) Due to the redistribution of the stress field around the mining excavation shear fractures may originate in the corners of the immediate roof and propagate upwards through a number of strata to intersect over the centre of the opening
- iv) The shear fractures propagating up from the corners of the excavation may intersect a weak bedding plane leading to the collapse of the immediate roof
- v) Tensile stresses due to buckling are generated in the centre of the roof which may lead to fracturing followed by falls if horizontal weakness plane exist
- vi) Failure of the roof due to complex interactions of roof, pillars and floor. The roof may deform due to the heaving or buckling of the floor. The resulting deformation of the floor under the ribs, softens the ribs. As a consequence the effective span of the immediate roof increases. In addition horizontal load previously carried by the floor is partially transferred into the roof.

Displacement downwards into the mining excavation of blocks or wedges of rock under the influence of gravity can occur where the intersections of the discontinuity planes and the free surface defined by the coal mine roof is unfavourable. In order for this mechanism to operate it is necessary for the block to be separated from the surrounding rock mass by at least three intersecting structural discontinuities (Hoek and Brown 1980). Block failure is a major process in the collapse of shallow tunnels and mining excavations where the in-situ stress field is to low to generate stress failure of the rock mass (Hoek and Brown 1980).

Where the vertical stress is high in relation to the horizontal stress, shear stresses acting in a vertical direction are generated in the corner of the roadway. This can lead to the propagation upwards from the corner of the excavation of vertical shear fractures. This phenomena has been termed cutter roof in the USA (Figure 3.17) (Su and Peng 1986).

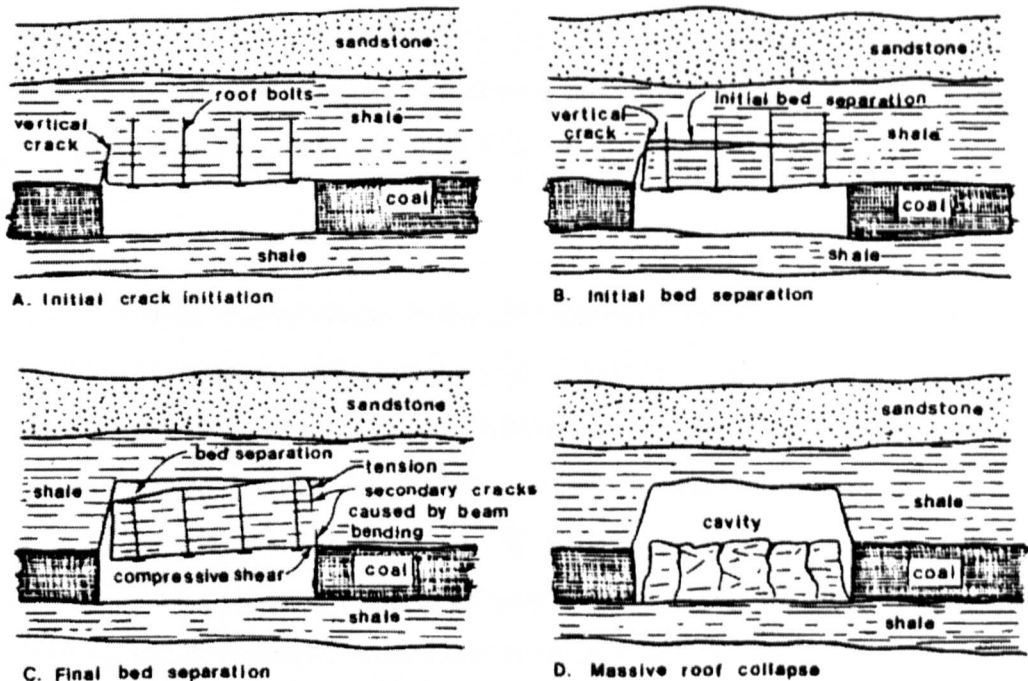


Figure 3.17 Failure of a coal mine roadway due to cutter roof

(After Su and Peng 1986)

### 3.4.2 Floor Deformation Mechanisms

Floor strata is often of a weak nature consisting of clayey seatearth that contains smooth, undulating low friction listric planes. Clay rich seatearths are also susceptible to swelling and reduced shear strength in the presence of water. In roadways which have weak floors the majority of height loss within the roadway can be attributed to floor heave (Holmes 1982).

#### 3.4.2.1 The Effect of Water on Clay Rich Mudrocks

The mineral content of seatearth is such that it is usually affected by water leading to a substantial decrease in the seatearth strength with a resulting swelling and cracking of the rock mass (Krishna and Whittaker 1973).

Bolt (1956) divided the swelling processes into either mechanical and physico-chemical. Void spaces within a claystone or mudrock vary in size and in general the smaller voids are important in the physico-chemical process whilst the larger voids are associated with mechanical swelling. The rate of swelling in both cases is related

to the permeability of the rock mass. The permeability of mudrocks is dependant on jointing, strata planes and the degree of interconnectivity of pores and pore size (Bell et al 1986). Physico-chemical swelling occurs as intra-crystalline swelling of clay minerals which have weak binding forces between individual clay crystals. Examples of such clay minerals within the UK Coal Measures are known as mixed clay minerals.

Figure 3.18 shows the percentages of the different clay minerals evaluated for tailings samples from 57 different British mine sites (Taylor and Spears 1970). In physico-chemical swelling water molecules and hydrated cations are adsorbed onto the surface of the negative charged platy clay crystal. An overlapping double layer of water and cations exist between two clay plates. In a state of equilibrium, the repulsion associated with the positively charged cations is equal to the effective contact stress. On unloading an out of balance cation concentration will be created and water drawn into the system by osmosis to restore equilibrium leading to swelling and associated reduction in shear strength (Taylor and Smith 1986).

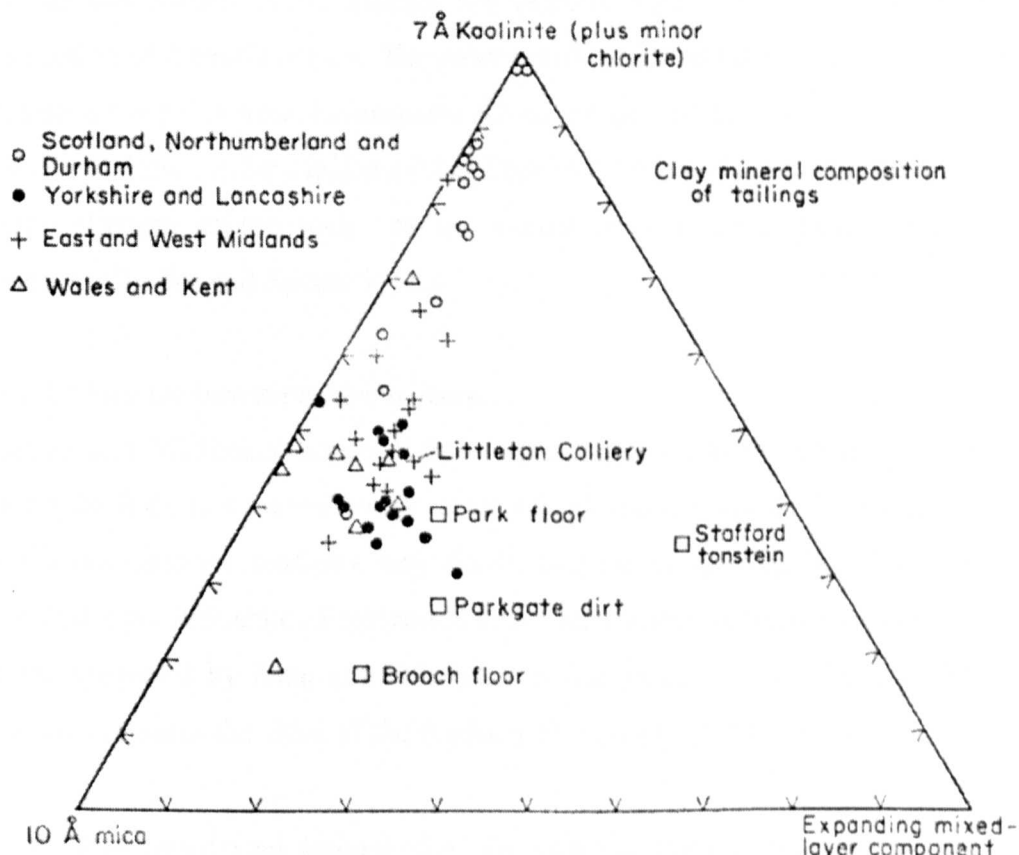


Figure 3.18 Mineralogy of UK Coal Measure Spoil  
(after Taylor and Spears 1970).

Mechanical swelling occurs in response to unloading which is brought about by stress relief around underground excavations (Taylor and Smith 1986). Relaxation of the mean stress ( $p$ ) in a mudrock sets up a negative (suction) pressure ( $u_s$ ) in the pore water of about the same magnitude as the mean stress (Equation 3.18)

$$u_s \approx p = \frac{1}{3} (\sigma_v' + 2\sigma_h') \quad (3.18)$$

The suction pressure draws water into the pores from adjacent voids leading to swelling of the rock.

Fluctuating air humidity or repeated wetting and drying of claystones and mudstones exposed within the roof floor or rib of a roadway has been observed to lead to breakdown of the rock and a corresponding increase in roof falls (Chugh and Missavage 1981). This process of breakdown has been termed slaking or air breakage (Taylor and Spears 1986). During dry periods high suction pressure develops and desiccation of the rock occurs. The outer macro voids and discontinuities will be filled with air during this time. Subsequent saturation causes this air to become pressurized as water is drawn in by capillary (Van Eeckhout 1976). If the air pressure exceeds the tensile strength of the rock failure occurs usually along predisposed planes of weakness (Taylor and Spears 1986).

### 3.4.2.2 Floor Deformation Mechanisms

Krishna and Whittaker outlined three mechanisms of floor lift in mine roadways. Where the floor is weak relative to the rib, plastic extrusion of the floor from under the rib side into the roadway may occur. In more competent floors buckling of the floor under the influence of horizontal stress may occur. A further mechanism of floor failure suggested by King and Whittaker is the penetration of the floor by the arch legs. This releases the sides of the roadway floor leading to floor lift.

If the stress transferred through the ribs into the floor is greater than the bearing capacity of the floor failure of the floor beneath the ribs followed by penetration of the floor by the rib will occur. Soil mechanics bearing capacity theory, though not

generally applicable to discontinuous brittle rocks can be applied to weak seatearths because they behave in a similar manner to soils (ECSC 1987).

The deformation behaviour of the floor within gate roads in Betws Colliery, South Wales indicated that the floor may consist of two zones of strata (ECSC 1987). The upper zone was found to be usually 1 to 2 metres in thickness and was susceptible to physical and chemical weathering processes initiated by machine travel, ingress of water, temperature variations and oxidation. Characteristically this zone deformed by swelling and plastic deformation. The lower zone presumably of more competent rock behaved as a brittle beam and deformed by buckling and brittle fracture.

A mechanism of floor deformation was proposed based on a study of floor heave in Smoot mine , West Virginia USA (Peng et al 1992). The results of the study indicate that floor heave goes through the following three stages:

#### **Stage 1 Elastic deformation.**

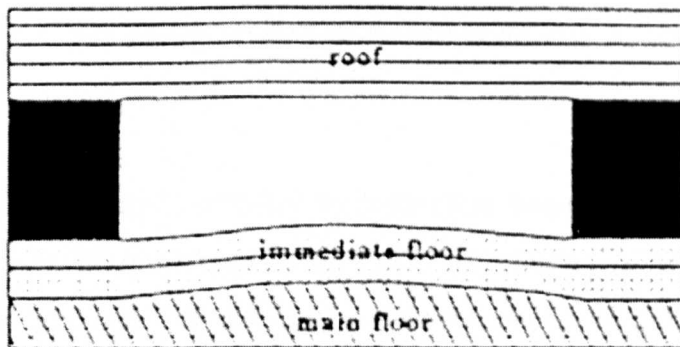
The floor under increasing abutment loading continuously deforms but maintains its continuity. Shear stress and bending moments continually build up in the floor unit the shear or tensile strength of the floor strata is reached. (Figure 3.19)

#### **Stage 2 Failure initiation.**

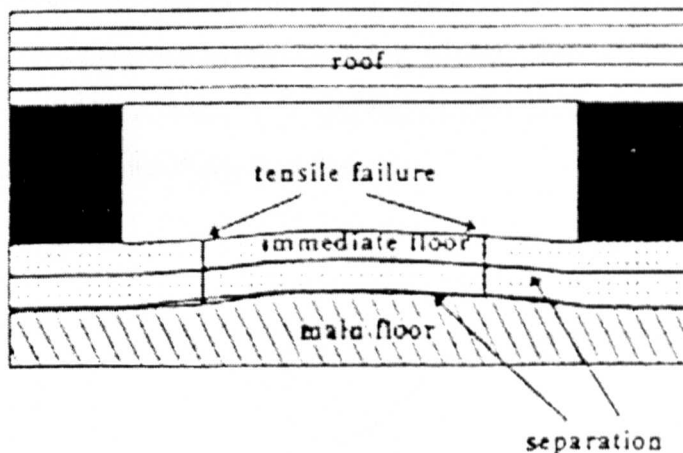
Shear and tensile fractures create discontinuities in the floor and cause separation on bedding surfaces, as a result the bending moment in the floor is released (Figure 3.19).

#### **Stage 3 Failure propagation.**

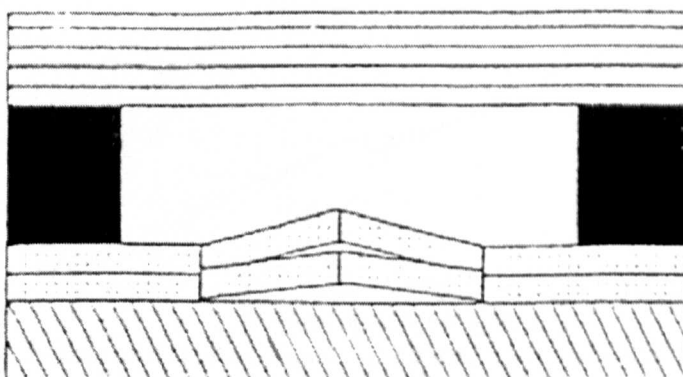
The horizontal stress continues to increase in the floor unit the floor fails in buckling. Finally the floor heaves up at the centre releasing the horizontal stress (Figure 3.19).



Stage 1 Elastic Deformation



Stage 2 Failure Initiation



Stage 3 Failure Propagation

Figure 3.19 Mechanism of deformation of a coal mine floor (after Peng et al 1992)

### 3.4.3 Rib Deformation Mechanisms

Gate road ribs are mainly situated in the coal seam being extracted whilst the top and bottom of the rib may be situated in the strata directly overlying and underlying the coal seam.

Rib side deformation is affected by both cleat frequency and the orientation of the cleat planes to the free face (ECSC 1987). The higher the cleat frequency generally the weaker the coal,. The relationship between the orientation of the cleat planes and roadway is a major influencing factor on deformation process that occur within the ribs (Holmes 1982 )(Figure 3.20). Where the cleat planes form an angle of less than  $25^{\circ}$  to the roadway large deformations can occur as a result of fracturing and dilation preferentially occurring along the cleat planes. The slabbing of the sides of the roadway in a process known as spalling is also characteristic of cleat planes being roughly parallel to the roadway sides.

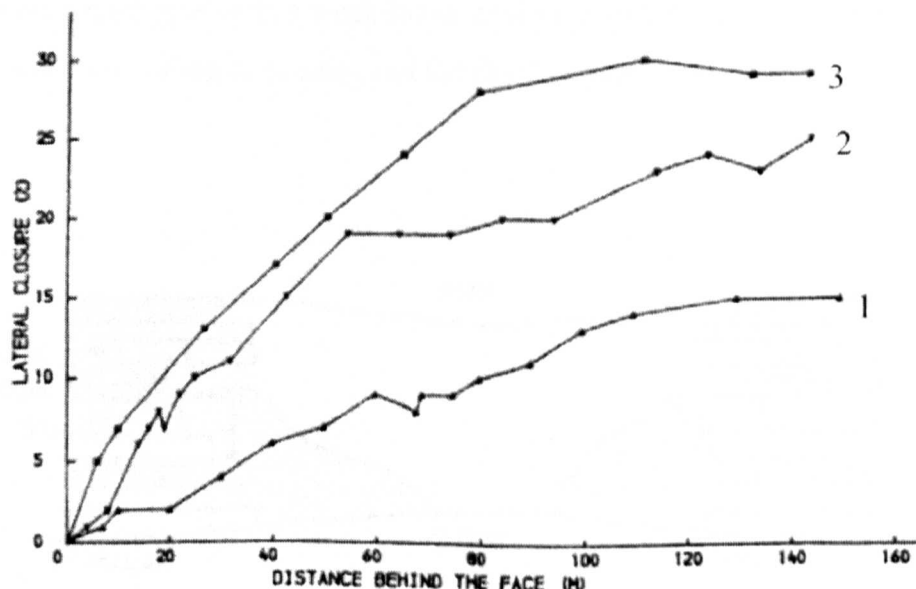


Figure 3.20 Lateral gateroad closure expressed as a percentage of the original width  
1)  $\theta = 55^{\circ}$ , 2)  $\theta = 30^{\circ}$  and 3)  $\theta = 8^{\circ}$  where  $\theta$  = angle between trend of cleat and trend of roadway (After Holmes 1982)

Extrusion of the rib side into the roadway is also influenced by the presence of weakness planes parallel to bedding. Where a weakness plane exists between two strata units of different stiffness the plane acts as a release surface allowing the unit with a lower stiffness to slide along.

The effect of banded structures of soft and hard layers in coal seams is to produce three types of deformation based on the number, relative thickness and parting shear strengths which are as follows (After ECSC 1987):

- (1) The extrusion of individual coal layers due to their different physical properties, the amount of extrusion of each layer being dependant on physical properties and the friction effect between layers (Figure 3.21).
- (2) Simultaneous extrusion of all coal layers mainly confined to homogeneous coal seams, the extrusion being influenced by the inelastic properties of all layers present, and the frictional effect between the coal seam and the roof and floor strata (Figure 3.22).
- (3) Differential extrusion within a thick coal seam containing a major hard and soft bed, the amount of extrusion dependant on physical properties of the beds and proximate roof and floor strata. Such extrusion occurs with a strong upper coal beneath a hard roof with a weak lower coal on a soft floor, resulting in extrusion of lower coal pulling or pushing out the floor (Figure 3.23).

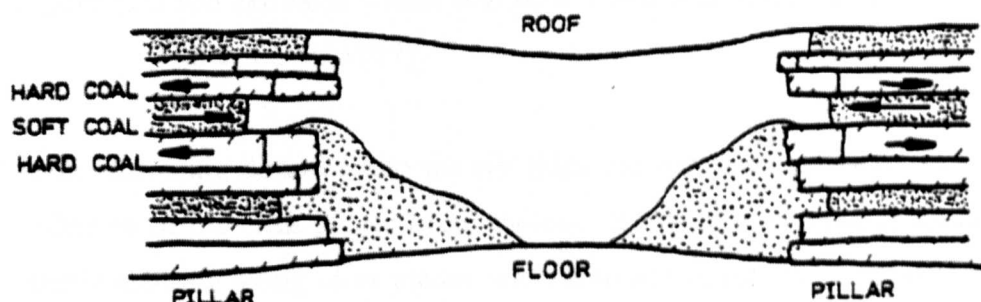


Figure 3.21 Rib extrusion with layers of different engineering properties  
(After ECSC 1987)

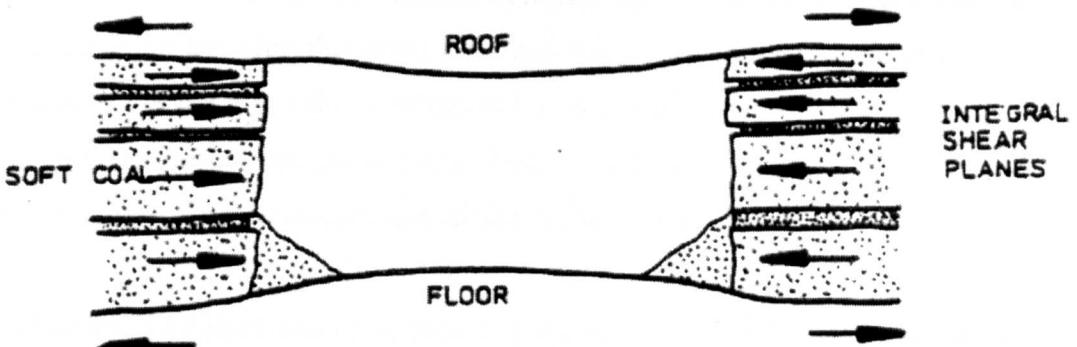


Figure 3.22 Rib extrusion within homogeneous coal seams

(After ECSC 1987)

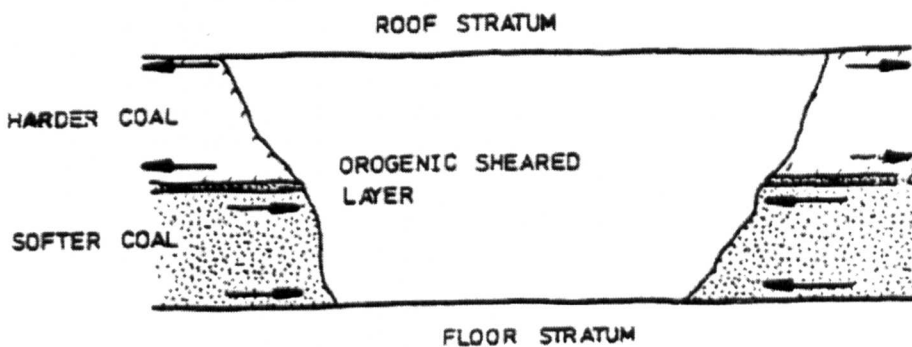


Figure 3.23 Rib extrusion within coal seam consisting of hard and soft layers

(after ECSC 1987)

With increasing distance into the rib sides the confining pressure increases and the influence of the cleat planes becomes less significant. At some distance into the rib tensile splitting along cleat planes will cease to become the critical mode of failure and will be replaced by the development of shear planes through the rock material. The shear strength of the rock material now becomes the most important factor influencing failure and deformation of the rock material.

### 3.5 CONCLUSIONS

The majority of the underground coal produced in the United Kingdom is by deep highly mechanised longwall mining methods. The characteristic features of this method, such as panel extraction and roadway formation generate a redistribution of

the in-situ stress field. New zones of stress concentrations or zones of stress relief are formed. Interaction between the stress field and the Coal Measure strata lead to the deformation of the strata and the development of zones of rock failure or yield. These zones in turn can affect the stress redistribution. Supports are installed within the roadway to reduce the deformation and failure of the rock strata.

The mechanisms of deformation and failure of the rock strata immediately adjacent to the roadway and coal face have been reviewed. These mechanism can be logically divided into those that occur with the roof strata, those that occur in the rib strata, those that occur in the ribs and those that occur adjacent to the face line. These mechanism of failure and deformation are influenced by the nature of the installed support, by the in-situ stress field and by the engineering properties of the rock strata.

## **CHAPTER 4**

### **CHARACTERISATION OF THE MECHANICAL PROPERTIES OF ROCK AND ROCK MASSES**

#### **4.1 INTRODUCTION**

Analytical and numerical methods of underground excavation design require, as input parameters, the mechanical i.e. the strength and stiffness, properties of the rock mass. As has been indicated in Chapter 2, rock mass as an engineering material is complex and contains numerous discontinuities in the form of bedding, jointing and faults etc. It is not practical to determine the strength and stiffness properties of a rock mass by direct testing. Therefore to determine realistic properties it is often necessary to apply reduction factors to the intact strength and stiffness values to account for the influence of any discontinuities and environmental factors. Surprisingly, it has been found that the intact properties of the rock have been frequently used as input parameters in numerical models by some researchers (Mohammad 1998). It is reasonable to assume that the strength and stiffness properties used in these models would have been significantly overestimated.

Engineering rock mass classification systems provide methodologies for quantifying the rock mass condition. Empirical relationships developed between the reduction factors and the classification value provide the most meaningful method of predicting the strength and stiffness properties of a rock mass.

This chapter describes the mechanical behaviour of intact rock and reviews the various methods that have been developed for predicting the mechanical properties of intact rock and rock masses. The final section of the chapter describes various engineering rock mass classification systems with an emphasis on those classifications that have been developed for or applied to coal mining environments.

#### **4.2 MECHANICAL PROPERTIES OF INTACT ROCK**

Intact rock refers to hand sized samples of rock free from bedding and joints. However smaller scale features, comprising the rock's fabric, such as lamination planes, cleavage and micro-fractures may be present. Strength and deformation

properties of intact rock are frequently used as a basis for obtaining rock mass strength and stiffness properties.

#### 4.2.1 Stress-Strain Behaviour Of Intact Rock

A typical stress-strain curve for a compression test undertaken on an intact rock sample is shown in Figure 4.1. The shape of the curve is evidence of the mechanisms of deformation and failure of rock. Region I in Figure 4.1 is slightly convex upwards and is associated with the closure of pre-existing micro cracks. Region II is linear and the rock is this region behaves in an elastic manner. Region III is typically concave downwards, which is a manifestation of random small crack formation, crack growth and sliding along existing crack interfaces. The point of maximum stress marks the beginning of stage IV. The maximum stress represents the peak strength of the material and this point is known as the failure point. Region IV is characterised by the negative slope of the stress strain curve and is associated with the gradual reduction of strength of the rock with increasing deformation. This is attributed to the development of a large number of small fractures parallel to the direction of loading which eventually coalesce along a plane. During this stage the rock undergoes irrecoverable (plastic) deformation.

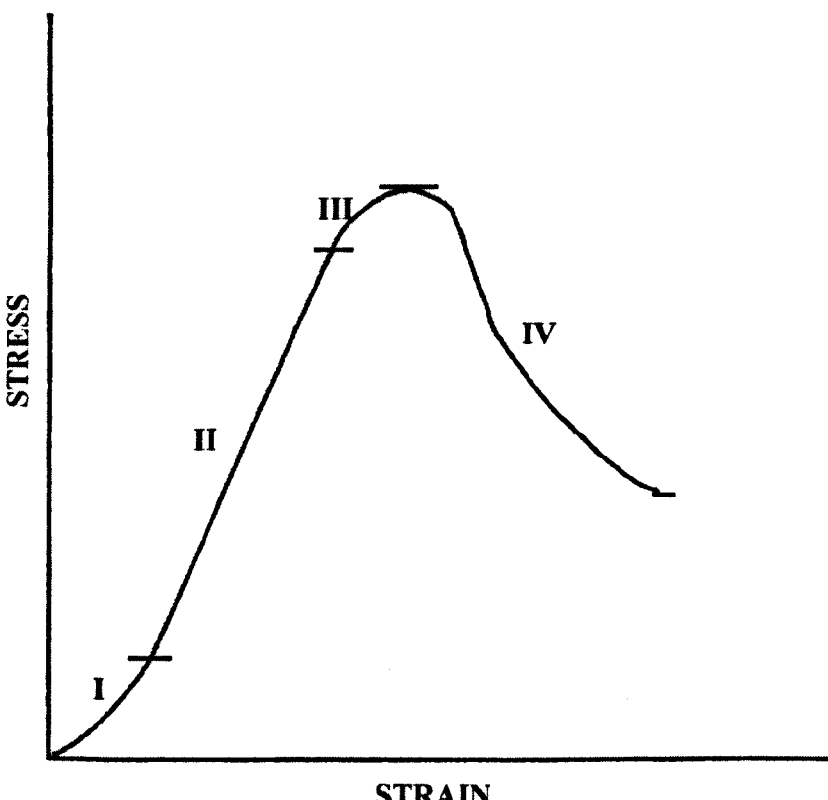


Figure 4.1 Typical stress-strain behavior of intact rock (After Jaeger and Cooke 1979)

A material is said to behave in a brittle manner when after the peak strength has been reached and the ability to resist load decreases rapidly with increasing deformation. The brittleness of the rock can be defined as the magnitude of the greatest slope of region IV (Jaeger and Cook 1979). The loss in strength associated with brittle rocks may lead to sudden and catastrophic failure in the form of rock bursts. Conversely a rock is said to behave in a ductile manner when it can sustain permanent deformation without losing its ability to resist load.

Four simplified types of stress-strain behaviour often commonly exhibited by rocks are shown as Figure 4.2 to 4.5.

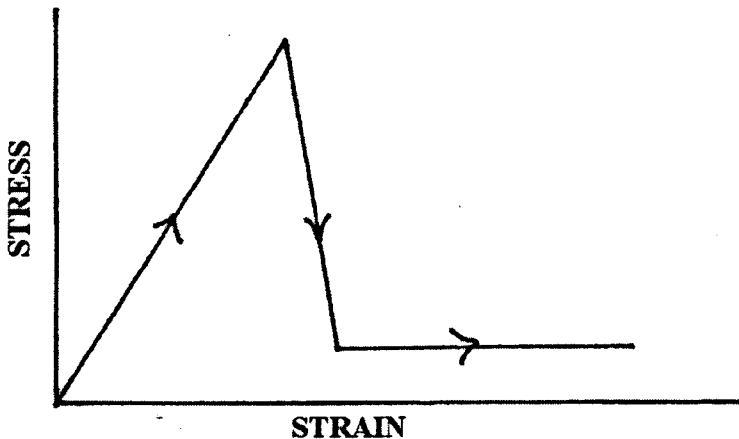


Figure 4.2 Stress-strain curve for a brittle material.

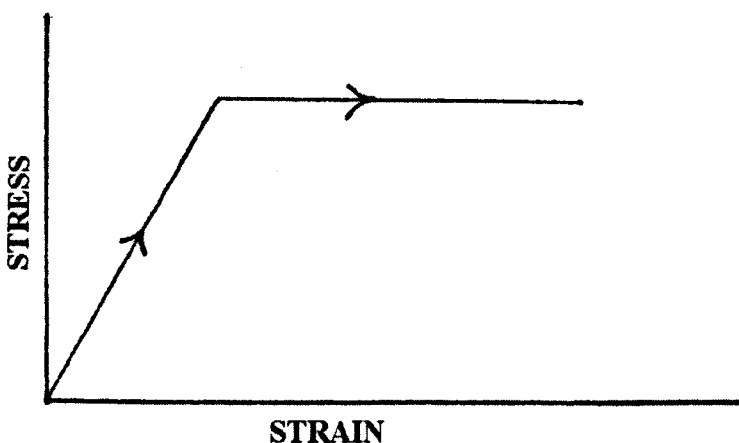


Figure 4.3 Stress-strain curve for an elastic-perfectly plastic material

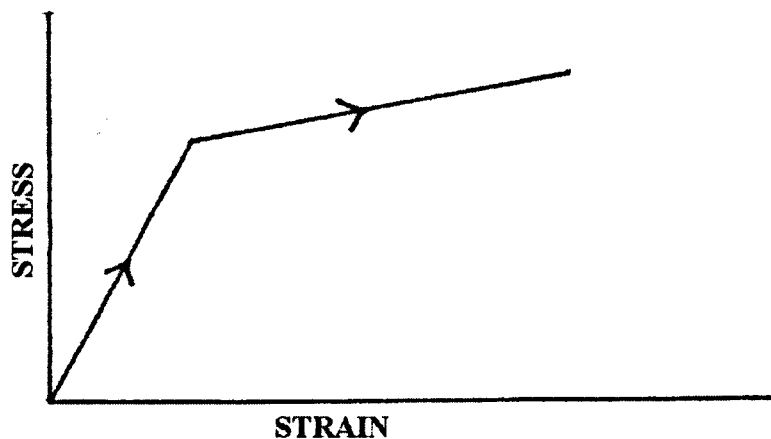


Figure 4.4 Stress-strain curve for an strain hardening material

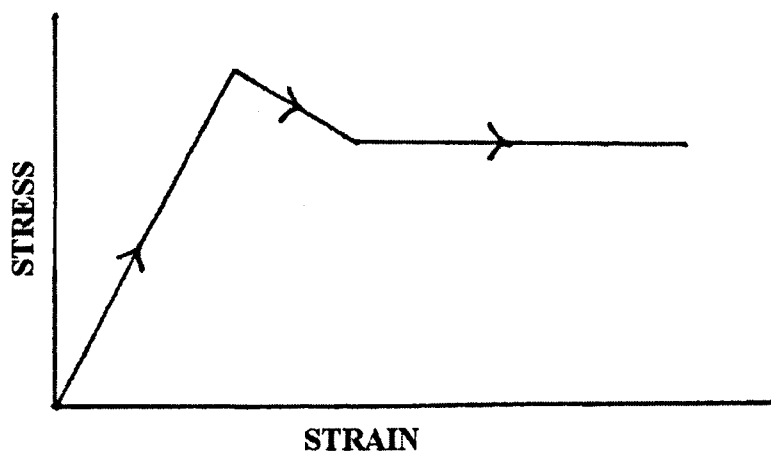


Figure 4.5 Stress-strain curve for a strain softening-perfectly plastic material

#### 4.2.2 Elastic Properties Of Intact Rock

Within the linear elastic region of the stress-strain curve produced by the uniaxial compression testing of a rock sample the constant ( $E$ ) in the stress-strain relationship is called the Young's Modulus (Equation 4.1).

$$\sigma = E\varepsilon \quad (4.1)$$

For an isotropic rock the only other constant required to fully characterise its elasticity is Poisson's Ratio.

### **4.2.3 Intact Rock Failure**

#### **4.2.3.1 Influencing Parameters**

The strength of intact rock is influenced by a number of factors. Ramamurthy (1985) divided these factors into geological, lithological, physical, mechanical and environmental factors (Table 4.1).

<b>Geological</b>	<b>Lithological</b>	<b>Physical</b>	<b>Mechanical</b>	<b>Environmental</b>
Geological age Weathering and other alterations	Mineral Composition Cementing Material Texture and Fabric Anisotropy	Density/specific Gravity Void index Porosity	Specimen preparation Specimen geometry End contact/restraint Type of testing machine Rate of loading	Moisture content Nature of pore Fluids Temperature Confining pressure

Table 4.1 Factors influencing the strength of intact rock (After Ramamurthy 1986)

Sample size also effects the strength of the intact rock sample with a general decrease in strength with increasing sample size (Hoek and Brown 1980).

As the mechanical factors are independent of the rock properties standardisation of the sample preparation and testing procedures has been developed to enable test results to be comparable. Although no British Standard as yet exist for rock testing, procedures for preparation and testing are given in International Standards for Rock Mechanics (ISRM 1981) and the American Standards for Testing of Materials.

##### *4.2.3.1.1 Confining pressure*

If a standard test procedure is undertaken the dominant parameter affecting the strength of a rock is confining pressure. It has been known for over a century that if the lateral displacement of a rock sample is resisted by applying confinement to its sides it will become stronger and more ductile (Jaeger and Cook 1979). The confining pressure also influences the type of fracture developed within a rock specimen. In

uniaxial compression the sample can often fail by longitudinal splitting. Under a moderate amount of confining pressure a single plane of fracture inclined at an angle to the direction of loading often develops. This is a typical failure mechanism under compressive stresses and is known as a shear fracture. Under high confining pressures a network of shear fractures develop and the rock behaves as a ductile material (Price 1966).

#### 4.2.3.2 Failure Criteria

Failure criteria define a locus of stress conditions where the rock strength is obtained. Normally, for simplicity, failure criteria are expressed in terms of a biaxial stress field defined by the maximum and minimum principal stresses and the intermediate principal stress is not considered (Hoek and Brown 1980). Although there is evidence that the intermediate principal stress does have an effect on the strength of the rock (Jaeger and Cooke 1979, Sheorey 1997) it is believed to be not as significant as the maximum and minimum principal stresses. Due to the increase in difficulty of testing and the increased complexity of analysis to include the intermediate stress for most practical cases it is ignored (Hoek and Brown 1980).

Failure criteria have been developed for intact rock, rock containing single planes of weakness and for rock masses containing multiple joint sets (Sheorey 1997, Hoek and Brown 1980). Testing of intact rock to determine the failure criterion is relatively simple, however experimental difficulties increase significantly for rock with one set of discontinuities. Testing of a rock mass with multiple joint sets is extremely difficult and very expensive. Because of this very little experimental data is available for rock masses and rock mass failure criteria tend to be based on empirical reductions of the intact failure envelope.

There are two basic types of failure criteria, which are theoretical failure criteria that are derived from assumptions concerning the mode of failure and empirical failure criteria that are developed directly from laboratory testing.

#### 4.2.3.3 Theoretical Failure Criteria

Though these criterion have little practical use within rock engineering as they do not provide very good predictions to actual strength properties of intact rock (Sheorey

1997) they are of fundamental importance for understanding the state of stress within a rock mass and the process of rock failure.

#### *4.2.3.3.1 Coulomb's theory and criterion*

This simple but important theory was originally developed in the 18<sup>th</sup> Century (Jaeger and Cooke 1979). Coulomb stated that failure would occur in a material when the maximum shear stress at a point in the material reaches a specific value ( $S_o$ ) known as the shear strength of the material. If  $\sigma_1$  and  $\sigma_3$  are the principal stresses in a material Coulomb's Theory states that the maximum shear stress is given by Equation 4.2

$$\tau = \frac{1}{2} (\sigma_1 - \sigma_3) \quad (4.2)$$

Thus failure occurs when the shear stress has the magnitude:

$$S_o = \frac{1}{2} (\sigma_1 - \sigma_3) \quad (4.3)$$

According to Coulomb's theory the failure plane will bisect at an angle between the maximum and minimum principal stresses. However in reality the failure plane forms an angle of less than 45° with the major principal stress. Navier modified Coulomb's theory by allowing for an increase in shear resistance of the material proportional to the magnitude of the normal stress acting across the plane of failure. The modified Coulomb criterion is given as Equation 4.4, where respectively  $\sigma_\theta$  and  $\tau_\theta$  are the normal and shear stresses acting on the failure plane.

$$\tau_\theta = S_\theta - \mu \sigma_\theta \quad (4.4)$$

The term  $\mu \sigma_\theta$  is analogous to the frictional force resisting sliding on an inclined plane due to a normal stress and thus the constant  $\mu$  is called the coefficient of internal friction.

The magnitude of the shear and normal stress acting on a plane is dependent on the orientation of that plane to the principal stresses. The stress conditions on a plane orientated at an angle  $\theta$  to the direction of major principal stress (Figure 4.6) if plotted on normal stress - shear stress axis lies on a circle with a centre  $(\sigma_1 + \sigma_3)/2$  and radius  $(\sigma_1 - \sigma_3)/2$  (Figure 4.7).

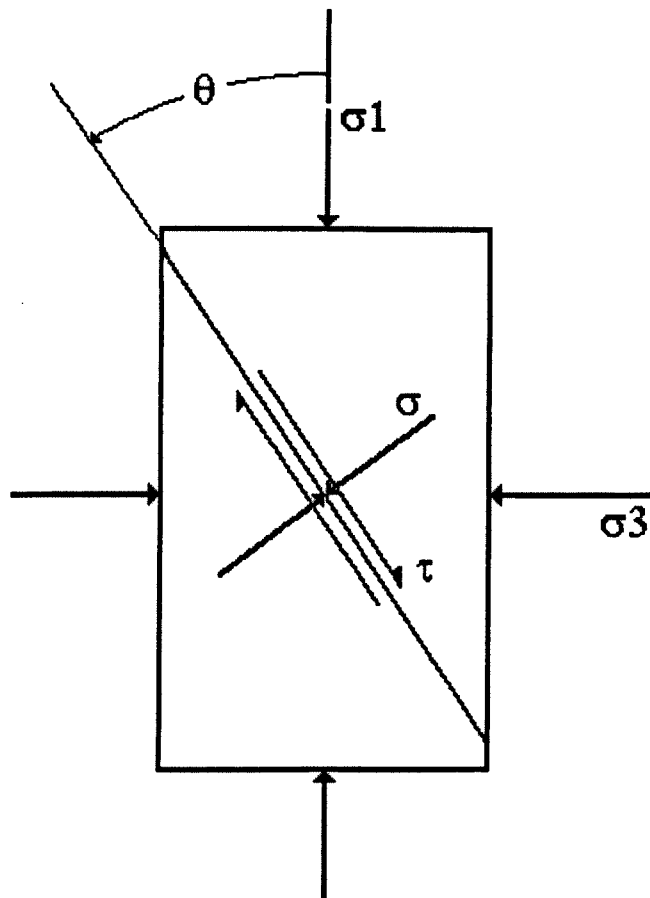


Figure 4.6 Stress Conditions in a Biaxial Stress field

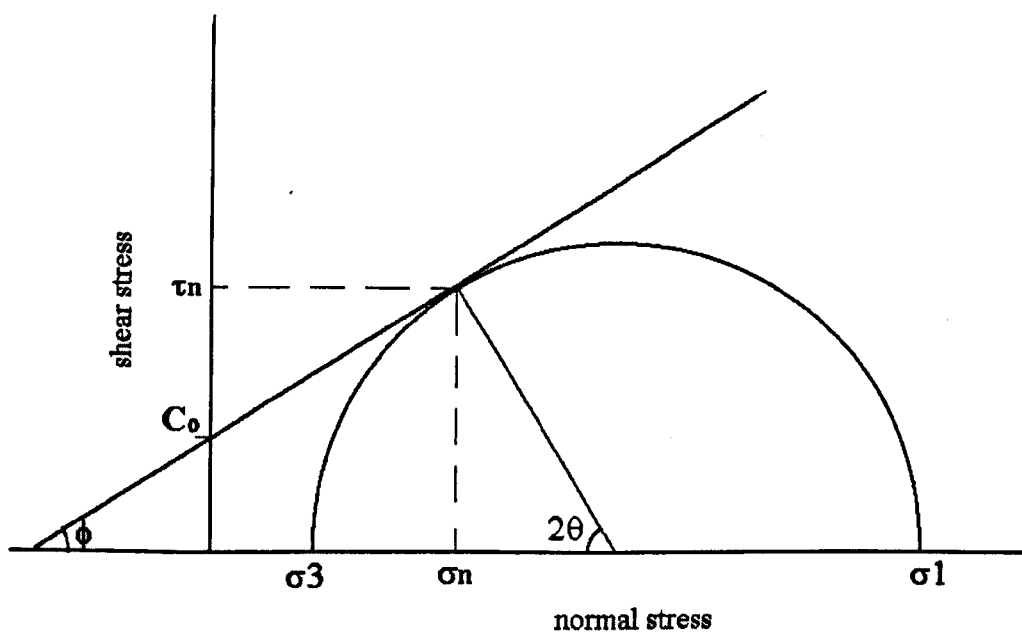


Figure 4.7 Coulomb-Navier Failure envelope

The normal and shear stresses acting on a plane of angle  $\theta$  to the maximum principal stress can be derived from Equations 4.5 and 4.6 respectively.

$$\sigma_\theta = \frac{\sigma_1 + \sigma_3}{2} + \frac{\sigma_1 - \sigma_3}{2} \cos 2\theta \quad (4.5)$$

$$\tau_\theta = \frac{\sigma_1 - \sigma_3}{2} \sin 2\theta \quad (4.6)$$

#### 4.2.3.3.2 Mohr's failure criterion

Mohr's theory of failure states that failure will occur when the shear stress on the potential fracture plane has increased to a value which depends on the normal stress acting across the plane. This is expressed mathematically as Equations 4.7.

This relationship is represented in Figure 4.8 by a curve A-B in the  $\sigma$ - $\tau$  plane.

$$\tau_\theta = f(\sigma_\theta) \quad (4.7)$$

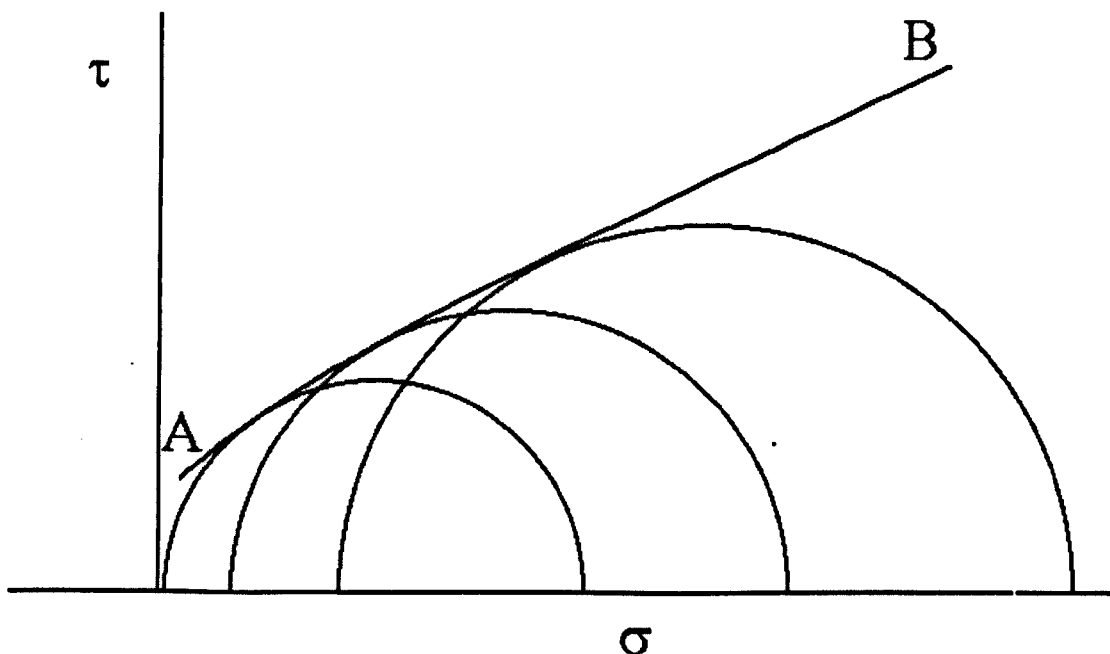


Figure 4.8 Mohr's Failure Envelope

The curve is not defined by explicit formulae but is obtained by constructing an envelope to the Mohr's circles of stress for failure under a variety of confining stresses.

The angle between the failure plane and the maximum principal stress is equal to half the angle between the normal to the tangent of the failure envelope and the x axis (Figure 4.6). For the state of stress represented by a Mohr's circle lying completely within the envelope the rock will not fail.

#### *4.2.3.3 Griffith's theory and criterion for brittle fracture*

Griffith working in the 1920's developed a failure criterion for a brittle material based on mechanisms of microscopic tensile failure within the material. Griffith observed that there was a large difference between the theoretical tensile strength of a material predicted from the calculation of forces required to break atomic bonds and the observed tensile strength of the materials (Murrell 1965). He hypothesised that crystalline materials contain randomly orientated microcracks and that stress concentrations develop at the end of some of these cracks causing the cracks to propagate and finally contribute to the development of a macroscopic failure plane. Griffith based his hypothesis on an energy instability concept. He stated that a crack will only extend when the total potential energy within the rock due to the applied forces decrease or remains constant with an increase in crack length (Brady and Brown 1985) . Considering a thin elastic strip of unit thickness with an elliptical hole orientated with its long axis perpendicular to an applied tensile stress Griffith determined that the reduction of energy in the strip due to the elliptical crack is as follows (Equation 4.9)

$$W_e = \frac{\pi c^2 \sigma_o^2}{E} \quad (4.9)$$

Where  $W_e$  is elastic strain energy stored around the crack,  $c$  is half crack length,  $E$  is the Young's Modulus.  $\sigma_o$  is the applied tensile stress

He also stated that the upon extension of the crack strain energy associated with stretching of atomic bonds prior to failure will be transferred into crack surface

energy. This surface energy is considered to be analogous to surface tension in a liquid. The equation he derived to calculate this surface energy ( $W_s$ ) is given as Equation 4.10.

$$W_s = 4cT \quad (4.10)$$

where  $T$  is the surface energy per unit of the crack surface

Hence the decrease in total energy due to the elliptical hole can be calculated from Equation 4.11

$$W = W_e - W_s = \frac{\pi c^2 \sigma_o^2}{E} - 4cT \quad (4.11)$$

The crack will propagate if  $\delta W / \delta c = 0$  i.e. if there is a reduction of potential energy with crack extension. The tensile strength ( $T_o$ ) is therefore: (Equation 4.12)

$$\sigma_o = T_o = \sqrt{\frac{2ET}{\pi c}} \quad (4.12)$$

Griffith extended his theory to the case of biaxial compression. Under biaxial compression tensile stresses can be shown to be generated in a zone around the elliptical crack where the radius of curvature is smallest (Figure 4.9).

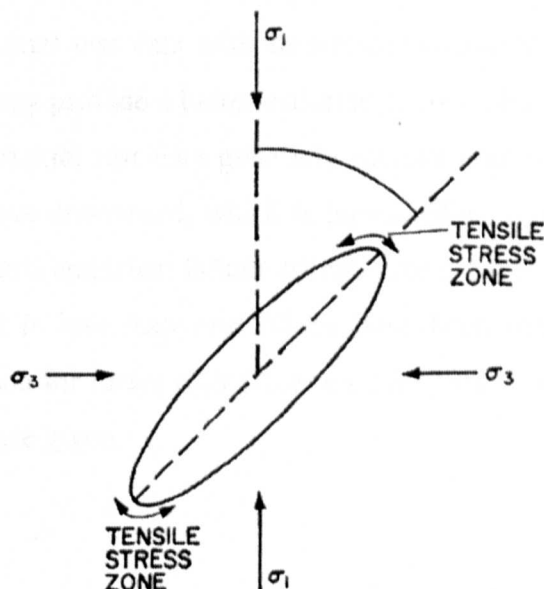


Figure 4.9 Griffith crack in a biaxial compressive stress field (After Price 1966)

Griffith assumed that the crack will propagate from the points of maximum tensile stress concentration and obtained a criterion for failure outlined (Equation 4.13, Equation 4.14) below:

if  $\sigma_1 + 3\sigma_3 > 0$

$$(\sigma_1 - \sigma_3)^2 - 8T_o(\sigma_1 + \sigma_3) = 0 \quad (4.13)$$

if  $\sigma_1 + 3\sigma_3 < 0$

$$\sigma_3 + T_o = 0 \quad (4.14)$$

Griffith's failure criterion produces a parabolic failure curve. Subsequently it has been found that this is the general shape of rock failure envelopes. Griffith's theory also predicts that the unconfined compressive strength is equal to 8 times the tensile strength, which again has been found to be approximately correct for rock. However the failure criteria is too general for fitting to actual test data. Modifications to Griffith's criteria include the consideration of frictional stresses generated across the face of cracks as they close due to compression. Mcintosh and Walsh (1963) developed a modified criterion to account for the friction. Closure only occurs under a compressive stress regime and in the tensile region Griffith's original theory are used.

#### 4.2.3.4 Empirical Failure Criteria

Empirical failure criteria have been developed solely on the basis of obtaining good fits to actual rock triaxial test data without any consideration of the mechanisms of failure of the rock. They provide a better estimate of rock strength properties than the theoretical criteria. Triaxial test data generally indicate that the failure envelope for rock material is concave downward, which is typical of a curve produced by a power relationship. Hence most empirical failure criteria take the form of a power law where the power coefficient is less than one. There have been many different empirical failure criteria proposed for intact rock (Hassani 1980) and here a review of only the better known criteria are given.

#### *4.2.3.4.1 Murrell's criterion*

The following empirical criterion was suggested by Murrell (1965) to fit triaxial tests results from a sandstone. The criteria applies for the range of stresses between uniaxial compression and the brittle ductile transition stress (Equation 4.15).

In terms of shear and normal stress acting on the plane of failure

$$\tau = \lambda \sigma^n \quad (4.15)$$

Where empirical constant  $\lambda \approx 2T_o^{0.5}$  and  $n \approx 0.61$

A limitation to Murrell's criterion is that it is only valid when  $\sigma_3 \geq 0$ .

Hobbs (1967) proposed, for sedimentary rocks, a similar criterion to that developed by Murrell. However Hobbs' criterion had the addition of a constant relating to the cohesion of the rock (Equation 4.16).

$$\tau = \tau_c + \mu \sigma^\alpha \quad (4.16)$$

Where  $\tau_c$ ,  $\mu$  and  $\alpha$  are material constants.  $0.5 \leq \alpha \leq 1$

#### *4.2.3.4.2 Bieniawski's criterion*

Bieniawski (1974) attempted to relate the variables, in two failure criterions, to the lithology of the rock type thus allowing the strength parameters to be estimated from the unconfined compressive strength and rock type only.

He reduced the failure criterions to a dimensionless form by dividing the principal stresses at failure by the uniaxial compressive strength. Normalising the data in this way has the advantage that since effects such as specimen size, environmental conditions and testing techniques are presumably similar in both numerator and denominator they are eliminated upon normalisation. Normalising also allows comparison of the failure envelopes of rock with different unconfined compressive strengths.

He derived rock type constants for the normalised form of Murrell's Criterion expressed in terms of principal stress (Equation 4.17) and for a criterion proposed by Hoek (1968) (Equation 4.18).

$$\frac{\sigma_1}{\sigma_c} = B \left( \frac{\sigma_3}{\sigma_c} \right)^A + 1 \quad (4.17)$$

Where  $B$  and  $A$  are material constants

$$\frac{\tau_m}{\sigma_c} = 0.1 + D \left( \frac{\sigma_m}{\sigma_c} \right)^C \quad (4.18)$$

Where

$$\sigma_m = \left( \frac{\sigma_1 + \sigma_3}{2} \right) \quad \tau_m = \left( \frac{\sigma_1 - \sigma_3}{2} \right)$$

$D$  is a constant dependant on rock type and  $C = 0.9$

Bieniawski considered constants that he derived had accuracy sufficient for practical purposes. Table 4.2 details the constants he derived.

Subsequently it has been found that the  $B$  parameter in the Criterion is not necessarily constant for a particular rock type but that there is a significant correlation between  $B$  and the unconfined compressive strength of the rock (Vutukuri and Hossaini 1992).

ROCK TYPE	Constant 'A' = 0.75	Constant 'B'	Constant 'C' = 0.9	Constant 'D'
Norite		5.0		0.8
Quartzite		4.5		0.78
Sandstone		4.0		0.75
Siltstone		3.0		0.7
Mudstone		3.0		0.7
ALL ROCK TYPES		3.5		0.75

Table 4.2 Material Constants (After Bieniawski 1974)

Hassani (1980) after undertaking extensive testing on UK Coal Measure lithologies attempted to fit a range of empirical failure criteria to the test data. He found that the power law given by Equation 4.17 produced the best fit. His proposed 'D' constants for UK Coal Measures is given as Table 4.3.

Rock type	Constant 'D'
sandstone	0.7714
mudstone	0.8588
siltstone	0.7829
seat earth	0.6939
coal	0.6145

Table 4.3 Material constants for UK Coal Measure Rocks (After Hassani 1980)

## 4.3 MECHANICAL PROPERTIES OF ROCK MASSES

### 4.3.1 Introduction

The transition from intact rock material to a heavily jointed rock mass is shown in Figure 4.10. With increasing sample size there is a general reduction in strength and stiffness of the rock due to the presence of discontinuities. At some critical rock volume the rock mass strength and deformation properties are obtained and there is no further reduction in strength or stiffness with increasing sample size. The rock mass strength and stiffness properties generally determine the stability of underground excavations.

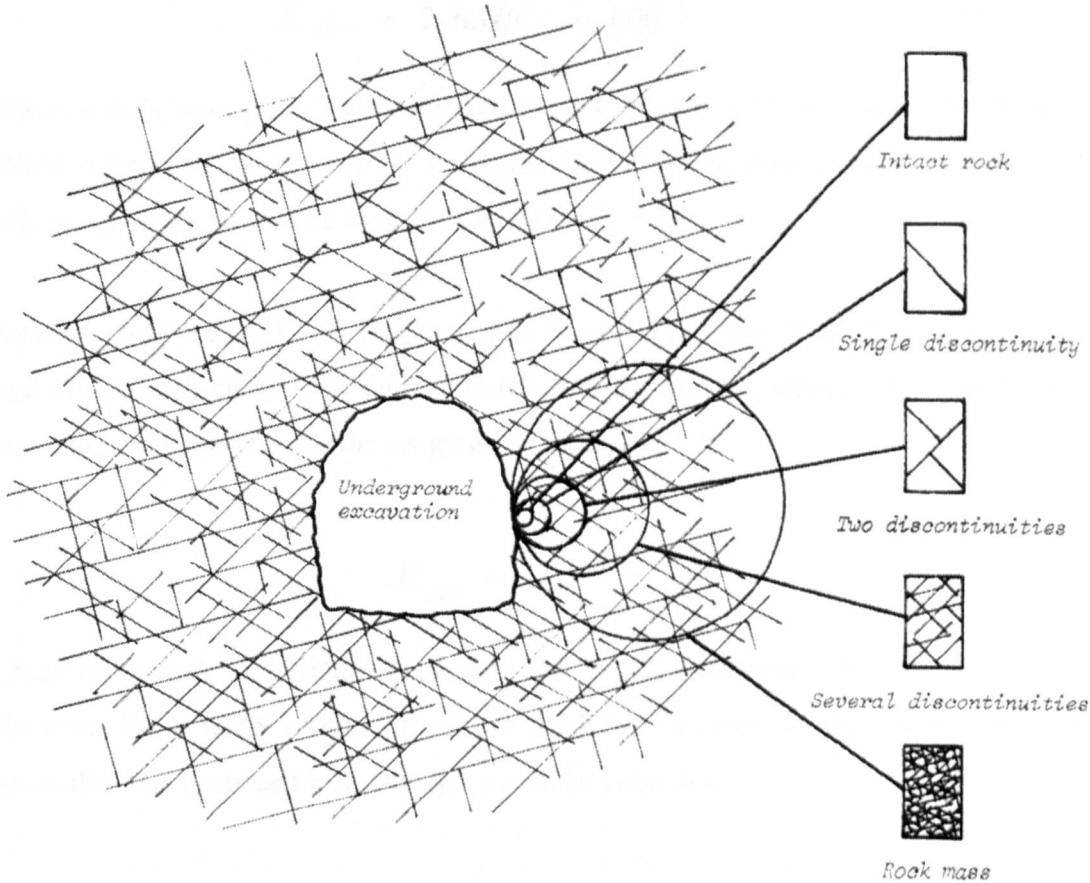


Figure 4.10 Transition from intact rock to a heavily jointed rock mass with increasing sample size (after Hoek and Brown 1980)

#### 4.3.2 Stiffness Properties Of Rock Masses

If it is assumed that heavily jointed rock masses can be considered to be isotropic (Hoek and Brown 1980) only the deformation modulus and Poisson's ratio are required to fully characterise its stress-strain behaviour prior to failure. In-situ determination of the deformation modulus can be undertaken using several types of tests but all are expensive, time consuming and difficult to interpret (Bieniawski 1978). This has led to the development of empirical equations that allow the deformation modulus to be estimated from rock mass classifications.

Bieniawski (1978) proposed the following relationship directly relating the rock mass rating (RMR) to the deformation modulus ( $E_{def}$ ) in GPa. The relationship was derived from the back analysis of a wide variety of case studies including coal mine pillars (Equation 4.19).

$$E_{def} = 2 RMR - 100 \quad (4.19)$$

Bieniawski's case studies were applied to rock masses with an RMR > 50. When the RMR is less than or equal to 50, corresponding to a fair, poor or very poor rock mass this relationship cannot be used as it leads to  $E_{def} < 0$ .

Serafim and Pereira (1983) supplemented Bieniawski's data with other case histories, mainly of back analysis of dam foundation deformations, where RMR was less than 50. Their proposed correlation is given as Equation 4.20.

$$E_{def} = 10^{(RMR-10)/40} \quad (4.20)$$

Chappell (1984) correlated RMR with the in-situ determined deformation modulus obtained for a wide variety of soft to hard rock masses of the Snowy mountains Australia. His proposed relationship is give in Table 4.4

RMR	Description	Rock Mass Deformability (GPa)	Recommended Poisson's Ratio
?	Extremely poor	<0.05	0.45
0-19	Very poor	0.05 to 0.5	0.4
20-39	Poor	0.5 to 1	0.35
40-59	Fair	1 to 5	0.3
60-79	Good	5 to 25	0.25
80-100	Very good	25 to 50	0.23
?	Extremely good	> 50	0.2

Table 4.4 relationship between RMR deformation modulus and Poisson's Ratio  
(after Chappell 1984)

Nicholson and Bieniawski (1990) developed a non-linear stress dependant deformation modulus. They found from laboratory testing on intact rock and rock fill that the deformation modulus is influenced by confining pressure. They also assumed

that the rock mass deformation modulus is related to the intact elastic modulus by a reduction factor dependant on rock mass quality.

Their proposed relationship is as follows (Equation 4.21):

$$E_{def} = \frac{\sigma_c \left( \frac{m \sigma_3}{\sigma_c} + s \right)^{0.5}}{\varepsilon_{1c} \left( a + \frac{b \sigma_3}{\sigma_c} \right)} \quad (4.21)$$

Where  $m$  and  $s$  are rock mass properties as defined in the Hoek-Brown failure criteria  
 $\varepsilon_{1c}$  is the strain at failure of an intact rock in the unconfined compressive test  
 $a$  and  $b$  are rock mass properties representing the effect of rock mass quality and confining pressure on the failure strain ( $a=1$  for intact rock).

Analysing Bieniawski's and Serafim and Pereira's data they proposed the following reduction factor to account for the effect of rock mass quality:

$$RF = 0.0028 (RMR)^2 + 0.9 \exp \left( \frac{RMR}{22.8} \right) \quad (4.22)$$

Thus where there is very low or no confinement the deformation modulus of the rock mass may be estimated by using the following relationship (Equation 4.23):

$$E_{def} = E(RF) \quad (4.23)$$

Mitri et al (1994) from case studies of hard rock mines proposed the following relationship between the intact elastic modulus and the deformation modulus of a rock mass (Equation 4.24):

$$E_{def} = 0.5E \left[ 1 - \left( \cos \left( \pi \frac{RMR}{100} \right) \right) \right] \quad (4.24)$$

Based upon practical observations and back analysis of excavation behaviour in poor quality rock masses Hoek and Brown (1997) proposed the following modification to Serafim and Pereira's equation for when the unconfined compressive strength is < 100 MPa

$$E_{def} = \sqrt{\frac{\sigma_c}{100}} 10^{(GSI - 10/40)} \quad (4.25)$$

Where *GSI* is Hoek and Brown's Geological Strength Index.

#### 4.3.3 Rock Mass Failure Criteria

Joints and weakness planes act in reducing the strength of the rock mass to some value less than the intact strength. It is usually not practical to determine directly the strength properties of the rock mass. Therefore rock mass failure criteria have been developed that allow estimation of the rock mass strength by reducing the intact strength envelope by an amount related to the degree of fracturing. Rock mass classifications quantify the quality of the rock mass in a systematic way and have been used by many workers as a basis for their rock mass failure criteria. Some of the most popular rock mass failure criteria are as follows:

##### 4.3.3.1 Hoek – Brown Failure Criterion

The Hoek-Brown failure criterion has become the most widely used rock mass failure criterion in use today (Carter et al 1991). First proposed in 1980, Hoek and Brown's philosophy behind developing the criteria was that it should satisfy the following requirements:

A It should adequately describe the response of an intact rock sample to the full range of stress conditions likely to be encountered underground. These conditions range from uniaxial tensile stress to triaxial compressive stress.

B It should be capable of predicting the influence of one or more sets of discontinuities upon the behaviour of a rock sample. This behaviour may be highly anisotropic; i.e. it will depend upon the inclination of the discontinuities to the applied stress direction.

C It should provide some form of projection, even if approximate for the behaviour of a full scale rock mass containing several sets of discontinuities.

Hoek and Brown developed their empirical failure criterion initially to fit triaxial data sets of intact rock. Their starting point was to base the criterion on a quasi-parabolic form predicted by the Griffith theory and by a process of trial and error defined a criterion in terms of principal stresses (Equation 4.26)

$$\frac{\sigma_1}{\sigma_c} = \frac{\sigma_3}{\sigma_c} + \left( m_i \frac{\sigma_3}{\sigma_c} + s \right)^{0.5} \quad (4.26)$$

Where  $m_i$  is a material constant for intact rock and  $s = 1$  for intact rock

Since its development Hoek and Brown have determined the material constant  $m_i$  values for a wide variety of rock types based on analyses of published triaxial test results on intact rock (Table 4.5)(Hoek et al 1995).

For heavily jointed rock masses i.e. containing 4 or more joint sets Hoek and Brown (1980) considered that the mass strength would be isotropic. Thus they proposed a rock mass failure criteria of the same form as the intact criteria but with reduced  $m$  and  $s$  parameters to account for the quality of the rock mass. Working with a limited supply of rock mass triaxial test data from the Panguna Andesite from the Island of Bougainville in Papua New Guinea they proposed approximate relationships between the quality of the andesite expressed in terms of classification values derived from Barton's Q system and Bieniawski's Rock Mass Rating system and a reduction factor to be applied to the constants  $s$  and  $m_i$ .

Hoek and Brown produced an updated version in 1988 which was based on the experience of using the criterion on a number of projects. This version allowed the rock mass material parameters to be determined directly from Bieniawski's 1976 rock mass rating classification that will be outlined later in this chapter.

Rock type	Class	Group	Texture				
			Course	Medium	Fine	Very fine	
SEDIMENTARY	Clastic		Conglomerate (22)	Sandstone 19	Siltstone 9	Claystone 4	
			← Greywacke → (18)				
	Organic		← Chalk → 7				
			← Coal → (8-21)				
	Non-Clastic	Carbonate	Breccia (20)	Sparitic Limestone (10)	Micritic Limestone 8		
		Chemical	Gypstone 16		Anhydrite 13		
METAMORPHIC	Non Foliated		Marble 9	Hornfels (19)	Quartzite 24		
	Slightly foliated		Migmatite (30)	Amphibolite 31	Mylonites (6)		
	Foliated*		Gneiss 33	Schists (10)	Phyllites (10)	Slate 9	
IGNEOUS	Light		Granite 33	Rhyolite (16)		Obsidian (19)	
			Granodiorite (30)	Dacite (17)			
			Diorite (28)	Andesite 19			
	Dark		Gabbro 27	Dolerite (19)	Basalt (17)		
			Norite 22				
Extrusive pyroclastic type			Agglomerate (20)	Breccia (18)	Tuff (15)		

Table 4.5  $m_i$  values for intact rock (parenthesis are estimates) (after Hoek et al 1995)

In 1992 Hoek-Brown proposed a modified criterion together with a simplified classification scheme for estimating the parameters for this criterion. The modified criterion eliminated the tensile strength of the rock mass as they considered the type of heavily jointed rock mass that the criterion applies to does not have a significant tensile strength.

A more general form of the criterion was published in 1995 which incorporated both the original and modified criterions, and is given as Equation 4.27 (Hoek et al 1995):

$$\frac{\sigma_1}{\sigma_c} = \frac{\sigma_3}{\sigma_c} + \left( m_b \frac{\sigma_3}{\sigma_c} + s \right)^a \quad (4.27)$$

Where  $m_b$  is a material parameter constant for the rock mass  
 $s$  and  $a$  are constants which depend upon the characteristics of the rock mass

They state that this criterion is applicable to intact or heavily jointed rock masses but may be used with extreme care when two joint sets of equal influence are present.

A Geological Strength Index (GSI), which can be determined from rock mass classification values, was proposed as a basis for calculating the material parameters  $m_b$ ,  $s$  and  $a$ . The value of GSI ranges from about 10 for extremely poor rock masses to 100 for intact rock. Hoek et al (1995) for undisturbed rock masses gave the following relationships between the material constants and GSI.

For  $GSI > 25$

$$\frac{m_b}{m_i} = \exp \left( \frac{GSI - 100}{28} \right) \quad (4.28)$$

$$s = \exp \left( \frac{GSI - 100}{9} \right) \quad (4.29)$$

$$a = 0.5$$

For  $GSI < 25$

$$s = 0$$

$$a = 0.65 - GSI/200$$

Hoek et al (1995) established relationships between their GSI and Bieniawski's 1976 and 1989 rock mass rating classification and Barton, Lein and Lunde's 'Q' Classification (1974) which are given as Equations 4.30, 4.31 and 4.32 respectively.

For Bieniawski's classification the rock mass is assumed to be dry and the joint orientation very favourable and for Barton's 'Q' value the rock mass should be assumed to be dry and subjected to medium stress conditions.

$$\text{For } RMR_{76} > 18 \quad GSI = RMR_{76} \quad (4.30)$$

For  $\text{RMR}_{76} < 18$       Equation 4.32 should be used

For  $\text{RMR}_{89} > 23$        $\text{GSI} = \text{RMR}_{89} - 5$       (4.31)

For  $\text{RMR}_{89} < 23$       Equation 4.32 should be used

$$\text{GSI} = 9\text{LOG}_e Q + 44 \quad (4.32)$$

#### 4.3.3.2 Bieniawski-Yudhibr Criterion

Yudhibr et al (1983) used Bieniawski criterion for intact rock as a basis for his rock mass failure criterion (Equation 4.33).

$$\frac{\sigma_1}{\sigma_c} = A + B \left( \frac{\sigma_3}{\sigma_c} \right)^{0.65} \quad (4.33)$$

Where  $A = 1$  for intact rocks

$$A = 0.0176Q^\alpha \text{ for rock masses}$$

Where  $Q = \text{Rock Quality Index of Barton et al (1974)}$

$\alpha = \text{variable}$

#### 4.3.3.3 Ramamurthy's Criterion

Ramamurthy (1986) proposed the following failure criteria for both intact rock

$$\frac{\sigma_1 - \sigma_3}{\sigma_3} = B_i \left( \frac{\sigma_c}{\sigma_3} \right)^{0.8} \quad (4.34)$$

Where  $B_i$  is a constant depending on rock type

This criterion is only applicable when  $\sigma_3 > 0$

From the analysis of triaxial test results Ramamurthy determined the following values of  $B_i$  for intact rock:

1.8 for siltstone

2.2 for shale, slate, mudstone, claystone and sandstone

2.4 for limestone, anhydrite and rocksalt,

2.6 for quartzite, andesite, diorite, norite, liprite and basalt

2.8 for marble and dolomite

3.0 for granite and charnockite

For a jointed rock mass the criterion is as follows (Equation 4.35)

$$\frac{\sigma_1 - \sigma_3}{\sigma_3} = B \left( \frac{\sigma_{cm}}{\sigma_3} \right)^{0.8} \quad (4.35)$$

Using Hoek and Brown's limited data set obtained for Panguna Andesite he developed the following rock mass constants.

$$B_m = B_i \exp \left( \frac{RMR - 100}{75.5} \right) \quad (4.36)$$

$$\sigma_{cm} = \sigma_c \exp \left( \frac{RMR - 100}{75.5} \right) \quad (4.37)$$

Where  $\sigma_{cm}$  = uniaxial compressive strength of rock mass  $B_m$  = rock mass parameter

#### 4.3.4 Application of Rock Mass Failure Criteria to the UK Coal Measure Strata

An investigation to identify the optimum failure criterion for predicting the strength of UK Coal Measure rock masses was undertaken as part of the research for this thesis. An initial evaluation was undertaken for each of the three failure criterions described in the previous section, namely the Ramamurthy, Bieniawski-Yudhibr and Hoek-Brown criterions. These criterions were applied to triaxial data sets for a variety of intact Coal Measure rocks. Hassani's (1980) extensive test data was used as a basis for the evaluation. It was considered that once the failure criterion that most accurately predicted the strength of the intact Coal Measure rock types was identified, reduction in the intact failure envelope to account for rock mass characteristics would then allow the most realistic estimate of the rock mass strength properties to be determined.

Appendix 2 Shows the application of the three criterions to the sets of triaxial data obtained by Hassani (1980) from the testing of a variety of UK Coal Measure rock types.

The plots shown in Appendix 2 indicated that Ramamurthy's Criterion was the least satisfactory of the three established criterions. This criterion can be seen to generally produces a poor fit and was not applicable in the low confining-tensile stress range. Bieniawski's criterion although producing a reasonable fit to the data was not applicable in the tensile range. The Hoek-Brown criterion was applicable in the low confinement and tensile stress range and generally produced a reasonable fit to the data. The Hoek-Brown Criterion was probably the most satisfactory of the three established criterions. However there was a tendency for the criterion to overestimate the strength in the low confinement range.

#### 4.3.4.1 Development of a Rock Mass Failure Criteria for UK Coal Measure Strata

The above studies indicated that none of the established rock mass failure criterions produced failure envelopes that closely fitted the triaxial data sets for intact Coal Measure rock types. Therefore studies were undertaken to develop a failure criterion that was more applicable to the typical triaxial data sets obtained for Coal Measure rock types. This new failure criterion was based on modifying the established Hoek-Brown failure criterion as this had been identified as being the most suitable existing rock mass failure criterion for predicting the strength of the Coal Measures.

Several workers have found that the material constant  $m_i$  within the Hoek-Brown Criterion varies as a function of confining pressure (Ramamurthy 1986, Vutukuri and Hassani 1992, Frith 1992). Carter et al (1991) and Branch (1987) had also stated that the Hoek-Brown failure criterion often produced a poor fit in the low confining stress-tensile region. This can be considered significant as the rock strata immediately adjacent to an underground excavation is often in low confinement.

It was found during the studies that the  $m_i$  parameter determined for Hassani's data sets was not a constant but varied as a function of confining pressure. Significantly improved failure envelope fits to the lower confining and tensile stress range was

achieved by allowing the  $m_i$  parameter to vary as a linear function of the confining pressure within the Hoek-Brown failure criterion.

The modified Hoek-Brown failure criterion (Coal Measure Failure Criterion) developed for UK Coal Measures is given as Equation 4.38 and the failure envelope plots predicted by the Coal Measure Failure Criterion are included within Appendix 2.

$$\frac{\sigma_1}{\sigma_c} = \frac{\sigma_3}{\sigma_c} + \left( \left( \left( \frac{\sigma_3}{\sigma_c} m_{i1} \right) + m_{i2} \right) \frac{\sigma_3}{\sigma_c} + s_i \right)^{0.5} \quad (4.38)$$

Where  $m_{i1}$  and  $m_{i2}$  and  $s_i$  are empirical material constants

The empirical material constants  $m_{i1}$ ,  $m_{i2}$  and  $s_i$  are found by fitting a quadratic curve to the results of triaxial tests when plotted on an axis of  $\sigma_3/\text{ucs}$  against  $(\sigma_1/\text{ucs} - \sigma_3/\text{ucs})^2$ . Such a curve is shown in Figure 4.11. The  $m_{i1}$  parameter value therefore represents the coefficient of the  $x^2$  term, the  $m_{i2}$  value represents the coefficient of the  $x$  term and the  $s_i$  value represents the y intercept value of the tangent to the quadratic curve.

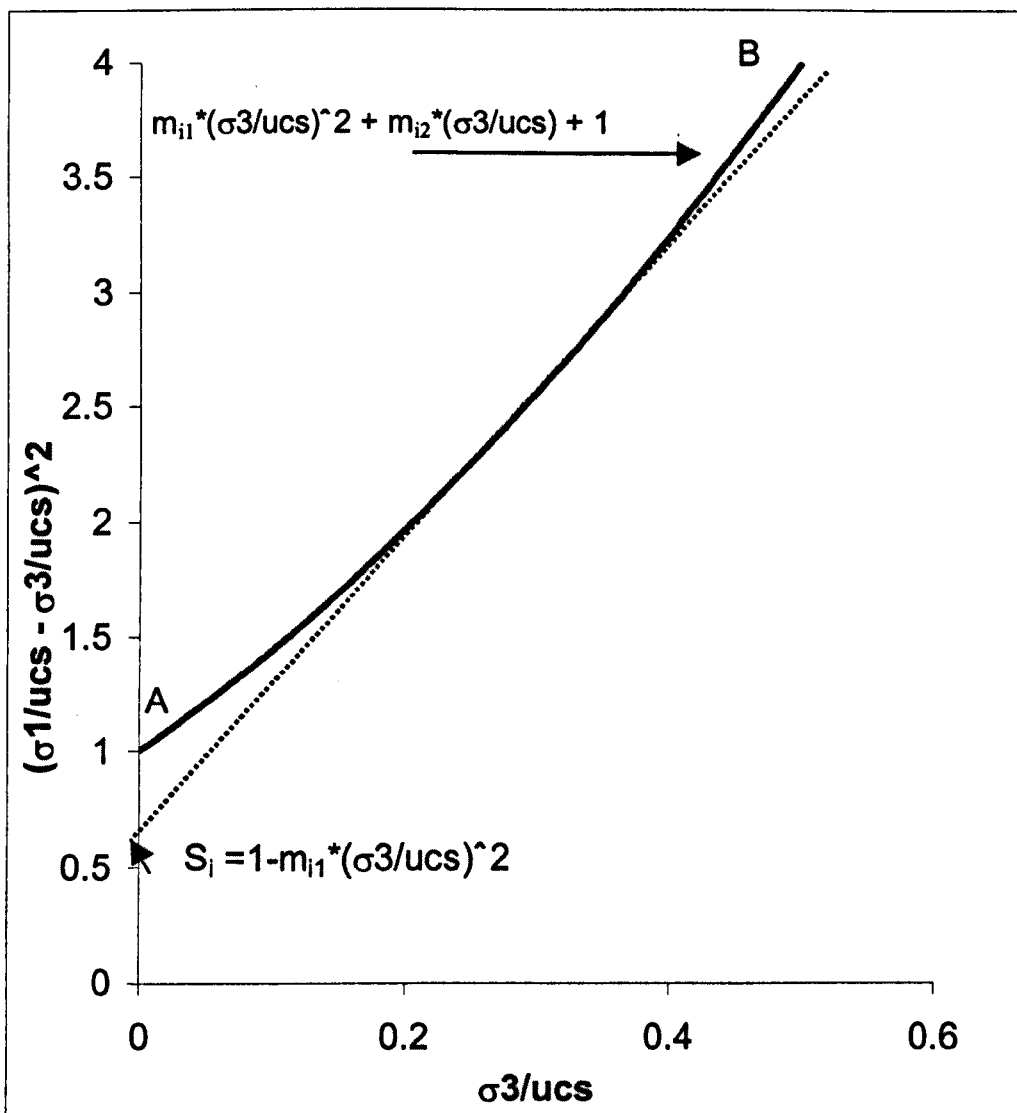


Figure 4.11 Plot of  $\sigma_3/\text{ucs}$  'v'  $(\sigma_1/\text{ucs} - \sigma_3/\text{ucs})^2$

#### 4.3.4.2 Evaluation of Most Suitable Criterion for Predicting Failure of Coal Measure Strata

From the application of the Coal Measure Failure Criterion to Hassani's data sets it could be seen that in all cases the Coal Measure Failure Criterion produced a better fit to the triaxial data than the Hoek-Brown failure criterion. This is illustrated by the higher correlation coefficients shown in Table 4.6.

ROCK TYPE	CoD	CoD	Number of sets of data
	Hoek-Brown Criterion	Coal Measure Failure Criterion	
Seatearth	0.8805	0.9726	4
Mudstone	0.9355	0.9809	5
Siltstone	0.9407	0.9834	8
Fine sandstone	0.9544	0.9569	6
Medium sandstone	0.9279	0.9423	9
Coarse sandstone	0.8911	0.9322	4

Table 4.6 Coefficients of determination (CoD) calculated for Hoek-Brown failure criterion and Coal Measure Failure Criterion

The Coal Measure Failure Criterion has also produced good fits for triaxial test results for rock types other than Coal Measures and has been found to fit particular well to triaxial results obtained for salt (Lloyd 1998). However the criterion is not suitable for fitting to sparse triaxial data or when there is a large degree of scatter in the triaxial results.

To determine the strength of Coal Measure rock masses using the new criterion the reduction factors based on GSI determined by Hoek and Brown were utilised to allow the following relationships to be derived for  $GSI > 28$ .

$$\frac{m_{b1}}{m_{i1}} = \exp\left(\frac{GSI - 100}{28}\right) \quad (4.39)$$

$$\frac{m_{b2}}{m_{i2}} = \exp\left(\frac{GSI - 100}{28}\right) \quad (4.40)$$

$$s_b = \exp\left(\frac{GSI - 100}{9}\right) - \frac{1}{2} m_{b1} \left(\frac{\sigma_3}{\sigma_c}\right)^2 \quad (4.41)$$

## **4.4 MECHANICAL PROPERTIES OF ANISOTROPIC ROCKS**

### **4.4.1 Introduction**

Coal measure rocks are often anisotropic as they characteristically exhibit strength and stiffness properties that vary with direction due to the presence of lamination, bedding other planes of stratification and joints. Anisotropy exist on a variety of scales. It is present within intact samples due to the presence of fissility and laminations and on a larger scale due to the presence of bedding and also due to alternating beds of different rock types (Amadei 1996). Jointing within the coal measures also create directional variation in the rock's properties. This is especially pronounced within coal which is often closely jointed in the form of cleat. The significance of anisotropy to the behaviour of the strata adjacent to underground excavations is in the relationship between the redistribution of stress due to the excavation and the directions of anisotropy. In a laminated or bedded roof, shear along these planes may occur or within a coal rib the orientation of the cleat planes in relation to the roadway is of great significance.

### **4.4.2 Elastic Properties Of Stratified Rocks**

Elastic deformation of stratified rocks can be modelled by assuming the material to be either orthotropic or transversely isotropic.

#### **4.4.2.1 Orthotropy**

Orthotropy implies that there are three orthogonal planes of elastic symmetry within the rock mass. Orthotropy is exhibited by coal for instance where the cleat and bedding planes are assumed to be planes of elastic symmetry. Nine independent elastic constants are needed to describe the deformability of the material. In an x,y,z coordinate system  $E_x$ ,  $E_y$  and  $E_z$  are the Young's moduli in the x,y and z directions respectively.  $G_{xy}$ ,  $G_{xz}$  and  $G_{yz}$  are the shear moduli in planes parallel to the xy, xz and yz planes, respectively. The symbol  $\nu_{ij}$  ( $i,j = x,y,z$ ) are the Poisson's ratios that characterise the normal strains in the symmetry directions j when a stress is applied in the symmetry direction i. However Poisson's ratio's  $\nu_{ij}$  and  $\nu_{ji}$  are such that  $\nu_{ij}/E_i = \nu_{ji}/E_j$  reducing the required Poisons ratio required to characterise the material to three.

#### 4.4.2.2 Transverse Isotropy

A transversely isotropic medium is characterised by a plane of elastic symmetry. The only other axis of isotropic symmetry is the line perpendicular to this plane (Figure 4.12). Transverse isotropy is exhibited by stratified rocks where the plane of stratification represents the plane of isotropy. There are also distinctly different elastic modulus perpendicular and parallel to the layers. Five unique constants are required to determine the elastic deformation of a transversely isotropic material.  $E_{xy}$  and  $E_z$  which are the Young's Modulus in the plane of stratification perpendicular to the plane of stratification respectively.  $v_{xy}$  and  $v_z$  which are the Poisson's Ratio in the plane of stratification and perpendicular to the plane of stratification respectively.  $G_{xy}$  which is the shear modulus in planes perpendicular to the plane of stratification.

The shear modulus between the plane of isotropy and normal plane can be very difficult to determine experimentally using direct testing methods, (Chen et al 1993). However the modulus is often expresses in terms of  $E_{xy}$ ,  $E_z$   $v_{xy}$  and  $v_z$  through the following empirical equation (Amadei 1992) (Equation 4.42).

$$\frac{1}{G_{xy}} = \frac{1}{E_{xy}} + \frac{1}{E_z} + 2 \frac{v_z}{E_z} \quad (4.42)$$

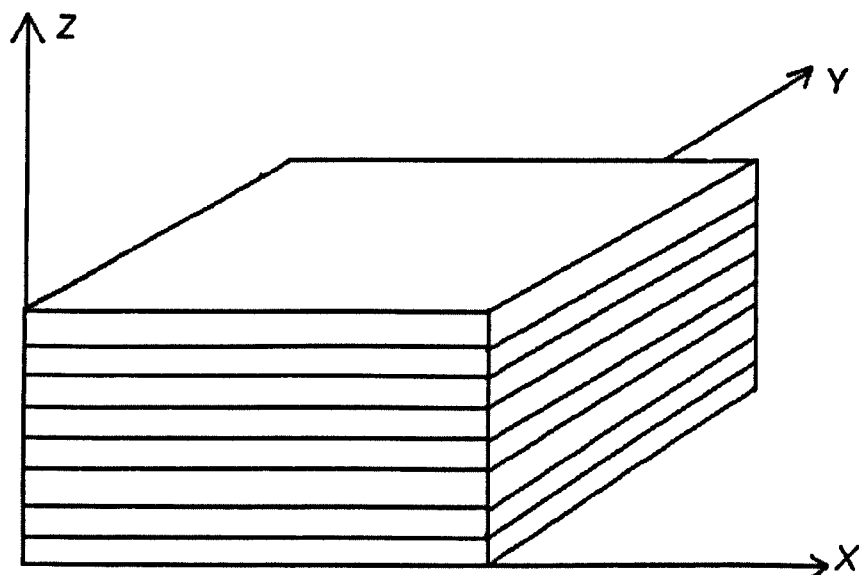


Figure 4.12 A transversely isotropic body for which the x,y plane is the plane of isotropy

#### 4.4.3 Failure Criteria For Anisotropic Rocks

Anisotropic failure theories have been developed by several authors to predict the strength of anisotropic rocks. Generally they are based on the presence of a single plane of weakness within intact rock. For simplicity the theories considered the situation to be two-dimensional and it would be more accurate to use the term transversely orthotropic (Yasar et al 1998).

Figure 4.13 shows the variation in strength with orientation of laminations ( $\beta$ ) to the maximum principal stress for a laminated siltstone. Four anisotropic failure criteria were fitted to determine the criterion that best fitted the test results. The four criterions were the Single Plane of Weakness theory (Jaeger, 1960) (SPW), Walsh-Brace theory (1964) (WB), the Continuously Variable Cohesive Strength theory (Jaeger, 1960) (CV) and Variable Friction Angle and Cohesive Strength theory (Donath, 1972) (VF/VC).

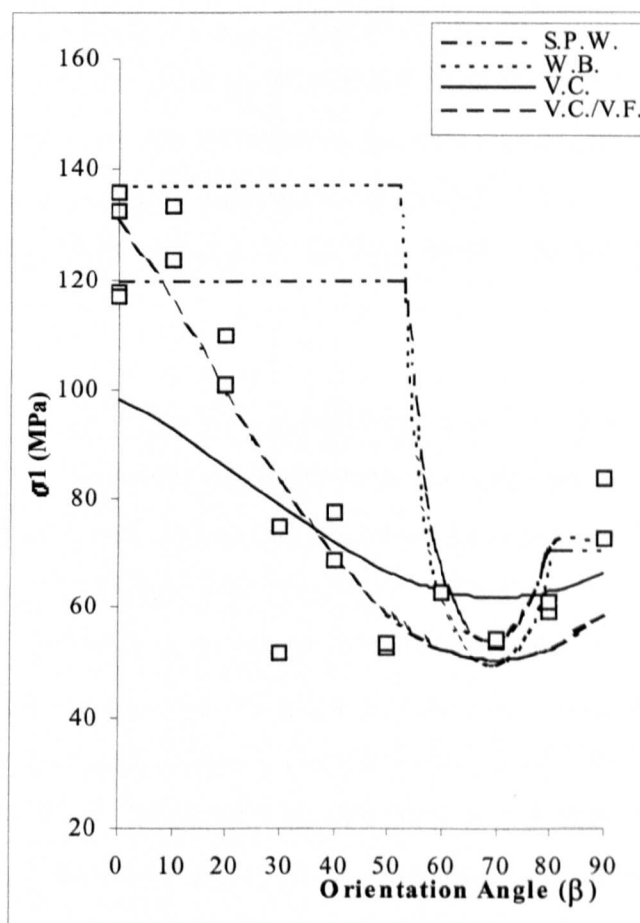


Figure 4.13 Application of anisotropic failure theories to a Middle Coal Measure laminated siltstone (After Yasar et al 1998)  $\sigma_3 = 4$  MPa

As the effect of the intermediate principal stress is not accounted for in these criteria they are unsuitable for predicting the strength of anisotropic rocks under more complex loading conditions that are normally found in-situ. Amadei (1989) developed a model to predict anisotropic rock mass strength that described the intact rock strength by the non-linear Hoek-Brown failure criteria and the joint surface by a linear Coulomb criteria. The criteria took into account the resolved stresses on the joint surface in a multiaxial stress state. The joint failure surface predicted by his model was conic in  $\sigma_1$ ,  $\sigma_2$ ,  $\sigma_3$  space..

## 4.5 ROCK MASS CLASSIFICATIONS

### 4.5.1 Introduction

Rock excavation design prior to modern day rock engineering was probably undertaken using rules of thumb with much depending on the engineers previous experience of constructing excavations in similar rock conditions. These engineers would have observed the success or otherwise of their excavation designs and used this knowledge in future projects. Rock mass classifications were developed to allow a common method of communicating the knowledge on rock mass conditions. Correlation of rock mass classification and installed support allowed the supports requirement for future projects to be empirically predicted from the rock mass classification.

The first widely used rock mass classification was developed over 50 years ago by Terzaghi. Terzaghi's (1946) classification was qualitative being based on broad descriptions of the rock mass. Subsequently quantitative classification, originally based on single parameters was developed. Modern rock mass classifications are typically multi-parameter more quantitative classifications. Such classifications were first introduced approximately 30 years ago and were originally validated on hard rock tunnelling. The output from multi-parameter classifications was usually a single numerical value. This value was originally used in empirical relationships to predict required support and stand-up times for unsupported excavations (Wickham et al 1974). Although it was originally envisaged that a multi-parameter classification should be general enough to be applied to all rock engineering projects subsequently

many rock mass classifications have been developed for specific applications. The increasing use of numerical modelling techniques within rock engineering has lead to the use of the classification values within empirical rock mass failure criteria to predict the strength and stiffness properties of the rock mass. The next section of this chapter reviews some of the better known and important classifications systems.

#### **4.5.2 Terzaghi's Rock Load Height Classification**

Terzaghi, using his experience of the behaviour of steel supported railway tunnels in the Alps proposed a simple classification for use in estimating the loads to be supported by the steel supports in tunnels. He based his rock mass classification on six broad rock mass conditions which are defined below:

*Intact rock contains neither joints nor hair cracks. Hence, if it breaks, it breaks across sound rock. On account of the injury to the rock due to blasting, spalls may drop off the roof several hours or days after blasting. This is known as a spalling condition. Hard, intact rock may also be encountered in the popping condition involving the spontaneous and violent detachment of rock slabs from the sides or roof.*

*Stratified rock consists of individual strata with little or no resistance against separation along the boundaries between strata. The strata may or may not be weakened by transverse joints. in such rock, the spalling condition is quite common.*

*Moderately jointed rock contains joints and hair cracks, but the blocks between joints are locally grown together or so intimately interlocked that vertical walls do not require lateral support. In rocks of this type, both spalling and popping conditions may be encountered.*

*Blocky and seamy rock consists of chemically intact or almost intact rock fragments which are entirely separated from each other and imperfectly interlocked. in such rock, vertical walls may require lateral support. Crushed but chemically intact rock has the character of a crusher run. If most or all of the fragments are as small as fine sand grains and no re-cementation has taken place, crushed rock below the water table exhibit the properties of a water-bearing sand.*

**Squeezing rock** slowly advances into the tunnel without perceptible volume increase. A prerequisite for squeeze is a high percentage of microscopic and sub-microscopic particles of micaceous minerals or of clay minerals with a low swelling capacity.

**Swelling rock** advances into the tunnel chiefly on account of expansion. The capacity to swell seems to be limited to those rocks which contain clay minerals such as montmorillonite, with a high swelling capacity.

Terzaghi used the above classification to estimate the rock load to be carried by the steel arches. He suggested that during tunnel construction relaxation of the rock mass will occur above and on the sides of the tunnel. His concept is illustrated in Figure 4.14 and Table 4.7.

The loosened rock within the area defined by acdb in Figure 4.14 will tend to move towards the tunnel. However frictional forces developed along the boundaries a-c and b-d resist this movement and in doing so transfer most of the overburden weight ( $W$ ) onto the rock mass on either side of the tunnel. The roof and sides of the tunnel are therefore required only to support the balance which is equivalent to a height  $H_p$

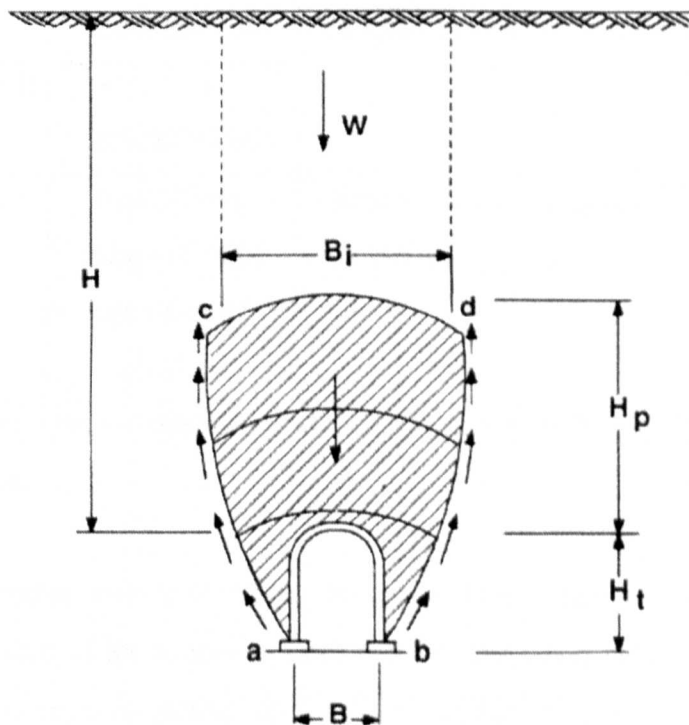


Figure 4.14 The tunnel rock-load concept of Terzaghi (1946)

Rock condition	Rock load height Hp in ft	Remarks
1. Hard and intact	Zero	Light lining required only if spalling or popping occurs
2 Hard stratified or schistose	0 to 0.5B	Light support, mainly for protection against spalls. Load may change erratically from point to point
3 Massive, moderately jointed	0 to 0.25B	
4. Moderately blocky and seamy	0.25B to 0.35(B+Ht)	No side pressure
5, Very blocky and seamy	(0.35 to 1.10)(B+ Ht)	Little or no side pressure
6 Completely crushed but chemically intact	1.10(B+Ht)	Considerable side pressure. Softening effects of seepage towards bottom of tunnel requires continuous support for lower ends of ribs or circular ribs
7 Squeezing rock, moderate depth	(1.10 to 2.10)(B+Ht)	Heavy side pressure, invert struts required. Circular ribs are recommended
8. Squeezing rock great depth	(2.10 to 4.50)(B+Ht)	
9. Swelling Rock	Upto 250 ft, irrespective of the value of (B+Ht)	Circular ribs are required. In extreme cases use yielding support.

Table 4.7 Terzaghi's recommendations of support in steel arch supported Tunnels.

The rock load heights were determined for the condition that the tunnel is located under the water table. If the tunnel is located above the water table the rock load for rock type 4 to 6 Terzaghi recommended that the load should be reduced by 50%.

#### 4.5.3 Lauffer's Classification

Lauffer's classification of 1958 has had a significant influence upon the development of later rock mass classifications. Lauffer based his work on earlier work by Stini who had emphasised the importance of structural defects in the rock mass and their orientation in relation to the tunnel orientation. He suggested that the time dependent stability of an unsupported tunnel was related to the condition of the rock mass. He introduced the concept of stand up time and active span. The stand up time is the length of time which an underground opening will stand unsupported after excavation while the active span is the largest unsupported span in the tunnel section between the face and supports. His relationship between active span rock mass class and stand-up time is shown in Figure 4.15. The letters refer to rock mass class with A being very good rock corresponding to Terzaghi's hard and intact rock while G is very poor rock corresponding to Terzaghi's squeezing or swelling rock (Hoek and Brown 1980). This concept has lead to the development of the modern New Austrian Tunnelling Method which is widely used to day. (Bieniawski 1989)

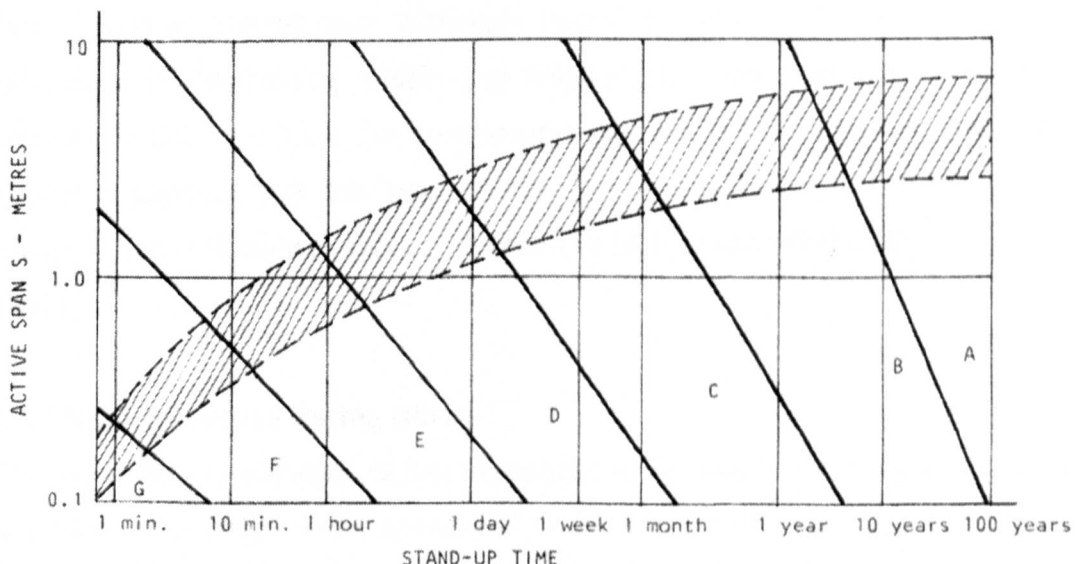


Figure 4.15 Relationship between active span, rock class and stand up time

#### 4.5.4 Rock Quality Designation (RQD) Index

The RQD Index (Deere 1964) was developed as a modified core recovery percentage. Since its introduction it is now standardly applied in drill core logging and forms a basic element of several rock mass classification schemes. The RQD Index was the first quantitative method of rock mass classification, assigning a numerical number to

the rock mass quality. The Index is calculated by summing the length of sound core pieces greater than 10 cm and expressing this length as a percentage of the total core run. Deere (1968) related the RQD to a basic description of rock quality (Table 4.8).

RQD	Rock quality
0 to 25 %	Very poor
25 to 50 %	Poor
50 to 75 %	Fair
75 to 90 %	Good
90 to 100 %	Excellent

Table 4.8 Relationship between RQD index and the engineering quality of the rock mass (Deere 1968).

The RQD Index has a number of drawbacks as a sole descriptor of rock quality. It does not account for rock strength, joint orientation, joint character or environmental factors such as groundwater. Although simple in concept, its application involves judgement in determining which core lengths are sound (Deere et al 1988). The arbitrary length of 10 cm for core lengths has also been questioned with various authors suggesting that this length should be a function of core diameter and no consideration is taken into account of core loss (Bikerman and Mantab 1986 , Hassagi 1969).

#### 4.5.5 Rock Structure Rating (RSR)

The Rock Structure Rating (RSR) classification developed by Wickham, Tiedeman and Skinner in 1972 can be considered as the first modern rock mass classification (Wickham et al 1974). The classification consists of three basic parameters that Wickham et al (1974) considered to influence the support requirement of rock tunnels. A feature of the RSR classification is that the parameter values are weighted with respect to their relative effect on the requirements of structural support in tunnels (Wickham et al 1974). This allowed a final qualitative rating to be assigned to the rock mass which consisted of the sum of the weighted ratings for each parameter. The rating system was determined on the basis of case histories as well as reviews of

books and technical papers dealing with the different aspects of ground support in tunnelling.

The three parameters 'A', 'B' and 'C' and their respective ratings are given in Tables 4.9, 4.10 and 4.11 respectively:

Parameter 'A' is a general appraisal of the rock structure through which the tunnel is driven. Parameter 'B' relates to the joint pattern (strike, dip and joint spacing) and the direction of drive. Parameter 'C' takes into consideration the following: 1) the overall quality of the rock as indicated by the numerical sum of values assigned to parameters 'A' and 'B' 2) the condition of the joint surfaces and 3) the anticipated amount of water inflow.

The classification was not intended to technically define specific support at a particular location in a tunnel, but rather to provide the means by which overall ground support requirements of a tunnel can be reasonably estimated prior to tunnel construction (Wickham et al 1974).

In order to correlate RSR values with actual support installations Wickham developed a Rib Ratio concept. For steel rib supports, which were commonly used in tunnelling at that time, he calculated theoretical spacing for various sized ribs and tunnel diameters based on roof loads calculated using Terzaghi's formula for determining roof loads in loose sand below the water table. The rib ratio for an actual tunnel was calculated by dividing the theoretical spacing by the actual spacing and multiplying by 100. Wickham et al (1974) empirically determined a relationship between Rock Structure Rating and Rib Ratio (RR) (Equation 4.41)

$$(RR + 80)(RSR + 30) = 8800 \quad (4.41)$$

Rib ratios varying between 0 (no support) and 100 (heavy support) and correspond to RSR values of 19 and 80 respectively.

Wickham et al (1974) also developed empirical relationships between rock load and RSR. He used this relationship to extend the use of the rating for predicting shotcrete

ROCK STRUCTURE RATING PARAMETER "A" GENERAL AREA GEOLOGY					MAX. VALUE 30
BASIC ROCK TYPE				GEOLOGICAL STRUCTURE	
IGNEOUS	HARD	MED	SOFT	DECOMP.	MASSTIVE
IGNEOUS	1	2	3	4	SLIGHTLY FAULTED OR FOLDED
METAMORPHIC	1	2	3	4	MODERATELY FAULTED OR FOLDED
SEDIMENTARY	2	3	4	4	INTENSELY FAULTED OR FOLDED
TYPE 1					30      22      15      9
TYPE 2					27      20      13      8
TYPE 3					24      18      12      7
TYPE 4					19      15      10      6

Table 4.9 Rock Structure Rating, Parameter A (after Wickham et al 1974)

ROCK STRUCTURE RATING PARAMETER "B" JOINT PATTERN DIRECTION OF DRIVE		MAX. VALUE 45					
		STRIKE $\perp$ TO AXIS		STRIKE $\parallel$ TO AXIS		DIRECTION OF DRIVE	
BOTH	WITH DIP	AGAINST DIP		BOTH		DIP OF PROMINENT JOINTS	
		FLAT	DIPPING	VERTICAL	DIPPING	FLAT	DIPPING
(1) VERY CLOSELY JOINTED	9	11	13	10	12	9	9
(2) CLOSELY JOINED	13	16	19	15	17	14	14
(3) MODERATELY JOINED	23	24	28	19	22	23	23
(4) MODERATE TO BLOCKY	30	32	36	25	28	30	28
(5) BLOCKY TO MASSIVE	36	38	40	33	35	36	34
(6) MASSIVE	40	43	45	37	40	40	38

NOTES: Flat 0 - 20°; Dipping 20° - 50°; Vertical 50° - 90°

Table 4.10 Rock Structure Rating, Parameter B (after Wickham et al 1974)

ROCK STRUCTURE RATING PARAMETER "C" GROUND WATER JOINT CONDITION		MAX. VALUE 25					
		SUM OF PARAMETERS A + B					
ANTICIPATED WATER INFLOW (GPM/1000')	13 - 44			45 - 75			
	GOOD	FAIR	POOR	GOOD	FAIR	POOR	
NONE	22	18	12	25	22	18	
SLIGHT (<200 gpm)	19	15	9	23	19	14	
MODERATE (200-1000 gpm)	15	11	7	21	16	12	
HEAVY (>1000 gpm)	10	8	6	18	14	10	

Joint Condition: Good = Tight or Cemented; Fair = Slightly Weathered or Altered; Poor = Severely Weathered, Altered, or Open

Table 4.11 Rock Structure Rating Parameter C (after Wickham et al 1974)

thickness and rock bolt spacing. However these relationships have not been properly validated with application to enough case studies and therefore the RSR concept was not recommended for selection of rock bolt and shotcrete support (Bieniawski 1989).

#### **4.5.6 Rock Mass Rating (Geomechanics Classification)**

In 1973 Bieniawski proposed a rock mass classification for estimating the necessary support measures required in rock tunnels (Bieniawski 1974). His classification was based on the following six parameters which after detailed studies he considered were the most significant parameters that influenced the engineering behaviour of rock masses:

- 1) uniaxial compressive strength of rock material
- 2) drill core quality (RQD)
- 3) spacing of joints
- 4) orientation of joints
- 5) conditions of joints
- 6) groundwater flow

The classification is applied to each different structural region within the rock mass. A structural region is defined by a zone of rock where the rock mass condition is uniform. Bieniawski considered that the boundaries of the structural regions will usually coincide with major geological features such as faults, dykes shear zones etc.

After the structural regions have been identified the classification parameters are measured to allow determination of the corresponding classification ratings. Bieniawski initially assigned importance ratings derived by Wickham et al (1974) to the different ranges of the parameters (Bieniawski 1973). The ratings for each of the classification parameters are summed to yield the basic RMR.

Adjustment to the basic RMR value is made to account for the influence of the strike and dip of the discontinuities in relation to the tunnel orientation.

Based on experience in applying the RMR system Bieniawski has made several changes, since 1973 to the importance weightings used in the classification, although

the classification parameters apart from the groundwater parameter have remained unaltered. Table 4.12 and 4.13 give the 1976 and most recent 1989 classification. Although originally developed for tunnelling, Bieniawski subsequently proposed joint adjustment ratings for foundations and slopes (Table 4.14) (Bieniawski 1976). To enable a decision to be made for the favourability of the joint orientation for tunnelling Bieniawski proposed Table 4.17 which is based on studies by Wickham et al (1974).

After the basic rock mass rating has been adjusted to account for joint orientation the rock mass can be classified into five groups in accordance with Table 4.15 and the practical meaning of each rock mass class is determined using Table 4.16.

The RMR classification concept has been developed further, by other workers, for a wide range of different mining and civil engineering applications. To be of use in the design of a structure, empirical relationships have been established between the RMR value and design parameters such as rock mass strength and stiffness, tunnel support requirements, factors of safety, stand-up times and support loads. Different parameters and importance weightings specific to the application have been incorporated within the RMR classification extensions. Table 4.18 lists major extensions of the RMR classification (after Hudson 1986).

<b>Originator and Date</b>	<b>Country of origin</b>	<b>Applications</b>
Laubscher, 1977	South Africa	Mining
Ghose and Raju, 1981	India	Coal mining
Kendorski et al, 1983	USA	Hard rock mining
Serafim and Pereira, 1983	Portugal	Foundations
Gonzales de Vallejo	Spain	Tunnelling
Unal, 1983	USA	Roof bolting/ coal
Romana, 1985	Spain	Slope stability
Newman, 1985	USA	Coal mining
Venkateswarlu, 1986	India	Coal mining
Robertson, 1988	Canada	Tunnelling

Table 4.18 Rock Mass Rating Extensions (after Hudson 1996)

PARAMETER			RANGES OF VALUES					
1	Strength of intact rock	Point load strength index	> 8 MPa	4-8 MPa	2-4 MPa	1-2 MPa	For this low range uniaxial compressive strength is preferred	
		Uniaxial compressive strength	> 200 MPa	100-200 MPa	50- 100 MPa	25-50 MPa	10- 25 MPa	3-10 MPa
	rating	15	12	7	4	2	1	0
2	Drill core quality	90%-100%	75%-90%	50%-75%	25%-50%	< 25%		
	rating	20	17	13	8	3		
3	Spacing of joints	> 3 m	1-3 m	0.3-1 m	50-300 mm	< 50mm		
	rating	30	25	20	10	5		
4	Condition of joints		Very rough surfaces. Not continuous , no separation, hard joint wall rock	Slightly rough surfaces. Separation < 1mm Hard joint wall rock	Slightly rough surfaces Separation < 1mm soft wall rock	Slickensides surfaces OR Gouge < 5mm thick OR joints open 1-5mm. Continuous joints	Soft gouge >5mm thick OR Joints open >5mm continuous joints	
	rating	25	20	12	6	0		
5	Ground water	Inflow per 10m tunnel length	None		< 25 litres/min	25-125 litres/min	> 125 litres/min	
		Ratio joint water pressure/major principal stress	0		0.0-0.2	0.2-0.5	>0.5	
		General conditions	Completely dry		Moist only (interstitial water)	Water under moderate pressure	Severe water problems	
	rating	10	4		7	0		

Table 4.12 1976 Rock Mass Rating System (after Beiniawski 1976)

PARAMETER			RANGES OF VALUES					
1	Strength of intact rock	Point load strength index	> 8 MPa	4-8 MPa	2-4 MPa	1-2 MPa	For this low range uniaxial compressive strength is preferred	
		Uniaxial compressive strength	> 200 MPa	100-200 MPa	50- 100 MPa	25-50 MPa	10- 25 MPa	3-10 MPa
	rating	15	12	7	4	2	1	0
2	Drill core quality	90%-100%	75%-90%	50%-75%	25%-50%	< 25%		
	rating	20	17	13	8	3		
3	Spacing of joints	> 3 m	1-3 m	0.3-1 m	50-300 mm	< 50mm		
	rating	20	15	10	8	5		
4	Condition of joints		Very rough surfaces. Not continuous , no separation, hard joint wall rock	Slightly rough surfaces. Separation < 1mm Hard joint wall rock	Slightly rough surfaces Separation < 1mm soft wall rock	Slickensides surfaces OR Gouge < 5mm thick OR joints open 1-5mm. Continuous joints	Soft gouge >5mm thick OR Joints open >5mm continuous joints	
	rating	30	25	20	10	0		
5	Ground water	Inflow per 10m tunnel length	None	<10	10- 25 litres/min	25-125 litres/min	< 25 litres/min	
		Ratio joint water pressure/major principal stress	0	<0.1	0.1-0.2	0.2-0.5	0.0-0.2	
		General conditions	Completely dry	damp	wet	dripping	flowing	
	rating	15	10	7	4	0		

Table 4.13 1989 Rock Mass Rating System (after Beiniawski 1989)

Strike and dip orientations of joints		Very favourable	favourable	fair	unfavourable	Very unfavourable
Ratings	tunnels	0	-2	-5	-10	-12
	foundations	0	-2	-7	-15	-25
	slopes	0	-5	-25	-50	-60

Table 4.14 Joint Orientation Adjustment rating (after Beiniawski 1976)

Rating	100 to 81	80 to 61	60 to 41	40 to 21	< 21
Class number	I	II	III	IV	V
Description	Very good rock	Good rock	Fair rock	Poor rock	Very poor rock

Table 4.15 Relationship between RMR and rock mass quality (after Beiniawski 1976)

Class number	I	II	III	IV	V
Average stand up time	10 years for 5 m span	6 months for 4 month span	1 week for 3 m span	5 hours for 1.5 m span	10 minutes for 0.5 m span
Cohesion of the rock mass	> 300 KPa	200-300 KPa	150-200 KPa	100-150 KPa	< 100 KPa
Friction angle of the rock mass	> 45°	40° – 45°	35° – 40°	30° – 35°	30°

Table 4.16 Stand up time and rock strength for different rock classes  
(after Beiniawski 1976)

Strike perpendicular to tunnel axis				Strike parallel to tunnel axis		Dip 0-20° irrespective of strike
Drive with dip		Drive against dip		Dip 45-90°	Dip 20-45°	
Dip 45- 90°	Dip 20– 45°	Dip 45-90°	Dip 20-45°	Dip 45-90°	Dip 20-45°	
Very favourable	favourable	fair	unfavourable	Very unfavourable	fair	unfavourable

Table 4.17 Joint orientations for tunneling

Bieniawski (1989) produced a summary chart of adjustments to the basic RMR value that should be considered for mining applications (Figure 4.16). This chart was based on Laubscher's (1977) and Kendorski's (1983) RMR extension classifications for hard rock mining.

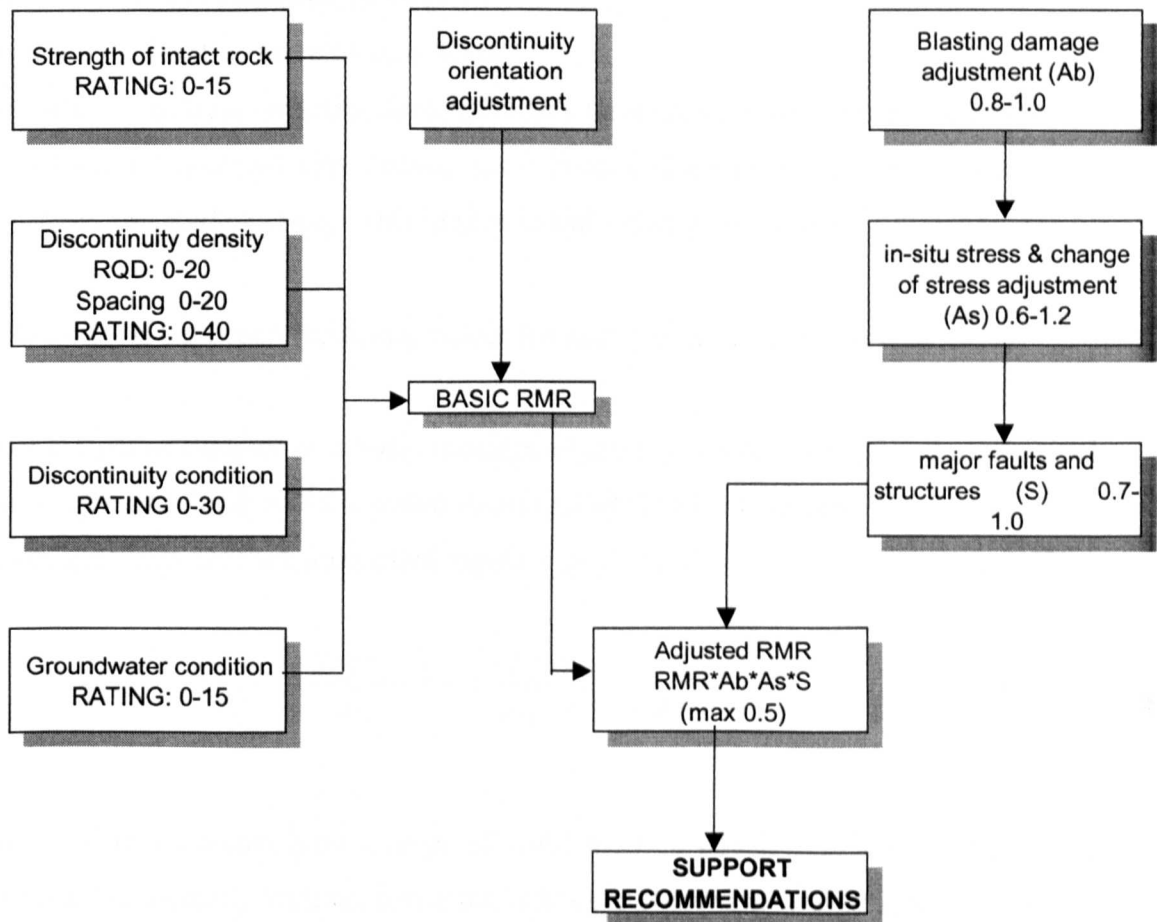


Figure 4.16 Adjustments to the RMR System for Mining (after Bieniawski 1989)

#### 4.5.7 NGI Tunnelling Quality Index ('Q' Index)

Barton, Lein and Lunde whilst working for the Norwegian Geotechnical Institute (NGI) proposed an index for the tunnelling quality of a rock mass that is now popular known as the 'Q' (quality) Index (Barton et al 1974). Their 'Q' Index was originally developed for and validated on hard rock tunnels in Scandinavia, but has become widely used for many other applications.

The ‘Q’ index is based on determining importance values for six parameters which are:

- 1) RQD is Deere’s Rock Quality Designation Index
- 2) Jn is joint set number
- 3) Jr is joint roughness number
- 4) Ja is joint alteration number
- 5) Jw is joint water reduction factor
- 6) SRF is a stress reduction factor; this is a measure of 1) loosening load in the case of shear zones and clay bearing rock 2) rock stress in competent ground and 3) squeezing and swelling loads in plastic and incompetent rock)

Table 4.19 gives descriptions and values for each parameter (Barton et al 1974).

The six parameters allow a basic measure of the block size ( $RQD/J_n$ ) , the interblock shear strength ( $J_r/J_a$ ) and the active stress ( $J_w/SRF$ ) to be determined.

Three quotients are then multiplied together to obtain the ‘Q’ Index (Equation 4.42)

$$Q = \left( \frac{RQD}{J_n} \right) \times \left( \frac{J_r}{J_a} \right) \times \left( \frac{J_w}{SRF} \right) \quad (4.42)$$

The ‘Q’ Index values have a range of 0.001 to 1000 which relate logarithmically to the rock mass quality with the lower the Index the poorer the quality of the rock mass.

To allow the Q index to be related to tunnels with different sizes, an equivalent dimension (ED) is defined for the excavation. The equivalent dimension which is a function of both the size and the purpose of the excavation is obtained by dividing the span, diameter or the wall height of the excavation by a quantity called the excavation support ratio (ESR) (Equation 4.43)

$$ED = \frac{\text{span - or - height (m)}}{ESR} \quad (4.43)$$

The ESR values which are related to the proposed use of the excavation and the degree of safety required have been listed in Table 4.20.

DESCRIPTION	VALUE	NOTES
<b>I. ROCK QUALITY DESIGNATION</b>	<b>RQD</b>	
A. Very poor	0 - 25	1) Where RQD is reported or measured as <= including 0 ), a nominal value of 10 is used to evaluate Q.
B. Poor	25 - 50	
C. Fair	50 - 75	
D. Good	75 - 90	
E. Excellent	90 - 100	2). RQD intervals of 5, i.e. 100, 95, 90 etc are sufficiently accurate.
<b>2. JOINT SET NUMBER</b>	<b>Jn</b>	
A. Massive, no or few joints	0.5 - 1.0	
B. One joint set	2	
C. One joint set plus random	3	
D. Two joint sets	4	
E. Two joint sets plus random	6	
F. Three joint sets	9	1. For intersections use (3 x Jn)
G. Three joint sets plus random	12	2. For portals use (2 x Jn)
H. Four or more joint sets, random, heavily jointed 'sugar cube', etc	15	
J. Crushed rock, earth-like	20	
<b>3. JOINT ROUGHNESS NUMBER</b>	<b>Jr</b>	
<i>a. rock wall contact and</i>		
<i>b. rock wall contact before</i>		
<i>10 cms shear.</i>		
A. Discontinuous joints	4	
B. Rough or irregular, undulating	3	
C. Smooth, undulating	2	
D. Slickensided, undulating	1.5	1. Add 1.0 if the mean spacing of the relevant joint set is greater than 3m.
E. Rough or irregular, planar	1.5	2. Jr = 0.5 can be used for planar, slick-slickensided joints having lineations, provided the lineations are orientated for minimum strength.
F. Smooth, planar	1.0	
G. Slickensided, planar	0.5	
<i>c. :no rock wall contact when sheared.</i>		
H. Zone containing clay minerals thick enough to prevent rock wall contact.	1.0	
J. Sandy, gravelly or crushed zone thick enough to prevent rock wall contact.	1.0	
<b>4. JOINT ALTERATION NUMBER</b>	<b>Ja</b>	$\phi r$ (approx.) Values of $r$ , the residual friction angle are intended as an approximate guide to the mineralogical properties of the alteration products if present
<i>a. Rock wall contact.</i>		
A. Tightly healed, hard, non-softening, impermeable filling	0.75	-
B. Unaltered joint walls, surface staining only	1.0	(25° - 35°)
C. Slightly altered joint walls non-softening mineral coatings, sandy particles, clay-free disintegrated rock, etc	2.0	(25° - 30°)
D. Silty, or sandy-clay coatings, small clay-fraction (non-softening)	3.0	(20°-25°)

E. Softening or low friction clay mineral coatings, i.e. kaolinite, mica. Also chlorite, talc, gypsum and graphite etc., and small quantities of swelling clays. (Discontinuous coatings, 1-2mm or less in thickness)	4.0	(8° - 16°)
<b>b. Rock wall contact before 10 cms shear.</b>		
F. Sandy particles, clay-free disintegrated rock etc	4.0	(25°-30°)
G. Strongly over-consolidated, non-softening clay mineral fillings (continuous, < 5mm thick)	6.0	(16° - 24°)
H. Medium or low over-consolidation, softening, clay mineral fillings, (continuous, < 5mm thick)	8.0	(12°-16°)
J. Swelling clay fillings, i.e. montmorillonite (continuous, < 5 mm thick ). Values of Ja depend on percent of swelling clay-size particles, and access to water	8.0-12.0	(6°-12°)
<b>c. No rock wall contact when sheared.</b>		
K. Zones or bands of disintegrated L, or crushed rock and clay (see M. G,H and J for clay conditions)	6.0 8.0 8.0 - 12.0	(6°-24 °)
N. Zones or bands of silty or sandy clay, small clay fraction, (non-softening)	5.0	
Q. Thick, continuous zones or P. bands of clay ( see G, H and R. J for clay conditions)	10.0-13.0 13.0-20.0	(6° -24 °)
<b>5. JOINT WATER REDUCTION FACTOR</b>		
A. Dry excavations or minor inflow, i.e. < 5 lit/min. locally	Jw 1.0	approx water pressure (Kgf/cm <sup>2</sup> ) <1.0
B. Medium inflow or pressure, occasional outwash of joint fillings estimates.	0.66	1.0- 2.5
C. Large inflow or high pressure in competent rock with unfilled joints	0.5	2.5 - 10.0
D. Large inflow or high pressure considerable outwash of fillings	0.33	2.5-10.0
E. Exceptionally high inflow or pressure at blasting, decaying with time		1. Factors C to F are crude Increase Jw if drainage measures are installed
F. Exceptionally high inflow or pressure continuing without decay		2. Special problems caused by ice are not considered
<b>6. STRESS REDUCTION FACTOR</b>		
<i>a. Weakness zones intersecting excavation, which may cause Loosening of rock mass when tunnel is excavated.</i>		
A. Multiple occurrences of weakness zones containing clay or chemically disintegrated rock, very loose surrounding rock (any depth) not	SRF 10.0	1. Reduce these values of SRF by 25-50% if the relevant shear zones only influence but do
B. Single weakness zones containing clay, or chemically disintegrated rock (excavation depth < 50m)	5.0	intersect the excavation
C. Single weakness zones containing clay, or chemically disintegrated rock (excavation depth > 50m)	2.5	2. See below
D. Multiple shear zones in competent rock (clay free), loose surrounding rock (any depth )	7.5	3. See below
E. Single shear zones in competent rock (clay free), (depth of excavation < 50m)	5.0	
F. Single shear zones in competent rock (clay free),	2.5	

(depth of excavation > 50m)	
G. Loose open joints, heavily jointed or 'sugar cube' (any depth)	5.0

**b. Competent rock, rock stress problems**

	$\sigma_c/\sigma_1$	$\sigma_t/\sigma_1$	SRF
H. Low stress, near surface	>200	>13	2.5
J. Medium stress	200-10	13-0.66	1.0
K. High stress, very tight structure (usually favourable to stability, may be unfavourable for wall stability)	10-5	0.66-0.33	0.5-2
L. Mild rock burst (massive rock)	5-2.5	0.33-0.16	5-10
M. Heavy rock burst (massive rock)	<2.5	<0.16	10-20

**c. Squeezing rock, plastic flow of incompetent rock under the influence of high rock pressure**

	SRF
N. Mild squeezing rock pressure	5-10
O. Heavy squeezing rock pressure	10-20

**d. Swelling rock, chemical swelling activity depending upon presence of water**

	SRF
P. Mild swelling rock pressure	5-10
R. Heavy swelling rock pressure	10-20

**2. For strongly anisotropic virgin stress field (if measures**

For strongly anisotropic virgin stress field (if measured) : when  $5 \leq \sigma_1/\sigma_3 \leq 10$ , reduce  $\sigma_c$  to  $0.8\sigma$  and  $\sigma_t$  to  $0.8\sigma_t$ . When  $\sigma_1/\sigma_3 > 10$ , reduce  $\sigma_c$  and  $\sigma_t$  to  $0.6\sigma_c$  and  $0.6\sigma_t$ , where  $\sigma_c$  = unconfined compressive strength, and

$\sigma_t$  = tensile strength (point load) and  $\sigma_1$  and  $\sigma_3$  are the major and minor principal stresses.

3. Few case records available where depth of crown below surface is less than span width. Suggest SRF increase from 2.5 to 5 for such cases (see H).

#### ADDITIONAL NOTES ON THE USE OF THESE TABLES

When making estimates of the rock mass quality (Q) the following guidelines should be followed, in addition to the notes listed in the tables:

1. When borehole core is unavailable, RQD can be estimated from the number of joints per unit volume, in which the number of joints per metre for each joint set are added. A simple relation can be used to convert this number to RQD for the case of clay free rock masses :

$$RQD = 115 - 3.3J_v \text{ (approx.)} \quad \text{where } J_v = \text{total number of joints per m}^3 \\ (RQD = 100 \text{ for } J_v < 4.5)$$

2. The parameter  $J_n$  representing the number of joint sets will often be affected by foliation, schistosity, slaty cleavage or bedding etc. If strongly developed these parallel "joints" should obviously be counted as a complete joint set. However, if there are few "joints" visible, or only occasional breaks in the core due to these features, then it will be more appropriate to count them as "random joints" when evaluating  $J_n$ .

3. The parameters  $J_r$  and  $J_a$  (representing shear strength) should be relevant to the weakest significant joint set or clay filled discontinuity in the given zone. However, if the joint set or discontinuity with the minimum value of  $(J_r/J_a)$  is favourably oriented for stability, then a second, less favourably oriented joint set or discontinuity may sometimes be more significant, and its higher value of  $J_r/J_a$  should be used when evaluating Q . The value of  $J_r/J_a$  should in fact relate to the surface most likely to allow failure to initiate.

4. When a rock mass contains clay, the factor SRF appropriate to Loosening Loads should be evaluated. In such cases the strength of the intact rock is of little interest. However, when jointing is minimal and clay is completely absent the strength of the intact rock may become the weakest link, and the stability will then depend on the ratio rock-stress/ rock-strength. A strongly anisotropic stress field is unfavourable for stability and is roughly accounted for as in note 2 in the table for stress reduction factor evaluation.

5. The compressive and tensile strengths ( $\sigma_c$  and  $\sigma_t$ ) of the intact rock should be evaluated in the saturated condition if this is appropriate to present or future in situ conditions. A very conservative estimate of strength should be made for those rocks that deteriorate when exposed to moist or saturated conditions

Table 4.19 The NGI Tunneling Quality ('Q' Index) rock mass classification  
(after Barton et al 1974)

Excavation Category	ESR	
Temporary mine openings	3 to 5	
Vertical shafts	Circular section	2.5
	Rectangular/square section	2.0
Permanent mine openings, water tunnels for hydroelectric power (excluding high pressure penstocks), pilot tunnels, drifts, and headings for large excavations	1.6	
Storage caverns, water treatment plants, minor highway and railroad tunnels, surge chambers, access tunnels	1.3	
Power stations, major highway or railroad tunnels, civil defense chambers, portals intersections	1.0	
Underground nuclear power stations, railroad stations, factories	0.8	

Table 4.20 ESR values (after Barton 1974)

The relationship between the ‘Q’ Index and the equivalent dimension  $D_e$  of an excavation that will stand unsupported is shown in Figure 4.17. Barton produced comprehensive guidelines on support requirements required in tunnels based on the ‘Q’ index and the equivalent dimensions (Barton et al 1974).

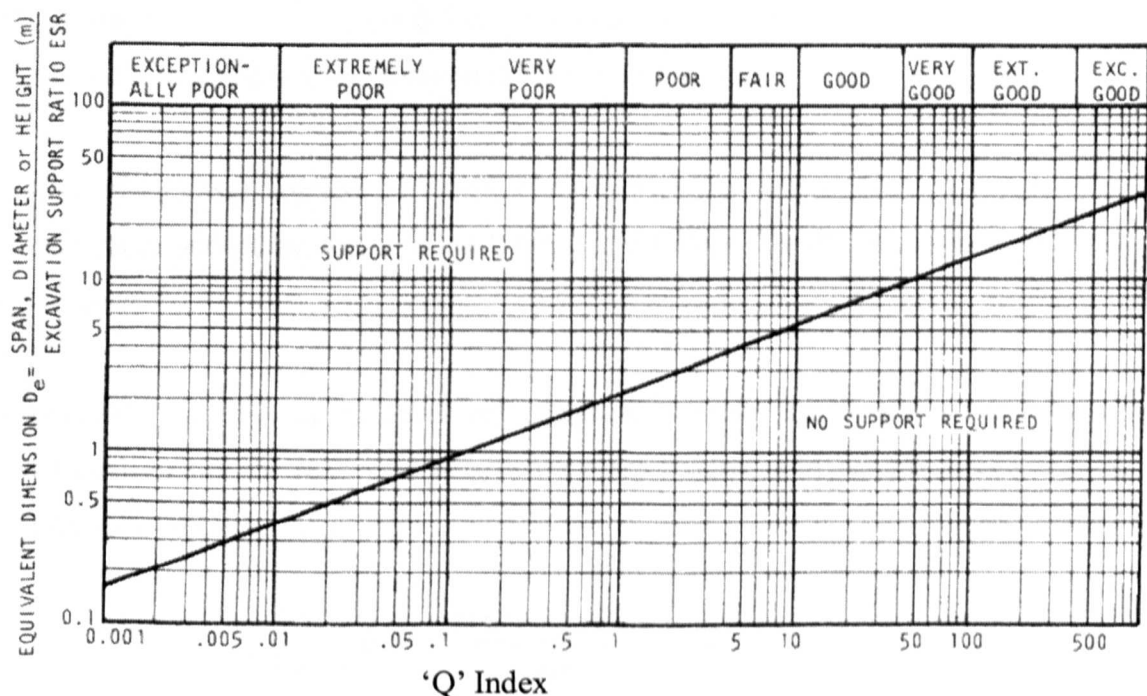


Figure 4.17 Relationship between the maximum equivalent dimension  $D_e$  of an unsupported excavation and the ‘Q’ Index. (after Barton et al 1974)

#### 4.5.8 The Utilisation Of Rock Mass Classification In Coal Mine Design

Existing classifications developed for civil engineering purposes are not readily adaptable to coal mining because they do not provide for the layered structure of coal measure strata and the fact that the dimensions and stability requirements of civil engineering tunnels are often very different than those in mines. Although existing classifications have been used within coal mines they have usually been modified to account for the different conditions experienced in coal mining. Classifications have also been developed specifically for predicting strata behaviour within coal mines.

Ghose and Raju (1981) proposed a four parameter rock mass classification developed for predicting cavability of the rock strata in Indian coal mines (Table 4.21)

<i>Parametric values for groups I-V</i>					
PARAMETERS	I	II	III	IV	V
UCS (MPa)	0-10	10-30	30-60	60-90	90-125
Average core size (mm)	0-50	50-90	90-130	130-160	160-200
Thickness (m)	0-0.5	0.5-1	1-2	2-3	3-6
Depth (m)	1000-720	720-480	480-240	240-80	80-0

Table 4.21 Cavability Classification (after Ghose and Raju 1981)

Bieniawski (1982) applied his RMR classification for determining safe roof span within room and pillar mines in the USA. He validated his classification on 60 coal mine cases.

Unal (1983) developed an empirical equation, between Bieniawski's 1979 RMR classification and the rock load height, for entry roadways in American coal mines, which is as follows:

$$h_t = \frac{100 - RMR}{100} B \quad (4.44)$$

Where  $h_t$  is rock load height,  $B$  is entry span and  $RMR$  is Bieniawski's 1979 rock mass rating.

He showed that the roof bolt length can be estimated as half the rock load height and prepared a series of design charts for mechanically tensioned and resin grouted bolts for application in US coal mines. The design charts take into consideration such factors as the use and life of entries and entry intersections.

Hart (1987) developed a classification scheme for Coal Measure Rocks as an aid in predicting the height of void migration above shallow mine workings. The source data for his classification scheme was rotary openhole borehole logs. Three basic sets of parameters were derived and are described as follows:

- (i) *Lithology*. Hart considered that the lithology profoundly influenced the compressive strength of Coal Measure rocks. He derived a lithology index ( $L_i$ ) based on the relative percentages of clay minerals (illite and kaolinite) to quartz and siderite (Equation 4.45).

$$L_i = \frac{\text{illite } (\%) + \text{kaolinite } (\%)}{\text{quartz } (\%) + \text{siderite } (\%)} \quad (4.45)$$

He correlated his  $L_i$  index to the uniaxial compressive strength ( $\sigma_c$ ) of water saturated rock and obtained a 75% correlation coefficient using the following relationship.

$$\sigma_c = \frac{L_i}{0.0783 \cdot L_i - 0.0355} \quad (4.46)$$

Hart determined typical lithological indices for a range of common Coal Measure rock types which are given as Table 4.22.

- (ii) *Degree of Weathering*. The degree of weathering was arbitrarily quantified by Hart by assigning a weathering index ( $W_i$ ) to the rock strata in accordance with Table 4.23.
- (iii) *Discontinuities*. Hart proposed a discontinuity index ( $D_i$ ) to represent the degree of discontinuity concentration. As the classification was developed for use with rotary openhole borehole information a description of drill

penetration performance was tentatively used to determine the discontinuity concentrations. The penetration performance was related to the in-situ discontinuity spacing (Table 4.24).

The values of  $L_i$ ,  $W_i$  and  $D_i$  were then combined to produce a Strata Quality Index ( $S_i$ ) (Equation 4.47).

$$S_i = L_i \times D_i + W_i \quad (4.47)$$

Hart stated that the plot of cumulative lithological unit thickness against cumulative Strata Quality Index through the sequence overlying a mining excavation would provide an indication of the potential for void migration towards the ground surface.

Lithology	Derived Lithological index, $L_i$	Lithology	Derived Lithological index, $L_i$
<u>Group A</u> Sandstone Siltstone Ganister Ironstone	1.0	<u>Group B</u> Any group A with minor interbeds of finer grained rocks: Silty mudstone Silty sandstone Seatearth	1.5
<u>Group C</u> Mudstone Any of Group A with minor interbeds of coarser rocks.	2.0	<u>Group D</u> Shale Fireclay	2.5

Table 4.22 Lithological Index Classification (after Hart 1987)

Weathering Grade BS 5930 (1981)	Derived Weathering Index $W_i$
Slightly	10
Moderately	20
Highly	100

Table 4.23 Weathering Index Classification (after Hart 1987)

Drill penetration Performance	Mean Discontinuity Spacing Ds (metres)	Derived Discontinuity Index, $Di = 1/Ds$ Discontinuities per metre	Equivalent Description BS5930 (1981)
Very hard drilling	0.20	5	Medium Spaced (RQD = 100%)
Hard drilling	0.10	10	Closely Spaced RQD = 100%
Firm or medium drilling	0.05	20	Very closely spaced
Loose or soft and very soft drilling	0.01	100	Extremely closely spaced

Table 4.24 Discontinuity Index Classification (after Hart 1987)

Choquet and Chorette (1988) investigated the suitability of six rock mass classifications for predicting the support requirements in 10 coal mines in Quebec, Canada. The classification they appraised were: Bieniawski's RMR, Laubscher's modified RMR for mining (MRMR) Barton's Q Index and a modified RMR (SRMR) developed by Brock. The final two classifications were formed by modifications to Laubsher's MRMR and Bieniawski's RMR. They concluded that the modified Launcher's MRMR and Barton's Q index most realistically predicted the support requirements within the coal mines. However they also recorded a large degree of scatter between these classification and the actual support installed indicating the none of the classification can be used as a sole predictor of support requirement.

Daws (1991) describes a system for initial bolt design based on RMR that may be used for British coal mines. Daws suggested an adjustment factor should be applied to the RMR to account for the direction of maximum horizontal stress (Figure 4.18).

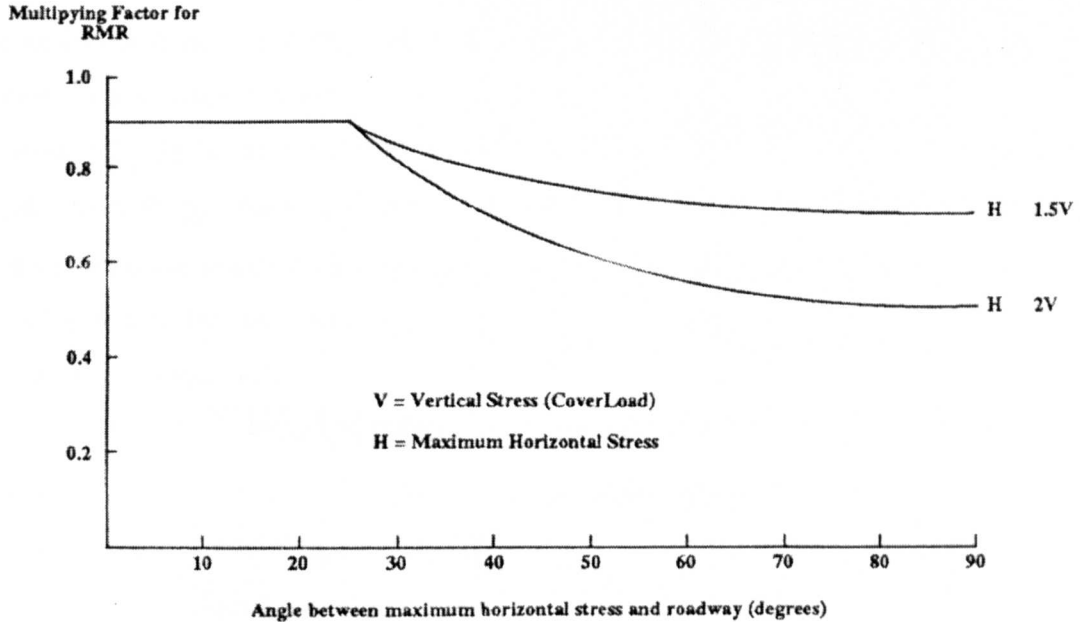


Figure 4.18 Adjustment to RMR to account for in-situ stress condition

(after Daws 1991)

Using Equation 4.44 to determine the rock load height he proposed that the load to be taken by the support system per meter length of tunnel to be as follows (Equation 4.48).

$$P = f \cdot h_t \cdot B \cdot \gamma \quad (4.48)$$

Where  $P$  = support load (tonnes)

$f$  = factor of safety

$\gamma$  = rock density (tonnes/m<sup>3</sup>)

$h_t$  = rock load height (m)

$B$  = width of tunnel (m)

He suggest that the roof bolt spacing ( $S$ ) can be determined using the following equation (Equation 4.49)

$$S^2 = \frac{qUT}{P} \quad (4.49)$$

Where  $q = \text{Tan}2(45 \times \phi/2)$

$U$  = yield load of rock bolt (tonnes)

$T$  = bolt length (m)

In order to predict the roof stability within Indian coal mines, Dhar et al (1992) developed a classification called the CMRS Geomechanic Classification of Coal Measure Rocks. From a detailed literature study they determined that layer thickness, rock strength, groundwater weathering and structural anomalies such as sandstone lenses were the major causes of roof failure. On the basis of a statistical analysis of available data the five parameters were given the following maximum importance weightings (Table 4.25).

PARAMETER	Importance weighting (%)
Layer thickness (RQD)	30
Structural features	25
Weatherability	20
Rock strength	15
Water seepage	10

Table 4.25 Parameter weightings CMRS Classification  
(after Dhar et al 1992)

Adjustment factors to be applied to the CMRS rating varying between 1.0 and 0.7 were devised to account for in-situ stress, mining induced stress and the method of excavation. The CMRS Rating was correlated to rock load height and roof bolt design.

Buddery and Oldroyd (1992) stated that there was a need for a dedicated rock mass classification for coal measures strata in South Africa coal mines because of the following drawbacks to existing well established classifications:

- i) The test or classification parameters may not relate directly to actual strata behaviour in coal mine roadways.
- ii) Sample preparation requirements and test procedures may make it impossible to test weak strata so that the behaviour of these strata has to be inferred from experience.
- iii) The tests are typically costly, time consuming and can only be conducted in specialist laboratories. This presents significant difficulties when very large

- numbers of tests are required such as during the feasibility stage of a major coal mining project.
- iv) Existing rock mass classification systems will frequently assign the same class to a wide range of coal mine roofs.

They developed separate classifications for coal mine roofs and floors with the parameters in each classification related to the expected mode of failure of the strata. The roof classification was devised to characterise the ability of the lamination and bedding planes to open and separate which they state was the major factor influencing roof failure. An impact splitting test was developed to determine lamination and bedding plane strength. The test consisted of a bolster chisel, with a 1.5 kg weight attached to it, that was mounted in such a way that it can be dropped onto core from a constant height. The blade of the chisel is aligned parallel to the planes of stratification and a test is carried out at 2 cm intervals. Fracture frequency per cm ( $f_s$ ) created by the test are determined for individual strata units. Using either Equation 4.50 or 4.51 an individual roof rating for each unit is determined.

$$\text{For } f_s \leq 5 \text{ RATING} = 4f_s \quad (4.50)$$

$$\text{For } f_s > 5 \text{ RATING} = 2f_s + 10 \quad (4.51)$$

The unit ratings were weighted in relation to their position within the roof (Equation 4.52)

$$\text{Weighted rating} = \text{rating} \times 2(2-h)t \quad (4.52)$$

Where  $h$  = mean unit height above the roof (m)

$T$  = thickness of unit (m)

The weighted ratings for all units are then summed to give the final roof rating.

Table 4.26 details Buddery and Oldroyd's proposed relationships between unit and roof rating and rock class.

<b>Unit rating</b>	<b>Rock class</b>	<b>Roof rating</b>
< 10	Very poor	<39
11-17	Poor	40-69
18-27	Moderate	70-99
28-32	Good	100-129
>32	Very good	>130

Table 4.26 Relationship between unit and roof rating and rock class.  
(after Buddery and Oldroyd 1992)

The floor classification was based on characterising the ability of the floor strata to swell and degrade in the presence of water, which they considered to be the main factor influencing the degradation of South African coal mine floors. They based the classification on unconfined swelling strain and slake durability tests. Table 4.27 gives the relationship between these parameters and the floor quality for individual floor units.

<b>RATING</b>	<b>Description</b>	<b>Swell index</b>	<b>Slake durability index</b>
A	Good	<1	<14
B	Moderate	1-3	14-26
C	Poor	3.1-15	26.1-36
D	Very poor	>15	>36

Table 4.27 Floor classification (after Buddery and Oldroyd 1992)

Bieniawski and Kalamaras (1993) revised Bieniawski's RMR classification to incorporate the structural properties of a coal seam. They replaced the groundwater parameter by a stratification parameter. Depending on the uniformity of stratification a rating of 5, 10 or 15 was proposed (Table 4.28).

<b>Stratification description</b>	<b>Rating</b>
Heterogeneous due to layering	5
Two discrete mechanical layers	10
Homogenous	15

Table 4.28 Stratification Parameter (after Bieniawski and Kalamaras 1993)

For the condition of discontinuities parameter they include the following types typical of bedding surfaces:

- (1) bedding surfaces that are clay free are given a rating of 20
- (2) bedding defined by thin clay or shale bands have a rating of 0.

An adjustment to account for the orientation of the face cleat within the coal seam was determined by Bieniawski and Kalamaras and is detailed in Table 4.29.

ADJUSTMENT FOR FACE CLEAT ORIENTATION					
Angle between strike of vertical face cleats and rib face (degrees)	<20	20-35	35-50	50-65	65-90
Rating for the face cleat orientation factor	-12	-10	-5	-2	0

Table 4.29 Adjustment for cleat orientation (after Bieniawski and Kalamaras 1993)

#### 4.5.9 USBM Coal Mine Roof Rating Classification

The United States Bureau of Mines Developed a system, named the Coal Mine Roof Rating (CMRR), to predict the roof performance of coal mines within the USA (USBM 1994, Mark and Molinda 1994). The CMRR has the same format as Bieniawski's RMR, summing various individual ratings to obtain a final CMRR on a scale of 0 to 100. The classification was developed to be applicable to all coal measure rocks regardless of depositional environment, age, rank or geographical location (USBM 1994). The CMRR classification has been used extensively across the USA from mines ranging from small to some of the largest longwall operations in the United States (USBM 1994). The classification has also been used as an input parameter in the analysis of longwall pillar stability where it has been found to increase the accuracy of the analysis.

To determine the CMRR the mine roof is first divided into structural units at least 15cm thick. A rating is the determined for each unit based primarily on an evaluation of the discontinuities and their characteristics (Figure 4.19). The CMRR is determined

by firstly obtaining ratings for each discontinuity set within the unit. Tables 4.30 and 4.31 are used to determine ratings for discontinuity shear strength and intensity respectively. These ratings are then summed to obtain individual discontinuity ratings. The most significant discontinuity is the one with the lowest individual rating. If more than one set is present a multiple discontinuity adjustment is applied (Table 4.32). Two other unit parameters incorporated within the CMRR classification are moisture sensitivity and strength. Tables 4.33 and 4.34 should be used to determine these ratings, which are then summed with the lowest discontinuity rating to obtain the unit rating. This is undertaken for each individual unit identified.

To obtain the CMRR for the roof as a whole, firstly, each of the unit ratings is multiplied by the thickness of that unit. These ratings are then summed and then divided by the total thickness to produce a thickness weighted rating for the roof. Adjustments are then made to the thickness weighted rating to account for strong beds, unit contacts, groundwater and surcharge.

ROUGHNESS	(1) Strong cohesion	(2) Moderate cohesion	(3) Weak cohesion	(4) slickensided
(1) Jagged	35	29	24	10
(2) Wavy	35	27	20	10
(3) Planar	35	25	16	10

*NOTE:- If unit has no bedding or discontinuities, then apply test to the intact rock.  
Strong cohesion implies that the discontinuities have no weakening effect on the rock.*

Table 4.30 CMRR cohesion-roughness rating (after USBM 1994)

Persistence m	(1) > 1.8 m	(2) 0.6 to 1.8 m	(3) 20 to 61 cm	(4) 6 to 20 cm	(5) < 6cm
(1) 0 to 0.9	35	30	24	17	9
(2) 0.9 to 3	32	27	21	15	9
(3) 3 to 9	30	25	20	13	9
(4) >9	30	25	20	13	9

*Note:- If unit has no bedding or discontinuities, then enter 35. If cohesion is strong then enter 35*

Table 4.31 CMRR spacing-persistence rating (after USBM 1994)

<b>Two lowest individual discontinuity ratings both lower than-</b>	<b>Adjustment</b>
30	-5
40	-4
50	-2

Table 4.32 CMRR Multiple discontinuity set adjustment (after USBM 1994)

<b>Strength (Mpa)</b>	<b>Rating</b>
(1) >103	30
(2) 55 to 103	22
(3) 21 to 55	15
(4) 7 to 21	10
(5) < 7	5

Table 4.33 CMRR strength rating (after USBM 1994)

<b>Moisture sensitivity</b>	<b>Rating</b>
(1) Not sensitive	0
(2) Slightly sensitive	-3
(3) moderately sensitive	-10
(4) Severely sensitive	-25

*Note:- Apply adjustment only if the unit is exposed as the immediate roof or flowing groundwater is present and if the anticipated service life of the entry is long enough to allow decomposition to occur*

Table 4.34 CMRR Moisture sensitivity rating (after USBM 1994)

The CMRR can be divided into 3 classes which are weak (CMRR 0-45), moderate (CMRR 45-65) and Strong (CMRR 65-100).

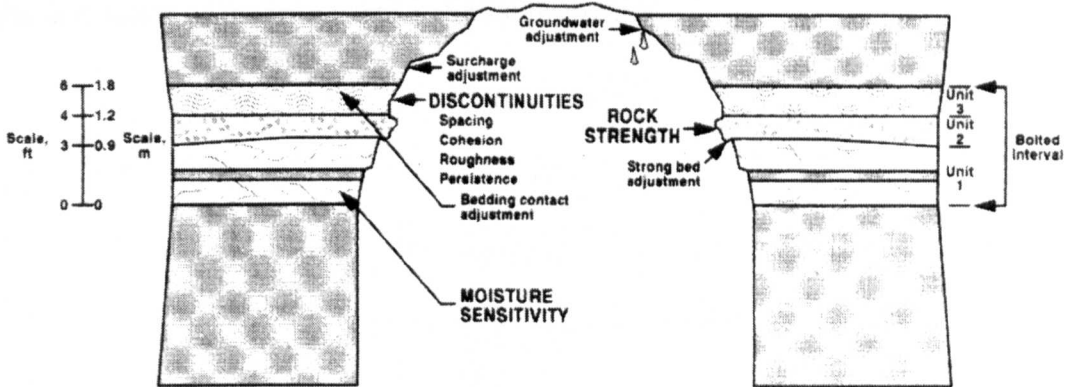


Figure 4.19 The different components of the coal mine roof rating (after USBM 1994)

#### 4.5.9.1 USBM Floor Quality Classification

A quality rating for predicting the behaviour of coal mine floors using a modified Coal Mine Roof Rating was proposed by Riefenberg (1995). Riefenberg modified the CMRR by eliminating the strong bed adjustment as she did not consider it important in influencing floor deformation mechanisms. A further modification was to increase the strength weighting from 30% to 50% and decrease the discontinuity weighting from 70% to 50% in order to reflect the assumption that rock strength may be as important a factor as the presence of discontinuities.

## 4.6 CONCLUSIONS

The engineering properties, i.e. the strength and stiffness properties of the in-situ rock strata are dependant on both the strength and stiffness of the intact rock and the nature, orientation and frequency of planes of weakness such as bedding planes and joints.

The engineering properties of the intact rock are important as they provide an upper limit to the rock mass properties. Failure and stiffness criteria for the intact rock can thus be reduced to allow the effect of the rock discontinuities and ground water effects.

Many rock mass classifications have been developed over the last sixty years for many applications and environments. Rock mass classifications developed specifically for Coal Measure rock types or validated with case histories for coal

mining environments are most meaningful and can be used as a basis deriving a reduction factor of the intact rock material properties.

**CHAPTER 5**  
**DEVELOPMENT OF A ROCK MASS CLASSIFICATION FOR UK COAL**  
**MINE DESIGN**

### **5.1 INTRODUCTION**

Existing rock mass classifications have limited applicability for use within UK coal mines as they have not been developed to account for the behaviour of weak stratified rock masses in a high stress environment, both features of which are characteristic of UK coal mining.

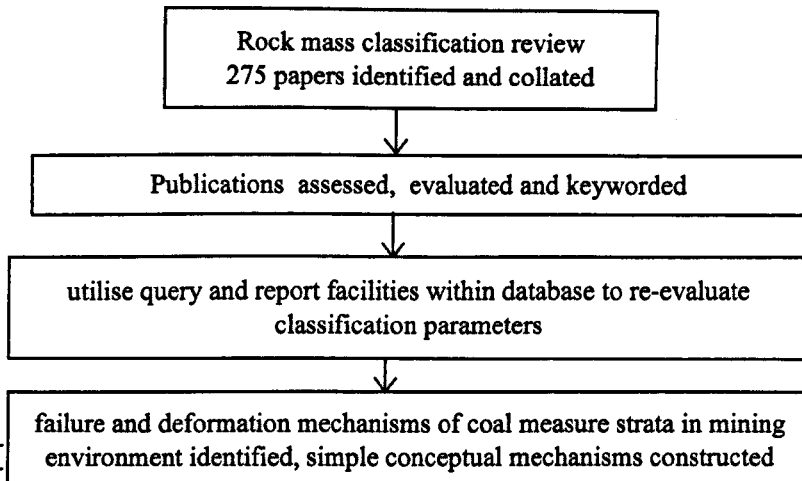
This chapter describes the development of a rock mass classification for use within UK coal mines. The classification parameters have been identified from a thorough assessment and evaluation of rock mass factors that influence typical strata deformation mechanisms that occur within UK coal mines. Existing established classifications and the specifically unique properties to the UK coal mining environment have provided a basis for the development of the classification. The classification has been developed so that it's output will provide a means of determining representative engineering properties of strata for use within numerical modeling techniques for underground roadway design in retreat face longwall mining. The overall methodology used to develop the classification is shown as Figure 5.1

### **5.2 SELECTION OF CLASSIFICATION STRUCTURE**

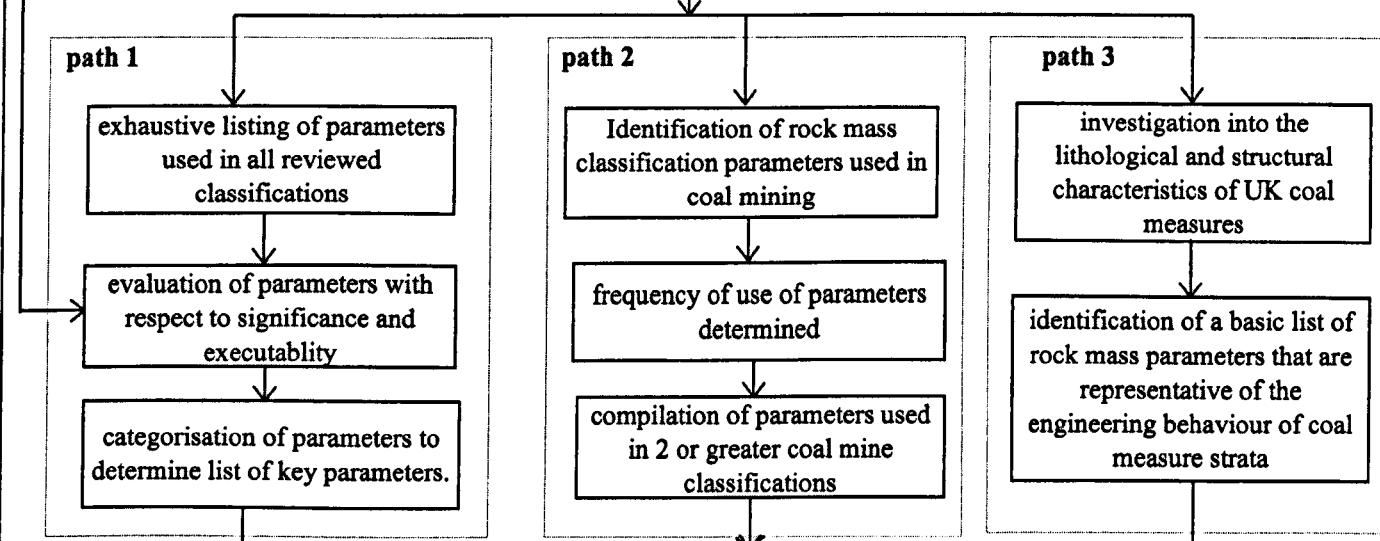
Existing classifications use a variety of systems or structures in the way they calculate the classification value of a rock mass. For instance the early classifications, such as Terzaghi's 1946 classification, require a simple qualitative assessment. Other classification derive a numerical quantitative value based on a single parameter such as the RQD system. Some structures are based on multi-parameter qualitative assessments of individual parameters and then the classification is derived by multiplying quotients of these values. Bieniawski's rock mass rating system involves the simple addition of ratings applied to a variety of influencing factors.

During the decision processes to select a classification structure for the proposed Coal Mine Classification it became apparent that all of the existing structures had disadvantages. The older qualitative classifications were considered unsuitable due to

## STAGE 1



## STAGE 2



## STAGE 3

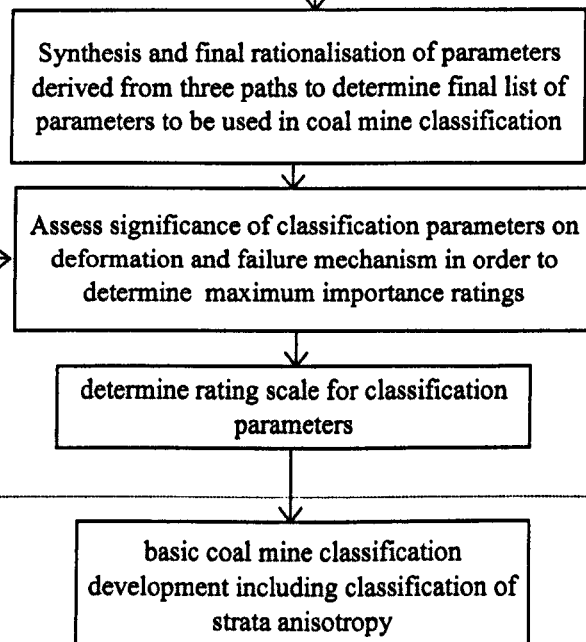


Figure 5.1 Coal Mine Classification Development

their subjective nature and broad groupings. Single parameter classifications were not considered suitable because no single parameter can characterise the engineering characteristics of a rock mass. Barton's structure utilised in the 'Q' Classification was considered difficult to interpret as the classification value was on a logarithmic scale which prevented a simple comparison of the rock quality between different rock masses. The Rock Mass Rating system of simply adding weighted importance ratings for individual parameter had the disadvantage that the relative importance weightings of the individual parameters had to be determined but had several advantages over other classification structures which are given as follows:

- i) The structure of the RMR classification system has been successfully utilised as a basis for most of the rock mass classifications in use today.
- ii) The RMR style classification has been found to be effective in differentiating rock masses of different qualities.
- iii) It is simple to apply and understand.
- iv) Reduction factors and adjustments can be applied to the basic rating to account for such features as joint orientation.
- v) The coal mine classification similar in structure to the RMR classification was considered desirable so that a direct correlation can be made between the rock mass rating and the rating produced by the coal mine classification.

It was therefore decided to use an RMR style structure for the coal mine classification.

### **5.3 IDENTIFICATION OF THE KEY CLASSIFICATION PARAMETERS**

#### **5.3.1 Introduction**

The strata behaviour around coal mine roadways can be considered to occur as a result of the interactions between the stress environment, the properties of the excavation such as size and shape etc, as well as the properties of installed support and the stress-strain properties of the different rock strata around the excavation. Time and changes in the strata properties due to weathering can also have a significant effect on strata behaviour.

As the rock mass classification is to be used to derive constitutive properties of the strata the factors relating to the stress environment, excavation characteristics and installed support have not been included within the classification.

It can be considered that parameters that significantly affect the strength and stiffness properties of the rock strata in the vicinity of underground excavations are those that are most actively involved with the process of deformation and failure (Smith and Rosenbaum 1993). As a basis of determining key parameters that will be used within the classification an evaluation has been made of the degree of influence a parameter has on the deformation characteristics of coal measure strata local to coal mine excavations.

### **5.3.2 Conceptual Mechanisms Of Strata Deformation**

To aid in a systematic evaluation of parameter significance a series of simple conceptual mechanisms representing the major mechanisms of deformation of rock strata local to UK coal mine roadways and face areas were developed. The mechanisms were conceptual but based on processes of deformation and failure that have been reported to occur in coal mines and which have been summarized in Chapter 3 of this thesis. Logically the areas where the mechanisms operate can be divided into four groups.

The groups were:

- a) roadway floor
- b) roadway roof
- c) coal face
- d) coal pillar/rib

The overall conceptual model of strata behaviour around a coal mine excavation can be considered to be constructed from individual mechanisms which operate simultaneously or in sequence. This infers interaction between individual mechanisms. These interactions influence both of the mechanisms which operate and the degree of effect that the mechanism has on the overall strata deformation adjacent to the excavation. To evaluate interactions and to determine which mechanism are dominant under a given set of strata and environmental conditions a systematic

analysis may be undertaken using an interactive matrix approach as developed by Hudson (1992).

In total 20 different conceptual mechanisms describing strata behaviour were identified and used in the assessment of parameter importance. A brief summary of each of the models is given below.

#### 5.3.2.1 Roadway Floor Deformation Mechanisms

##### i) *Buckling by horizontal stress* (Figure 5.2)

Horizontal stresses are redirected into the floor and roof strata when an excavation is formed. In the situation where a more deformable seatearth overlies a stiffer strata unit the horizontal stress can lead to the separation of the seatearth from the underlying strata allowing the seatearth to deform by buckling (Peng et al 1992). Tensile stresses develop in the centre of the buckled floor running parallel to the roadway. If these tensile stresses exceed the in-situ tensile strength of the seatearth fracturing will occur generating further deformation of the floor.

##### ii) *Swelling of seatearth floor* (Figure 5.3).

Rock units with a high percentage of clay minerals especially of the type montmorillonite and mixed clay are susceptible to uptake of water and a corresponding increase in volume and decrease in strength (Hart 1986). This mechanism is dominated by the capillary movement into the larger pores with a relaxation of tension forces in the water which help to bind the particles and by physico-chemical intra crystalline swelling of montmorillonite and mixed clay minerals.

##### iii) *Shear failure and deformation along shear planes.* (Figure 5.4)

Once the redistributed stresses around a mining excavation exceed the shear strength of the intact rock, shear planes will develop in the rock mass. These shear planes substantially reduce the strength of the rock mass and further deformation along the planes is likely.

iv) *Extrusion of seatearth into roadway floor* (Figure 5.5)

Under a constant stress generated by the stress abutments beneath the rib sides seatearths can behave as a viscous material and effectively flow from beneath the ribs into the excavation by creep processes (ECSC 1987).

v) *Bearing capacity failure* (Figure 5.6)

If the floor of a roadway is weaker than the overlying coal pillar/rib the stresses transmitted through the coal to the floor may exceed the floors bearing capacity. Failure of the floor strata may occur due to the development of rotational slip planes or by the punching of the rib or pillar into the softer floor (ECSC 1987).

### 5.3.2.2 Roadway Roof Deformation Mechanisms

i) *Buckling of roof beds under the influence of horizontal stresses* (Figure 5.7)

A secondary bending moment is generated across strata beds due to the presence of horizontal stress. Again this bending moment generates buckling of the roof strata (Afrouz 1992).

ii) *Self weight sagging of roof beds* (Figure 5.8)

In wide excavations where the roof strata is thinly bedded the bending moments generated across the individual beds due to the weight of the beds themselves generate bed deformation by buckling (Caudle 1984).

iii) *Shear failure of roof beds (initiating from the roadway corners)* (Figure 5.9)

The redistribution of the shear stresses around square shaped roadways generates high shear stresses in the corner of the excavation. If these shear stresses exceed the intact strength of the rock mass the shear failure will commence at the corner of the roof and propagate upwards towards the centreline of the roof (Frith et al 1991).

iv) *Shear joints/parting plane failure* (Figure 5.10)

Roof failure may occur if the shear planes formed by the mechanism described in iii) intersect a weak bedding horizon (Caudle 1974).

v) *Wedge/block failure* (Figure 5.11)

Joints and bedding planes may delineate blocks or rock wedges that can potentially fall out of the roof (Hoek and Brown 1980).

### 5.3.2.2 Coal Face Deformation Mechanisms

i) *Dilation of face and spalling of coal face* (Figure 5.12)

Cleat planes or mining induced cleavage planes that trend approximately parallel to a coal face will dilate towards the face due to the presence of tensile stresses generated by stress relief in the horizontal direction and induced by the vertical stresses (Holmes 1982). Weak bedding horizons at the roof/ floor interface and within the face allow shearing across the planes leading to increased dilation of the face.

ii) *Bearing capacity failure of floor beneath powered supports* (Figure 5.13)

The load transmitted through coal face powered supports may exceed the bearing capacity of weak material, seatearths especially (ECSC 1987). Bearing capacity failure in the form of rotational slips or punching failure of the seatearth floor may occur. The addition of water to the floor can lead to softening of the seatearth below the supports further reducing its bearing capacity (Hart 1986).

iii) *Collapse of immediate roof in front of supports* (Figure 5.14)

Well jointed, thinly bedded or fissile immediate roofs may collapse adjacent to the face immediately in front of the powered supports.

iv) *Cantilevering of beds over the goaf* (Figure 5.15)

Strong thickly bedded massive rock units may not collapse into the goaf immediately behind the support but may cantilever over the goaf. This creates large bending moments on the powered supports and immediate roof strata behind the coal face leading to greater fracturing of the immediate roof, proximate roof and coal.

v) *Wedge/ block failure of roof in front of supports* (Figure 5.16)

Wedges or blocks of strata may be formed by jointing and bedding within the rock mass. Block failure of the unsupported region in front of the powered support may occur

### 5.3.2.3 Pillar / Rib Side Deformation Mechanisms

#### i) *Side wall spalling by tensile cracking* (Figure 5.17)

Mining induced cleavage planes that trend approximately parallel to rib/pillar sides can be produced by tensile stresses acting perpendicular to the sides. The tensile stresses are generated by stress relief in the horizontal direction and induced by the vertical stresses. Weak bedding horizons at the roof/ floor interface and within the pillar/rib allow shearing across the planes leading to increased dilation of the face.

#### ii) *Side wall movement by coal cleat dilation* (Figure 5.18)

Cleat planes trending approximately parallel to the sides of the pillar/ rib will dilate under the influence of tensile stresses acting perpendicular to the sides of the excavation (Holmes 1982).

#### iii) *Shear failure and movement into roadways along shear planes* (Figure 5.19)

The stress transmitted into the coal pillar/rib via the roof and floor may exceed the shear strength of the coal. Shear planes will then develop in the coal pillar/rib.

#### iv) *Wedge/ block failure in pillar sides* (Figure 5.20)

The presence of joint sets and bedding planes may delineate the rock mass into wedges or blocks. Such wedges or blocks formed in the sides of the pillar/rib may fall-slide out of the sides into the excavation (Hoek and Brown 1980).

#### v) *Yield zone development* (Figure 5.21)

Redistribution of stresses occur around mining excavations generating high vertical stresses and low horizontal stresses within coal pillars and ribs. These stresses can exceed the in-situ shear strength of the coal and development of failure planes within the coal are possible. At the edges of the pillars and ribs where there is little confinement the coal may fail in tension to form vertical fractures. At greater depth in the rib/ pillar sides confining pressures occur and the coal will usually form inclined shear planes. The extent of the yield zone is dependant on the intact strength of the coal and the presence of cleat planes and weak bedding horizons (Wilson 1983).

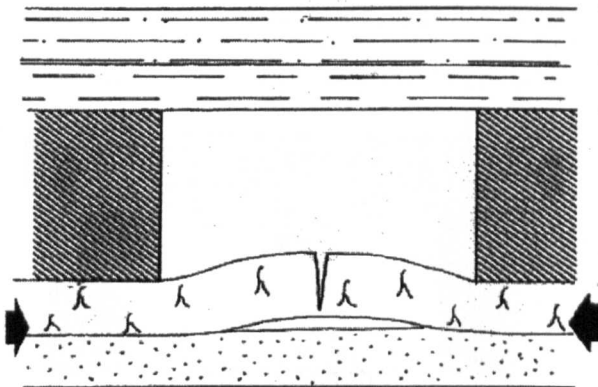


Figure 5.2 Buckling by horizontal stress

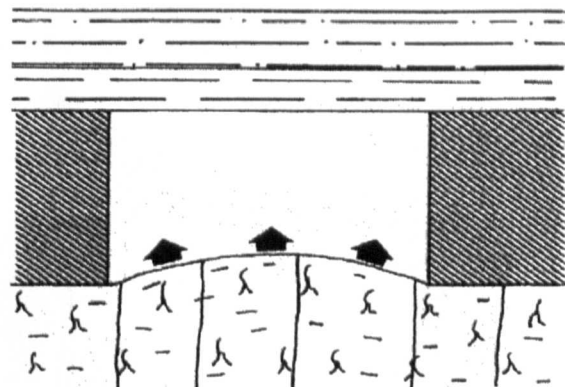


Figure 5.3 Swelling of seatearth

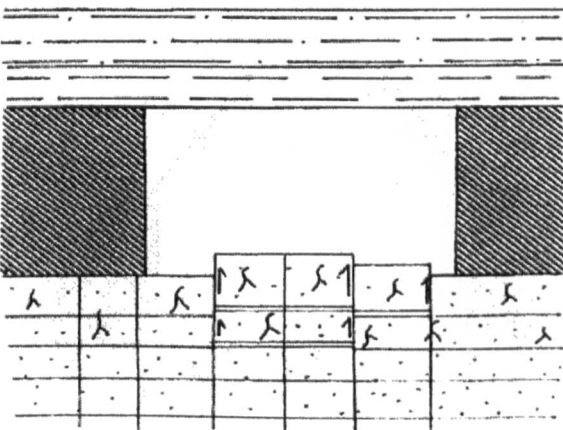


Figure 5.4 Deformation along shear planes

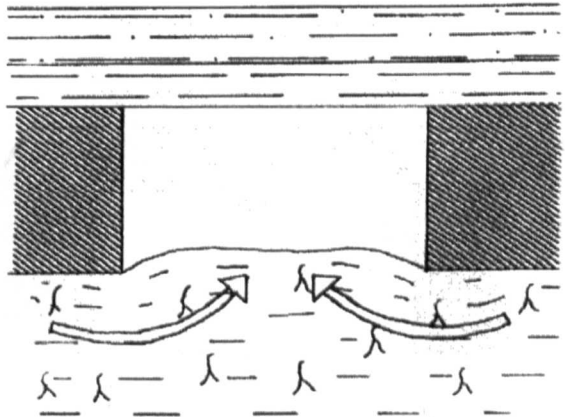


Figure 5.5 Extrusion of Seatearth into roadway

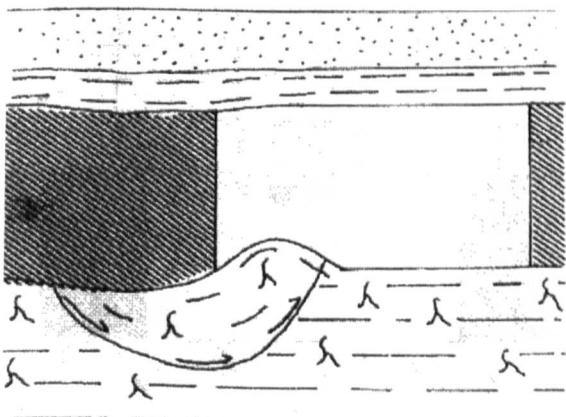


Figure 5.6 Bearing capacity failure

## ROADWAY ROOF DEFORMATION MECHANISMS

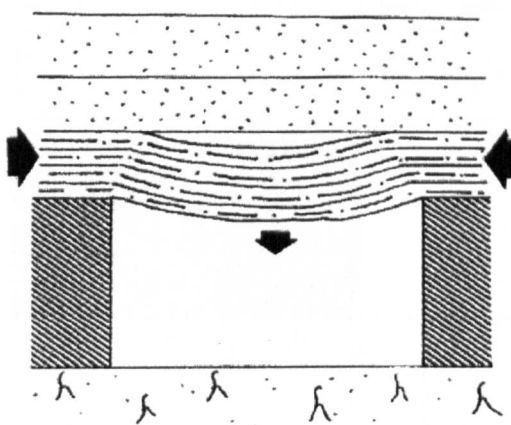


Figure 5.7 Buckling of roof beds

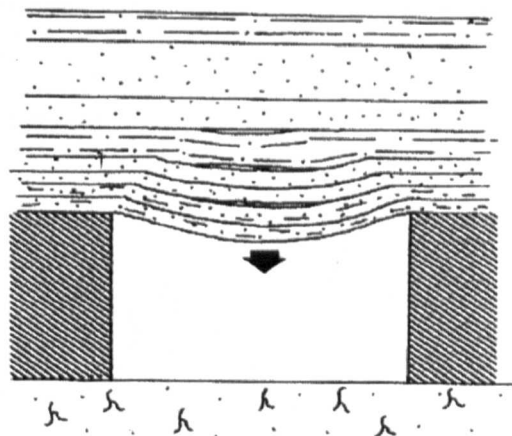


Figure 5.8 Self weight bending

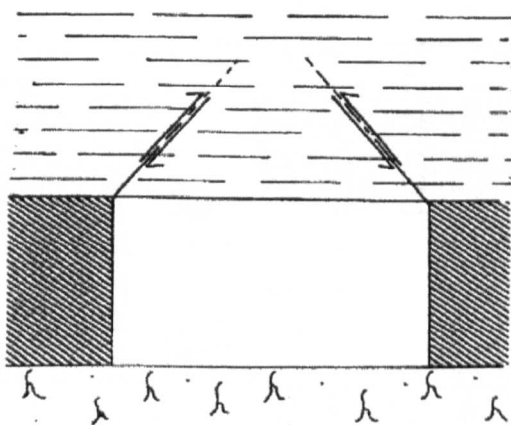


Figure 5.9 Shear failure

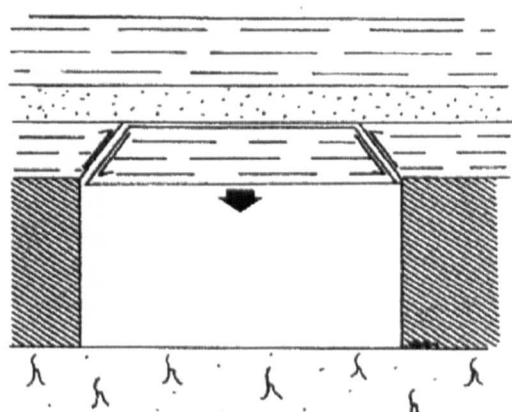


Figure 5.10 shear/parting plane failure

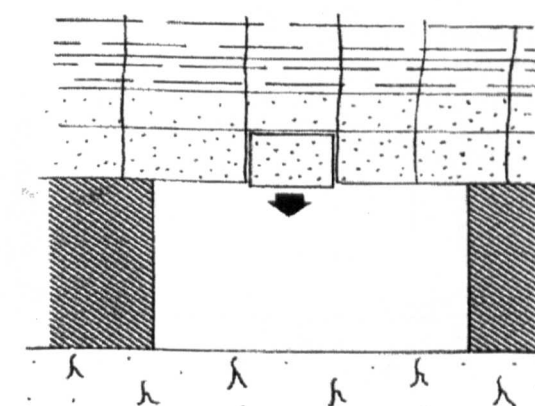


Figure 5.11 wedge/block failure

## COAL FACE DEFORMATION MECHANISMS

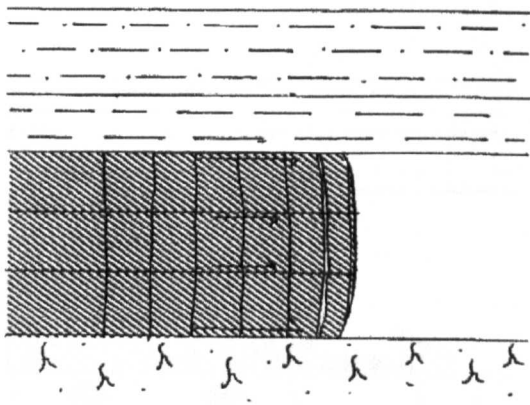


Figure 5.12 Spalling of coal face

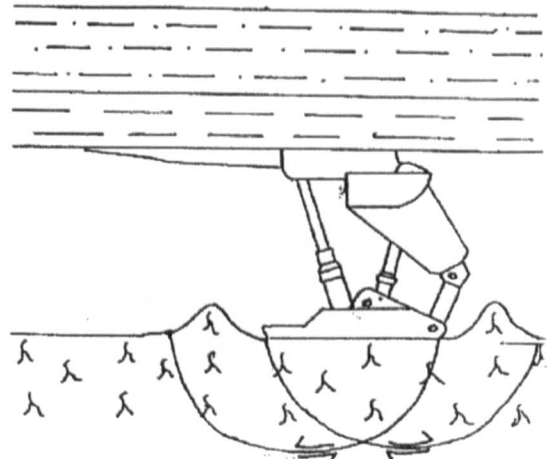


Figure 5.13 Bearing capacity failure

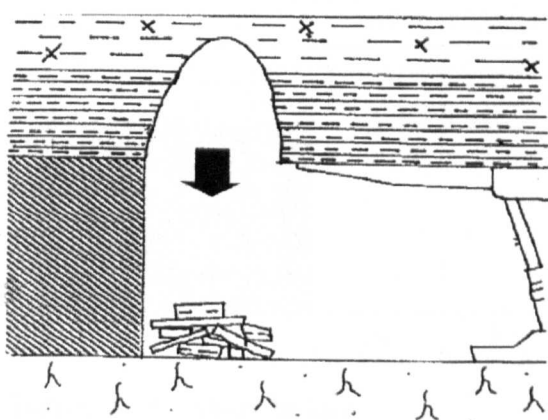


Figure 5.14 Collapse of immediate roof

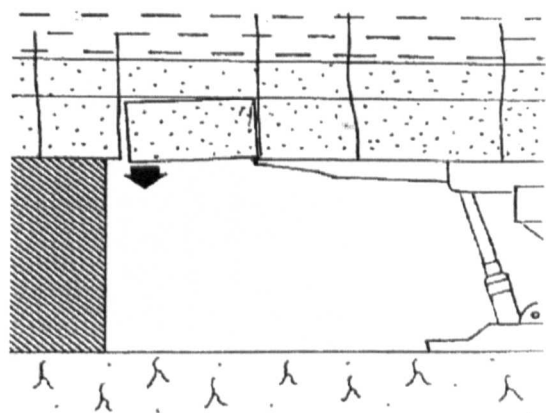


Figure 5.15 Wedge/block failure

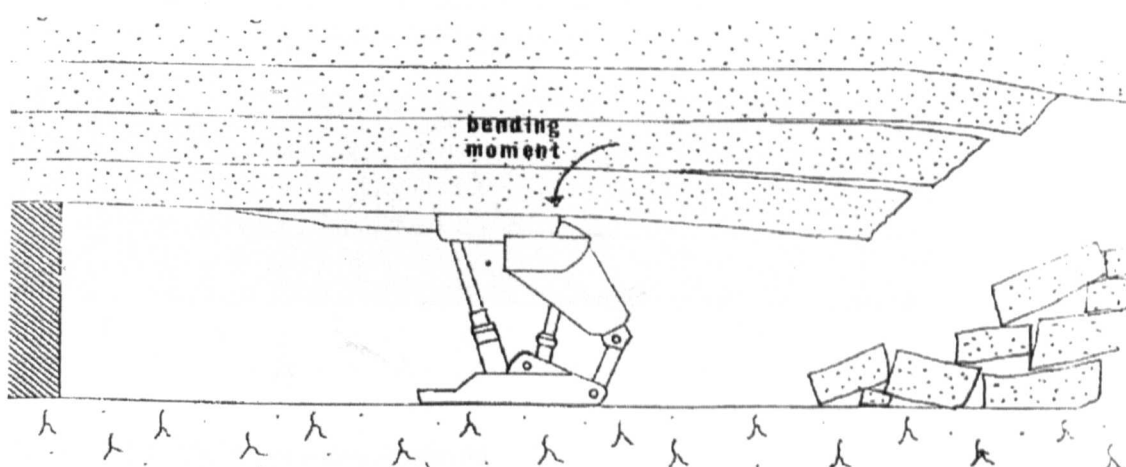


Figure 5.16 Cantilevering of beds

## ROADWAY RIB DEFORMATION MECHANISMS

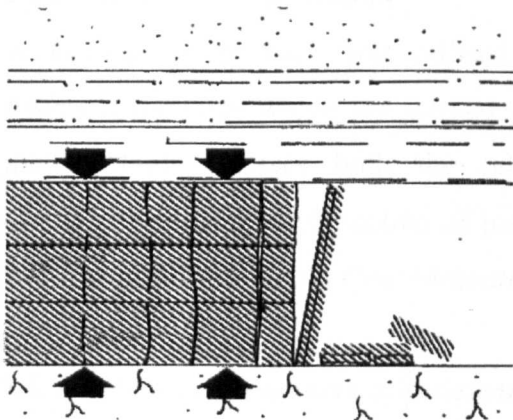


Figure 5.17 Tensile cracking

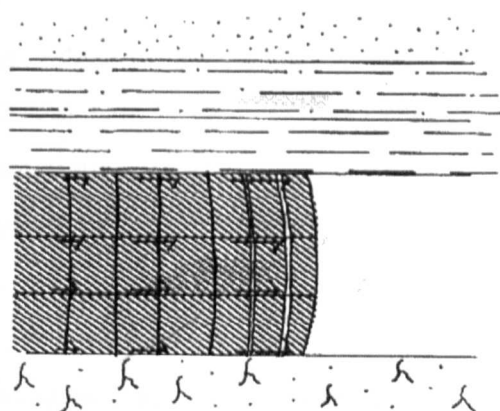


Figure 5.18 Coal cleat dilation

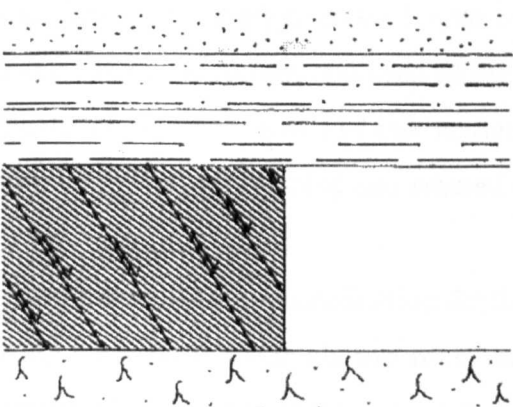


Figure 5.19 Shear failure

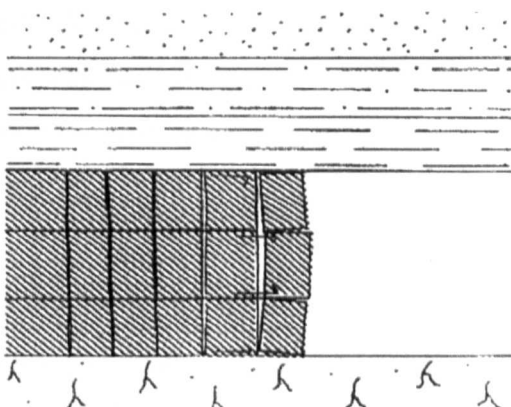


Figure 5.20 Wedge/block failure

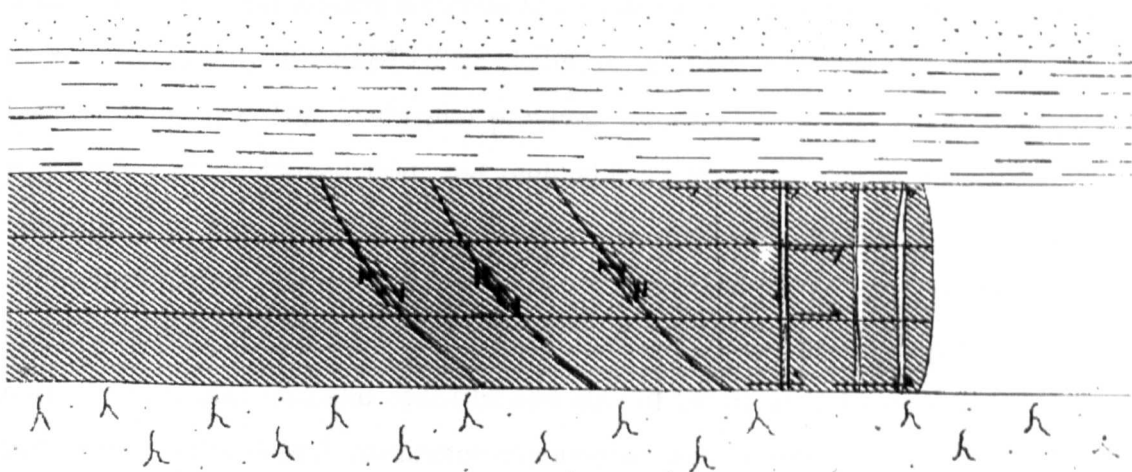


Figure 5.21 Yield zone development

### **5.3.3 Parameter Assessment**

A systematic approach was utilised for parameter selection consisting of three different methods which are termed path 1, path 2 and path 3 (Figure 5.1). This methodology assesses both the relevance of parameters used in preexisting classifications and identification of parameters not previously used in classifications but of significance to UK Coal Measure rock types.

#### **5.3.3.1 Path 1: Assessment of parameters used in existing rock mass classifications.**

An extensive literature search was undertaken to obtain a comprehensive list of publications that related the use of rock mass classifications to both mining and civil engineering rock mass environments. Each publication was reviewed and the most significant information entered onto a keyword form. A database was constructed using Microsoft Access and each of the keyword forms was entered as a record within the database. A total of 118 publications relating directly to rock mass classifications were reviewed, keyworded and entered into the database.

Using the rock mass classification database query function an exhaustive listing of the parameters used from all the rock mass classification publications reviewed was generated. 50 different classification parameters were identified and a systematic evaluation of each parameter was undertaken using the proforma shown as Figure 5.22. The evaluation process included an evaluation of the potential for the parameter to be meaningfully measured either in-situ, or by laboratory testing or derived from historical sources. This evaluation provided information on the likely sources the parameter can be derived from and highlighted parameters that will be difficult to measure. The second part of the evaluation was undertaken to assess the importance of the parameters .The parameter importance was evaluated in terms of its effect on the mechanisms of rock deformation and failure within the immediate roof, proximate roof, drivage, coal face and coal ribs and also its potential to be measured (derived from part 1). The overall parameter importance was classified on a scale of 1 to 6 with class 1 parameters being ‘very significant and executable’ and the class 6 parameters being ‘not significant and not executable’. 28 class 1 parameters were identified by this process. Rationalisation to avoid duplication was then undertaken as several of these parameters represented indices of a single rock characteristic. The final list of 16 parameters is given as Table 5.2.

**Param1**

Parameter:	[ ]
Comments:	[ ]
Type of Parameter:	[ ]
<b>POTENTIAL FOR MEASUREMENT</b>	
Executability:	[ ]
Executability (Lab):	[ ]
Executability (Field):	[ ]
Executability (History):	[ ]
Executability (Estimation):	[ ]
Significance:	[ ]
Significance (Lab):	[ ]
Significance (Field):	[ ]
Significance (History):	[ ]

<b>POTENTIAL FOR MEASUREMENT</b>	
Laboratory (New):	[ ]
Laboratory (History):	[ ]
Field Based (Index):	[ ]
Field Based (Large Scale New):	[ ]
Field Based (Large Scale History):	[ ]
Estimation:	[ ]
<b>IMPORTANCE FOR CLASSIFICATION</b>	
Immediate Strata:	[ ]
Proximate Strata:	[ ]
Borehole (new):	[ ]
Borehole (history):	[ ]
Driveage Face:	[ ]
Coal Face:	[ ]
Coal Rib:	[ ]

Figure 5.22 Parameter evaluation proforma

## Path 2: Assessment of Parameters Used in Existing Coal Mine Classifications

### Systems

On an international level several classifications have previously been developed for coal mining environments (Mark et al 1994, Buddery et al 1993, Bieniawski 1982).

As part of the literature search 18 rock mass classifications developed for coal mining were reviewed (Table 5.1). These classification have been developed for use in their country of origin and usually for a specific purpose which varied between predicting pillar behaviour, floor behaviour, roof stability and for use in the design of roof bolting layouts. The parameters used in each classification were listed and the number of times the parameter was used in the classifications recorded. This information was used to construct a histogram of the parameters and their corresponding frequencies of use (Figure 5.23). Seventeen different parameters were identified with 13 of these parameters appearing in more than one classification system. The reoccurrence of similar parameters in the coal mine classifications indicates that these parameters are of significant importance to the in-situ deformation behaviour of the strata around excavations in coal mines.

AUTHOR	DATE	SCOPE OF APPLICATION	COUNTRY OF ORIGIN
Z.T. Bieniawski	1982	Room and pillar coal mines	United States of America
Z.T. Bieniawski et al	1991	In-situ strength of coal	United States of America
P.S. Buddery et al	1993	Roof and floor classification	South Africa
G. Daws	1991	Coal mine roof bolting	United Kingdom
B.B. Dhar et al	1992	Support loads and surface subsidence	India
C.N. Ghose et al	1992	Rock loads in coal mine roadways	India
A.K. Ghose et al	1981	Rock bolting on coal mines	India
A.K. Ghose	1988	Longwall roof rock behaviour	South Africa
D.K. Hylbert	1978	Coal mine roof stability	South Africa
G.S. Kalamaras et al	1993	Mass strength of coal seams	United States of America
M. Karmis et al	1984	Coal mine roof stability	United States of America
C. Karpuz et al	1992	Mine roadway design	
C. Mark et al	1994	Coal mine roof stability	United States of America
D.C. Oldroyd et al	1992	Design and support of inclined shafts	South Africa
J. Riefenberg	1995	Floor quality in coal mines	United States of America
P.R. Sheory	1982	Mining stability	India
R. Shepard	1970	Strata displacement around roadways	United Kingdom
E. Unal et al	1990	Classification for clay bearing and stratified rock mass	Turkey

Table 5.1 Existing Classification Systems for Coal Mining

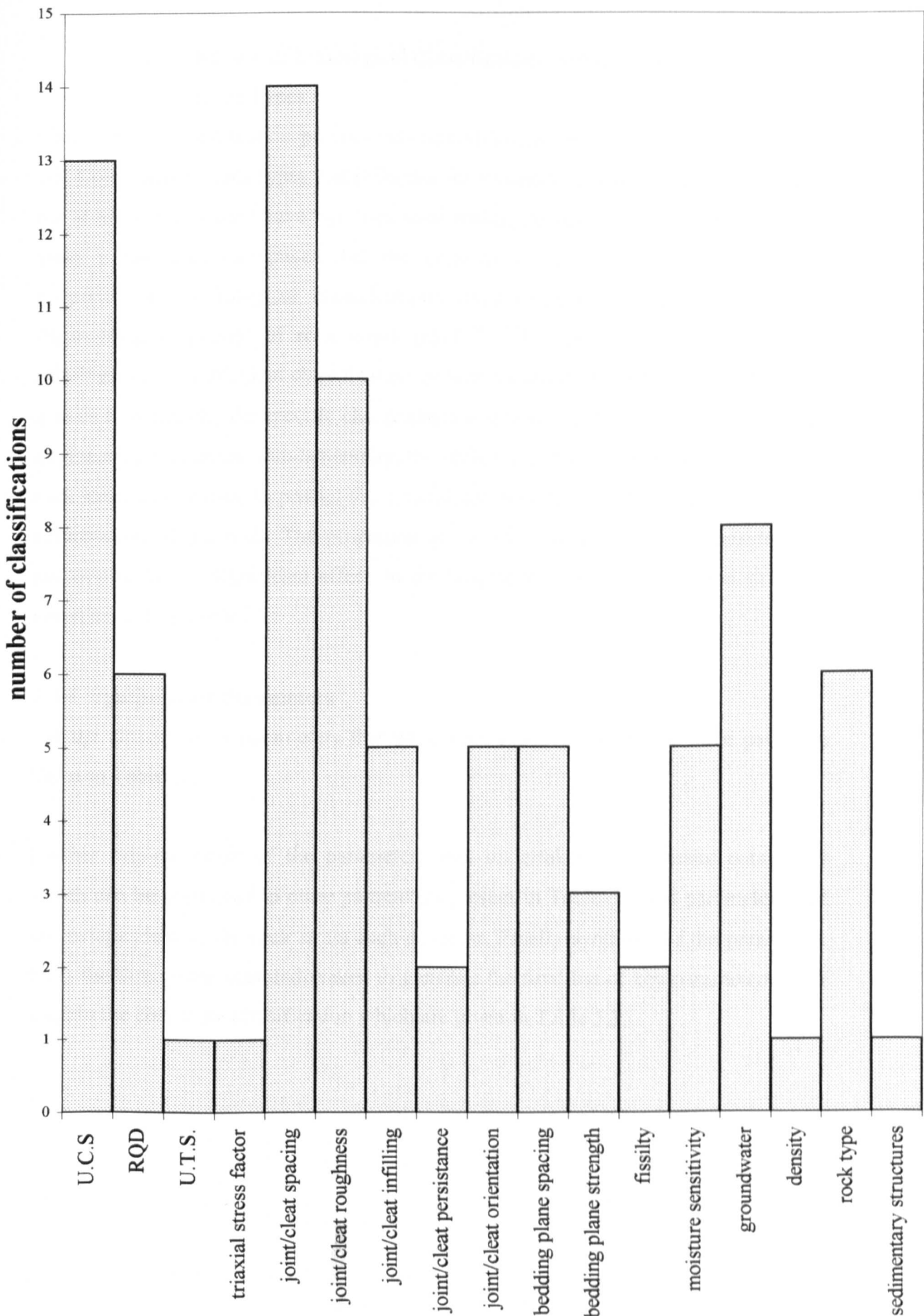


Figure 5.23 Rock mass parameters adopted within existing classifications developed for coal mining/coal measure strata

### **5.3.3.2 Path 3: Review of Lithological Classification Systems and Coal Measure**

#### **Rock Types.**

This part of the evaluation process was undertaken to determine basic properties of UK Coal Measure rock types that influence the strength and deformation properties of the strata and that may have not been used within existing classifications. For many years it has been recognised that the same rock types have similar engineering properties and lithological classifications have often been used to predict the engineering properties of rock strata (Hart 1987). The review of coal measure lithologies and lithological classification systems undertaken in Chapter 2 was used as a basis to determine the specific characteristics of coal measure strata that affect their engineering properties. Fundamentally, the review indicated that the grain size of the rock strata can be used to predict the mineralogy, sedimentary structure and degree of cementation of the rock. The properties of the strata that have been considered to potentially have a significant affect on the ‘engineering properties’ of the strata are given as part of Table 5.2:

### **5.3.4 Synthesis Of Parameters**

All the classification parameters that have been identified from the three paths are listed in Table 5.2.

Further rationalisation of the parameters was undertaken to eliminate parameters which can be correlated to other parameters present in Table 5.2 and parameters that are independent of the rock strata such as stress. Finally synthesis of the parameters from the three paths was undertaken to generate the final list of key parameters to be used in the coal mine classification which are given in Table 5.3.

Path 1		Path 2		Path 3			
UCS		UCS		Clay mineralogy			
Joint properties	Spacing	Joint properties	Orientation	Grain size			
	Set number		Aperture	cementation			
	Roughness		Set number	Mineral orientation			
	Fill		Spacing	Bed. / lam. properties			
	Orientation		Strength				
	Cohesion	Bed. / lam.	Spacing	spacing cohesion strength			
Bed. / lam. Properties	Spacing	Properties	Strength				
	Strength		Moisture sensitivity				
Rock density		Water flow					
Fissility		In-situ stress					
Water flow		Artificial support					
Elastic modulus		Mining induced stress					
Mining induced stress							
In-situ stress							

Table 5.2 Identified Potential Classification Parameters

Derived parameters for Coal Mine Classification	
Unconfined compressive strength	
Bedding / lamination properties	Spacing
	Strength
Joint properties	Set number
	spacing
	orientation
	strength
	Fissility
Water flow	
Moisture sensitivity	

Table 5.3 Final list of critical strata parameters

## **5.4 DESCRIPTION OF IDENTIFIED CLASSIFICATION PARAMETERS**

### **5.4.1 Introduction**

A discussion of the different parameters and their methods of evaluation is now given. For any practical classification system the methods of measurement should be based on simple laboratory and field based testing schedules together with field mapping (Bieniawski 1974). The aim is to generate indices of the rock parameters that can be used as a basis for determining weighted ratings for each parameter. It is envisaged that measurement of parameters for the coal mine classification will be largely undertaken on borehole cores and structural mapping of underground exposures. However it is also envisaged that in many cases where strata classification are required actual measured data may be unobtainable. The construction of databases of rock properties measured for specific lithologies would allow parameter values to be obtained for similar rock types where actual measurements are not available. Where data is lacking engineering judgment may have to be used to estimate parameter values thus increasing the level of uncertainty in the final classification rating.

### **5.4.2 Unconfined Compressive Strength (UCS)**

This is the most generally used measurement of rock strength. The UCS is a measurement of the strength of the intact rock and therefore represents the maximum unconfined strength the rock mass can obtain without considering the influence of discontinuities and other parameters that effect the engineering properties of the rock mass. The UCS has also been correlated to other engineering properties of the rock mass such as moisture sensitivity (Olivier 1979), elastic modulus (Wilson 1983) and joint spacing (Laderia and Price 1981).

#### **5.4.2.1 Point Load Test**

The uniaxial compressive strength for classification purposes can be obtained by means of a point load test. This test has the advantages of being relatively portable, simple to use and requires little in the way of sample preparation and allows many samples to be tested so that an average strength for the rock unit can be obtained. The test essentially involves compressing a piece of rock between two points. A typical point load testing system is shown as Figure 5.24.

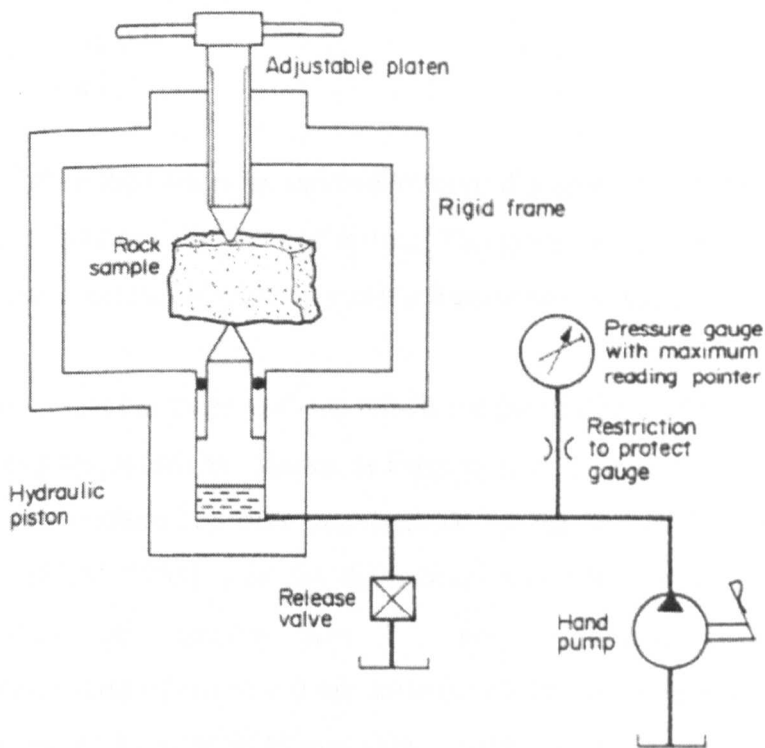


Figure 5.24 Point load test system (after Hudson 1995)

The initial development of the test has been attributed to Reichmuth who investigated the effects of specimen shape and size on results' (Hudson 1995). Broch and Franklin (1972) further developed the test so that it could be used as a convenient method for strength classification of rock materials. After extensive testing they proposed a simplified method of calculating the point load index and specified the test as being most applicable for rock cores.

The standard point load index,  $I_{s(50)}$ , (MPa) is calculated as the ratio of the applied load,  $P$ , (N) to the square of the distance,  $D$ , (mm) between the loading points (Equation 5.1)

$$I_{s(50)} = \frac{P}{D^2} \quad (5.1)$$

For the standard test  $D$  is the diameter of a diametrically tested core of 50mm diameter. For other core sizes the point load index ( $I_s$ ) is multiplied by a size correction factor ( $F$ ) to obtain the standard index (Equation 5.2).

$$I_{s(50)} = F \cdot I_s \quad (5.2)$$

Where  $F = \left(\frac{D}{50}\right)^{0.45}$

For shapes other than cores an equivalent core diameter,  $D_e$ , derived from the cross sectional area between the point of testing. The point load strength index can then be calculated and corrected if necessary using Equations 5.1 and 5.2.

The point load test has three variants which are the diametrical test, axial test and the irregular lump test which are shown as Figures 5.25, 5.26 and 5.27 respectively. The point load test method has been standardised by the International Society of Rock Mechanics (ISRM 1985). For the diametrical test core specimens should have a length/diameter ratio greater than 1.0. For axial test core specimens the length/diameter ratio of 0.3 to 1.0 are suitable whilst for the irregular lump test rock blocks or lumps of a size  $50 \pm 35$  mm with a width/length ratio being between 0.3 and 1.0 are suitable.

Many coal measure rock type are anisotropic and the UCS of the sample depends on the angle of bedding with respect to loading. For the coal mine classification the UCS is defined as representing the maximum strength of the rock strata and therefore the sample should be loaded perpendicular to any planes of stratification.

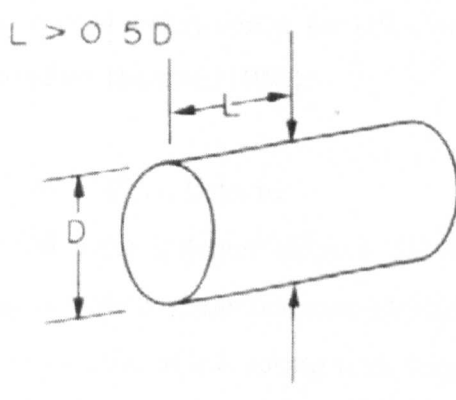


Figure 5.25 Diametrical point load test  
(after ISRM 1985)

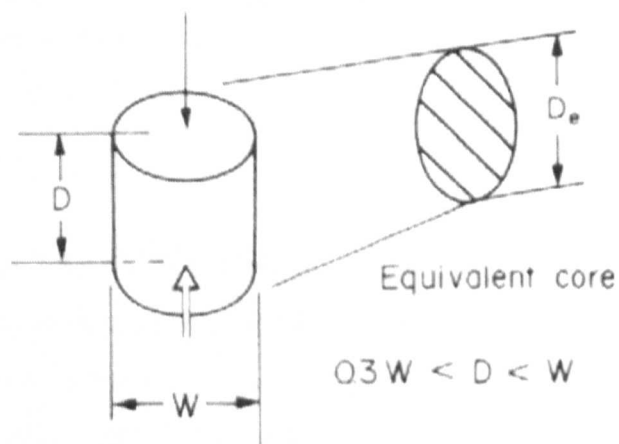


Figure 5.26 Axial point load test  
(after ISRM 1985)

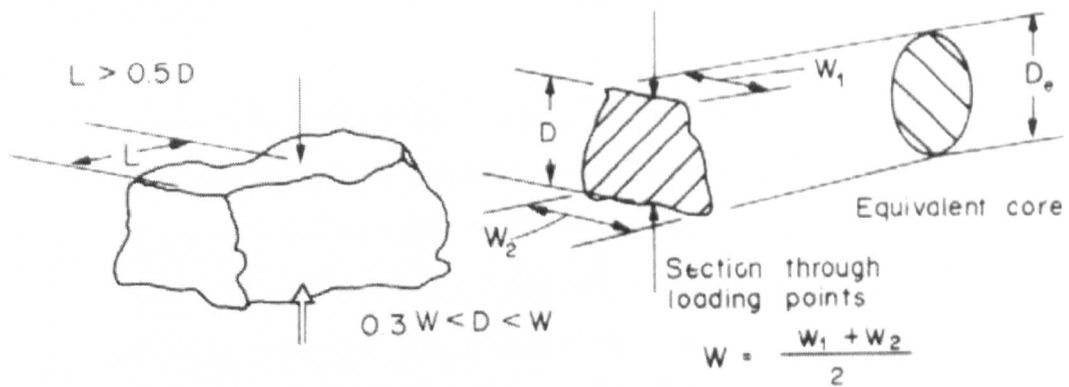


Figure 5.27 Point load lump test (after ISRM 1985)

When testing is carried out it is important that load is steadily increased such that failure occurs within 10 to 60 seconds (Bowden et al 1998). There should preferably be at least 10 test per sample and a test should be rejected as invalid if the fracture surfaces pass through only one loading point.

Broch and Franklin (1972) suggested the following relationship between the standard point load index and the UCS (Equation 5.3)

$$UCS = K \cdot I_{s(50)} \quad (5.3)$$

The correction factor,  $K$ , was suggested by Broch and Franklin (1972) and Bieniawski (1975) to be 24. However this value is not accurate for all rock types. For weaker rocks (<25 MPa) a lower value of  $K$  between 10 to 20 has been proposed (Bowden et al 1998) whilst for UK Coal Measure strata a value of  $K = 29$  has been suggested by Hassani (1980).

#### 5.4.2.2 NCB Cone Indenter

The NCB cone indenter (Figure 5.28), developed by the National Coal Board's Mining Research Establishment (MRDE) in the 1960's, is a portable instrument which is capable of measuring rock strength from a fragment of rock not larger than 12mm x 12mm x 6mm. The sample requires no special preparation apart from being clean and sound. The small sample size requirement offers a means of determining the

unconfined compressive strength of weak and fissile strata units, which often contain many parting horizons.

The instrument determines the hardness of a rock sample by measuring the resistance to indenting by a tungsten carbide cylinder with a conical tip that has a 40° cone angle. It is important that the condition of the point of the cone is maintained at a tip radius of 0.1mm ± 0.025 mm and it is not chipped or deformed (Hudson 1995). The standard test essentially involves the application of a predetermined force of 40 N which generates a spring deflection of 0.635 mm. To obtain the cone indenter number ( $I_s$ ) the cone penetration ( $P_s$ ) is compared to a spring deflection of 0.635mm (Equation 5.4).

$$I_s = \frac{0.635}{P_s} \quad (5.4)$$

Weak rocks may fracture when the standard cone indenter test is attempted, for such rocks the load applied is reduced to 12 N which generates a spring deflection of 0.23 mm. The weak rock cone indenter number ( $I_w$ ) is given by Equation 5.5.

$$I_w = \frac{0.23}{P_w} \quad (5.5)$$

A linear correlation between the cone indenter number and the uniaxial compressive strength of the rock exists. For the standard cone indenter number the relationship is given as Equation 5.6 where the uniaxial compressive strength is for a 25mm diameter cylindrical specimen with a height to diameter ratio of 2:1. For the weak cone indenter number the relationship is given by Equation 5.7. Both relationships have a standard deviation for an individual test of ± 13.5 MPa (MRDE 1977). It is therefore necessary to calculate the mean value for a number of tests to obtain an accurate value of the UCS.

$$\text{UCS} = 24.8.I_s \quad (\text{MPa}) \quad (5.6)$$

$$\text{UCS} = 16.5.I_w \quad (\text{MPa}) \quad (5.7)$$

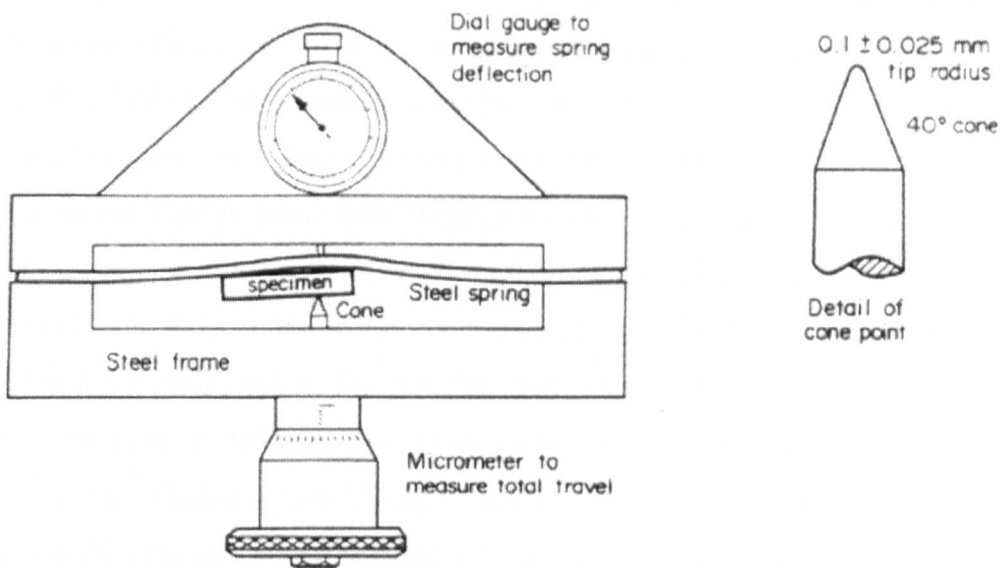


Figure 5.28 The NCB Cone Indenter (after MRDE 1977)

### 5.4.3 Joint Properties

Joint or cleat properties should be evaluated where possible from a line survey where a record should be made of orientation, persistence or dominance, roughness and distance along the survey line of each joint encountered in accordance with ISRM guidelines (ISRM 1981).

#### 5.4.3.1 Number of Joint/Cleat Sets

A joint set is a system of joints that have a common dip amount and direction. The number of joint sets occurring within the rock mass influences the blockiness of the rock mass. Ideally the joint/cleat set number should be determined from a stereographic plot of the joint orientations determined from a line survey. Where the strata unit being classified cannot be inspected in-situ as in the case of roof and floor strata it is possible to infer the joint set number from adjacent exposures such as rib side exposures. Commonly in UK Coal Measure rocks there are generally 2 main vertical / subvertical joint sets orientated at 90 degrees to each other (Price 1966, Moseley and Ahmed 1967, Gross 1993).

#### 5.4.3.2 Joint Spacing

The mean of the joint spacing in a joint set provides an index that represents the degree of fracturing of the rock strata produced by that joint set. The lower the mean spacing of the joints within a set the lower the in-situ strength and elastic modulus of the rock mass. The first step in determining the joint spacing is to attribute each joint on the line survey to a set. The average spacing of the joints in each set is then derived by determining the average perpendicular distance between each joint in the set. Line surveys usually cannot be undertaken for roof and floor strata within coal mines as the strata is unexposed and only borehole cores are taken. It is difficult to evaluate joint spacing in vertical boreholes due to the fact that most joints have a near vertical or vertical dip. Approximate relationships exist between joint spacing and strata properties such as bed thickness and Young's modulus as described in Chapter 2 of this thesis, or engineering judgement may have to be used to assume a joint spacing where data is lacking.

#### 5.4.3.3 Joint Roughness

Joint plane surfaces can vary between being smooth with slickensides through to being very rough undulating or stepped surfaces. Generally the rougher the surface the greater the shear strength of the joint. The most commonly used index to represent surface roughness is Barton's (1974) Joint Roughness Coefficient (JRC). The joint roughness coefficient varies between 1 and 20 with a JRC of 1 being smooth and a JRC of 20 being very rough. Barton produced a chart as an aide to determining the JRC by visual inspection (Figure 5.29).

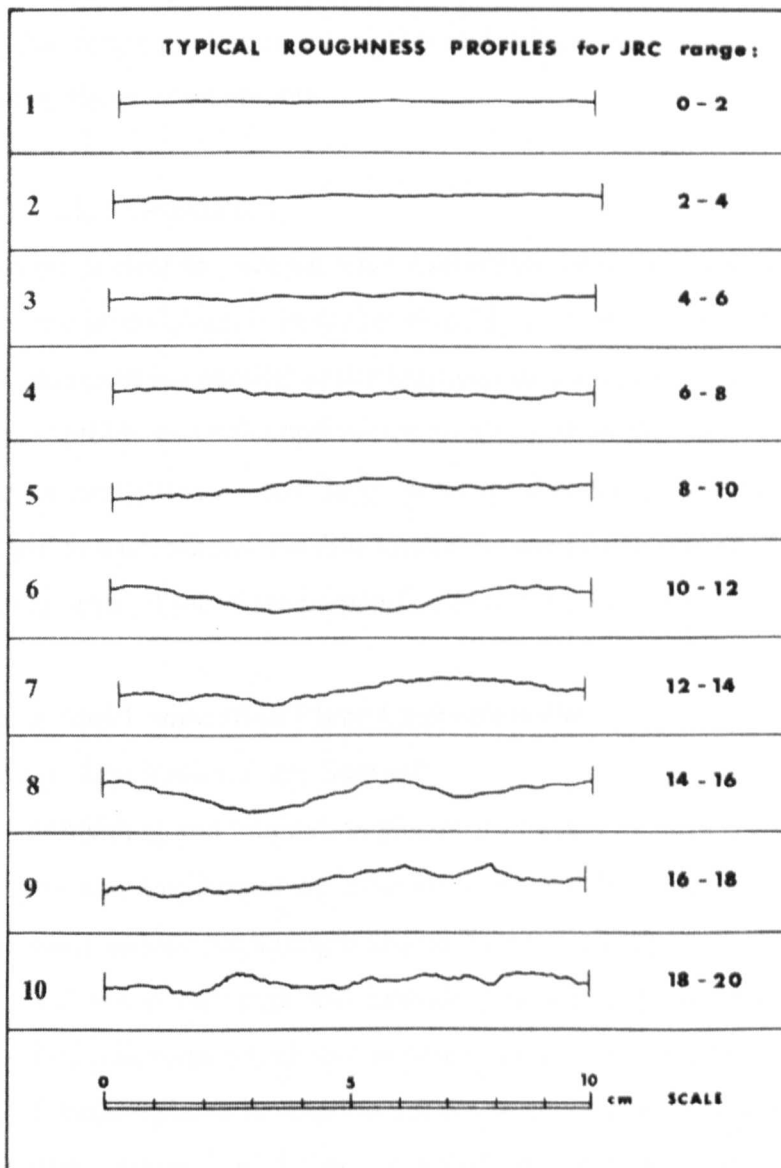


Figure 5.29 Barton's Joint Roughness Coefficient, JRC (after Barton 1974)

#### 5.4.3.4 Joint Persistence

Persistence of a joint plane is a measurement of the lateral extent of the joint plane. Joints may extend over a few centimetres to hundreds of metres. For coal mine excavations the persistence of the joint planes in relation to the dimensions of the roadway is of particular importance.

#### 5.4.3.5 Cleat Dominance

Cleat planes that are typically well defined, planar and transgress other sets of cleat are identified as the dominant planes. Other sets of cleat which are typically less well

developed, curved, not persistent and often terminate at the dominant planes are subordinate. The dominant planes are weaker and reduce the strength and stiffness of the rock mass by the greatest amount.

#### 5.4.3.6 Joint / Cleat Orientation

The planes within a cleat or joint set have a common trend or strike. The importance of the trend of the joints/cleats is in the relationship with the orientation of the mining excavation. Joints trending parallel to the long axis of a roadway or parallel to the coal face create most problems whilst optimum stability is often the case when joints trend perpendicular to the roadway / coal face. However face and gate roads are generally orientated at 90° to each other, so stable conditions in one can often lead to degrees of instability in the other, if joints are perpendicular to the face or roadway.

### 5.4.4 Bedding And Lamination Plane Characteristics

#### 5.4.4.1 Bedding / Lamination Plane Strength

The strengths of bedding and lamination planes are related to surface roughness, large scale topography and the degree of cohesion between the bedding surfaces. Weak planes substantially reduce the strength and stiffness of a rock mass in the vicinity of underground coal mine workings and provide potential separation horizons in the immediate roof of roadways which can seriously effect stability. Within a strata unit the strength of bedding and lamination planes will vary with some planes being cemented whilst others exist as preexisting partings. The strength of bedding/lamination surfaces may be obtained by compression testing on angle cores or testing in a shear box. However for classification purposes this would be impractical as it involves sample preparation and laboratory testing facilities. The natural variability in bedding plane and lamination plane strength within a strata unit also requires a large amount of testing to be undertaken and the large scale topographic features of the bedding surface would not be accounted for. It was considered that an index relating to the anisotropic strength perpendicular and across bedding/lamination surfaces could be quickly obtained by point load testing of cores samples across the bedding/lamination surface in accordance with ISRM guidelines (ISRM 1985). The UCS value obtained from point load testing across the bedding surface could be related to the UCS perpendicular to bedding to obtain an anisotropic

strength index (ISRM 1985). For foliated rocks Tsidiz (1990) proposed the following classification of point load strength anisotropy:

Strength anisotropy index	Descriptive term
> 3.5	Very highly anisotropic
3.5 – 2.5	Highly anisotropic
2.5-1.5	Moderately anisotropic
1.5-1.1	Fairly anisotropic
<1.1	Quasi-anisotropic

Table 5.4 Classification of point load strength anisotropy for foliated rocks  
(after Tsidiz 1990)

Using this test it was envisaged that a representative sample of bedding/lamination surfaces could be obtained so that the mean bedding/lamination strength index could be determined. It was considered that preexisting parting horizons within the strata unit are of extra significance as they form natural bedding separation horizons and horizontal shear horizons and a record should be made of the frequency of such horizons within each strata unit.

#### 5.4.4.2 Bedding / Lamination Spacing

Bedding spacing can be defined as the mean perpendicular distance between the bedding surfaces within a strata unit. The closer the bedding spacing the lower the strength and elastic modulus of the rock mass. The bedding spacing influences strata mechanisms that occur in the roof and floor strata of a coal mine roadway as closely spaced bedding planes form thin beams of rock, which under the effect of horizontal stresses may buckle and fail in tension.

#### 5.4.5 Fissility

The preferred orientation of clay minerals that frequently occurs in argillaceous rocks leads to a reduction in the strength parallel to the orientation. Very poor rock mass conditions can occur where fissility is well developed (shales). For classification purposes the strength anisotropic point load index test is considered a representative

measurement of the degree of fissility. The anisotropic index should be determined for the intact rock between any bedding planes. In laminated strata this is not possible due to the closeness of the lamination planes and for this case the rock can be treated as unfissile.

#### **5.4.6 Groundwater Flow**

Groundwater movement through a rock mass exerts stresses on to the sides of joints and planes within the rock mass. This reduces the normal stresses across the fractures lowering the shear strength of the joints. Close to an excavation the confining stresses across a joint or bedding plane may be low, in such cases the movement of groundwater may lead to large dilation of the joints / bedding planes leading to large inflows of water and collapse of the strata into the excavation. An area of groundwater flow in the mining excavation should be recorded and the groundwater condition determined by comparing observations of the moisture condition, seepage and inflows.

#### **5.4.7 Moisture Sensitivity**

As described in Chapter 4, several Coal Measure rock types are susceptible to swelling, slaking and a reduction in shear strength in the presence of water. Moisture sensitivity is of importance to predominately argillaceous rocks such as seatearths which are exposed in the floor, roof and sidewalls of coal mining excavations. Some sandstones that contain a clay matrix are also susceptible to large reductions in strength with additions of small amounts of water (Hawkins and McConnell 1992). The potential for in-situ swelling, reduction in strength and slaking is related to both the intact strength and the swelling potential. Several moisture sensitivity/ mudrock durability tests have been developed (ISRM 1981, Olivier 1979, Mark 1994). Olivier (1979) proposed the geodurability classification which is based on the free swelling coefficient and uniaxial compressive strength (Figure 5.30). The classification was developed primarily to assess the durability of mudrocks and poorly cemented sandstones during tunneling operations in South Africa but can be used internationally and has been applied in a limited manner to UK Coal Measure mudstones (Bell et al 1997).

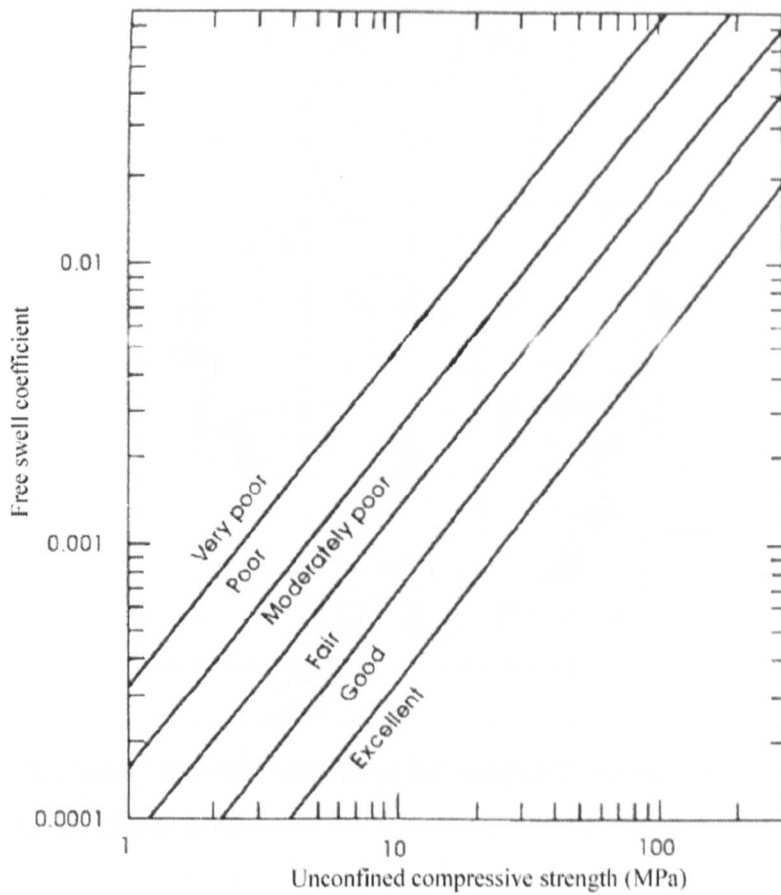


Figure 5.30 Geodurability classification (After Olivier 1979)

To determine the free swell the rock sample should be oven dried at a temperature of 105°C for a minimum period of 12 hours and also immersed in water for a minimum period of 12 hours during which the swelling is carefully monitored by dial gauges. The free swell coefficient ( $E_d$ ) can then be calculated using Equation 5.8:

$$E_d = \frac{\Delta L}{L} \quad (5.8)$$

Where  $\Delta L$  = change in length after swelling

$L$  = initial length of specimen

The ISRM (1981) recommended a cell and dial gauge assembly for measuring free swell is that shown as Figure 5.31

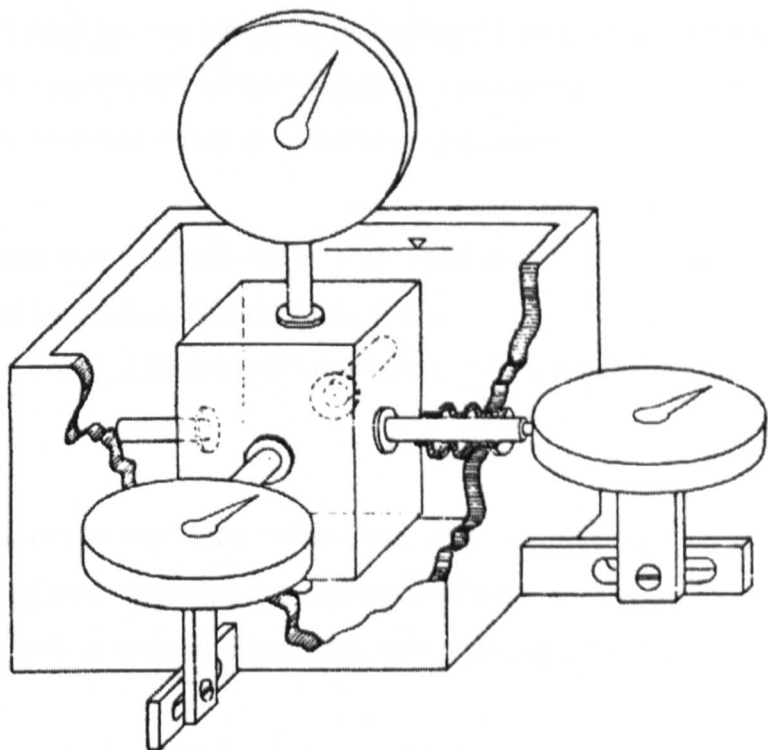


Figure 5.31 Cell and specimen assembly for unconfined swelling test.

(after ISRM 1981)

## 5.5 DERIVATION OF PARAMETER IMPORTANCE RATINGS

### 5.5.1 Introduction

The selected parameters do not all have the same degree of influence on the strength and stiffness properties of the rock strata. In most existing classification systems this has been taken into account by attributing importance ratings relative to the assessed importance of each individual parameter (Bieniawski 1989). In the Rock Mass Rating system and its hybrids the final classification rating is given as the sum of individual parameter ratings (Bieniawski 1989).

Due to the cyclic nature of the UK Coal Measures, at any one locality within an underground excavation there could usually be several strata units of different lithological and structural properties influencing the overall strata deformation adjacent to the excavation. This means that to determine the importance of the individual classification parameters using statistical techniques a large amount of classification and monitoring data for a wide variety of strata and mining conditions was required. Such information was not available and to obtain preliminary ratings for the coal mine classification parameters an alternative methodology has been

developed. The methodology was based on evaluating the relative importance of each of the classification's parameters to the conceptual mechanisms of strata failure and deformation that has previously been described in this chapter.

The derivation of importance ratings can be considered as two parts, which are:

- 1) the derivation of the maximum importance rating
- 2) the construction of rating scales representing the variation of rating value against parameter value.

In the RMR classification structure, which has been adopted by the Coal Mine Classification, the importance ratings are expressed as a percentage with the summed value of the parameter's maximum importance ratings being therefore 100%.

### **5.5.2 Maximum Importance Rating**

The maximum rating for a parameter can be considered as a representation of the relative importance of the parameter in processes of failure and deformation of the in-situ strata. The maximum deformation occurs when the parameter value is most unfavourable. For instance a UCS of 10 MPa would be considered unfavourable as the rock with such a low strength would fail and deform extensively under typical UK coal mining depths of between 600 and 1000m.

The relative importance of each individual classification parameter was determined for each conceptual mechanism. This was undertaken by estimating, for each parameter, the degree of deformation produced by an unfavourable parameter value. The parameters were then given importance ratings relative to the predicted degree of deformation produced. Using this method reasonable assessments could usually be made of the relative importance of the individual parameters. The methodology used is outlined in Figure 5.32 and the percentage importance ratings for the roof, floor, rib and face localities are shown as Tables 5.5, 5.6, 5.7 and 5.8 respectively.

To obtain the overall importance rating for an individual parameter the parameter's importance rating for each mechanism was averaged. Differences in joint and bedding ratings determined for strata within the rib/coal faces and roof/floor were apparent. It was therefore decided to produce two sets of importance ratings with one set for

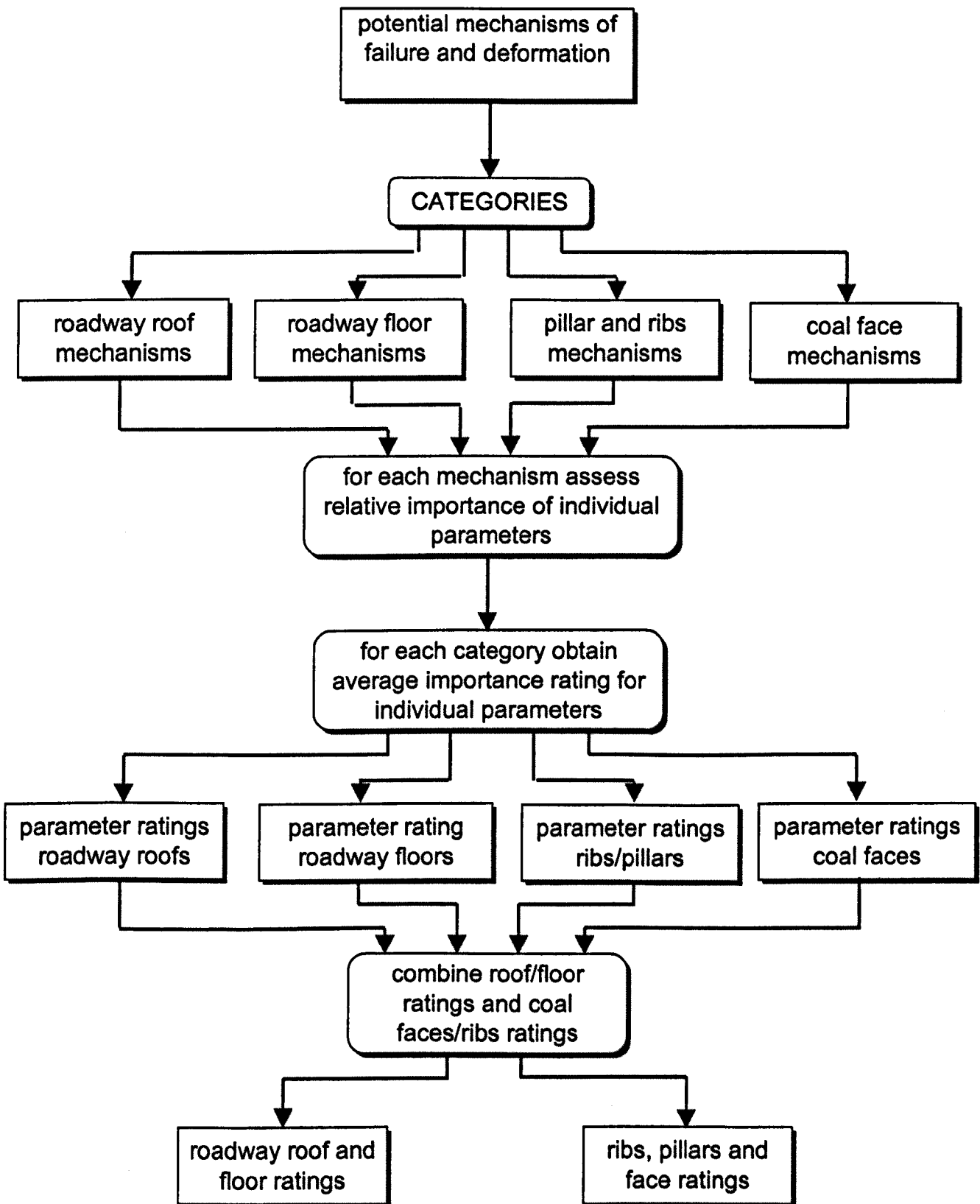


Figure 5.32 Methodology developed to determine maximum importance ratings

PARAMETERS	<i>buckling by horizontal stress</i>		<i>swelling of seatearth floor</i>		<i>shear along joints and bedding</i>		<i>asymetrical plastic deformation</i>		<i>failure beneath pillar</i>						
UCS	10%		5%		5%		20%		35%						
no. joint sets	7% 7% 3% 3%	20%	7% 7% 3% 3%	20%	10% 10% 5% 5%	30%	7.50% 7.50% 5% 5%	7.50% 7.50% 5% 5%	25%						
joint spacing															
joint profile															
joint persistancce															
joint orient.	R.F		R.F		R.F		R.F		R.F						
no. cleat sets	not applicable		not applicable		not applicable		not applicable		not applicable						
cleat spacing	not applicable		not applicable		not applicable		not applicable		not applicable						
cleat profile	not applicable		not applicable		not applicable		not applicable		not applicable						
cleat orient.	not applicable		not applicable		not applicable		not applicable		not applicable						
bedding spacing	25% 15%	40%	10% 10%	20% 20%	15% 15%	30%	15%	30%	7%	15%					
bedding strength															
fissility	15%		15%		15%		15%		10%						
water flow	10% 5%	15% 15%	15% 25%	40%	10% 5%	15%	3% 7%	10%	10%	15%					
moist. sensivity															

Table 5.5 Importance ratings for rock mass parameters within roadway floor

PARAMETERS	<i>self weight sagging</i>		<i>strata buckling</i>		<i>shearing from roof corners</i>		<i>shear/parting plane interaction</i>		<i>wedge failure</i>		<i>asymetrical deformation</i>					
UCS	10%		10%		35%		30%		10%		20%					
no. joint sets	7% 7% 3% 3%	20%	7% 7% 3% 3%	20%	3.50% 3.50% 1.5% 1.50%	30%	3.50% 3.50% 1.5% 1.50%	30%	10%	10%	7.50% 7.50% 5% 5%					
joint spacing																
joint profile																
joint persistancce																
joint orient.	R.F		R.F		R.F		R.F		R.F		R.F					
no. cleat sets	not applicable		not applicable		not applicable		not applicable		not applicable		not applicable					
cleat spacing	not applicable		not applicable		not applicable		not applicable		not applicable		not applicable					
cleat profile	not applicable		not applicable		not applicable		not applicable		not applicable		not applicable					
cleat orient.	not applicable		not applicable		not applicable		not applicable		not applicable		not applicable					
bedding spacing	25% 15%	40%	25% 15%	40% 40%	20% 10%	30%	20%	30%	15%	30%	15% 15%					
bedding strength																
fissility	15		15		15		15		10		10					
water flow	10% 5%	15% 15%	10% 5%	15% 15%	10% 5%	15%	10% 5%	15%	15%	3% 7%	10%					
moist. sensivity																

Table 5.6 Importance ratings for rock mass parameters within roadway roof

PARAMETERS	<i>spalling of coal seam out of face</i>		<i>failure beneath supports</i>		<i>collapse of roof in front of supports</i>		<i>cantilevering of roof over supports</i>		<i>wedge/block failure of roof</i>	
UCS	20%		30%		20%		25%		10%	
no. joint sets	not applicable not applicable not applicable not applicable	5% 6% 2% 2%	10% 10% 5% 5%	30%	10% 10% 30% 30%	30%	10% 10% 5% 5%	30%	10%	30%
joint spacing										
joint profile										
joint persistancce										
joint orient.	not applicable		R.F		R.F		R.F		R.F	
no. cleat sets	10% 10% 6% 4%	30%	not applicable not applicable not applicable not applicable	8% 8% 5% 5%	not applicable not applicable not applicable not applicable					
cleat spacing										
cleat profile										
cleat dominance										
cleat orient.	R.F		not applicable		not applicable		not applicable		not applicable	
bedding spacing	11% 9%	20%	8% 7.5%	15% 15%	10% 10%	20%	13% 12.5%	25%	15% 15%	30% 30%
bedding strength										
fissility	15%		8%		10%		10%		15%	
water flow	10% 5%	15% 15%	12% 18%	30%	8% 7%	20%	10% 5%	15%	8% 7%	15% 15%
moist. sensivity										

Table 5.7 Importance ratings for rock mass parameters within coal face

PARAMETERS	sidewall spalling		sidewall cleat dilation		shear along joint planes		wedge/block failure in pillar sides	yield zone development
UCS	45%		10%		10%		10%	20%
no. joint sets	not applicable		not applicable		not applicable		not applicable	not applicable
joint spacing	not applicable		not applicable		not applicable		not applicable	not applicable
joint profile	not applicable		not applicable		not applicable		not applicable	not applicable
joint persistance	not applicable		not applicable		not applicable		not applicable	not applicable
joint orient.	not applicable		not applicable		not applicable		not applicable	not applicable
no. cleat sets	4%	13%	15%	40%	10%	30%	11%	12%
cleat spacing	3%		15%		10%		12%	
cleat profile	3%		5%		5%		4%	
cleat dominance	2%		5%		5%		3%	
cleat orient.	R.F		R.F		R.F		R.F	R.F
bedding spacing	6%	12%	12.5%	25%	15%	30%	15%	10%
bedding strength	6%		12.5%		15%		15%	
fissility	15%		15%		15%		15%	15%
water flow	10.0%	15%	7.5%	10%	8.0%	15%	10.0%	8.0%
moist. sensivity	5%		2.5%		5%		5%	
							15%	15%

Table 5.8 Importance ratings for rock mass parameters within roadway rib or coal pillar

PARAMETERS	AVERAGE RATING (%)	
UCS	18	
no. joint sets	8	
joint spacing	7	
joint profile	4	23
joint persistance	4	
joint orient.	R.F	
bedding spacing	16	
bedding strength	12	28
fissility	13	
water flow	9	
moist. sensivity	9	18
<b>TOTAL = 100</b>		

Table 5.9 Average importance ratings  
roof/floor (coal face and roadway)

PARAMETERS	AVERAGE RATING (%)	
UCS	18	
no. cleat sets	10	
cleat spacing	11	30
cleat profile	5	
cleat dominant	4	
cleat orient.	R.F	
bedding space	12	
bedding strength	11	23
fissility	13	
water flow	9	
moist. sensivity	5	14
<b>TOTAL = 100</b>		

Table 5.10 Average importance ratings  
coal pillar/rib/face

R.F. denotes reduction factor

rib/face line classification, and one set for roof/floor classification. The final maximum classification ratings for the roof/floor classification are given in Table 5.9 and for the rib/face line classification in Table 5.10.

### 5.5.3 Rating Scales

Consideration of the mechanisms of strata deformation and failure indicates that a range of parameter values which are significant in terms of their effect on the mechanisms exist. The end limits of the importance ratings have been evaluated with the parameter value which generates the least deformation or failure being given the maximum rating and the parameter value which produces the most failure and deformation is given a rating of zero. The relationship between parameter values and their corresponding rating was obtained by undertaking a parametric sensitivity analysis on each of the mechanism's models. The analysis encompassed established rock mechanics methodologies in the case of strata buckling, block failure and bearing capacity failure. Where this was not possible engineering judgement was used together with considerations of the scales used in previous rock mass classifications.

Two basic types of scales were identified from the analysis, simple linear scales (Figure 5.33) where a change in a parameter value produces a corresponding linear change in the deformation in the rock mass, and non-linear scales (Figure 5.34) where a change of a parameter value produces a non-linear change in the deformation or where the possibility of failure is more likely over one part of the parameter range. For instance in the roof buckling by horizontal stresses there is a theoretical negative exponential effect between the bed thickness the amount of buckling produced.

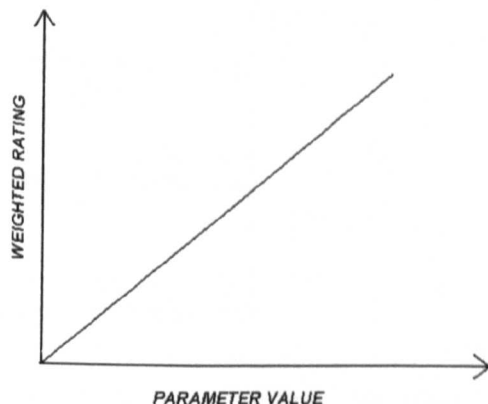


Figure 5.33 Linear scales

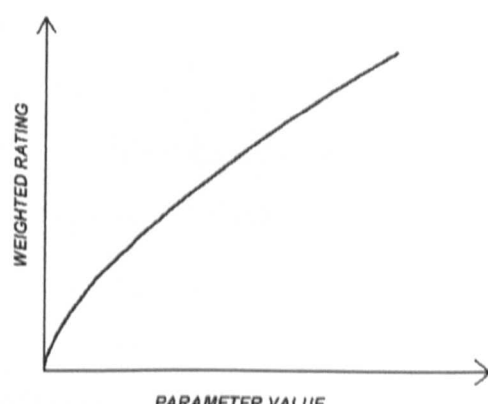


Figure 5.34 Non-linear Scales

The derived relationships between parameter values and ratings are included as Figures 5.35 to 5.44 and Tables 5.11 to 5.15.

#### 5.5.4 Adjustment Ratings For Joint/Cleat Orientation

The preliminary adjustment rating for joint orientation within floor and roof strata is shown in Figure 5.43 and for cleat and joint orientation within the rib sides and coal face are shown in Figure 5.44. It was considered that the strata within the coal ribs/coal face would be more affected by joint/cleat orientation than the roof or floor strata and hence have been given a bigger range of ratings. Negative ratings were given to cleat/joint sets with an unfavourable orientation i.e. the angle formed between the strike of the joints and the rib sides being less than  $45^\circ$  and positive ratings were given to favourably orientated cleat/joint sets i.e. orientated greater than  $45^\circ$ . The orientation of the dominant closely spaced joints were considered as potentially having a greater effect on strata deformation than widely spaced joint sets, and the adjustment ratings was related to the joint/cleat rating of the set.

### 5.6 OUTLINE OF THE COAL MINE CLASSIFICATION

#### 5.6.1 Introduction

The structure of the Coal Mine Classification system is shown in Figure 5.45.

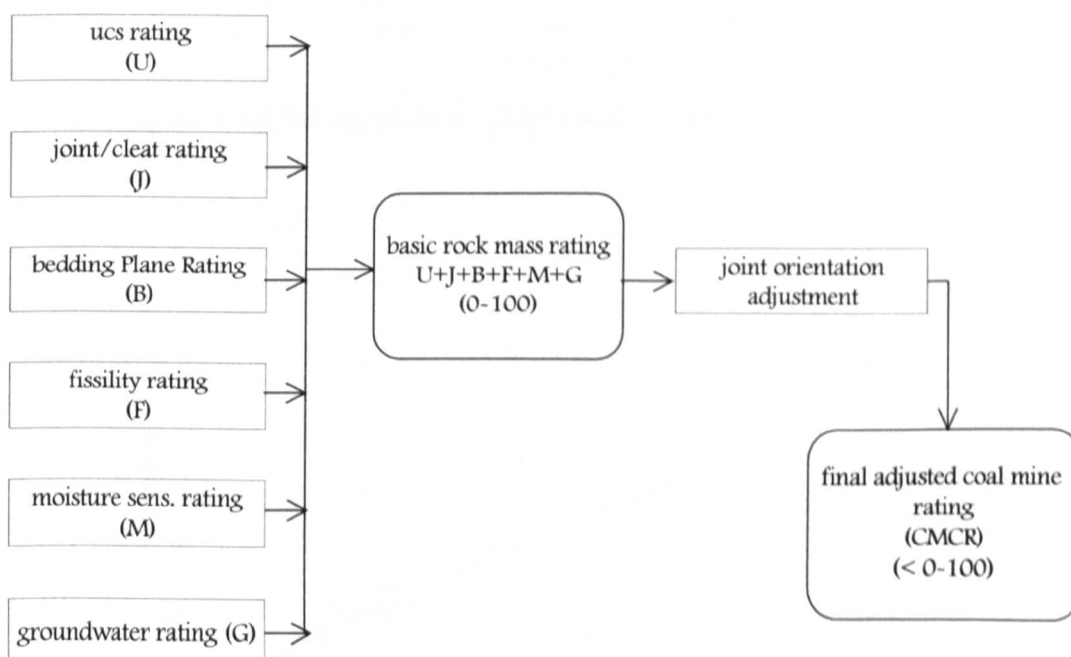


Figure 5.45 Structure of the Coal Mine Classification System

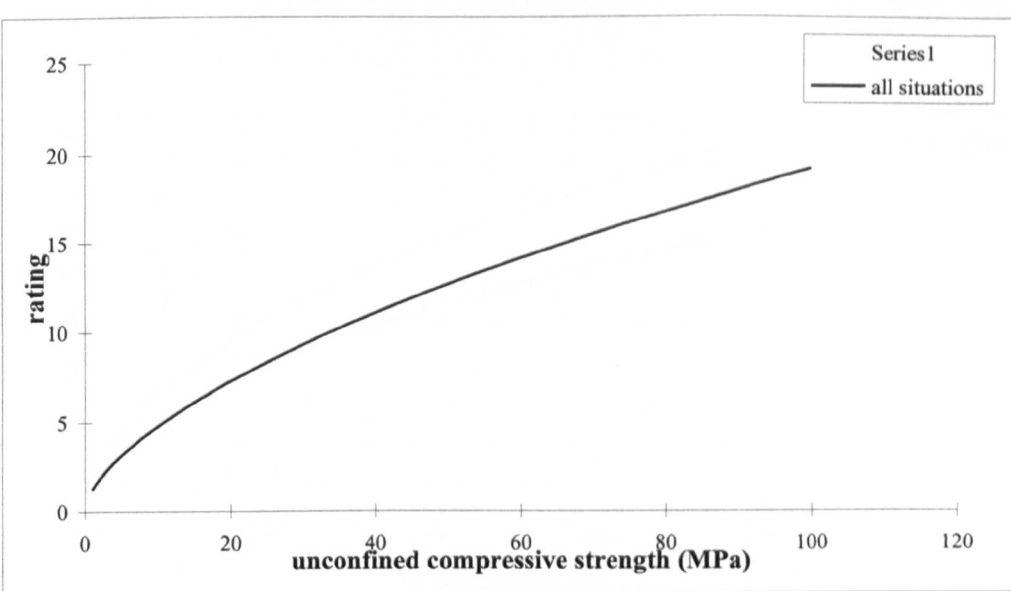


Figure 5.35 Rating scale for unconfined compressive strength

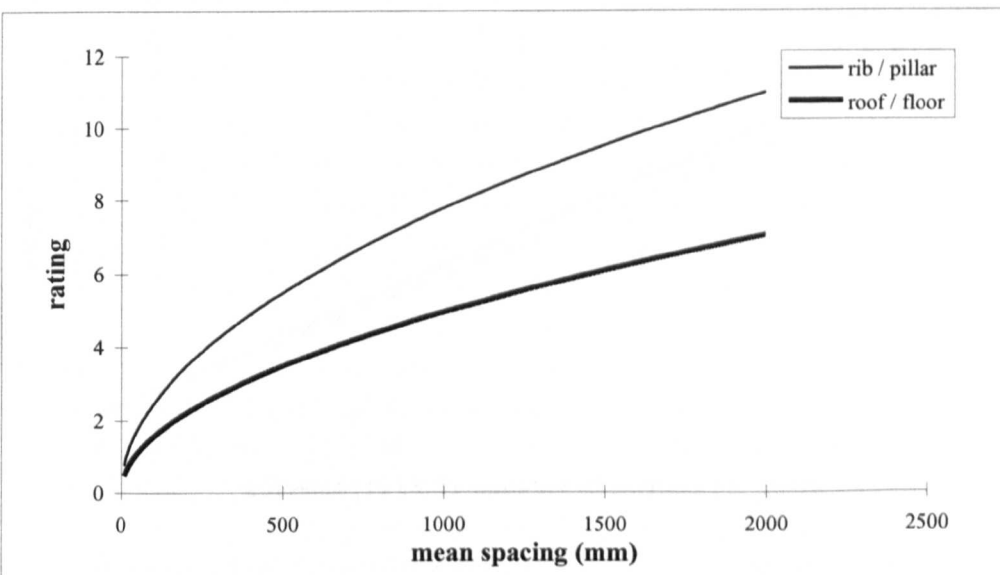


Figure 5.36 Rating scale for joint/cleat spacing

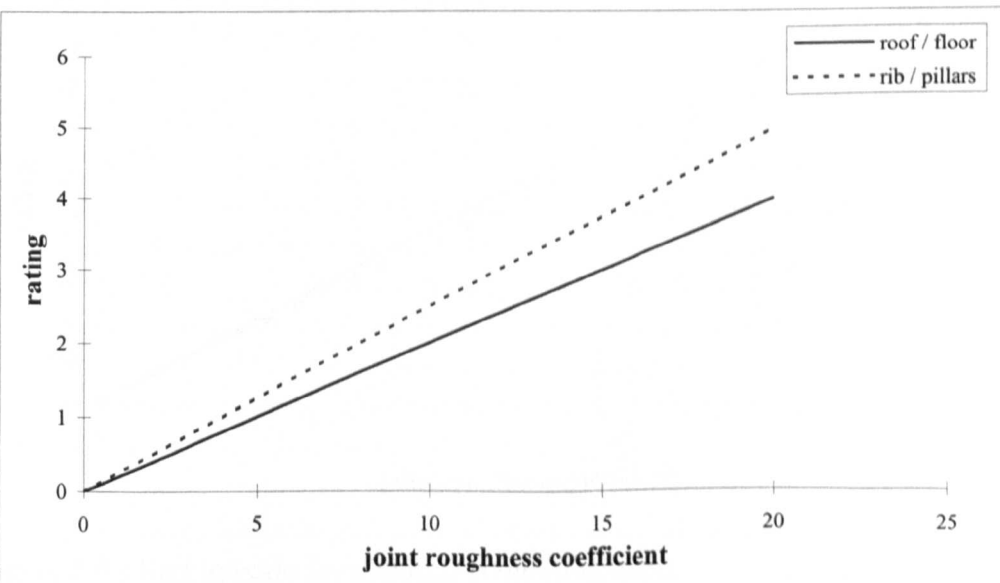


Figure 5.37 Rating scale for joint/cleat roughness

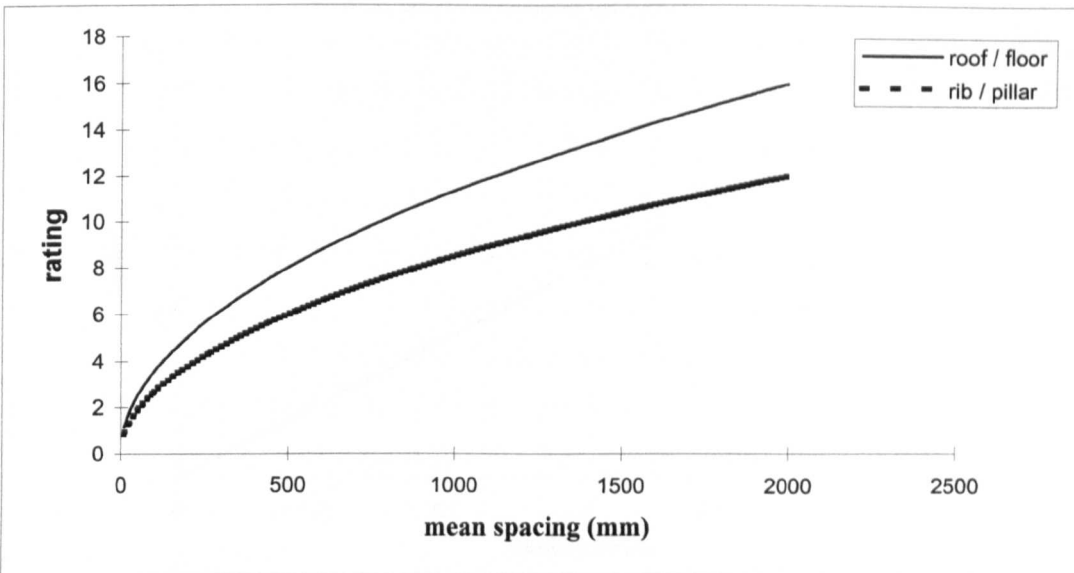


Figure 5.38 Rating scale for bedding plane spacing

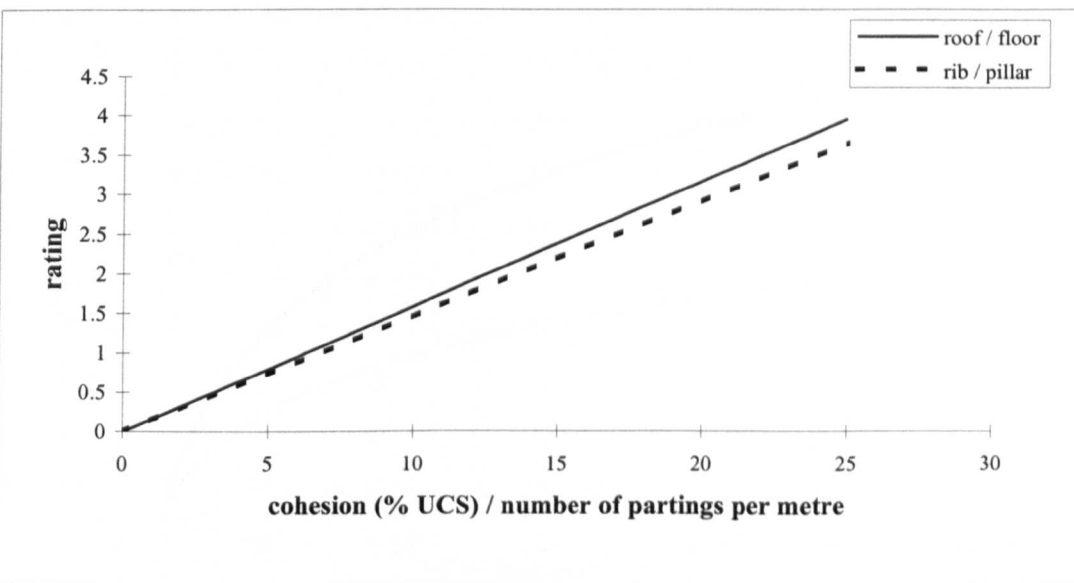


Figure 5.39 Rating scale for bedding plane cohesion

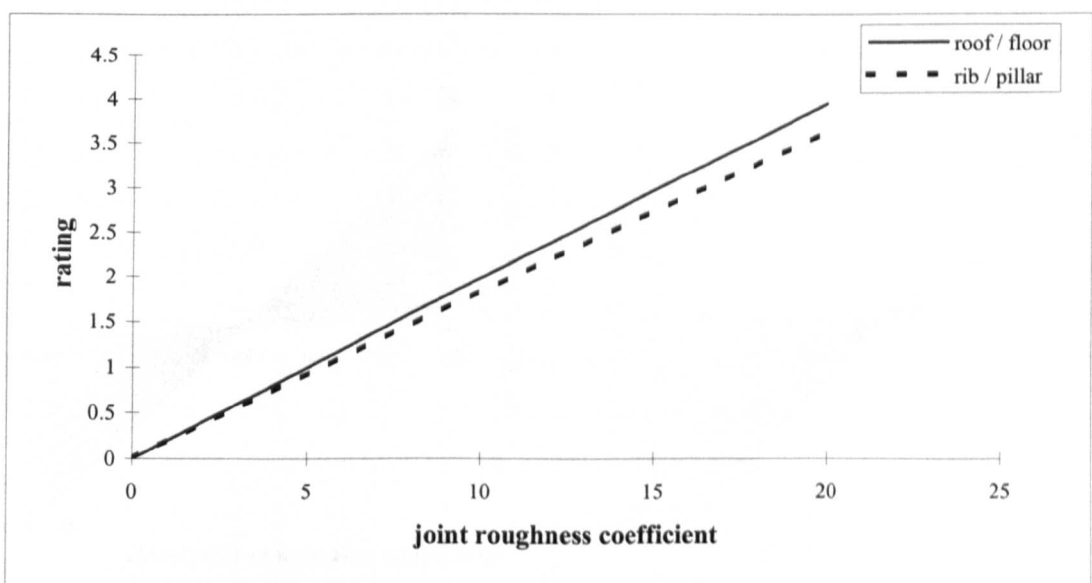


Figure 5.40 Rating scale for bedding plane roughness

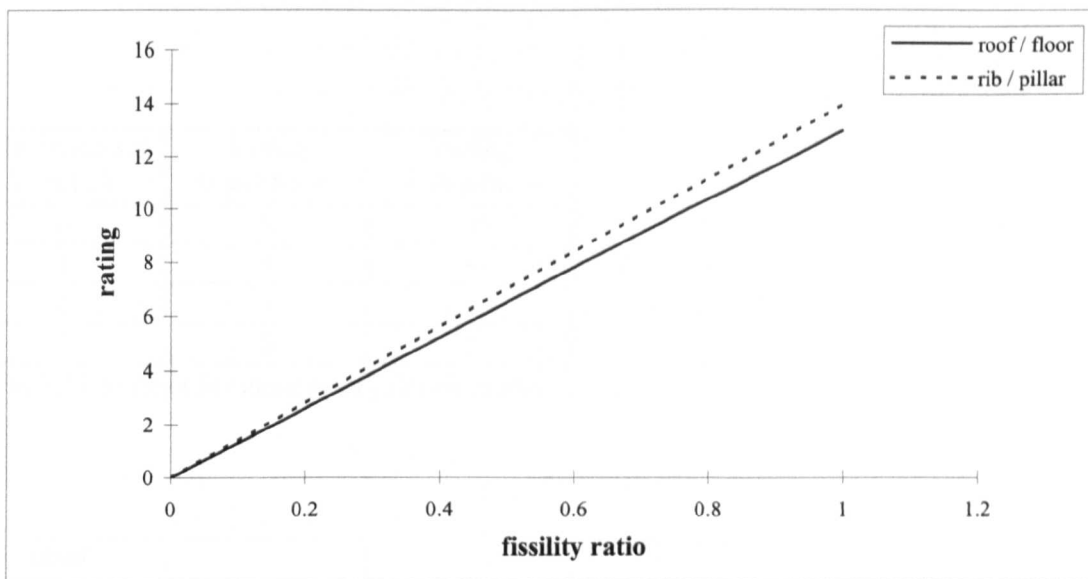


Figure 5.41 Rating scale for the fissility

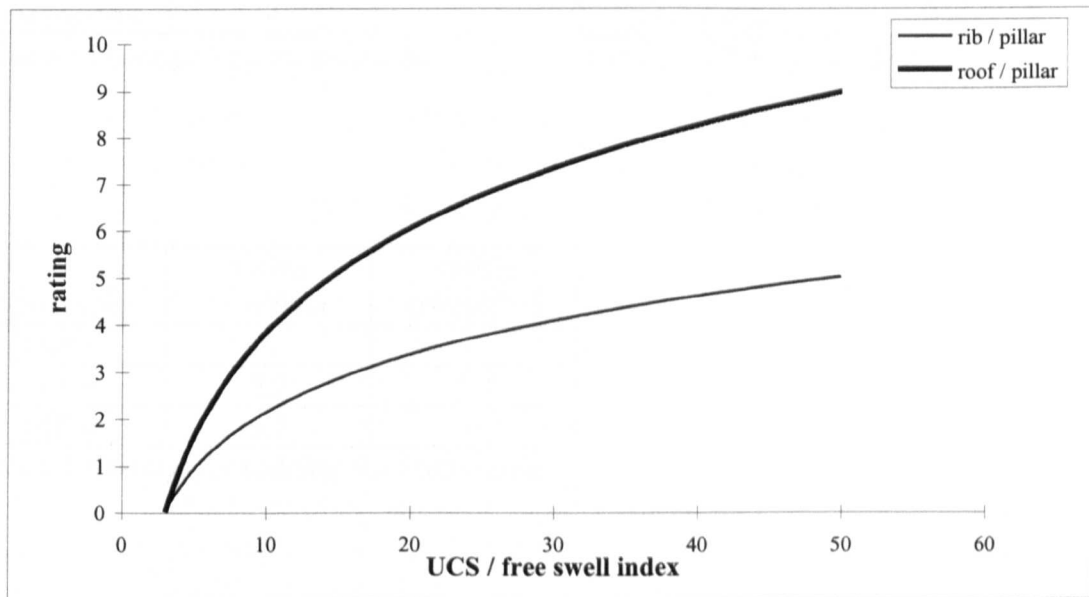


Figure 5.42 Rating scale for the moisture sensitivity

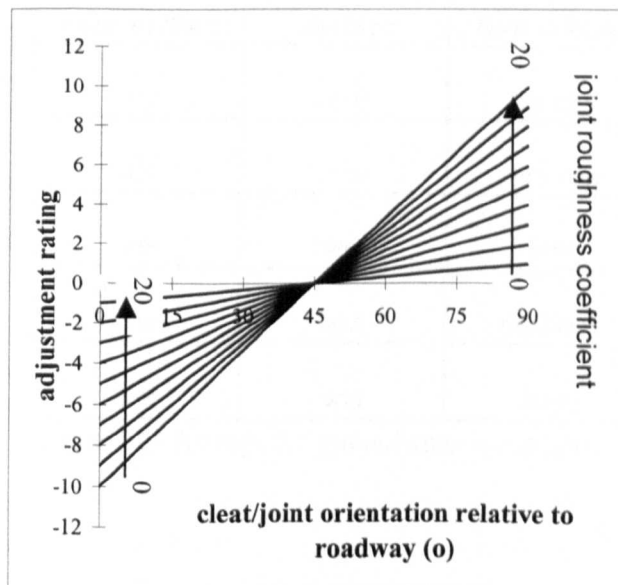


Figure 5.43 Adjustment rating for cleat/joint orientation in rib/pillar

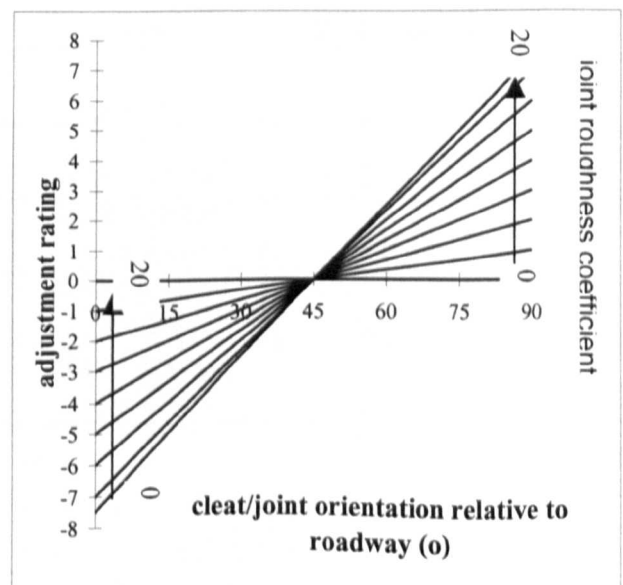


Figure 5.44 Adjustment rating for cleat/joint orientation in roof/floor

joint/cleat set number	rating (roof/floor)	rating (rib/pillar)
0	8	10
1	5	6
2	3	3
3	0	0

Table 5.11 Ratings for number of joint/cleat sets

joint persistence	rating
persistent	0
impersistent	4

Table 5.12 Ratings for joint persistence

cleat dominance	rating
dominant	0
not dominant	4

Table 5.13 Ratings for cleat dominance

topography	rating (roof/floor)	rating (rib/pillar)
planar	0	0
wavy	2.2	2.4
diffuse	3.7	4

Table 5.14 Ratings for bedding plane topography

rock surface	discontinuity surface	flow volume	observation of flow	RATING
dry	dry	none	none	9
dry	wet	very low	none visible	7
wet	wet	low	light seepage /dripping	5
wet	wet	medium	steady seepage /flowing	2
wet	wet	large	heavy seepage /gushing	0

Table 5.15 Ratings for groundwater conditions

The basic Coal Mine Classification Rating (CMCR) for a strata unit is derived as a summation of the ratings attributed to each measured parameter. The rating can vary between 0 to 100 with extremely poor rock mass conditions and 100 suggesting a very strong rock mass with no weakness planes. When applying the classification adjustments can be made where required to the basic rating to account for the effect of joint / cleat orientation relative to the orientation of the rib sides or coal face.

### **5.6.2 Characterisation of Anisotropy Using the Coal Mine Classification Rating.**

The directional nature of the Coal Mine Classification's stratification and jointing parameters infers that a directional variation in the CMCR may exist and thus a directional variation in the strength and stiffness properties of the rock mass.

Simplistically the structure of the strata may be considered as consisting of three sets of orthogonal planes formed by two sets of vertical joints and the horizontal planes of weakness parallel to bedding. Directional variation in the CMCR can be evaluated by determining ratings for the strata along imaginary lines parallel to and perpendicular to bedding.

#### **Rating perpendicular to bedding. $R_{(v)}$**

This is determined by summing the ratings for the stratification parameters and parameters that are considered non-directional such as the unconfined compressive strength, moisture sensitivity and groundwater with directional parameters such as bedding properties and Fissility. The joint parameters are assigned the maximum ratings (Figure 5.46)

#### **Rating parallel to bedding. $R_{(h)}$**

This is determined by summing the ratings for the joint/cleat parameters including the joint orientation adjustment rating and parameters that are considered non-directional such as the unconfined compressive strength, moisture sensitivity and groundwater. The stratification parameters are assigned the maximum ratings (Figure 5.47).

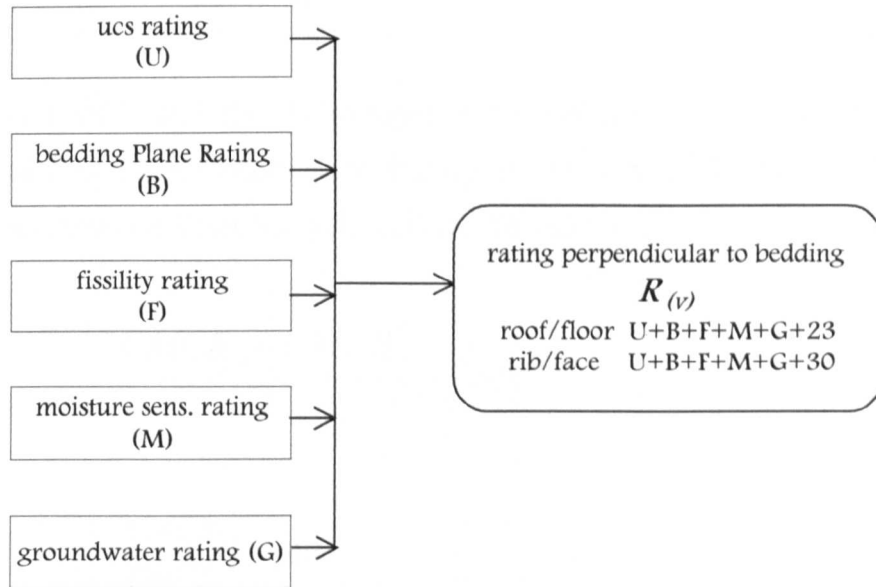


Figure 5.46 Calculation of rating perpendicular to bedding.

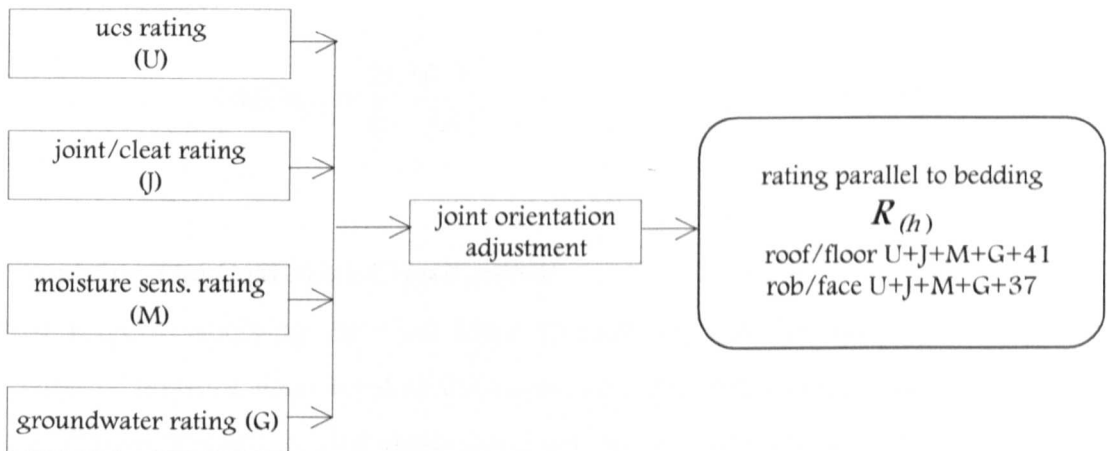


Figure 5.47 Calculation of rating parallel to bedding

The ratio between these two ratings can be considered as representing the degree of anisotropy of the strata and has been termed the Anisotropic Ratio (AR). The anisotropic ratio is defined in Equation 5.9:

$$AR = \frac{R_{(v)}}{R_{(h)}} \quad (5.9)$$

The adjusted CMCR and the Anisotropic Ratio can then be used to determine representative Coal Mine Classification Ratings in the vertical direction ( $CMCR_{(v)}$ ) and horizontal direction ( $CMCR_{(h)}$ ) (Equation 5.10 and 5.11)

$$\frac{CMCR_{(v)} + CMCR_{(h)}}{2} = CMC \quad (5.10)$$

$$\frac{CMCR_{(v)}}{CMCR_{(h)}} = AR \quad (5.11)$$

$$CMCR_{(v)} = \frac{2CMCR}{\left(1 + \frac{1}{AR}\right)} \quad (5.12)$$

$$CMCR_{(h)} = \frac{2CMCR}{\left(1 + AR\right)} \quad (5.13)$$

### 5.6.2 Applying The Coal Mine Classification

The first stage of applying the Coal Mine Classification is the identification and subdivision of the rock mass local to the excavation into strata units where the rock mass has similar properties. This subdivision will usually be undertaken with respect to the rock type and bedding or lamination plane characteristics. The presence of faults, joint characteristics and groundwater conditions also form important classification boundaries. Individual strata units should be greater than 0.25 metres thick with horizons less than this incorporated into an adjacent unit. Prior to classification the strata units should be identified in accordance with the lithological classifications detailed earlier in this thesis and given a brief engineering description in accordance with the recommended methods described in BS 5930 (1981).

Where units of < 0.25 metres are considered to potentially have a significant effect on the stability of the excavation, as for example clay bands or thin fractured fault zones or sheared smooth major discontinuities the unit should be considered separately from the rock mass classification and the effect of the feature assessed using analytical techniques.

A data sheet has been constructed that allows the parameter values of up to seven strata units to be entered onto the same sheet (Figure 5.48). A Coal Mine Classification computer application has also been developed using Microsoft Visual Basic. The application exists as an executable program that together with its support files can be run on a 1.44 MB disc used in the Windows environment. The application allows rapid calculation of the Coal Mine Classification Rating for a strata unit. File saving accommodates the logical storage of all classification data so that a database can be gradually built up of the strata properties for different mine sites.

## 5.7 CONCLUSIONS

An appraisal of existing rock mass classification structures indicates that the most suitable structure to be utilised for an engineering classification of UK Coal Measure strata was a Rock Mass Rating system where weighted importance ratings are summed.

Existing rock mass classifications have limited applicability for use for the engineering classification of rock strata within UK coal mines. Identification of the key parameters to be used within the classification was undertaken using conceptual mechanisms of typical strata deformations and by examining parameters used in established classifications previously applied to coal measure strata types and also by consideration of the lithological characteristics of the Coal Measure rock types.

The key parameters that have been identified were the unconfined compressive strength, bedding plane characteristics, jointing and cleat characteristics, moisture sensitivity and groundwater.

An initial set of importance ratings for each of the parameters has been derived and

produced as a series of graphs and tables. The characterisation of anisotropy was found to be typical of coal measure strata and has been included within the classification to obtain independent ratings both parallel and perpendicular to bedding.

# COAL MINE CLASSIFICATION DATA SHEET

	mine panel panel orientation	gate	coal seam metre mark					
	unit number	1	2	3	4	5	6	7
	height above seam roof							
	basic rock type							
	UCS (MPa)							
bedding/ lamination properties	bed/lam spacing (m)							
	topography							
	roughness (JRC)							
	cohesion (% ucs)							
	parting planes (No.)							
	joint/cleat set no.							
joint persistence/ cleat dominance	set 1							
	set 2							
	set 3							
joint/cleat roughness	set 1							
	set 2							
	set 3							
average spacing	set 1							
	set 2							
	set 3							
strike orient (0-180)	set 1							
	set 2							
	set 3							
	fissility ratio (0 to 1)							
moisture sensitivity	not required							
	Free Swell Coefficient.							
	groundwater condition							

Figure 5.48 Coal Mine Classification data entry sheet

## **CHAPTER 6**

### **APPLICATION OF THE COAL MINE CLASSIFICATION TO UK COAL MINES**

#### **6.1 INTRODUCTION**

This chapter describes the application of the Coal Mine Classification to sites at three different UK coal mines. For each of the mine sites a variety of data including roof cores, surface to seam borehole logs, in-situ stress measurements, mine layout plans, laboratory test data, details on installed supports and extensometer monitoring data for both the roadway roof and rib sides has been gathered. These data sets have been used in the application of the Coal Mine Classification at each case study locality. Validation of the effectiveness of the classification in predicting the strength and stiffness properties of the strata using numerical modeling techniques is fully described in Chapter 7 of this thesis.

##### **6.1.1 Data Uncertainty**

The data gathering process revealed that several aspects of the strata properties that have been identified in this thesis as significantly effecting the deformation of the roadways are not routinely recorded by the mines geotechnical personnel. For instance the spacing and orientation of the cleats and joints within the coal seam and adjacent strata are not measured and the geotechnical personnel could only indicate an approximate direction of cleat for the case study regions. For this preliminary validation of the Coal Mine Classification approximate values for the joint and cleat parameters have been determined using engineering judgement and historical sources. However this does increase the degree of uncertainty of the values of certain classification parameters and final strata rating than could be obtained with better parameter ratings.

#### **6.2 APPLICATION OF THE COAL MINE CLASSIFICATION TO RICCALL MINE, NORTH YORKSHIRE.**

##### **6.2.1 Introduction**

Riccall mine forms one of 6 mines that comprise the Selby complex which is situated in the Vale of York to north of the town of Selby. All the mines in the complex work the Barnsley seam which varies between 300 metres depth in the west of the area to

approximately a 1000 metres at the North Selby, Riccall and Whitemoor mines in the east and north of the complex. As the seam is comparatively near to the surface at its western edge access to the seam was developed by means of drift tunnels (Pyne 1984). These drift tunnels were driven in the solid beneath the Barnsley seam and extended across the complex allowing the 5 satellite mines of North Selby, Riccall, Stillingfleet, Whitemoor and Wistow to be linked to a single coal handling plant at the Gascoigne Wood Drift Mine (Houghton 1992).

Riccall Mine started production in 1988 (Siddall 1989) and by 1993 was producing coal at the rate of 2.5 million tonnes a year (Houghton 1993). The depth of cover varies from 600 to 1100 metres across Riccall's reserve area and the thickness of the Barnsley seam varies from 1.9 to 2.4 metres. Like all mines within the Selby complex coal is extracted using retreat mining techniques (Houghton 1992).

### **6.2.2 General Strata Sequence Adjacent To The Barnsley Seam**

The Skipwith No. 1 surface to seam borehole log, supplied by RJB Mining Ltd (RJB 1997 (a)), provides details on the lithological sequence above and below the Barnsley seam within the general vicinity of the case study localities. The section of the log detailing the strata sequence within the vicinity of the Barnsley seam is given in Table 6.1

### **6.2.3 Location Of Case Studies**

Case study information and roof rock cores were obtained for a total of twelve localities within the gate roads of panels H438, H478 and H505. The localities are detailed in Table 6.2 and shown in Figures 6.1 to 6.3.

Strata description		Depth of top below GL (m)
Banded siltstone, ripple bedded		873.57
Grey siltstone with ironstone bands		874.90
Grey shaly mudstone with ironstone bands		876.30
Dark grey shale		878.32
Grey shaly mudstone with ironstone bands		878.35
Black shale		879.76
DULL SEAM	Inferior dull coal (10 cm)	879.88
	COAL (17.5 cm)	
	Dull coal (29.5 cm)	
	Inferior coal (3 cm)	
Grey mudstone-seatearth with rootlets		880.48
Dark grey mudstone seatearth		880.76
Inferior coal		880.89
Grey mudstone seatearth with rootlets and ironstone nodules		880.93
Grey silty mudstone-seatearth with ironstone nodules, rootlets and plants		882.50
Grey silty mudstone with ironstone nodules and plants		883.30
Grey siltstone with ironstone nodules and plants		885.15
Banded siltstone		892.92
Banded sandstone		894.13
Pale grey sandstone		894.83
Banded siltstone with ironstone nodules		896.00
Grey silty mudstone with ironstone lenses and plants		898.47
Grey mudstone with ironstone nodules and plant debris		901.80
Dark grey mudstone with coal streaks and plants		902.15
BARNESLEY SEAM	Inferior coal (1.5cm)	902.28
	Coal (76.5cm)	
	Inferior dull coal (1.5cm)	
	Coal (73 cm)	
	Inferior dull coal (8 cm)	
	Coal (52cm)	
	Coal with pyrites (2.5cm)	
Grey mudstone-seatearth, weak and friable		904.43
Dark grey siltstone seatearth with rootlets		904.90
Dark grey siltstone		905.20
Grey silty mudstone seatearth with rootlets		905.40
Grey silty mudstone with scattered rootlets		905.60
Grey siltstone		906.00
Banded siltstone, cross-bedded		906.53
Grey silty mudstone with ironstone bands		907.77
Grey shaly mudstone		908.42
Coal		908.57
Carbonaceous mudstone-seatearth with coal streaks		908.76
Dark grey silty mudstone with plant debris		908.90
Grey silty mudstone-seatearth with rootlets		908.95
Banded siltstone with ironstone nodules and rootlets		909.20
Dark grey silty mudstone with plant debris		909.63
Grey mudstone with plant debris		910.00
Banded siltstone cross bedded		910.16
Dark grey silty mudstone with plant debris		914.41

Table 6.1 Section of Skipwith No.1 borehole adjacent to Barnsley seam, Riccall

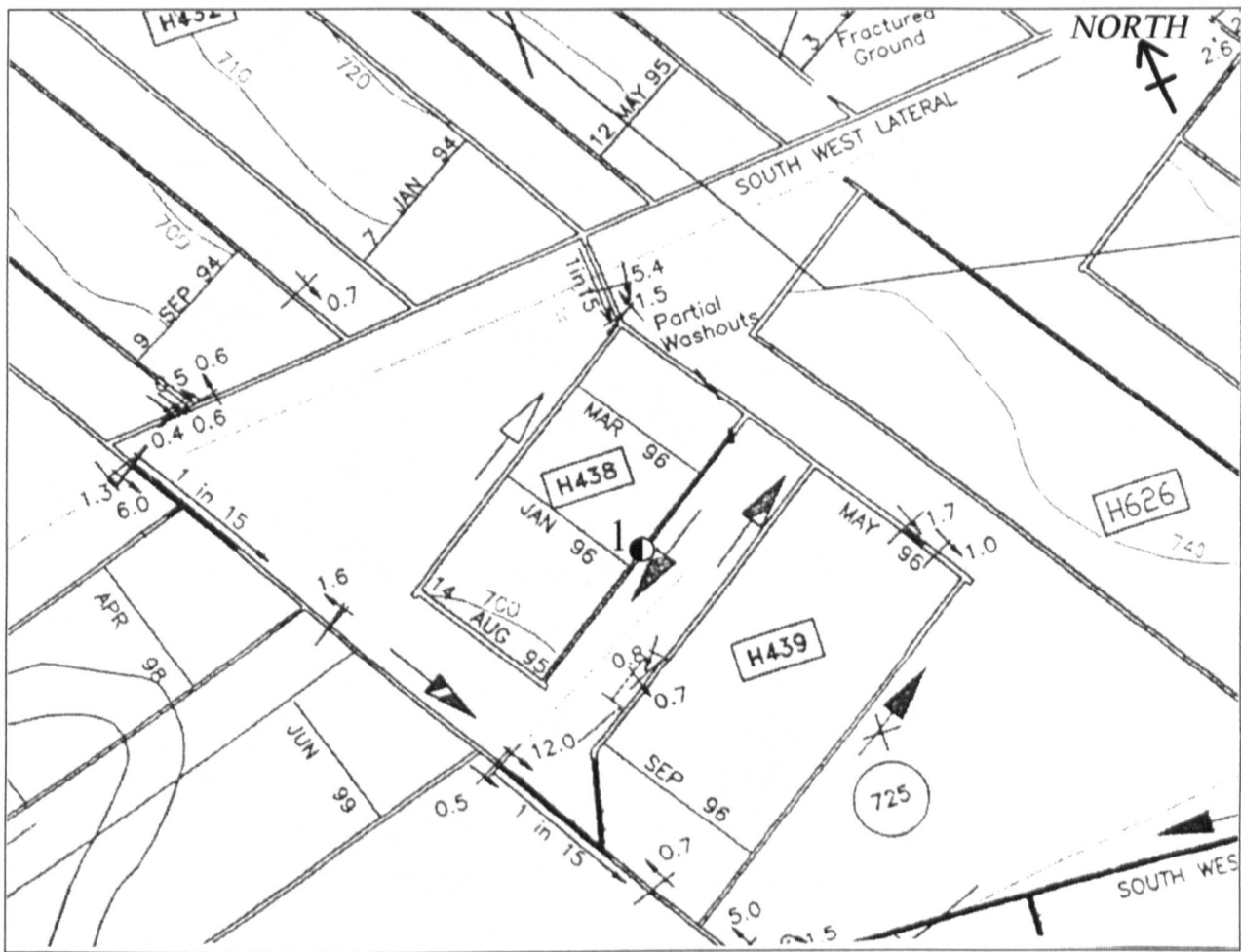


Figure 6.1 Riccall Mine, Panel 438 Layout

1 ● case study locality 1

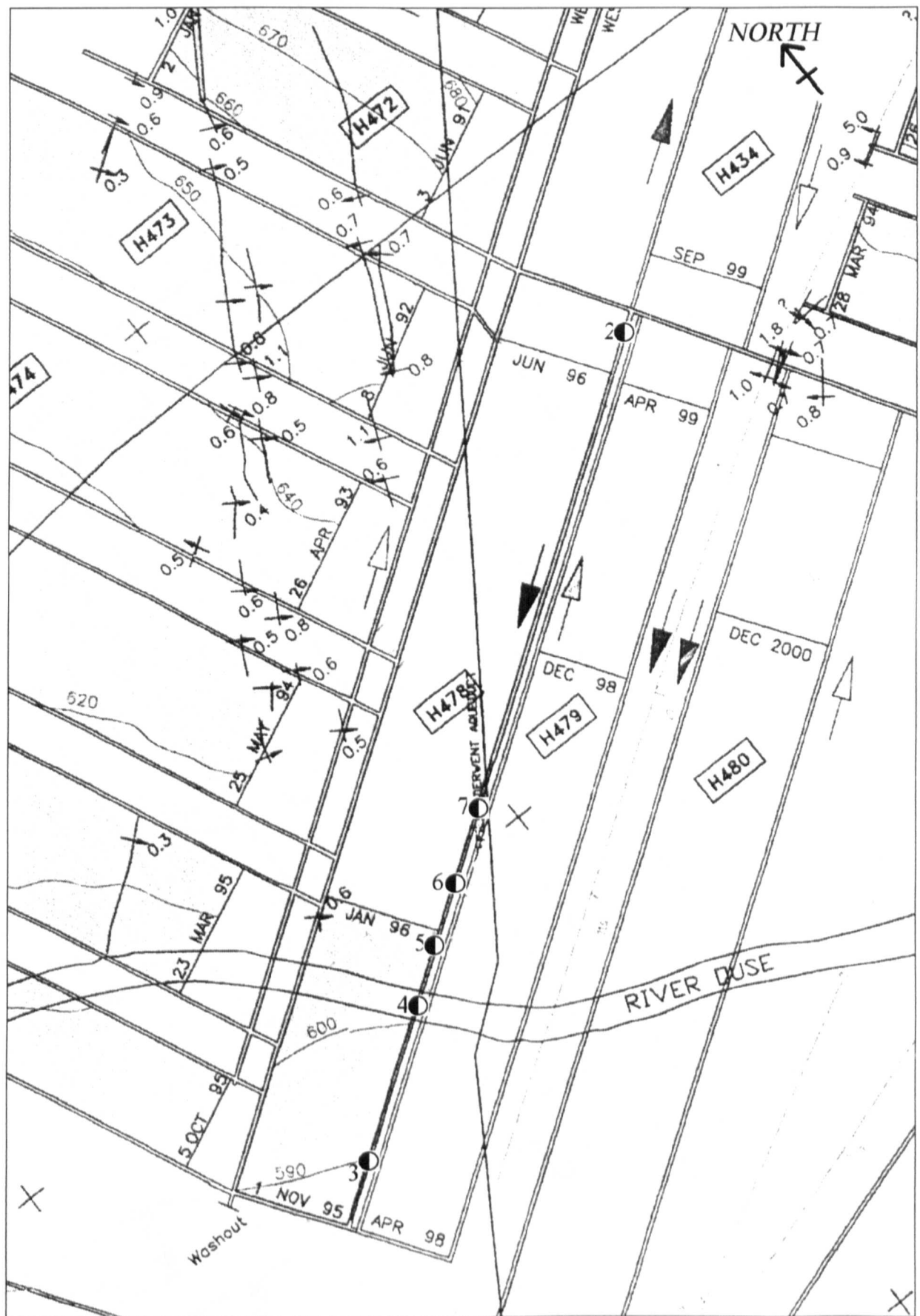


Figure 6.2 Riccall Mine, Panel 478 Layout  
**2 ●** case study locality 2

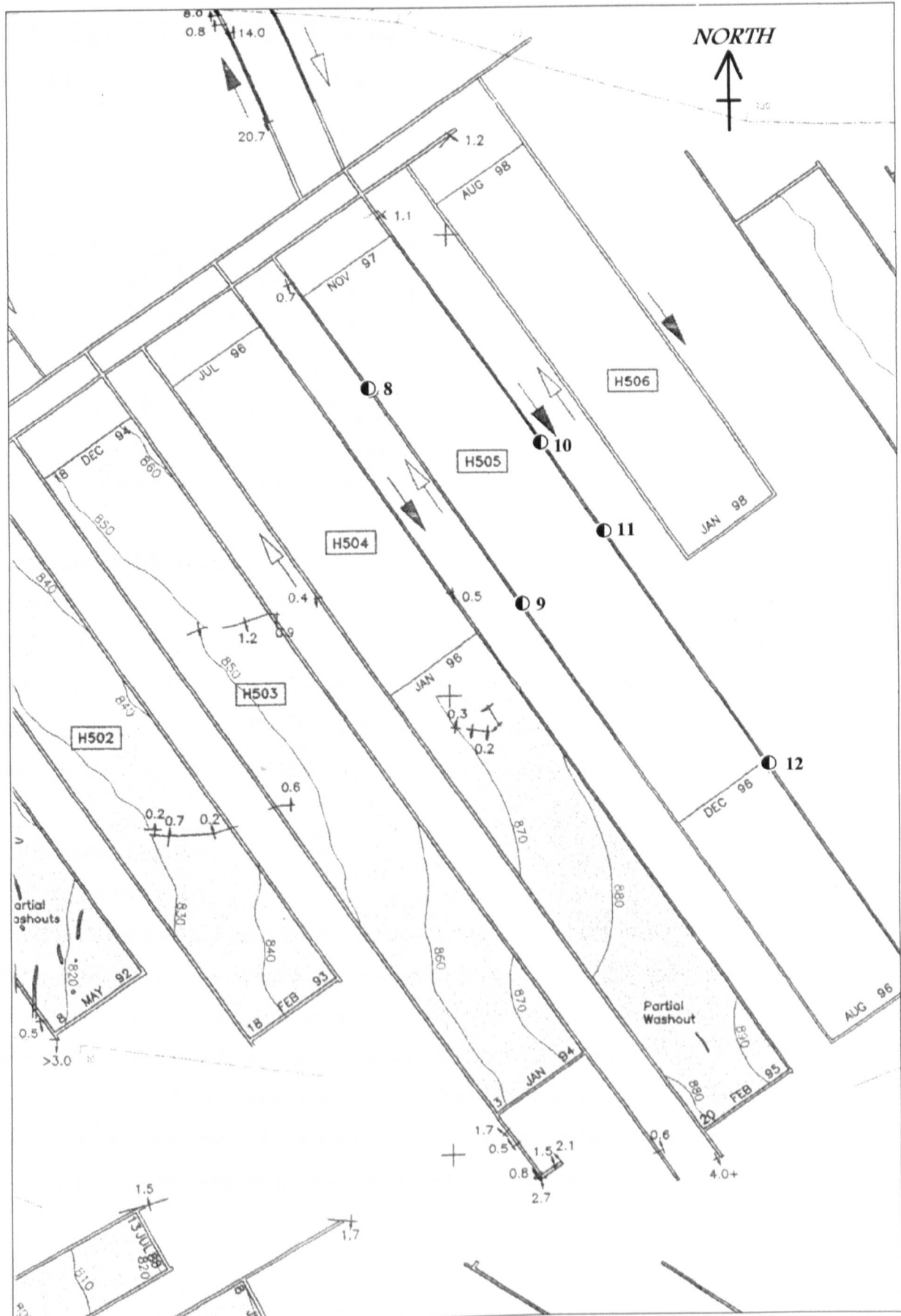


Figure 6.3 Riccall Mine, Panel 505 layout

● 8 case study locality 8

<b>Locality number</b>	<b>Panel</b>	<b>Gate</b>	<b>Metre mark</b>
1	438	Main	214
2	478	Main	31
3	478	Main	110
4	478	Main	387
5	478	Main	486
6	478	Main	587
7	478	Main	710
8	505	Tail	353
9	505	Tail	922
10	505	Main	669
11	505	Main	902
12	505	Main	1583

Table 6.2 Case study locations Riccall Mine

#### **6.2.4 Roadway Dimensions**

The roadways in panels H438, H478 and H505 are rectangular in section and approximately 5 metres wide by 3 metres high. The roadways were driven in seam and the logs for roof boreholes indicate that the roof elevation was typically formed at an horizon within the immediate roof approximately 1 metre above the seam top. This was due to the weak nature of the fissile mudstones directly overlying the coal.

#### **6.2.5 Installed Supports**

##### **6.2.5.1 Primary Support**

The primary support pattern used within the gateroads is shown in Figure 6.4. The pattern consisted of seven steel 22mm diameter 2.4 metre long full column grouted rockbolts and steel roof straps were equally spaced across the roof with each line of rockbolts being at 1 metre intervals. Rib supports in the panel were provided by 2 x 1.8 metres long rockbolts horizontally installed into the rib sides and fitted with steel ribstraps. In the face side 2 x 1.8 metres long rib fibreglass bolts were installed to prevent damage to the coal cutting equipment during coal extraction.

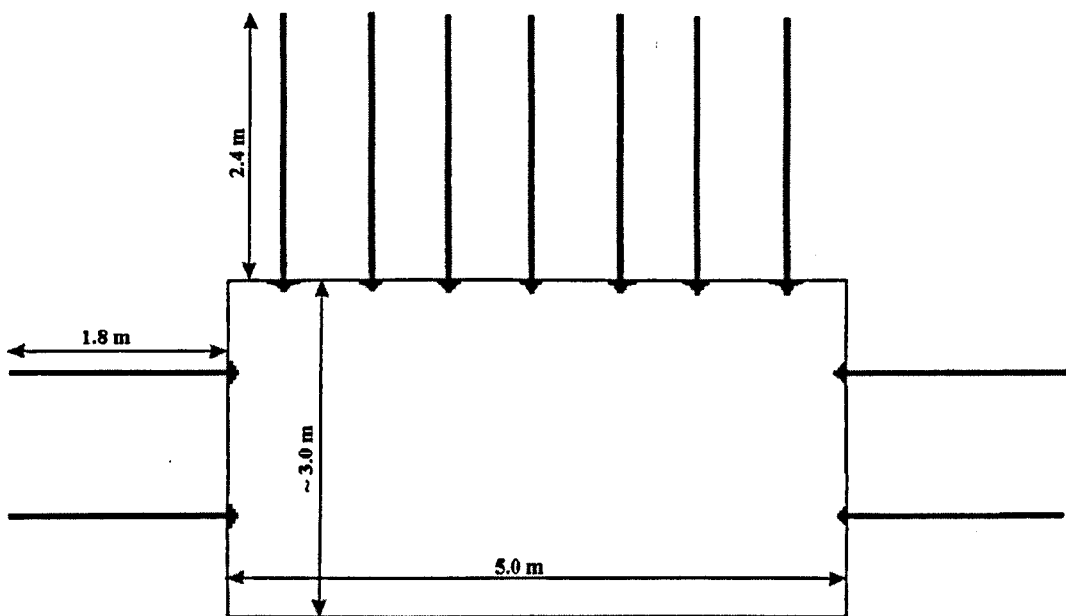


Figure 6.4 Primary supports, Riccall Mine

#### 6.2.5.6 Secondary Support

Where movement in excess of 25 mm had occurred, either within the bolted horizon or from the top of the bolted horizon to a height in the roof of 4.8 metres, secondary supports have been installed in the form of 2 x 4.8 metre long double bird cage cable bolts every 1 metre along the length of the roadway. The cable bolts were installed into 55mm diameter holes in a staggered pattern across the roof in between the line of primary rock bolts.

#### 6.2.6 Monitoring Data

Monitoring results were obtained from multi-horizon sonic extensometers installed in the centre line of the roof at regular intervals for Panels H478 and H505 and have been provided by RJB Mining. The extensometers measured roof displacement to a distance of approximately 5 metres into the roof of the roadway. No such equivalent monitoring data was available for panel H438.

#### 6.2.7 In-Situ Stress

In-situ stress measurements, undertaken using the CSIRO overcoring technique have been obtained for panel 505's tail gate (RMT 1996). The results of the measurement obtained in the roof strata at a lateral distance of 10.9 metres from the roadway was conjectured to represent the virgin in-situ stress conditions. The measurement

indicated that the maximum stress resolved into the horizontal plane acted in a direction of 82° (Table 6.3). However this result contradicted visual evidence at Riccall, and previous measurements in the Selby coal field, which suggested that the maximum horizontal stress has a bearing of approximate 340° (RMT 1996).

The measured stress resolved into the vertical direction was 24 MPa which closely corresponds to the expected overburden stress at this locality.

	Magnitude	Direction
Vertical stress	24 MPa	
Major horizontal stress	23 MPa	82°
Minor horizontal stress	16.7 MPa	353°

Table 6.3 In-situ stress results 505 panel tail gate (after RMT 1996)

Due to the uncertainty in the in-situ stress measurements for the Riccall mine it is assumed that for the purpose of numerical modeling the in-situ stress is lithostatic i.e. the three principal stresses are equal to the expected overburden stress at each locality.

#### **6.2.8 Mining Interaction**

The Barnsley seam has not been under or over worked. Inspection of the dates of panel extraction indicated on the mine layout plans and the dates of roof extensometer measurements indicates that the localities were not influenced by the front stress abutment of the retreating panel at the time of the measurement or from adjacent panels during the period of monitoring.

#### **6.2.9 Intact Rock Properties**

Testing of the rock core samples has been undertaken to obtain the intact triaxial envelopes and Young's modulus for each of the basic lithologies identified. Limitations and the size requirements of the core restricted the amount of test work that could be undertaken.

### 6.2.9.1 Triaxial Strength

The triaxial strength was determined for a range of low confining stresses for each of the basic lithologies in order to simulate the stress conditions adjacent to roadways. The samples were prepared and tested in accordance with the procedure outlined by the ISRM (1981). The tensile strength was determined by the Brazilian disc test again in accordance with ISRM procedure (ISRM 1981). The test results are given in Appendix 3. The data was analysed using a computer program developed from this research to determine the strength properties of intact rock and rock masses. The Hoek-Brown material parameter,  $m_i$ , was determined for each of the data sets (Table 6.4). The computer generated triaxial envelopes for mudstone, massive siltstone, laminated siltstone and sandstone are shown in Figure's 6.5 to 6.10.

Lithology	$m_i$ value
Mudstone	9.2
Massive siltstone	16.6
Laminated siltstone	11.1
Sandstone	15.6

Table 6.4 Hoek-Brown  $m_i$  variables for Riccall Lithologies

### 6.2.9.2 Young's Modulus

Determination of the Young's modulus was undertaken on samples prepared for triaxial testing. The testing was undertaken in accordance with ISRM (1981) guidelines, however the tests were terminated at an approximate axial stress of 25 MPa in order to prevent damage to the specimen prior to triaxial testing. The Young's Modulus was determined as the gradient of the linear portion of the curve formed by plotting the stress against the strain. The stress strain curve for each specimen tested are given in Appendix 2 and the calculated Young's Modulus for each basic rock type are outlined in Table 6.5.

MUDSTONE: panel 478, main gate, 710mm

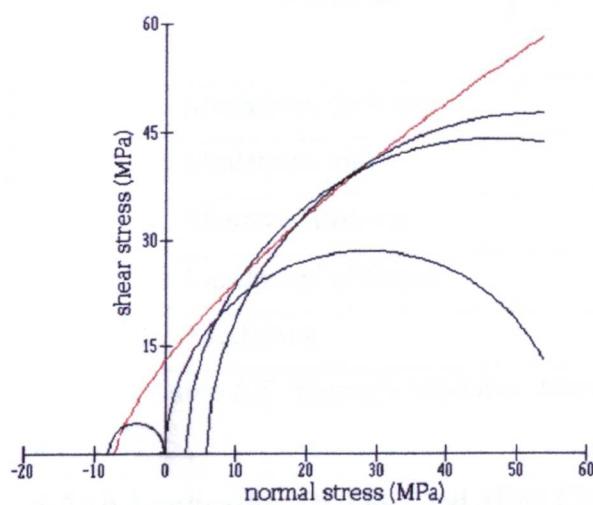


Figure 6.5. Mudstone, Riccall, 478 panel

MUDSTONE: Riccall, panel 505, main gate, 1583mm

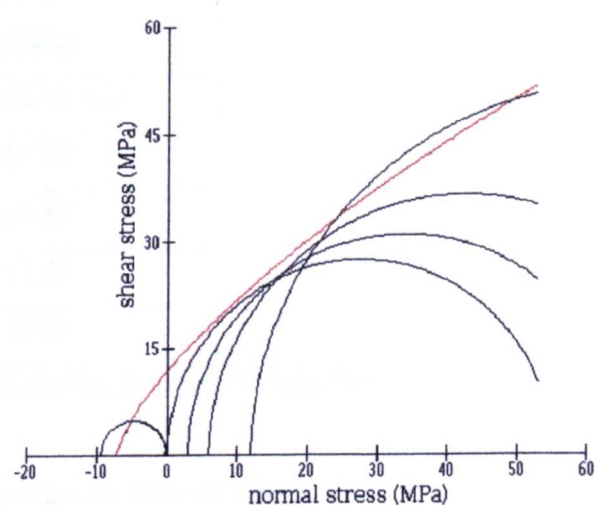


Figure 6.6 Mudstone, Riccall 505 panel

SILTSTONE: Riccall, panel 478, main gate, 31mm

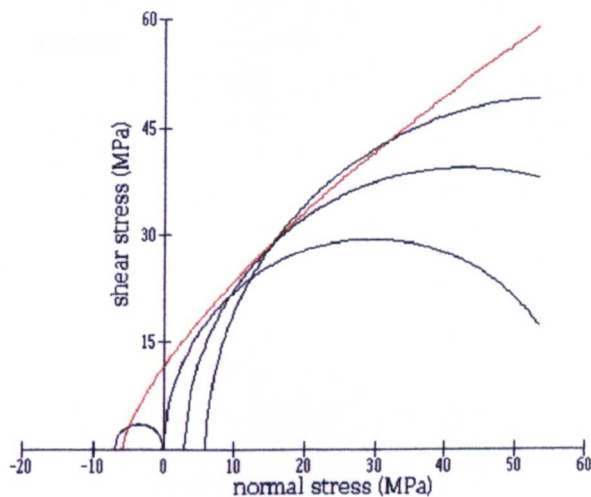


Figure 6.7 Siltstone, Riccall, 478 Panel

SILTSTONE: panel 505, main gate, 669mm

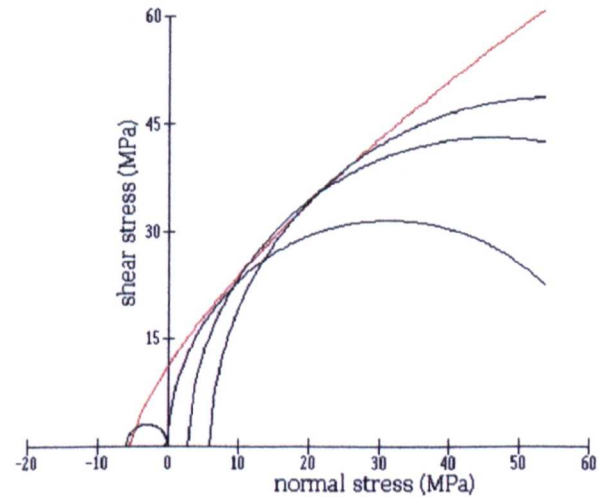


Figure 6.8 Siltstone, Riccall, 505 panel

LAMINATED SILTSTONE: Riccall, 478 panel main gate  
486mm

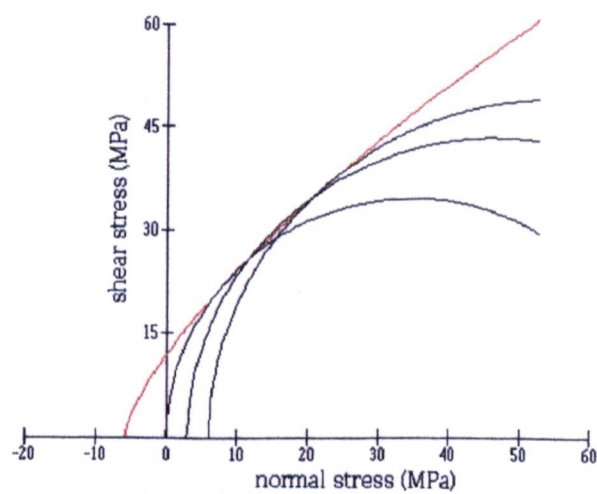


Figure 6.9, Laminated siltstone, Riccall, 478 panel

SANDSTONE: 478 panel, main gate, 710mm

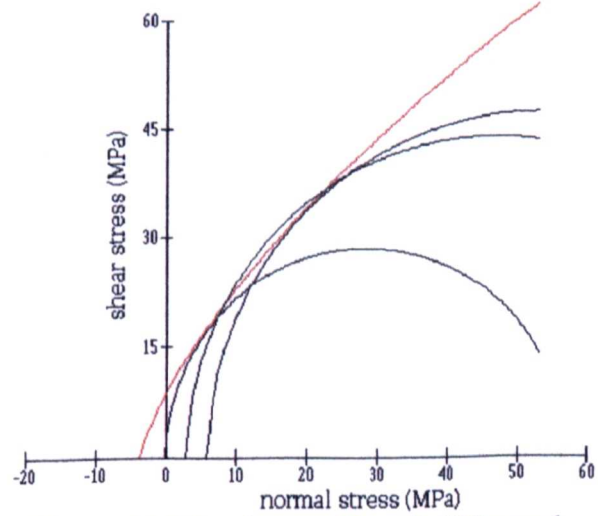


Figure 6.10 Sandstone, Riccall 478 panel.

Lithology	Young's Modulus (GPa)
Mudstone, dark grey	Unable to test
Mudstone, silty	15.82
Massive siltstone	14.87
Laminated siltstone	12.36
Sandstone	9.37

Table 6.5 Young's Modulus determined for Rock Strata Within Riccall Mine

#### 6.2.10 Application Of The Coal Mine Classification to Riccall Mine

The Coal Mine Classification was applied to the strata units identified from roof cores which have been obtained for each of the twelve localities from RJB Mining Ltd. The following pages describes how the parameter ratings were obtained for each of the cores:

#### 6.2.10.1 Case Study locality 1: Panel H438, Main Gate 214 Metre Mark

The borehole core was 4.92 metres long and is shown as Figure 6.11.



Figure 6.11 Roof core from the main gate of Panel H438 at 214 metre mark

Four strata units were identified and the classification applied to each unit. The unconfined compressive strengths for strata units 2, 3 and 4 were obtained by axial point load tests of the core. The UCS was estimated from the point load index using Equation 5.1. A conversion factor (K) of 24 (Bieniawski 1975) was used in the calculation. No suitable sized samples for point load testing could be obtained for strata unit 1 and the UCS for this unit was estimated using the cone indenter. To predict the UCS the cone indenter test was repeated five times on the same sample and the readings averaged. The bedding/lamination parameters of spacing, roughness and cohesion were determined in accordance with the procedures described in Chapter 5. The number of preexisting parting planes was recorded for each strata unit and care was taken that the partings represented natural breaks. As for all case study localities, no information in relation to the joint properties could be obtained. The mine geotechnical staff indicated the general orientation of the main and butt cleat across the mine site. This was used to infer the general orientation of the major and

minor joint sets within the roof. A joint spacing of 1 metre was assumed for each joint set which corresponds to the “wide spacing” of the ISRM classification of joint spacing (ISRM 1981). A joint roughness coefficient of 4 was assumed for joint roughness, corresponding to a slightly rough joint. The mine site is recorded to be dry with no water problems. The classification data sheet and the test results are included within Appendix 3. The basic rating, orientation adjusted rating, anisotropic ratio and vertical and horizontal coal mine ratings were obtained for each strata unit using the procedure described in Chapter 5. These coal mine ratings are given in Table 6.6.

<b>Unit</b>	<b>Distance above top of coal seam (m)</b>	<b>Description</b>	<b>Basic rating</b>	<b>CMR</b>	<b>AR</b>	<b>CMR vertical</b>	<b>CMR horizon</b>
1	0.12 to 0.72	MUDSTONE: grey many parting horizons, occasional smooth lenticular low angle joint	42	42	1.33	36	48
2	0.72 to 1.06	MUDSTONE: grey, silty occasional low angle joint,	44	44	1.32	38	50
3	1.06 to 4.01	MUDSTONE: grey, silty, Fissile parting band at 1.47 to 1.49	46	46	1.30	40	52
4	4.01 to 5.04	MUDSTONE: grey, silty, frequent parting planes	46	46	1.30	40	52

Table 6.6 Classification ratings for roadway roof of panel H438 at 214 metre mark

#### 6.2.10.2 Case Study Locality 2: Panel H478, Main Gate 31 Metre Mark

The borehole core was 5.0 metres long and is shown as Figure 6.12.

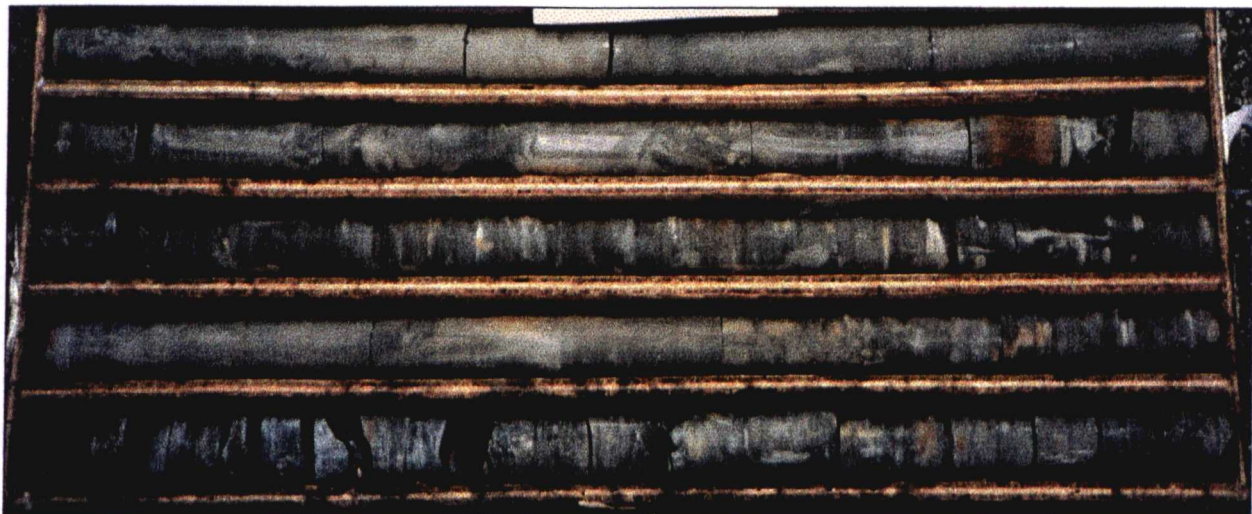


Figure 6.12 Roof core from the main gate of Panel H478 at 31 metre mark

Three distinctive strata units were identified and the Coal Mine Classification was applied to each unit in the same manner as has been described for case study 1. The classification data sheet and the test results are included within Appendix 3. The determined Coal Mine Classification ratings are given in Table 6.7.

<b>Unit</b>	<b>Distance above top of coal seam (m)</b>	<b>Description</b>	<b>Basic rating</b>	<b>CMR</b>	<b>AR</b>	<b>CMR Vertical</b>	<b>CMR horizon</b>
1	0.4 to 0.74	MUDSTONE: grey, silty	47	47	1.29	41	53
2	0.74 to 1.4	MUDSTONE: grey silty	49	49	1.28	43	55
3	1.4 to 5.4	SILTSTONE: grey, massive	60	60	1.13	57	62

Table 6.7 Coal Mine Classification Ratings main gate Panel H478 at 31 metre mark

### 6.2.10.3 Case study locality 3: Panel H478, main gate 110 metre mark

The roof core obtained for this locality was 5.0 metres long. Three distinctive strata units were identified and the Coal Mine Classification was applied to each in the same manner as has been described for case study 1. The classification data sheet and the test results are included within Appendix 3. The Coal Mine Classification Ratings are given in Table 6.8.

<b>Unit</b>	<b>Distance above top of coal seam (m)</b>	<b>Description</b>	<b>Basic rating</b>	<b>CMR</b>	<b>AR</b>	<b>CMR Vertical</b>	<b>CMR Horizon</b>
1	0.2 to 0.55	MUDSTONE: dark grey	37	37	1.39	31	43
2	0.55 to 1.05	MUDSTONE: grey silty	46	46	1.30	40	52
3	1.05 to 5.2	SILTSTONE: grey, massive	64	64	1.00	64	64

Table 6.8 Coal Mine Classification Ratings main gate of Panel H478 at 110 metre mark

#### 6.2.10.4 Case study locality 4: Panel H478, Main Gate 387 Metre Mark

The roof core obtained for this locality was 4.92 metres long and is shown as Figure 6.13.

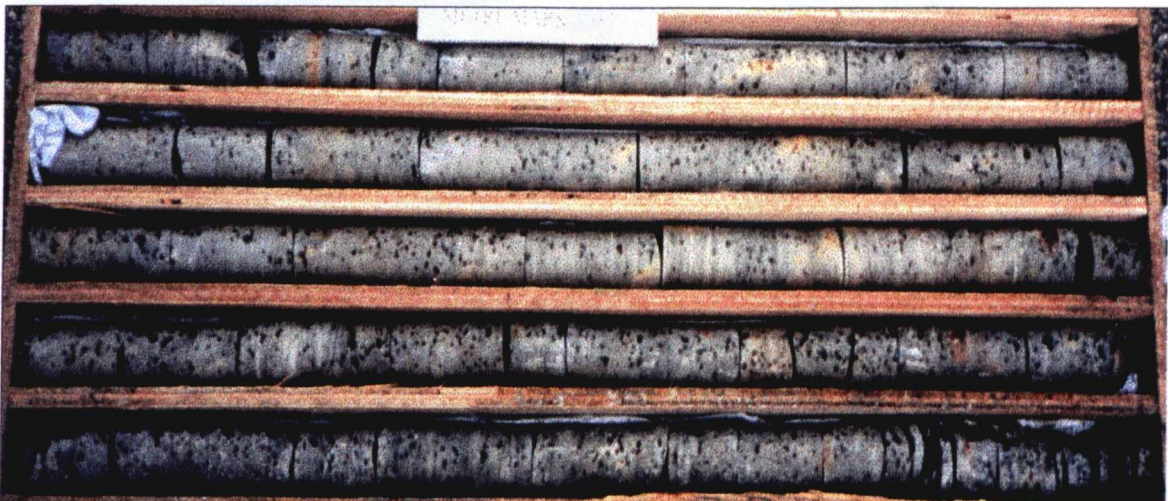


Figure 6.13 Roof core from the main gate of Panel H478 at 387 metre mark

Four distinctive strata units were identified and the Coal Mine Classification was applied to each in the same manner as has been described for case study 1. The classification data sheet and the test results are included within Appendix 3. The classification ratings are given in Table 6.9.

<b>Unit</b>	<b>Distance above top of coal seam (m)</b>	<b>Description</b>	<b>Basic rating</b>	<b>CMR</b>	<b>AR</b>	<b>CMR Vertical</b>	<b>CMR Horizon</b>
1	0.4 to 1.13	MUDSTONE: grey, silty	49	49	1.28	43	55
2	1.13 to 1.45	MUDSTONE: dark grey	40	40	1.35	34	46
3	1.45 to 2.00	MUDSTONE: grey, silty	52	52	1.24	46	57
4	2.00 to 5.32	SILTSTONE: grey, massive	53	53	1.21	48	58

Table 6.9 Coal Mine Classification Ratings main gate, Panel H478 at 387 metre mark

#### 6.2.10.5 Case Study Locality 5: Panel H478, Main Gate 486 Metre Mark

The roof core obtained for this locality was 4.84 metres long and is shown as Figure 6.14.



Figure 6.14 Roof core from the main gate of Panel H478 at 486 metre mark

Four distinctive strata units were identified and the Coal Mine Classification was applied to each in the same manner as has been described for case study 1. The classification data sheet and the test results are included within Appendix 3. The classification ratings given in Table 6.10.

<b>Unit</b>	<b>Distance above top of coal seam (m)</b>	<b>Description</b>	<b>Basic rating</b>	<b>CMR</b>	<b>AR</b>	<b>CMR Vertical</b>	<b>CMR Horizon</b>
1	0.56 to 1.26	SILTSTONE: grey, massive	64	64	1.07	62	66
2	1.26 to 2.26	SILTSTONE: grey, laminated	60	60	1.07	58	62
3	2.26 to 4.50	SILTSTONE: grey, laminated	61	61	1.07	59	63
4	4.50 to 5.40	SILTSTONE: grey, laminated	61	61	1.07	59	63

Table 6.10 Coal Mine Classification Ratings main gate, Panel H478, 486 metre mark

#### 6.2.10.6 Case Study Locality 6: Panel H478, Main Gate 587 Metre Mark

The roof core obtained for this locality was 5.54 m long and is shown as Figure 6.15.



Figure 6.15 Roof core from the main gate of Panel H478 at 587 metre mark

Seven distinctive strata units were identified and the Coal Mine Classification was applied to each in the same manner as has been described for case study 1. The classification data sheet and the test results are included within Appendix 3. The classification ratings are given in Table 6.11.

unit	Distance above top of coal seam (m)	Description	Basic rating	CMR	AR	CMR Vertical	CMR Horizon
1	0.6 to 1.6	MUDSTONE: grey, silty	50	50	1.22	45	55
2	1.6 to 2.13	SILTSTONE: grey, laminated	62	62	1.07	60	64
3	2.13 to 2.35	SILTSTONE: grey, laminated	57	57	1.15	53	61
4	2.35 to 3.02	SILTSTONE: grey, laminated	60	60	1.11	57	63
5	3.02 to 3.97	SILTSTONE: grey, laminated	58	58	1.15	54	62
6	3.97 to 4.53	SILTSTONE: massive, grey	61	61	1.07	59	63
7	4.53 to 6.14	SILTSTONE: grey, laminated	59	59	1.11	56	62

Table 6.11 Coal Mine Classification Ratings main gate, Panel H478, 587 metre mark

#### 6.2.10.7 Case study locality 7: Panel H478, Main Gate 710 Metre Mark

The roof core obtained for this locality was 5 metres long and is shown as Figure 6.16.



Figure 6.16 Roof core from the main gate of Panel H478 at 710 metre mark

Four distinctive strata units were identified and the Coal Mine Classification was applied to each in the same manner as has been described for case study 1. The classification data sheet and the test results are included within Appendix 3. The classification ratings given in Table 6.12

<b>Unit</b>	<b>Distance above top of coal seam (m)</b>	<b>Description</b>	<b>Basic rating</b>	<b>CMR</b>	<b>AR</b>	<b>CMR Vertical</b>	<b>CMR Horizon</b>
1	0.6 to 1.28	MUDSTONE: dark grey	41	41	1.41	34	48
2	1.28 to 2.63	MUDSTONE: grey, silty	57	57	1.11	54	60
3	2.63 to 4.8	SILTSTONE: grey, massive	61	61	1.10	58	64
4	4.8 to 5.6	SANDSTONE: pale brown	60	60	1.07	58	62

Table 6.12 Coal Mine Classification Ratings main gate Panel H478, 710 metre mark

#### 6.2.10.8 Case Study Locality 8: Panel H505, Tail Gate, 353 Metre Mark.

Panel 505 was oriented at an angle of 147° from the north.

The roof core obtained for this locality was 5 metres long and is shown as Figure 6.17.

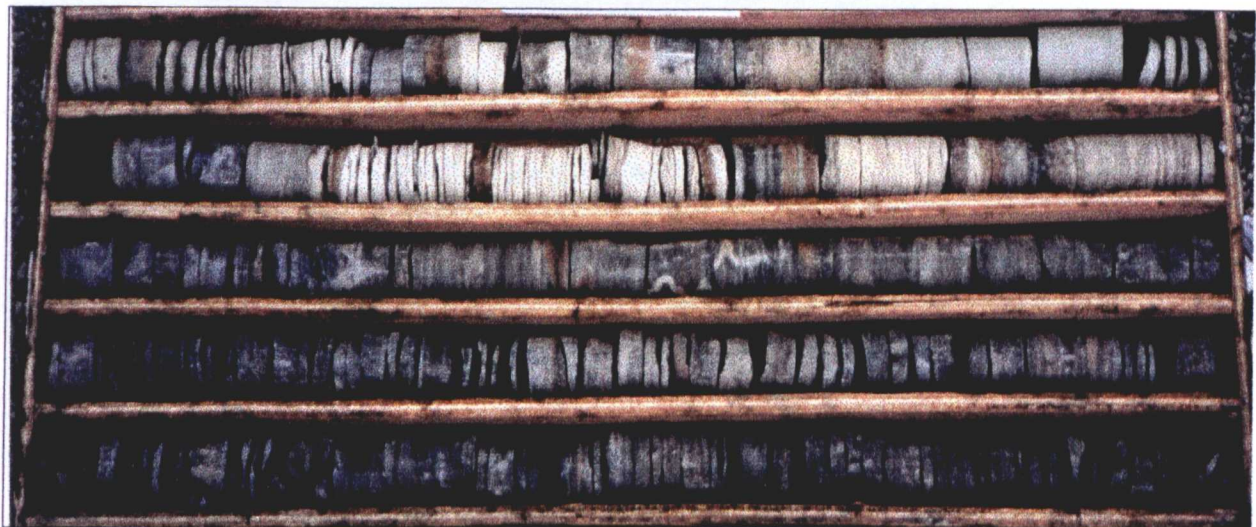


Figure 6.17 Roof core from the tail gate of Panel H505 at 353 metre mark

Four distinctive strata units were identified and the Coal Mine Classification was applied to each in the same manner as has been described for case study 1. The classification data sheet and the test results are included within Appendix 3. The classification ratings are given in Table 6.13

Unit	Distance above top of coal seam (m)	Description	Basic rating	CMR	AR	CMR Vertical	CMR Horizon
1	0.6 to 2.8	MUDSTONE: dark grey	40	40	1.42	33	47
2	2.8 to 3.7	SILTSTONE: grey, laminated	49	49	1.28	43	55
3	3.7 to 4.9	SILTSTONE: grey, laminated	45	45	1.39	38	52
4	4.9 to 5.6	SILTSTONE: grey, laminated	51	51	1.32	44	58

Table 6.13 Coal Mine Classification Ratings tail gate of Panel H505, 353 metre mark

#### 6.2.10.9 Case Study Locality 9: Panel H505, Tail Gate, 922 Metre Mark

The roof core obtained for this locality was 4.96 metres long and is shown as Figure 6.18.



Figure 6.18 Roof core from the tail gate of Panel H505 at 922 metre mark

Six distinctive strata units were identified and the Coal Mine Classification was applied to each in the same manner as has been described for case study 1. The classification data sheet and the test results are included within Appendix 3. The Coal Mine Classification Ratings are given in Table 6.14.

<b>Unit</b>	<b>Distance above top of coal seam (m)</b>	<b>Description</b>	<b>Basic rating</b>	<b>CMR</b>	<b>AR</b>	<b>CMR Vertical</b>	<b>CMR Horizon</b>
1	0.94 to 2.32	MUDSTONE: dark grey	39	39	1.44	32	46
2	2.32 to 3.06	MUDSTONE: grey, silty	44	44	1.38	37	51
3	3.06 to 3.9	SILTSTONE: grey, massive	46	46	1.30	40	52
4	3.9 to 5.12	MUDSTONE: grey silty	42	42	1.40	35	49
5	5.12 to 5.68	MUDSTONE: grey, silty	48	48	1.29	42	54
6	5.68 to 5.9	MUDSTONE: grey, silty	47	47	1.35	40	54

Table 6.14 Coal Mine Classification Ratings tail gate of Panel H505, 922 metre mark

#### 6.2.10.10 Case Study Locality 10: Panel H505, Main Gate, 669 Metre Mark.

The roof core obtained for this locality was 5.00 metres long and is shown as Figure 6.19.



Figure 6.19 Roof core from the main gate of Panel H505 at 669 metre mark

Four distinctive strata units were identified and the Coal Mine Classification was applied to each in the same manner as has been described for case study 1. The classification data sheet and the test results are included within Appendix 3. The derived Coal Mine Classification Ratings are given in Table 6.15.

unit	Distance above top of coal seam (m)	Description	Basic rating	CMR	AR	CMR Vertical	CMR Horizon
1	0.75 to 1.18	MUDSTONE: dark grey	39	39	1.44	32	46
2	1.18 to 2.3	MUDSTONE: grey, silty	44	44	1.38	37	51
3	2.3 to 2.82	SILTSTONE: grey, massive	46	46	1.30	40	52
4	2.82 to 5.75	MUDSTONE: grey silty	42	42	1.40	35	49

Table 6.15 Coal Mine Classification Ratings main gate Panel H505, 669 metre mark

#### 6.2.10.11 Case study locality 11: Panel H505, main gate 902 metre mark.

The roof core obtained for this locality was 4.95 metres long and is shown as Figure 6.20.



Figure 6.20 Roof core from the main gate of Panel H505 at 902 metre mark

Four distinctive strata units were identified and the Coal Mine Classification was applied to each in the same manner as has been described for case study 1. The classification data sheet and the test results are included within Appendix 3. The derived Coal Mine Classification Ratings are given in Table 6.16.

<b>unit</b>	<b>Distance above top of coal seam (m)</b>	<b>Description</b>	<b>Basic rating</b>	<b>CMR</b>	<b>AR</b>	<b>CMR Vertical</b>	<b>CMR Horizon</b>
1	1.0 to 2.2	MUDSTONE: dark grey	42	42	1.40	35	49
2	2.2 to 4.54	MUDSTONE: grey, silty	47	47	1.35	40	54
3	4.54 to 5.00	SANDSTONE: grey, thinly bedded	52	52	1.26	46	58
4	5.00 to 5.95	MUDSTONE: grey silty	49	49	1.28	43	55

Table 6.16 Coal Mine Classification Ratings main gate Panel H505, 902 metre mark

#### 6.2.10.12 Case study locality 12: Panel H505, main gate 1583 metre mark.

The roof core obtained for this locality was 4.90 metres long and is shown as Figure 6.21.

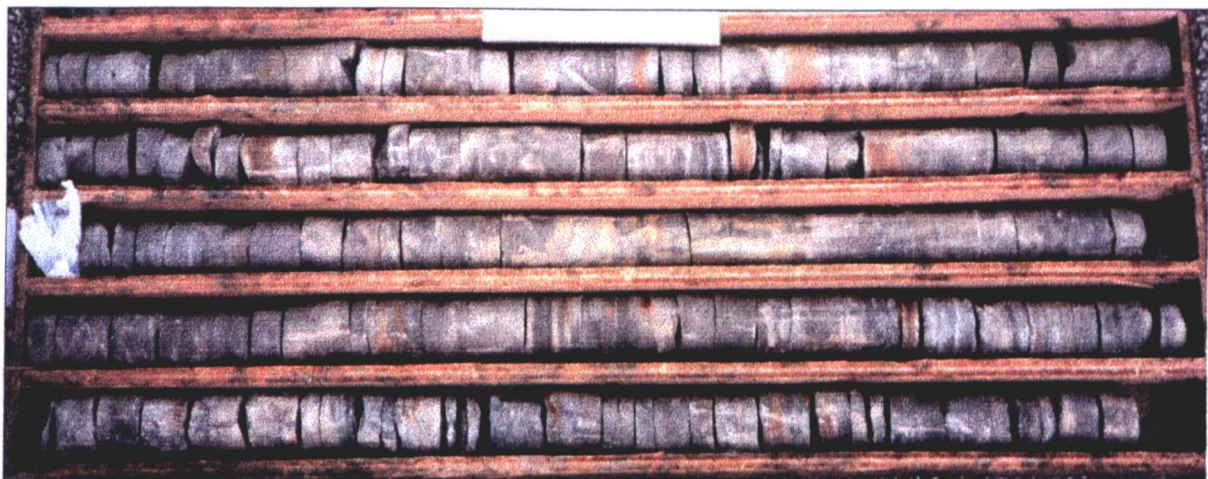


Figure 6.21 Roof core from the main gate of Panel H505 at 1583 metre mark

Six distinctive strata units were identified and the Coal Mine Classification was applied to each in the same manner as has been described for case study 1. The classification data sheet and the test results are included within Appendix 3. The derived Coal Mine Classification Ratings are given in Table 6.17.

<b>unit</b>	<b>Distance above top of coal seam (m)</b>	<b>Description</b>	<b>Basic rating</b>	<b>CMR</b>	<b>AR</b>	<b>CMR Vertical</b>	<b>CMR Horizon</b>
1	0.74 to 1.54	MUDSTONE: dark grey	46	46	1.24	41	51
2	1.54 to 2.96	MUDSTONE: grey, silty	48	48	1.29	42	54
3	2.96 to 3.81	SILTSTONE: grey, massive	55	55	1.2	51	59
4	3.81 to 4.35	MUDSTONE: grey, silty	49	49	1.16	43	55
5	4.35 to 4.89	SILTSTONE: grey, massive	49	49	1.28	43	55
6	4.89 to 5.6	MUDSTONE: grey silty	50	50	1.27	44	56

Table 6.17 Coal Mine Classification Ratings, main gate panel H505, 1583metre mark.

## **6.3 APPLICATION OF THE COAL MINE CLASSIFICATION TO DAW**

### **MILL MINE, WARWICKSHIRE**

#### **6.3.1 Introduction**

Daw Mill Mine is located in the Warwickshire coalfield and works the Warwickshire Thick Seam. Case study data was collected to enable the Coal Mine Classification to be applied to the coal gate of panel 94. The case study location is shown in Figure 6.22.

#### **6.3.2 General Strata Sequence Adjacent To The Warwickshire Thick Seam**

Figure 6.23 illustrates the generalised lithology sequence in the vicinity of the Warwickshire thick seam (Garratt 1997). The Hillfield surface to seam borehole drilled in the southern area of Daw Mill Colliery indicates that the roof sandstone/siltstone horizon is approximately 8 metres thick and is overlain by mixed coal measure strata of siltstones, mudstones and thin coal seams.

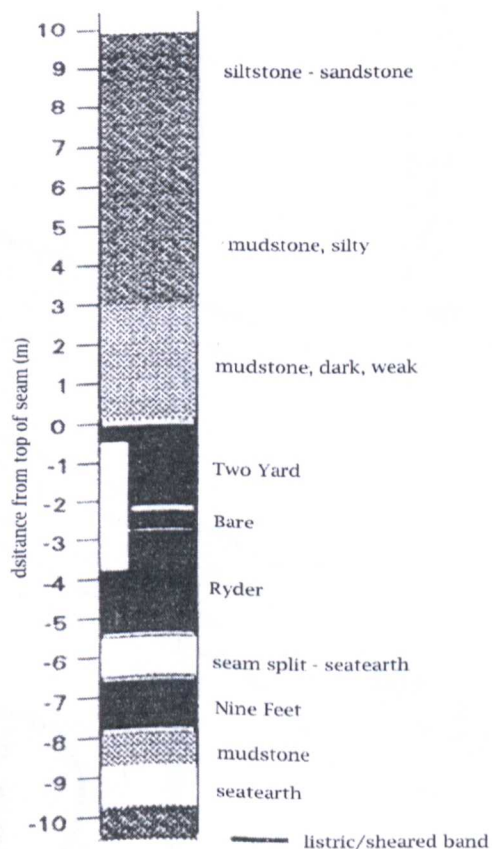


Figure 6.23 Generalized Lithology 90's Area (After Garratt 1997)

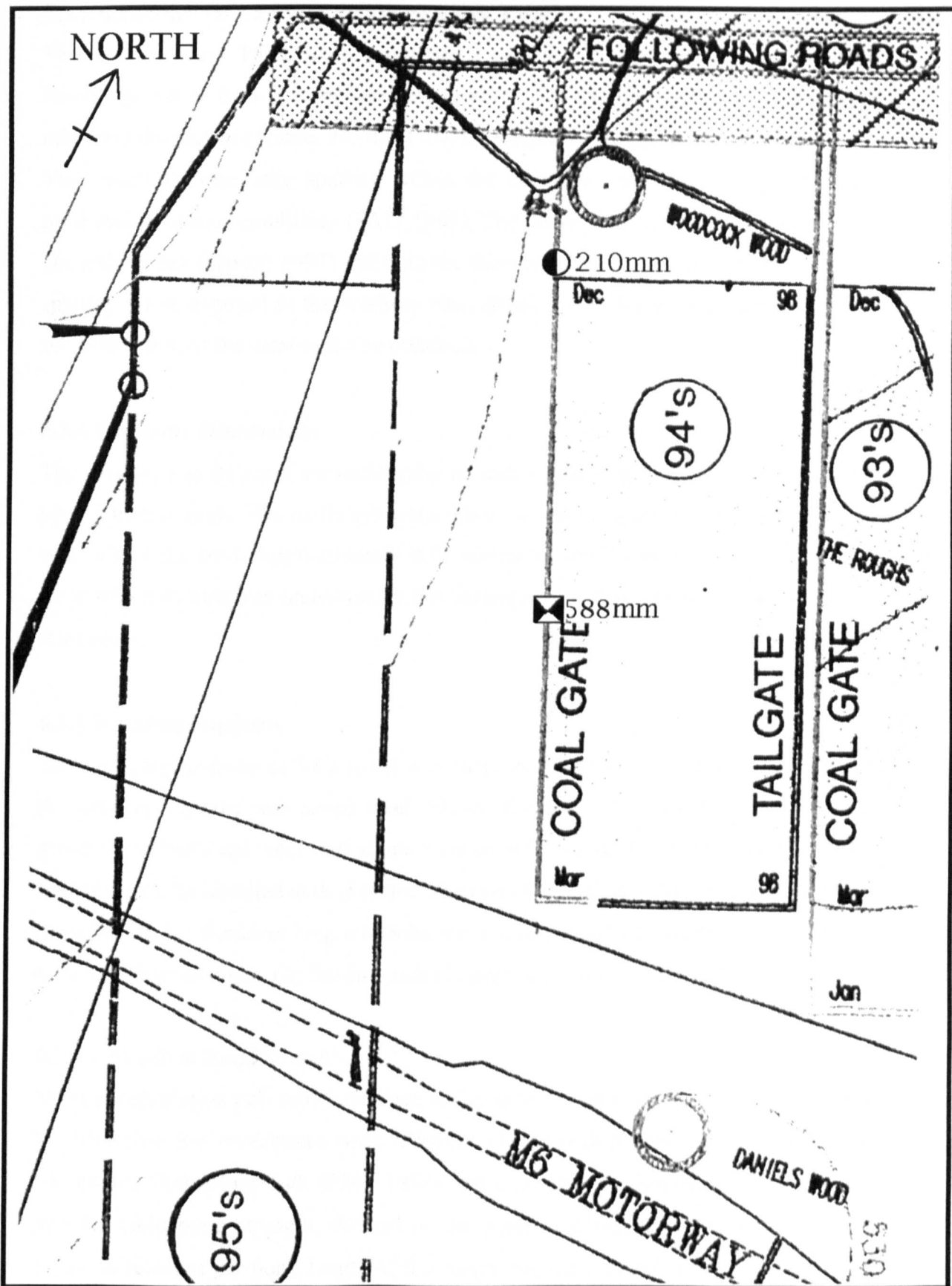


Figure 6.22 Daw Mill Mine panel 94 layout, showing case study localities

Position of extensometer, Position of roof borehole

### **6.3.3 Structure Of The Warwickshire Thick Coal**

The Warwickshire Thick seam comprises a number of separate seams which have come together to form a composite seam with a total thickness of approximately 7.5 metres in the region of panel 94 (RMT 1998) (Figure 6.23). Typically the higher, Two Yard seam showed little spalling within the rib sides and where left in the roof produced good roof conditions (RMT 1998). The lower, Bare Coal was recorded to be generally weak (Garratt 1997) and both the Bare and Ryder coals usually experienced spalling when exposed in the roadway ribs. (RMT 1998) No information relating to the orientation of the cleat could be obtained.

### **6.3.4 Roadway Dimensions**

The roadways in 94 panel are rectangular in section and approximately 5 metres wide by 3.7 metres high. The roadways were driven leaving approximately 0.8 metres of coal within the roof. Approximately 0.75 metres of the Ryder seam was left in the floor which in turn was underlain by the seatearth split between the Ryder and Nine Foot seam.

### **6.3.5 Installed Supports**

The coal gate roadway of 94's panel was supported entirely by rockbolts. In the roof the primary support was seven steel 22mm diameter 2.4 metre long full column grouted rockbolts and steel roof straps were equally spaced across the roof with each line of rockbolts installed at 0.65 metre intervals (RMT 1998). Rib reinforcement was provided by 3, 1.8 metres long rockbolts horizontally installed into the rib sides every 0.65 metres of advance. On the face side rib fibreglass bolts were installed.

#### **6.3.5.1 Rockbolt Bond Strength.**

Short encapsulation pull tests have been undertaken within in the roof of 95's tail gate to determine the resin/strata bond strength of the rock/rockbolt system by Rock Mechanics Technology Ltd. (RMT 1998). Four horizons within the roof were tested and the yield bond strength, defined as the point at which the bond stiffness falls below 20KN/mm per bond length of 0.3 metre was determined at each horizon. The results of the test are summarised in Table 6.18.

<b>Test Horizon</b>	<b>Mean bond stiffness (KN/mm/m)</b>	<b>Mean yield bond strength (KN/m)</b>
0.5 to 0.8	230	294
1.2 to 1.5	249	387
2.0 to 2.3	237	424
2.7 to 3.0	363	378

Table 6.18 Summary of pull test data for 95 tail gate roof strata (After RMT 1998)

### 6.3.6 Monitoring Data

Monitoring results have been obtained from a multi-horizon sonic extensometer installed in the roof of 94's coal gate at the 588 metre mark (RMT 1998). The roof displacement for different monitoring dates is shown as Figure 6.24.

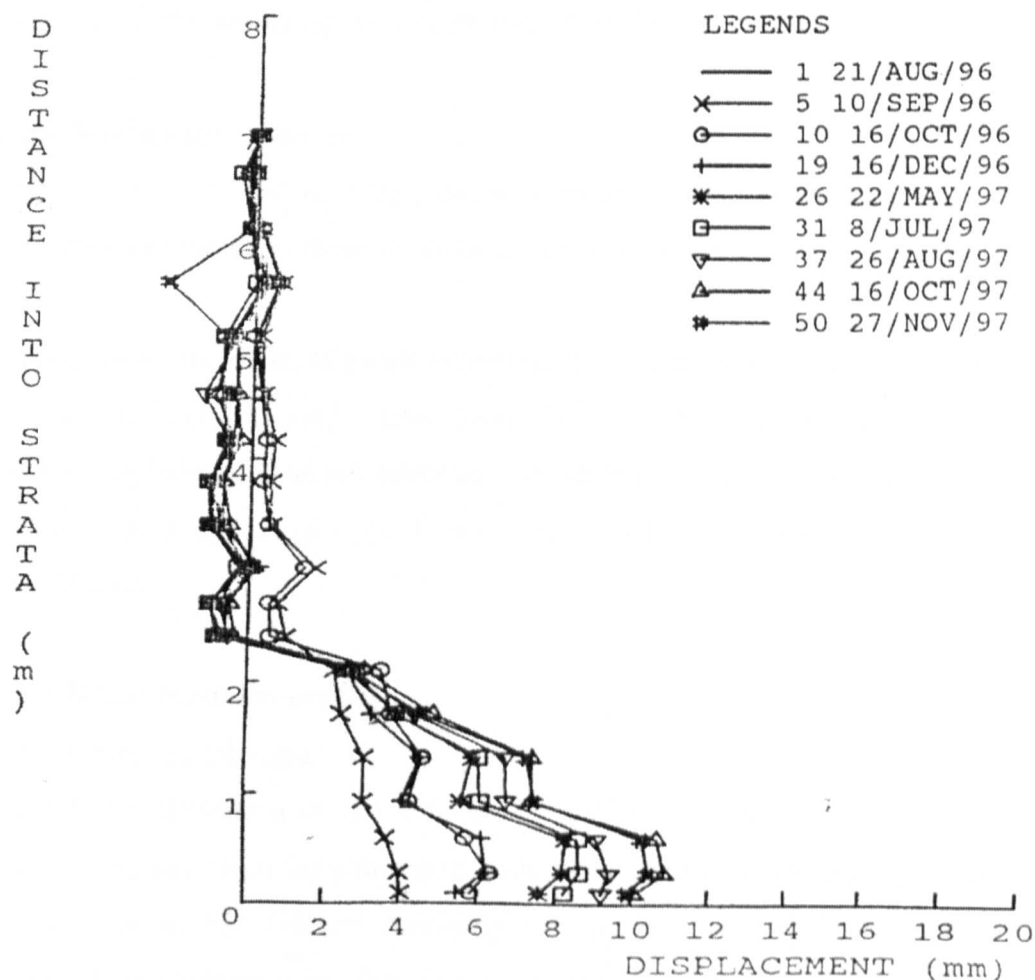


Figure 6.24 Roof Displacement, Daw Mill, 94's coal gate, 588 metre mark.

### **6.3.7 In-Situ Stress**

In-situ stress measurements obtained by overcoring have been determined for the tail gate of 90's panel (ECSC 1995) (Table 6.19). The measurements indicate that the maximum horizontal stress has a bearing of 336° which is in general accordance with the angle inferred from borehole breakouts obtained elsewhere at Daw Mill Colliery (ECSC 1995).

	<b>Magnitude</b>	<b>Direction</b>
Major horizontal stress	15.1 MPa	336°
Minor horizontal stress	11.1 MPa	54°

Table 6.19 In-situ stress results 90's tail gate (after ECSC 1995)

The depth of the seam in the vicinity of 94's panel is approximately 660 metres. The anticipated vertical stress due to the overlying strata, within 94's panel, was calculated to be 16.5 MPa, assuming an average density of 25 KN/m<sup>3</sup> for the overlying strata.,

### **6.3.8 Mining Interactions**

There are no recorded workings above or below the Warwickshire Thick seam in the 94's area and therefore there no vertical interactions were found (RMT 1998).

Inspection of the dates of panel extraction and location indicated on the mine layout plan and the dates of roof extensometer the available measurements indicate that the monitoring location was not adversely influenced by the front abutment stress caused by the retreating face or from the adjacent 93, 95 and 78 panels during the period of monitoring.

### **6.3.9 Intact Rock Properties**

#### **6.3.9.1 Triaxial Strength**

Published information on the triaxial strength of siltstone-sandstone, mudstone and coal lithologies from 90's tail gate have been used to determine the average axial stress at failure for different confining pressures for each of the rock types (Garratt 1998). These values were then input into the software package developed for this research to calculate the Coal Measure Failure Criterion parameters  $m_{i1}$  and  $m_{i2}$  (Table

6.20). The corresponding computer generated Mohr-Coulomb failure envelope for each of the rock types are shown as Figure 6.25 to 6.27.

Lithology	$m_{i1}$	$m_{i2}$
Coal	8	-5
Siltstone-sandstone	13	-31
Mudstone	15	-16

Table 6.20 Coal Measure Failure Criterion material parameters  $m_{i1}$  and  $m_{i2}$

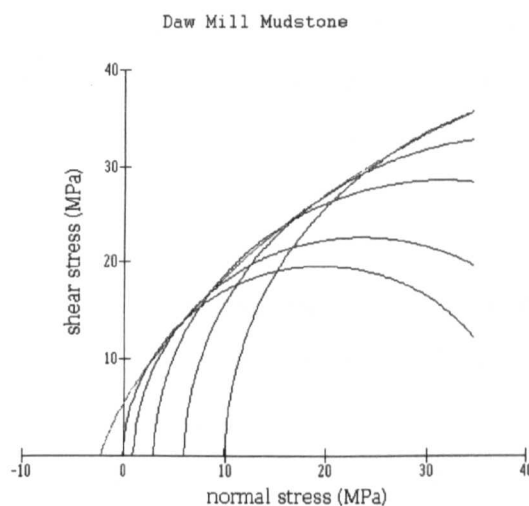


Figure 6.25 Failure envelope for Daw Mill  
Mudstone.

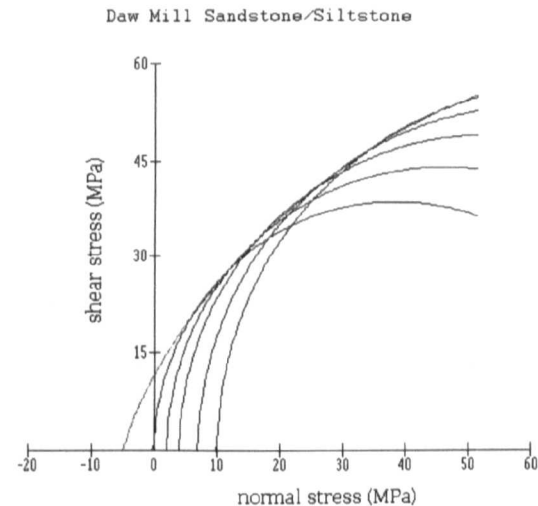


Figure 6.26 Failure envelope for  
Sandstone/siltstone.

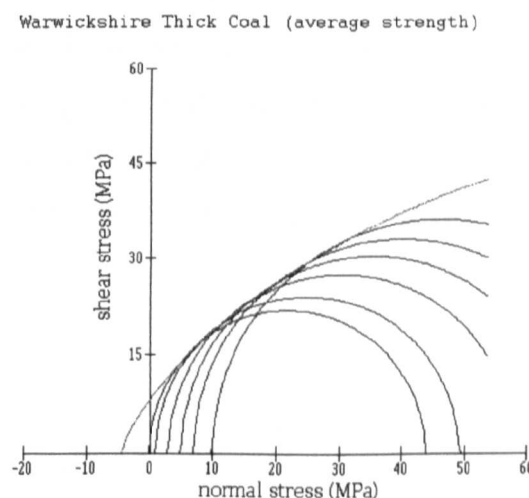


Figure 6.27 Failure envelope for the Warwickshire  
Thick Seam.

### **6.3.9.2 Young's Modulus**

No measurement of the Young's Modulus of the roof strata for 94's panel could be obtained. The empirical relationship  $E = 310 * \text{UCS}$  (after Wilson 1983) has been used to estimate the Young's Modulus for each of the strata units apart from the coal where the modulus has been assumed to be 4 GPa (Wilson 1983).

### **6.3.10 Application Of The Coal Mine Classification**

The Coal Mine Classification was evaluated for the strata units identified from the geotechnical core obtained in the roof of 94's coal gate at the 210 metre mark (RMT 1998). The borehole core was 5.0 metres long and the geotechnical log is shown as Figure 6.28. Ten strata units were identified and the classification evaluated for each unit. The unconfined compressive strength for each unit was obtained from the average for each strata unit. The bedding/lamination parameters of spacing, roughness and cohesion was estimated from the lithological descriptions. The fissility ratio was determined by evaluating typical fissility ratios for the basic lithologies in the Riccall case study and using these values for similar lithologies recorded in the log. No information in relation to the joint properties could be obtained. The general orientation of the major and minor joint sets within the roof was inferred from the trend of faults within the vicinity of panel 94. A joint spacing of 1 metre was assumed for each joint set which corresponds to the "wide spacing" of the ISRM classification of joint spacing (ISRM 1981). A joint roughness coefficient of 4 was assumed. The mine site is recorded to be dry with no water problems. The classification data sheet is included within Appendix 3. The basic rating, orientation adjusted rating, anisotropic ratio and vertical and horizontal coal mine ratings were obtained for each strata unit using the procedure described in Chapter 5 of this thesis. These Coal Mine Classification Ratings are given in Table 6.21.

$\frac{L}{D}$	Log	Sample No	S MPa	E GPa	S /E	Bond Strngth
SANDSTONE-SILTSTONE Dark grey siltstone finely interlaminated with pale grey sandstone, parting along carbonaceous/micaceous laminae with small plant fragments. Continues to top of borehole at 5.15m	5	7	71 67			
		6	71 71	17 7	4.03	
		F	125 1			
OTHER IRONSTONE BAND Listricated surface at top		5	59 5			4
MUDSTONE Dark grey smooth, with occasional listricated surfaces	4					
		4	42 46			
		E	22.81			
MUDSTONE Grey, silty, fine grained, homogeneous		3	77.08	-		
SANDSTONE-SILTSTONE Sandy siltstone, finely laminated, with plant fragments and dark carbonaceous laminae	3	2	62 97	-		3
		D	15.4			
SILTSTONE Grey, fine grained, with plant fragments and occasional listricated surfaces		C	20 46			2
MUDSTONE Grey, smooth, weak, occasional thin ironstone bands, 2cm soft clay band at top	2	B	13 05			2
		A	20 9			1
		1	39 84			1
MUDSTONE Dark grey, weak, homogeneous						1
COAL Broken	1					90
MUDSTONE Dark grey, weak, homogeneous						60
MUDSTONE Black/carbonaceous, broken with listricated surfaces, 1cm soft clay band at top						30
OTHER MISSING core - Coal fragments, WARRICKSHIRE THICK SEAM						
OTHER NOT CORED Bottom of borehole starts 0.80m below top of Warwickshire Thick Seam	0					

Figure 6.28 Geotechnical Roof Log, 94's coal gate, 210 metre mark  
 (After Rock Mechanics Technology 1998 (a))

<b>Unit</b>	<b>Distance above top of coal seam (m)</b>	<b>Description</b>	<b>Basic rating</b>	<b>CMR</b>	<b>AR</b>	<b>CMR vertical</b>	<b>CMR horizon</b>
1	-0.67 to 0	COAL (Two Yard Seam)	62	61	0.97	62	60
2	0 to 0.17	MUDSTONE: black, carbonaceous, soft clay band at top	38	37	1.39	31	43
3	0.17 to 0.92	MUDSTONE: dark grey weak with thin coal	40	38	1.30	33	43
4	0.92 to 2.13	MUDSTONE: grey fine grained, weak 2cm thick clay	37	36	1.40	30	42
5	2.13 to 2.59	SILTSTONE: grey, fine grained	56	55	1.11	52	58
6	2.59 to 2.79	SANDSTONE/SILTSTONE: Finely dark carbonaceous laminae	63	62	1.07	60	64
7	2.79 to 3.36	MUDSTONE: grey, silty	45	44	1.26	39	49
8	3.36 to 3.56	MUDSTONE: dark grey smooth with lenticular planes and ironstone band	38	37	1.39	31	43
9	3.56 to 3.79	SANDSTONE, pale grey medium grained	54	53	1.26	47	59
10	3.79 to 4.35	SANDSTONE/SILTSTONE: Finely interlaminated	63	62	1.07	60	64

Table 6.21 Classification ratings for roadway roof of the tail gate of panel 94 at 210 metre mark

## **6.4 APPLICATION OF THE COAL MINE CLASSIFICATION TO ROSSINGTON MINE, SOUTH YORKSHIRE**

### **6.4.1 Introduction**

Rossington Mine is located approximately 5 miles to the south east of the town of Doncaster, South Yorkshire and works the Barnsley/Dunsil seam of the Yorkshire coalfield.

The Coal Mine Classification was applied to a case study of Rossington's, B3 panel the location of which is shown in Figure 6.29. B3 panel is a retreat panel with a short face length of 80 metres. Directly overlying the Barnsley seam in this panel is a

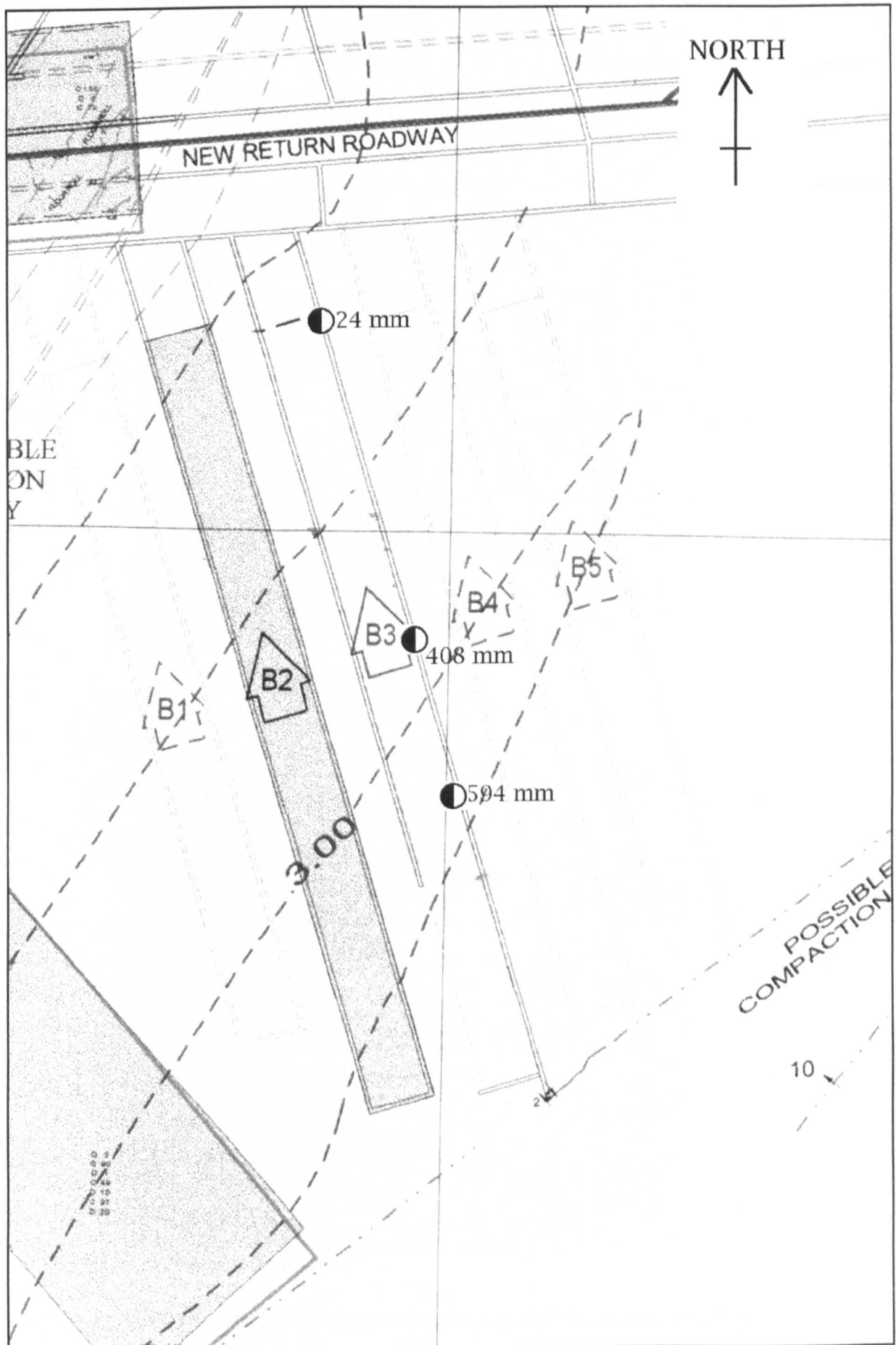


Figure 6.29 Rossington Mine, Panel B3 layout

● 24 is the case study locality at 24 metre mark

Inferior COAL	4 cm }			
COAL	14 cm }	18	923	24
Grey mudstone-seatearth with rootlets		26	923	50
Grey siltstone-seatearth with rootlets		09	923	59
Light grey sandstone with scattered rootlets		16	923	75
Banded siltstone		55	924	30
Grey siltstone with scattered rootlets		72	925	02
Finely bedded light grey sandstone		30	925	32
Banded siltstone, cross-bedded in parts	1	58	926	90
Grey siltstone	1	00	927	90
Grey silty mudstone with ironstone bands		37	928	27
ironstone, cone-in-cone structure, mussels near base		13	928	40
Dark grey mudstone with mussels		03	928	43
Grey mudstone with occasional mussels		07	928	50
Grey siltstone		25	928	75
Grey shaly mudstone, ironstone bands, occasional mussels		46	929	21
Dark grey mudstone with mussels		02	929	23
Grey mudstone, ironstone bands and scattered mussels		23	929	46
Light grey sandstone, small-scale cross- bedding		60	930	06
Banded siltstone, contorted bed in parts		79	930	85
Grey siltstone, a few sandy laminae		62	931	47
Banded siltstone		86	932	33
Grey siltstone		52	932	85
Grey silty mudstone with ironstone bands	2	90	935	75
Grey shaly mudstone with ironstone lenses		99	936	74
Ironstone		07	936	81
Dark grey shaly mudstone with ironstone bands		76	937	57
Black shale with fish scales, canneloid in parts		83	938	40
Dark grey shale		17	938	57
Grey shaly mudstone		20	938	77
Dark grey shaly mudstone		13	938	90
Grey shaly mudstone with ironstone bands and lenses		85	939	75
Grey silty mudstone with ironstone bands	2	59	942	34
Grey siltstone		32	942	66
Grey silty mudstone with scattered plants and ironstone nodules	1	54	944	20
Grey shaly mudstone with ironstone nodules and plant debris at top		90	945	10

### Roof strata

Dark grey shaly mudstone		02	945	12
COAL	40 cm }			
Grey mudstone-seatearth	2 cm			
Inferior COAL	5 cm			
COAL with thin dull bands	26,5 cm			
CANNEL	45 cm			
COAL	84 cm >	3	38	948
Dark grey mudstone-seatearth	3,5 cm			50
Inferior COAL	2,5 cm			
COAL	51,5 cm			
Fusain and COAL	1 cm			
COAL with dull band in middle	77 cm			
Carbonaceous mudstone		06	948	56
Grey mudstone-seatearth with rootlets, plants and ironstone nodules		24	949	30
Grey silty mudstone with ironstone nodules and bands, scattered rootlets	1	05	950	35
Black silty mudstone with coal streaks		02	950	37
Dark grey silty mudstone, ironstone bands and plant debris		53	950	90
Grey siltstone with scattered rootlets		10	951	00
Grey silty mudstone with scattered rootlets		10	951	10
Grey silty mudstone-seatearth with rootlets		17	951	27
Grey silty mudstone with scattered rootlets		28	951	55
Grey shaly mudstone		35	951	90
Dark grey shaly mudstone with ironstone nodules		46	952	36
Black shale with scattered fish scales		03	952	39
Canneloid shale		05	952	44
Grey mudstone-seatearth with rootlets		31	952	76
Grey siltstone-seatearth with rootlets		10	952	85
Mudstone, silty	3	65	956	50
Siltstone and sandstone	3	00	959	50
Mudstone, silty	4	00	963	50
Siltstone and sandstone	4	00	962	50
Mudstone, silty in parts	2	70	970	20

### Seam section and floor strata

Figure 6.30 Section close to Barnsley seam, Finningley No.2 Borehole, Rossington

mudstone unit. Interpolation of the thickness of the mudstone from isopachytes shown on the mine layout plan (Figure 6.29) indicates that the thickness varies along B3's main gate from 1.0 metre at 200 metre mark to 2.30 metres at 590 metre mark and 2.0 metres at 819 metre mark. The mudstone underlies more competent siltstone and where the siltstone lies at less than 1.4 metres above the coal the roof of the roadway was formed at the horizon between these two units. When the thickness of the mudstone unit became greater than 1.4 metres the roof was formed within the less competent mudstone. Some coal has been left in the floor in order to reach the higher siltstone horizon (R.J.B. 1997 (a)). Where the roof horizon is formed within the mudstone elevated levels of immediate roof deformation, relative to where the roof is formed in the siltstone have been measured. In order to evaluate the effectiveness of the Coal Mine Classification to differentiate between the weaker mudstone and more competent siltstone three localities have been selected within B3's main gate. The localities are at metre marks 24, 408, and 594. The roof at 24 metre mark has been formed at an horizon 1.0 metre above the Barnsley seam within the siltstone, whilst at the 410 metre mark and the 594 metre mark 1.2 m and 1.6 m of mudstone is present in the immediate roof.

#### **6.4.2 General Strata Sequence Adjacent To The Barnsley Seam**

The Finningley No.2 surface to seam borehole log, supplied by R.J.B. Mining Ltd., was located approximately 2000 metres to the west of B3 panel and was the closest surface to seam borehole to B3 panel. Details on the lithological sequence above and below the Barnsley seam taken from the borehole log are given in Figure 6.30.

#### **6.4.3 Roadway Dimensions**

The main gate in B3 panel is rectangular in section and approximately 5 metres wide and 3 metres high. The roof of the roadway was formed at a horizon varying between 0.45 and 2.00 metres above the top of the Barnsley seam (R.J.B 1997 (a)).

#### **6.4.4 Installed Supports**

The roadways of B3 panel are supported entirely by rockbolts. In the roof the primary support comprised seven steel 22mm diameter 2.4 metre long full column grouted Advanced Technology (AT) rockbolts installed through 4.5m long roof straps set at 1.0 metre intervals along the roadway supplemented by one additional spot bolt

installed through the roof straps on the face side of the roadway. Rib reinforcement was provided by rows of 4, 1.8 metres long rockbolts horizontally installed into the rib sides every 1 metre.

#### 6.4.5 Monitoring Data

##### 6.4.5.1 Roof displacement

Monitoring results have been obtained from a multi-horizon sonic extensometer installed in the roof of B3's main gate at the 24, 408 and 594 metre mark (RMT 1998 (b)). The roof displacement for these three localities are shown as Figure 6.31, 6.32 and 6.33 respectively.

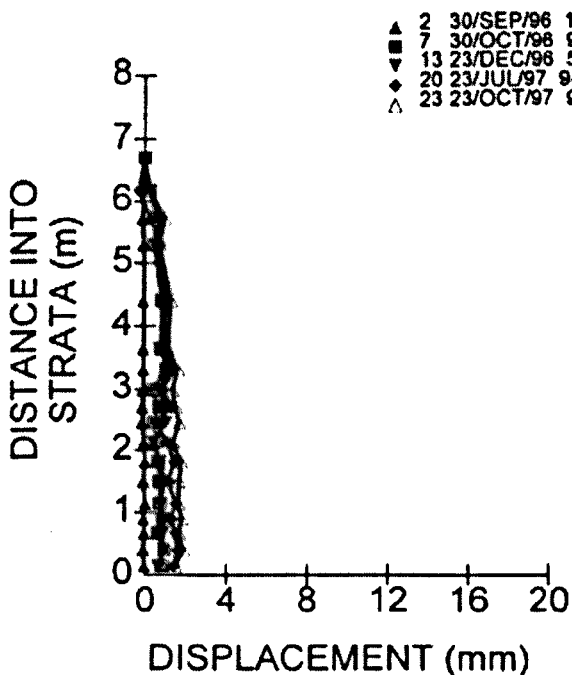


Figure 6.31 Roof displacement,  
24 metre mark (RMT 1998 (b))

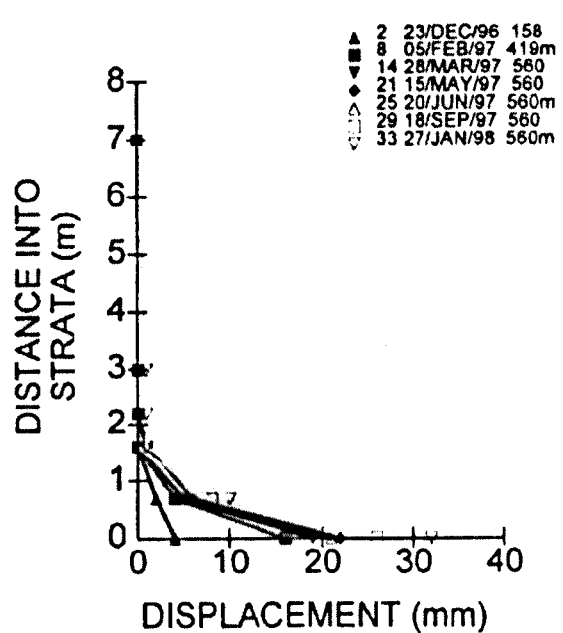


Figure 6.32 Roof displacement  
408 metre mark (RMT 1998 (b))

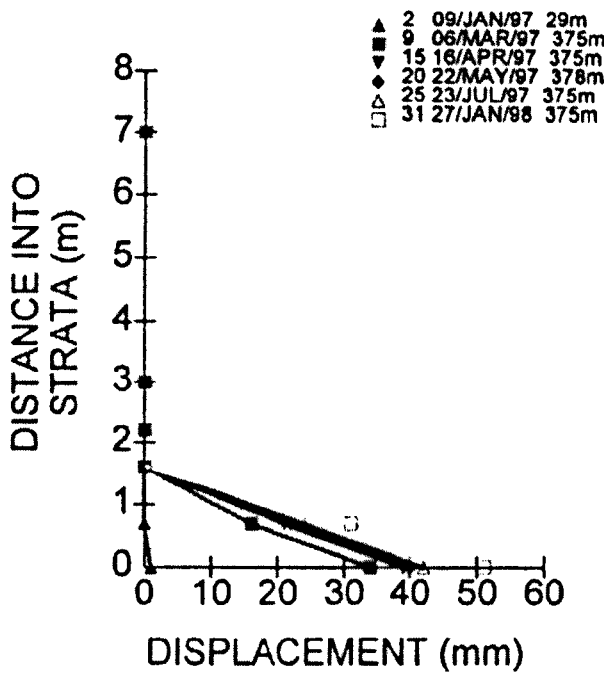


Figure 6.33 Roof displacement, 594 metre mark (RMT 1998 (b))

#### 6.4.5.2 Rib displacement

Rib displacements were monitored within B3's main gate at the 24 and 408 metre mark for both the left and right ribs by extensometers horizontally installed to a depth into the ribs of 5 metres (RMT 1998 (b)). The results of this monitoring are presented as time displacement curves in Figures 6.34 to 6.37.

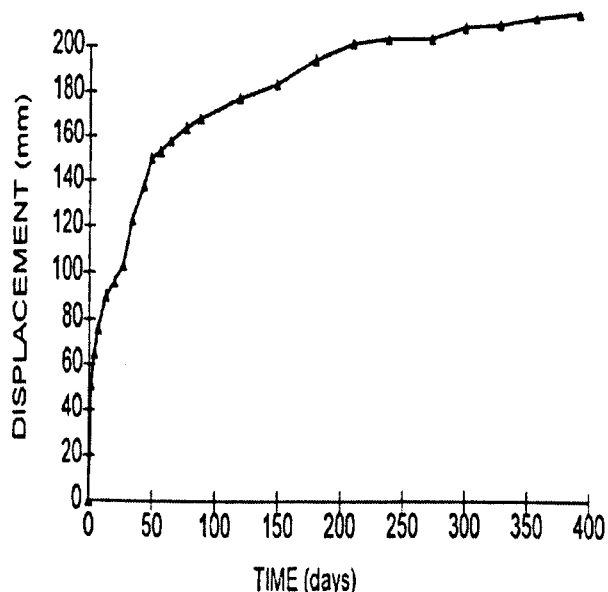


Figure 6.34 Left rib, 24 metre mark

B3's main gate (RMT 1998(b))

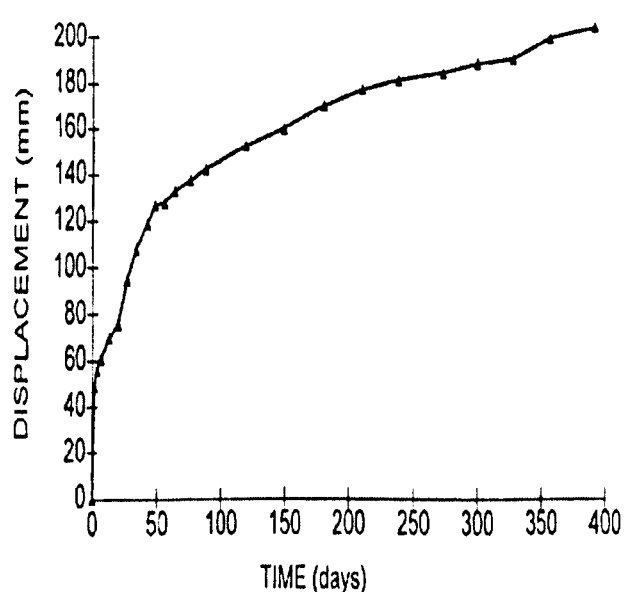


Figure 6.35 Right rib, 24 metre mark

B3's main gate (RMT 1998(b))

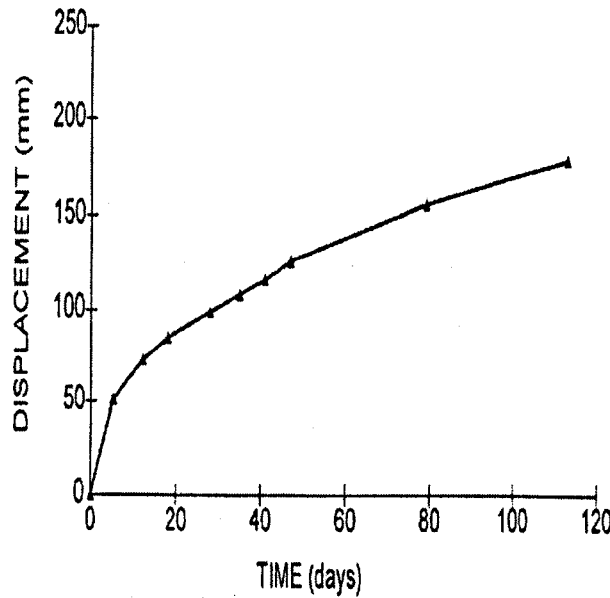


Figure 6.36 Left rib 415 metre mark  
B3's main gate (RMT 1998(b))

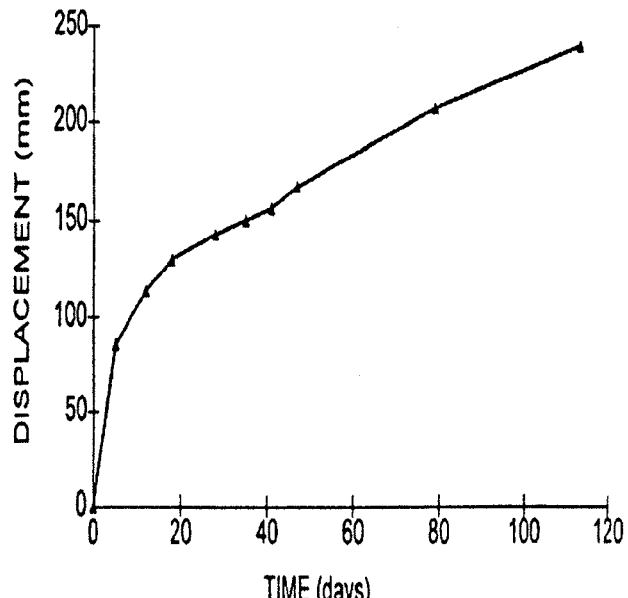


Figure 6.37 Right rib, 415 metre mark  
B3's main gate (RMT 1998(b))

#### 6.4.6 In-Situ Stress

Based on in-situ stress measurements in Rossington B96's main gate approximately 1000m to the north of B3 panel and Markham colliery approximately 3000m from B3's gateroads Rock Mechanics Technology (RMT 1997 (b)) proposed the following magnitudes and directions of the principal stresses for Rossington (Table 6.22)

<b>Vertical stress</b>	23 MPa (cover load)	
<b>Max. horizontal stress</b>	15-20 MPa	335° bearing
<b>Min. horizontal stress</b>	12-15 MPa	25° bearing

Table 6.22 In-situ stresses, Rossington Mine (RMT 1997 (b))

The horizontal stresses are relatively moderate in magnitude relative to the depth of working. The ratio between the horizontal stress components is low indicating that directional stress effects may not be very significant at Rossington (RMT 1997 (b)).

During the period of monitoring there should have been no horizontal interaction effects between adjacent panels.

#### 6.4.8 Intact Rock Properties

##### 6.4.8.1 Triaxial strength of Roof Strata

Intact material parameters for the Hoek-Brown failure and Coal Measure Failure Criterions have been determined from triaxial test data. The triaxial data sets were obtained from testing of roof core samples taken from Rossington B100 panel (RMT 1997 (b)). Both the Hoek-Brown failure criterion and the Coal Measure Failure Criterion were fitted to the triaxial data sets. The fit of the failure envelopes were very similar in both cases so it was decided, in this instance, to use the simpler Hoek-Brown criterion. The average material parameter,  $m_i$ , for each of the roof lithologies are given in Table 6.23.

Lithology	$m_i$
MUDSTONE:	6.0
MUDSTONE: silty	4.6
SILTSTONE: massive	4.7

Table 6.23 Hoek-Brown  $m_i$  parameter for Rossington roof strata

##### 6.4.8.2 Triaxial Strength of the Barnsley Seam

Triaxial testing of the Barnsley seam has been undertaken by Pomeroy (Pomeroy et al 1971) who tested the coal at various orientations to the cleat planes. The Coal Measure Failure Criterion was determined for Pomeroy's data for triaxial strength normal to the cleat planes as the effect of the cleat would be allowed for in the Coal Mine Classification. The intact Mohr-Coulomb envelope determined from the Coal Measure failure criterion is shown as Figure 6.38.

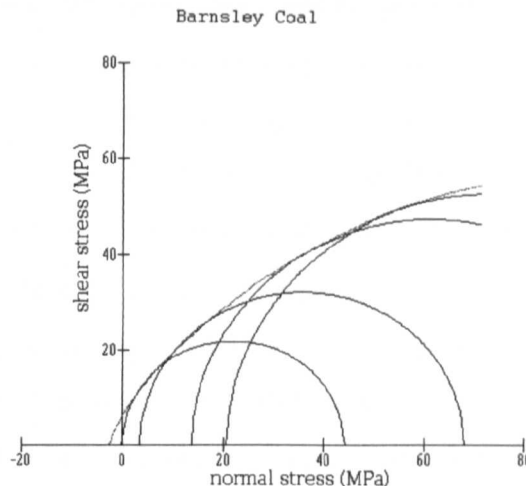


Figure 6.38 Intact failure envelope for the Barnsley coal.

#### 6.4.8.3 Elastic Modulus

Intact Young's Modulus was obtained for each of the samples used for triaxial testing and the average Young's modulus for each of the basic lithologies is given as Table 6.24 (RMT 1998(b)).

Lithology	Young's Modulus (GPa)
MUDSTONE:	15.2
MUDSTONE: silty	14.6
SILTSTONE: massive	19.1

Table 6.24 Typical Young's Modulus of Rossington roof strata  
(after RMT 1997(b))

The Young's modulus perpendicular to the cleat for the Barnsley seam has been determined as being 8.3 GPa by Pomeroy et al (1971).

#### 6.4.9 Application Of The Coal Mine Classification

##### 6.4.9.1 Classification of the Roof Strata

The Coal Mine Classification was evaluated for the strata units identified from the geotechnical core obtained in the roof of the adjacent shortwall panel B2's tailgate at 865 metre mark (R.J.B. 1997 (a)).

The borehole core was 7.0 metres long and the geotechnical log is included as Figure 6.39. Seven strata units were identified and the classification evaluated for each unit. The unconfined compressive strength for each unit was obtained from the geotechnical log. The bedding/lamination parameters of spacing, roughness and cohesion was determined from the fracture log and lithological descriptions. The fissility ratio was determined by evaluating typical fissility ratios for the basic lithologies in the Riccall case study and using these values for similar lithologies recorded in the log. The general orientation of the major and minor joint sets within the roof was inferred from the orientation of the cleat within the Barnsley seam. The main cleat is recorded to have a trend direction of 148° within the Barnsley seam at Rossington Mine (Holmes 1982). A joint spacing of 1 metre was assumed for each joint set which corresponds to the “wide spacing” of the ISRM classification of joint spacing (ISRM 1981). A joint roughness coefficient of 4 was assumed for joint roughness. The mine site is recorded to be dry with no water problems. The classification data sheet is included within Appendix 3. The basic rating, orientation adjusted rating, anisotropic ratio and vertical and horizontal coal mine ratings were obtained for each strata unit using the procedure described in Chapter 5. These coal mine ratings are given in Table 6.25.

Unit	Distance above top of coal seam (m)	Description	Basic rating	CMR	AR	CMR Vertical	CMR horizon
1	0 to 0.53	MUDSTONE: silty, grey	44	41	1.28	36	46
2	0.53 to 0.88	MUDSTONE: grey, plant fragments	41	38	1.31	33	43
3	0.88 to 1.8	MUDSTONE: silty, grey	48	45	1.25	40	50
4	1.8 to 5.2	SILTSTONE: fine grey	63	60	1.00	60	60
5	5.2 to 5.88	MUDSTONE: silty grey	49	46	1.24	41	51
6	5.88 to 6.64	MUDSTONE: grey, weak and fissile, thin clay band at base	39	36	1.32	31	41
7	6.64-7.01	MUDSTONE: black, carbonaceous	45	42	1.27	37	47

Table 6.25 Classification Ratings for roadway roof of the tailgate of B2 Panel,  
865 metre mark, Rossington Mine

GRAHAM DAWS ASSOCIATES				Geotechnical Borehole Log			
Rossington Colliery B2's Tail Gate		Equipment		Wombat Rig with diamond core barrel water flush cores 44mm diam			
Date Drilled	24/9/95	Core Run	Discontinuities	Lithology		Description	
U.C.S. (MPa)	Core Run (m)	Core Run (m)	Discontinuities	Depth (m)	Log	Log	Description
Location	Sample Number	Sample Number	Core Run (m)	Core Run (m)	Core Run (m)	Core Run (m)	Core Run (m)
22.71	4.8	13.33	7.01	TD	7.00	7.01	Top of Borehole
Distance	865m		6.84				
			9.00				
				6.00			
					6.64		MUDSTONE, smooth, basic, slightly carbonaceous, occasional spores.
					6.50		IRONSTONE, pale brown, bandred.
					6.29		MUDSTONE, smooth, medium to dark grey, fissile, irregular top.
					6.24		IRONSTONE, pale brown.
					6.00		MUDSTONE, smooth, grey, weak end fissile
					5.95		CAY, grey, soft and plastic.
					5.90		MUDSTONE, silty, grey, occasional plant detritus; slight ferruginous film 5.45 to 5.95, slightly salty above.
					5.85		
					5.80		
					5.75		
					5.70		
					5.65		
					5.60		
					5.55		
					5.50		
					5.45		
					5.40		
					5.35		
					5.30		
					5.25		
					5.20		SILTSTONE, grey, passage cap.
					5.15		
					5.10		
					5.05		
					5.00		

Figure 6.39 Geotechnical log for B2's tail gate 865mm 0.00m - 5.00m (R.J Budge Mining Ltd, 1997 (a))

GRAHAM DAWS ASSOCIATES							Geotechnical Borehole Log		
Rossington Colliery B2's Tail Gate			Equipment						
Site	Date Drilled	24/9/95	Discontinuities		Lithology				
			Core Run	Feature	E	S	D	Log	Description
U.C.S. (MPa)	Distance 865m	Sample	Core Run	<30° North Normal	>30° North Normal	Log			
Lithostratigraphic Section	Thickness mm	Location	Depth m	Depth m	Depth m				
64.69	10.42	6.14	F	100	4.44				rare diffuse sandstone laminae above 4.40m;
65.16	10.23	6.25	E	3.91	4.00	4.00	4.00		SILTSTONE, fine, grey, diffuse ferruginous patches from 2.45 to 2.55m.
				3.78					
					1.00				
						2.99	3.00	3.00	
						2.98	2.98	2.98	
						1.00			
							2.30	2.30	
							2.12	2.12	
							2.00	2.00	
							1.98	1.98	
							1.96	1.96	
							1.94	1.94	
							1.92	1.92	
							1.90	1.90	
							1.88	1.88	
							1.86	1.86	
							1.84	1.84	
							1.82	1.82	
							1.80	1.80	
							1.78	1.78	
							1.76	1.76	
							1.74	1.74	
							1.72	1.72	
							1.70	1.70	
							1.68	1.68	
							1.66	1.66	
							1.64	1.64	
							1.62	1.62	
							1.60	1.60	
							1.58	1.58	
							1.56	1.56	
							1.54	1.54	
							1.52	1.52	
							1.50	1.50	
							1.48	1.48	
							1.46	1.46	
							1.44	1.44	
							1.42	1.42	
							1.40	1.40	
							1.38	1.38	
							1.36	1.36	
							1.34	1.34	
							1.32	1.32	
							1.30	1.30	
							1.28	1.28	
							1.26	1.26	
							1.24	1.24	
							1.22	1.22	
							1.20	1.20	
							1.18	1.18	
							1.16	1.16	
							1.14	1.14	
							1.12	1.12	
							1.10	1.10	
							1.08	1.08	
							1.06	1.06	
							1.04	1.04	
							1.02	1.02	
							1.00	1.00	
							0.98	0.98	
							0.96	0.96	
							0.94	0.94	
							0.92	0.92	
							0.90	0.90	
							0.88	0.88	
							0.86	0.86	
							0.84	0.84	
							0.82	0.82	
							0.80	0.80	
							0.78	0.78	
							0.76	0.76	
							0.74	0.74	
							0.72	0.72	
							0.70	0.70	
							0.68	0.68	
							0.66	0.66	
							0.64	0.64	
							0.62	0.62	
							0.60	0.60	
							0.58	0.58	
							0.56	0.56	
							0.54	0.54	
							0.52	0.52	
							0.50	0.50	
							0.48	0.48	
							0.46	0.46	
							0.44	0.44	
							0.42	0.42	
							0.40	0.40	
							0.38	0.38	
							0.36	0.36	
							0.34	0.34	
							0.32	0.32	
							0.30	0.30	
							0.28	0.28	
							0.26	0.26	
							0.24	0.24	
							0.22	0.22	
							0.20	0.20	
							0.18	0.18	
							0.16	0.16	
							0.14	0.14	
							0.12	0.12	
							0.10	0.10	
							0.08	0.08	
							0.06	0.06	
							0.04	0.04	
							0.02	0.02	
							0.00	0.00	

#### 6.4.9.2 Classification of the Barnsley Seam.

In order to provide an initial validation of the Coal Mine Classification for the use in determining properties of strata within coal ribs, classification ratings were evaluated for the Barnsley seam and overlying strata exposed in the ribs of B3 panel. Along B3 main gate the seam thickness varies between 2.75 m and 3.0 m and has a well developed main cleat (R.J.B. 1997 (a)). A seam section produced for the Barnsley Seam from the Blaxton Common borehole (NCB 1982) records the Barnsley seam as comprising mainly of bright coal bands on average 20 to 30 cm thick. Although no measured cleat spacing was available for the coal exposed in B3's ribs the average spacing of cleat within bright coal types in Yorkshire coal seams has been recorded to be approximately 60 mm (Macrae and Lawson 1956). The trend of the main cleat has been recorded to be 148° at Rossington (Holmes 1982). Fillingley No2. Borehole (Figure 6.30) indicates the presence of two dirt partings consisting of dark grey mudstone approximately 10 cm thick. The intact unconfined compressive strength for the Barnsley seam has been determined to be 44 MPa (Pomeroy et al 1971).

Using the above information Coal Mine Classification Ratings were determined for the rib strata. Six strata units have been identified within the rib sides. The classification data sheet has been included in Appendix 3. The calculated classification ratings are given below in Table 6.26.

<b>Unit</b>	<b>Distance above top of coal seam (m)</b>	<b>Description</b>	<b>Basic rating</b>	<b>CMR</b>	<b>AR</b>	<b>CMR vertical</b>	<b>CMR horizon</b>
1	1.0 to 0.0	MUDSTONE: dark grey	49	47	1.24	42	52
2	0.0 to -0.4	COAL:	57	52	0.89	55	49
3	-0.4 to -0.5	MUDSTONE: dark grey (dirt parting)	47	45	1.25	40	50
4	-0.5 to -1.8	COAL	57	52	0.89	55	49
5	-1.8 to -1.9	MUDSTONE: dark grey (dirt parting)	47	45	1.25	40	50
6	-1.8 to -2.8	COAL	57	52	0.89	55	49

Table 6.26 Estimated Classification Ratings for the rib strata (Barnsley seam),  
B3 Panel, Rossington Mine

## **6.5 CONCLUSIONS**

This chapter described the application of the Coal Mine Classification to case study data obtained for three existing mine sites that were namely Riccall, Daw Mill and Rossington mines.

The data obtained for each of the mine sites also included data required to allow the construction of numerical models to be used as a method of validating the efficacy of the Coal Mine Classification.

Whilst deriving the Coal Measure Classification ratings for each of the individual strata units it became apparent the existing data collected by the geotechnical staff of the mines on the characteristics of the rock strata was often limited. Several of the parameters that have been identified as key influencing parameters as part of this research were not measured. Therefore to allow the Coal Mine Classification to be applied assumptions have had to be derived using engineering judgement. This was considered to increase the degree of uncertainty in the classification values.

The Coal Mine Classification ratings prior to adjustment for joint orientation were found to vary between 38 and 63 with the majority of the ratings lying between 40 and 60. The ratings appeared to be lithology dependant with a ratings between 38 and 42 typical of a weak, dark grey fissile mudstone and ratings of 60 or more being typical of moderately strong, pale grey laminated siltstones and sandstone's. The highest rating of 63 was derived for a very strong, laminated sandstone/siltstone.

To allow the efficacy of the Coal Mine Classification to be evaluated other factors that influence the deformation within roadways had to be quantified. This data was quite extensive and includes information on the nature of installed supports, the size and shape of the roadway, the in-situ stress field and the effects of the interaction between adjacent workings.

## **CHAPTER 7** **NUMERICAL MODELLING STUDIES**

### **7.1 INTRODUCTION**

A wide variety of techniques have been developed to calculate the stresses, displacements and failure zones that develop within the rock mass adjacent to underground excavations. These techniques vary from numerical techniques such as closed form solutions and limit equilibrium methods, photo-elastic techniques and the use of physical models. The computer revolution which has occurred within the last twenty or so years and the availability of affordable, powerful personal computers within the last ten years has lead to the development of computer modelling programs specifically developed to simulate the complex behaviour of multi-layered rock masses adjacent to underground excavations.

This chapter begins with a review of the analytical techniques mentioned above. The philosophy behind computer modelling in rock engineering is then described. The second half of the chapter describes the numerical modelling of the case study localities described in Chapter 6 using the Fast Lagrangian Analysis of Continua (FLAC) finite difference code. Material properties of the rock strata that are required as input parameters for the computer code have been determined using the Coal Mine Classification Ratings. The efficacy of the Coal Mine Classification for accurately predicting the in-situ material properties of the Coal Measure rocks is then evaluated by comparing the model results with in-situ monitoring obtained for the case study localities.

### **7.2 STRATA MODELLING TECHNIQUES**

#### **7.2.1 Closed Form Techniques**

These are the equations derived from classical stress analysis that relate the stress and displacement distributions within a body. The solution for a problem has to satisfy a set of mathematical conditions (Brady and Brown 1980). These governing conditions have been previously described in Section 3.2.2. Closed form solutions represent a state of stress and displacement equilibrium within the body and hence represent a closed system with no redistribution of stresses into adjacent bodies. Solutions have been published for excavations of various shapes and some work has been undertaken

into incorporating plastic failure within the solution (Hoek et al 1991). However the solutions are limited to very simple geometries and constitutive relations.

### **7.2.2 Limit Equilibrium Techniques**

These techniques determine the likelihood of failure along surfaces of weakness such as joints or bedding planes. In the analysis the gravitational stresses acting on a rigid block or wedge separated from the surrounding soil or rock mass by intersecting discontinuities are calculated and are checked against the shear resistance generated by the contact surfaces to determine whether the block can slide. The ratio between the restraining forces (shear resistance) and disturbing forces (gravitational force acting on the block) gives a factor of safety against failure. Factors of safety greater than 1 represent stable conditions and less than 1 instability. This technique is widely used in soil stability analyses (Smith 1985) and for the prediction of structurally controlled failure within rock slopes or near surface underground excavations (Hoek and Brown 1980).

However since confining stresses are difficult to incorporate into a limit equilibrium model this technique is limited to analyses in which the surrounding stress field can be ignored (Hoek et al 1991) and hence has limited applicability to the high stress environment present within UK coal mines.

### **7.2.3 Photo-Elastic Techniques**

Stress analysis using photo-elastic techniques involves the construction of a 2-D model of the structure within a material such as glass or plastic. The model material must become birefringent when strained i.e. exhibit the property of double refraction. The modelling technique involves passing a beam of polarised light through the stressed material. The beam is split into two component beams. The two components emerge from the material polarised in the planes of the principal stresses in that material. One of the beams is also slowed down relative to the other by a time difference proportional to the difference in the magnitude between the principal stresses. The two emergent beams are then passed through a further polarising filter known as an analyser. Interference between the two resolved components generates an optical pattern that can be seen by the observer. A series of bands or fringes of light extinction and enhancement is produced. The fringes, known as isochromatics,

represent contour lines of constant principal stress difference. Thus the fringe pattern represents a mapping of contours of maximum shear stress through the medium. Calibration of the model allows the shear stress magnitudes to be determined and from this mathematical manipulation allows the development of contour plots of the principal stresses throughout the domain. As stresses are independent of the material elastic modulus and the size of the excavation the stress predicted by the photo-elastic model relate directly to those for similar shaped underground excavations.

Photo-elastic techniques have several disadvantages for modelling coal mine excavations. Firstly only a single homogeneous elastic material can be modelled. This limits its use as a predictive tool for stress analysis with Coal Measures consisting of strata units of different rock properties. Also under the influence of the high in-situ stress field associated with deep coal mining in the UK the rock strata behaves in a non-linear manner.

#### **7.2.4 Physical Modelling Techniques**

Physical modelling involves the construction of scale models of the strata and installed supports. The physical model is then loaded into a test rig where the in-situ stress conditions are simulated by loading from hydraulic cylinders at the top and sides. For the physical model to provide useful information on deformation and failure mechanisms of the actual rock strata, scale factors have to be applied to the properties of the modelling material and to the properties representing length, time and stress. These properties must be scaled so that the theoretical equations that describe the behaviour of the materials being considered remain the same in both the actual case and in the model. Body forces should also be an inverse ratio to the geometric scale factor between model and prototype dimensions. For similitude between the actual excavation and the model the strength and deformation properties of the model are scaled with respect to the geometric scale factor, density scale factor and time. Once the material parameters have been scaled the model is said to be made of equivalent materials. Two basic types of materials used in geomechanics modelling are non-granular and granular material (Stimpson 1970). Although physical models have been used extensively to study the behavior of the strata around mining excavations (Roberts 1994) they have several disadvantages which include the following:

- (i) The construction of the model itself is very time consuming and requires careful preparation of the equivalent materials that represent the individual strata layers.
- (ii) A conventional physical model of a structure yields little or no information on stresses and displacements in the interior of the medium.
- (iii) The length of time to construct single models prohibits the systematic assessment of the effect of changing parameter properties on the deformation and failure mechanisms.
- (iv) The loading on external boundaries as opposed to internally is an approximation to reality.

## **7.3 COMPUTER BASED NUMERICAL MODELLING METHODS**

### **7.3.1 Introduction**

Computer based numerical modelling techniques have been developed over the last 20 to 30 years for the application to the modelling of geomechanical materials. The use of computer modelling for rock mechanics problems is now very popular (Starfield and Cundall 1988, Itasca 1998). The development of such methods has allowed, for the first time, a way of predicting the stresses, displacements and failure zones around structures formed within rock masses that exhibit complex non-linear constitutive behaviour. Several different numerical solution methods have been adopted for use within geotechnical modelling but all methods have utilised the same approach of dividing the area into smaller physical and mathematical components which are usually called elements (Hoek et al 1991). Each element is effectively a single body where the material properties are constant. The physical quantities such as stress and displacement within or on the boundaries of a body are governed by a set of mathematical equations. The physical quantities of the element interact with adjacent or all other elements in order to bring the overall modelling system into a state of equilibrium.

### **7.3.2 Solution Techniques**

The most common method of solution of the series of equations generated in this process is to formulate them as a series of simultaneous equations. The simultaneous equations may then be constructed into matrices and vectors and solved using matrix algebra. The element matrices are often combined into a large global stiffness matrix. This is known as the matrix or implicit solution technique. This solution is most efficient when used for modelling materials with comparatively simple constitutive behaviour. However where behaviour is more complex the solution would require multiple steps and matrix reformulation and this lowers the efficiency for the solution.

An alternative technique for solution, known as explicit or dynamic relaxation technique, is based on the assumption that a disturbance at a point in space is initially only felt by points in its immediate vicinity. With time ( i.e. computational steps) the disturbance spreads from point to point throughout the model until equilibrium is established. This method requires the damping of numerical oscillations and is relatively slow for simple problems. However it does not require the formulation or solution of a matrix and becomes the most efficient method when modelling material with complex constitutive relationships.

### **7.3.3 Numerical Modelling Methodologies**

There are four main types of numerical modelling methodologies used in rock engineering. The characteristics of each of the main types is described below.

#### **7.3.3.1 Boundary Element Method**

In this method only the boundaries of the model geometry such as the excavation surfaces are divided into elements. The rock mass is represented within the model as a mathematical infinite continuum. The boundary-element method utilises a fundamental solution for determining the stress and displacement at any point within the infinite medium. This solution is used as a basis for determining the relationship between conditions on the surface of the boundary elements and the conditions of all points within the remaining medium. Within the model each boundary element can have an effect on all the other boundary elements. To calculate the interaction effects a system of linear equations is assembled into a matrix, termed the coefficient matrix,

which represents the influence of one element on another. As each element can influence every other element the coefficient matrix is said to be fully populated. This means that the solution time increases exponentially with respect to the number of elements. As the state at any point in the medium is determined solely by the conditions on the discretized boundaries it is not necessary to approximate the far field stresses. However boundary element models have limited capability in modelling heterogeneous and non-linear materials.

#### 7.3.3.2 Distinct Element Method

In the distinct element method the rock mass is considered as being discontinuous. The rock mass is considered to consist of discrete interacting particles, free to move except during contact with neighbouring objects. (Dorfmann et al 1997). Particles can undergo large displacements, large rotations and are typically used to model failure of weakly cemented discrete systems under high loads (Dorfmann et al 1997) The particles or blocks are usually considered as rigid bodies with the rock mass deforming by interactions at the blocks contacts with the surrounding blocks (Hoek et al 1991). The distinct element method model this by constructing data structures that represent the blocky nature of the system being analysed. The blocky rock mass behaves in a highly non-linear manner and hence explicit solution techniques are usually favoured for distinct element methods (Hoek et al 1991). This allows the constitutive modelling of joint behaviour with little increase in computational effort and results in the computing time being only linearly dependant on the number of elements used. A disadvantage of using this method is that the results can be sensitive to the assumed values of modelling parameters (Hoek et al 1991) i.e. the properties of the discontinuities. This is major disadvantage for the modelling of coal mine excavations as the joint properties of the rock mass are often not known. UDEC is a commonly used, commercially available distinct element code (Itasca 1995).

#### 7.3.3.3 Finite Element Method

In the finite element method the entire modelled rock material is divided into elements. The elements are connected at nodal points, with the elements and nodal points constituting the finite element mesh. During the solution process the loads and displacements at the nodal points are determined from the load and displacement conditions within the finite area enclosed by the nodal points i.e. within the elements.

A central requirement for the finite element method is that the field quantities (stress, displacements) vary throughout in accordance with the governing equations. The solution is obtained by adjusting the parameters used in the equations to minimise error terms on local or global energy (Hoek et al 1991).

The finite element model is suitable for modelling heterogeneous or non-linear materials as the material behaviour in each element is individually calculated. Prior to solving the model, boundary conditions are usually required to be applied to the models outer edges. The model mesh needs to be extended beyond the zone of influence of the excavation and the boundary conditions applied therefore represent the in-situ far field conditions. Although finite element methods analyse the rock mass as a continuum, discontinuities can be explicitly represented. However for a heavily discontinuous rock mass it is more efficient to use the distinct element method. The model is solved using an explicit solution technique. Material non-linearity is accounted for by modifying the material stiffness properties within the global stiffness matrix in an iterative manner. The matrix itself is solved for each iteration and this can be time consuming for materials with complex non-linear behaviour as many iterations of the matrix calculation may be required to bring the model into equilibrium (Coetzee et al 1993).

#### 7.3.3.4 The Finite Difference Method

The finite difference model is constructed in the same manner as a finite element model. The mesh, manner of prescribing boundary conditions and material properties are similar. However for solving the problem the finite difference method uses an explicit solution technique. This technique involves the direct replacement of every derivative in the set of governing equations with an algebraic expression written in terms of the field variables (e.g. stress and displacement) at discrete points in space (Coetzee et al 1993). In this manner the large matrices which are a feature of the finite element method are not formed. The finite difference solution is analogous to a time stepping process with each calculation wave representing one timestep. The general calculation sequence used in the FLAC finite difference code is shown as Figure 7.1.

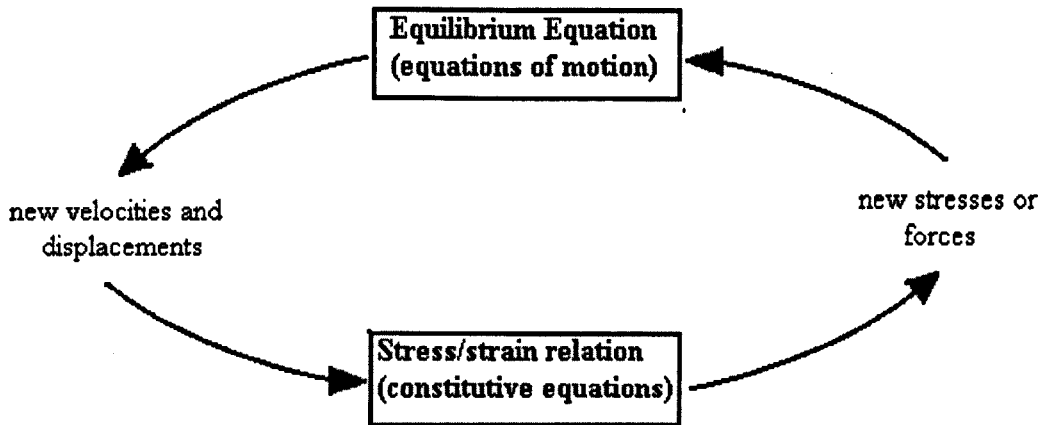


Figure 7.1 Sequence of Calculation, Finite Difference Method

(after Coetze et al 1993)

In the calculation sequence equations of motion are first invoked to derive velocities and displacements from stresses and forces. Strain rates are derived from the velocities and new stresses from the strain rates. During one calculation sequence the values are fixed and not effected by the values calculated for adjacent localities. For instance the velocities associated with the locality are not affected by stresses calculated for adjacent points. It is therefore necessary to represent each calculation loop as a very small time step. However after each cycle interaction occurs between adjacent points and after several cycles disturbances can propagate across several elements as they would in a natural system. No iteration process is required to compute stress from strains and this method is the best method to use for modelling non-linear, large strain systems, such as excavations in Coal Measure rocks.

## 7.4 FAST LAGRANGIAN ANALYSIS OF CONTINUA (FLAC)

### 7.4.1 Introduction

FLAC is an explicit, finite difference program that performs a Lagrangian analysis (Itasca 1995). FLAC Version 3.3 has been used extensively within the School of Chemical, Environmental and Mining Engineering for the computer modelling of coal mining environments. The code has successfully used to model large scale subsidence effects (Mohammad 1998) and intermediate scale environments, for instance stress distribution above the goaf of longwall panels (Lloyd 1998). FLAC has

also been used extensively within rock mechanics consultancies to model strata deformation around roadways within UK coal mines (Garratt 1998).

FLAC models the rock strata as a continuum however interfaces which allow the strata to slide and separate may be explicitly modelled. A variety of functions allow supports such as roof bolts and steel arches to be incorporated into the model. Figure 7.2 illustrates the major components of a FLAC model. FLAC Version 3.3 is a 2D code and thus 3D effects such as stress notching and roadway face end behaviour are difficult to model in two dimensions. The FLAC model is constructed using a series of FLAC commands that are written using a normal text editor and saved as a FLAC data file. The sequence of commands within the data file corresponds closely with the physical sequence they represent. As FLAC solves the problem using an explicit time marching scheme the model problem may be constructed on a time related basis with for instance incremental stages of excavation or the time related installation of supports (Coatzee et al 1993).

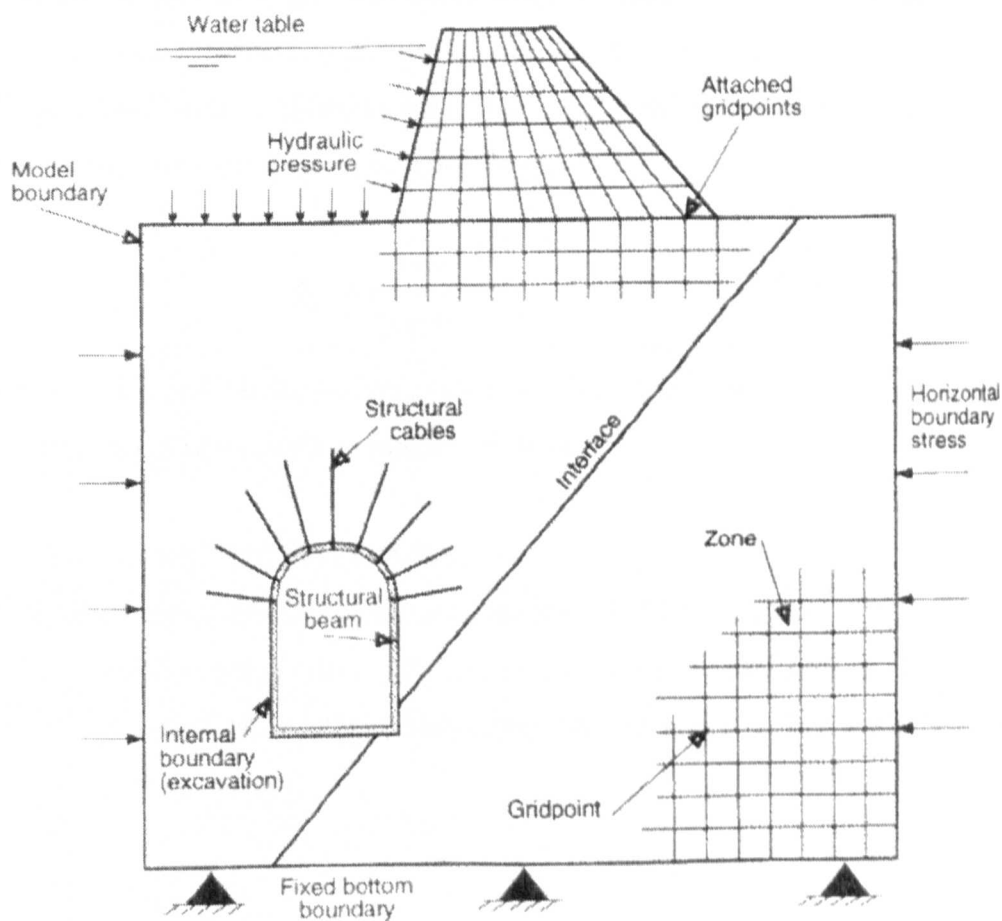


Figure 7.2 FLAC model Components (After Coetze et al, 1993)

#### **7.4.2 The Finite Difference Grid**

The first stage in the construction of a FLAC model is the discretisation of the problem by the construction of finite difference grid. The grid or mesh is organized in a row and column fashion. The size of the grid is specified by the number of zones i required in the horizontal (x) direction and the number of zones j required in the vertical (y) direction. Each zone is identified by a pair of i,j coordinates. The vertices of the zones meet at grid points which are called nodes. Also each node is also identified by a pair of ij coordinates. The grid is sized and distorted to model the physical situation by mapping the ij node coordinates to xy space which represents the dimensions of the real environment. This mapping process allows the FLAC grid to be distorted and graded. Finer grids lead to more accurate results as they provide a better representation of high stress gradients. However as the grid is made finer the number of zones increases which increases the computational time and computer RAM requirements. Grading the grid allows a finer grid to be constructed near the excavation and an increasingly coarse grid with distance from the excavation. This has the benefit of a finer grid but with a reduced number of zones. A useful equation that can be used to determine the aspect ratio i.e. the ratio between the dimensions of each successive zone is given as Equation 7.1. To retain accuracy the aspect ratios should be kept reasonably close to unity (Itasca 1995).

$$S_n = a_1 \frac{1-r^n}{1-r} \quad (7.1)$$

Where  $S_n$  = the total distance to be graded,  $a_1$  = length of zone 1,

$r$  = aspect ratio, and  $n$  = number of zones

#### **7.4.3 FLAC CONSTITUTIVE MODELS**

Nine standard constitutive models are provided in FLAC version 3.3 (Itasca 1995) and these can be arranged into null, elastic and plastic model groups (Itasca 1995). Constitutive models and material properties can be assigned individually to every zone within a FLAC model.

##### **7.4.3.1 Null Model**

A null material model is used to represent material that is removed or excavated.

### 7.4.3.2 Elastic Model Group

#### 7.4.3.2.1 *Elastic isotropic model*

This is the simplest FLAC constitutive model and represents the material as an linear elastic isotropic medium with infinite strength. This model is valid for homogeneous, isotropic, continuous material that exhibit linear stress strain behaviour with no hysteresis on unloading. To characterise the elastic material FLAC requires as input parameters the Bulk (K) and Shear (G) moduli of the material. These moduli are calculated from the Young's modulus (E) and Poisson Ratio ( $\nu$ ) using Equations 7.2 and 7.3.

$$G = \frac{E}{2(1+\nu)} \quad (7.2)$$

$$K = \frac{E}{3(1-2\nu)} \quad (7.3)$$

#### 7.4.3.2.2 *Elastic, transversely isotropic model*

FLAC can model the material as an elastic, transversely isotropic medium.

### 7.4.3.3 Plasticity Models

All FLAC's plasticity models involve the potential to model both linear-elastic deformations and permanent, path dependant plastic deformations. Stress strain relations within the plasticity models are as a consequence non-linear. The different plastic models within FLAC are characterised by their yield function, hardening softening functions and flow rule. The yield functions define the stress conditions at which plastic flow takes place. FLAC's plastic models are based on plane strain conditions. The plasticity models can also produce localisation. Localisation is the development of families of discontinuities such as shear bands in material that starts as a continuum (Itasca 1995).

#### 7.4.3.3.1 *Mohr-Coulomb Model*

This is the conventional model used to represent shear failure in soils and rocks. The yield function for this model corresponds to a Mohr Coulomb Failure Criterion (shear yield function) with a tension cutoff (tensile yield function). The input parameters

required by FLAC to determine the yield function are the Mohr-Coulomb parameters of material friction and cohesion and the tensile strength of the material. At yield FLAC calculates the plastic flow within the medium. The flow rule within FLAC assumes that the total strain increment may be divided into elastic and plastic parts with only the elastic part contributing to an incremental change in stress which is calculated by means of an elastic law. The Mohr-Coulomb model models the material as an elastic perfectly plastic medium.

#### *7.4.3.3.2 Ubiquitous joint model*

This model accounts for the presence of a orientation of weakness (weakness planes) within a FLAC Mohr-Coulomb model. Yield may occur in either the solid or along the weak plane or both depending on the stress state, the orientation of the weak plane and the material strength properties of the solid and weak plane. The input parameters required by FLAC to characterise the material are those of the Mohr-Coulomb model plus the friction angle, cohesion, tensile strength and orientation of the weakness planes.

#### *7.4.3.3.3 Strain-softening model*

This constitutive model is based on the FLAC Mohr-Coulomb model as described earlier. However the difference lies in the possibility that the cohesion, friction, dilation and tensile strength may harden or soften after the onset of plastic yield. Within the Mohr-coulomb model these properties are assumed to remain constant. Within the strain-softening model the user can define the cohesion, friction, dilation properties as a piecewise linear softening law dependant on the shear strain increment. The tensile strength can also be prescribed in terms of another hardening parameter measure termed the plastic tensile strain.

#### *7.4.3.3.4 Other plastic models provided for in FLAC*

A Drucker-Prager model allows the simulation of the behaviour of soft clays with low friction angles but is not generally applicable to geologic materials.

FLAC's double yield model is intended to represent materials in which there may be irreversible compaction in addition to shear yielding such as hydraulically placed back fill or lightly cemented granular material.

A modified cam clay model may be used to model material where the change in volume of the material influence the bulk property and shear strength as in the case of overconsolidated clays.

#### **7.4.4 Model Boundary Conditions**

The boundary conditions are the constraints or controlled conditions which are applied to the boundary of the finite difference grid. The two main types of mechanical conditions that can be applied at model boundaries are prescribed stress and prescribed displacement. Boundaries may either represent real or artificial boundaries. Real boundaries are boundaries within the model that also exist in the physical situation being modelled, for instance excavation surfaces or the ground surface. Artificial boundaries represents the models extent of the physical situation. There are two categories of artificial boundary which are lines of symmetry and lines of truncation. Lines of symmetry take advantage of a line or axis of symmetry within the model to reduce the model size by modelling only one side of the mirror image. Lines of truncation allows the detailed modelling of the zone of interest within a large physical situation, such as the modelling of a roadway within a deep coal mine. The artificial boundaries should be positioned sufficiently far from the area of interest so that the behaviour in that area is not greatly affected.

#### **7.4.5 Initial Stress Conditions**

Underground rock masses exist in a stressed state prior to excavation due to the presence of in-situ stresses. This in-situ state is reproduced within FLAC by setting initial stress conditions. Prior to the solution of the model problem the prescribed initial conditions and the imposed boundary conditions have to be brought into equilibrium representing field conditions.

#### **7.4.6 FLAC Modelling Methodology**

Unlike in other branches of engineering, rock engineering problems tend to be characterised by a lack of information relating to the structure and properties of the material being modelled (Starfield and Cundall 1988). This is due to the complex nature of rock masses and the difficulty of investigating its structure (Pan and Hudson 1991).

Whyatt and Julien (1988) described four styles of implementing numerical models within rock engineering design which are as follows:

**(1) Ultimate Design Tool**

In this style numerical modelling is used as a precise prediction technique. For numerical models to be used in such a way the properties of the system being modelled should be fully defined. Using numerical modelling as an ultimate design tool has been successful in the mechanical and aerospace engineering industry but has limited applicability in rock engineering due to the lack of data and the variability of rock as an engineering material.

**(2) Method of Last Resort**

This style is used when the numerical model is used to establish some basis for design when empirical methods are not available or not known to the design engineer.

**(3) Aid to Judgement**

Numerical models are used in studies to identify the most threatening failure mechanisms and/or to assess the relative merits of alternative designs. This includes parametric studies to assess the sensitivity of the model to changes in parameter values. This style is suitable for data limited situations typical of rock engineering problems.

**(4) Calibrated Model**

In this style models are adjusted or ‘fudged’ to fit measurements taken from existing excavations. The calibrated model analysis requires a detailed numerical model often based on extensive laboratory and insitu tests that are combined with observations of field displacement and stress redistribution. The laboratory results are adjusted until the model behaviour is similar to the field measurements. This readjustment is a reflection of the fact that rock mass behaviour often deviates significantly from that predicted from laboratory tests. This style has been used for the numerical modelling of coal mine excavations within UK coal mines (Garratt 1997) where often a calibrated model is developed for a region and is utilised as a basis for parametric studies undertaken as an aid to judging support requirements within that region.

Starfield and Cundall (1988) suggested that a distinctive modelling methodology that is both purposeful and effective should be developed for rock mechanics modelling. Using a classification proposed by Holling for the use of modeling ecological problems they stated that modelling problems can be divided into four groups dependant on the level of data and understanding of the project.

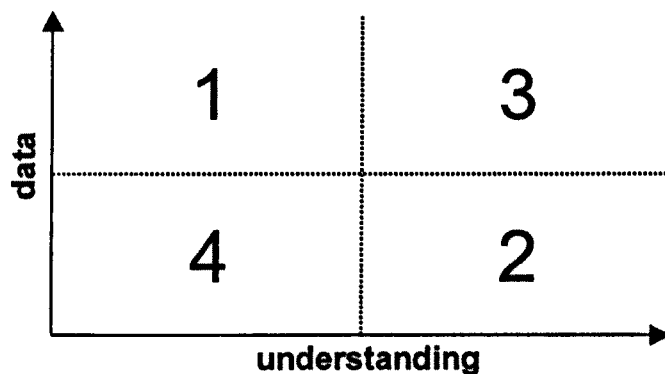


Figure 7.3 Holling's Conceptual Classification of Modelling problems  
(after Starfield and Cundall 1988)

Modelling problems that lie within region 1 in Figure 7.3 have good data but little understanding and this is where statistics is the most approximate modelling tool. In region 3 modelling problems are characterised by good data and good understanding of the problem. For models situations falling in this zone, models can be constructed, validated and used with conviction. Modelling problems that lie within regions 2 and 4 are characterised by limited data, due either to the data not being available or easily obtained. Starfield and Cundall (1988) stated that rock mechanics problems fall into the data limited categories and that there is not enough information about a rock mass to model it unambiguously. They state that one should attempt not to try to incorporate complex detail within a rock mechanics model but the designer should use the simplest model that will allow the important mechanism to occur. They consider that the validation of a data limited model may be impossible. Therefore instead of attempting to use the model as a fully predictive tool the models should be used to discover the potential mechanism of failure and deformation within the rock mass.

Coetzee et al (1993) state that there is a continuous spectrum of modelling situations with respect to the data and that FLAC use may vary from an investigating mechanism to being used as a fully predictive tool (Figure 7.4).

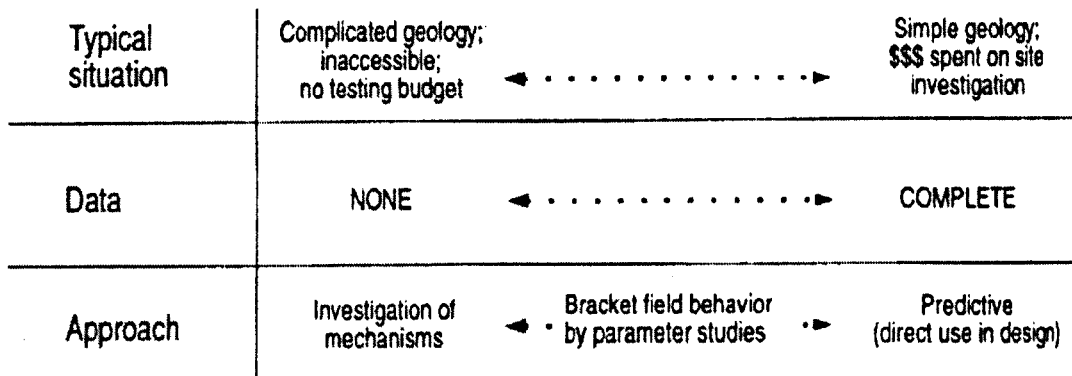


Figure 7.4 Spectrum Of Modelling Situations (After Coetzee et al 1993)

## 7.5 NUMERICAL MODELLING OF GATE ROAD DEFORMATIONS WITHIN UK COAL MINES

### 7.5.1 Introduction

Extensive numerical modelling using the finite difference continuum code FLAC Version 3.3 was undertaken for Riccall, Daw Mill and Rossington mine sites at the case study locations detailed in Chapter 6.

The objective of the FLAC modelling was to validate the Coal Mine Classification as a means of predicting representative strata properties for input into computer based numerical models. Prior to the validation of the classification a basic modelling methodology that would allow the simulation of the typical strata deformation and failure mechanisms that have been observed to occur in coal mine roadways had to be developed. A FLAC constitutive material model was chosen in order to represent the deformation behaviour of the strata at the case study localities. Complex constitutive models that required a large number of input parameters to characterise the material behaviour were avoided as assumptions, or else back analysis would be required to determine input parameters. An attempt was made to identify a less complex constitutive model that would model the major deformation and failure mechanisms

of the rock mass in-situ but with a reduced number of input parameters which could be evaluated from the Coal Mine Classification Ratings.

### **7.5.2 Numerical Modelling Of Gateroad Deformation, Riccall Colliery**

Computer modelling has been undertaken of the twelve case study localities, detailed in Chapter 6, within the gateroads of panels H505, H478 and H438.

#### **7.5.2.1 Establishment of a Modelling Methodology**

A provisional modelling methodology was developed and applied in the form of FLAC modelling of the gateroads. The methodology was initially developed by the modelling and analysis of roof deformations for the roof strata at the 922 metre mark of the tail gate of Panel H505. The modelling methodology developed for this locality was established as the optimum modelling methodology that was then applied in all the other localities.

##### ***7.5.2.1.1 Roof Deformation Characteristics,***

###### ***922 metre mark, Tail Gate, H505 Panel Riccall***

The roof monitoring data at the 922 metre mark is shown as Figure 7.5. The displacement readings show less than 1 mm of deformation occurring between 1.8 m and 5 m height within the roof. Below 1.8 m the strata has been measured to have deformed by approximately 60 mm in the 6 month period from the time of installation of the extensometer. The extensometer readings also indicate a slow time dependant deformation within the immediate roof. (Figure 7.5).

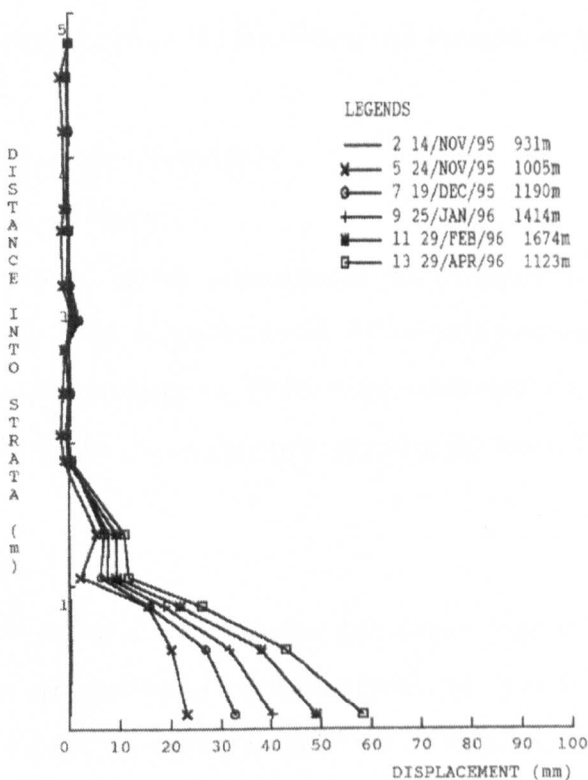


Figure 7.5 Roof Extensometer 922mm, Tail gate 505 Panel, Riccall

(after R.J.B. 1997)

#### *7.5.2.1.2 Selection of constitutive material model*

The in-situ stress redistributed around the excavation upon development would be expected to exceed the strength of the material. A yield zone would develop around the excavation with possible strain softening of the yielded strata. A manifestation of failure would be the development of large strains within the rock material. Previous workers have identified a shear strain increment of 10mm/m as representing failure and subsequent onset of strain softening (RMT 1997). Figure 7.5 indicates that large strains have occurred within the immediate roof at this locality with a significant vertical displacement of the rock strata upto a height of approximately 1 or 2 metres into the roof. To simulate the elastic and plastic deformations of the roof strata an elastic-perfectly plastic constitutive model was selected. Strain softening was not incorporated within the constitutive behaviour as the degree of post yield strain softening of the rock strata was unknown.

The Coal Mine Classification Ratings for the roof strata indicates that there are different material properties in the vertical and horizontal directions due to the presence of laminations, bedding planes etc. FLAC the ubiquitous joint constitutive model was selected to simulate the directional strength properties.

### 7.5.2.2 Modelling Input Parameters

#### 7.5.2.2.1 *Elastic parameters*

The ubiquitous joint model characterises the material as an isotropic linear elastic material upto the onset of plastic yield. The elastic parameters required in this model are the bulk and shear modulus. These were calculated from the deformation modulus ( $E$ ) and Poisson's ratio ( $\nu$ ) of the material using Equation 7.2 and 7.3 respectively.

#### *Poisson's Ratio*

Poisson's Ratio assumed for non-coal lithologies was 0.25 and for coal 0.3. These value has been determined to be characteristic of Coal Measure Rock types (Wilson 1980). FLAC modelling has been found not to be particularly sensitive to changes in Poisson's Ratio (Mohammad 1998).

#### *Deformation modulus*

Three methods of empirical prediction of the rock mass deformation modulus were evaluated in order to determine the optimum method. The methods evaluated were Serafim and Pereira's (Equation 4.20), Nicholson and Bieniawski (Equation 4.22) and Mitri et al (Equation 4.24). Assuming a typical Coal Measure Young's Modulus of 20 GPa the deformation modulus was estimated using each of the methods for a variety of rock mass conditions corresponding to a rock mass rating range of 25 to 75. The results of the evaluation are shown as Figure 7.6. From Figure 7.6 it is apparent that Serafim and Pereira's method suggests that the deformation modulus is greater than the intact modulus within the upper range of RMR values. Nicholson and Bieniawski's method predicts very low deformation modulus for the range of RMR values. Mitri's method predicts higher deformation modulus values than Nicholson and Bieniawski's method and as the deformation modulus is related to the intact modulus it does not exceed the intact value above a certain threshold value. From this initial appraisal it was concluded that Mitri's method provided the most appropriate

way of reducing the intact Young's Modulus for rock mass conditions using the Coal Mine Classification Rating.

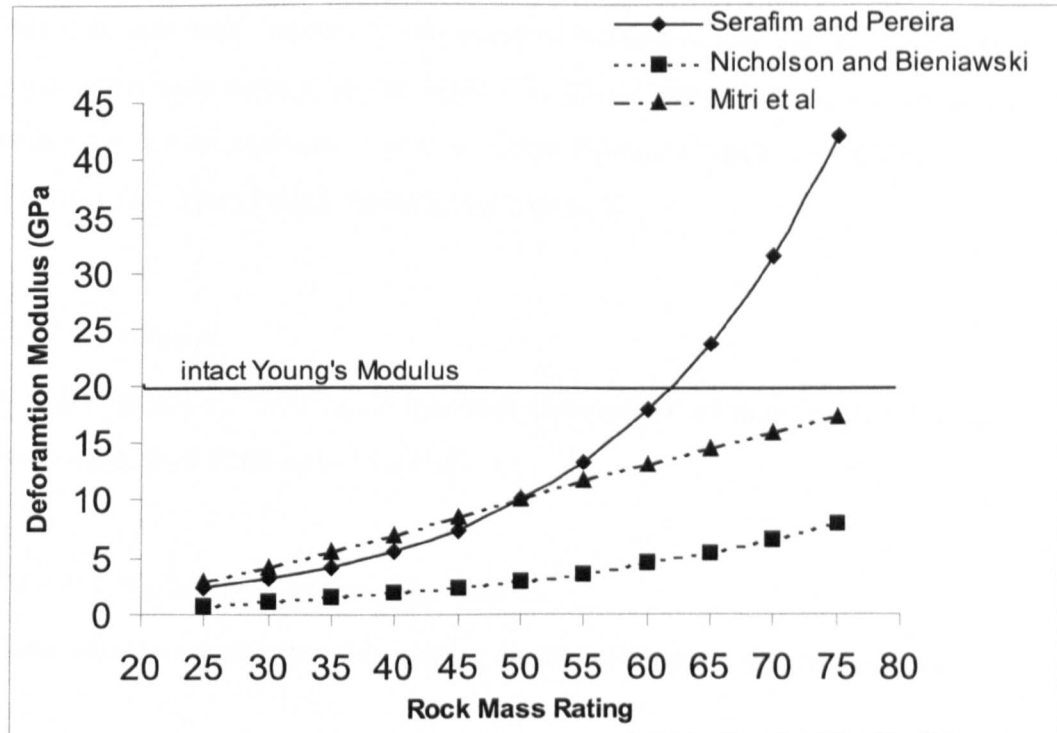


Figure 7.6 Relationship Between Rock Mass Ratings and Deformation Modulus  
(Young's Modulus = 20 GPa)

The deformation modulus calculated for each of the classified strata units using Mitri's method is given in Table 7.1.

Strata properties		Strata unit number					
		1	2	3	4	5	6
CMC Rating		35	43	45	42	48	47
CMCR (Vert.)		32	37	40	35	42	40
CMCR (Horiz.)		46	51	52	49	54	54
Intact UCS (MPa)		20	41	43	34	48	52
Intact Young's modulus (GPa)		5.2	10.7	10.2	8.9	12.6	13.6
Deformation modulus (GPa)		1.4	4.2	4.3	3.3	5.9	6.2
Strength parallel to bedding	Friction ( $^{\circ}$ )	22	29	34	27	32	32
	Cohesion (MPa)	0.85	1.18	1.42	1.07	1.35	1.35
	Tension (MPa)	0.1	0.1	0.1	0.1	0.1	0.1
Strength right angle to bedding	Friction ( $^{\circ}$ )	26	33	38	31	35	36
	Cohesion (MPa)	1.03	1.49	1.71	1.33	1.71	1.77
	Tension (MPa)	1	1	1	1	1	1

Table 7.1 Strata Properties: immediate roof, 922 metre mark, tail gate, H505, Riccall

#### *7.5.2.2.2 Strength properties*

The ubiquitous joint model requires the Mohr-Coulomb strength properties of friction, and cohesion both parallel to the plane of weakness and for the solid. The strength parameters have been given in Table 7.1. These parameters were evaluated from the intact triaxial strength and the Coal Mine Ratings  $CMR_{(h)}$  and  $CMR_{(v)}$  using Hoek-Brown Rock Mass Failure Criterion (Chapter 4).

#### *7.5.2.2.3 Density*

A strata density of  $2500 \text{ kg/m}^3$  has been assumed for all non-coal Coal Measure strata and a density of  $1500 \text{ kg/m}^3$  for coal.

#### *7.5.2.2.4 Modelling of support elements.*

FLAC has the capability of simulating structural supports within the model.

##### *Cable Elements*

Rock bolts and cable bolts can be modelled within FLAC using cable elements. Cable elements are linear features with no diametrical shear strength and are defined by the segments of a line connected at i,j nodal points. The constitutive behaviour of the cables and their interaction with the surrounding rock mass are defined by a set of parameters which relate to the diameter, yield strength, elasticity modulus of the cable, the shear stiffness of the grout and the shear strength of the grout/rock interface. These parameters are illustrated in Figure 7.7. The maximum shear stress that can be developed in the cable element is dependant on the strength of the grout/rock interface as shear failure is typically observed to occur at this interface (St. John and Van Dillen 1983). The strength of the interface has three components which are; adhesion, mechanical interlock and friction (St John and Van Dillen 1983). With increasing radial confinement the shear strength of this interface is considered to increase (Hyett et al 1992) . The strength of the grout/rock bond within FLAC is given by defining per length of element, the cohesive force of the grout/rock interface ( $S_{\text{bond}}$ ) and the stress dependant frictional resistance of the grout/rock interface ( $S_{\text{friction}}$ ) (ITASCA 1995).

These parameters can be obtained directly from the load displacement curves obtained from in-situ pull test data. Where this information is unavailable the shear strength can be estimated as being the lowest of either the shear strength of the rock or the shear strength of the grout (Itasca 1995, St. John and Van Dillen 1983).

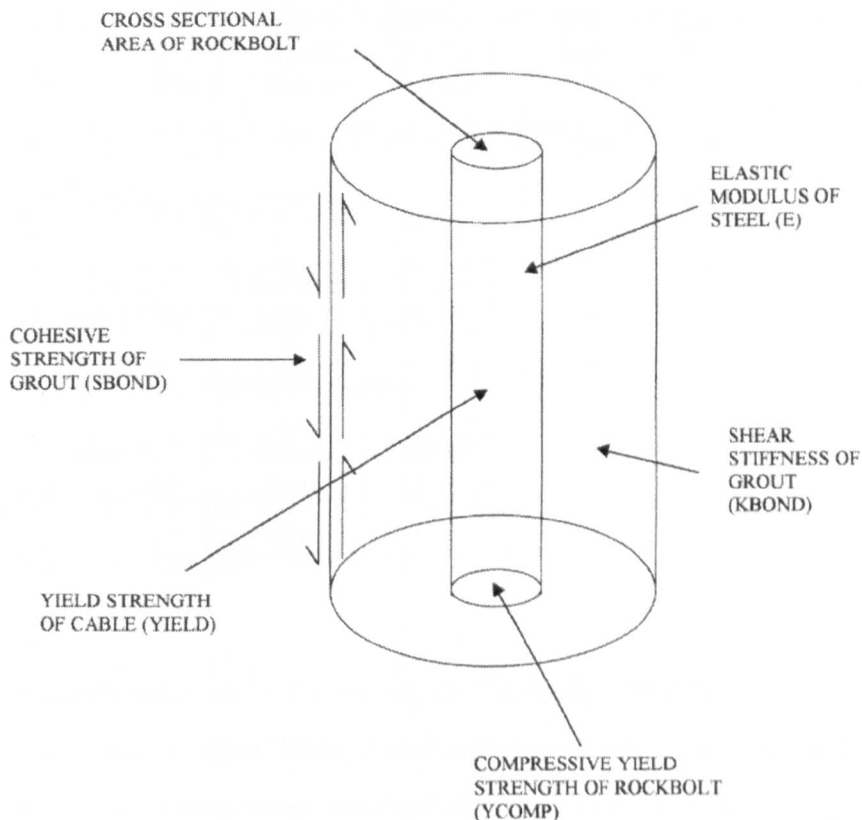


Figure 7.7 FLAC's Cable Bolt Parameters

#### *Installed primary supports within panel 505 main gate at 922 metre mark*

Properties of roof bolts, rib bolts, roof straps and end plates for this locality are given as Table 7.2 and 7.3 respectively. The properties relating to the strength and dimensions of the bolts have been determined from published information (Bigby et al 1996). As no pull test data was available  $S_{bond}$  and  $S_{fric}$  representing the shear strength of the grout rock interface have been determined for individual strata units from the rock mass strength properties. The dimensions of the roof straps and end plates (RJB 1997) together with the Young's modulus determined from the typical Young's modulus of steel are given in Tables 7.4 and 7.5 respectively.

Strata unit no.	BOLT DIAM (mm)	HOLE DIAM (mm)	MODULUS OF BOLT (GPa)	Kbond (GN)	S <sub>bond</sub> (kN)	S <sub>fric</sub>	Y <sub>comp</sub> (MPa)	ultimate strength (kN)
1	22	27	217	13.56	87	26	640	309
2	22	27	217	13.56	126	33	640	309
3	22	27	217	13.56	145	38	640	309

Table 7.2 Steel roof bolts 2.4 metres long

Strata unit no.	BOLT DIAM (mm)	HOLE DIAM (mm)	MODULUS OF BOLT (GPa)	Kbond (GN)	S <sub>bond</sub> (kN)	S <sub>fric</sub>	Y <sub>comp</sub> (MPa)	ultimate strength (kN)
Barnsley Coal	22	27	47	13.56	424	0	640	350

Table 7.3 Rib bolts 1.8 metres long

Young's modulus (GPa)	Thickness (mm)	Width (mm)
200	2	100

Table 7.4 Roof strap properties

Young's modulus (GPa)	Thickness (mm)	Width (mm)
200	14	100

Table 7.5 End plate properties

### Secondary Supports

A displacement of >25 mm within the bolted interval at this site was recorded by the roof extensometers. Therefore it is expected that 6 metre long double birdcaged cable bolts would have been installed at this locality as a form of secondary support. The properties of the cable bolts are given in Table 7.6 (Kent et al 1997). The S<sub>bond</sub> and S<sub>fric</sub> representing the shear strength of the grout rock interface have been determined for individual strata units from the rock mass strength properties.

Strata unit no.	HOLE DIAM (mm)	MODULUS OF BOLT (GPa)	Kbond (GN)	S <sub>bond</sub> (kN)	S <sub>fric</sub>	Y <sub>comp</sub> (MPa)	ultimate strength (kN)
1	55	150	8.49	178	26	320	600
2	55	150	8.49	257	33	320	600
3	55	150	8.49	295	38	320	600
4	55	150	8.49	230	31	320	600
5	55	150	8.49	295	35	320	600
6	55	150	8.49	306	36	320	600
7	55	150	8.49	359	41	320	600

Table 7.6 Properties of cable bolts (after Kent et al 1997)

#### *7.5.2.2.5 The finite difference grid*

A finite difference grid representing an area 50 metres high by 30 metres wide was constructed for the modelling. The model of the roadway can be considered as being symmetrical about a vertical axis that passes through the center of the roadway. It was therefore necessary to only model half the problem and an axisymmetric grid was constructed. Within the immediate zone surrounding the excavation the grid represents 10 cm square elements. Grading of the grid with distance from the excavation has been undertaken to reduce the number of elements with the mesh. The grid is shown schematically as Figure 7.8

#### *7.5.2.2.6 Boundary conditions*

Vertical stress was applied to the top boundary with the vertical stress being calculated from the depth of cover. Horizontal stresses representing the in-situ horizontal stress conditions were applied to the right hand boundary and in the out of plane direction. Both the top and right boundaries were free to displace in both the x and y directions. The left hand boundary was allowed to displace in the y direction but fixed in the x direction whilst the bottom boundary was free to displace in the x direction but fixed in the y direction (Figure 7.8).

#### *7.5.2.2.7 Running the simulation.*

The simulation consisted of the following sequence of steps

##### *(1) Initialise stresses*

Prior to excavation the in-situ rock mass was pre-stressed in accordance with the applied boundary conditions.

##### *(2) Removal of excavation*

FLAC's null constitutive model for zones representing the excavation.

##### *(3) Run model for 50 steps.*

The model was run prior to the installation of supports for 50 steps. This was to represent the period of time in the real situation after tunnel excavated but before the installation of supports and roof extensometers. The actual amount of deformation

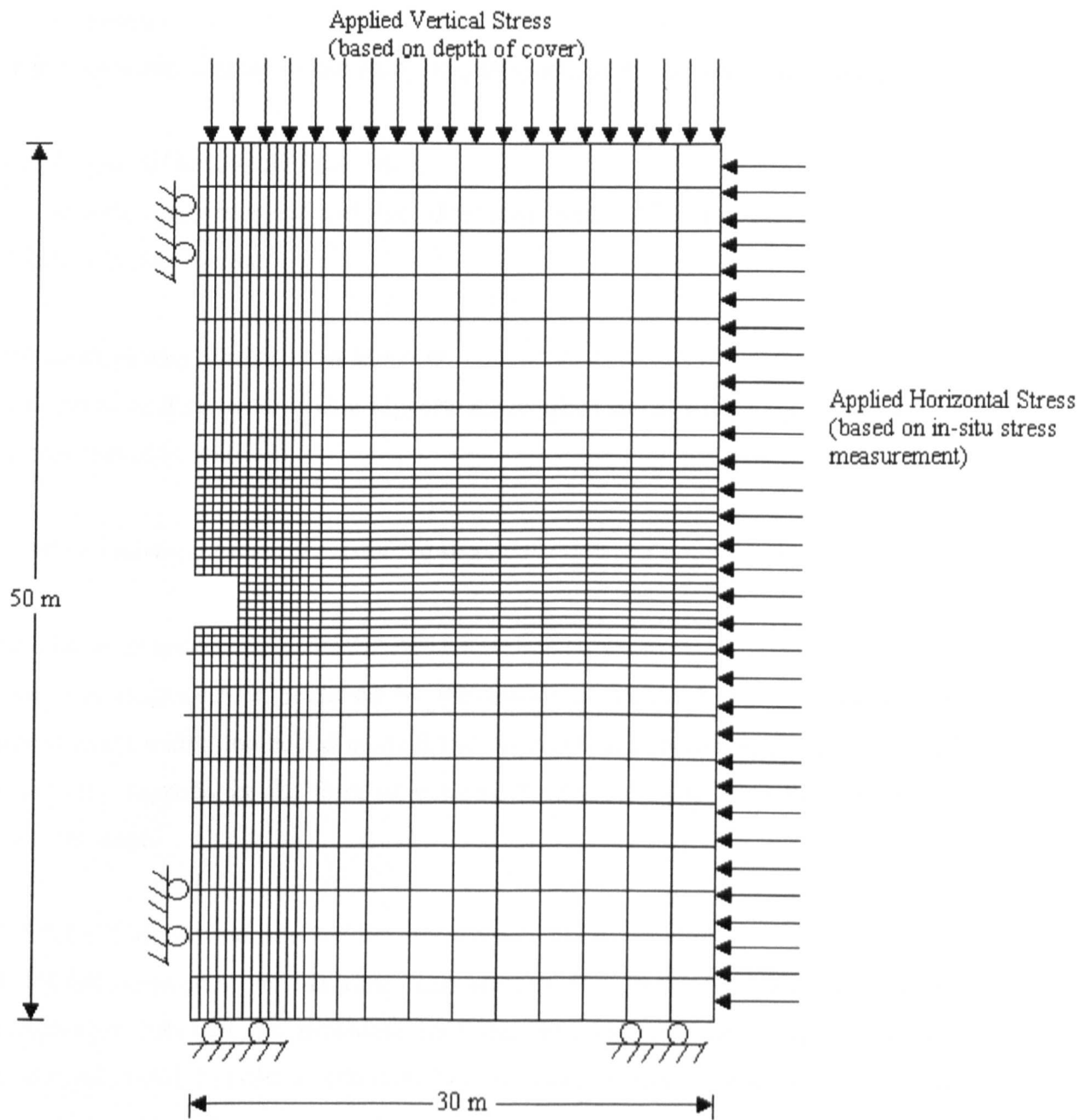


Figure 7.8 Schematic of the Finite Difference Grid Used in Modelling Coal Mine Gateroads

occurring prior to the installation of the monitoring equipment is not clearly understood and further work is required in this aspect.

*(4) Installation of primary roof and rib bolt primary supports together with roof and rib straps.*

Cable elements utilised within FLAC model to simulate roof and rib bolts supports.

*(5) Run model for 20,000 FLAC steps.*

Initial preliminary runs indicated that 20000 steps were sufficient to reach a quasi static solution to the problem

*(6) Analysis roof displacement histories.*

To determine if secondary cable supports are required and at what stage (step number) cables should be installed.

*(7) Rerun model if necessary installing secondary supports at correct stage.*

#### *Secondary Supports*

The roof displacement predicted by the initial run indicated that 25 mm of roof deformation within the bolted interval had occurred. The model was then re-run and secondary supports in the form of 6 metre long cable bolts were installed at the relevant stage.

#### *7.5.2.2.8 Time dependency*

A FLAC simulation of the roof extensometer was constructed to allow direct comparison between the measured roof displacement and that predicted by the numerical model. In order to minimise time dependant effects such as creep which the FLAC simulation does not model, the FLAC prediction was compared to the roof displacement approximately six months after installation of the extensometer.

#### *7.5.2.2.9 Analysis of results*

##### *Total Displacement*

The comparison between the FLAC prediction and actual measured data is shown as Figure 7.9. The final roof displacement predicted by the FLAC model is 49 mm whilst

the monitored data suggest that the roof displacement to be 58 mm. As there was uncertainty in several of the rock mass classification parameters and the boundary conditions it was considered that this was a reasonable prediction of the total roof displacement.

### *Displacement Pattern*

Comparison with the displacement pattern within the roof of the roadway indicated by the extensometers and that predicted by the FLAC simulation shows that both the extensometer data and the FLAC simulation show an increased degree of displacement below 2.00 metres height. However the degree of displacement is lower in the FLAC simulation. This may be attributed to the constitutive behaviour within the FLAC model that does not incorporate post peak strain softening.

The extensometer measurements indicate that no displacement had occurred between the heights into the roof of 2 and 5 metres.

#### 7.5.2.3 Numerical Modelling of Case study Localities at the Riccall Mine Site

The numerical model methodology i.e. the methodology developed for the modeling of panel 505 922 metre mark, was applied to 10 other case study localities for the Riccall mine site. The strata strength and stiffness parameters for each of the strata units to be present within the immediate roof of each of these localities was determined from the Coal Mine Classification Ratings in the same manner as for the roof strata at the 922 metre mark.

##### *7.5.2.3.1 Analysis of results*

The comparisons between the FLAC simulation and the measured roof displacements for the Riccall case study locations shown in Figures 7.10, 7.11, 7.12, 7.13, 7.14, 7.15, 7.16, 7.17, 7.18 and 7.19.

Generally the Figures indicate that the roof displacements predicted from the FLAC modelling corresponds to the in-situ monitored displacements. Both the FLAC predictions and the in-situ monitoring shows that an increased dilation of the strata frequently occurs to an approximate depth of 1.5 to 2 metres into the roof. This is illustrated for instance in Figures 7.9, 7.15, 7.16, 7.17, 7.18 and 7.19.

## 922 Metre Mark, Tail Gate, H505, Riccall

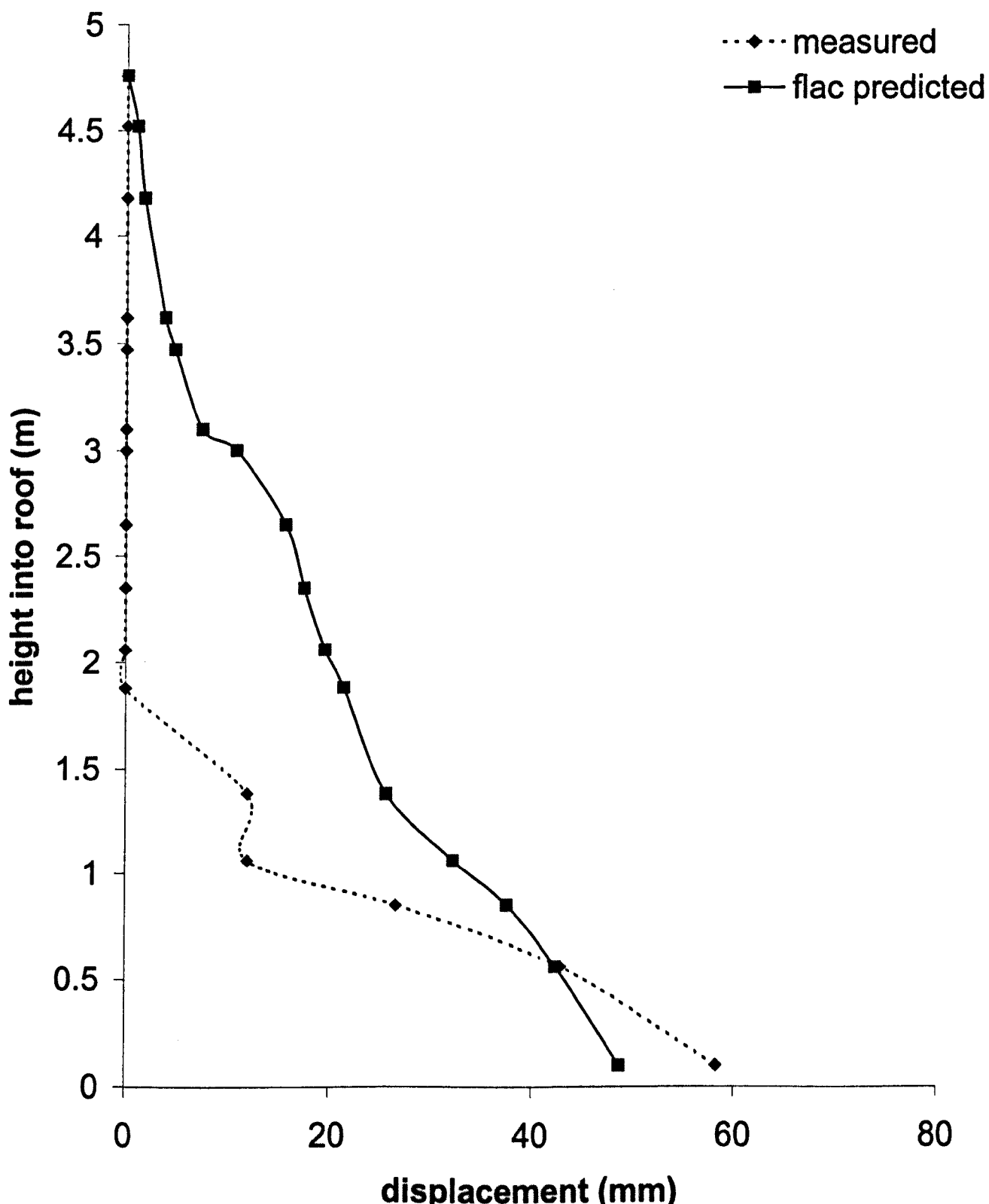


Figure 7.9 Comparison Between Flac Prediction and Actual Roof Displacement at 922 Metre Mark, H505 Panel, Riccall

### 31 Metre Mark, Main Gate, H478, Riccall

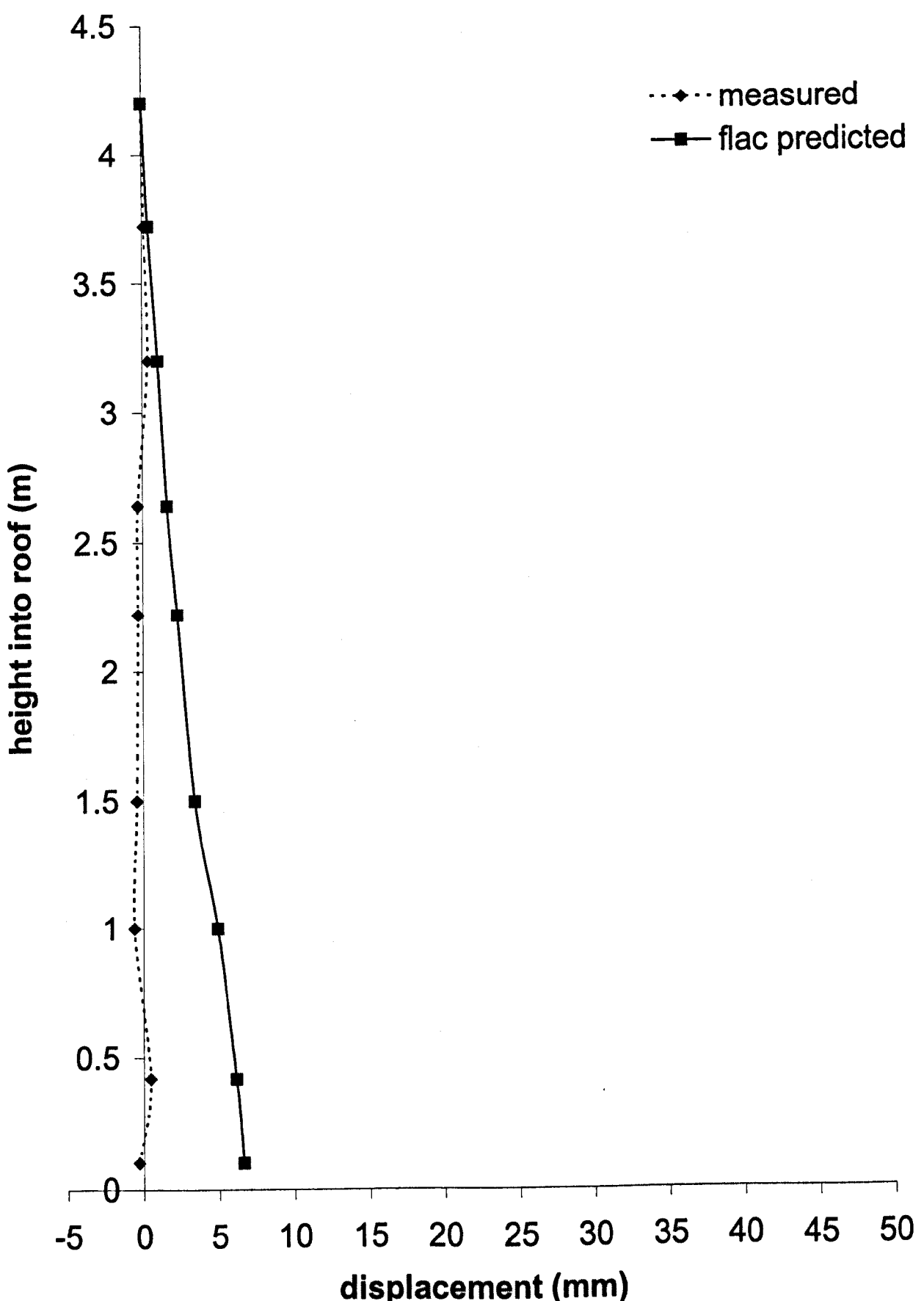


Figure 7.10 Comparison Between FLAC Prediction and Monitoring data at 31 Metre Mark, Main Gate, H478 Panel, Riccall  
266

**Riccall, H478, Main Gate, 110 Metre Mark**

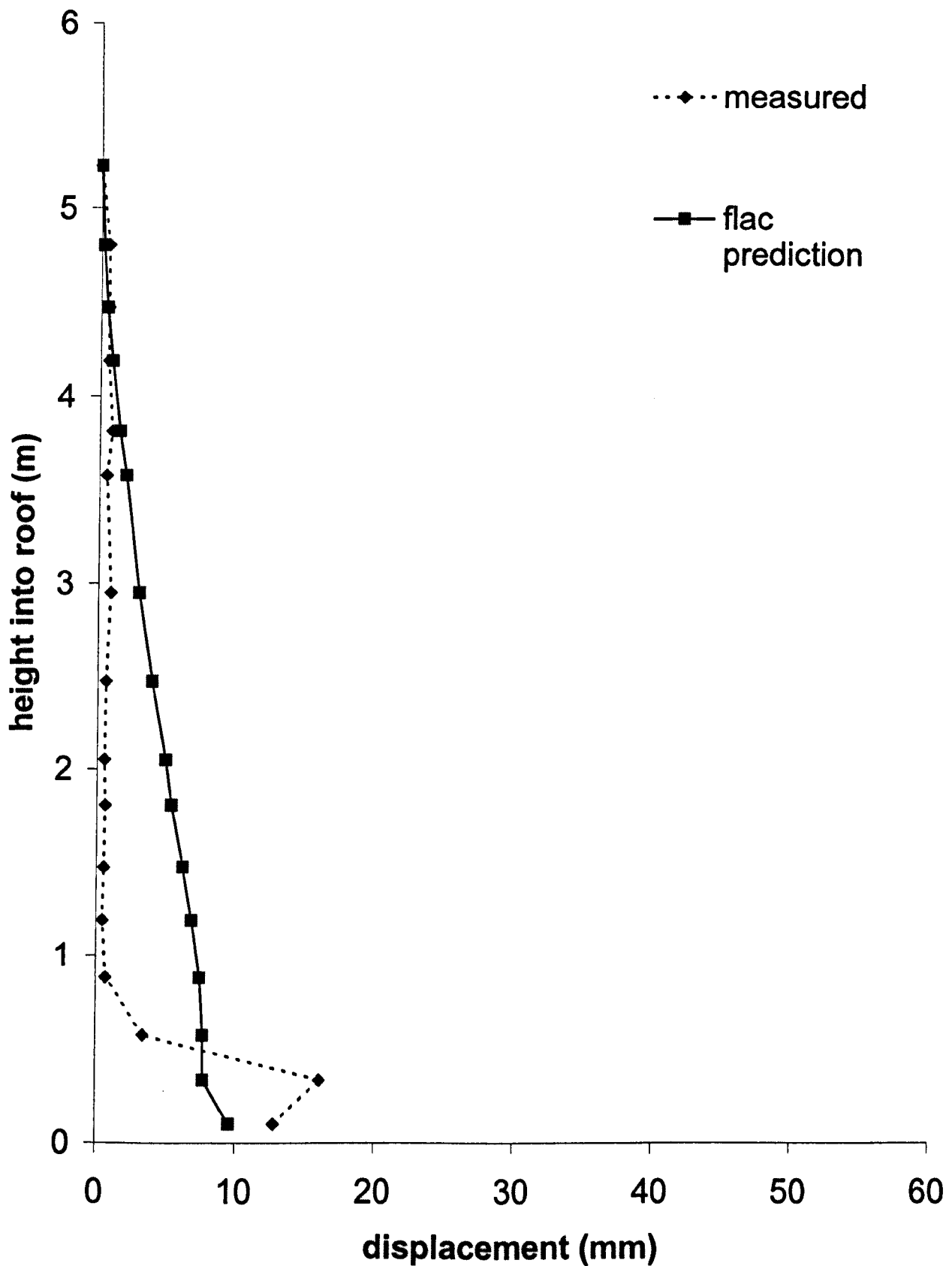


Figure 7.11 Comparison between Flac Prediction and Monitoring Data at 110 metre mark, main gate of Panel H478, Riccall

**Riccall, H478, Main Gate, 387 Metre Mark**

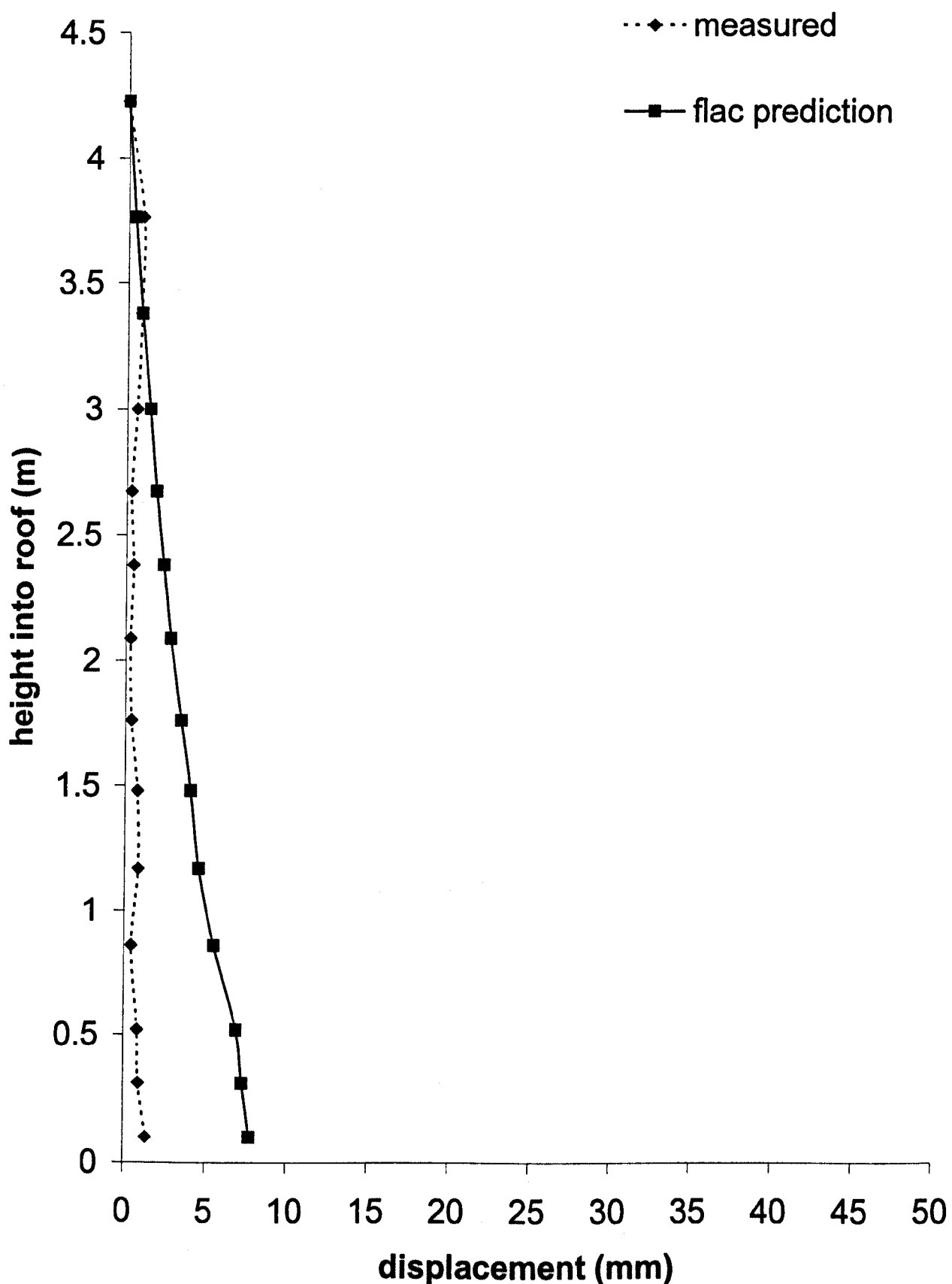


Figure 7.12 Comparison Between Flac Prediction and Monitored Roof Displacement at 387 Metre Mark, Main Gate, H478 Panel, Riccall.

**Riccall, H478, Main Gate, 486 Metre Mark**

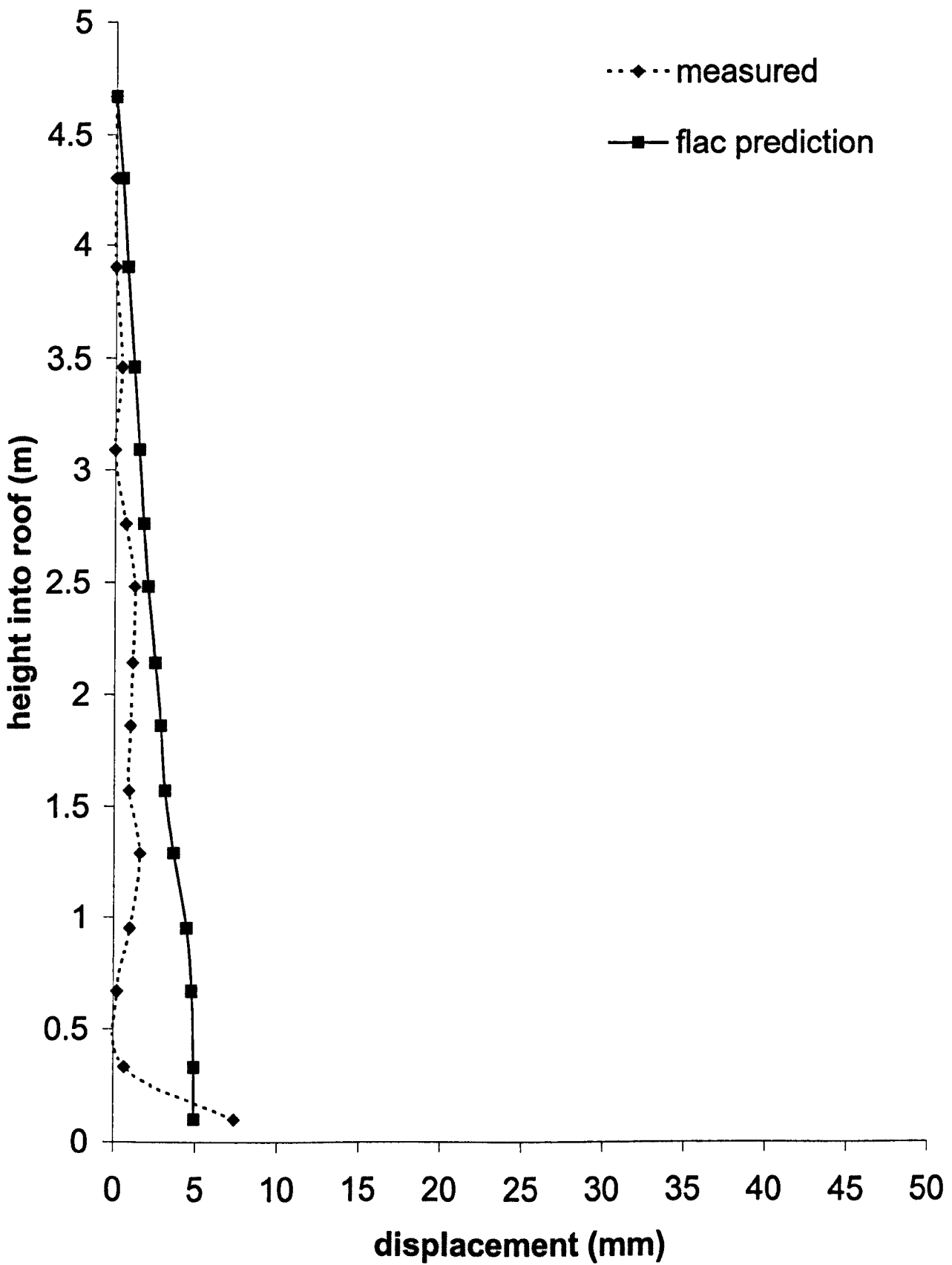


Figure 7.13 Comparison Between FLAC Prediction and Monitored Roof Displacement at 486 Metre Mark, Main Gate, H478 panel, Riccall

**Riccall, H487, Main Gate, 587 Metre Mark**

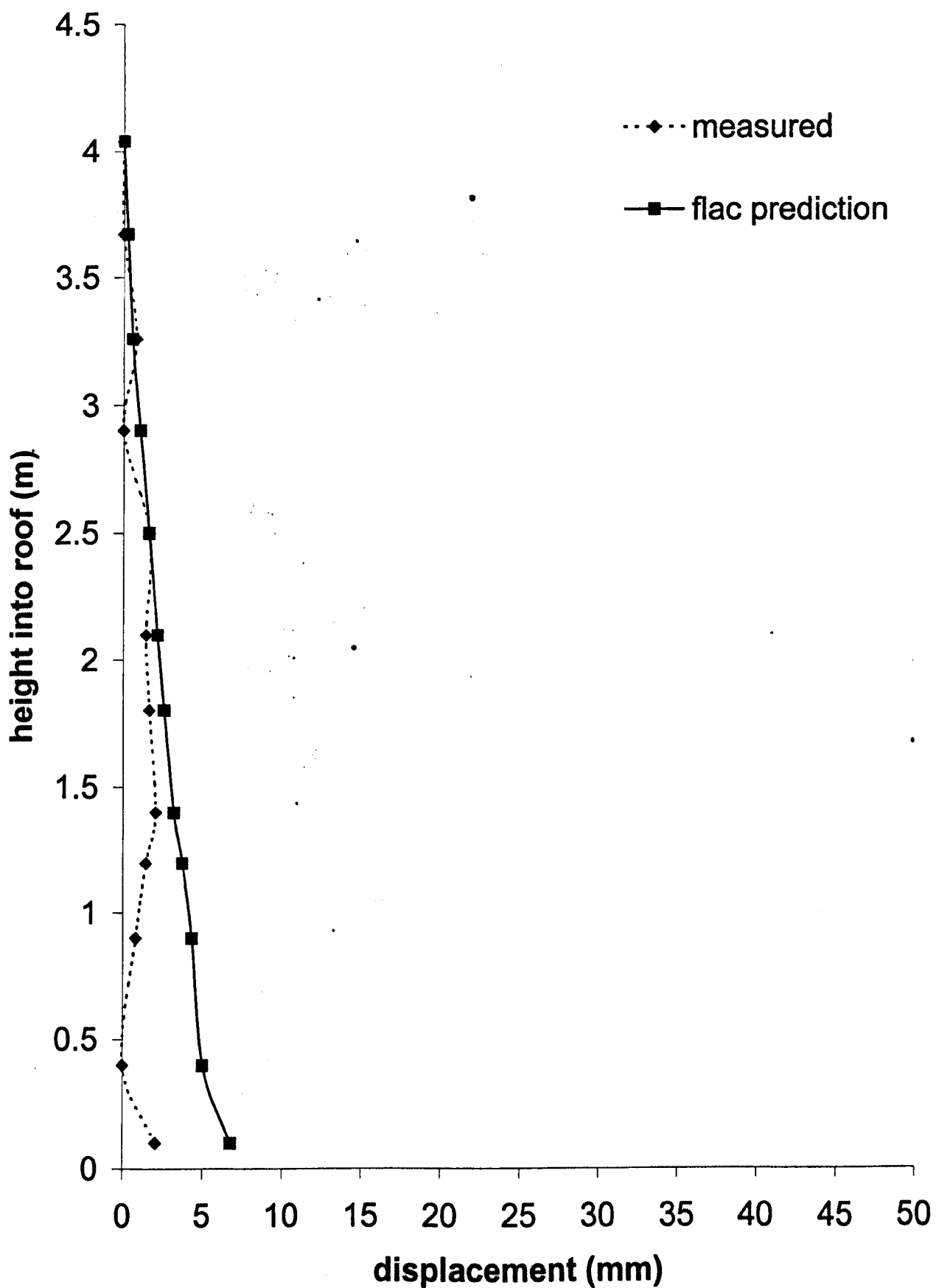


Figure 7.14 Comparison Between FLAC Prediction and Monitored Roof Displacement, 587 Metre mark, Main gate, H487 Panel, Riccall

## Riccall, H478, Main Gate, 710 Metre Mark

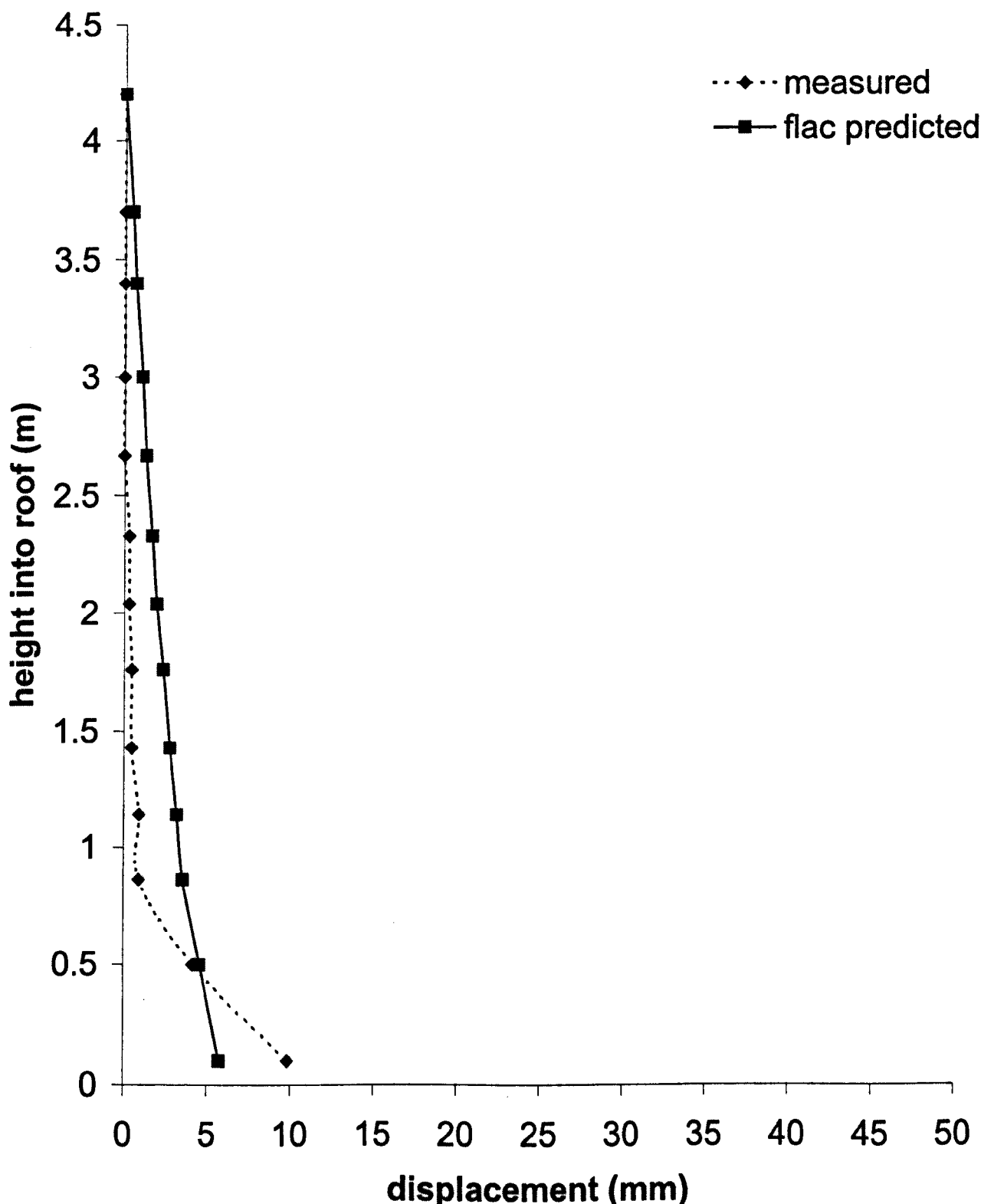


Figure 7.15 Comparison Between FLAC Prediction and Monitored Roof Displacement, 710 Metre mark, Main Gate, H478 Panel, Riccall.

**Riccall, H505, Tail Gate, 353 Metre Mark**

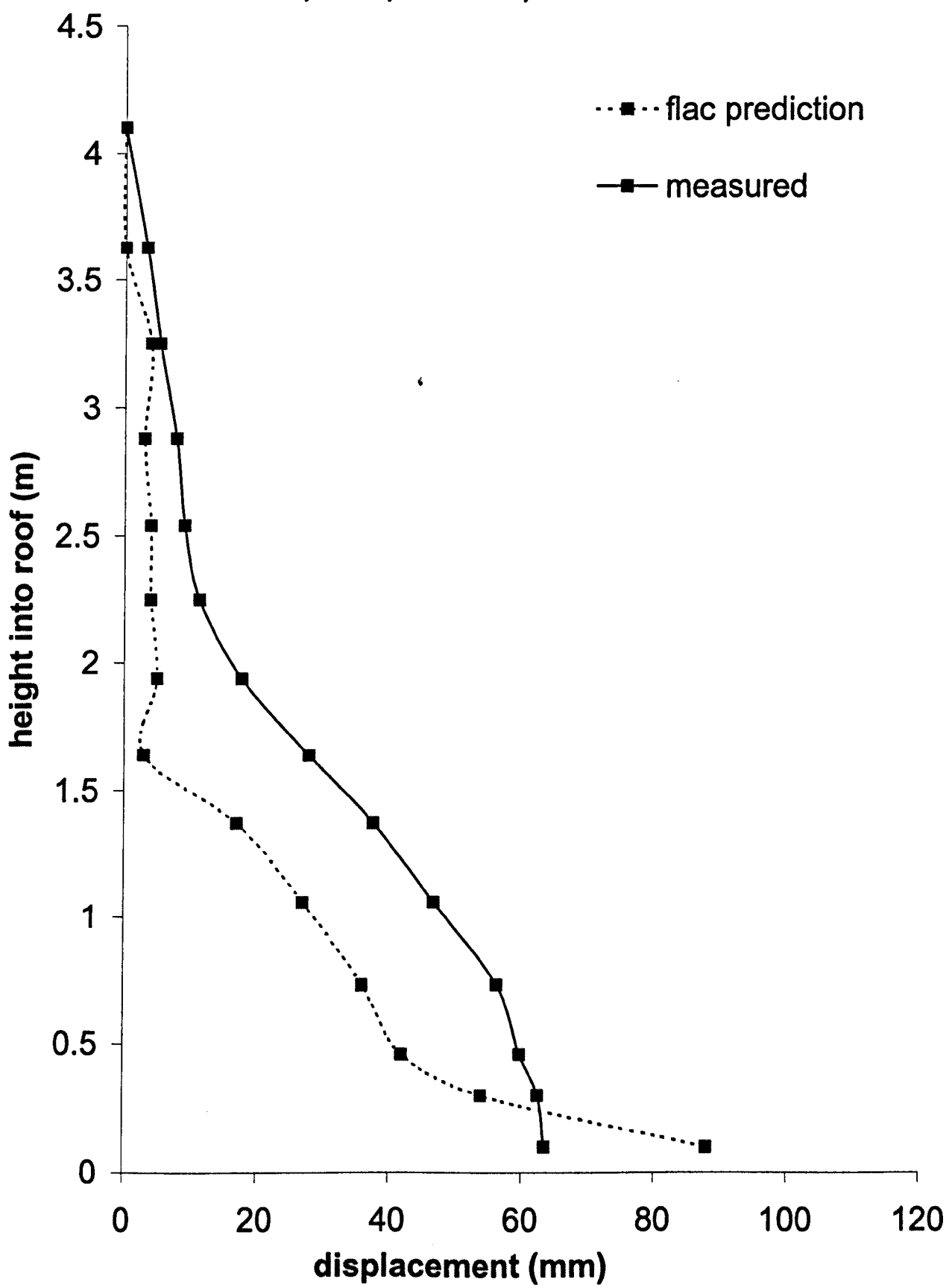


Figure 7.16 Comparison Between FLAC Prediction and Monitored Roof Displacement at 353 Metre Mark, Tail Gate, H505 Panel, Riccall

## Riccall, H505, Main Gate, 669 Metre Mark

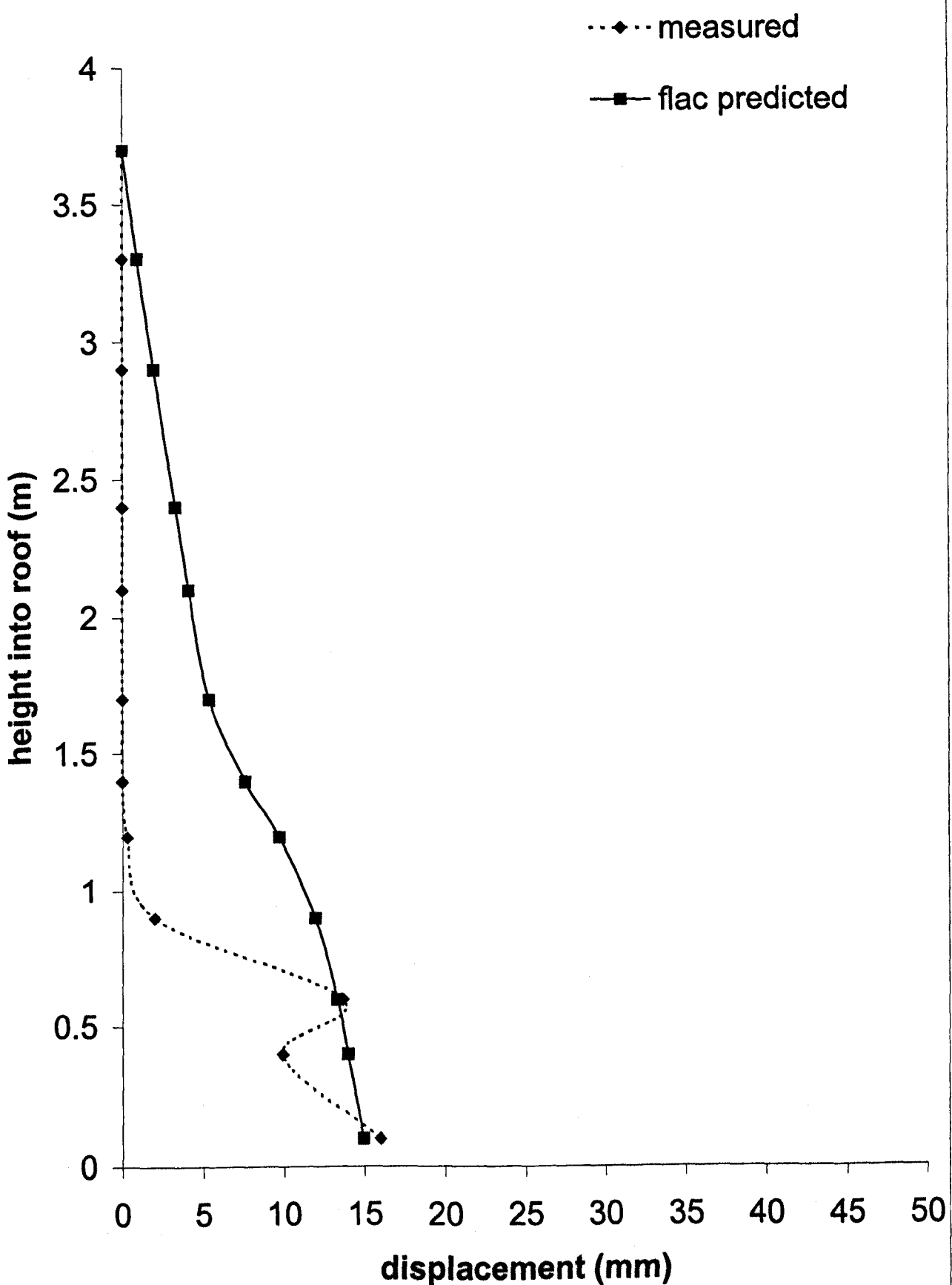


Figure 7.17 Comparison Between FLAC Prediction and Monitored Roof Displacement 669 Metre Mark, Main Gate, H505 Panel, Riccall

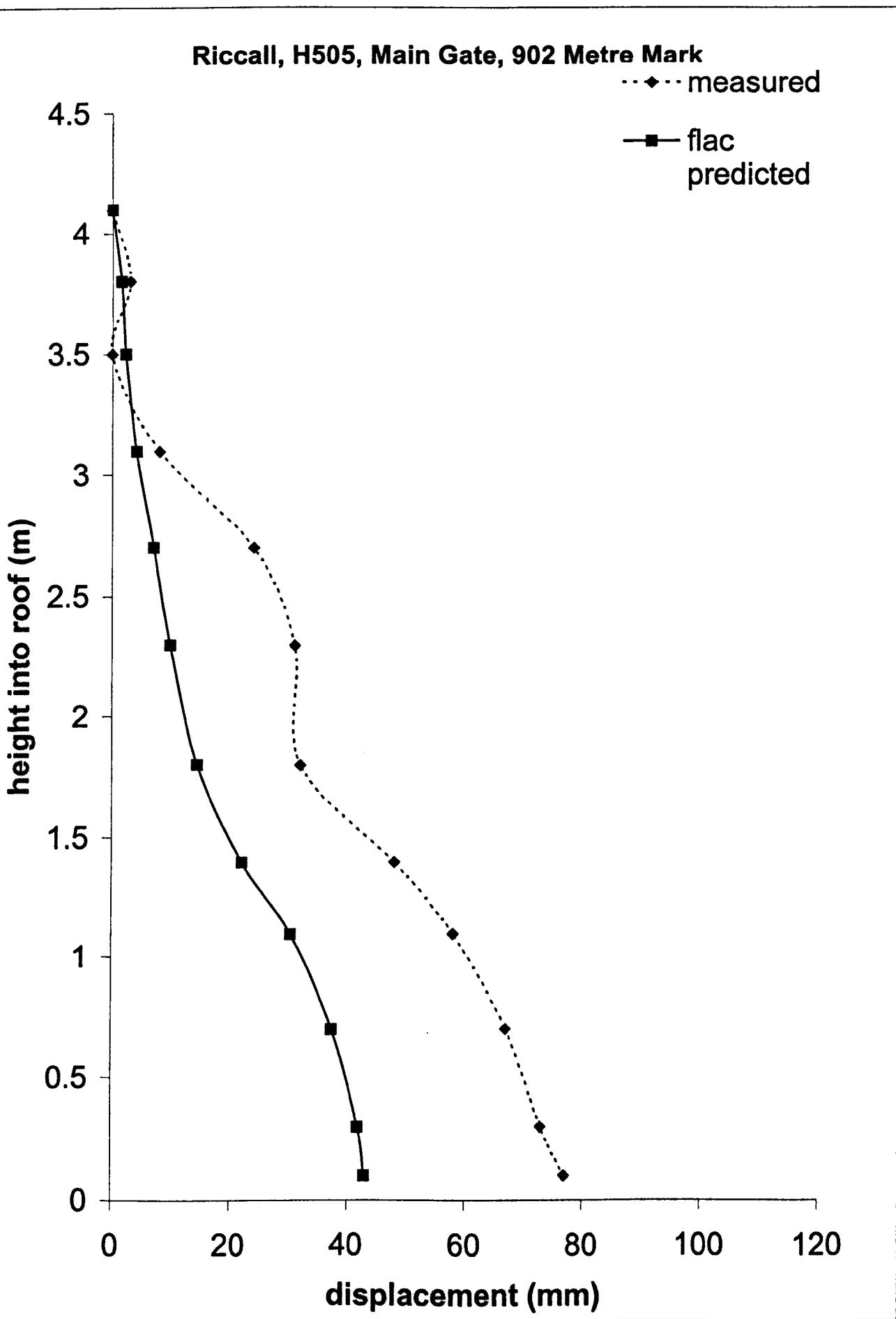


Figure 7.18 Comparison Between FLAC Prediction and Monitored Roof Displacement at 902 Metre Mark, Main Gate, H505 Panel, Riccall

### Riccall, H505, Main Gate, 1583 Metre Mark

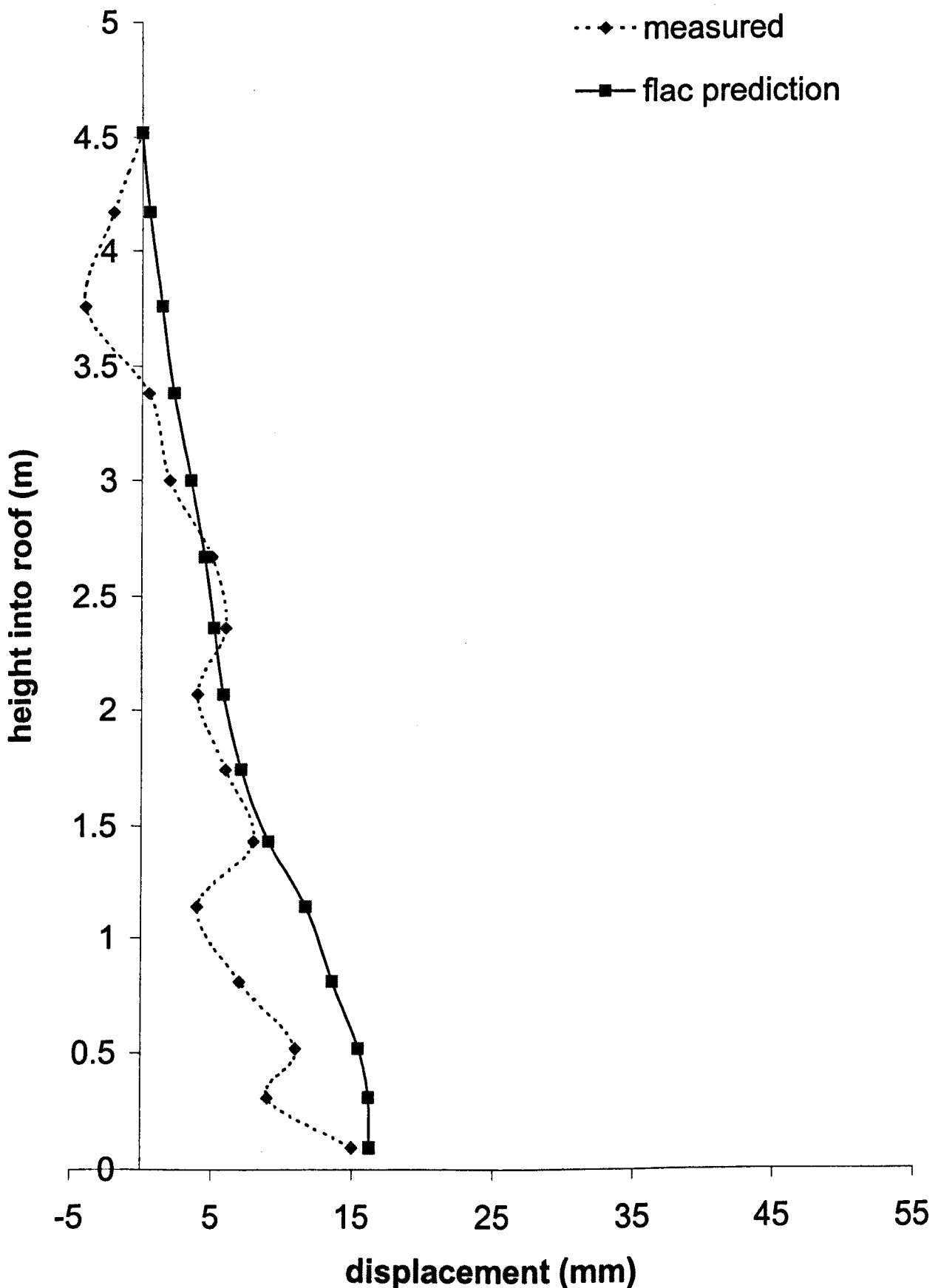


Figure 7.19 Comparison Between Flac predcition and Monitoring Data at 1583 Metre Mark, Main Gate, H505 Panel, Riccall

The FLAC simulation often predicted larger roof displacements above 1.5 meters in the immediate roof than the measured data indicates. Very low roof displacements within this region was often indicated by the monitored data with zero or 1 mm of displacement shown to have occurred in 9 out of the 11 localities (Figures 7.9, 7.10, 7.11, 7.12, 7.13, 7.14, 7.15, 7.16 and 7.17). It is considered that under the stress conditions at this locality some displacement would be expected to occur within this region. It is conjectured that the displacement occurred prior to the installation of the extensometers. This displacement may have occurred at two different stages during the development of the roadway prior to the installation of the roof extensometers. The stages are as follows:

*(1) immediately in front of the face end of the tunnel*

The displacement in the region adjacent to the face end of the tunnel excavation is dependant on the restraint provided by the side walls and the face of the tunnel itself (Hoek and Brown 1980). Initial tunnel displacement within the immediate strata is therefore influenced by the three dimensional effects from formation of the tunnel. Redistribution of in-situ stresses in front of the advancing tunnel generate displacements perpendicular to the tunnel walls. Displacement of more than 35% of the total elastic displacement may occur within the immediate strata prior to excavation. (Hanafy and Emery 1980, Brady and Brown 1993). This displacement would not be recorded on the extensometers. As the FLAC simulation was two dimensional all the strata displacement was predicted to occur after the excavation had been removed. The elastic deformation of the roof strata would be expected to be higher in the FLAC model than in that recorded by the extensometers

*(2) Displacement after the tunnel had been excavated but prior to installation of the roof extensometers.*

The rate of strata displacement is greatest immediately behind the tunnel face. Installation of the roof extensometers can occur behind the tunnel face line some time after excavation. Delays in the installation of the roof extensometers would mean that displacement especially of the immediate elastic nature would not have been recorded by the extensometers.

### 7.5.3 Numerical Modelling of Gateroads: Daw Mill Colliery, Warwickshire

The basic modelling methodology developed for the Riccall case studies was utilised for the numerical modelling of a case study site at Daw Mill Colliery. The case study location was the coal gate of panel 94 (Figure 6.33). The characteristics of the location and application of coal mine classification to the locality has been described in Section 6.3. The strength and stiffness properties for the immediate roof have been determined from the Coal Mine Classification Ratings for the immediate roof (Section 6.3.10), triaxial strength (Section 6.3.9.1) and Young's Modulus (Section 6.3.9.2) using Mitri's relationship to determine the deformation modulus and the modified Hoek Brown Failure Criterion for rock mass strength. These properties are given in Table 7.7.

Strata properties		Strata unit number									
		1	2	3	4	5	6	7	8	9	10
CMC Rating		61	37	39	36	55	62	44	37	53	62
CMCR (vert)		60	43	43	42	58	64	49	43	59	64
CMCR (horiz)		62	31	33	30	52	60	39	32	47	60
Intact Youngs Modulus (Gpa)		4	7.7	9.3	8.7	19.5	22.3	13.0	7.7	38.8	22.3
Intact UCS (MPa)		60	25	30	28	63	72	42	25	125	72
Deformation modulus (GPa)		2.7	2.3	3.1	2.5	11.2	15.5	5.3	2.3	21.2	15.2
Strength right angles to bedding	Friction (°) Cohesion (MPa) Tension (MPa)	34 2.2 0.1	27 1.1 1	29 1.2 1	28 1.2 1	37 2.1 1	39 2.8 1	33 1.5 1	27 1.1 1	42 3.4 1	39 2.8 1
Strength parallel to bedding	Friction (°) Cohesion (MPa) Tension (MPa)	34 2.4 1	24 0.9 0.1	26 1 0.1	25 1 0.1	35 1.8 0.1	38 2.5 0.1	30 1.2 0.1	24 0.9 0.1	39 2.3 0.1	38 2.5 0.1

Table 7.7 Strata Properties, Roof Strata, 94 Panel, Daw Mill

#### 7.5.3.1 Installed Roadway Supports

Within Daw Mills Panel 94 coal gate the roof was supported by seven steel 22 mm diameter 2.4 metre roof bolts installed at 1 metre intervals along the roadway. Short encapsulation pull test data was available for this gateroad and has been detailed in Section 6.3.5.1. This data was used to calculate the FLAC input parameters ( $S_{bond}$  and  $S_{friction}$ ) of the roof bolt grout/ rock interface. In order to compare the effect of estimating  $S_{bond}$  and  $S_{friction}$  using the rock mass strength and using actual pull test data  $S_{bond}$  and  $S_{friction}$  parameters were also evaluated using the method outlined for Riccall case studies in Section 7.5.2.3.6.

### 7.5.3.2 Results of Numerical Modelling

The modelled vertical displacement at intervals in the immediate roof corresponding to roof extensometer measurements, were plotted and compared with the actual roof extensometer data. The comparison is shown as Figure 7.20. Figure 7.20 shows that the FLAC simulation predicts 18 mm total roof displacement. In-situ extensometer data indicates a total vertical displacement of the immediate roof of 8 mm. However the pattern of roof displacement is similar in both cases with an increase in roof displacement predicted below approximately 2.3 m by the FLAC simulation and indicated by the monitoring data. Both the FLAC simulation and roof monitoring data indicate vertical roof displacement of approximately 9 mm between 0 and 2.3 metres height into the roof. The FLAC prediction produces a roof displacement between 2.3 metres and 7 metres height into the roof of approximately 8 mm whilst the monitoring data indicates that 0 mm displacement has incurred in this interval.

### 7.5.3.3 Sensitivity of Model to Shear Strength of Rock/Grout Bond

For the Riccall case study localities no actual in-situ test data in the form of pull test information was available for the grout/rock shear strength parameters ( $S_{fric}$  and  $S_{bond}$ ). In the FLAC modelling these parameters were evaluated from the shear strength of the rock mass adjacent to the bolts using the methodology detailed in 7.2.3.6. For the Daw Mill localities pull test data was available which allowed both the  $S_{fric}$  and  $S_{bond}$  parameters to be determined from actual test data. A further study was undertaken to compare the roof displacement using  $S_{fric}$  and  $S_{bond}$  calculated from pull test data and estimated from the rock mass strength. The results of this comparison are shown as Figure 7.21. Virtually identical displacements were obtained which tentatively indicates that  $S_{bond}$  and  $S_{fric}$  parameters may be estimated from the rock mass strength with reasonable confidence.

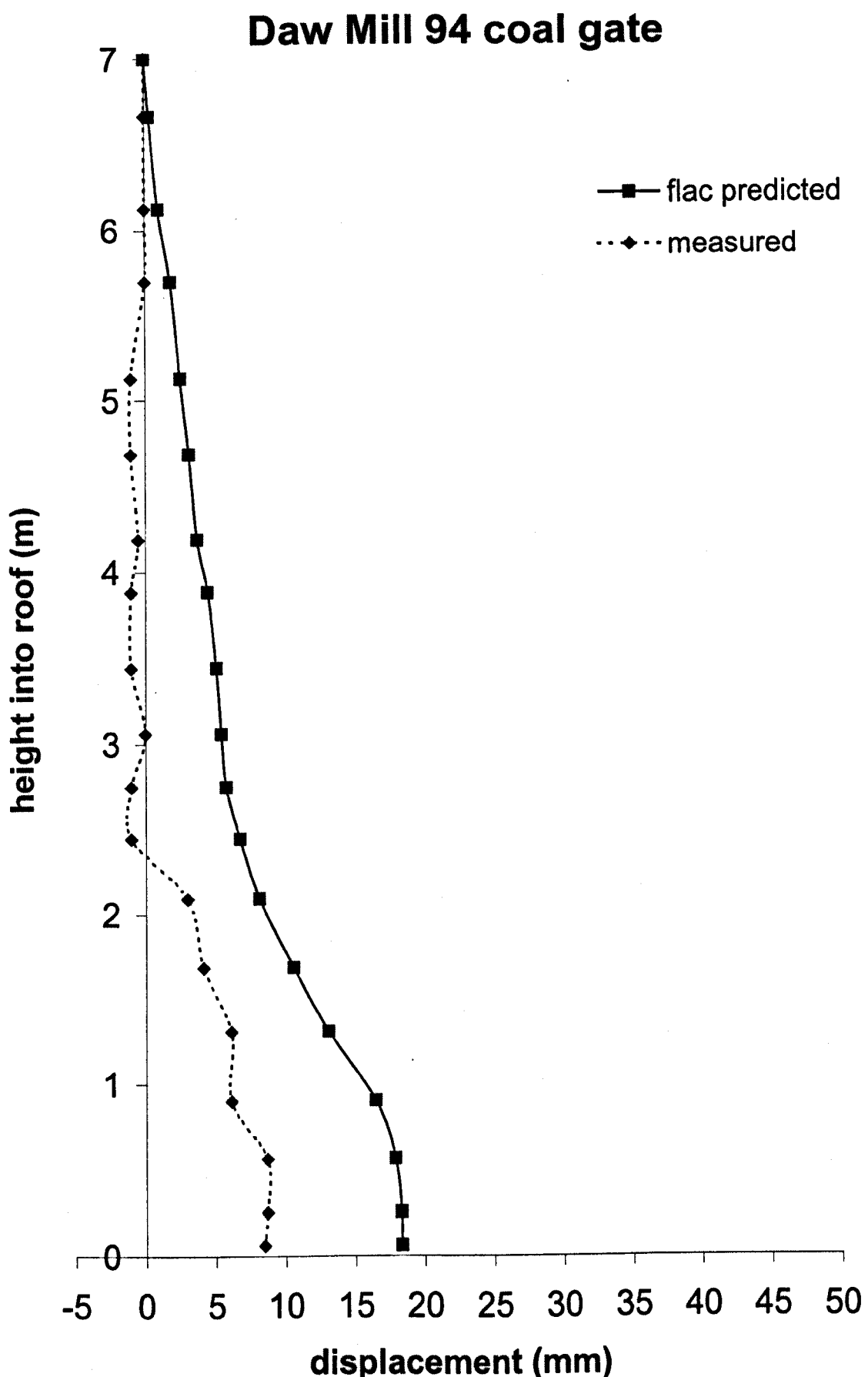


Figure 7.20 Comparison between FLAC prediction and monitored roof displacement coal gate of 94 Panel, Daw Mill

## Daw Mill 94 coal gate

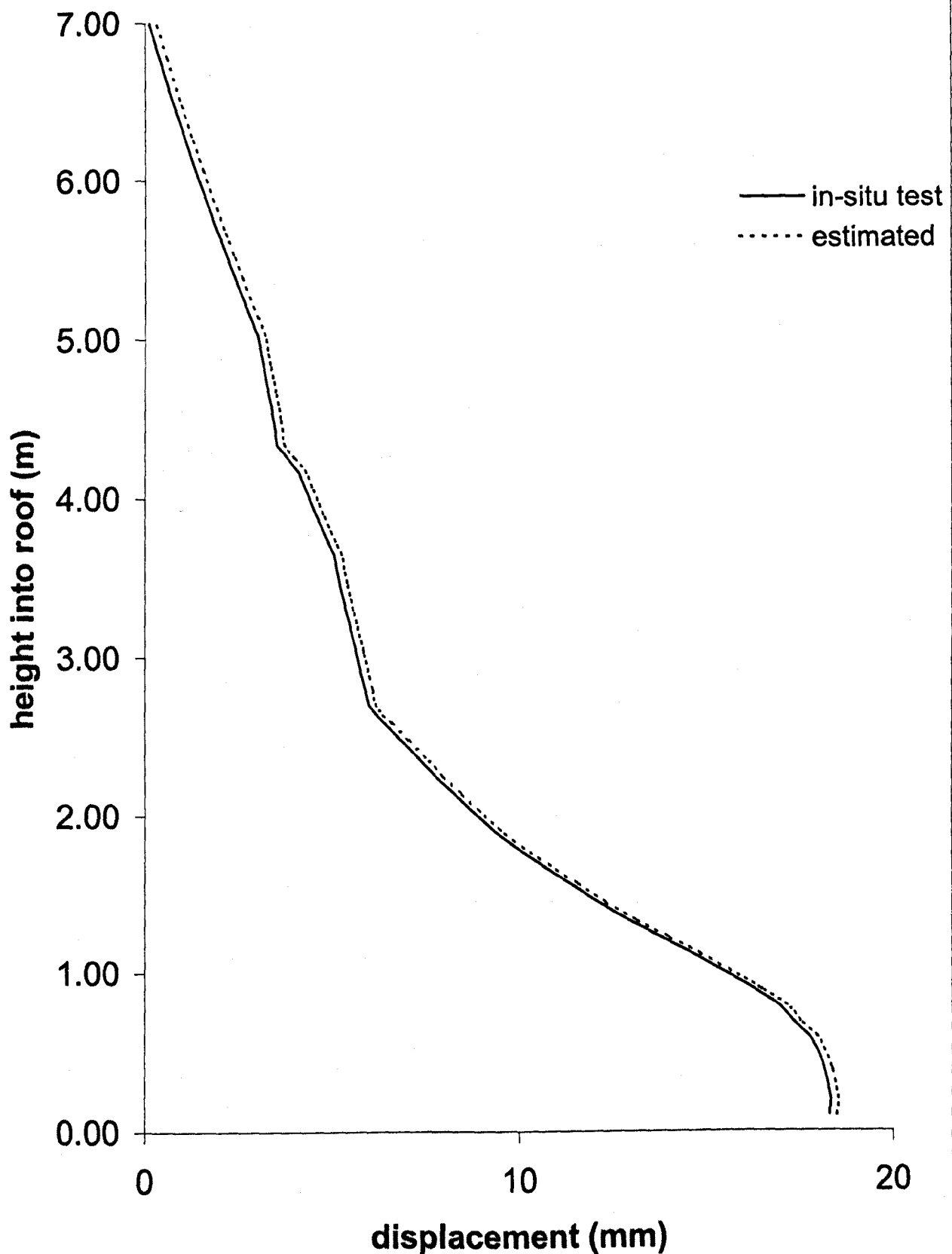


Figure 7.21 Roof Displacement coal gate of 94 Panel, Daw Mill. Roof Bolt's SFRIC and SBOND Calculated From (a) Pull Test Data and (b) Rock Mass Strength 280

## 7.5.4 Numerical Modelling of the Tail Gate, B3 Panel, Rossington Colliery, Yorkshire

### 7.5.4.1 Introduction

The immediate roof strata of B3 panel tail gate consisted of a mudstone horizon underlying a more competent siltstone. Where possible the roof was extended through the mudstone to be formed in the siltstone. However this was only possible up to approximately the 200 metre mark as the mudstone horizon increased in thickness in-bye. The amount of roof displacement was indicated by roof extensometers to increase with increasing thickness of mudstone within the immediate roof. Where the roof was formed within the siltstone horizon the amount of roof displacement was very low with only a few mm of displacement being recorded.

Three locations along the tail gate of B3 Panel were modelled. These localities were at the 24 metre mark, 408 metre mark and 594 metre mark and the Coal Mine Classifications for the identified strata units within the immediate roof, the intact strength and stiffness properties, in-situ stress conditions, installed supports and other data have been described in Chapter 6. The rock mass strength and stiffness properties have been determined by reduction from the intact properties by utilising the strata's Coal Mine Classification ratings within empirical relationships in the same manner as undertaken for the Riccall and Daw Mill case studies. The strata in-situ mass strength properties and mass stiffness properties are given in Table 7.8.

Strata properties		Strata unit number						
		1	2	3	4	5	6	7
CMC Rating		41	38	45	60	46	36	45
Anisotropic ratio		1.28	1.31	1.23	1.02	1.24	1.34	1.23
CMCR (vert)		36	33	40	60	41	31	37
CMCR (horiz)		46	43	50	60	51	41	47
Intact UCS (MPa)		43	30	56	70	67	30	52
Intact Young's Modulus (GPa)		15.2	15.2	14.6	19.1	15.2	15.2	15.2
Deformation modulus (GPa)		5.5	4.8	6.2	12.5	6.6	4.4	6.4
Strength parallel to bedding	Friction ( $\phi$ ) Cohesion (MPa) Tension (MPa)	24 0.85 0.1	22 0.85 0.1	26 1.17 0.1	32 2.45 0.1	28 1.32 0.1	21 0.82 0.1	25 1.04 0.1
Strength right angles to bedding	Friction ( $\phi$ ) Cohesion (MPa) Tension (MPa)	26 1 1	24 1 1	28 1.51 1	32 2.45 1	30 1.73 1	24 0.97 1	28 1.14 1

Table 7.8 Roof Strata Properties, B3 Panel, Rossington

#### **7.5.4.2 Modelling of B3 Panel, Main Gate, 24 Metre Mark**

At this location the immediate roadway roof was formed entirely within the more competent siltstone horizon. A FLAC model was constructed using the data described in Section 6.4 and rock mass strata properties selected from Table 7.8. The model was run for 20,000 steps.

The comparison between the simulated roof extensometer determined from the FLAC model and the roof extensometer monitoring data is shown as Figure 7.22. The simulated extensometer predicts approximately 13 mm total roof deformation whilst the monitoring data indicates approximately 2 mm total deformation. The small amount of displacement measured by the extensometer indicates little limited plastic deformation of the roof strata and that the roof displacement would occur as elastic deformation. This is also predicted by the FLAC simulation where shear strain within the roof was calculated to be less than 10mm/m (Figure 7.23). It is conjectured that the majority of the elastic strain within the roof would have occurred in front of the excavation or prior to the installation of the extensometer in the manner described in Section 7.5.2.2.3.

#### **7.5.4.3 Modelling of B3 Panel, Main Gate, 408 Metre Mark.**

At the 408 metre mark the immediate roadway roof consisted of 1.2 metres of mudstone which was overlain by the more competent siltstone horizon. Rock mass strata properties were selected from Table 7.8 to allow construction of the immediate roof within the model. The model was then run for 20,000 steps.

The comparison between the simulated roof extensometer determined from the FLAC model and the roof extensometer monitoring data is shown as Figure 7.24. The simulated extensometer predicts approximately 19 mm total roof deformation whilst the monitoring data indicates approximately 22 mm total deformation. The strain within the roof is shown to increase below approximately 1.6 metres in both the prediction and actual case, representing the change from the more competent siltstone to the less competent mudstone. The FLAC model predicts that a total of approximately 11mm of vertical displacement occurs between 1.6 metres and 7 metres depth into the roof whilst the monitored data indicates less than 2mm displacement. This again may be attributed to the elastic deformation occurring prior

## Rossington B3 main gate 24 metre mark

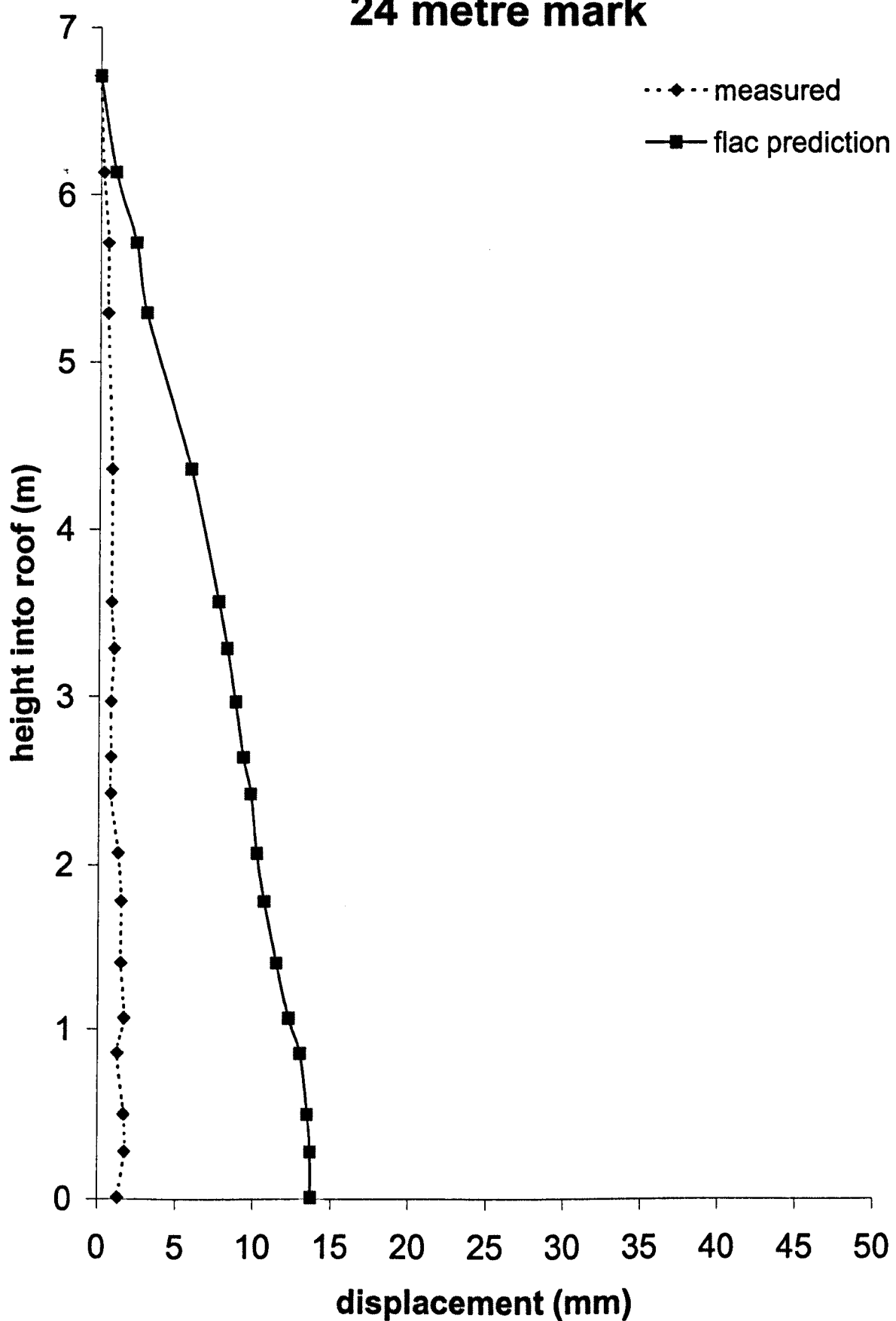


Figure 7.22 Comparison Between FLAC prediction and Monitored Roof Displacement at 24 Metre Mark, Main gate, B3 Panel, Rossington

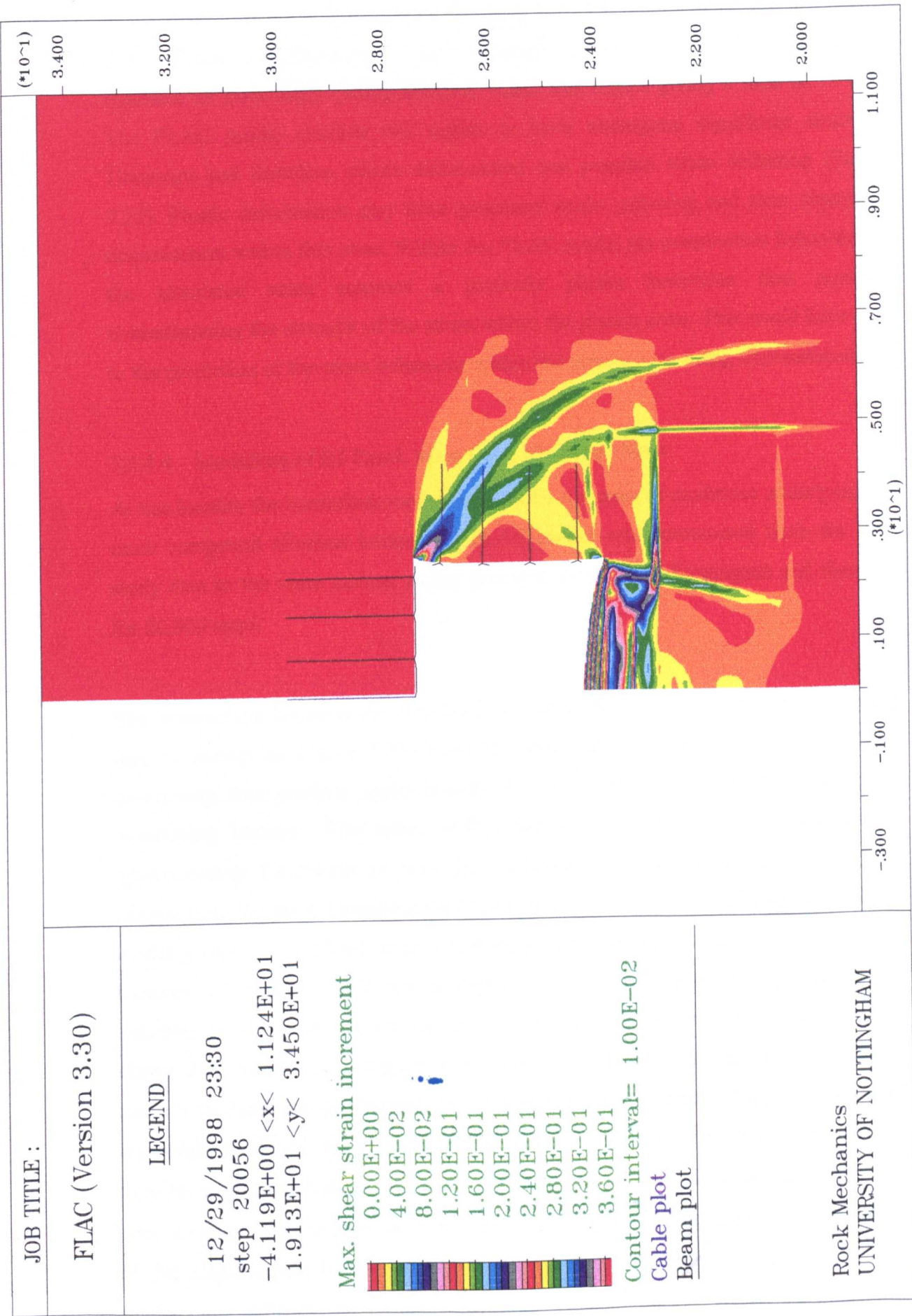


Figure 7.23 Predicted Shear Strains 24 mm, Main Gate, B3 Panel, Rossington (Shear Strain Intervals 10mm/m)

to installation of the extensometers. Between 0 to 1.6 metres depth the monitoring data indicates a displacement of approximately 20 mm whilst the FLAC prediction indicates an extra 8mm of displacement within this region giving a total of 18 mm. The FLAC model predicts this region to have undergone significant strain ( $> 10\text{mm/m}$ ) and therefore plastic deformation and possible strain softening (Figure 7.25). Plastic deformation may have generated strain softening and time dependant displacement within this zone. Within the FLAC model the constitutive behaviour of the simulated strata assumes a perfectly plastic behaviour thus possibly overestimating the strength of the strata within the plastic zone. This could have lead to the prediction of the strata behaviour within the plastic zone being underestimated.

#### 7.5.4.4 Modelling of B3 Panel, Main Gate, 594 Metre Mark

At this locality the immediate roof consisted of 1.6 metres of mudstone underlying the more competent siltstone horizon. A FLAC model was constructed from the case study data in the same manner as the previous localities at Rossington and then run for 20,000 steps.

The comparison between the simulated roof and the roof extensometer monitoring data is shown as Figure 7.26. Both the simulated extensometer and the actual monitoring data predicts approximately 42 mm total roof deformation within the monitoring horizon. The strain within the roof is shown to increase below approximately 1.8 metres in both the predicted and actual case, representing the change from the more competent siltstone to the less competent mudstone. The FLAC model predicts that a total of approximately 11mm of vertical displacement occurs between 1.8 metres and 7 metres depth into the roof whilst the monitored data indicates no displacement within this region. This again may be attributed to the elastic deformation occurring prior to installation of the extensometers. Between 0 and 1.8 m depth the monitoring data indicates a displacement of approximately 42 mm whilst the FLAC prediction indicates 31mm of displacement. Plastic deformation may have generated strain softening and time dependant displacement within this zone which was not incorporated into the FLAC model leading to an underestimation of the displacement by the model. Plastic deformation within the immediate roof mudstone is indicated by the degree of measured displacement within the mudstone.

## Rossington B3 main gate 408 metre mark

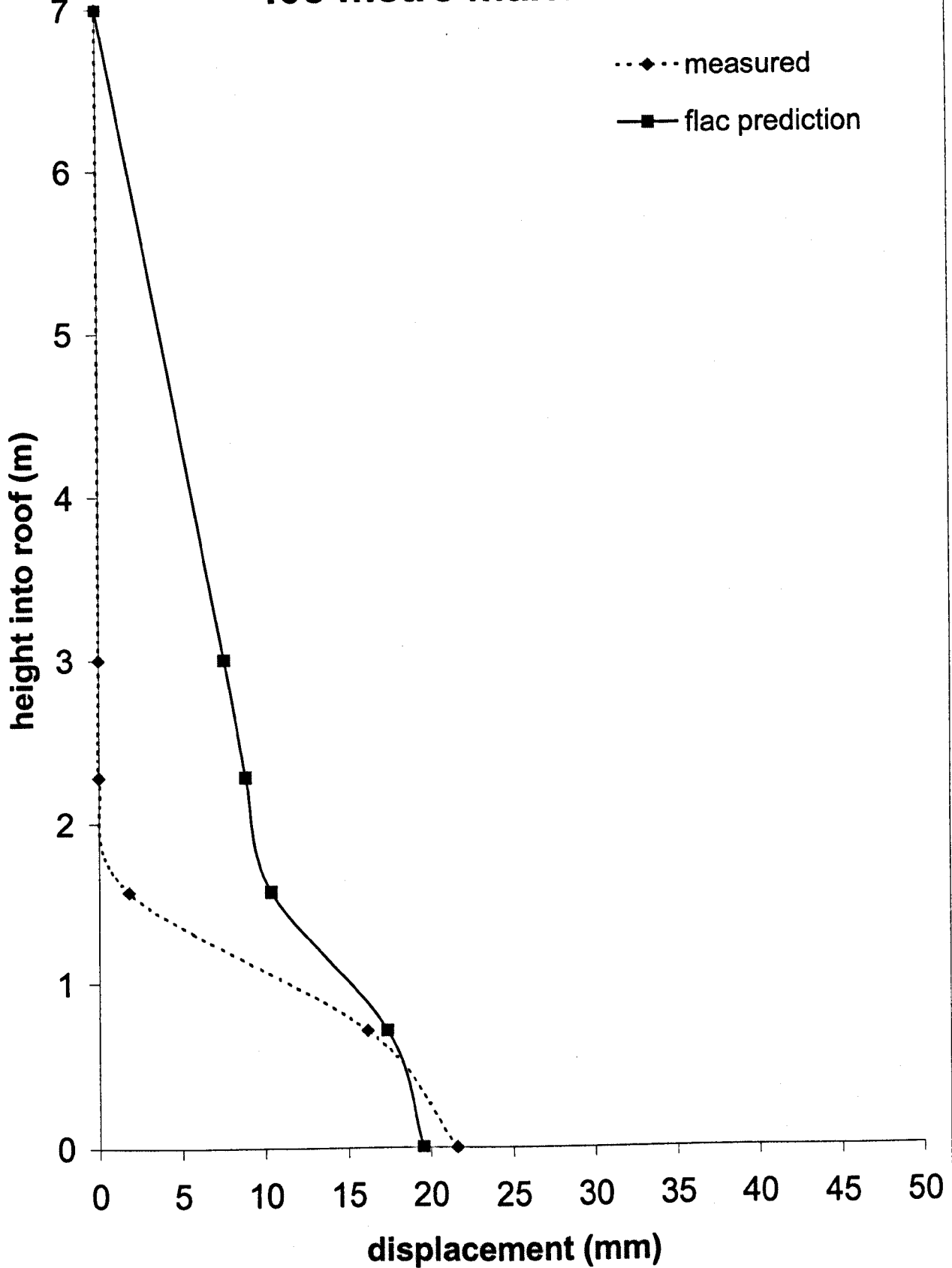


Figure 7.24 Comparison Between FLAC Prediction and Monitored Roof Displacement at 408 Metre Mark, Main gate, B3 Panel, Rossington

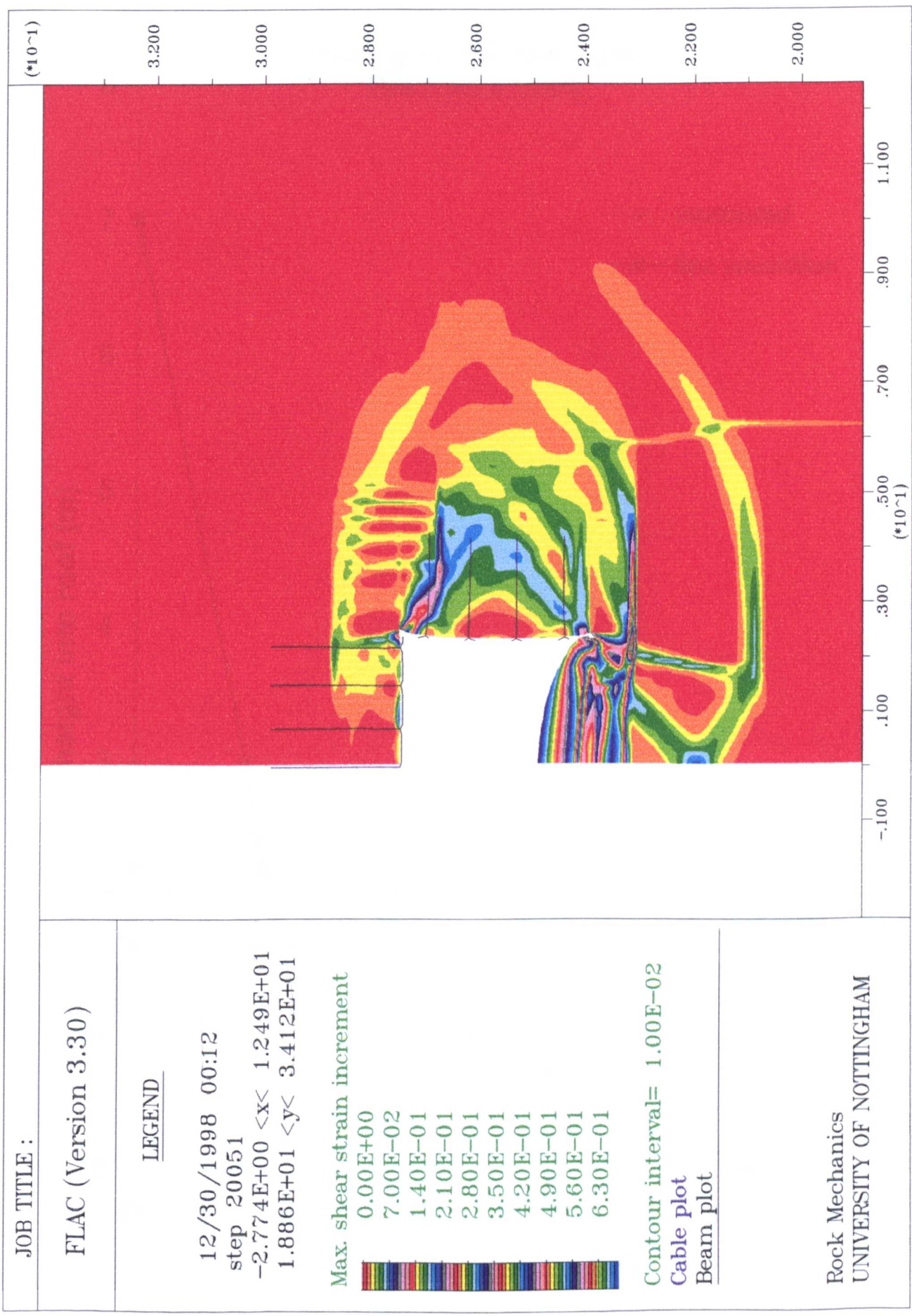


Figure 7.25 Predicted Shear Strains 408 mm, Main Gate, B3 Panel, Rossington (Shear Strain Intervals 10mm/m)

**Rossington B3 main gate  
594 metre mark**

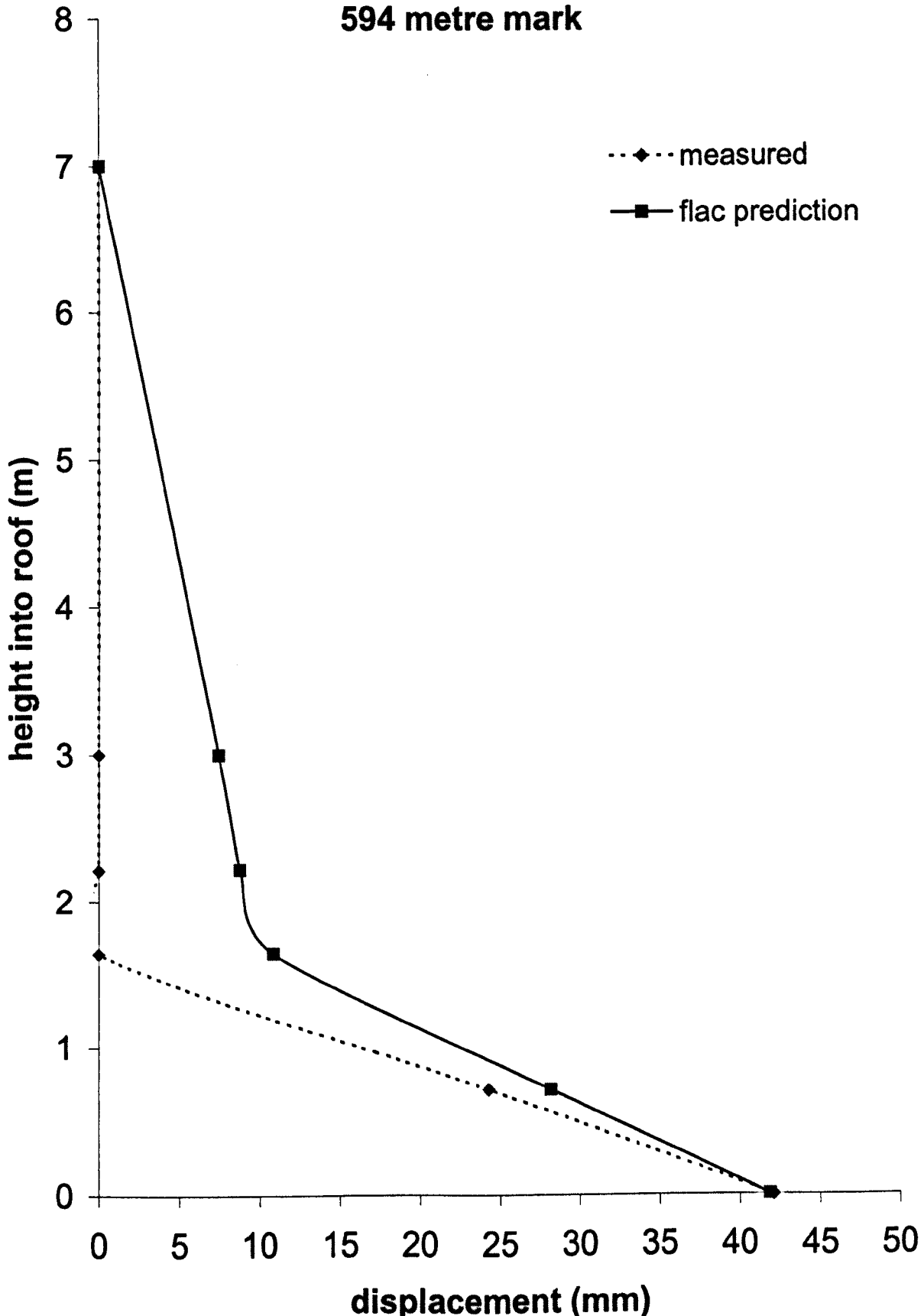


Figure 7.26 Comparison Between FLAC Prediction and Monitored Roof Displacement at 594 Metre mark, Main Gate, B3 Panel, Rossington

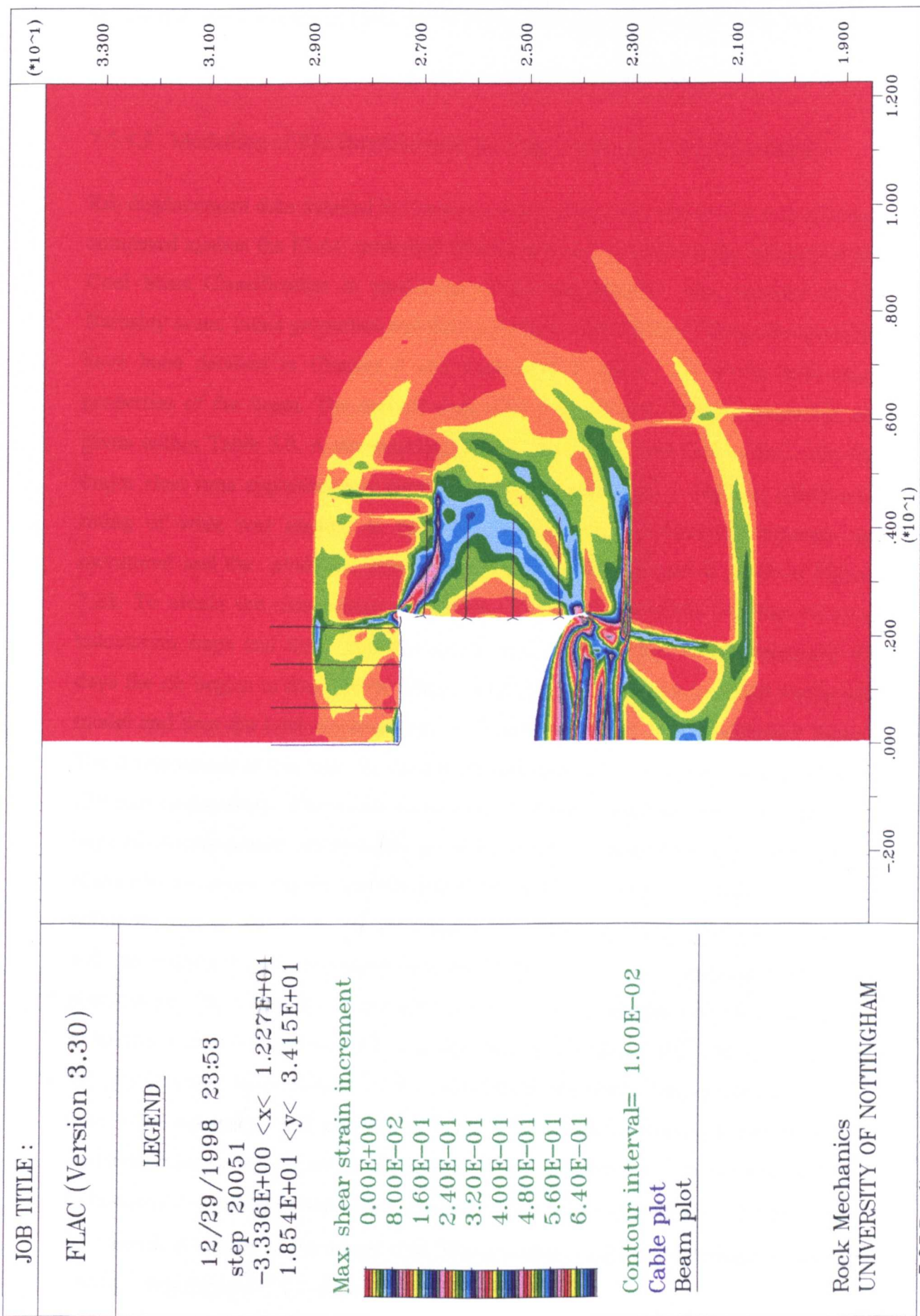


Figure 7.27 Predicted Shear Strains 594 mm, Main Gate, B3 Panel, Rossington (Shear Strain Intervals 10mm/m)

The FLAC model also predicts plastic behaviour within the mudstone. The extent of the plastic zone determined from the FLAC modelling is shown as Figure 7.27.

#### 7.5.4.5 Modelling of Rib Displacement, B3 Panel, Main Gate, 24 Metre Mark.

Rib displacement data detailed in Section 6.4 and shown as Figure 6.47 and 6.48 was compared against the FLAC modelled rib displacement to evaluate the efficacy of the Coal Mine Classification in predicting ribside deformation. The structure of the Barnsley seam, intact properties and the Coal Mine Classification Rating for the seam have been detailed in Chapter 6 and were used to derive the in-situ rock mass properties of the Seam. The derived rock mass strength and stiffness properties are given within Table 7.9. A characteristic of the seam within the gate roads is that the major cleat runs approximately parallel to the gateroads thus a negative adjustment rating of what was applied to the CMC Ratings. The comparison between the monitored and the predicted time related total rib displacement is given in Figure 7.28. To obtain the comparison a tentative correlation was made between FLAC's calculation steps and time. The monitoring data indicates that at approximately 60 days the rib begins to displace by creep. Creep behavior was not included within the model and thus the total displacement at 60 days was taken as a comparison figure. The displacement at this time for the left rib and right rib was approximately 160 and 130 mm respectively. The initial FLAC run predicted approximately 100 mm. The large rib displacements are probably a manifestation of extensive plastic deformation of the rib side strata. This is also illustrated by the high shear strain predicted to occur within the ribs by the FLAC model (Figure 7.23). The difference between the model and the monitoring displacements can be attributed to strain softening within the plastic zone. The orientation of the cleat in relation to the rib sides has been identified as having a large influence on rib side deformation (Holmes 1982) and the extent of the plastic zone. Reevaluation of the orientation adjustment ratings within the rib sides was undertaken and the models rerun. The predicted displacements with the readjusted ratings are shown as Adjustment B and Adjustment C within Figure 7.28. Adjustment C prediction indicates a rib displacement of approximately 150mm at 60 days which is similar to the actual data. The orientation adjustment ratings for the rib sides for Adjustment C are shown as Figure 7.29.

### Rossington B3 main gate 24 metre mark; rib displacement

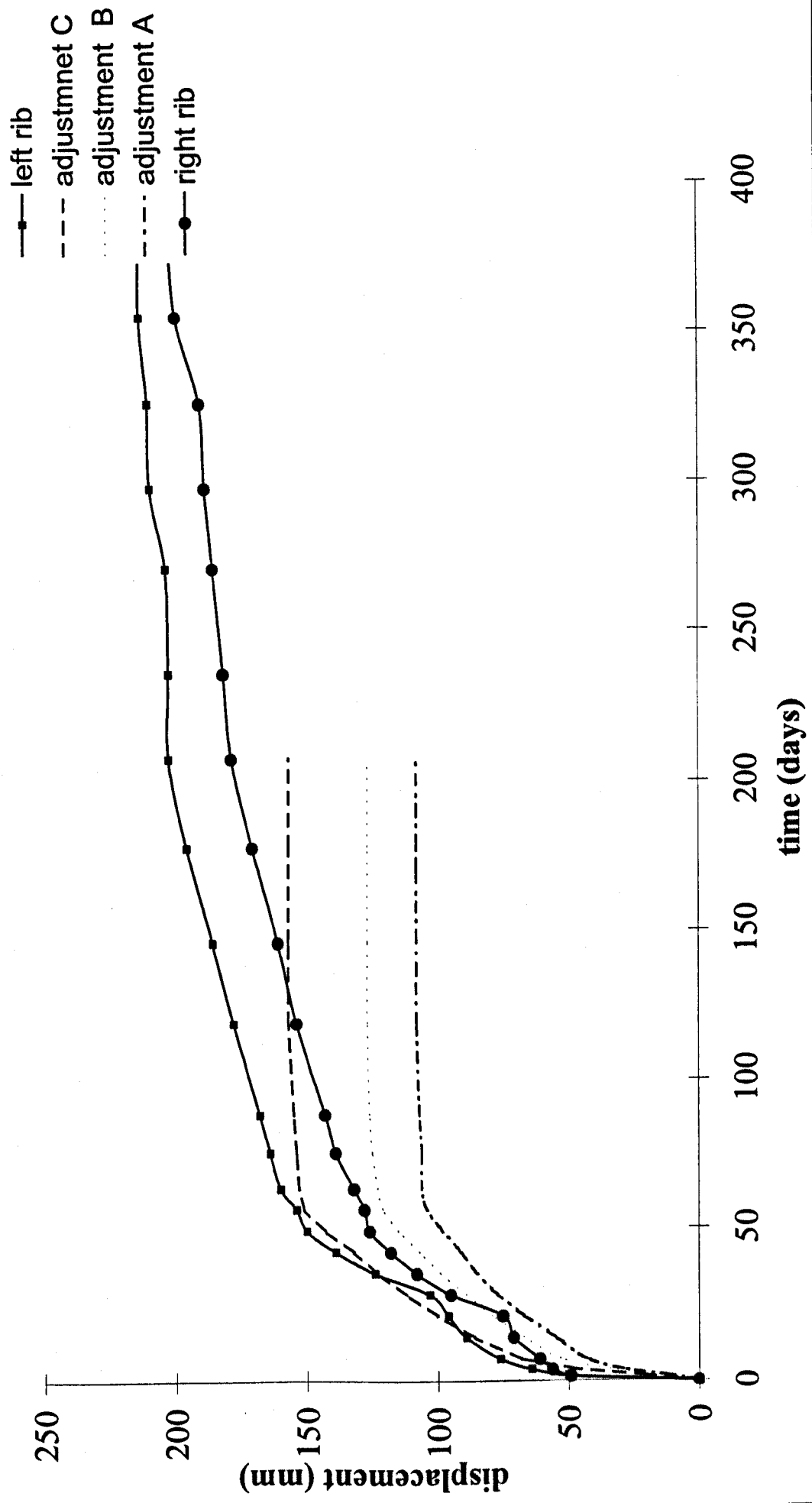


Figure 7.28 Comparison Between FLAC Prediction and Monitored Rib Displacement at 24 Metre Mark, Main Gate, B3 Panel, Rossington.

Strata Properties		Strata Unit Number					
		1	2	3	4	5	6
Unadjusted CMC Rating		45	52	43	52	43	52
Cleat/joint adjustment rating		-14	-24	-14	-24	-14	-24
Adjusted CMC Rating		31	28	29	28	29	28
Anisotropic ratio		1	0.61	1	0.61	1	0.61
CMCR (vert)		31	35	29	35	29	35
CMCR (horiz)		31	21	29	21	29	21
Intact UCS (MPa)		30	40	20	40	20	40
Intact Young's Modulus (GPa)		15.2	8.3	15.2	8.3	15.2	8.3
Deformation modulus (GPa)		3.3	1.5	2.9	1.5	2.9	1.5
Strength parallel to bedding	Friction (°)	26	25	25	25	25	25
	Cohesion (Mpa)	1.2	1.37	1.1	1.37	1.1	1.37
	Tension (GPa)	1	1	1	1	1	1
Strength right angles bedding	Friction (°)	26	24	25	24	25	24
	Cohesion (MPa)	1.2	1.18	1.1	1.18	1.1	1.18
	Tension (GPa)	0.1	0.1	0.1	0.1	0.1	0.1

Table 7.9 Strata properties, Coal Ribs, B3 Panel, Rossington (Barnsley Seam)

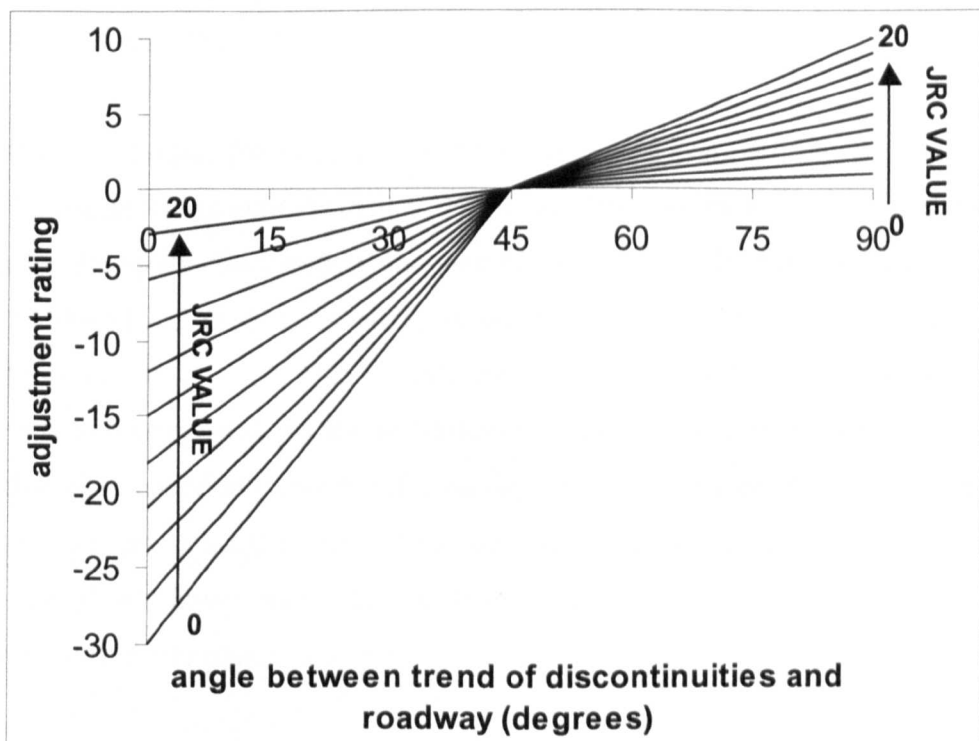


Figure 7.29 Revised orientation adjustment ratings for rib side strata

#### **7.5.4.6 Modelling of Rib Displacement in B3 Panel, Main Gate, 415 Metre Mark.**

The revised adjustment ratings were applied to the unadjusted Coal Mine Classification Ratings for rib side strata at this locality and the strength and stiffness properties calculated (Table 7.9) The comparison between the monitored total rib side displacement and the modelled displacement is shown as Figure 7.30. The FLAC model indicates that displacement ceases at approximately 75 days with a predicted total displacement of approximately 160 mm. The monitored data indicates that after 75 days the left rib has displaced approximately 150 mm and the right rib approximately 200 mm. Figure 7.30 illustrates that the time-displacement curve predicted by FLAC is similar to the monitoring data.

## **7.6 CONCLUSIONS**

The Fast Lagrangian Analysis of Continua (FLAC) method was utilised for the computer modelling of the case study localities described within Chapter 6.

FLAC's ubiquitous joint constitutive model was utilised to best represent the behaviour of the Coal Measure strata. The engineering properties of the strata were determined from the Coal Mine Classification ratings in conjunction with the intact properties of the strata.

The computer models for each case study locality was compared to the monitoring data. The comparisons indicate that the FLAC models provide a reasonable method of predicting the strata deformation characteristics of the rock strata. It was however observed the FLAC prediction tended to over predict the deformation of the upper part of the immediate roof. This is attributed to the initial elastic deformation of the roof strata occurring prior to the installation of the roof extensometers. The FLAC prediction also tended to under predict the degree of deformation occurring within the lower part of the immediate roof. This was attributed to strain softening occurring within the plastic lower roof. The constitutive model used assumes the material to behave as a perfectly plastic material.

### Rossington B3 main gate 415 metre mark; rib displacement

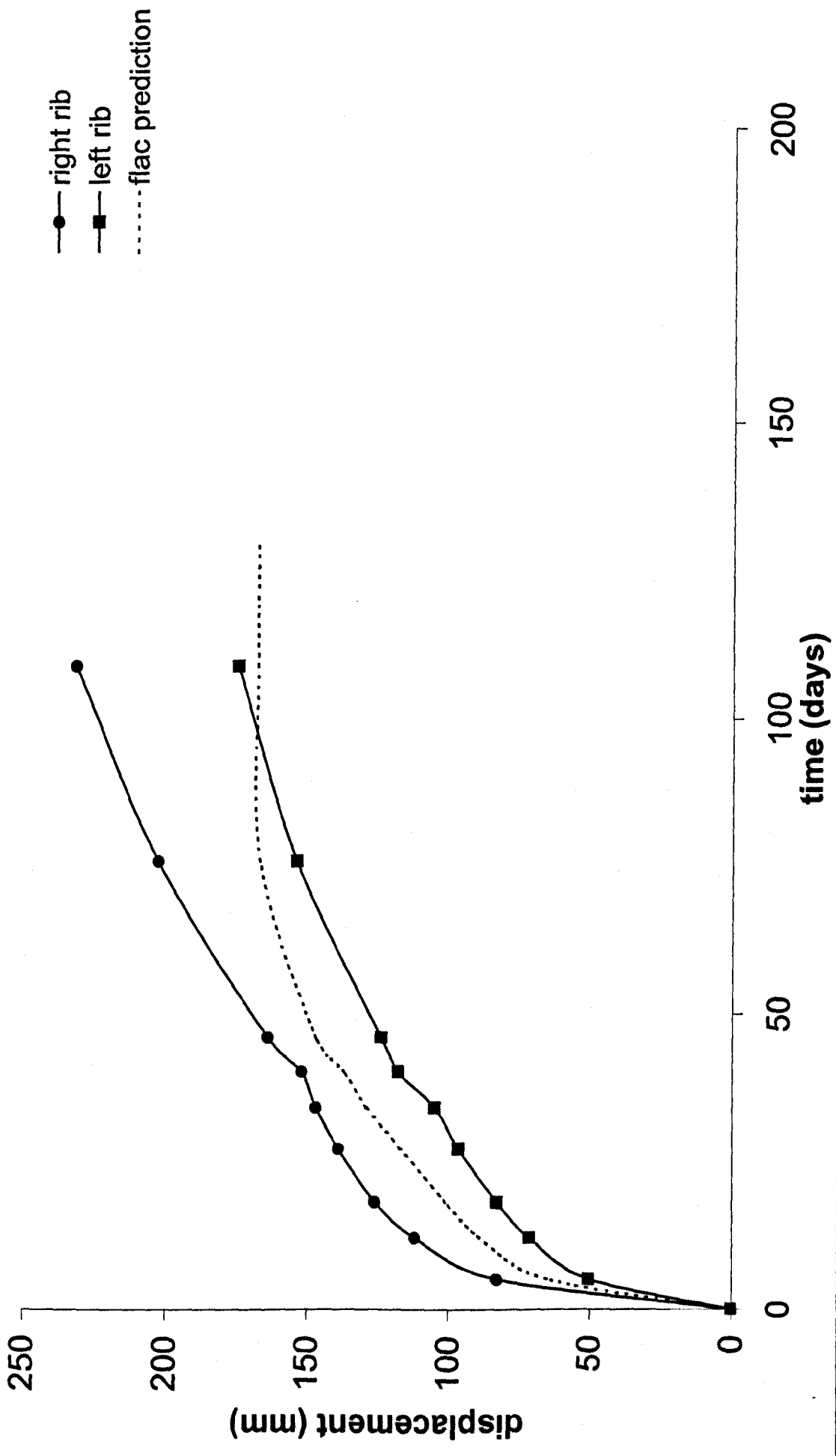


Figure 7.30 Comparison Between FLAC Prediction and Monitored Rib Displacement at 415 Metre Mark, Main gate, B3 Panel, Rossington

## **CHAPTER 8**

### **GENERAL CONCLUSIONS AND RECOMMENDATIONS**

In this final chapter the conclusions from each of the earlier chapters are summarised and recommendations for future work that would usefully progress this field of research are suggested.

#### **8.1 GENERAL CONCLUSIONS**

Chapter 2 describes the geological history of the UK Coal Measures and details how the typical characteristic features of the coal measures are a product of its depositional, diagenetic and post diagenetic history. The chapter highlighted the fact that the Coal Measures typically consist of mudstones, siltstones and sandstones with lesser amounts of coal laterally extensive but vertically variable. Internal horizontal features such as bedding, laminations and fissility are mainly due to depositional and diagenetic processes whilst the nearer vertical inclined features, such as faults and joints are usually due to post diagenetic process associated with periods of compression and of tensional tectonic activity.

Chapter 3 described typical methods of mining within the UK. This chapter describes how new zones of stress are generated due to the redistribution of the in-situ stresses upon extraction of the mining excavations. The chapter also describes how the interaction between the redistributed stress field and the rock strata leads to the deformation and failure of the rock strata. The chapter highlights, by reviewing the typical mechanism of failure and deformation recorded to occur around coal mine excavations, the importance of the geological characteristics on the affect of the mechanisms of deformation and failure and consequently on the stability of coal mine excavations. It was found that the mechanisms can be logically divided into those that occur in the roof, the rib or the floor of a coal mine excavation. The chapter also revealed that the selection of rock reinforcement is dependant on the geological conditions and that fully grouted rock bolts have been identified as the most suitable bolt type for coal measure strata.

The engineering properties of the coal measure strata are determined by the strength and stiffness of the intact rock, and the nature, orientation and frequency of planes of weakness present within the strata. These planes of weakness included both

horizontally inclined features such as bedding and laminations and more vertically inclined features such as joints.

In order to be able to characterise rock masses in terms of the likely engineering behaviour rock mass classification systems have been developed and empirically validated. There have been many rock mass classifications that have been developed for a wide variety of different uses. Whilst several have been developed for classifying coal measure rock types none have been developed for the specific use of predicting the strength and stiffness properties of coal measure rock strata.

Chapter 5 describes the development of a rock mass classification for characterising the engineering properties of coal measure strata found within UK coal mines. This proposed classification has been named the Coal Mine Classification. It was observed that during the review of deformation mechanisms of the rock strata that typically occurred within UK coal mines that the mechanisms that occurred were dependant on the structural characteristic of the rock strata. The construction of conceptual mechanisms of strata behaviour was used as a basis of determining the key parameters for the Coal Mine Classification. The key parameters that would be incorporated within the Coal Mine Classification were identified using a systematic approach. This approach included exhaustive listings of all parameters used in existing rock mass classifications and then assessment of the importance of each of these parameters by assessing their significance to the conceptual mechanism of strata deformation. To account for the significance of parameters previously identified as having a significant effect on behaviour of coal measure rock types an assessment of the parameters used in previous classifications developed for coal measure strata was undertaken. To account for any lithological and structural properties that may be significant to the engineering properties of the strata but not previously identified the lithological and structural characteristics of the strata were taken into consideration.

The identified parameters were synthesised and the following key parameters were identified:

- Unconfined Compressive Strength
- Bedding/ Lamination Properties
  - Spacing
  - Strength
- Joint Properties
  - Set Number
  - Spacing
  - Orientation
  - Strength
- Fissility
- Water Flow
- Moisture Sensitivity

A provisional assessment of the relative importance weightings and ratings was undertaken using a systematic approach based on their assessed significance to the conceptual mechanisms of deformation and failure. These ratings have been produced as a series of tables and charts that allow the evaluation of the individual parameter ratings.

The conceptual mechanism of failure and deformation indicated that there was a difference in strata properties both perpendicular and parallel to bedding. The anisotropic nature of the coal measure strata was accounted for by the incorporation into the classification of separate ratings for the strata properties both parallel to and perpendicular to bedding,

Case study data was collected for Riccall, Daw Mill and Rossington mines in order to apply and validate the Coal Mine Classification. Whilst deriving the Coal Mine Classifications ratings for the case study localities it was observed that several of the structural parameters that have been identified as significantly influencing the strata deformation were not routinely measured by the mines geotechnical staff.

Coal Mine Classification ratings were derived from individual strata units identified from either rock cores taken from the immediate roof strata for the Riccall mine or from geotechnical logs of rock cores taken from the immediate roof strata for the Daw Mill and Rossington mine sites. The Coal Mine Classification Ratings were found to

vary between 38 and 93 with the majority of the ratings lying between 40 and 60. The ratings appeared to be lithology dependant with ratings of approximately 40 or less typically determined for a weak, dark grey, fissile mudstone and ratings of 60 or greater being derived typically for moderately strong to very strong, pale grey laminated siltstones and sandstones.

In order to validate the Coal Mine Classification as a means of predicting strata properties the finite difference numerical modelling technique was utilised. Commercially available software known as FLAC was used to model the strata deformation at the case study localities. Roof extensometer data was provided and enabled a comparison to be undertaken between the actual roof deformation and the roof deformation predicted by the model. The engineering properties of the rock strata were determined from the Coal Mine Classification Rating.

A disadvantage in numerical modelling of the coal mine roadways was that the required input parameters for each model was very extensive. Apart from the engineering properties of the rock strata a knowledge of the in-situ stress, size and shape of the excavation, the amount and properties of installed supports and an assessment of the effect on the in-situ stress field of mining interactions are all required.

The most suitable constitutive model of strata behaviour was assessed, evaluated and selected so that the in-situ behaviour of the rock strata could be representatively simulated. A ubiquitous joint material model was utilised as this would allow strata yielding and the incorporation of anisotropic behaviour.

The detailed FLAC model simulations for the case study localities provided a reasonable prediction of the roof strata deformation as indicated by comparisons between the in-situ roof extensometers measurements and the FLAC simulation. It was however observed that the FLAC prediction tended to over predict the deformation of the upper part of the immediate roof. This may be attributed to the initial immediate elastic deformation of the roof strata occurring prior to the installation of the roof extensometers. The FLAC prediction also tended to under predict the amount of deformation occurring within the lower part of the immediate roof. This may be attributed to strain softening occurring within the plastic lower roof.

## **8.2 RECOMMENDATIONS FOR FUTURE STUDIES**

This research describes the initial development of a rock mass classification that was proposed for use in predicting the engineering properties of Coal Measure rock types. This work included an initial validation of the Coal Mine Classification on case study localities at three different mine sites and provides a basis for further validation work to prove the efficacy of the classification. Rock mass classification systems are empirically established and the effectiveness of the classification is in part due to parameters and structure of the classification and in part a function of the number of case studies that the classification has been validated on.

It is considered that further case study validation would be desirable with preferably a wide range of strata and mining conditions. For instance all the case studies described in this thesis the mine localities were all dry and therefore the groundwater and moisture sensitivity parameters require further validation. Further adjustment of the proposed parameter ratings may therefore be required.

This research has also highlighted that the joint and cleating structure of the strata are not recorded as part of the geotechnical appraisal. These parameters have been identified as having an important effect on strata deformation. It is therefore recommended that structural mapping should be incorporated into the geotechnical appraisal of a roadway.

### *Numerical modelling*

The FLAC modelling of the roadways localities within the Riccall, Daw Mill and Rossington mines have identified aspects of the modelling techniques where further development will be required.

The FLAC simulations often predicted larger roof displacements above 1.5 metres in the immediate roof than the measured roof displacements. This may be due to displacement occurring within the roof prior to the installation of the extensometers. Such displacements may have occurred within the strata in front of the face end of the roadway or within the strata after the roadway has been excavated but prior to the installation of the extensometers. It is recommended that further work investigating these aspects be carried out. It is envisaged this work would be best undertaken using

a 3-D numerical modelling methodology to allow the 3-D effects associated with the face ends of the roadways to be simulated.

The FLAC prediction also tended to under predict the degree of deformations occurring within the lower part of the immediate roof. This may be attributed to strain softening occurring within the plasticised immediate roof. The constitutive model that was utilised for the FLAC modelling for this research was a perfectly plastic model. This model was chosen in order to remove the requirement of determining post peak stress strain relationship of the in-situ strata. Incorporating strain softening within the FLAC model is therefore recommended. In order to conduct this further work an evaluation of the constitutive behaviour of the post peak in-situ strata behaviour would be required

## REFERENCES

Afrouz A.A. (1992) "Practical Handbook of Rock Mass Classification Systems and Modes for Ground Failure", Published by CRC Press.

Amadei B. and Savage W.Z. (1989) "Anisotropic Nature of Jointed Rock Mass Strength", A.S.C.E. Journal of Engineering Mechanics, Vol.115, No.3, pp525 to 542.

Amadei B. (1996) "Importance of Anisotropy When Estimating and Measuring In-Situ Stresses in Rock", International Journal of Rock Mechanics, Mining Science and Geomechanical Abstracts, Vol.33, No.3, pp293 to 325.

Anderton R., Bridges P.H., Leeder M.R. and Sellwood B.W. (1979) "A Dynamic Stratigraphy of The British Isles", Published by George Allen and Unwin, ISBN 0-04-551028-8.

Anonymous (Geological Society Engineering Group Working Party) (1970) "The Logging of Rock Cores for Engineering Purposes", Quarterly Journal of Engineering Geology, Vol.3, pp 1 to 24.

Barton N, Lein R and Lunde J. (1974) "Analysis of Rock Mass Quality and Support Practice in Tunneling, and a Guide for Estimating Support Requirements", Internal report, Norges Geotekniste Institutt, pp 1 to 74.

Bell F.G. (1986) "A Review of the Engineering Behavior of Soils and Rock with Respect to Groundwater", in Proceedings of Groundwater in Engineering Geology Conference, held by Geological Society of London, Engineering Group, pp1 to 23.

Bell F.G. (editor) (1987) "Ground Engineers Reference Book", published by Butterworths

Bell F.G, Entwistle D.C. and Culshaw M.G. (1997) "A Geotechnical Survey of Some British Coal Measure Mudstones with Particular Emphasis on Durability", Engineering Geology, Vol. 46, pp115 to 129.

Bieniawski Z.T. (1974) "Geomechanics Classification of Rock Masses and its Application to Tunneling", Proceedings of the 3<sup>rd</sup> International Congress on Rock Mechanics, ISRM, Denver, Vol. II A, pp27 to 32.

Bieniawski Z.T. (1975) "The Point Load Test in Engineering Practice", Engineering Geology Vol. 9, pp1 to 11.

Bieniawski Z.T. (1976) "Rock Mass Classification in Rock Engineering", Proceedings of the Symposium on Exploration for Rock Engineering, Johannesburg, AA Balkema, Vol.1, pp97 to 106.

Bieniawski Z.T. (1978) "Determining Rock Mass Deformability-Experience from Case Histories", International Journal of Rock Mechanics, Mining Science and Geomechanics Abstracts, Vol. 15, pp237 to 247.

Bieniawski Z.T. (1982) "Improved Design of Room and Pillar Coal Mines for U.S. Conditions", Proceedings 1<sup>st</sup> International Conference on Stability in Underground Mining, pp19 to 47.

Bieniawski Z.T. (1989) "Engineering Rock Mass Classification: A Complete Manual for Engineers and Geologists in Mining, Civil and Petroleum Engineering", Published by John Wiley and Sons, ISBN 0-471-60172-1

Bieniawski Z.T. and Kalamaras G.S. (1993) "Determination of the In-Situ Strength of a Coal Seam Based on Coal Strata Stratification", Proceedings 11<sup>th</sup> Annual Workshop, Generic Mineral Technology Centre, Mine Systems Design and Ground Control, Alabama, pp 3 to 14.

Bigby D.N., Cassie J.W. and Ledger A.R. (1992) "Absolute Stress and Stress Change Measurements in British Coal Measures", ISRM Symposium: Eurock '92, Ed by Hudson J.A., Published by Thomas Telford, pp 390 to 395.

Bigby D.N. (1997) "Developments in British Rockbolting Technology" in Coal International, pp111 to 116.

Bikerman D.J. and Mahtab M.A. (1986) "Use and Abuse of RQD in Underground Mine Design", Proceedings of Mining Latin America Conference, Chile, Published by IMM London, pp51 to 56.

Bowden A.J, Lamont-Black J. and Ullyott S. (1998) "Point Load Testing of Weak Rock with Particular Reference to Chalk", Quarterly Journal of Engineering Geology, Vol. 31, Part 2, pp95 to 103.

Brady B.H.G. and Brown E.T. (1993) "Rock Mechanics for Underground Mining" 2<sup>nd</sup> Edition, published by Chapman and Hall, London, ISBN 0-412-47550-2.

Branch D. (1987) "Study of Mine Tunnel Stability with Reference to Stress Conditions and Deformational Response of Associated Carboniferous Rocks", PhD Thesis, University of Nottingham.

Brereton N.R. and Evans C.J. (1987) "Rock Stress Orientations in the United Kingdom from Borehole Breakouts", British Geological Survey Report RG 87/14.

Bridges M.C. (1976) "Presentation of Fracture Data for Rock Mechanics", 2<sup>nd</sup> Australian-New Zealand Conference on Geomechanics, pp144 to 148.

Broch E. and Franklin J.A. (1972) "The Point Load Strength Test", International Journal of Rock Mechanics and Mining Science, Vol.9, pp669 to 697.

British Standards Institution, BS 5930 (1981) "Site Investigations"

British Standards Institution, BS 7861 (1996) "Strata Reinforcement Support System Components Used in Coal Mines"

Buddery P.S and Oldroyd D.C. (1992) "Development of a Roof and Floor Classification Applicable to Collieries" ISRM Eurock'92, Ed. by Hudson, J.A. Published by Thomas Telford. Chapt. 35, pp197 to 202.

Bush D.D. and Meyer B.S. (1988) "In-Situ Stress Magnitude Dependency on Lithology", Key Questions in Rock Mechanics, Published By Balkema, pp 729 to 730.

Carter B.J., Duncan E.J. and Lajtai E.Z. (1991) "Fitting Strength Criteria to Intact Rock", Geotechnical and Geological Engineering, Vol.9, pp73 to 81.

Caudle R. (1974) "Mine Roof Stability" in USBM Report Ref. IC 8630, Ground Control Aspects of Coal Mine design.

Chappell B.A (1984) "Determination of Rock Mass Modulus", Proceedings of the 4<sup>th</sup> Australia – New Zealand International Conference on Geomechanics, Perth, May'84. pp514 to 518.

Chen, D.H., Zaman M.M. and Kukreti, A.R., (1993) "Laboratory Testing and Constitutive Modelling of Coal Including Anisotropy", In: Structure and Properties of Engineering Materials, Vol. 48, pp 349-354.

Choquet P. and Charette F. (1988) "Applicability of Rock Mass Classification in the Design of Rockbolt Support in Mines", 15<sup>th</sup> Canadian Rock Mechanics Symposium, University of Toronto, pp39 to 48.

Chugh Y.P and Missavage R.A. (1981) "Effects of Moisture on Strata Controls in Coal Mines", Engineering Geology, Vol. 17, pp241 to 255.

Clark C.A and Newson S. (1985) "A Review of the Monolithic Pumped Packing System", The Mining Engineer, March 1985, pp491 to 495

Clarke A.M. (1963) "A Contribution to the Understanding of Washouts, Swilles, Splits and other Seam Variations and the Amelioration of their effects on Mining in South Durham", The Mining Engineer, June 1963, pp 667 to 691.

Coetzee M.J., Hart R.D., Varona P.M. and Cundall P.A. (1993) "FLAC Basics", Published by Itasca Consulting Group Inc.

Creuels F.H. and Hermes J.M. (1956) "Measurement of the Changes in Rock Pressure in the Vicinity of a Working Face", Proceedings of the International Strata Control Congress, Essen, October 1956, Paper Ref. C + E .

Daws G. (1973) "Mine Layout: A Review of Factors Influencing the Choice", Colliery Guardian, Vol 221, pp185 to 189.

Daws G. (1991) "The Use of the Goemechanics Rock Mass Classification System in the Design of Coal Mine Roof Bolting Systems", Nottingham University Mining Journal, Vol. XLII, pp57 to 61.

Daws G. (1997) "Shotcreteing and the Use of Other Alternatives in Strata Control", Symposium on Developments in Ground Control, University of Nottingham, April '97.

Deere D.U. (1964) "Technical Descriptions of Rock Cores for Engineering Purposes", Rock Mechanics and Engineering Geology, Vol.1, No.1, pp 17 to 22

Deere D.U. and Deere D.W. (1988) "The RQD Index in Practice" Proceedings of the Symposium on Rock Classification Systems for Engineering Purposes, Cincinnati, (Ed. By Kirkaldie, L.) ASTM Special Technical Publication 984.

Dhar B.B, Saxena N.C. and Singh U.K. (1992) "Rock Mass Characterization for Estimation of Support in Underground Galleries and for Prediction of Surface Subsidence in Indian Coalfields", ISRM Eurock'92, Edited by Hudson, J.A., Published by Thomas Telford.

Dick J.C. and Shakoor A. (1992) "Lithological Controls on Mudrock Durability", Quarterly Journal of Engineering Geology, Vol. 25, pp 31-46.

Donath F.A. (1972) "Effects of Cohesion and Granularity on Deformational Behaviour of Anisotropic Rock", Geological Society of America, Memoir Vol. 135, pp95 to 128.

ECSC (1987) "Control of Soft Floor Conditions at Face Ends and in Gateroads", Final Report on Research Project 7220-AC/823.

ECSC (1995) "Lateral Stress Relief for Longwall Access and Truck Roadways", Final Report of Research Project No. 7220-AB/834.

Farmer IW, Price A.M. and Youdan D. (1972) "Design of Tunnels in Coal Measure Rocks", The Mining Engineer?, p13 to 27.

Fookes P.G. (1997) "Geology for Engineers: The Geological Model, Prediction and Performance", Quarterly Journal of Engineering Geology, Vol. 30, pp293 to 424.

Frith R.C., Reddish D.J. and Watson T.P. (1990) "Roadway Support and Design in the New UK Coal Industry", The Mining Engineer, p124 to 128.

Garratt M.H. (1997) "Computer Modelling as a Tool for Strata Control and Reinforcement Design", Symposium on Developments in Ground Control, University of Nottingham, April'97.

Ghose A.K. and Raju N.M. (1981) "Characterisation of Rock Mass Vis a Vis Application of Rock Bolting-Modelling of Indian Coal Mines", Proceedings of the 22<sup>nd</sup> U.S. Symposium on Rock Mechanics, pp452 to 457.

Gross M.R. (1993) "The Origin and Spacing of Cross Joints: Examples from the Monterey Formation, Santa Barbara Coastline, California", Journal of Structural Geology, Vol. 15, No. 6, pp 737 to 751.

Graham Daws Associates (1995) "Core Log, B2's Tail gate, Rossington Colliery"

Hallam A. and Sellwood B.W. (1976) "Middle Mesozoic Sedimentation in Relation to Tectonics in the British Area", Journal of Geology, Vol. 84, pp301 to 321

Hanafy E.A and Emery J.J. (1980) "Advancing Face Simulation of Tunnel Excavations and Lining Placement", in: Underground Rock Engineering:CIM Special Publication, Vol. 22, pp119 to 125.

Hart P.A (1986) "Investigation into the Role of Groundwater in Promoting Floor Heave in Coal Mine Gateroads", in Groundwater in Engineering Geology, Geological Society, Engineering Geology Special Publication, No.3, pp115 to 126.

Hart P.A (1987) "Application of Lithic and Structural Geological Data to the Assessment of Ground Stability above Shallow Coal Mines", In: Planning and Engineering Geology, Geological Society, Engineering Geology Special Publication, No.4, pp137 to 149.

Hassagi (1974) " A Method of Determining the Degree of Fissuration of Rock", International Journal of Rock Mechanics and Mining Science, Vol.11, pp 379 to 388.

Hassanii F.P. (1980) "A Study of the Physical and Mechanical Properties of Rocks and Their Discontinuities Associated with Open-cast Operations", PhD Thesis, University Of Nottingham.

Hawkins A.B. and McConnell B.J. (1992) "Sensitivity of Sandstone Strength and Deformability to Changes in Moisture Content", Quarterly Journal of Engineering Geology, Vol. 25, No.2, pp115 to 130.

Hawkins A.B. and Pinches G.M. (1992) "Engineering Description of Mudrocks", Quarterly Journal of Engineering Geology, Vol. 25, pp 17-30.

Health and Safety Executive. (1994), "Extensive Fall of Roof at Bilston Colliery", HMSO Publication, ISBN 0-7176-0700-3.

Hobbs D.W. (1967) "The Formation of Tension Joints in Sedimentary Rocks: An Explanation", N.C.B. Mining Research Establishment Report No. 2305.

Hoek E and Brown E.T. (1980) "Underground Excavations in Rock", published by Institution of Mining and Metallurgy, London.

Hoek E, Grabinsky M.W. and Diederichs M.S. (1991) "Numerical Modelling for Underground Excavation Design", Transactions of the Institute of Mining and Metallurgy, Vol.100, pp A22 to A30.

Hoek E., Wood D and Shah S. (1992) "A Modified Hoek-Brown Failure Criterion for Jointed Rock Masses", ISRM Eurock'92, Edited by Hudson, J.A., Published by Thomas Telford, London, pp209 to 214.

Hoek, E., Kaiser, P.K. and Bawden, W.F. (1995) "Support of Underground Excavations in Hard Rock", Published by Balkema, Rotterdam, ISBN 90-5410-186-5.

Hoek E. and Brown E.T. (1997) "Practical Estimates of Rock Mass Strength", International Journal of Rock Mechanics, Mining Sciences and Geomechanics Abstracts, Vol. 34, No. 8, pp1165 to 1186.

Holmes P. (1982) "Relations Between Geology and the Stability of Faces and Roadways in the Barnsley Seam", in Proceedings of the Symposium on Strata Mechanics, University of Newcastle, 1982, Ed by I.W. Farmer, pp118 to 123.

Houghton A (1993) "Development is the Key", Mining Engineer, September 1993, pp73 to 83.

Hudson J.A. and Cooling (1988) "In-Situ Rock Stresses and their Measurement in the UK – Part 1. The Current State of Knowledge", International Journal of Rock Mechanics, Mining Science and Geomechanics Abstracts, Vol. 25, No.6, pp 363-370.

Hudson J.A. (1992) "Rock Engineering Systems: Theory and Practice", Published By Ellis Horwood, Chapter 7, pp110 to 123, ISBN 0-13-782624-9.

Hudson J.A. (1993) "Rock Mass Classifications", in: Comprehensive Rock Engineering: Principles, Practices and Projects. Vol.3, Published by Ellis Horwood, ISBN 0-08-035931-0.

ISRM (International Standards for Rock Mechanics) (1981) "Rock Characterisation, Testing and Monitoring: ISRM Suggested Methods", Edited by Brown E.T., Pergamon Press, ISBN 0-08-027308-4.

ISRM (International Standards for Rock Mechanics) (Anon) (1985) "Suggested Method for Determining Point Load Strength", International Journal of Rock Mechanics Mining Science and Geomechanics Abstracts, Vol. 22, p51 to 60.

ITASCA (1995) "Fast Lagrangian Analysis of Continua, Version 3.3", Itasca Consulting Group Inc., Minneapolis, Minnesota, USA

Jacobi O. (1956) "The Pressure on Seam and Goaf", Proceedings of the International Strata Control Congress, Essen, October 1956, Paper Ref. JAC E.

Jaeger J.C (1960) "Shear Failure of Anisotropic Rocks", Geological Magazine, Vol.97, No.1, pp65 to 72.

Jaeger J.C. and Cook N.G.W. (1979) "Fundamentals of Rock Mechanics" 3<sup>rd</sup> Edition, published by Chapman and Hall, ISBN 0-412-22010-5.

Kendall P.F. and Briggs H. (1933) "The Formation of Rock Joints and the Cleat of Coal", Proceedings of the Royal Society of Edinburgh, pp 164 to 187.

Kendorski F and Cummings R.A (1983) "Rock Mass Classification for Block Caving Mine Support", in: Proceedings of 5<sup>th</sup> Congress of the International Society of Rock Mechanics, Australia, Published by A.A. Balkema.

Kent F.L., Hurt K.G. and Coggan J.S. (1997) "Design and Application of Cable Bolt Reinforcement in United Kingdom Coal Mine Roadways", Mineral Industry International Nov. 1997, pp44 to 50.

Klein R.J. and Brown E.T. (1983) "The State of Stress in British Rocks", Interim Report to The Department of the Environment OE (DOE/RW/83.8).

Krishna R. and Whittaker B.N. (1973) "Floor Lift in Mine Roadways-Recent Investigations and Modern Methods of Control", Colliery Guardian.

Ladeira F.L. and Price N.J. (1981) "Relationship Between Fracture Spacing and Bed Thickness", Journal of Structural Geology, Vol. 3, No., 2 pp179-183.

Larsen G. and Chilingar G.V. (1979) "Developments in Sedimentology, 25A, Diagenesis in Sediments and Sedimentary Rocks", published by Elseveir Scientific Publishing Company, ISBN 0-444-41657-9.

Laubsher D.H. (1977) "Geomechanics Classification of Jointed Rock Masses in Mining Applications", Transactions Institute of Mining and Metallurgy, Vol. 86, pp A1 to A8.

Lloyd P. (1998) Personal Communication.

Macrae J.C. and Lawson W. (1956) "The Incidence of Cleat Fractures in Some Yorkshire Coal Seams", Transactions of the Leeds Geological Association, Vol. 6, pp227 to 242.

Mark C. and Molinda G.M. (1994) "Evaluating Roof Control in Underground Coal Mines with the Coal Mine Roof rating", Proceedings 13<sup>th</sup> Conference on Ground Control in Mining, West Virginia, pp252 to 260.

Massey C.T (1977) "Retreat Mining", Mining Engineer, Vol. 137, pp39 to 43.

McLamore R. and Gray K.E. (1967) "The Mechanical Behaviour of Anisotropic Sedimentary Rocks", Transactions of the ASME, pp62 to 76.

McIntock F.A. and Walsh J.B. (1963) "Friction on Griffith's Cracks in Rocks Under Pressure", Proceedings 4th US National Congress of Applied Mechanics, pp1015 to 1021

McQuillian H. (1973) "Small-Scale Fracture Density in Asmari Formation of Southwest Iran and its Relation to Bed Thickness and Structural Setting", Bulletin of the American Association of Petroleum Geology, Vol. 57, pp2367 to 2385.

Mills L.J. (1985) "Retreat Mining Vs Advancing Faces", Colliery Guardian, Vol. 233, pp242 to 244.

Mines and Quarries Act 1954, HMSO Publication, ISBN X-76-079054-9.

Mitri H.S., Edrissi R. and Henning J. (1994) "Finite Element Modelling of Cable Bolted Stopes in Hard Rock Underground Mines", Presented at the SME Annual Meeting, Albuquerque, New Mexico, Feb. '94, Paper No. 94-116.

Mogi K (1966) "Pressure Dependence of Rock Strength and Transition from Brittle Fracture to Ductile Flow", Bulletin of the Earthquake Research Institute., Japan, Vol. 44, pp 215-232.

Mohammad N. (1998) "Subsidence Modelling of Weak Rock Masses", PhD Thesis, University of Nottingham.

Molinda G.M. and Mark C. (1994) "Coal Mine Roof Rating (CMRR); A Practical Mass Classification for Coal Mines", USBM Report IC 9387, pp83.

Moore D (1958) "The Yoredale Series of Upper Wensleydale and Adjacent Parts of the North-West Yorkshire", Proceedings of the Yorkshire Geology Society, No. 31, p 127-134.

Murrell S.A.F. (1962) "A Criterion for Brittle Fracture of Rocks and Concrete under Triaxial Stresses and the Effect of Pore Pressure on the Criterion", in: Rock Mechanics; Proceedings of the 5<sup>th</sup> Symposium on Rock Mechanics, Minnesota, pp 563 to 578.

NCB (1972) "Design of Mine Layouts with Particular Reference to Geological and Geometrical factors", NCB Working Party Report.

NCB (1977) "NCB Cone Indenter", MRDE Handbook No.5.

NCB (1982) "Blaxton Common Borehole Log and Seam Section."

NCB (1984) "Procedures in Coal Mining Geology", Published by: National Coal Board, Mining Department, 241 p.

Nicholson G.A. and Bieniawski Z.T. (1990) "A Non-Linear Deformation Modulus Based on Rock Mass Classification", International Journal Of Mining and Geological Engineering, No.8, pp 181 to 202.

Olivier H.J. (1979) "A New Engineering Geological Rock Durability Classification", Engineering Geology, Vol.14, p255 to 297.

Oram J.S. and Ponder C.G. (1995) "Measurement of the Effects of Interaction and Influence on Mine Layout at Maltby Colliery", 16<sup>th</sup> Conference on Ground Control in Mining, pp 16 to 24.

Park R.G. (1982) "Foundations of Structural Geology" Published by Blackie, ISBN 0-412-00181-0.

Park R.G. (1988) "Geological Structures and Moving Plates", Published by Blackie, ISBN 0-412-01621-4.

Peng S.S. and Chiang H.S. (1983) "Longwall Mining", Published by Wiley, New York, ISBN 0-471-86881-7.

Peng S.S., Tsang P. and Wang Y.J. (1992) "Mechanism of Floor Heave; A Case Study", Proceedings 10<sup>th</sup> Annual Workshop, Generic Mineral Technology Center, Mine Systems Design and Ground Control, Idaho, Nov'92. pp 53 to 63.

Pomeroy C.D., Hobbs D.W. and Mahmoel A. (1971) "The Effect of Weakness Plane Orientation on the Fracture of Barnsley Hards by Triaxial Compression", International Journal of Rock Mechanics and Mining Science, Vol.8, pp227 to 238.

Price N.J. (1959) "Mechanics of Jointing in Rocks", Geological Magazine, Vol. 96.

Price N.J. (1966) "Fault and Joint Development in Brittle and Semi-Brittle Rock"  
Published by Pergamon Press, ISBN 0-08-011275-7.

Priest S.D. and Hudson J.A (1976) "Discontinuity Spacing in Rock", International Journal of Rock Mechanics and Mining Sciences, Vol.13, pp134 to 153.

Pyne R. (1984) "Roadway Drivage on the Selby Complex", Mining Engineer, July 1984, pp57 to 62.

Ramamurthy T. (1986) "Stability of Rock Masses", Indian Geotechnical Journal, Vol.16, Jan. 86, pp1 to 74.

Reading H.G. (1982) "Sedimentary Environments and Facies", Published by Blackwell Scientific Publications, ISBN 0-632-01572-1.

Reifenberg J. (1995) "Towards a Method of Determining Floor Quality in an Underground Coal Mine", 14<sup>th</sup> Conference on Ground Control in Mining, pp200.

Rice R.J. (1977) "Fundamentals of Geomorphology" Published by Longman Group

RJB Mining PLC (1997) (a) " Skipwith No.1 Surface to Seam Borehole Log", Personnel communication.

RJB Mining PLC. (1997) (b) "Geological Report, Rossington Colliery, B3's Main Gate", Internal Report.

RJB Mining PLC. (1999) "Personal Communication", RJB Mining PLC, Geotechnical Department, Harworth.

Roberts B.H. (1994) "A Study of small Scale Coal Mining with particular Reference to the Longwall System and its Means of Support", PhD Thesis, University of Nottingham.

Rock Mechanics Technology (1996) "Rock Stress Measurement in 505's Loadergate, Barnsley Seam, Riccall Mine". RMT Report Ref 014-JO.

Rock Mechanics Technology (1997) (a) "Assessment of Retreat Options and Maingate Support requirements for Rossington with Initial Application to B100's Unit", Interim Report-Stage 1, May 1997.

Rock Mechanics Technology Ltd. (1997) (b) "Stress Measurements in B96's Main Gate, Barnsley/Dunsil Seam, Rossington Colliery", May 1997, Report Ref. RJBN/ROSS 5200AL01.

Rock Mechanics Technology Ltd (1998)(a) "Geotechnical Appraisal for Rockbolting in 95's Tail Gate, Warwickshire Thick Seam, Daw Mill Colliery", Report Ref. RJBS/DAWMILL/7419BC01, January 1998.

Rock Mechanics Technology Ltd, (1998)(b) "Geotechnical Appraisal for Rockbolting B100's Tail Gate, Barnsley Seam, Rossington Colliery", April 1998, Report Ref: RJBN/ROSS/5200PC05.

Selley R.C. (1982) "An Introduction to Sedimentology; 2<sup>nd</sup> Edition", published by Academic Press, ISBN 0-12-636360-9.

Serafim J.L. and Pereira J. (1983) "Consideration on the Geomechanical Classification of Bieniawski", Proceedings of the International Symposium on Engineering Geology and Underground Constructions, Portugal, Vol. 1, pp ii.33 to ii.44.

Sheorey P.R. (1997) "Empirical Failure Criteria for Rock", Published by A.A. Balkema, Netherlands.

Siddall R.G. (1989) "Selby-An Update on Progress", Mining Engineer, December 1989, pp227 to 234.

Siddall R.G. and Gale W.J. (1992) "Strata Control: A New Science for an Old Problem", Mining Engineer, Vol 151, No. 369, pp341 to 353.

Smart B.G.D and Haley S.M. (1987) "Further Development of the Roof Strata Tilt Concept for Pack Design and the Estimation of Stress Development in a Caved Waste", Mining Science and Technology, Vol.5, pp121 to 130.

Smith G.J. and Rosenbaum M.S. (1993) "Abandoned Mine Workings in Chalk: Approaches for Appraisal and Evaluation", Quarterly Journal of Engineering Geology, Vol. 26, No.4, pp281 to 292.

St. John C.M and Van Dillen D.E (1983) "Rockbolts: A New Numerical Representation and its Application in Tunnel Design", proceedings of the 24<sup>th</sup> U.S. Symposium on Rock Mechanics, June 1983, pp13 to 23.

Starfield A.M. and Cundall P.A. (1988) "Towards a Methodology for Rock Mechanics Modelling", International Journal of Rock Mechanics, Mining Science and Geomechanics Abstracts, Vol.25, No.3 pp 99 to 106.

Stimpson B. (1970) "Modelling Materials for Engineering Rock Materials", International Journal of Rock Mechanics and Mining Science, Vol.7, pp77 to 121.

Su W.H and Peng S.S, (1986) "Cutter Roof and its Causes", Mining Science and Technology, Paper Ref No. MIN00107, p20.

Taylor R.K. and Spears D.A (1970) "The Breakdown of British Coal Measure Rocks", International Journal of Rock Mechanics and Mining Science, Vol. 7, pp481 to 501.

Taylor R.K. and Smith T.J. (1986) "The Engineering Geology of Clay Minerals: Swelling, Shrinkage and Mudrock Breakdown", Clay Minerals, Vol.21, pp235 to 260.

Taylor R.K. (1988) "Coal Measure Mudrocks: Composition, Classification and Weathering Process", Quarterly Journal of Engineering Geology, Vol. 21, pp 85-99.

Terzaghi K. (1946) "Rock Defects and Loads on Tunnel Supports", in: Rock Tunneling with Steel Supports, Editors Proctor R.V. and White T. Published by Commercial Shearing and Stamping Co, pp 15 to 99.

Terzaghi K. and Ricard F.E. (1952) "Stresses in Rock about Cavities", Geotechnique, Vol. 3, pp57 to 90.

Timoshenko S.P. and Goodier J.N. (1970) "Theory of Elasticity", 3<sup>rd</sup> Edition, Published by McGraw-Hill, ISBN 0-07-064720-08.

Tsidz K.E.N. (1990) "The Influence of Foliation on Point Load Strength Anisotropy of Foliated Rocks.", Engineering Geology, Vol.29, pp49 to 58.

Tucker M.E. (1981) "Sedimentary Petrology; An Introduction", Published by Blackwell Scientific Publications, ISBN 0-632-00074-0.

U.S.B.M. (United States Bureau Of Mines) (1984) "Cleat in Bituminous Coal", Report Ref: RI 7910 1974.

Unal E. (1983) "Design Guidelines and Roof Control Standards for Coal Mines Roofs", PhD Thesis, Pennsylvania State University.

Van Eeckhout E.M. (1976) "The Mechanics of Strength Reduction Due to Moisture in Coal Mine Shales", International Journal of Rock Mechanics, Mining Science and Geomechanics Abstracts, Vol.13, pp61 to 67.

Vutukri V. and Hossaini S. (1992) "Assessment of Applicability of Strength Criteria for Rock and Rock Mass to Coal Pillars", Proceedings 11<sup>th</sup> Conference on Ground Control in Mining, Australia, July'92, pp1 to 8.

Waite K (1997) "Problems Solutions and the Future in Strata Control", Symposium on Developments in Ground Control, University of Nottingham.

Walsh J.B. and Brace W.F. (1964) "A Fracture Criterion for Brittle Anisotropic Rock", Journal of Geophysics Research, Vol.69, pp3449 to 3456.

Whittaker B.N. and Hodgson D.R. (1971) "Design and Layout of Longwall workings" Mining Engineer, Vol. 131, pp79 to 91.

Whittaker B.N. (1974) "An Appraisal of Strata Control Practice", Mining Engineer, Vol.134, No.166, pp9 to 24.

Whyatt J.K. and Julien M. (1988) "A Fundamental Question: The Role of Numerical Methods in Rock Mechanics Design" Key Questions in Rock Mechanics, Edited by Cundall, Published by A.A. Balkema, pp311 to 315.

Wickham G.E., Tiedeman H.R. and Skinner E.H. (1974) "Ground Support Prediction Model. RSR Concept", Proceedings of the Rapid Excavation and Tunneling Conference, San Francisco, California, pp691 to 707.

Williamson I.A. (1967) "Coal Mining Geology", published by Oxford University Press, ISBN B67-22457.

Wilson A.H. and Ashwin D.P. (1972) "Research into the Determination of Pillar Size", Mining Engineer, No. 141, Vol. 131, pp409 to 427.

Wilson A.H. (1983) "The Stability of Underground Workings in the Soft Rocks of the Coal Measures", International Journal of Mining Engineering, Vol. 1, pp91 to 187.

Wing S.P. (1997) "Practical Implications of the Proposed Mines (Control of Ground Movement) Regulations", Symposium on Developments in Ground Control, University of Nottingham, April'97.

Yasar E, Whittles D.N., Lloyd P and Reddish D.J. (1998), "Anisotropic Strength and Stiffness Properties of Some UK Coal Measure Siltstones", unpublished paper, (submitted to the Quarterly Journal of Engineering Geology).

Yudhibir, Lemanza W and Prinzl F. (1983) "An Empirical Failure Criterion for Rock Masses", Proceedings of 5<sup>th</sup> ISRM International Congress on Rock Mechanics, Balkema, Melbourne, 1:B1 to B9.

## **ACKNOWLEDGEMENT**

The author would like to express his sincere thanks and gratitude to the following people and establishments who were of help in producing this thesis:

Dr D.J. Reddish for his supervision, help and encouragement, for proof reading the text of this thesis and for his arrangements for providing the funding for this research.

Dr P.W. Lloyd for his supervision, help, encouragement and advice given during the duration of the research for this thesis and for proof reading and reviewing the text of this thesis.

Dr L.R.Stace for his help in obtaining case study information.

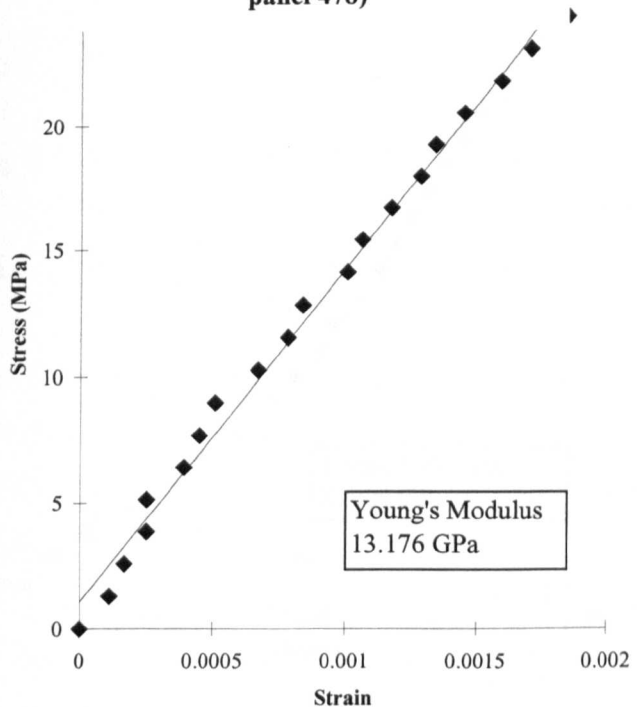
RJB Mining Ltd for the provision of samples and information and allowing case studies to be undertaken on locations within their mines.

The European Coal and Steel Community for providing the funding for this research.

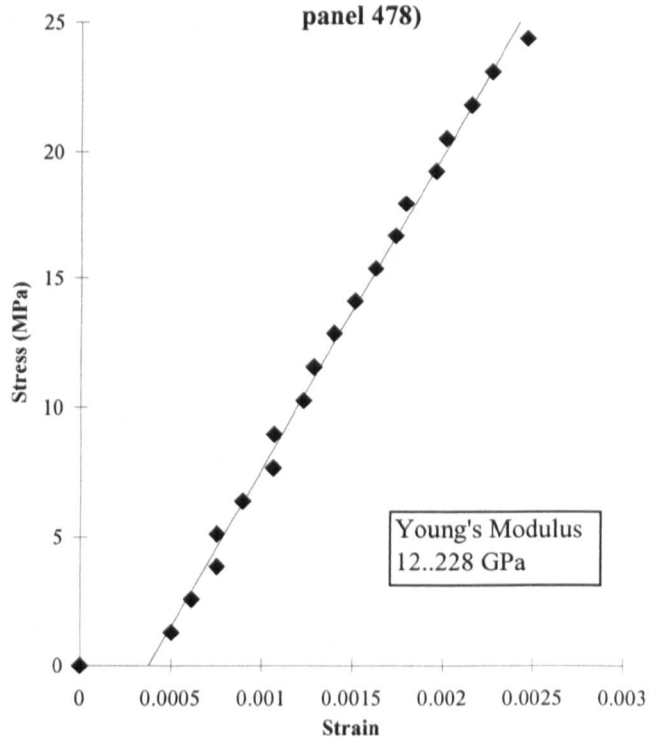
## **APPENDIX 1**

Stress Strain Plots For Roof Strata Samples, Panels 478 and 505, Riccall Mine

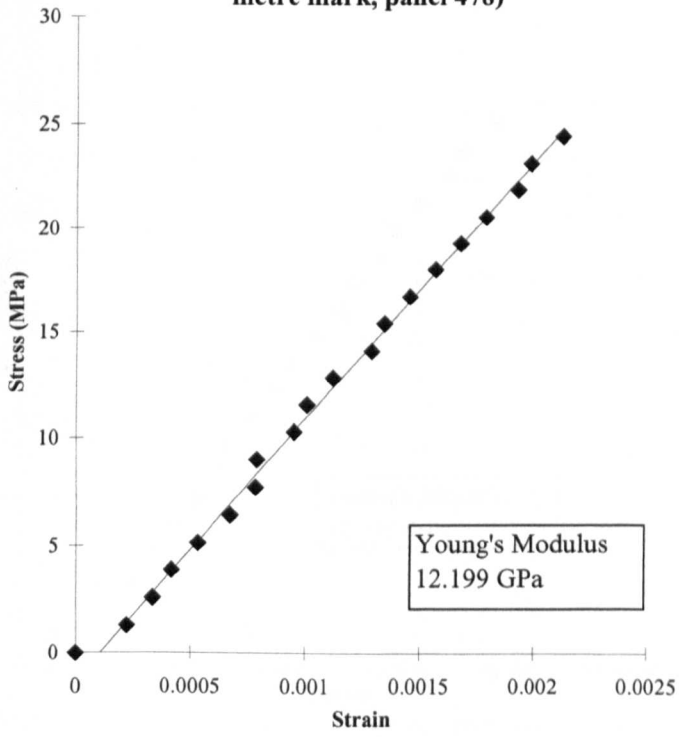
**MASSIVE SILTSTONE**  
(from roof core main gate 31 metre mark,  
panel 478)



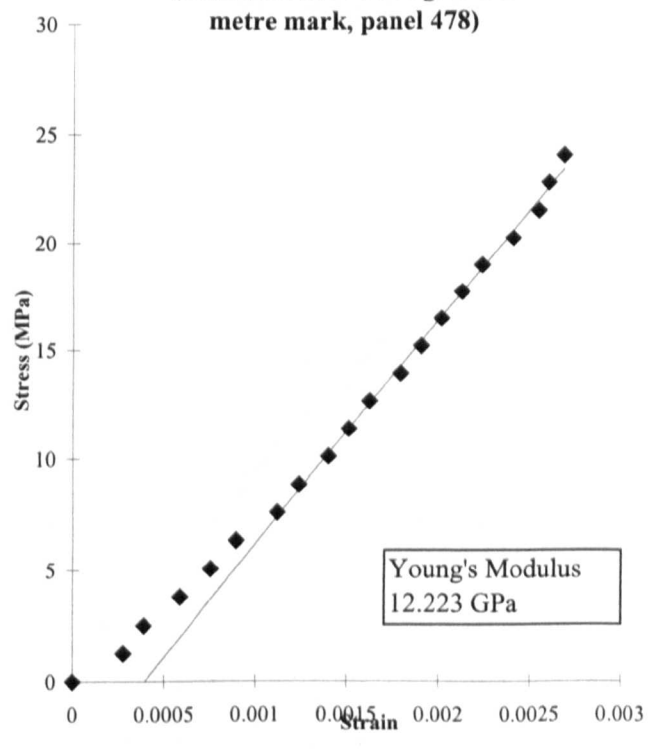
**MASSIVE SILTSTONE**  
(from roof core main gate 31 metre mark,  
panel 478)



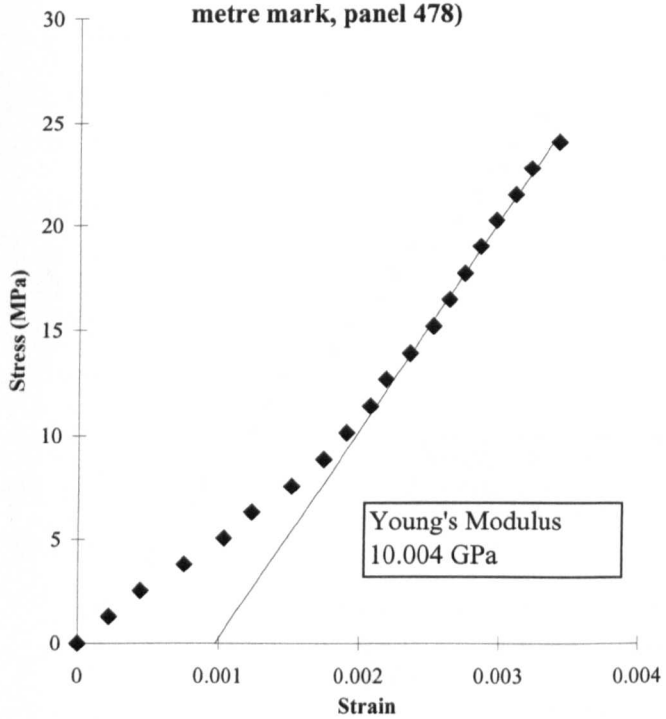
**MASSIVE SILTSTONE**  
(from roof core main gate 31  
metre mark, panel 478)



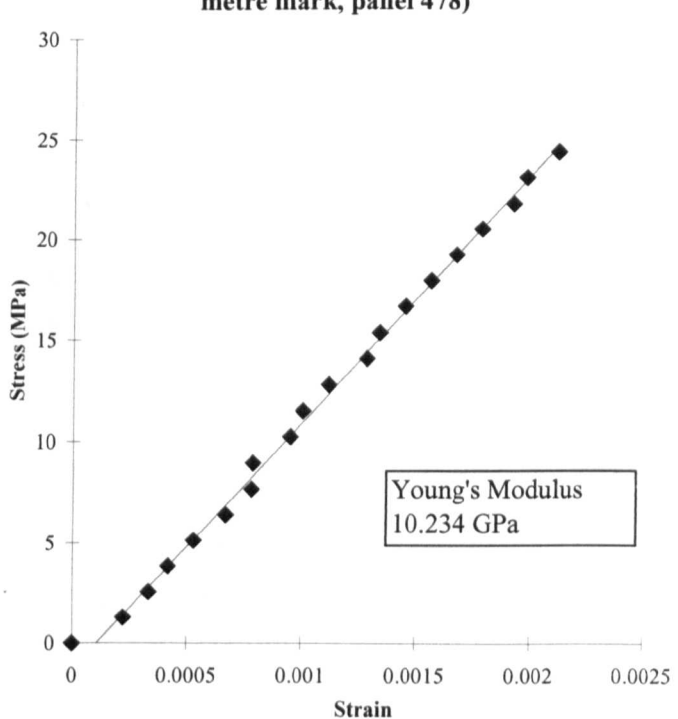
**SANDSTONE**  
(from roof core main gate 710  
metre mark, panel 478)



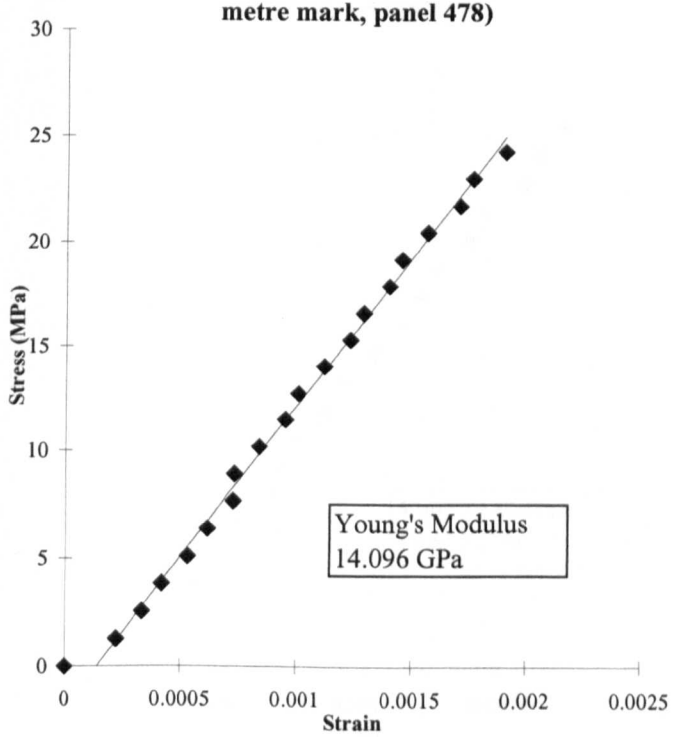
**SANDSTONE**  
(from roof core main gate 710  
metre mark, panel 478)



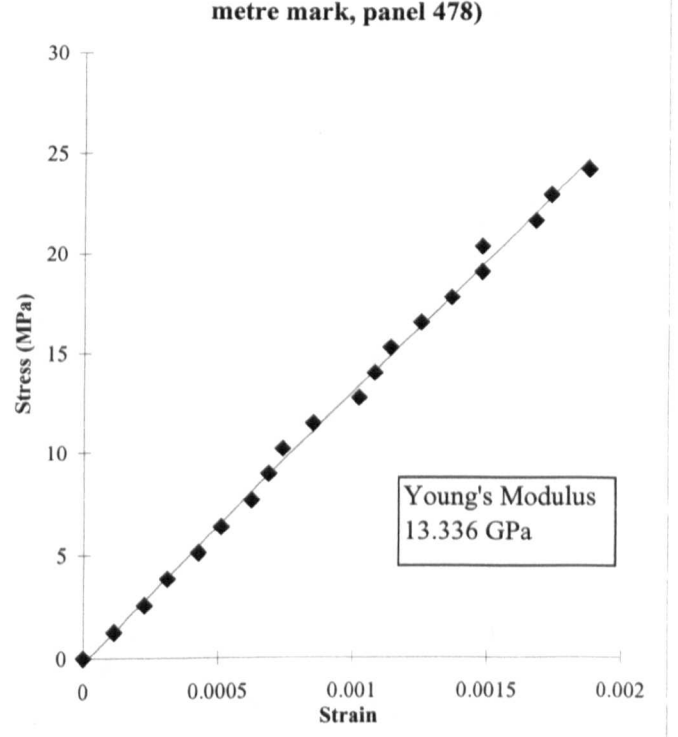
**MASSIVE SILTSTONE**  
(from roof core main gate 31  
metre mark, panel 478)



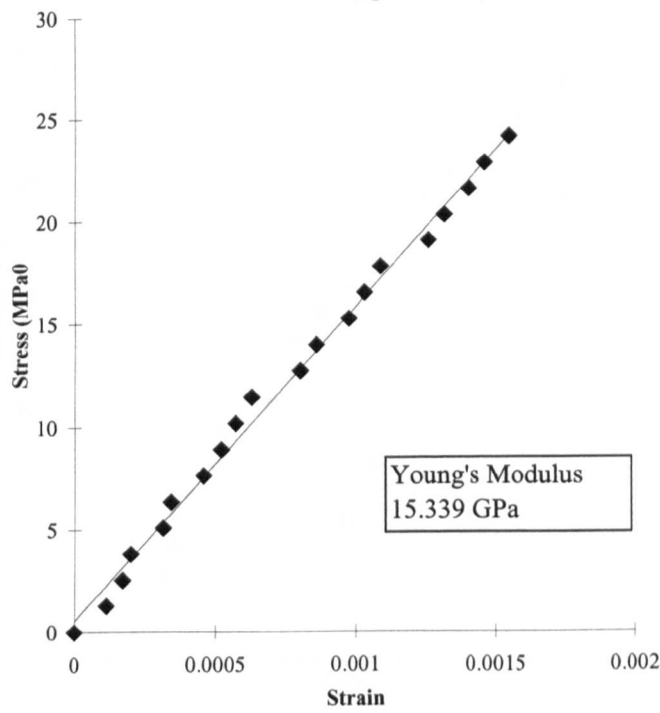
**LAMINATED SILTSTONE**  
(from roof core main gate 486  
metre mark, panel 478)



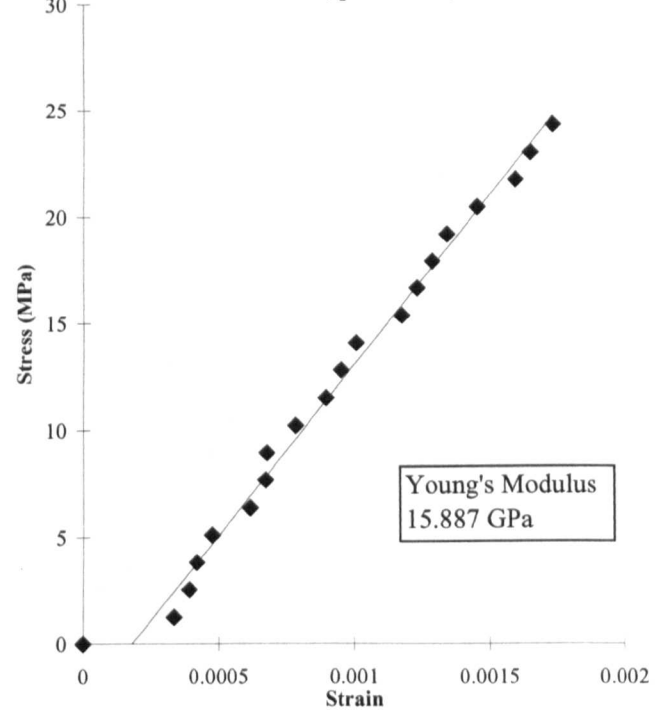
**LAMINATED SILTSTONE**  
(from roof core main gate 486  
metre mark, panel 478)



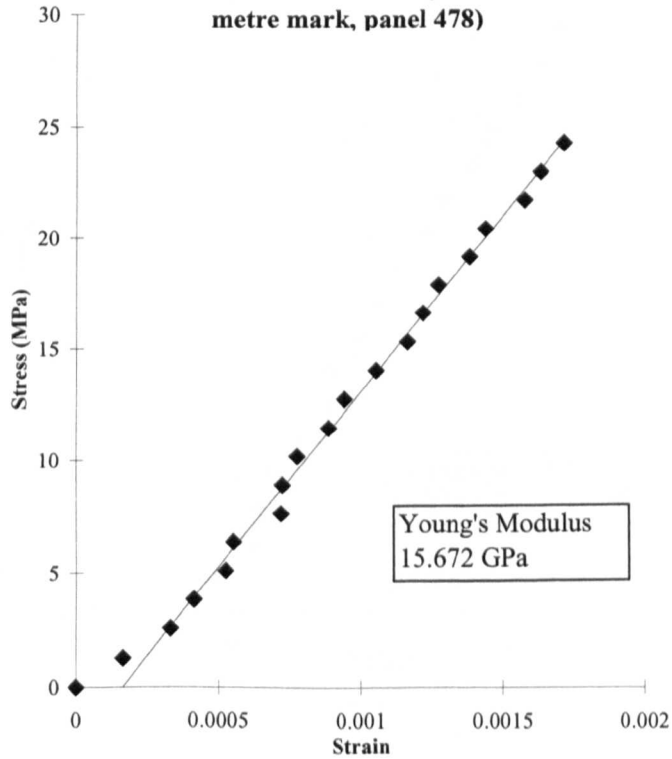
**MUDSTONE**  
(from roof core main gate 710  
metre mark, panel 478)



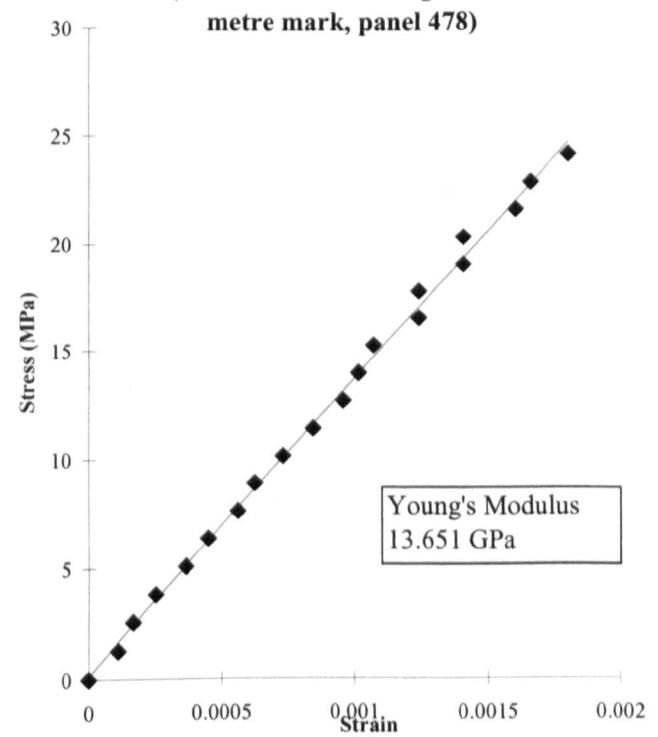
**MUDSTONE**  
(from roof core main gate 710  
metre mark, panel 478)



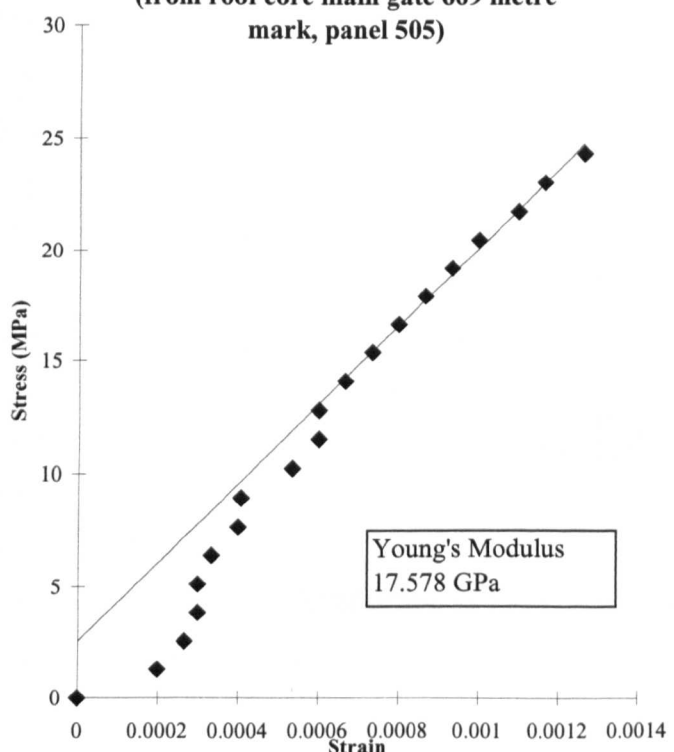
**MUDSTONE**  
(from roof core main gate 710  
metre mark, panel 478)



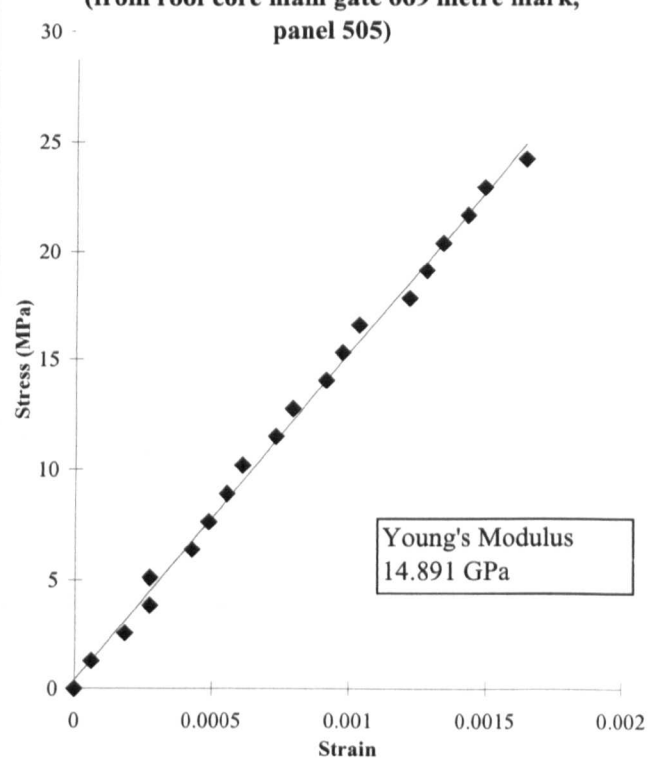
**MUDSTONE**  
(from roof core main gate 710  
metre mark, panel 478)



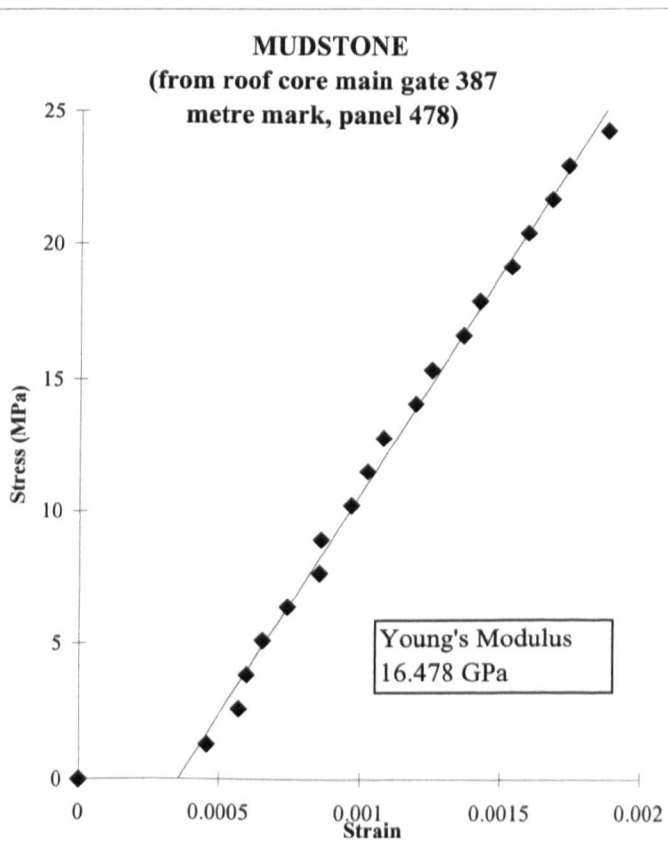
**MUDSTONE**  
(from roof core main gate 669 metre  
mark, panel 505)



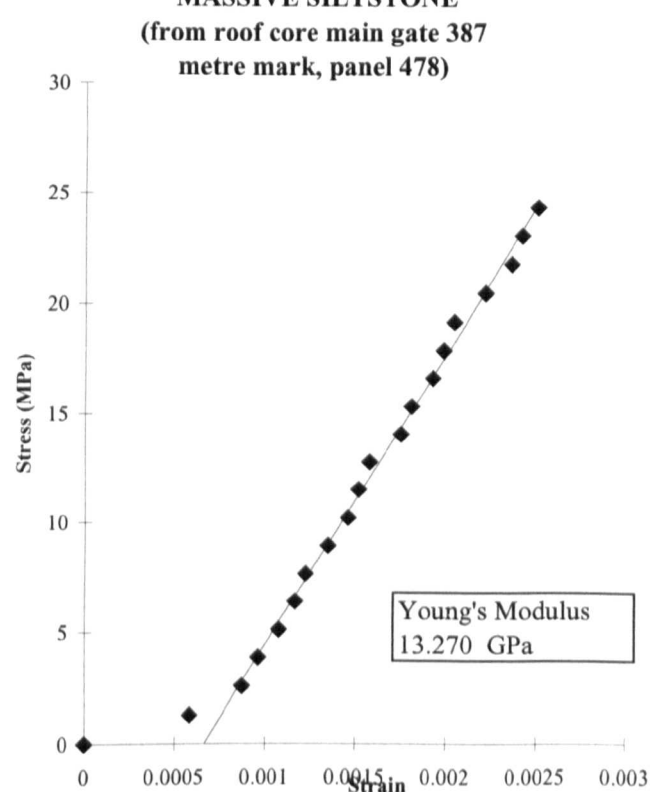
**MUDSTONE**  
(from roof core main gate 669 metre mark,  
panel 505)



**MUDSTONE**  
(from roof core main gate 387  
metre mark, panel 478)



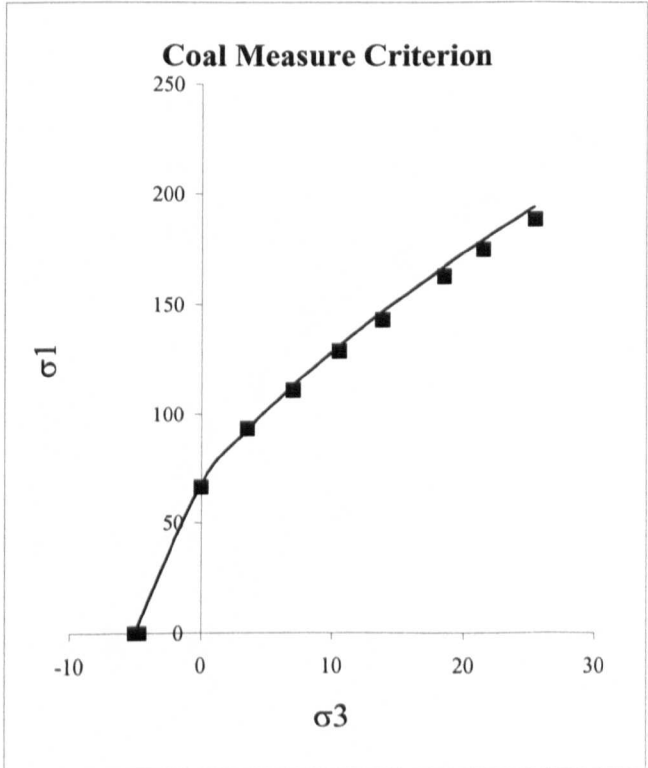
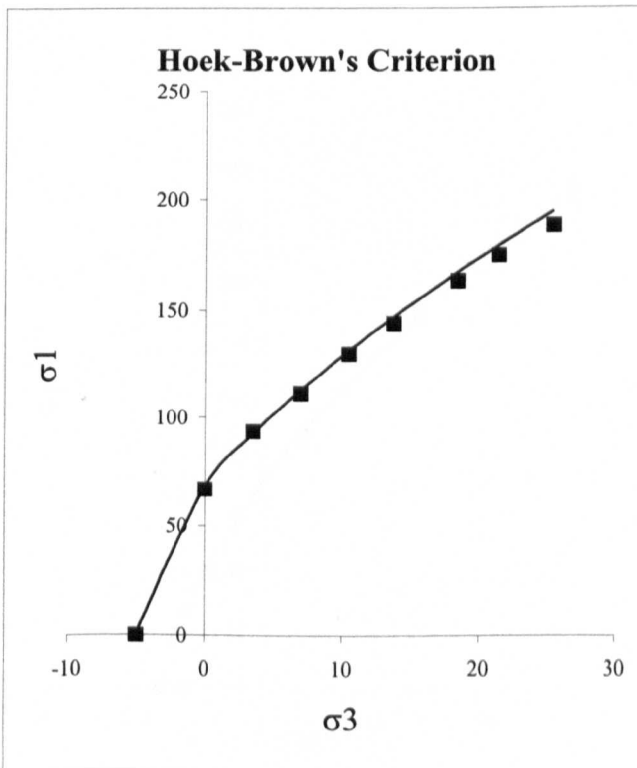
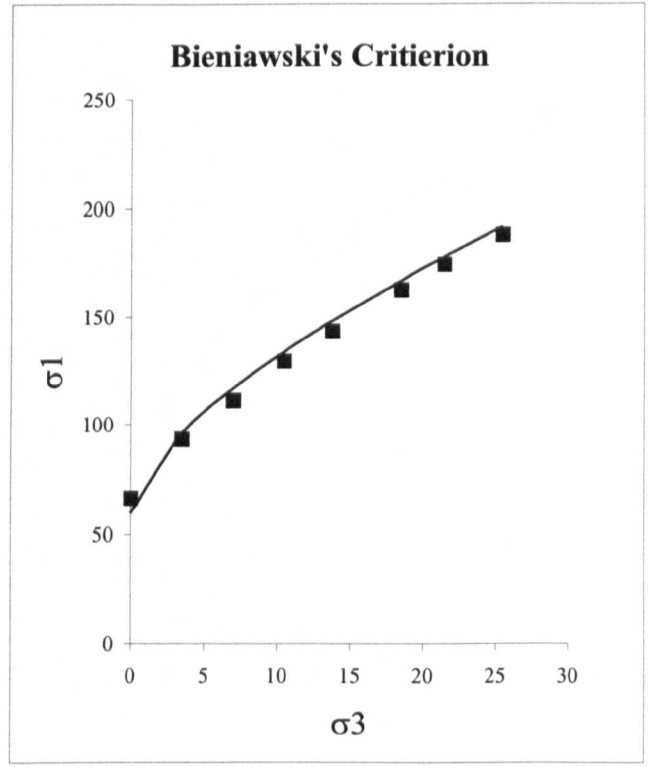
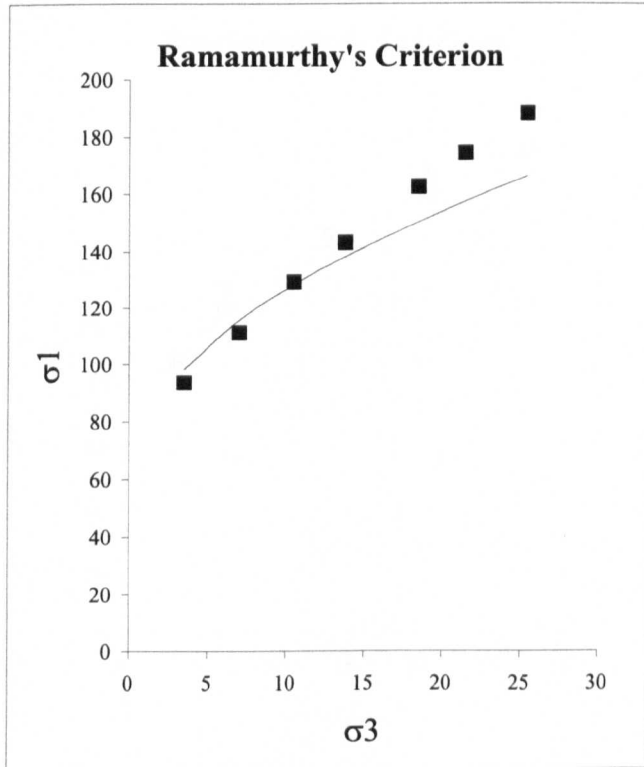
**MASSIVE SILTSTONE**  
(from roof core main gate 387  
metre mark, panel 478)



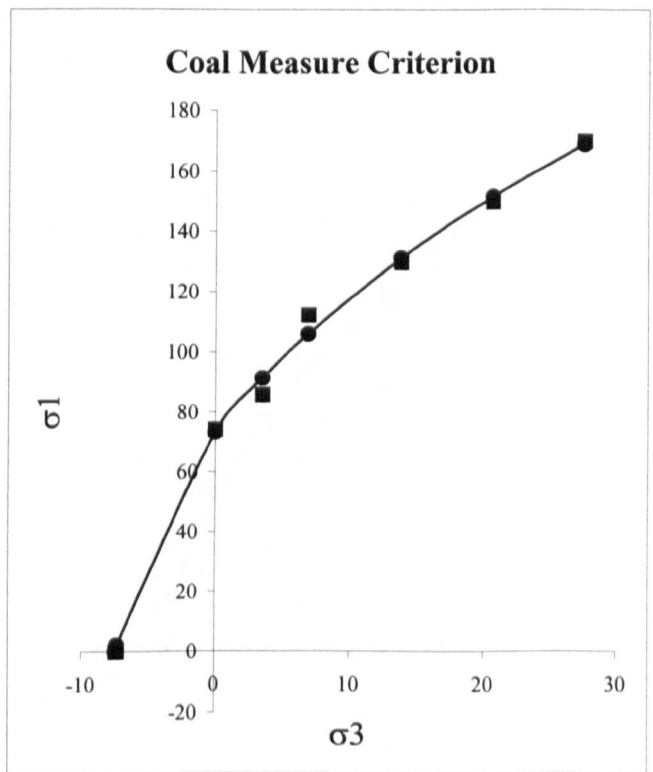
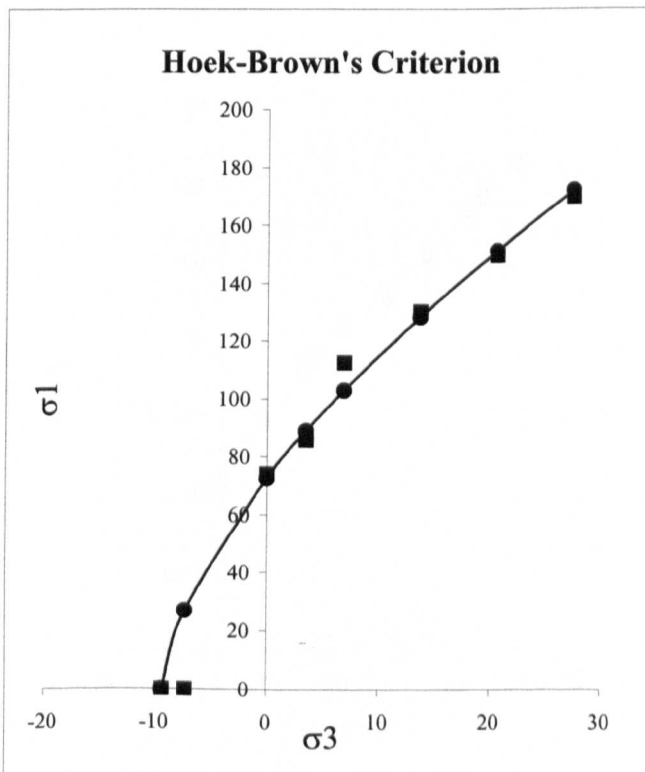
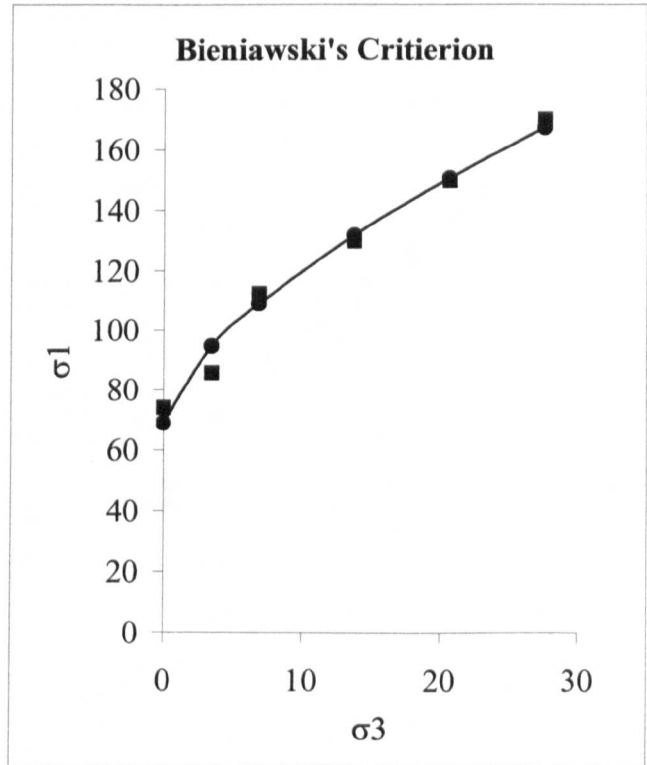
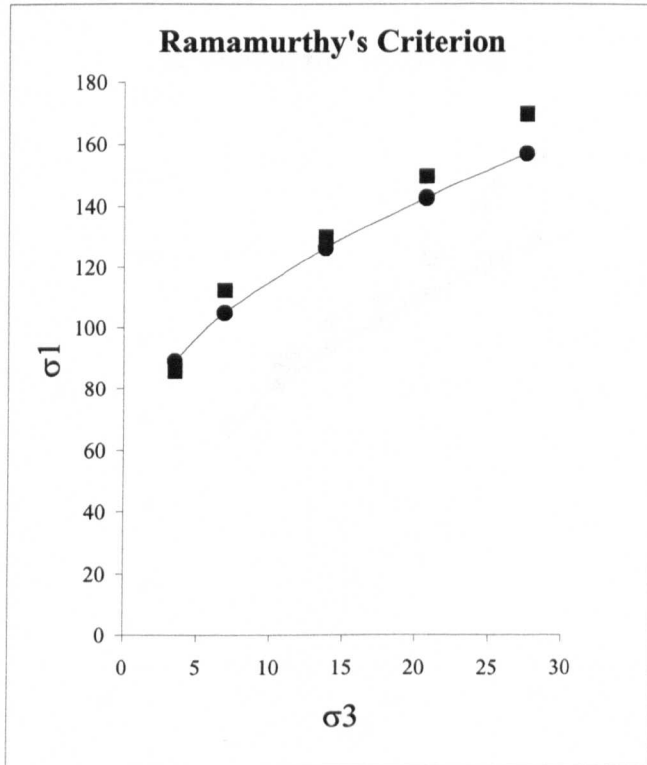
## **APPENDIX 2**

Application of Rock Mass Failure Criteria to Triaxial Data

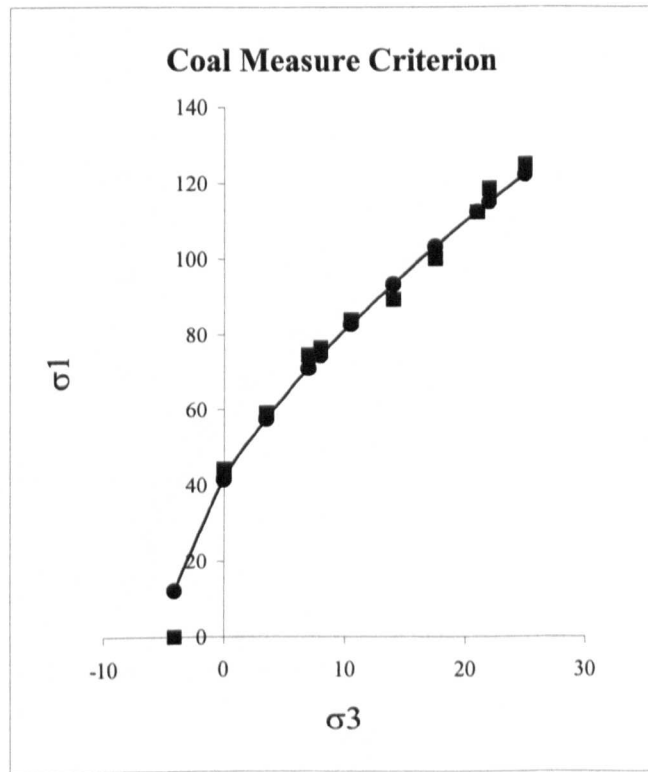
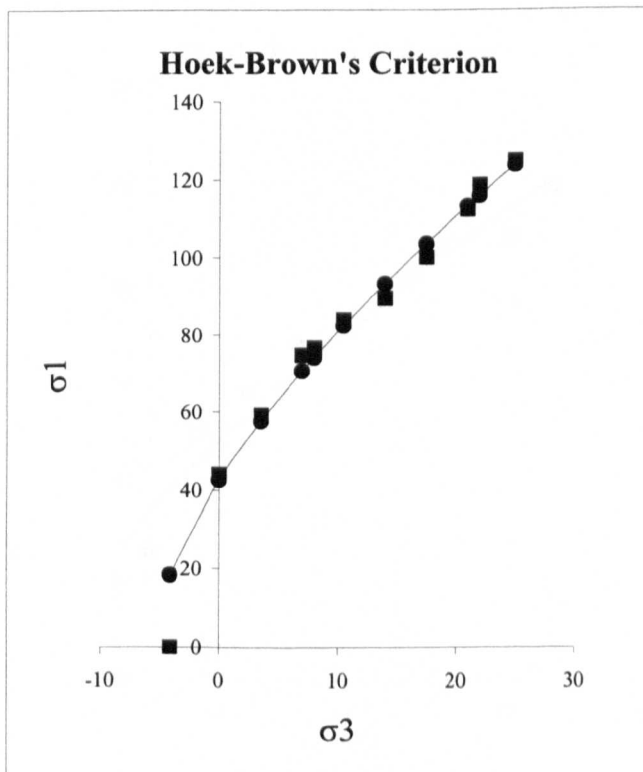
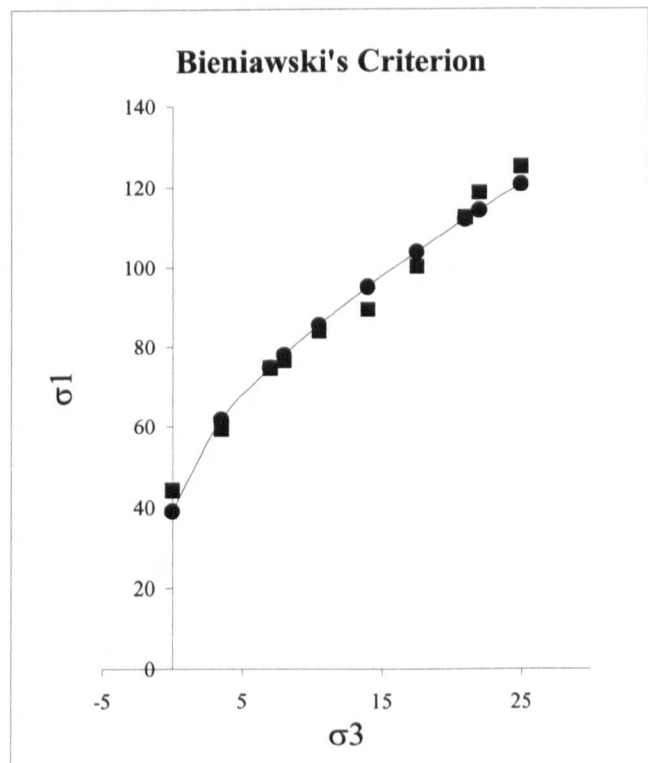
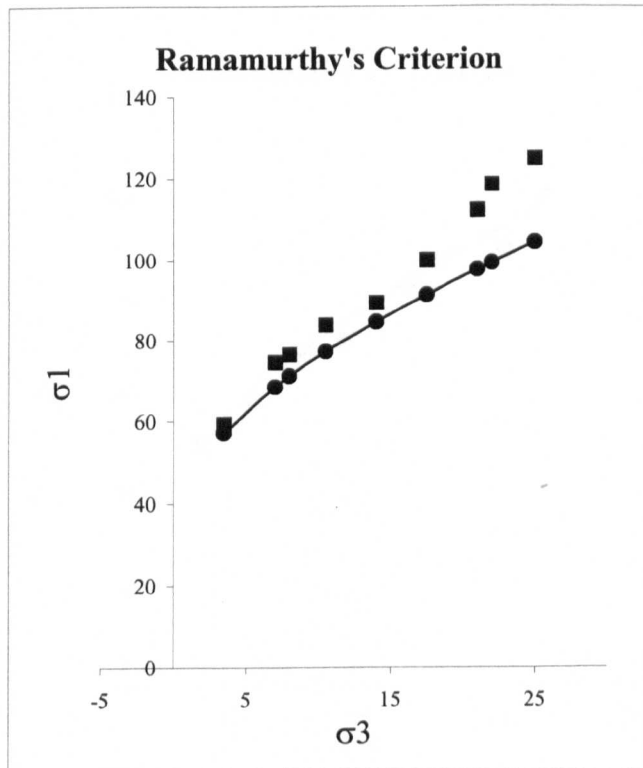
## Coal Measure Siltstone (Park Meadow)



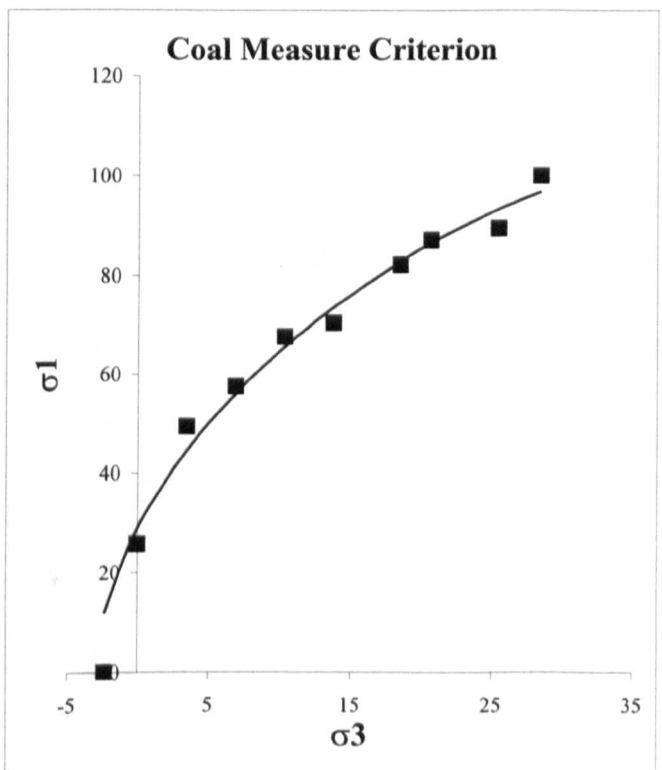
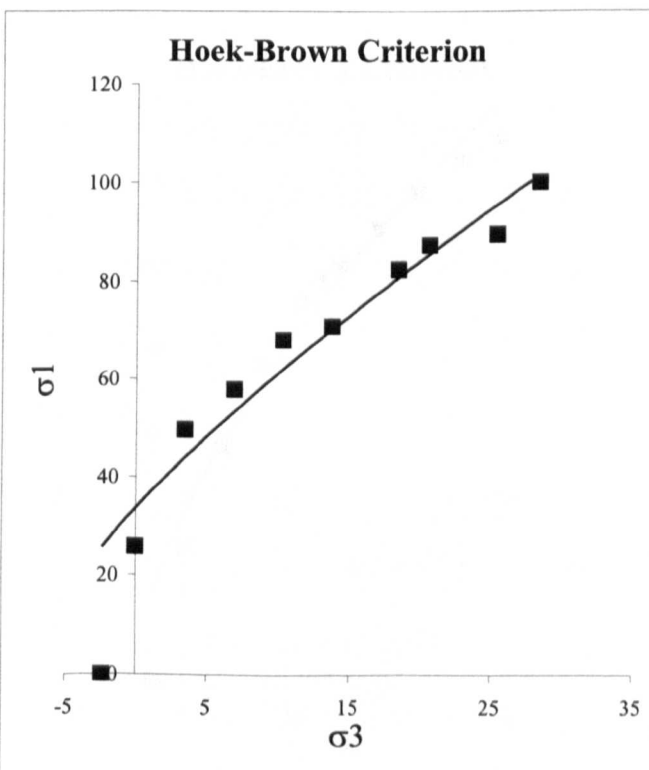
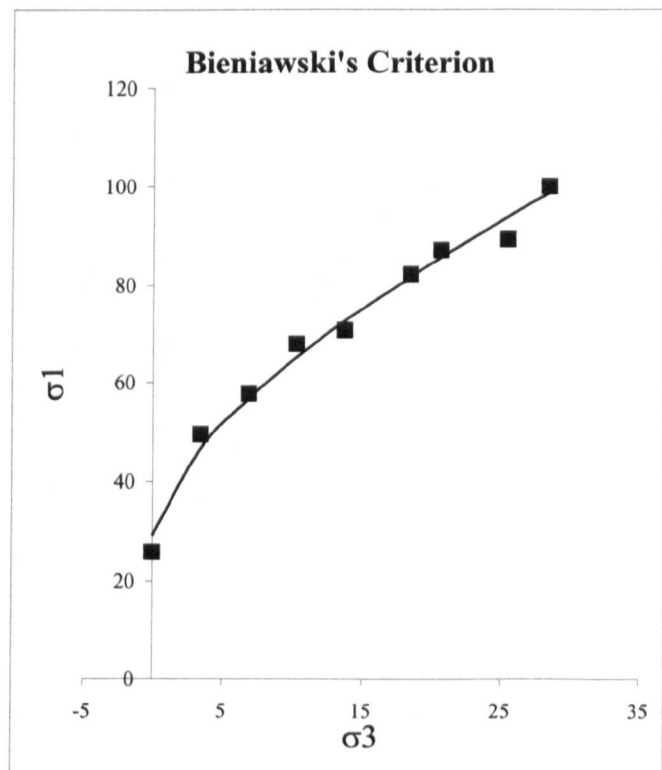
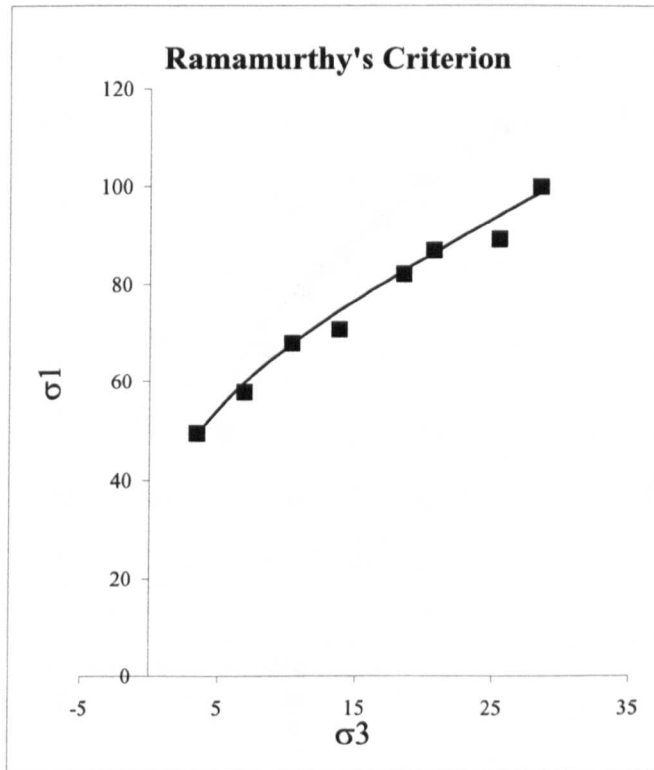
## Siltstone (East Midlands)



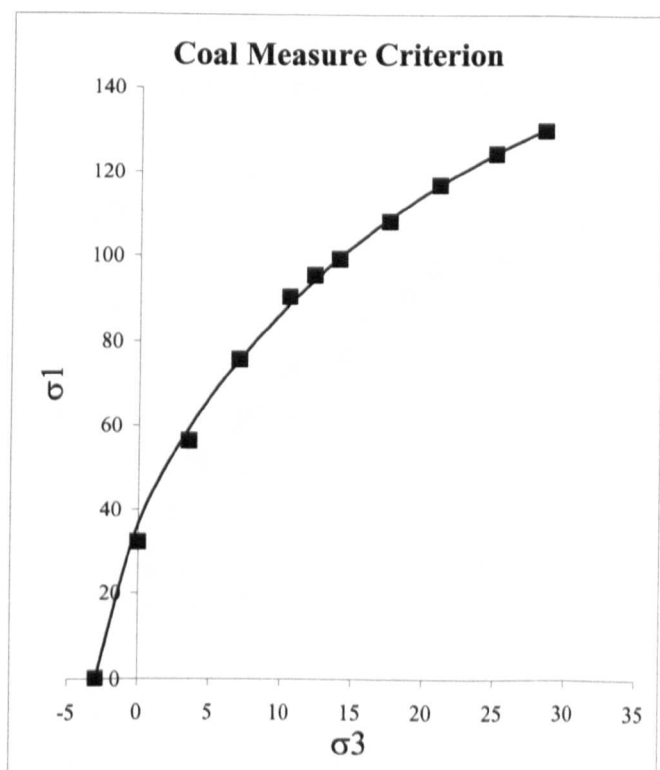
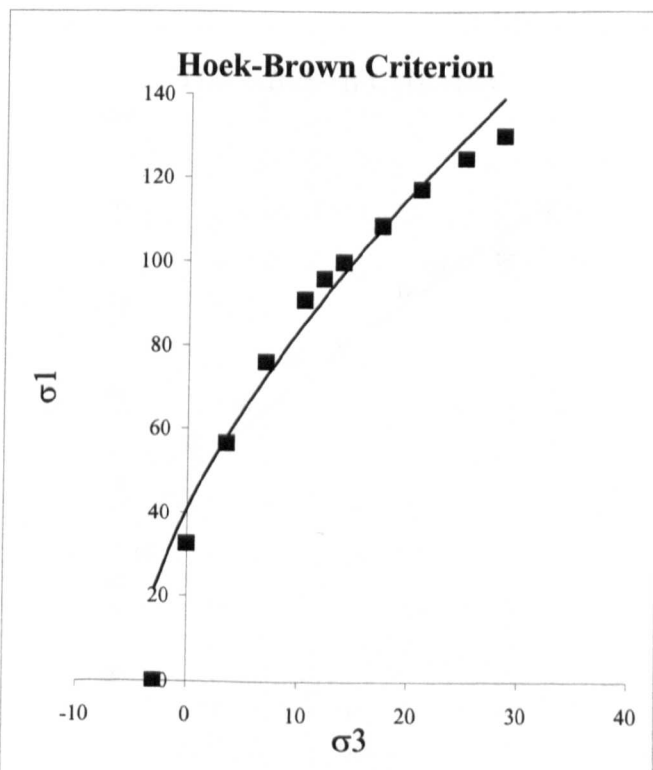
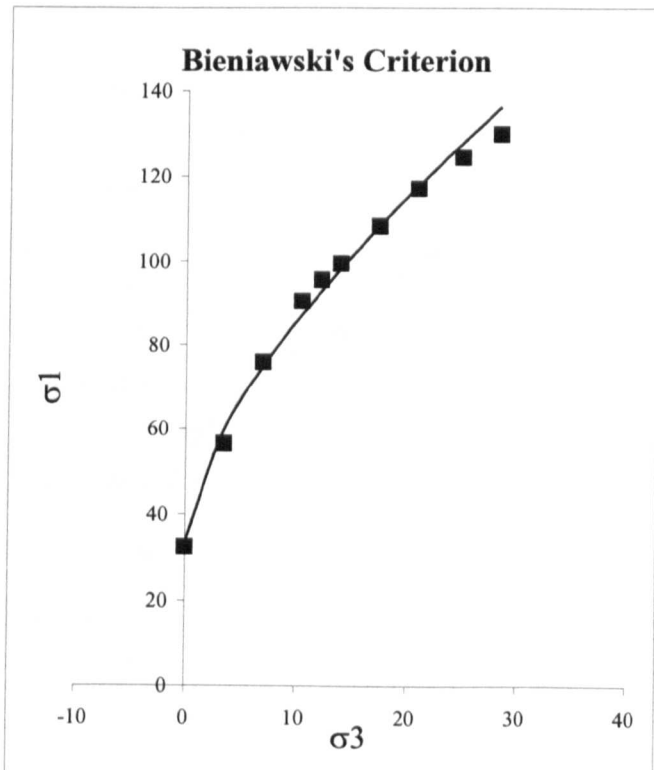
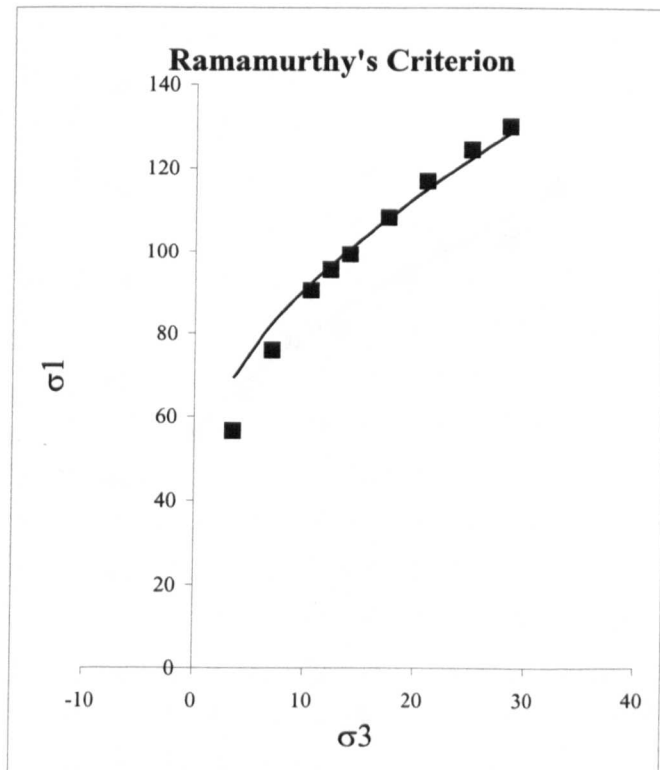
## Seatearth (Spondon)



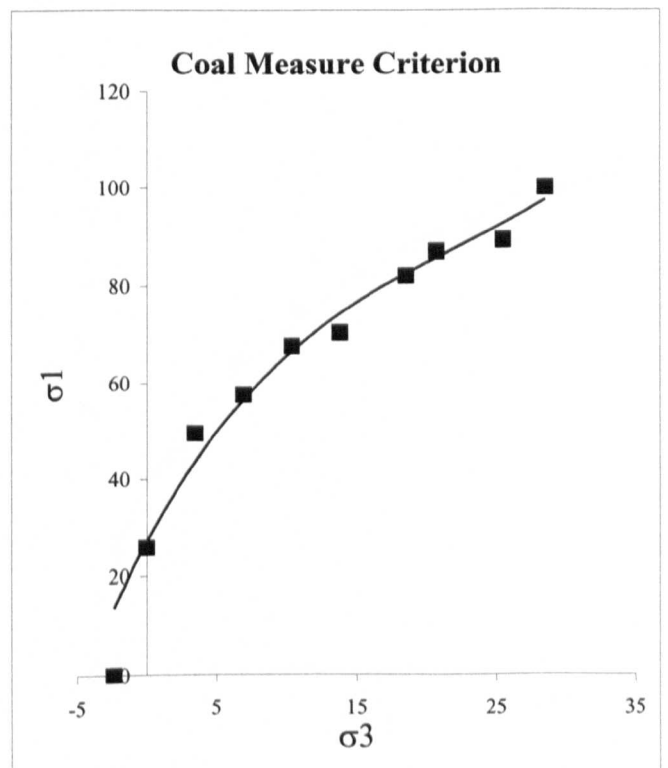
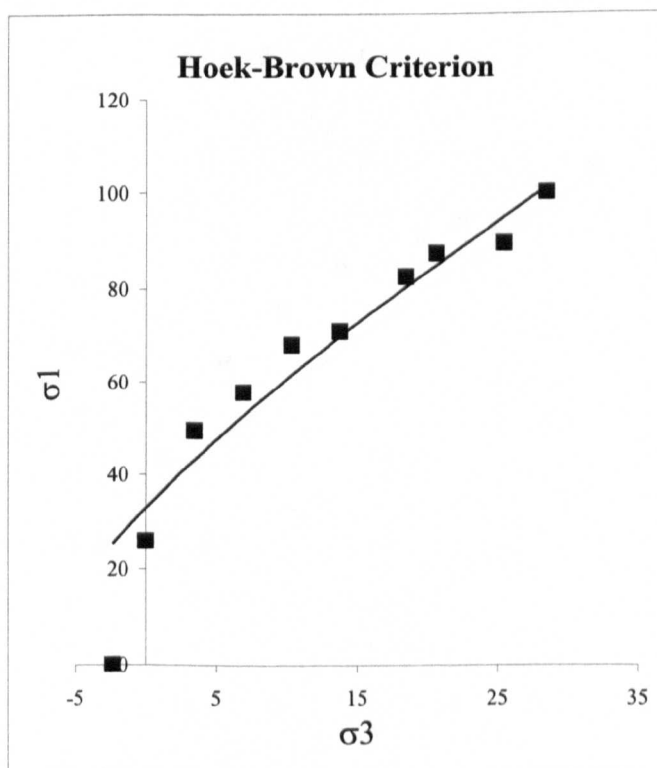
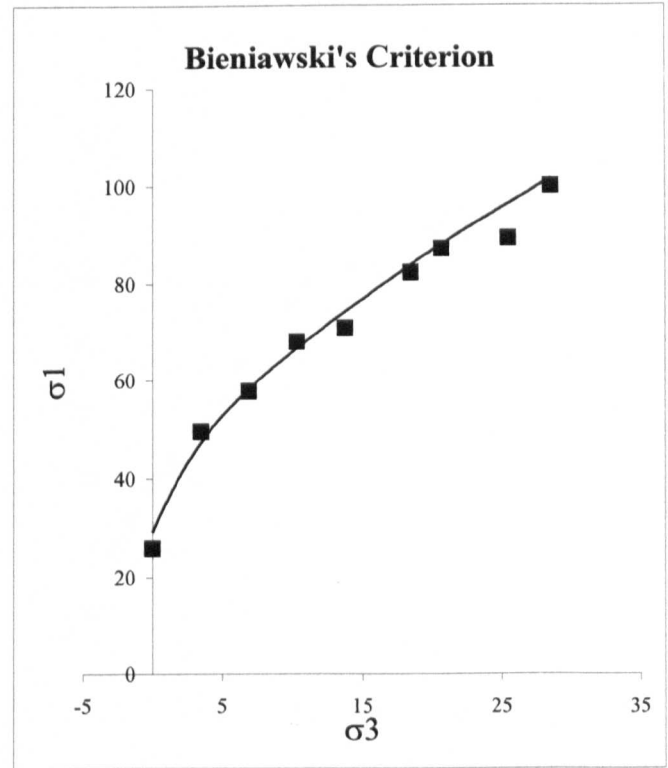
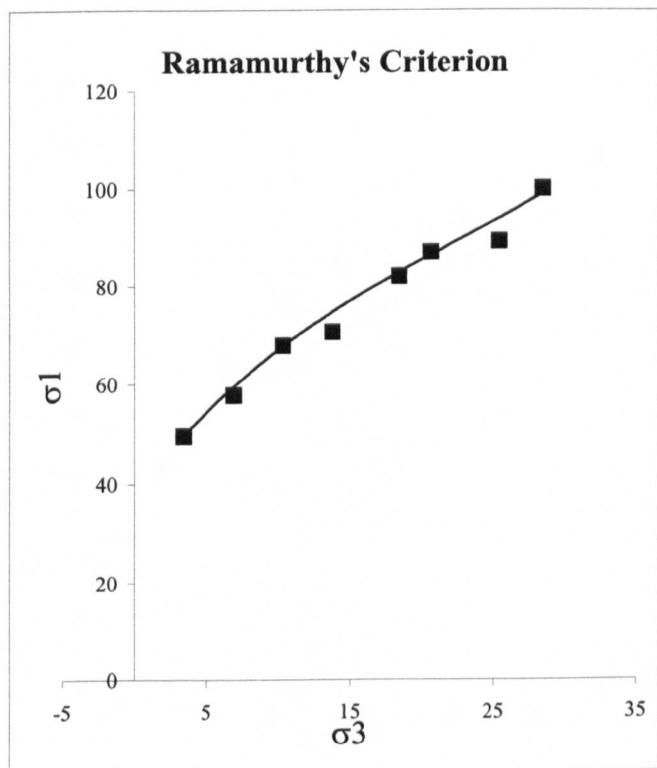
## Coal Measure Seatearth (Pye Hill)



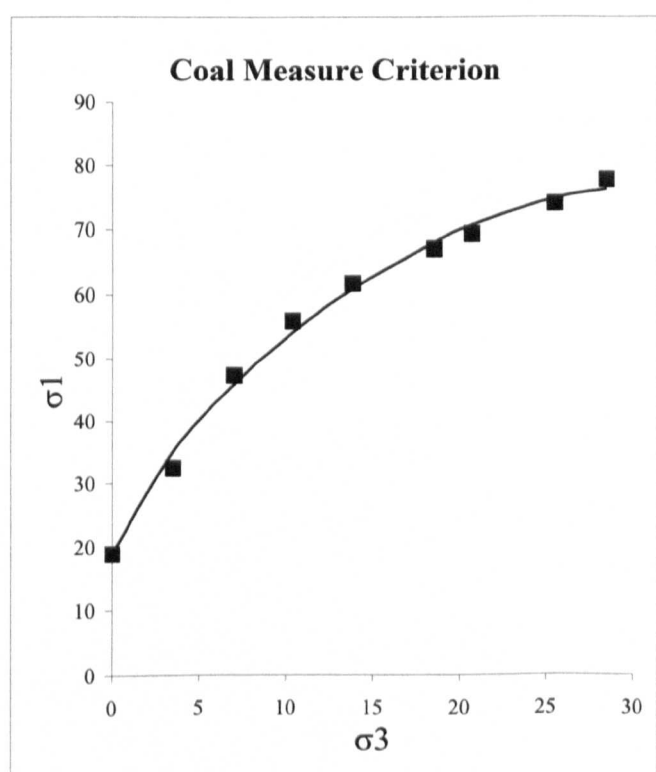
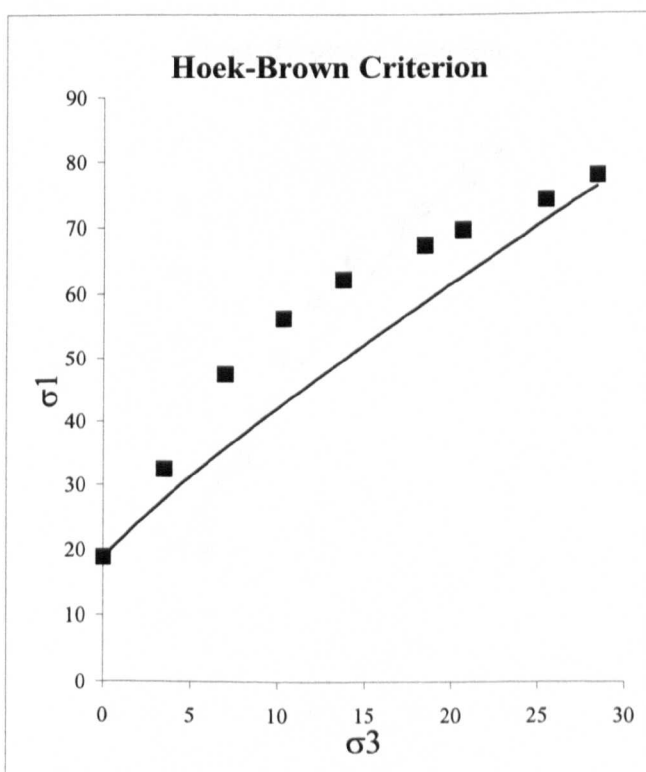
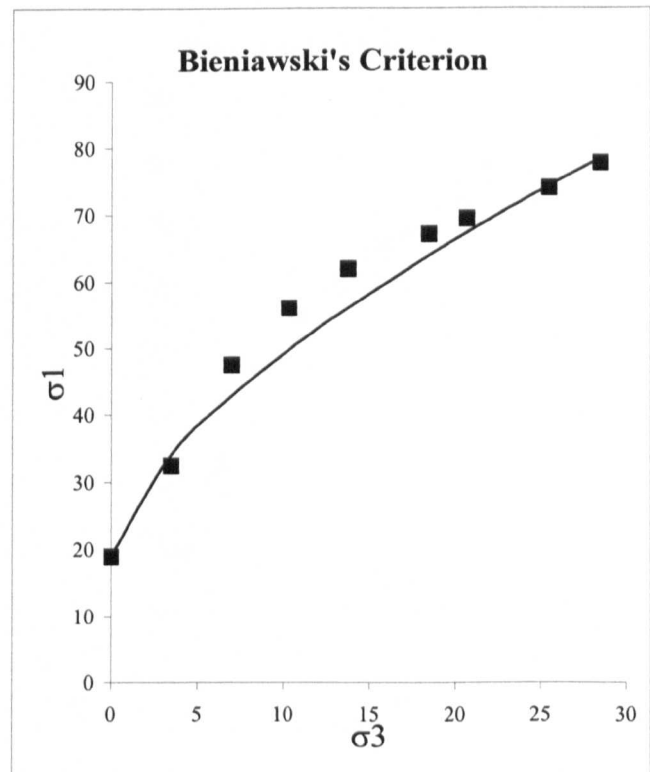
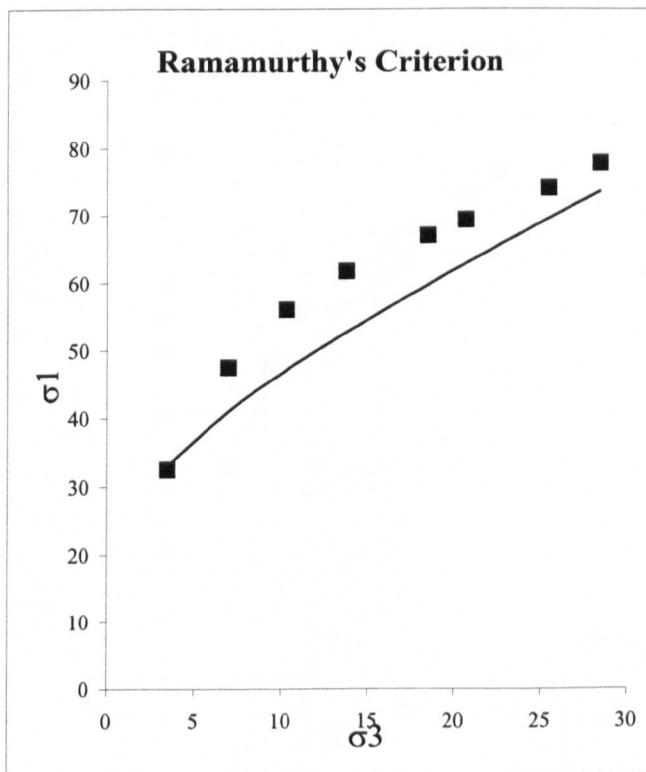
## Coal Measure Seatearth (North West 2)



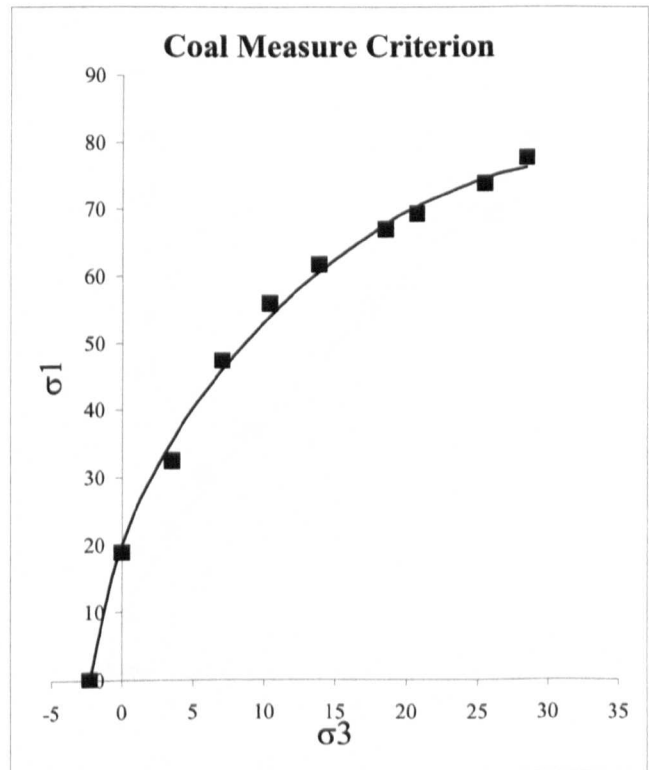
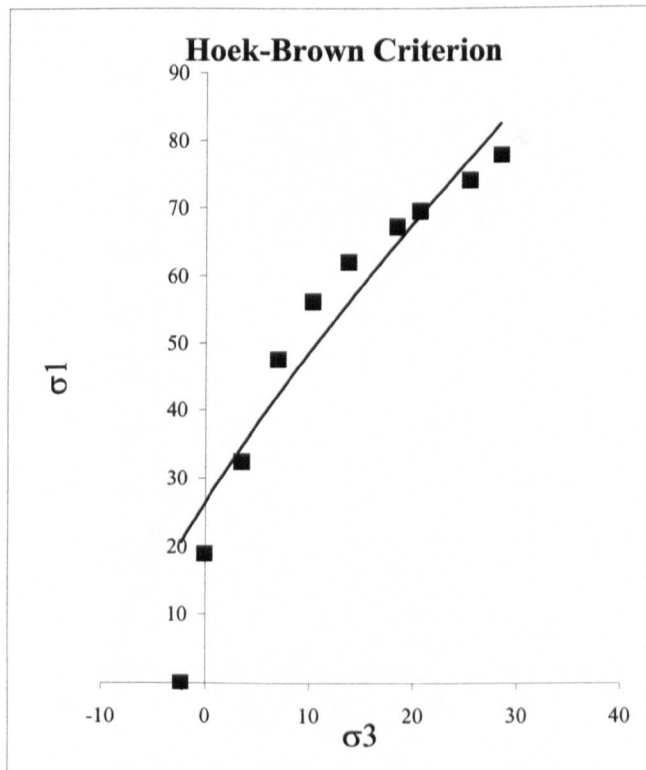
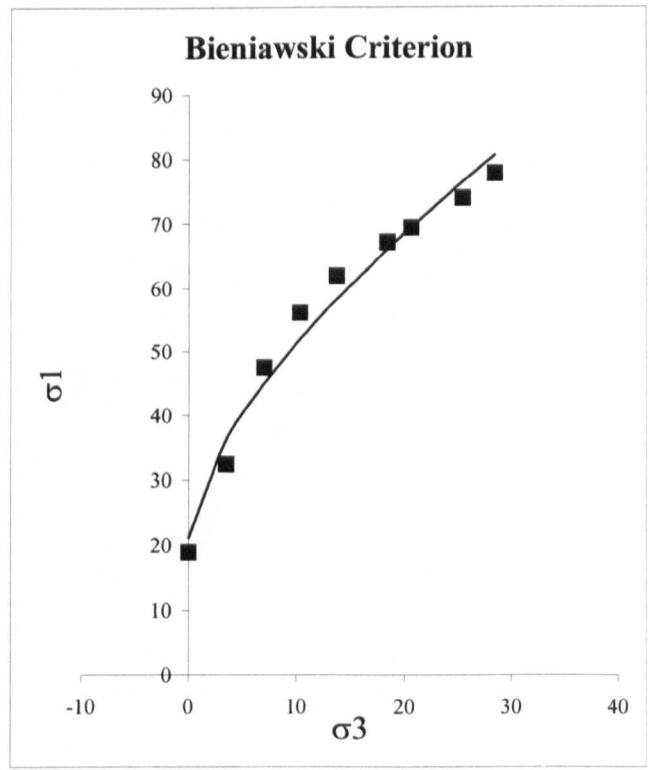
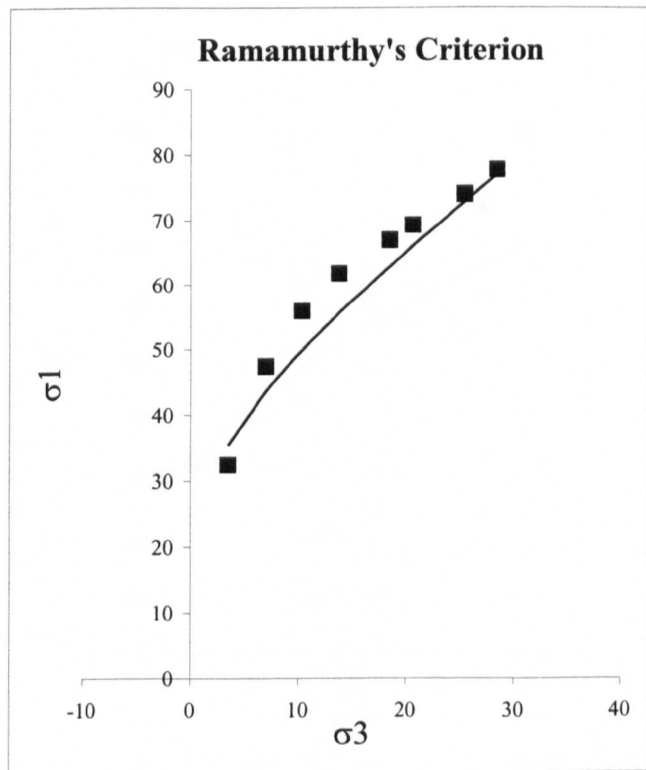
### Coal Measure Seatearth (North West 1)



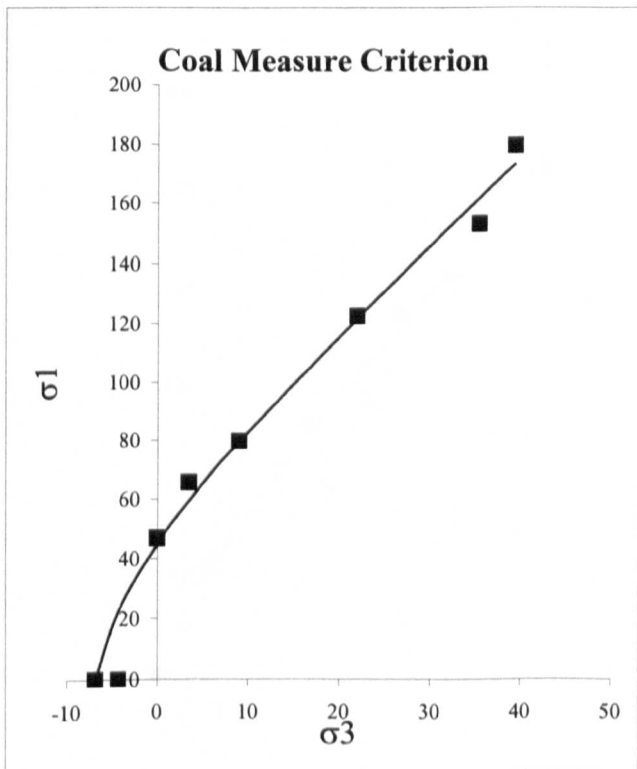
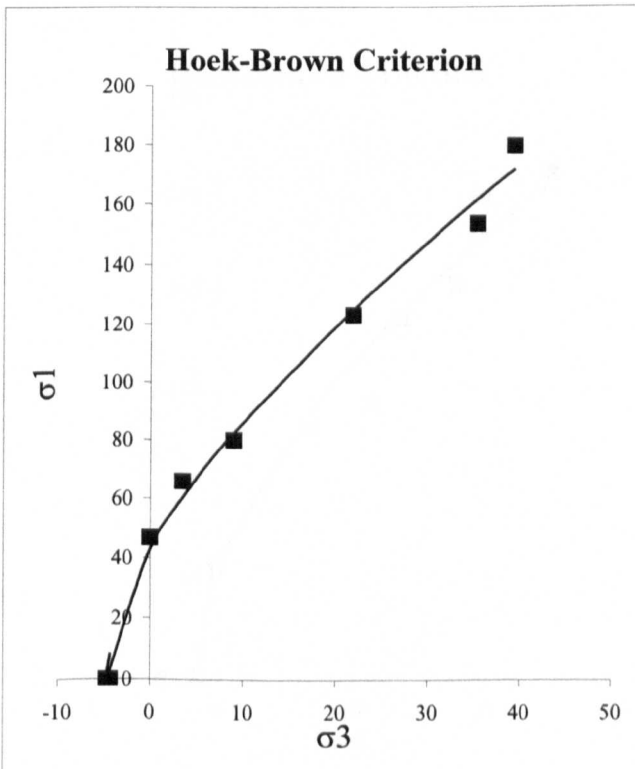
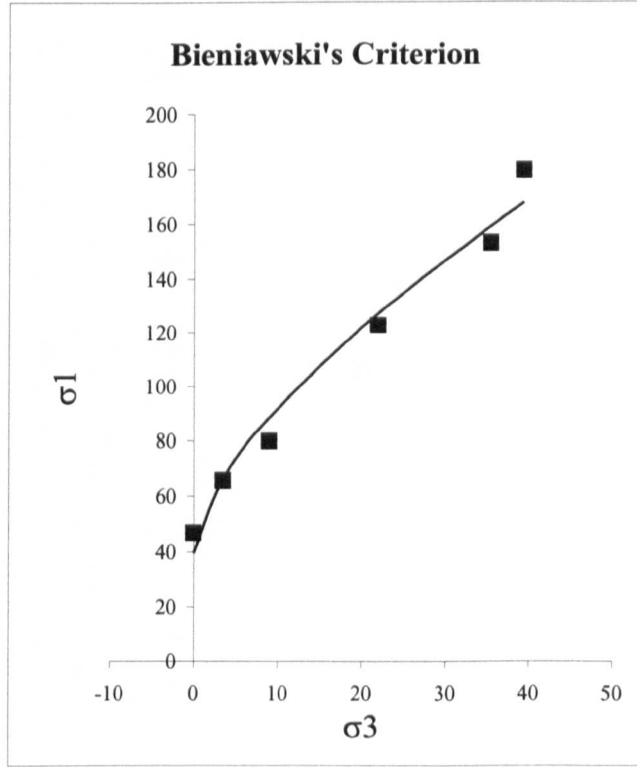
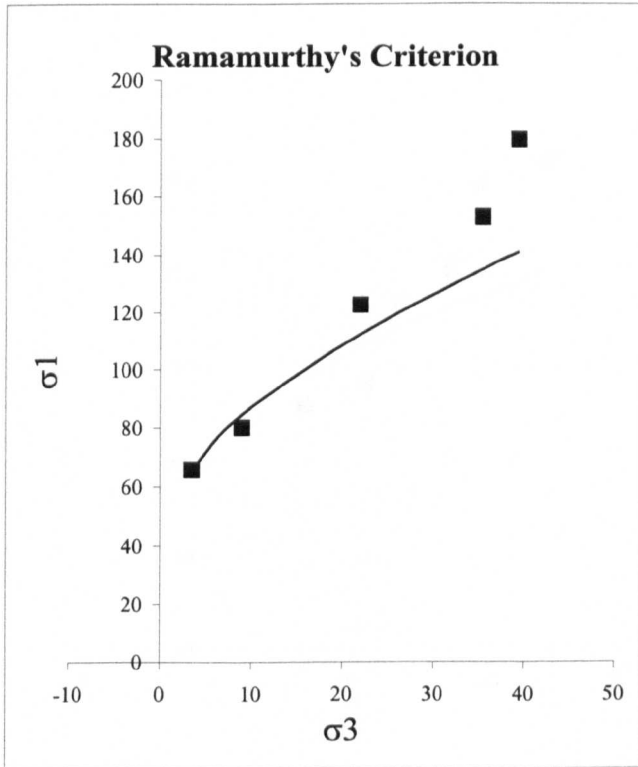
## Coal Measure Seatearth (East Midlands 2)



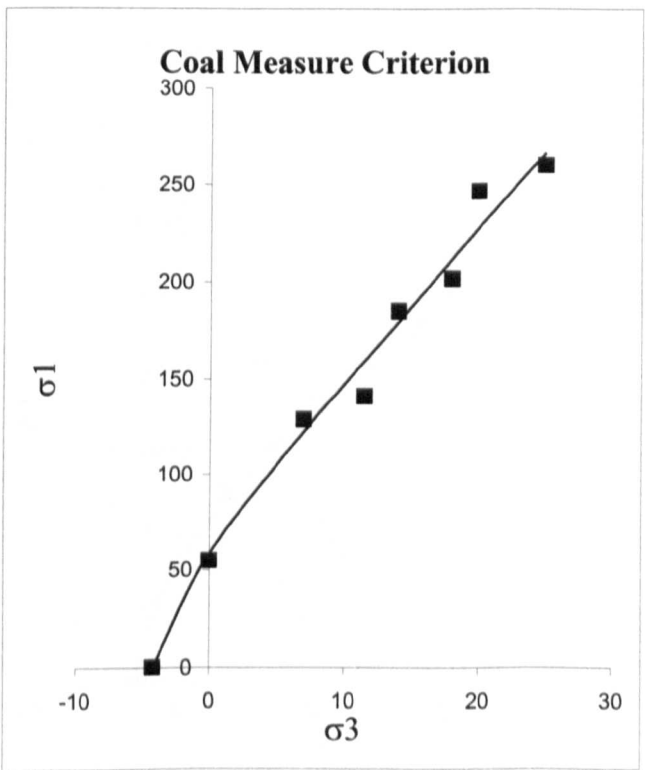
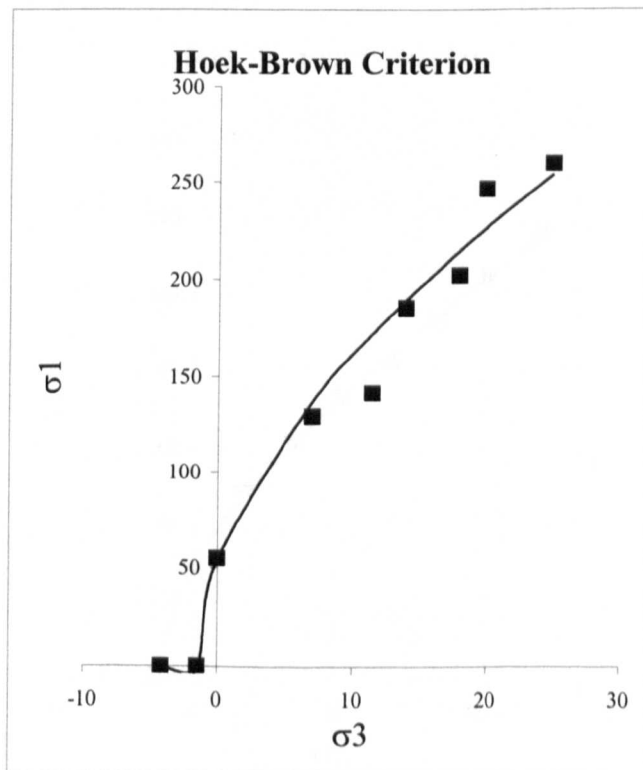
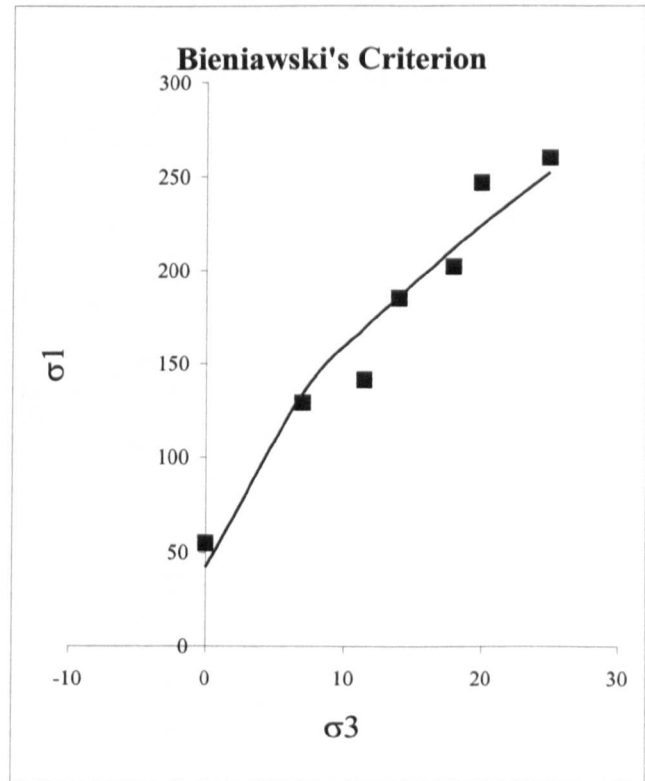
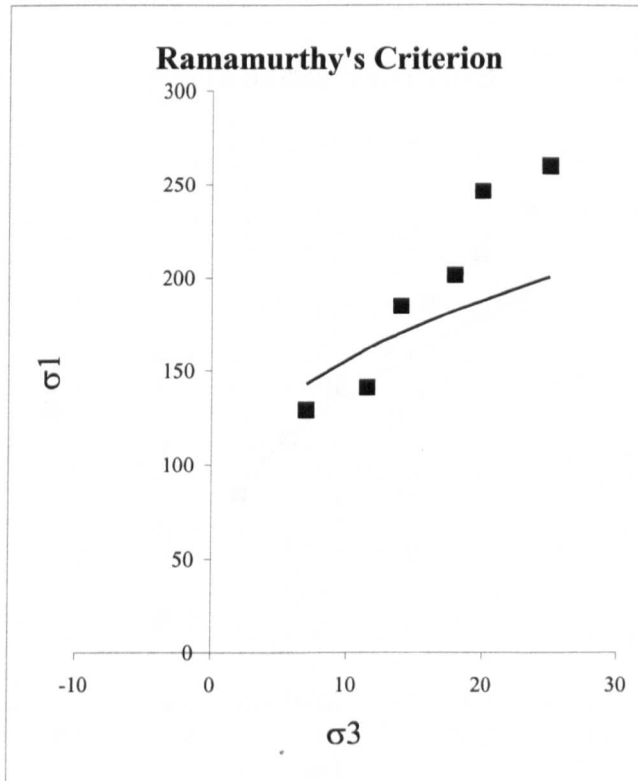
## Coal Measure Seat earth (East Midlands)



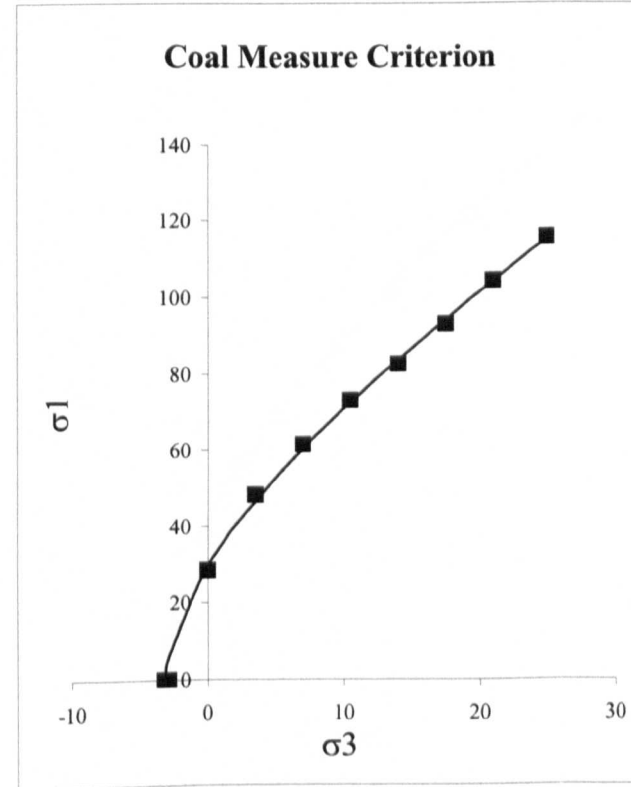
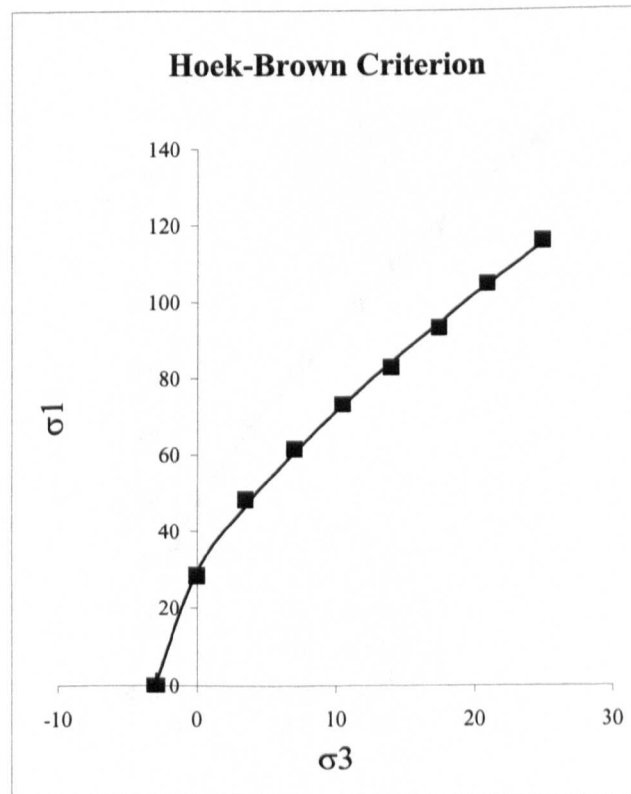
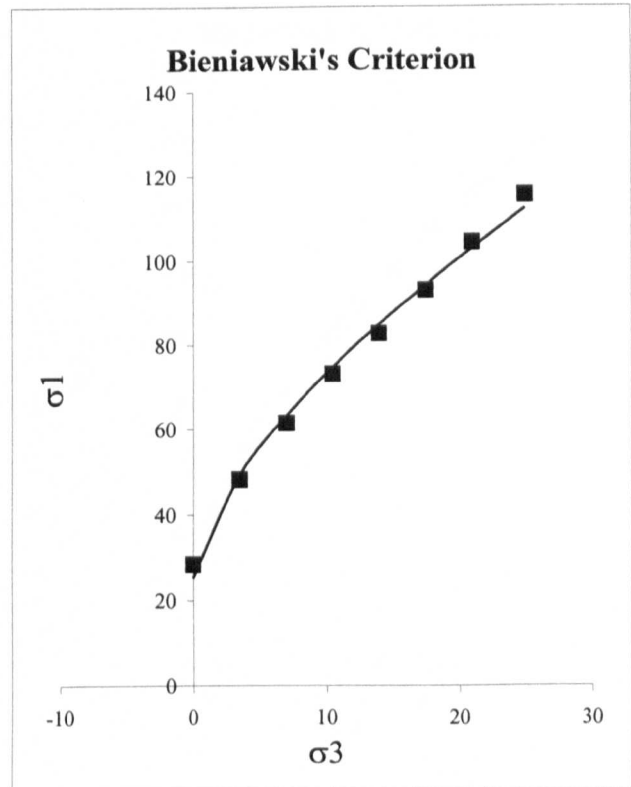
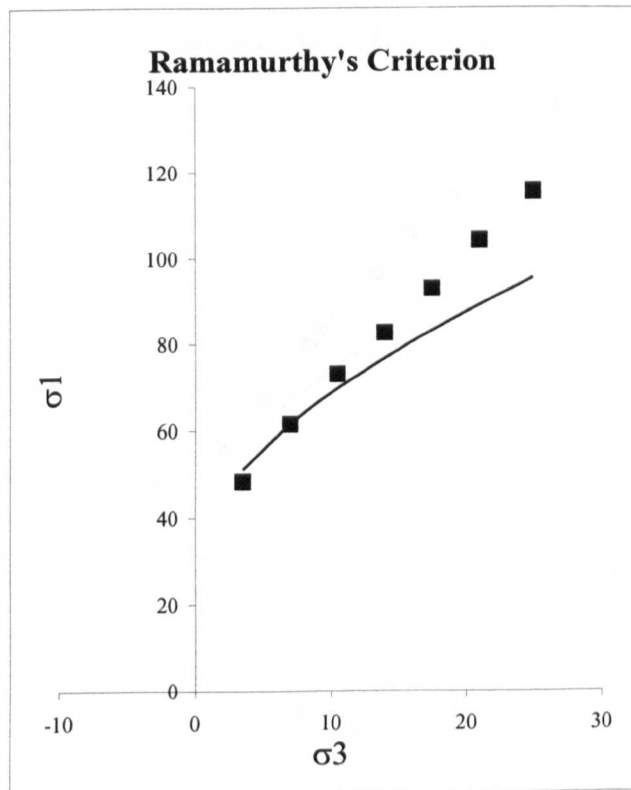
## Coal Measure Mudstone (Westfield 2)



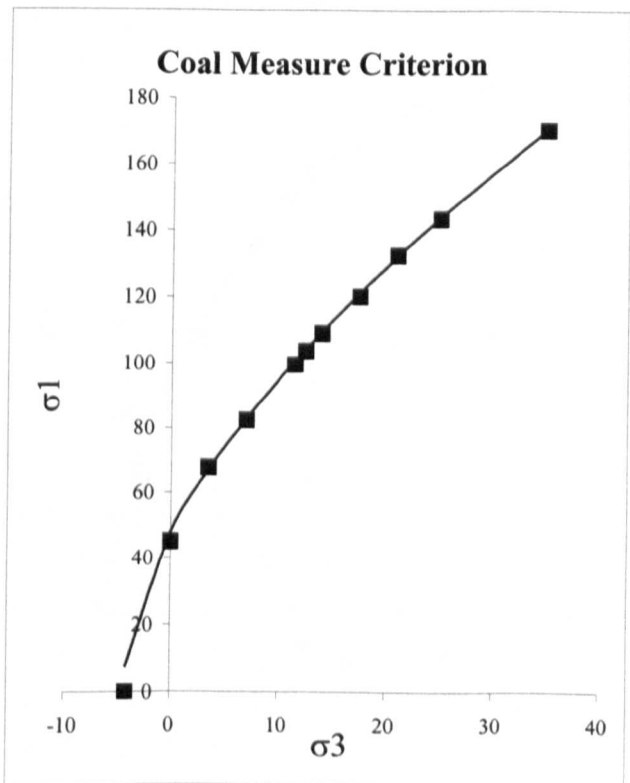
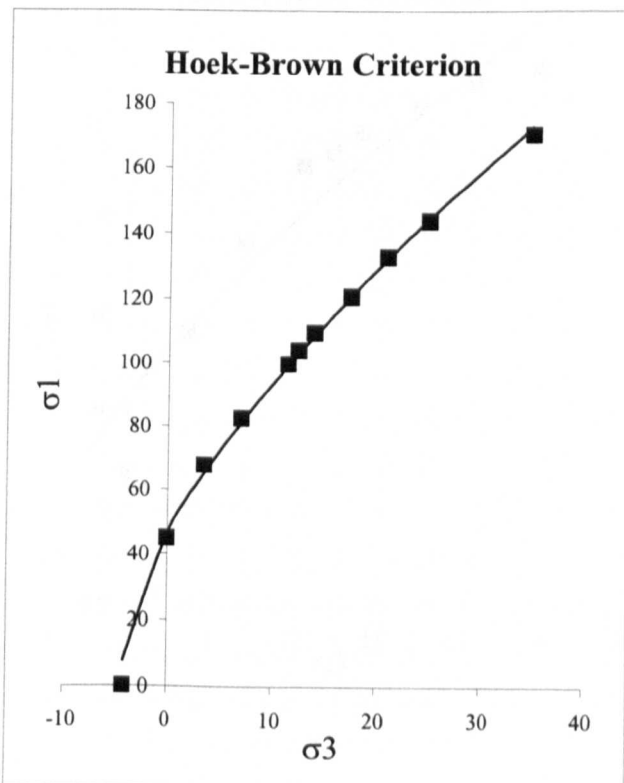
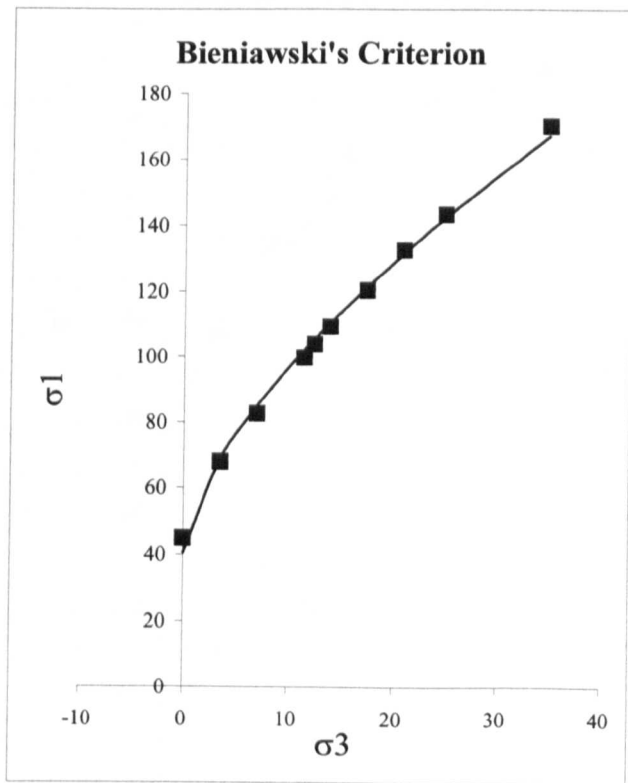
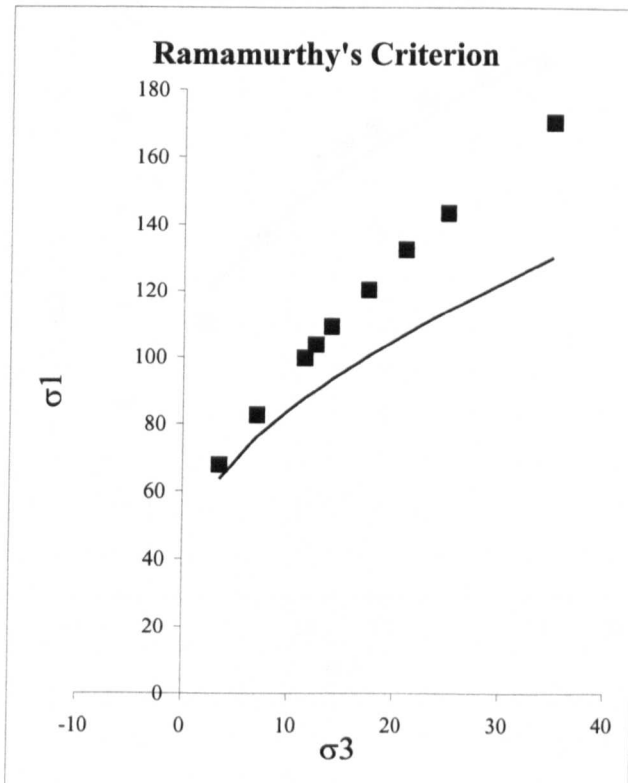
## Coal Measure Mudstone (Westfield 1)



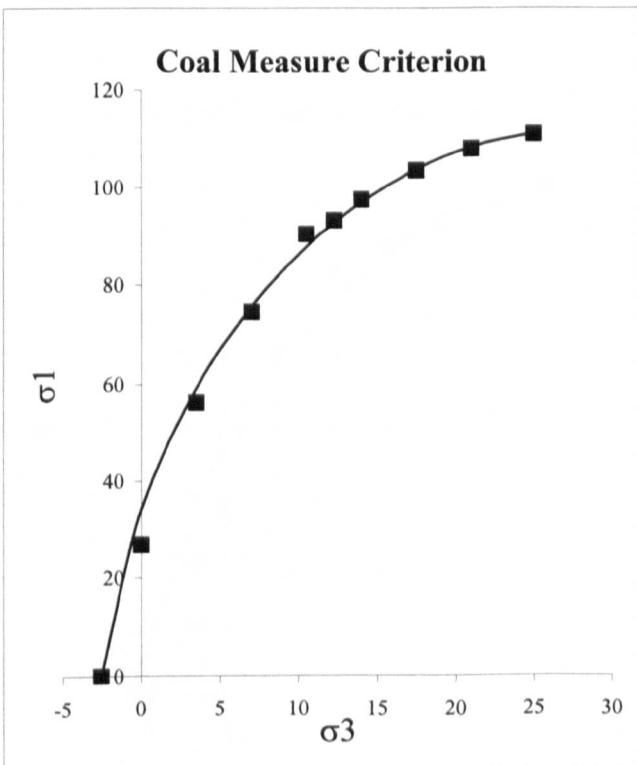
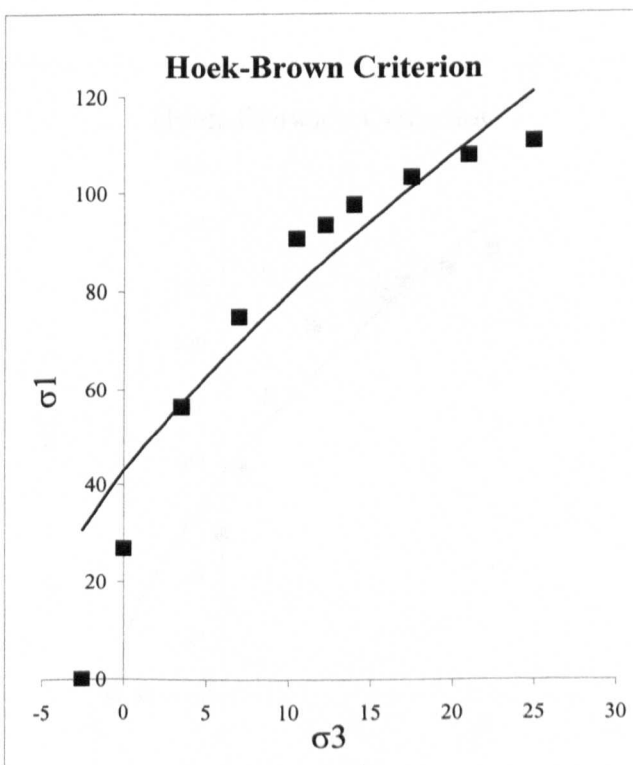
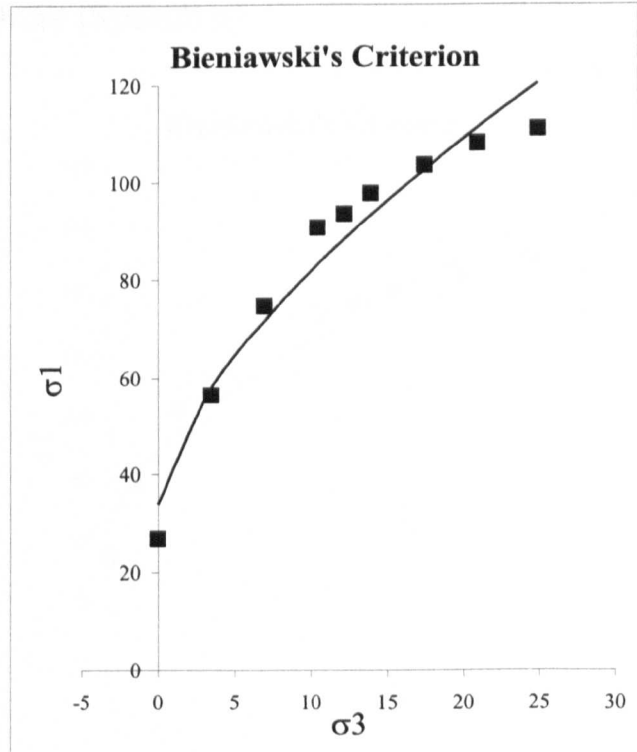
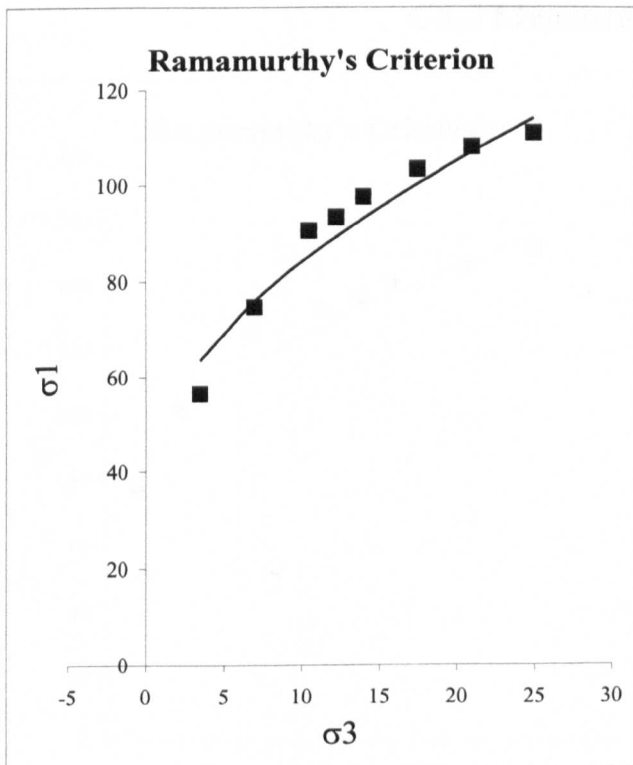
### Coal Measure Mudstone (Shipley)



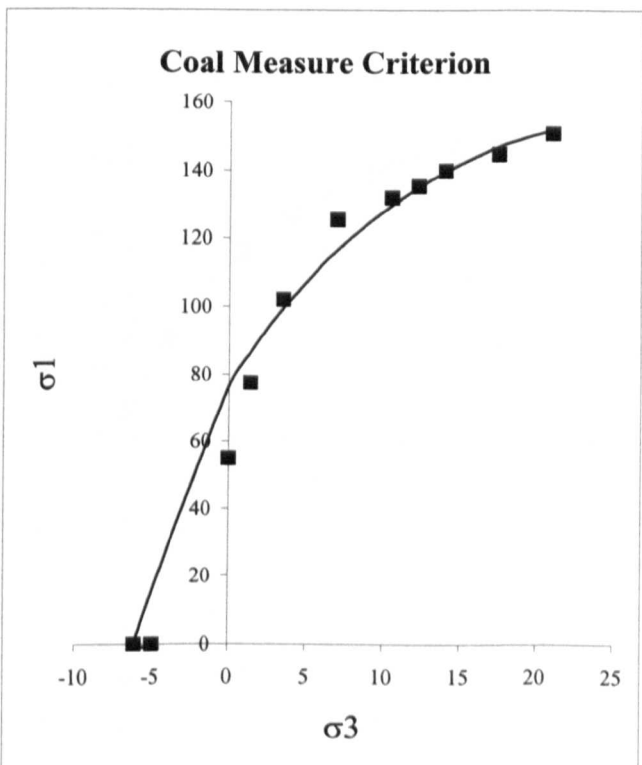
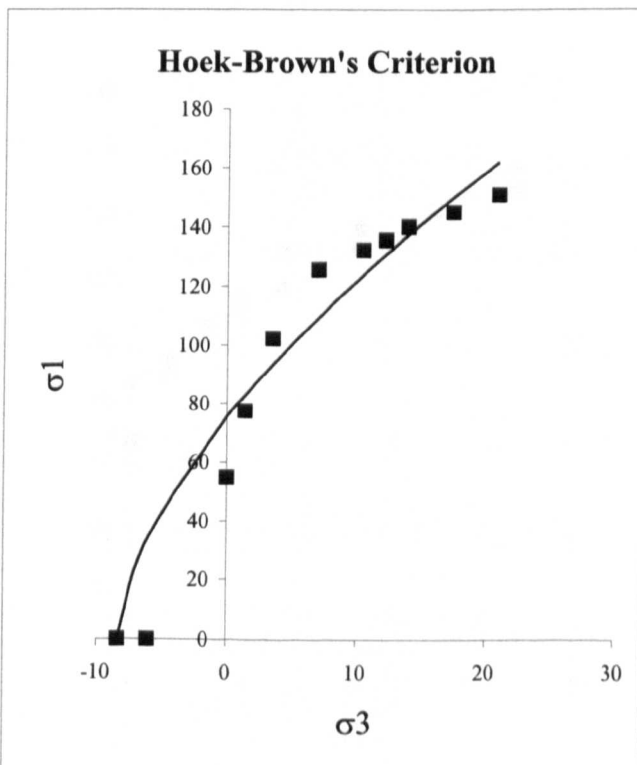
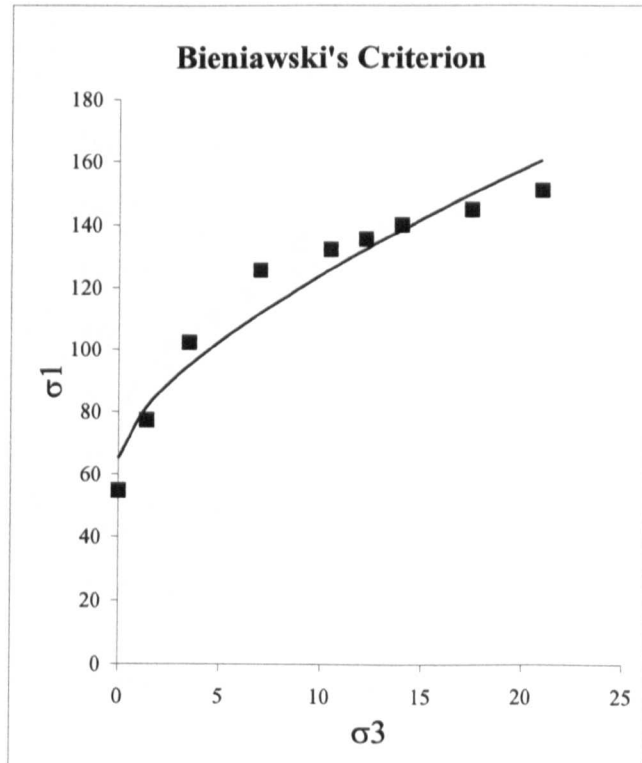
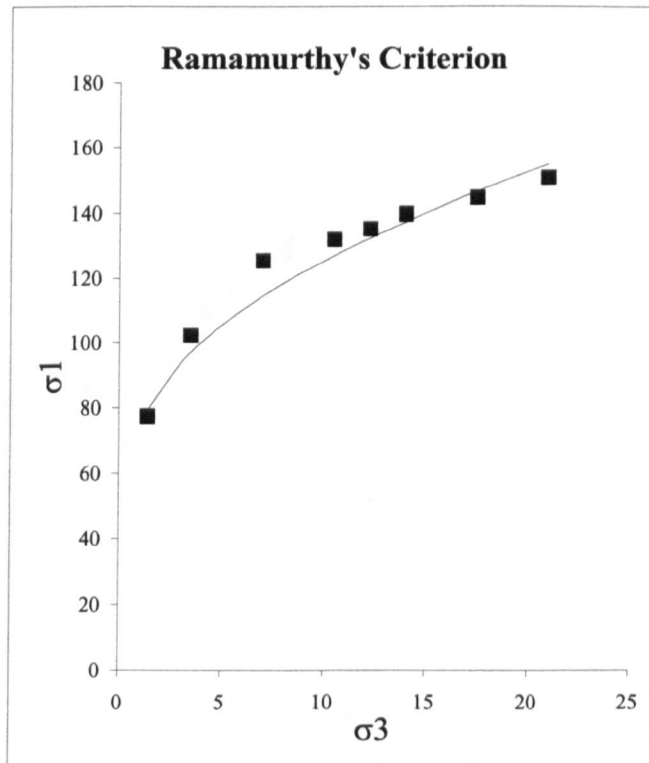
## Coal Measure Mudstone (Pye Hill)



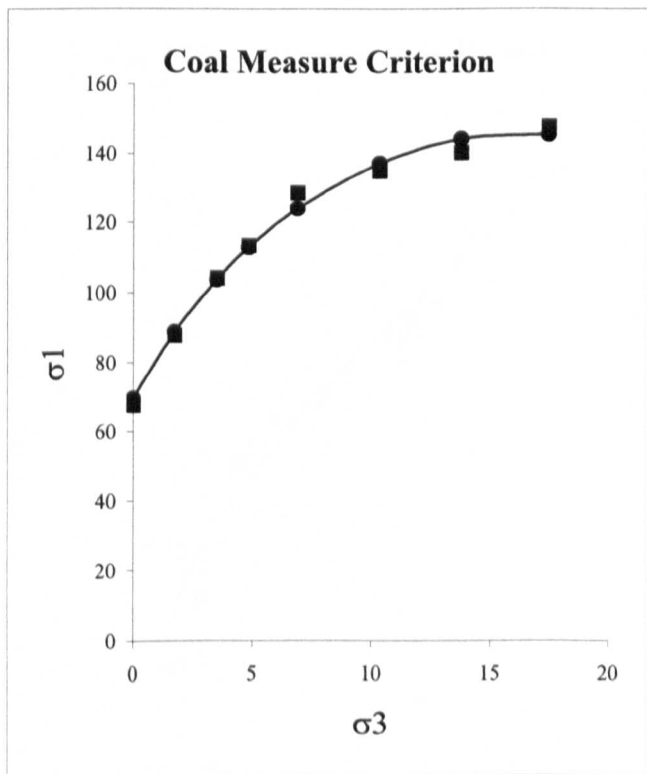
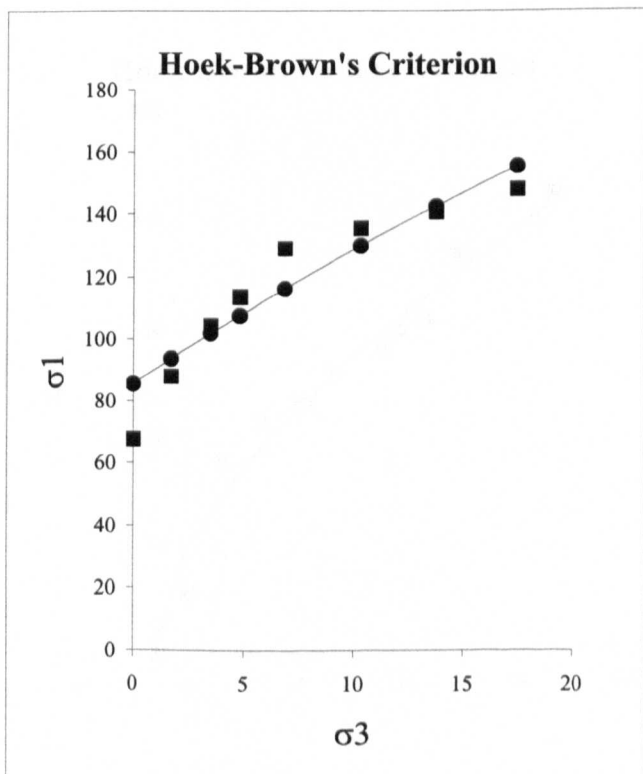
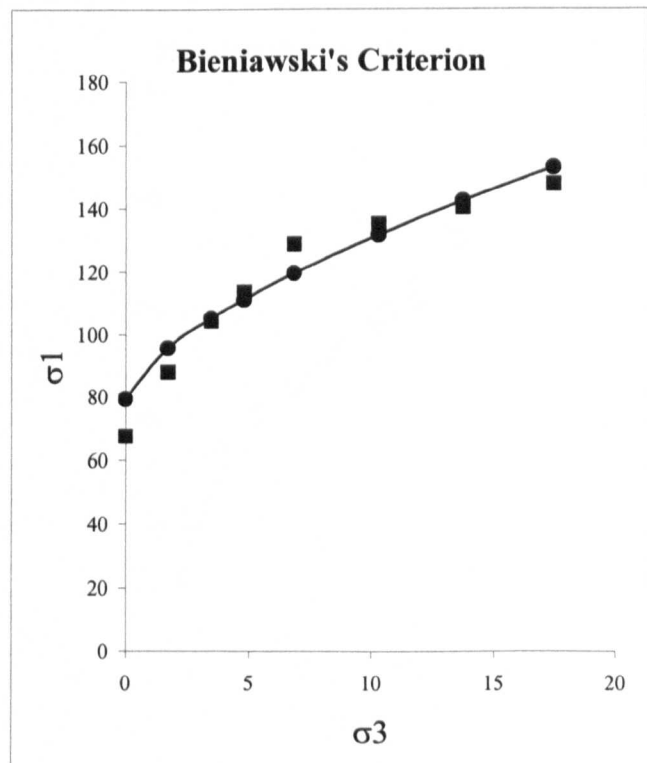
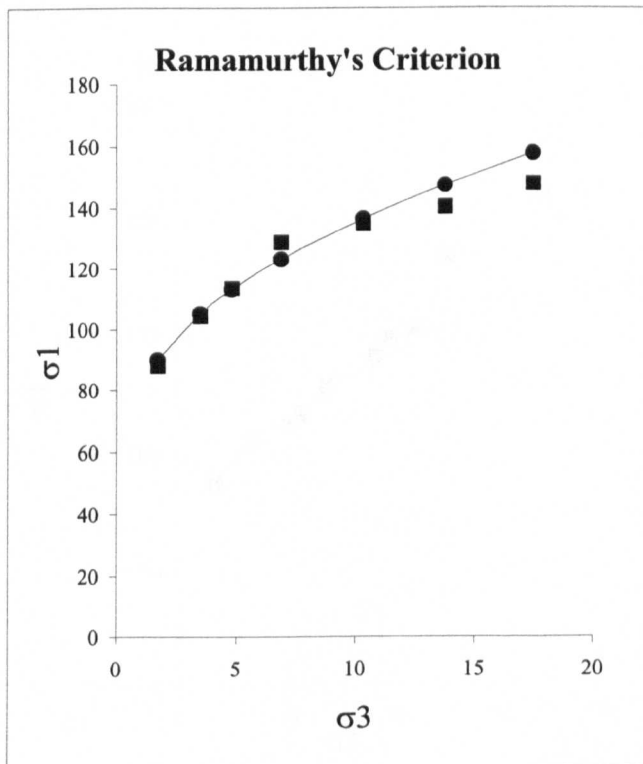
## Coal Measure Mudstone (Morrell's Wood)



## Coal Measure Siltstone (Spondon)

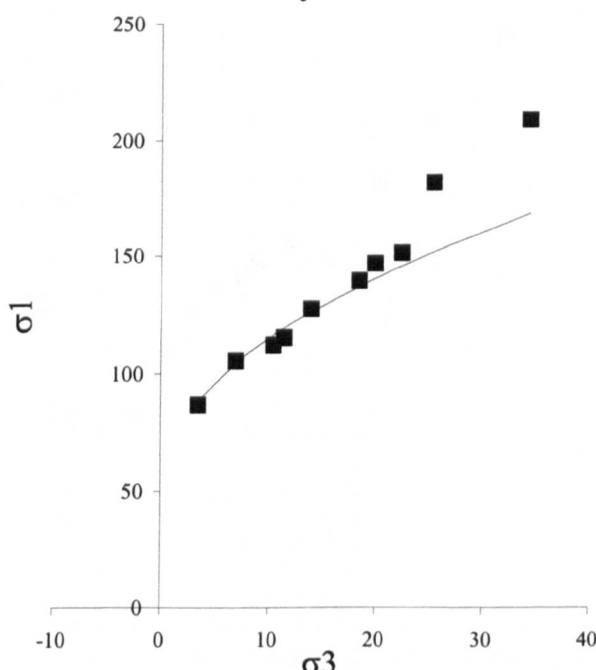


## Coal Measure Siltstone (Shipley)

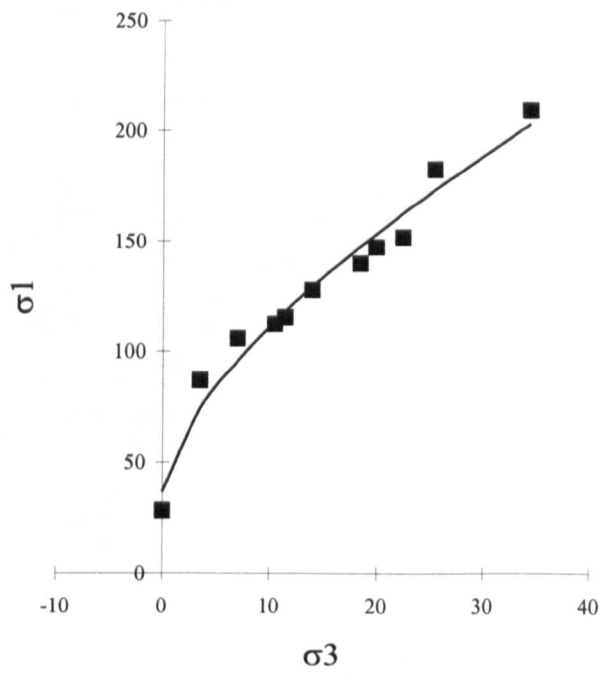


## Coal Measure Medium Grained Sandstone (Westfield)

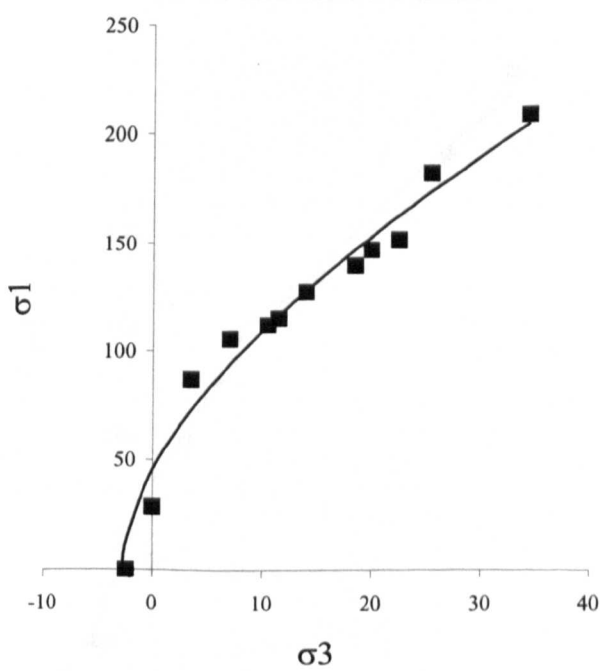
**Ramamurthy's Criterion**



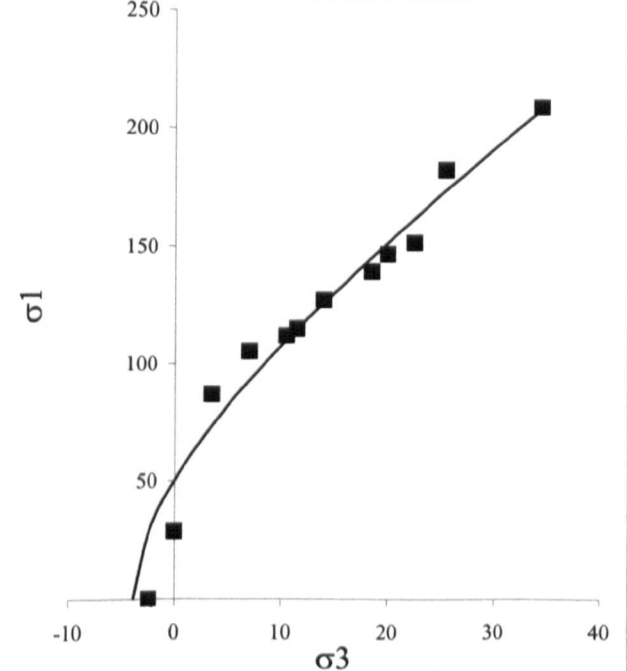
**Bieniawski's Criterion**



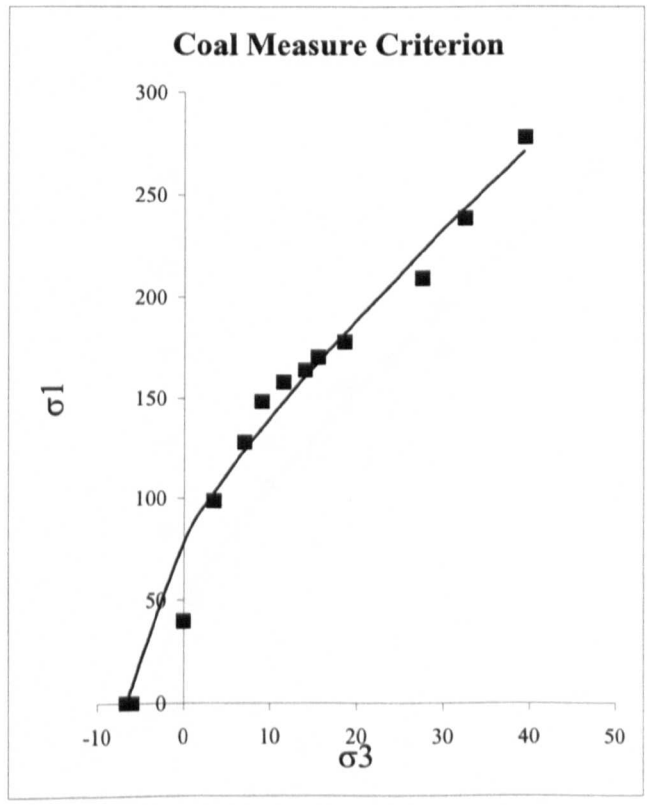
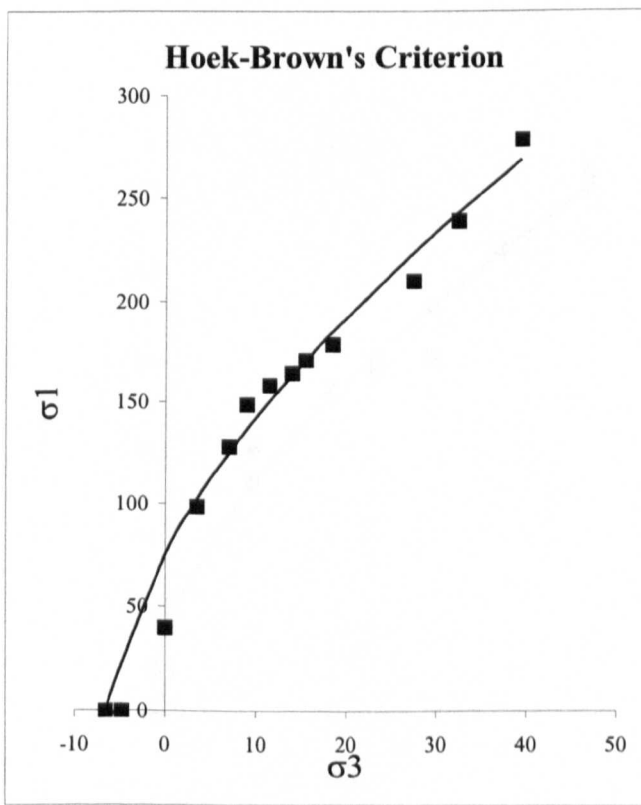
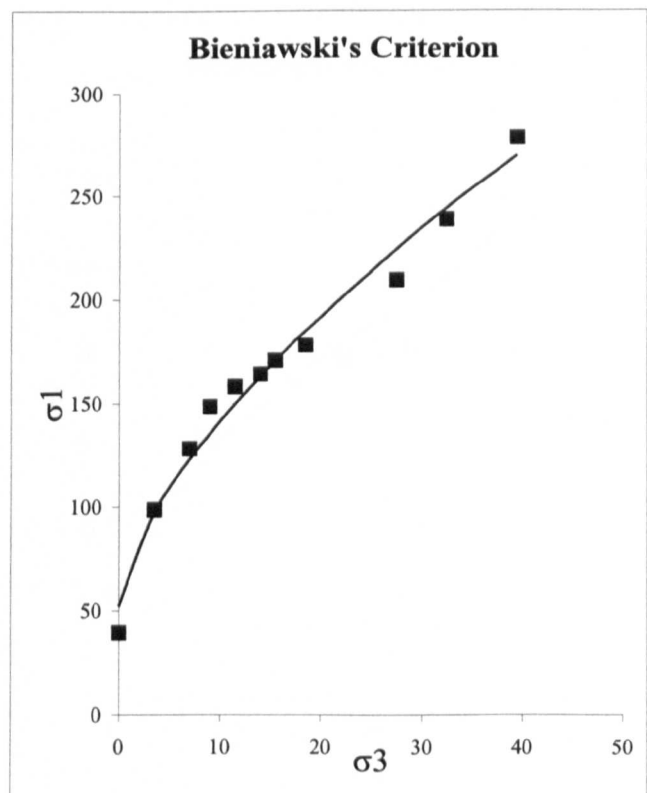
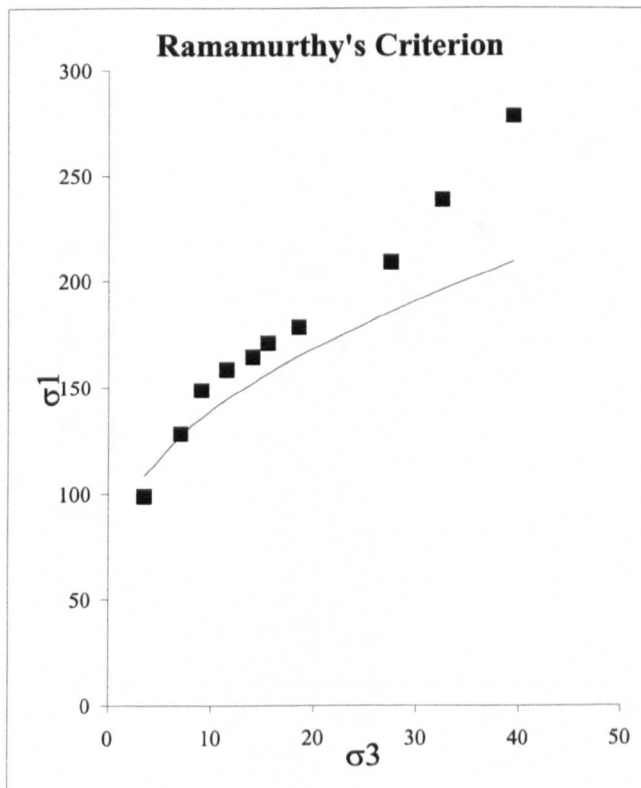
**Hoek-Brown Failure Criterion**



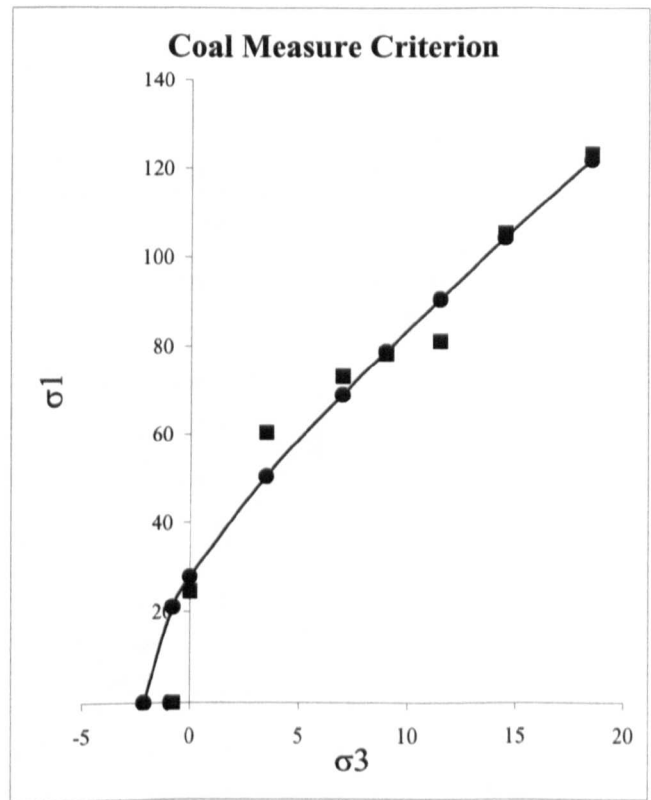
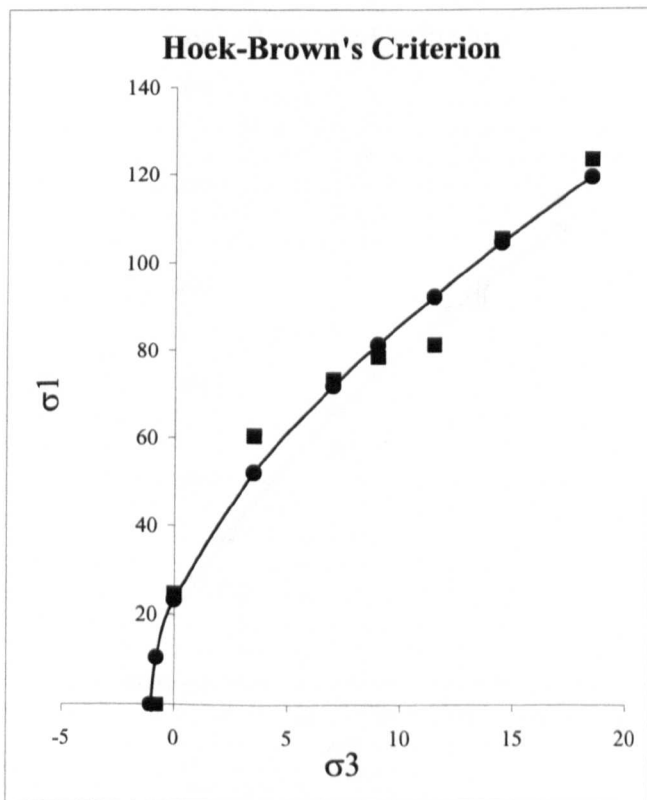
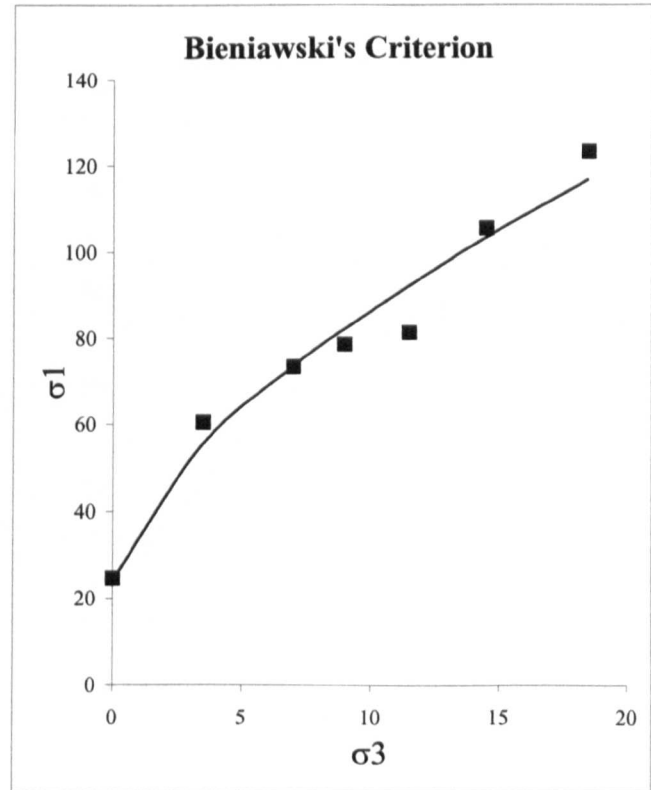
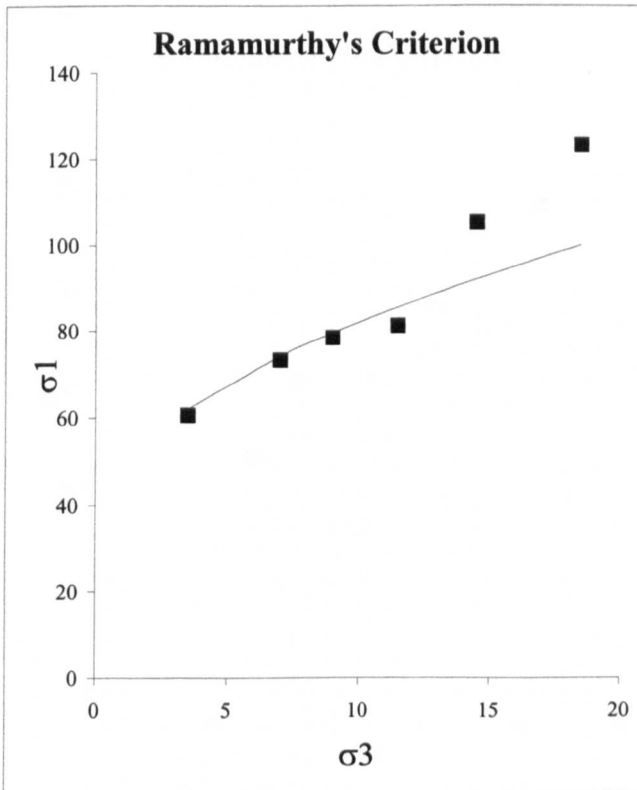
**Coal Measure Failure Criterion**



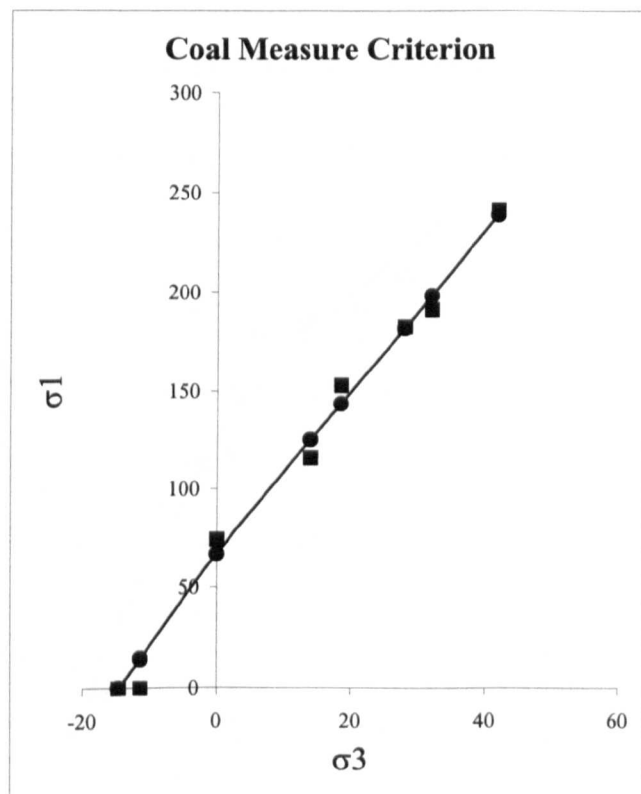
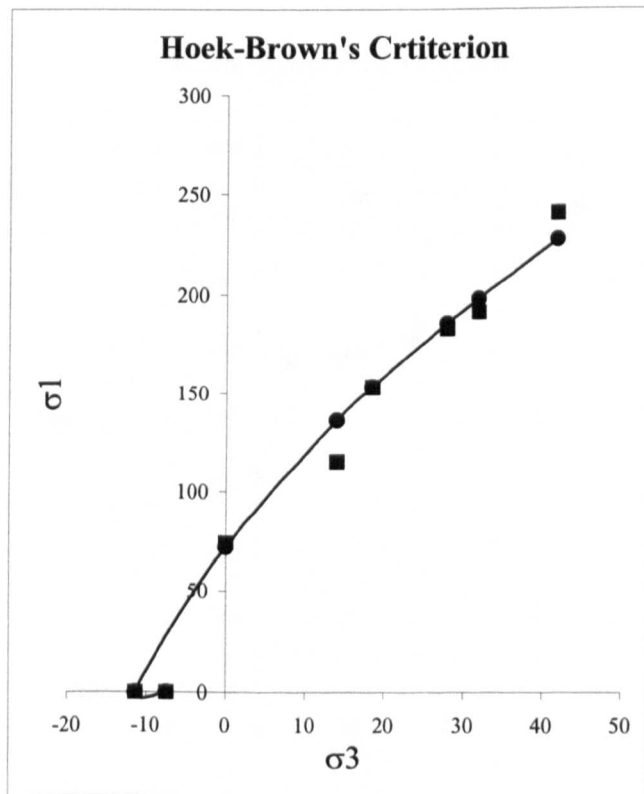
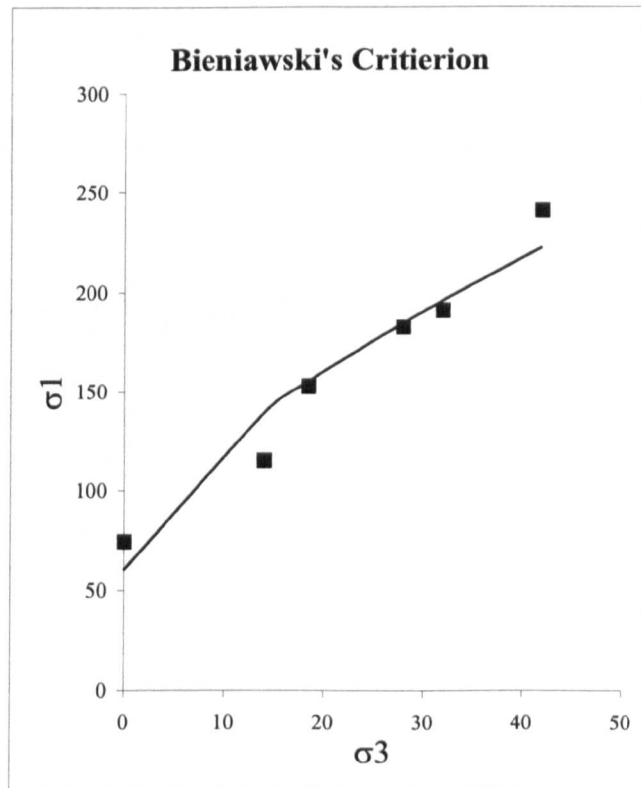
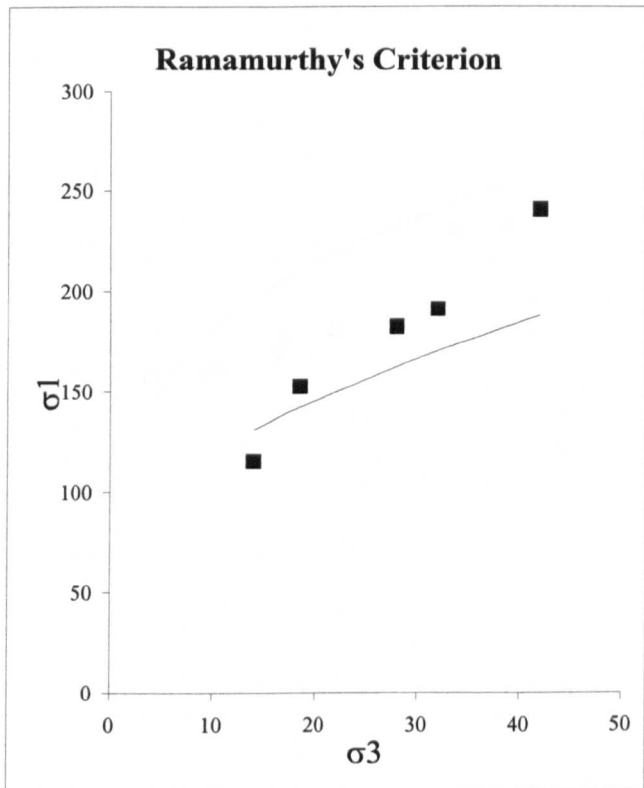
### Coal Measure Sandstone (Westfield)



### Coal Measure Coarse Grained Sandstone (Westfield)

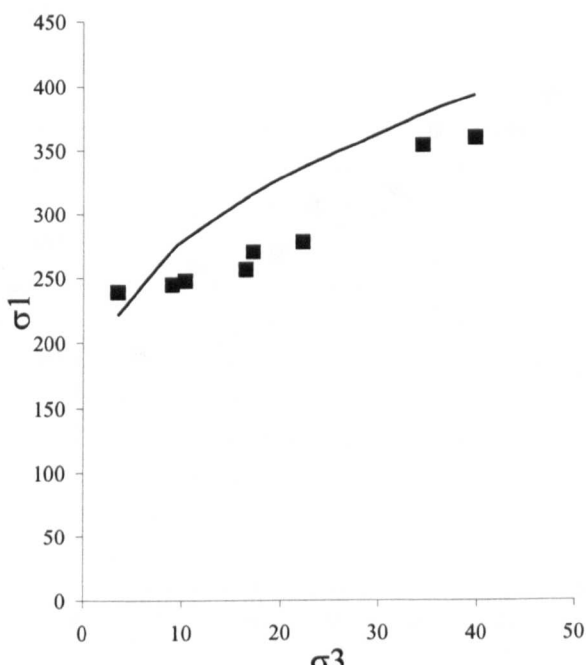


## Coal Measure Medium Grained Sandstone (Shipley)

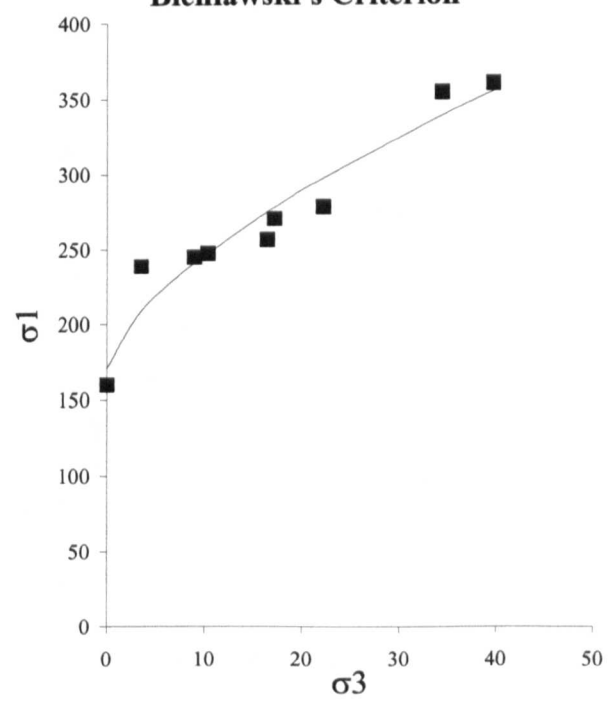


## Coal Measure Sandstone (Pennant Grit)

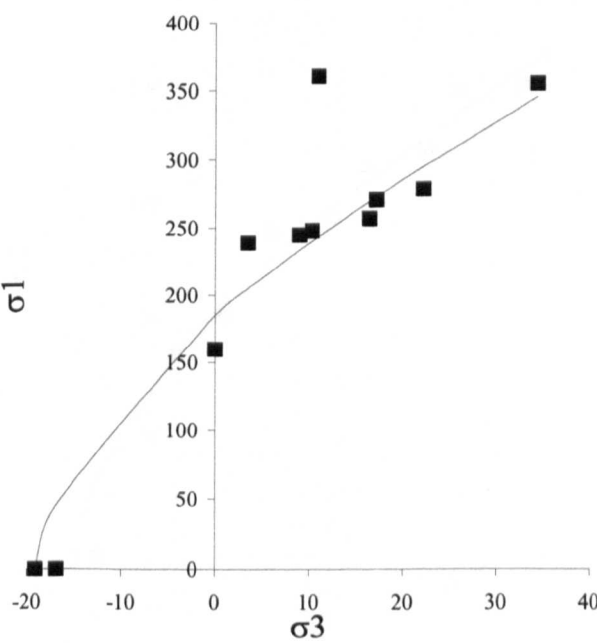
Ramamurthy's Criterion



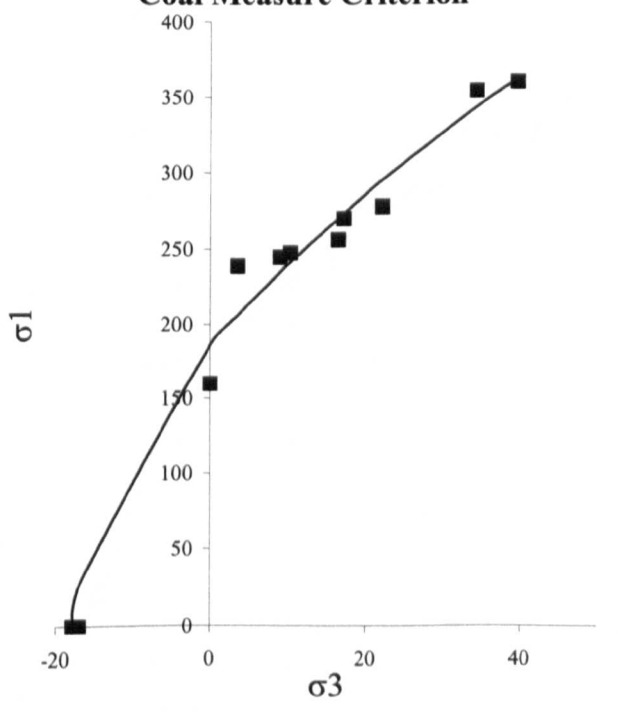
Bieniawski's Criterion



Hoek-Brown's Criterion

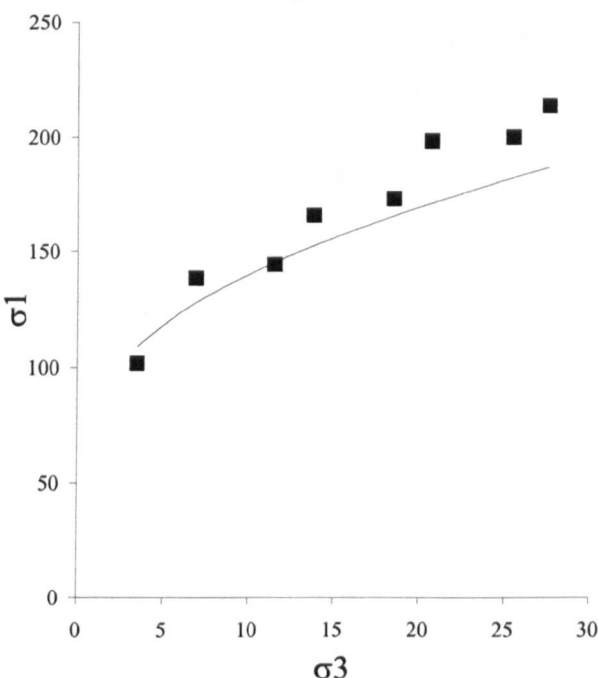


Coal Measure Criterion

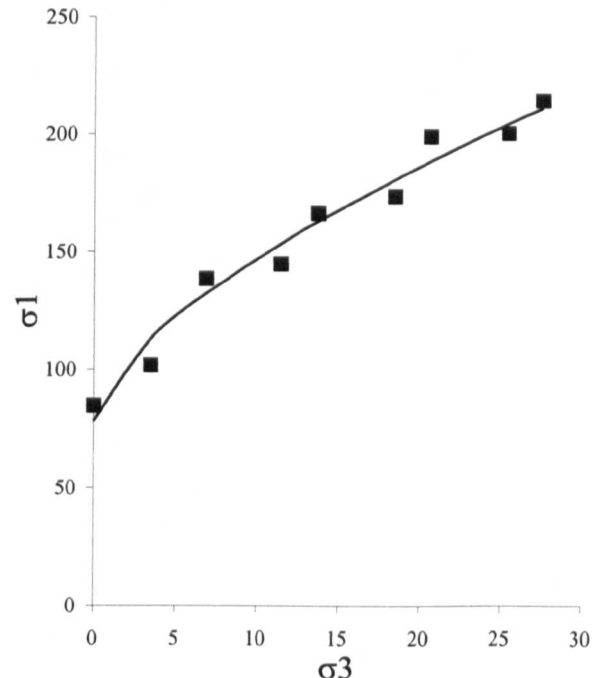


## Coal Measure Fine Grained Sandstone (More Green)

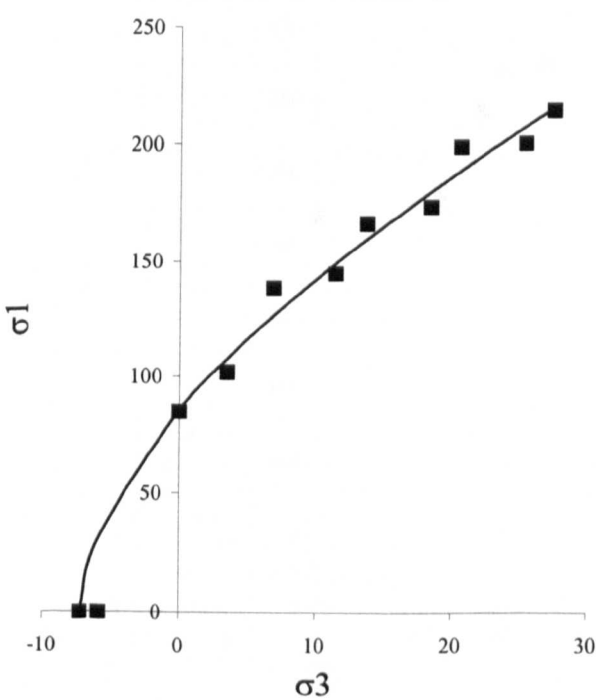
Ramamurthy's Criterion



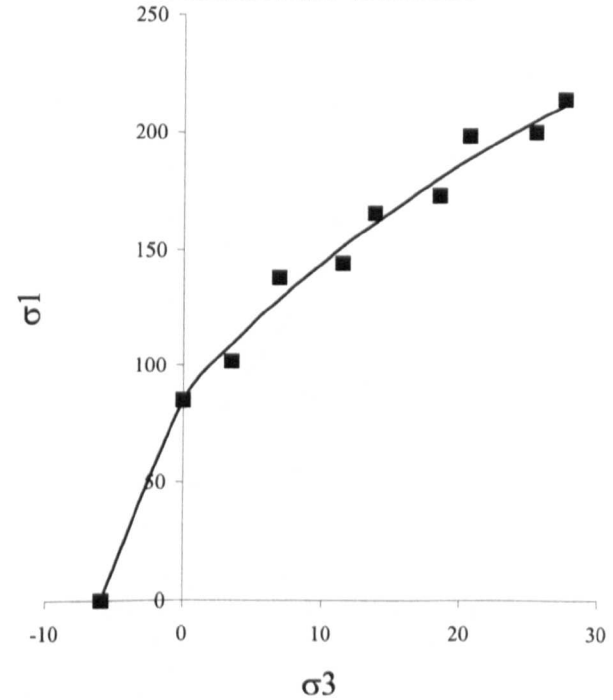
Bieniawski's Criterion



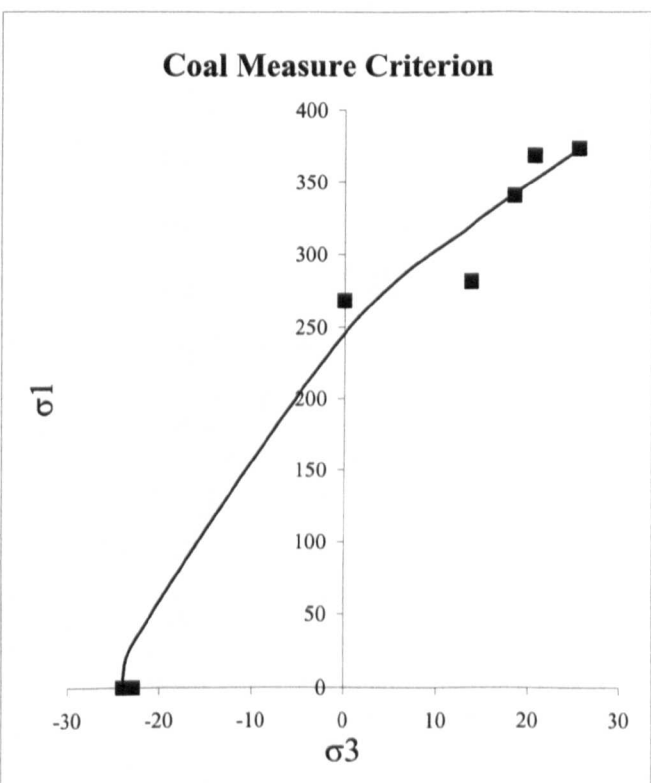
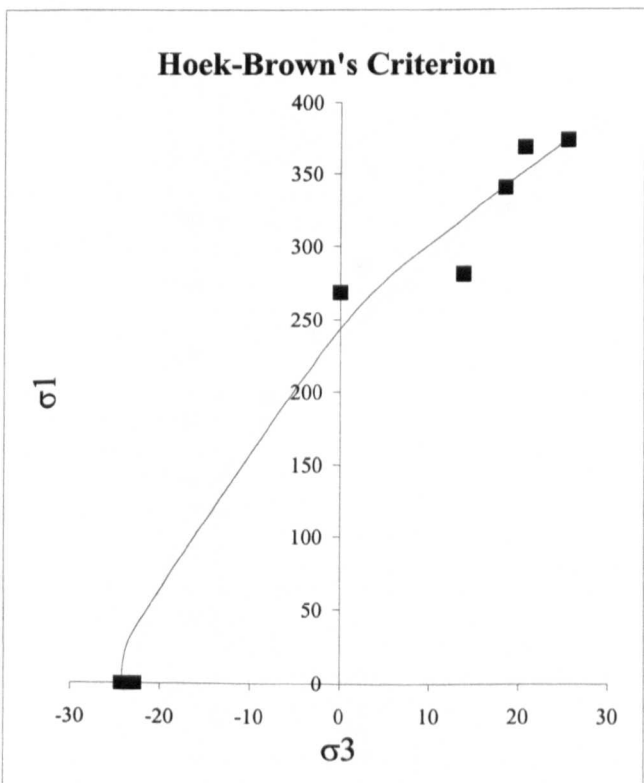
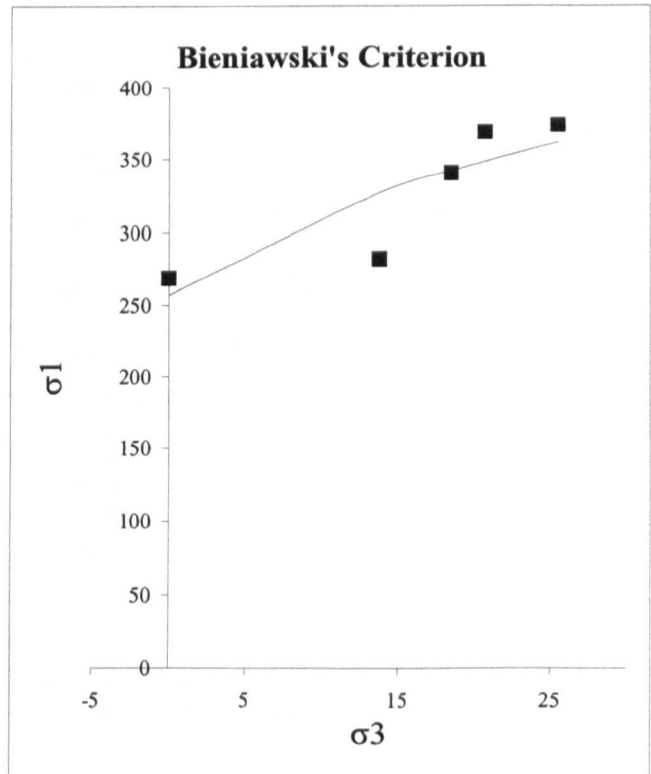
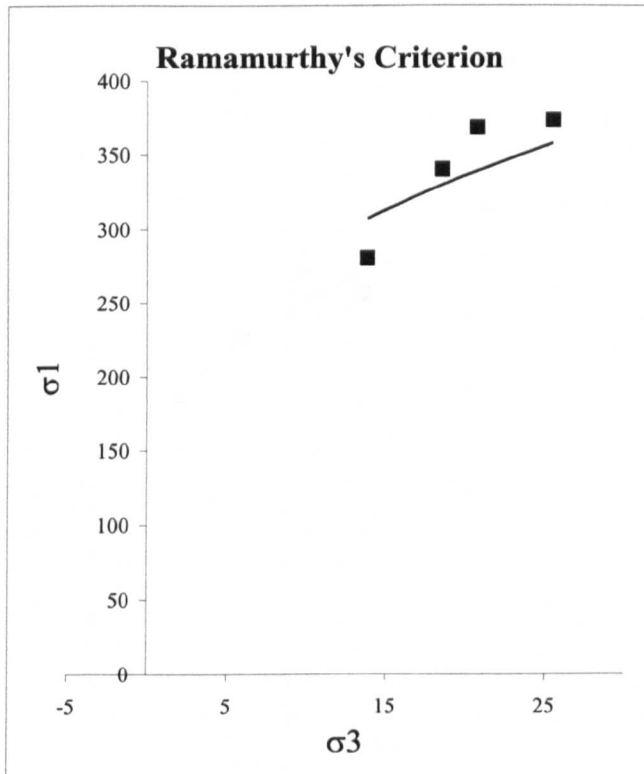
Hoek-Brown's Criterion



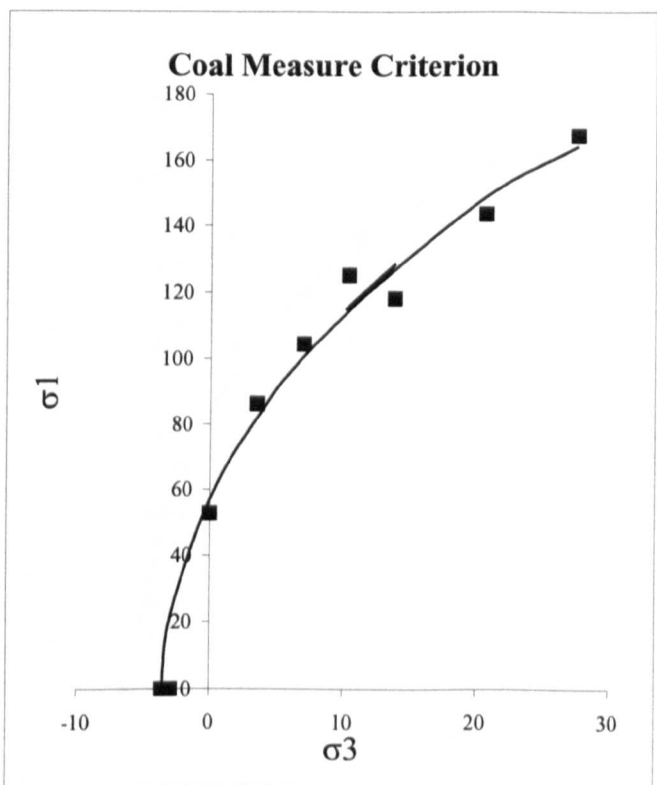
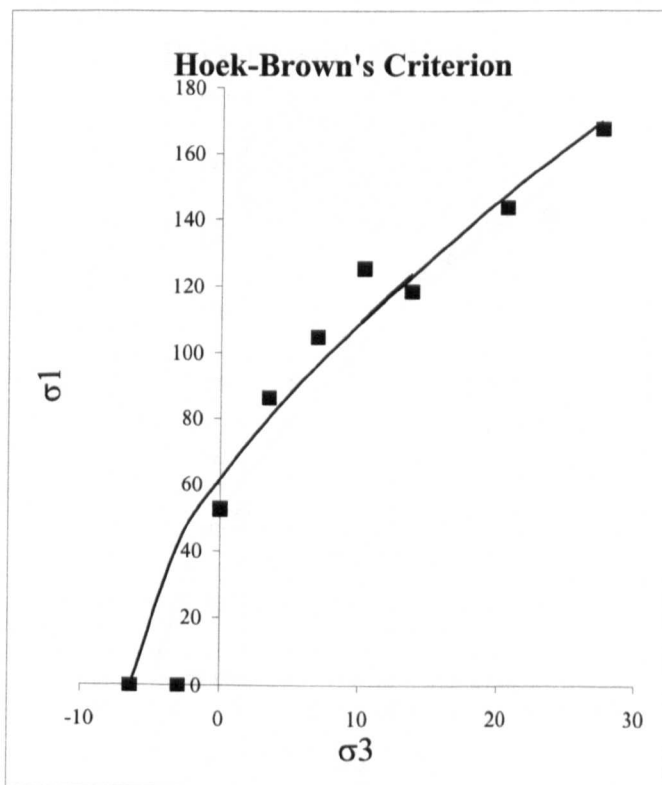
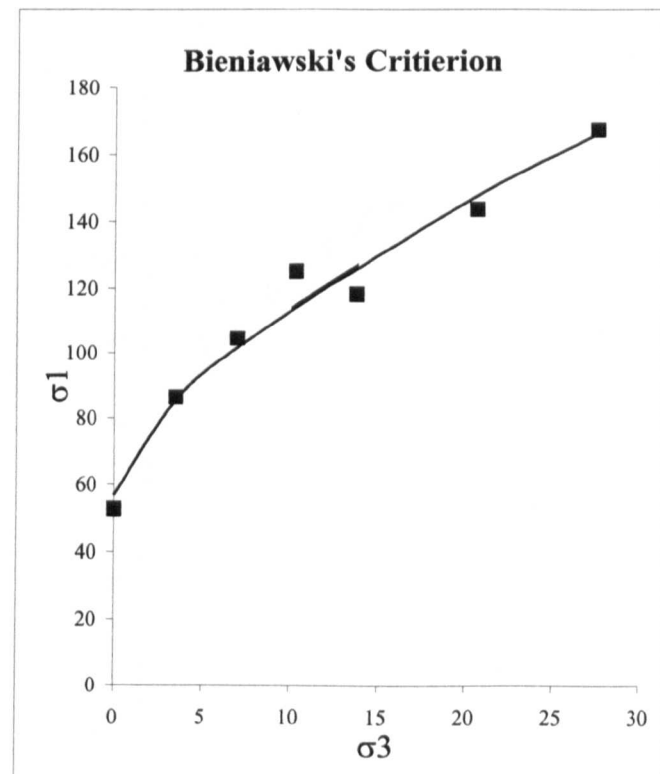
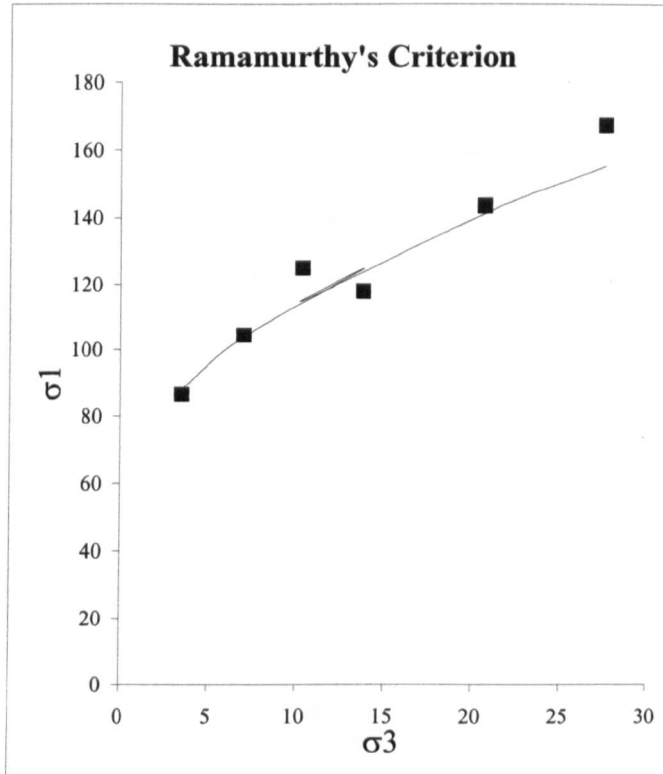
Coal Measure Criterion



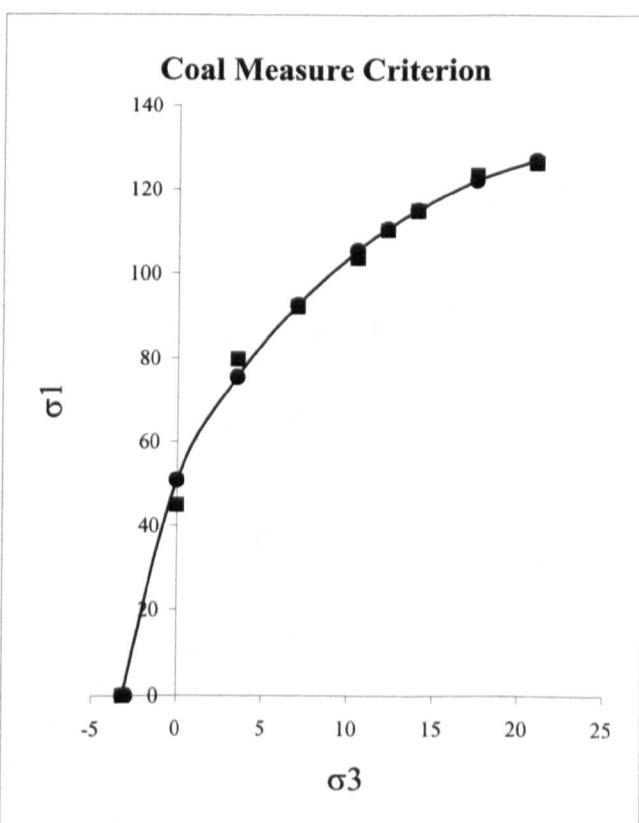
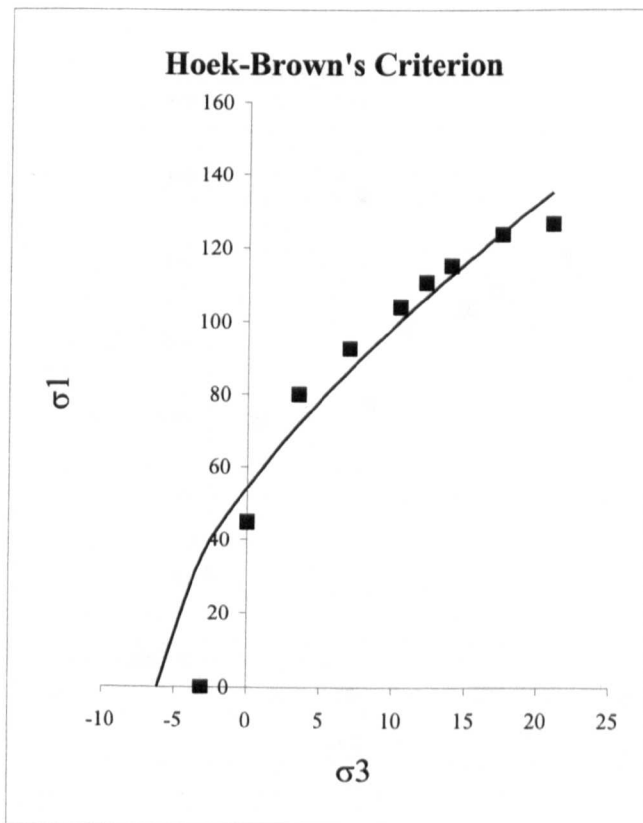
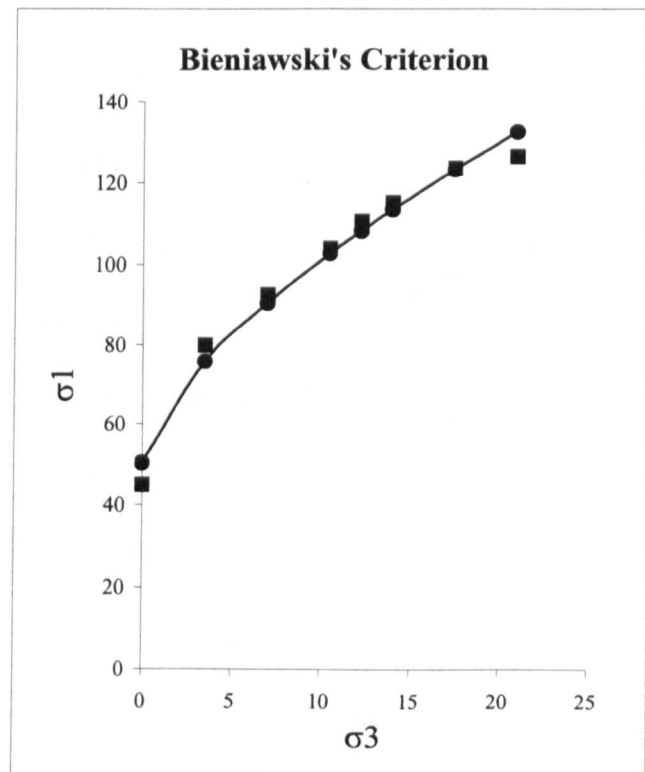
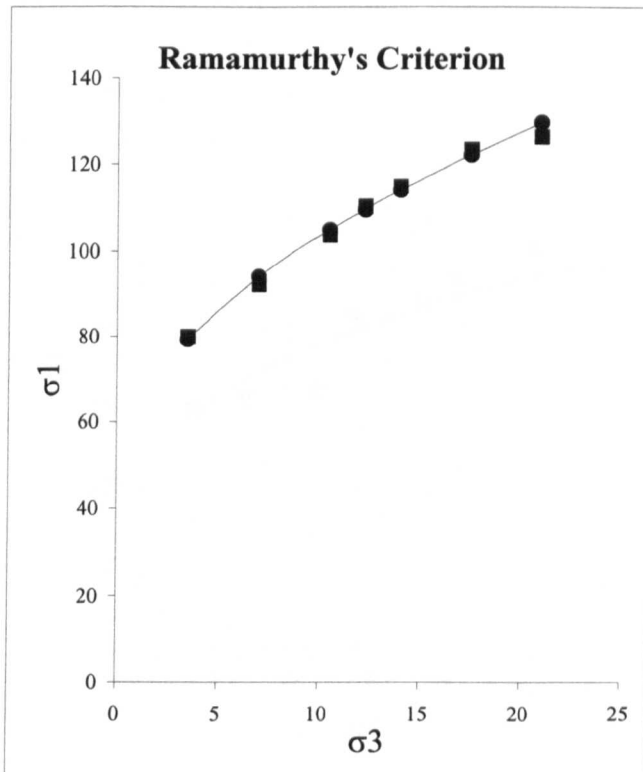
## Coal Measure Sandstone (Meadowgate)



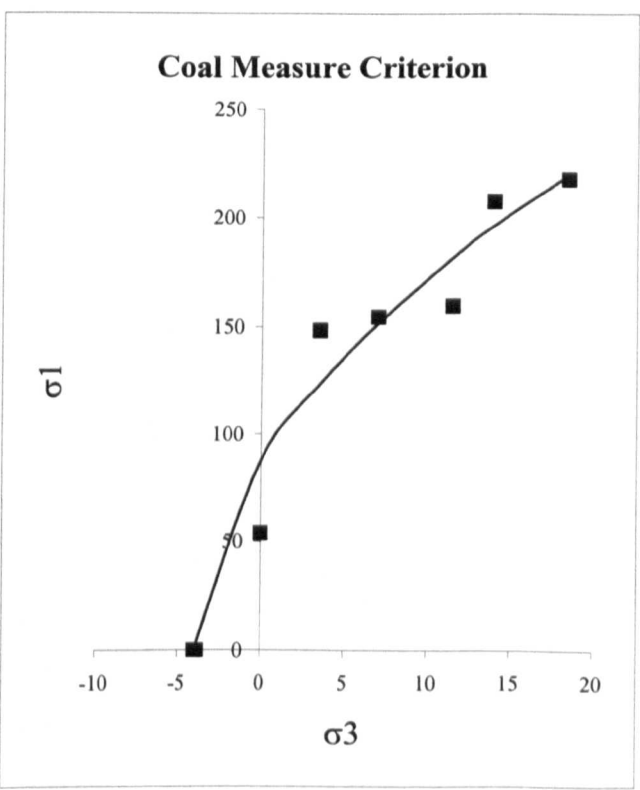
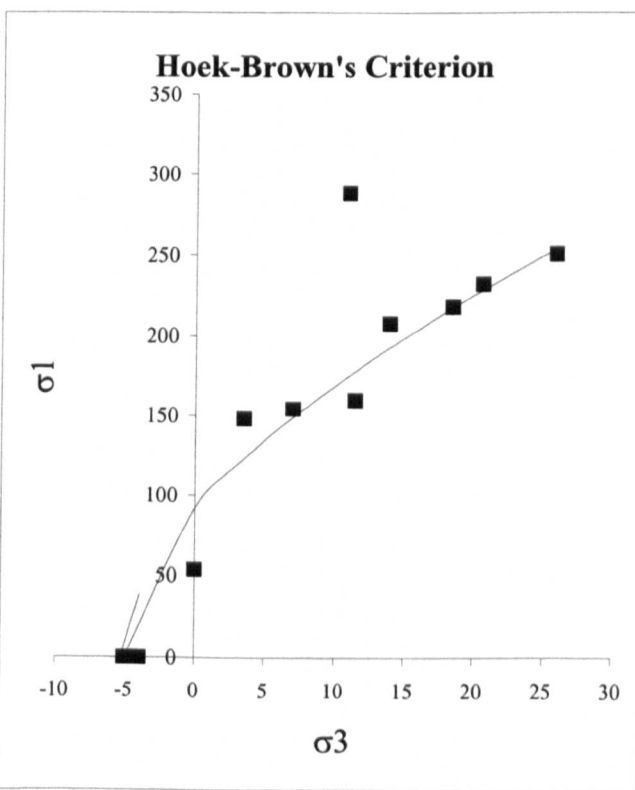
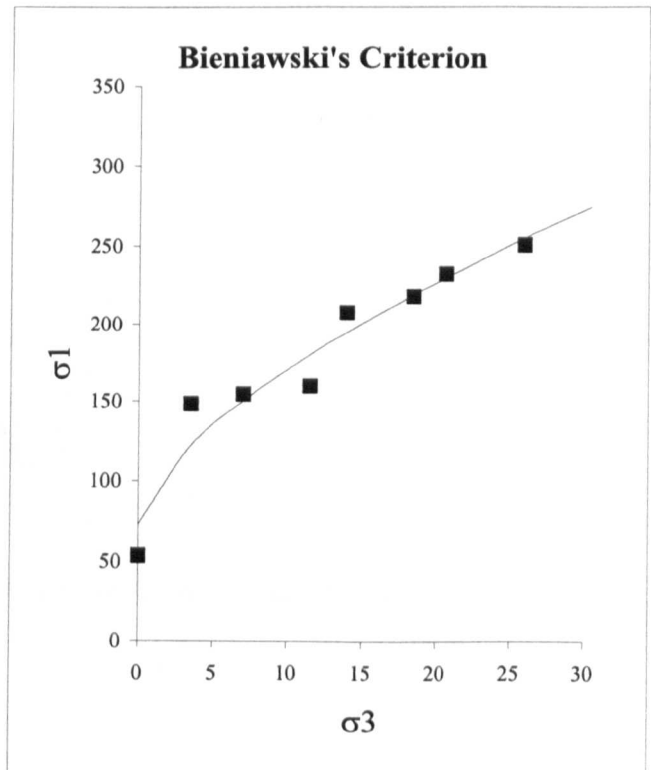
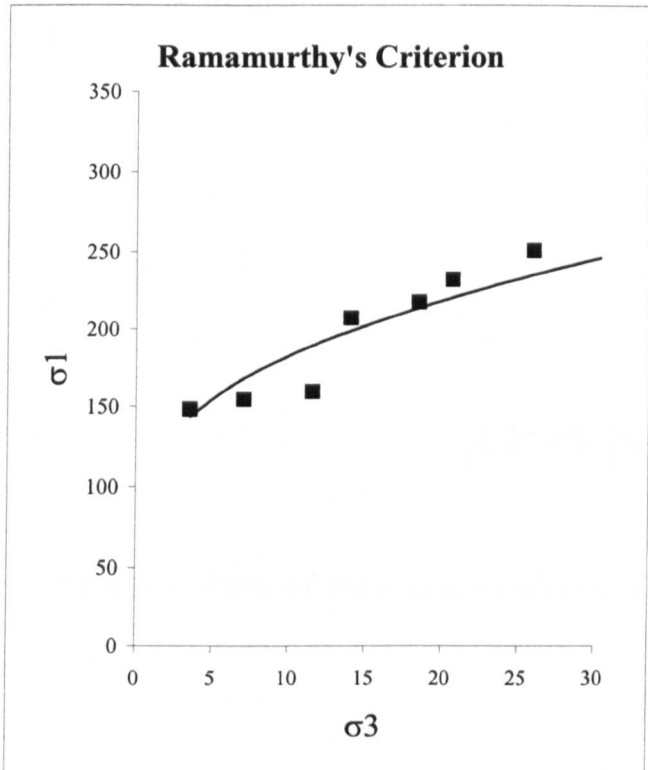
## Coal Measure Medium Grained Sandstone (Lynmouth)



### Coal Measure Sandstone (Low Close)



## Coal Measure Sandstone (Darley Dale)



## **APPENDIX 3**

Summary Sheets of Rock Test Results and Coal Mine Classification Data Sheets

LOCATION: Riccall Mine, Panel 438 main gate 214 metre mark

LOCATION: Riccall Mine, Panel 478, main gate, 31 metre mark

LOCATION: Riccall Mine, Panel 478, main gate, 110 metre mark

**LOCATION:** Riccall Mine, Panel 478 main gate 387 metre mark

LOCATION: Riccall Mine, Panel 478, main gate, 486 metre mark

LOCATION: Riccall Mine, Panel 478, main gate, 587 metre mark

**LOCATION:** Riccall Mine, Panel 478 main gate 710 metre mark

LOCATION: Riccall Mine, Panel 505, tail gate, 353 metre mark

LOCATION: Riccall Mine, Panel 505, tail gate, 922 metre mark

LOCATION: Riccall Mine, Panel 505 main gate 669 metre mark

LOCATION: Riccall Mine, Panel 505, main gate, 902 metre mark

LOCATION: Riccall Mine, Panel 505, main gate, 1528 metre mark

**CLASSIFICATION DATA SHEET**

mine	RICCALL	coal seam	BARNESLEY
panel	438	gate	MAIN
panel orientation	56	metre	214

		unit number	1	2	3	4
	height above seam roof	0.12 to 0.72	0.72 to 1.06	1.06 to 4.01	4.01 to 5.04	
	basic rock type	grey mudstn	grey mudstn	grey mudstn	grey mudstn	
	UCS (MPa)	41	48	57	53	
bedding/ lamination properties	bed/lam spacing (m)	0.017	0.031	0.038	0.031	
	topography	planar	planar	planar	planar	
	roughness (JRC)	4	4	4	4	
	cohesion (% ucs)	0	0	0	0	
	parting planes (No.)	25	28	3	15	
	joint/cleat set no.	2	2	2	2	
joint persistence/ cleat dominance	set 1	p	p	p	p	
	set 2	np	np	np	np	
	set 3	-	-	-	-	
joint/cleat roughness	set 1	4	4	4	4	
	set 2	4	4	4	4	
	set 3	-	-	-	-	
average spacing	set 1	1000	1000	1000	1000	
	set 2	1000	1000	1000	1000	
	set 3	-	-	-	-	
strike orient (0-180)	set 1	98	98	98	98	
	set 2	17	17	17	17	
	set 3	-	-	-	-	
	fissility ratio (0 to 1)	0.3	0.3	0.32	0.42	
moisture sensitivity	not required	*	*	*	*	
	Duncan's Free Swell Coeff.					
	groundwater condition	dry	dry	dry	dry	

**CLASSIFICATION DATA SHEET**

mine	RICCALL	coal seam:	Barnsley
panel	478	gate	MAIN
panel orientation	55	metre	31

		unit number	1	2	3	
		height above seam roof	0.4 to 0.74	0.74 to 1.4	1.4 to 5.4	
		basic rock type	grey m.stone	grey m.stone	mass. siltstn	
		UCS (MPa)	51	52	57	
bedding/ lamination properties	bed/lam spacing (m)	0.034	0.11	1		
		planar	planar	planar		
	topography	5	4	4		
		0	0	0		
	roughness (JRC)	10	6	4		
		parting planes (No.)	2	2	2	
joint persistence/ cleat dominance	set 1	p	p	p		
		np	np	np		
		-	-	-		
joint/cleat roughness	set 1	4	4	4		
		4	4	4		
		-	-	-		
average spacing	set 1	1000	1000	1000		
		1000	1000	1000		
		-	-	-		
strike orient (0-180)	set 1	98	98	98		
		17	17	17		
		-	-	-		
		fissility ratio (0 to 1)	0.46	0.46	0.73	
		not required	*	*	*	
moisture sensitivity	Duncan's Free Swell Coeff.					
	groundwater condition		dry	dry	dry	

**CLASSIFICATION DATA SHEET**

mine	RICCALL	coal seam	BARNESLEY
panel	478	gate	MAIN
panel orientation	55	metre	110

		unit number	1	2	3
		height above seam roof	0.2 to 0.55	0.55 to 1.05	1.05 to 5.2
		basic rock type	drkgrey m.stone	grey m.stone	mass. siltstn
		UCS (MPa)	21	49	54
bedding/ lamination properties		bed/lam spacing (m)	0.022	0.125	2.07
		topography	planar	planar	planar
		roughness (JRC)	4	4	3
		cohesion (% ucs)	0	0	0
		parting planes (No.)	16	4	2
		joint/cleat set no.	2	2	2
joint persistence/ cleat dominance		set 1	p	p	p
		set 2	np	np	np
		set 3	-	-	-
		set 1	4	4	4
joint/cleat roughness		set 2	4	4	4
		set 3	-	-	-
		set 1	1000	1000	1000
average spacing		set 2	1000	1000	1000
		set 3	-	-	-
		set 1	98	98	98
strike orient (0-180)		set 2	17	17	17
		set 3	-	-	-
		fissility ratio (0 to 1)	0.2	0.32	0.67
moisture sensitivity		not required	*	*	*
		Duncan's Free Swell Coeff.			
		groundwater condition	dry	dry	dry

**CLASSIFICATION DATA SHEET**

mine	RICCALL	coal seam	BARNESLEY
panel	478	gate	MAIN
panel orientatio	55	metre	387

		unit number	1	2	3	4	
		height above seam roof	0.4 to 1.13	1.13 to 1.45	1.45 to 2.00	2.00 to 5.32	
		basic rock type	grey m.stone	drk grey m.stone	grey m.stone	massive siltstn	
		UCS (MPa)	56	30	69	57	
bedding/ lamination properties		bed/lam spacing (m)	0.09	0.026	0.11	0.13	
		topography	planar	planar	planar	planar	
		roughness (JRC)	4	4	4	4	
		cohesion (% ucs)	0	0	0	0	
		parting planes (No.)	8	12	5	25	
		joint/cleat set no.	2	2	2	2	
joint persistence/ cleat dominance		set 1	p	p	p	p	
		set 2	np	np	np	np	
		set 3	-	-	-	-	
		set 1	4	4	4	4	
joint/cleat roughness		set 2	4	4	4	4	
		set 3	-	-	-	-	
		set 1	1000	1000	1000	1000	
		set 2	1000	1000	1000	1000	
		set 3	-	-	-	-	
average spacing		set 1	98	98	98	98	
		set 2	17	17	17	17	
		set 3	-	-	-	-	
		fissility ratio (0 to 1)	0.5	0.2	0.5	0.73	
moisture sensitivity		not required	*	*	*	*	
		Duncan's Free Swell Coeff.					
		groundwater condition	dry	dry	dry	dry	

**CLASSIFICATION DATA SHEET**

mine	RICCALL	coal seam	BARNESLEY
panel	478	gate	MAIN
panel orientation	55	metre	486

		unit number	1	2	3	4	
		height above seam roof	0.56 to 1.26	1.26 to 2.26	2.26 to 4.5	4.5 to 5.4	
		basic rock type	mass	lami	lami	lami	
		UCS (MPa)	73	56	69	51	
bedding/ lamination properties	bed/lam spacing (m)	0.05	0.02	0.005	0.05		
		planar	planar	planar	planar		
	roughness (JRC)	10	10	10	10		
		64	55	81	82		
	parting planes (No.)	3	4	9	4		
		joint/cleat set no.	2	2	2	2	
joint persistence/ cleat dominance	set 1	p	p	p	p		
		np	np	np	np		
		-	-	-	-		
joint/cleat roughness	set 1	4	4	4	4		
		4	4	4	4		
		-	-	-	-		
average spacing	set 2	1000	1000	1000	1000		
		1000	1000	1000	1000		
		-	-	-	-		
strike orient (0-180)	set 1	98	98	98	98		
		17	17	17	17		
		-	-	-	-		
		fissility ratio (0 to 1)	1	1	1	1	
		not required	*	*	*	*	
moisture sensitivity	Duncan's Free Swell Coeff.						
	groundwater condition	dry	dry	dry	dry		

**CLASSIFICATION DATA SHEET**

mine	RICCALL	coal seam	Barnsley
panel	478	gate	MAIN
panel orientation	55	metre	587

		unit number	1	2	3	4	5	6	7
		height above seam roof	0.6 to 1.6	1.6 to 2.13	2.13 to 2.35	2.35 to 3.02	3.02 to 3.97	3.97 to 4.53	4.53 to 6.14
		basic rock type	grey m.stone	lamin siltstn	lamin siltstn	lamin siltstn	lamin siltstn	mass. siltstn	lamin siltstn
		UCS (MPa)	52	68	83	66	73	71	78
bedding/ lamination properties		bed/lam spacing (m)	0.1	0.02	0.005	0.01	0.003	0.56	0.005
		topography	planar	planar	planar	planar	planar	planar	planar
		roughness (JRC)	4	8	4	6	8	6	8
		cohesion (% ucs)	0	75	46	85	58	0	73
		parting planes (No.)	10	1	8	2	16	1	21
		joint/cleat set no.	2	2	2	2	2	2	2
joint persistence/ cleat dominance		set 1	p	p	p	p	p	p	p
		set 2	np	np	np	np	np	np	np
		set 3	-	-	-	-	-	-	-
joint/cleat roughness		set 1	4	4	4	4	4	4	4
		set 2	4	4	4	4	4	4	4
		set 3	-	-	-	-	-	-	-
average spacing		set 1	1000	1000	1000	1000	1000	1000	1000
		set 2	1000	1000	1000	1000	1000	1000	1000
		set 3	-	-	-	-	-	-	-
strike orient (0-180)		set 1	98	98	98	98	98	98	98
		set 2	17	17	17	17	17	17	17
		set 3	-	-	-	-	-	-	-
		fissility ratio (0 to 1)	0.52	1	1	1	1	0.92	1
moisture sensitivity		not required	*	*	*	*	*	*	*
		Duncan's Free Swell Coeff.							
		groundwater condition	dry	dry	dry	dry	dry	dry	dry

**CLASSIFICATION DATA SHEET**

mine	RICCALL	coal seam	BARNESLEY
panel	478	gate	MAIN
panel orientation	55	metre	710

		unit number	1	2	3	4
		height above seam roof	0.6 to 1.28	1.28 to 2.63	2.63 to 4.8	4.8 to 5.6
		basic rock type	drkgrey m.stone	grey m.stone	mass. siltstn	s.stone
		UCS (MPa)	38	62	81	57
bedding/ lamination properties	bed/lam spacing (m)	0.031	0.27	0.79	0.3	
	topography	planar	planar	planar	planar	
	roughness (JRC)	2	3	3	6	
	cohesion (% ucs)	0	0	0	0	
	parting planes (No.)	22	5	4	2	
	joint/cleat set no.	2	2	2	2	
joint persistence/ cleat dominance	set 1	p	p	p	p	
	set 2	np	np	np	np	
	set 3	-	-	-	-	
joint/cleat roughness	set 1	4	4	4	4	
	set 2	4	4	4	4	
	set 3	-	-	-	-	
average spacing	set 1	1000	1000	1000	1000	
	set 2	1000	1000	1000	1000	
	set 3	-	-	-	-	
strike orient (0-180)	set 1	98	98	98	98	
	set 2	17	17	17	17	
	set 3	-	-	-	-	
	fissility ratio (0 to 1)	0.2	0.81	0.64	1	
	not required	*	*	*	*	
moisture sensitivity	Duncan's Free Swell Coeff.					
	groundwater condition	dry	dry	dry	dry	

**CLASSIFICATION DATA SHEET**

mine	RICCALL	coal seam	BARNESLEY
panel	505	gate	Tail
panel orientation	147	metre	353

		unit number	1	2	3	4
		height above seam roof	0.6 to 2.8	2.8 to 3.7	3.7 to 4.9	4.9 to 5.6
		basic rock type	drkgrey m.stone	grey m.stone	s.stone	s.stone
		UCS (MPa)	22	46	47	134
bedding/ lamination properties	bed/lam spacing (m)	0.022	0.053	0.014	0.07	
		topography	planar	planar	planar	planar
		roughness (JRC)	4	4	6	4
	cohesion (% ucs)	0	0	0	0	
		parting planes (No.)	101	15	87	10
	joint/cleat set no.	2	2	2	2	
joint persistence/ cleat dominance	set 1	p	p	p	p	
		np	np	np	np	
		-	-	-	-	
	set 2	4	4	4	4	
		4	4	4	4	
joint/cleat roughness	set 3	-	-	-	-	
		4	4	4	4	
		-	-	-	-	
	set 1	1000	1000	1000	1000	
average spacing	set 2	1000	1000	1000	1000	
		-	-	-	-	
	set 3	98	98	98	98	
strike orient (0-180)	set 2	17	17	17	17	
		-	-	-	-	
	set 3	98	98	98	98	
		fissility ratio (0 to 1)	0.2	0.49	0.2	0.16
		not required	*	*	*	*
moisture sensitivity		Duncan's Free Swell Coeff.				
		groundwater condition	dry	dry	dry	dry

**CLASSIFICATION DATA SHEET**

mine	RICCALL	coal seam	BARNESLEY
panel	505	gate	Tail
panel orientation	147	metre	922

		unit number	1	2	3	4	5	6
		height above seam roof	0.94 to 2.32	2.32 to 3.06	3.06 to 3.9	3.9 to 5.12	5.12 to 5.68	5.68 to 5.9
		basic rock type	drkgrey m.stone	grey m.stone	mass. siltstn	grey m.stone	grey m.stone	grey m.stone
		UCS (MPa)	20	41	43	28	48	52
bedding/ lamination properties	bed/lam spacing (m)	0.026	0.03	0.084	0.045	0.146	0.02	
		topography	planar	planar	planar	planar	planar	planar
		roughness (JRC)	4	4	4	4	4	4
	cohesion (% ucs)	0	0	0	0	0	0	0
		parting planes (No.)	53	24	10	27	4	11
joint persistence/ cleat dominance	joint/cleat set no.	2	2	2	2	2	2	2
		p	p	p	p	p	p	p
		set2	np	np	np	np	np	np
	set 3	-	-	-	-	-	-	-
		set1	4	4	4	4	4	4
joint/cleat roughness	set 2	4	4	4	4	4	4	4
		set 3	-	-	-	-	-	-
		set1	1000	1000	1000	1000	1000	1000
average spacing	set 2	1000	1000	1000	1000	1000	1000	1000
		set 3	-	-	-	-	-	-
		set1	98	98	98	98	98	98
strike orient (0-180)	set 2	17	17	17	17	17	17	17
		set 3	-	-	-	-	-	-
		fissility ratio (0 to 1)	0.2	0.3	0.43	0.34	0.41	0.4
moisture sensitivity	not required	*	*	*	*	*	*	*
	Duncan's Free Swell Coeff.							
	groundwater condition	dry	dry	dry	dry	dry	dry	dry

**CLASSIFICATION DATA SHEET**

mine	RICCALL	coal seam	BARNESLEY
panel	505	gate	MAIN
panel orientation	147	metre	669

		unit number	1	2	3	4	
		height above seam roof	0.75 to 1.18	1.18 to 2.3	2.3 to 2.82	2.82 to 5.75	
		basic rock type	grey m.stone	drk grey m.stone	grey m.stone	massive siltstn	
		UCS (MPa)	30	41	59	54	
bedding/ lamination properties	bed/lam spacing (m)	0.031	0.033	0.065	0.068		
		topography	planar	planar	planar	planar	
		roughness (JRC)	4	4	4	4	
	cohesion (% ucs)	0	0	0	0		
		parting planes (No.)	14	33	8	43	
		joint/cleat set no.	2	2	2	2	
joint persistence/ cleat dominance	set 1	p	p	p	p		
		set2	np	np	np	np	
		set 3	-	-	-	-	
joint/cleat roughness	set 1	4	4	4	4		
		set 2	4	4	4	4	
		set 3	-	-	-	-	
		set 1	1000	1000	1000	1000	
		set 2	1000	1000	1000	1000	
		set 3	-	-	-	-	
strike orient (0-180)	set 1	98	98	98	98		
		set 2	17	17	17	17	
		set 3	-	-	-	-	
		fissility ratio (0 to 1)	0.2	0.44	0.25	0.44	
moisture sensitivity	not required	*	*	*	*		
	Duncan's Free Swell Coeff.						
		groundwater condition	dry	dry	dry	dry	

**CLASSIFICATION DATA SHEET**

mine	RICCALL	coal seam	BARNESLEY
panel	505	gate	MAIN
panel orientation	147	metre mark	902

		unit number	1	2	3	4
		height above seam roof	1.0 to 2.2	2.2 to 4.54	4.54 to 5.00	5.00 to 5.95
		UCS (MPa)	33	62	86	60
bedding/ lamination properties	bed/lam spacing (m)	0.025	0.06	0.008	0.136	
	topography	planar	planar	planar	planar	
	roughness (JRC)	6	5	7	5	
	cohesion (% ucs)	0	0	0	0	
	parting planes (No.)	48	39	21	7	
		joint/cleat set no.	2	2	2	2
joint persistence/ cleat dominance	set 1	p	p	p	p	
	set 2	np	np	np	np	
	set 3	-	-	-	-	
joint/cleat roughness	set 1	4	4	4	4	
	set 2	4	4	4	4	
	set 3	-	-	-	-	
average spacing	set 1	1000	1000	1000	1000	
	set 2	1000	1000	1000	1000	
	set 3	-	-	-	-	
strike orient (0-180)	set 1	98	98	98	98	
	set 2	17	17	17	17	
	set 3	-	-	-	-	
		fissility ratio (0 to 1)	0.2	0.25	0.29	0.34
moisture sensitivity	not required	*	*	*	*	
	Duncan's Free Swell Coeff.					
		groundwater condition	dry	dry	dry	dry

**CLASSIFICATION DATA SHEET**

mine	RICCALL	coal seam	BARNESLEY
panel	505	gate	TAIL
panel orientation	147	metre	1583

		unit number	1	2	3	4	5	6
		height above seam roof	0.70 to 1.54	1.54 to 2.96	2.96 to 3.81	3.81 to 4.35	4.35 to 4.89	4.89 to 5.6
		basic rock type	drk. grey mudstn	grey mudstn	massive siltstn	grey mudstn	massive siltstn	grey mudstn
		UCS (MPa)	35	56	53	55	60	52
bedding/ lamination properties	bed/lam spacing (m)	0.034	0.051	0.028	0.036	0.054	0.054	
		planar	planar	planar	planar	planar	planar	
		4	4	4	4	4	4	
	roughness (JRC)	0	0	0	0	0	0	
	cohesion (% ucs)	25	28	3	15	10	13	
		parting planes (No.)	2	2	2	2	2	2
joint persistence/ cleat dominance	set 1	p	p	p	p	p	p	
		np	np	np	np	np	np	
		-	-	-	-	-	-	
joint/cleat roughness	set 1	4	4	4	4	4	4	
		4	4	4	4	4	4	
		-	-	-	-	-	-	
average spacing	set 1	1000	1000	1000	1000	1000	1000	
		1000	1000	1000	1000	1000	1000	
		-	-	-	-	-	-	
strike orient (0-180)	set 1	98	98	98	98	98	98	
		17	17	17	17	17	17	
		-	-	-	-	-	-	
		fissility ratio (0 to 1)	0.57	0.38	0.74	0.52	0.41	0.58
moisture sensitivity	not required	*	*	*	*	*	*	*
	Duncan's Free Swell Coeff.							
		groundwater condition	dry	dry	dry	dry	dry	dry

## ***COAL MINE CLASSIFICATION DATA SHEET***

mine Daw Mill                            coal seam: Warwickshire Thick  
 panel 94 gate coal                        metre mark 210  
 panel orientation 172

mine	ROSSINGTON	coal seam	BARNESLEY
panel	B2	gate	TAIL
panel orientation	160	metre	865

unit number		1	2	3	4	5	6	7
distance above top of coal seam		0 to 0.53	0.53 to 0.88	0.88 to 1.8	1.8 to 5.2	5.2 to 5.88	5.88 to 6.64	6.64 to 7.01
UCS (MPa)		43	30	56	70	67	25	43
bedding/ lamination properties	bed/lam spacing (mm)	20	20	115	1800	60	30	52
	topography	planar	planar	planar	planar	planar	planar	planar
	roughness	4	4	4	4	4	4	4
	cohesion (% ucs)	0	0	0	0	0	0	0
	parting planes (No.)	26	16	8	2	11	20	7
joint/cleat set no.		2	2	2	2	2	2	2
joint persistence/ cleat dominance	set 1	p	p	p	p	p	p	p
	set 2	np	np	np	np	np	np	np
	set 3							
joint/cleat roughness	set 1	4	4	4	4	4	4	4
	set 2	4	4	4	4	4	4	4
	set 3							
average spacing	set 1	1000	1000	1000	1000	1000	1000	1000
	set 2	1000	1000	1000	1000	1000	1000	1000
	set 3							
strike orient (0-180)	set 1	160	160	160	160	160	160	160
	set 2	70	70	70	70	70	70	70
	set 3							
fissility ratio (0 to 1)		0.35	0.3	0.35	0.5	0.35	0.2	0.35
moisture sensitivity	not required	x	x	x	x	x	x	x
	Duncan's Free Swell Coeff.							
groundwater condition		dry	dry	dry	dry	dry	dry	dry

mine	ROSSINGTON	coal seam	BARNESLEY
panel	B2	gate	TAIL
panel orientation	160	metre	865

	unit number	1	2	3	4	5	6
	distance above top of coal seam	1 to 0	0 to 0.4	-0.4 to -0.5	-0.5 to -1.8	-1.8 to -1.9	-1.9 to -2.8
	UCS (MPa)	30	40	20	40	20	40
bedding/ lamination properties	bed/lam spacing (mm)	20	60	10	60	10	60
	topography	planar	planar	planar	planar	planar	planar
	roughness	4	4	4	4	4	4
	cohesion (% ucs)	0	50	0	50	0	0
	parting planes (No.)	50	0	2	0	2	0
	joint/cleat set no.	2	2	2	2	2	2
joint persistence/ cleat dominance	set 1	p	p	p	p	p	p
	set 2	np	np	np	np	np	np
	set 3						
joint/cleat roughness	set 1	4	4	4	4	4	4
	set 2	4	4	4	4	4	4
	set 3						
average spacing	set 1	1000	60	1000	60	1000	60
	set 2	1000	60	1000	60	1000	60
	set 3						
strike orient (0-180)	set 1	160	160	160	160	160	160
	set 2	70	70	70	70	70	70
	set 3						
fissility ratio (0 to 1)		0.2	1	0.2	1	0.2	1
moisture sensitivity	not required	x	x	x	x	x	x
	Duncan's Free Swell Coeff.						
groundwater condition		dry	dry	dry	dry	dry	dry